NASA Contractor Report

STRAIN ENERGY RELEASE RATE AS A FUNCTION OF TEMPERATURE AND PRELOADING HISTORY UTILIZING THE EDGE DELAMINATION FATIGUE TEST METHOD

Richard S. Zimmerman and Donald F. Adams

Composite Materials Research Group
University of Wyoming
Laramie, Wyoming 82071

Contract NAG-1-674

February 1989

(NASA-CR-184966) STRAIN ENERGY RELEASE RATE AS A FUNCTION OF TEMPERATURE AND PRELOADING HISTORY UTILIZING THE EDGE DELAMINATION FATIGUE TEST METHOD Contractor Report, Jul. 1986 - Oct. 1988 (Wyoming Univ.) 270 p   N89-21286

G3/39   Unclas 0204574

NASA
National Aeronautics and Space Administration

Report Documentation Page

1. Report No.	2. Government Accession No.	3. Recipient's Catalog No.

4. Title and Subtitle
Strain Energy Release Rate as a Function of Temperature and Preloading History Utilizing the Edge Delamination Fatigue Test Method

5. Report Date
February 1989

6. Performing Organization Code

7. Author(s)
Richard S. Zimmerman and Donald F. Adams

8. Performing Organization Report No.
UW-CMRG-R-89-106

10. Work Unit No.

9. Performing Organization Name and Address
Composite Materials Research Group
University of Wyoming
P. O. Box 3295
Laramie, WY 82071

11. Contract or Grant No.
NAG-1-674

13. Type of Report and Period Covered
Contractor Report
July 1986 - October 1988

12. Sponsoring Agency Name and Address
National Aeronautics and Space Administration
NASA-Langley Research Center
Hampton, VA 23665

14. Sponsoring Agency Code

15. Supplementary Notes
Technical Monitor:
Dr. T. Kevin O'Brien
Fatigue and Fracture Branch - NASA-Langley Research Center

16. Abstract

Static laminate and tension-tension fatigue testing of IM7/8551-7 composite materials was performed. The Edge Delamination Test (EDT) was utilized to evaluate the temperature and preloading history effect on the critical strain energy release rate (G_c). Static and fatigue testing was performed at room temperature and 180°F (82°C). Three preloading schemes were used to precondition fatigue test specimens prior to performing the normal tension-tension fatigue EDT testing. Computer software was written to perform all fatigue testing while monitoring the dynamic modulus to detect the onset of delamination and record the test information for later retrieval and reduction.

17. Key Words (Suggested by Author(s))
edge delamination test (EDT)
strain energy release rate (G_C)
tension-tension fatigue
modulus decay
carbon fiber-reinforced/epoxy composite

18. Distribution Statement

19. Security Classif. (of this report)	20. Security Classif. (of this page)	21. No. of pages	22. Price
		270	

REPORT UW-CMRG-R-89-106

STRAIN ENERGY RELEASE RATE AS A FUNCTION OF TEMPERATURE AND PRELOADING HISTORY UTILIZING THE EDGE DELAMINATION FATIGUE TEST METHOD

RICHARD S. ZIMMERMAN
DONALD F. ADAMS

FEBRUARY 1989

TECHNICAL REPORT
NASA-LANGLEY RESEARCH CENTER
GRANT NO. NAG-1-674

COMPOSITE MATERIALS RESEARCH GROUP
DEPARTMENT OF MECHANICAL ENGINEERING
UNIVERSITY OF WYOMING
LARAMIE, WYOMING 82071-3295

PREFACE

This final report presents the results of a research program, initiated in July 1986, sponsored by the National Aeronautics and Space Administration under Grant No. NAG-1-674 (University of Wyoming Project No. 5-32474). The NASA Technical Monitor was Dr. T. Kevin O'Brien, Fatigue and Fracture Branch, Materials Division, NASA-Langley Research Center.

All work was performed by the Composite Materials Research Group (CMRG) within the Department of Mechanical Engineering at the University of Wyoming. Co-principal investigators were Mr. Richard S. Zimmerman, Staff Engineer, and Dr. Donald F. Adams, Professor. Making significant contributions to this program were Mr. Michael Borgman and Ms. Janice Atkins, undergraduate students in Mechanical Engineering and members of the CMRG.

Use of commercial products or names of manufacturers in this report does not constitute official endorsement of such products or manufacturers, either expressed or implied, by the National Aeronautics and Space Administration.

TABLE OF CONTENTS

SECTION 1

INTRODUCTION

The edge delamination test (EDT) is a mixed-mode fracture test method comprised of components of a tensile mode and a sliding or interlaminar shear mode of delamination (Mode I and Mode II). It was initially developed by Pagano and Pipes to characterize interlaminar fracture toughness in composite laminates and provide a method to determine their relative damage tolerance and toughness [1,2]. The EDT has been further developed by O'Brien and most recently has been proposed as a standard test method by the American Society for Testing and Materials (ASTM) [3,4].

The edge delamination specimen develops interlaminar normal stresses at the free edges when loaded in tension. These stresses, caused by large Poisson's ratio mismatches between plies, cause the specimen to delaminate at the ply interface with the highest interlaminar normal stress. The delamination is controlled by a combination of Mode I and Mode II. Several different laminate types have been used to perform this test, with varying percentages of Mode I and Mode II components based on the layup and material system [2,3]. O'Brien has also developed a finite element computer program to quantify the contribution of each mode in the EDT for the purpose of predicting material behavior related to damage tolerance and fracture toughness [3].

The EDT method is normally performed under static tensile loading but can be performed under tension-tension fatigue loading. Fatigue loading allows the determination of dynamic fracture toughness properties due to the cyclic loading. The purpose of this study was to measure effects of temperature and preloading history on critical strain energy release rate (G_C) determined using the edge delamination test method (EDT) in tension-tension fatigue. Tension-tension fatigue testing at two test temperatures was performed on IM7/8551-7 carbon fiber-reinforced epoxy composite specimens laid up in the $[\pm35/0/90]_s$ orientation. Some edge delamination specimens were fatigue tested with no preconditioning while others were preconditioned using one of two methods, i.e., a high mean load for 1000 cycles or a high spike load. Static tests to determine in-plane lamina properties and static edge delamination tests were also performed on IM7/8551-7 material.

SECTION 2

SUMMARY

All test specimens were fabricated and tested by the Composite Materials Research Group (CMRG) from cured panels supplied by NASA-Langley. The complete test matrix is given in Tables 1 and 2.

Static lamina testing was performed to generate in-plane material properties necessary to calculate the critical strain energy release rate (G_C) values measured in edge delamination tests (EDT). Static EDT were conducted to allow comparisons with dynamic EDT results. Transverse coefficient of thermal expansion (CTE) tests were also performed. Tension-tension fatigue testing was performed using the EDT method with three types of preconditioning of the test specimens.

Average axial and transverse tensile, edge delamination, and in-plane Iosipescu shear results are presented in Figures 1 through 4 as a function of test temperature. Average tabulated data are given in Section 4 and individual specimen data and stress-strain plots are presented in Appendix A.

Figure 1 shows the axial tensile test results for the IM7/8551-7 carbon fiber-reinforced/epoxy material. Figures 1a through 1c show that there were minimal differences in the longitudinal material properties between the two test temperatures. Figure 2 presents the transverse tensile material properties measured. Slightly more variation was seen in the transverse tensile material properties because of specimen configuration and material variations at the two test temperatures. These differences are discussed in detail in Section 4. Critical strain energy release rate (G_C) calculated from the static EDT results

TABLE 1

Test Matrix for Static Tests

Test Method	Test Temperature (°F) 75	180
	Test Replicates	
Axial Tension	5	5
Transverse Tension	5	5
In-Plane Iosipescu Shear	5	5
$[\pm 35/0/90]_s$ Edge Delamination	5	5
Transverse Coefficient of Thermal Expansion (-40°F to 250°F)	3	
	43 Specimens	

TABLE 2

Test Matrix for Edge Delamination Fatigue Tests at 10 Hz, R = 0.1

Fatigue Curve Type	Test Temperature (°F)	Specimen Replicates
Baseline Sine Wave (no preconditioning)	75	20
	180	20
High Load Spike in 1st Cycle (70 percent of ultimate load)	75	20
	180	20
High Mean Load Sine Wave (First 1000 cycles at 70 percent of ultimate peak load)	75	20
(First 1000 cycles at 60 percent of ultimate peak load)	180	20
Runout to 10^6 Cycles Typical Runout to 10^7 Cycles One Test/Curve		120 Specimens

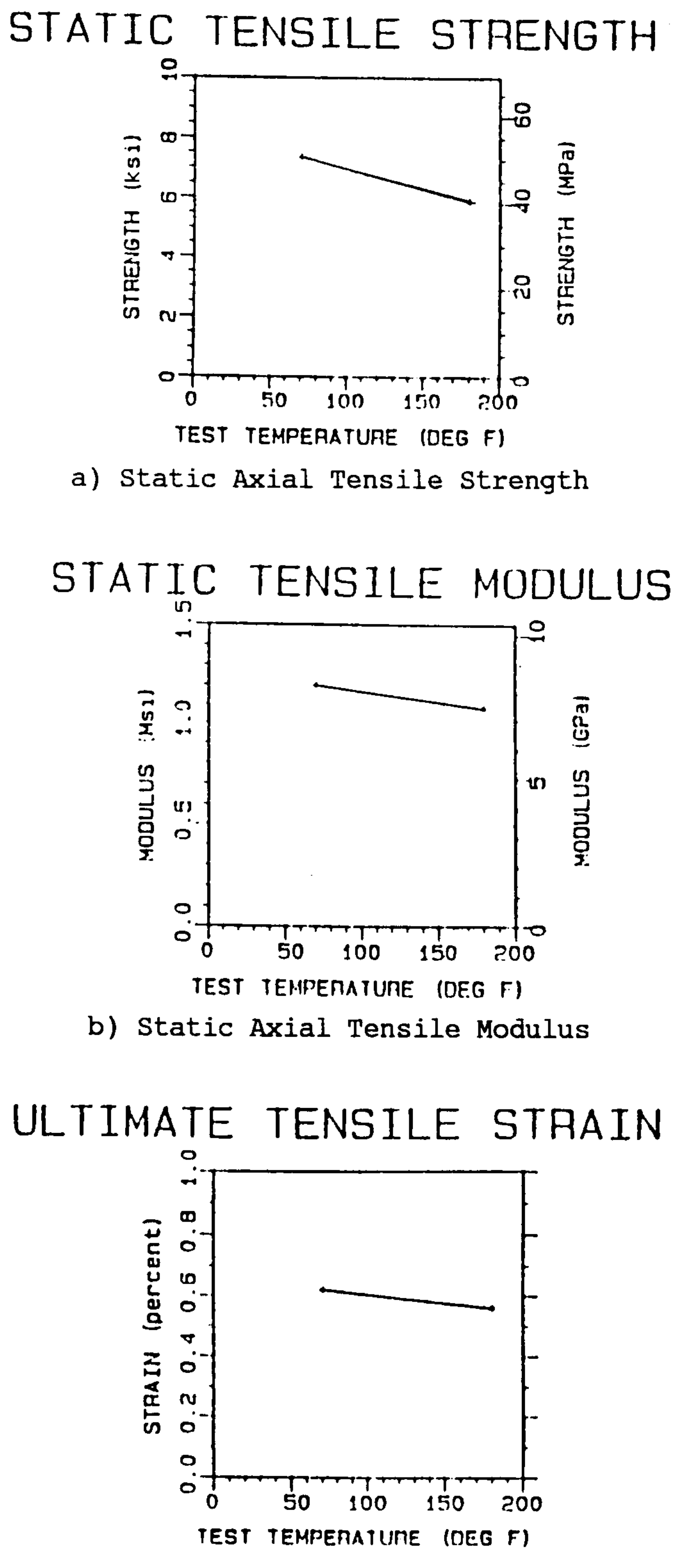

a) Static Axial Tensile Strength

b) Static Axial Tensile Modulus

c) Static Axial Tensile Ultimate Strain

Figure 1. Average Static Axial Tensile Results for the IM7/8551-7 Carbon/Epoxy Unidirectional Composite as a Function of Temperature.

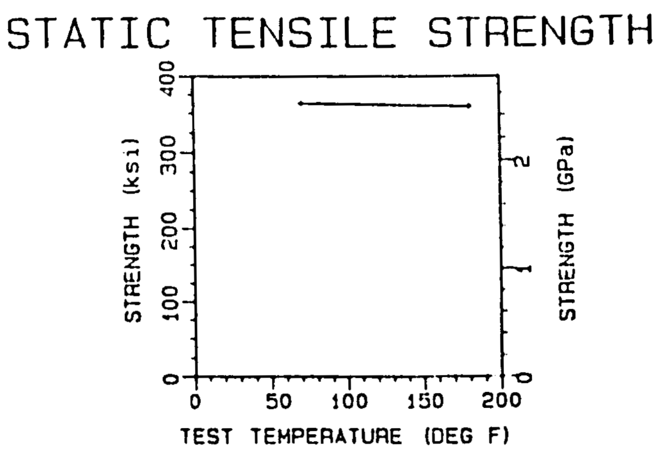

a) Static Transverse Tensile Strength

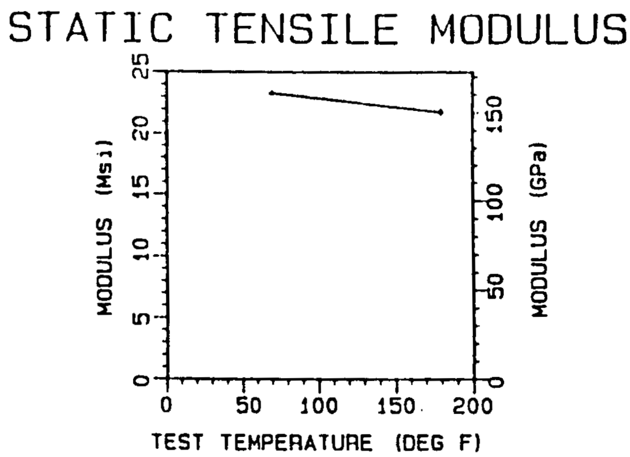

b) Static Transverse Tensile Modulus

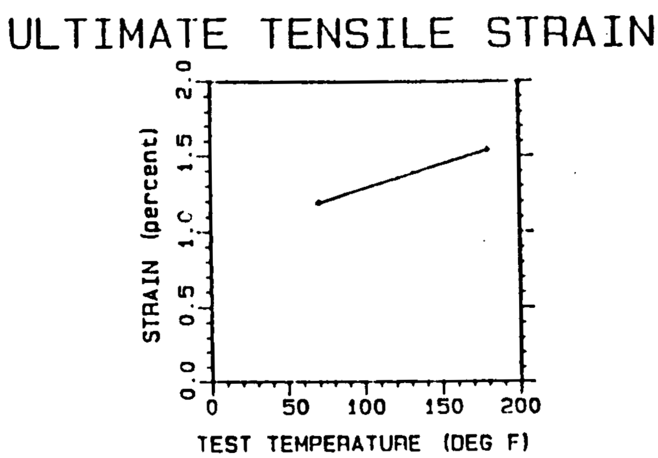

c) Static Transverse Tensile Ultimate Strain

Figure 2. Average Static Transverse Tensile Results for the IM7/8551-7 Carbon/Epoxy Unidirectional Composite as a Function of Temperature.

decreased slightly at the higher test temperature, as seen in Figure 3. In-plane Iosipescu shear properties are shown in Figure 4. Shear strength and modulus values decreased slightly at the higher test temperature. Ultimate shear strain variation with temperature could not be determined due to saturation of the strain gage rosettes at both test temperatures. Transverse CTE was measured for the IM7/8551-7 material.

Six complete fatigue curves were generated using EDT specimens. Three fatigue curves were generated at room temperature and three at 180°F (82°C), all at 10 Hz, using a sinusoidal waveform and a load ratio R equal to 0.1. Three preconditioning load histories (described in Section 3) were used to determine their effects on G_C. A laminated plate computer program (AC3) was used to calculate the sub-laminate modulus required for the calculation of the stiffness contribution in the strain energy release rate equation [12]. Cycles to delamination were reduced significantly after specimens had been preconditioned with the 1000 cycle high mean loading. Less effect on number of cycles to delamination was measured when a high spike loading precondition was performed prior to the fatigue loading. Values of G_C were higher at the elevated test temperature when the same precondition history fatigue curves were compared. This effect on G_C was the reverse of that seen in the static G_C data.

Section 3 discusses the test procedures and test apparatuses for all testing performed. Section 4 presents average test results for static and fatigue testing performed. Conclusions are given in Section 5. Individual test results are given in Appendices A and B.

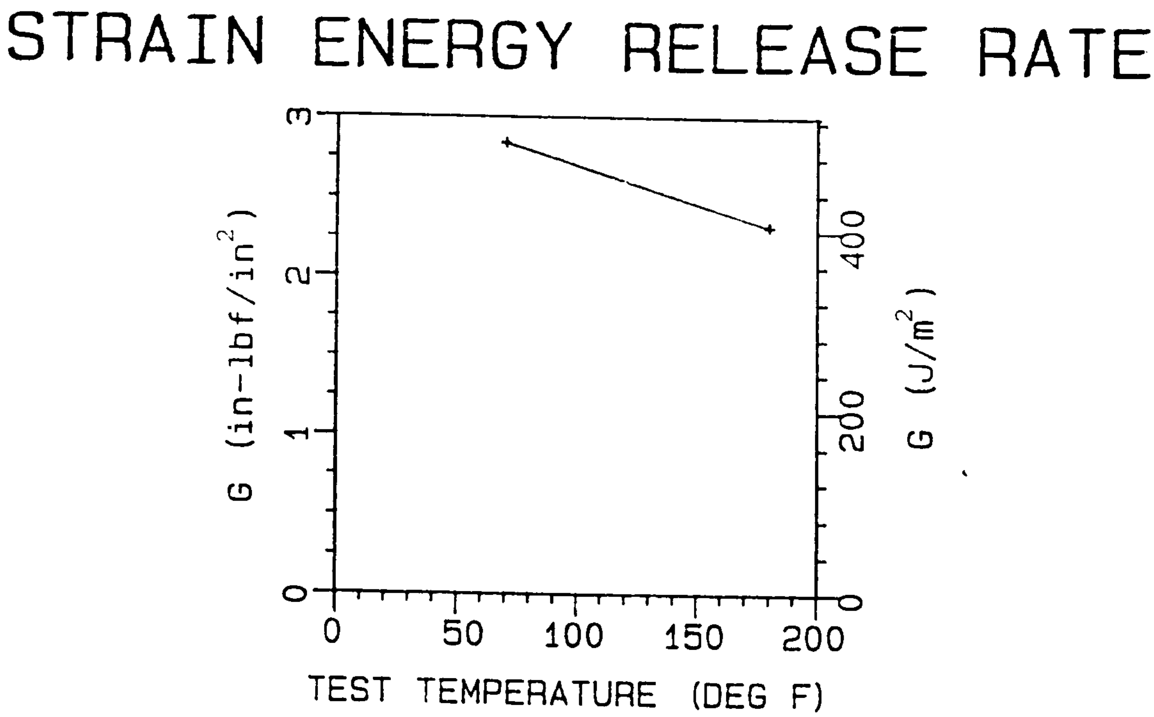

Figure 3. Average Static Critical Strain Energy Release Rate for IM7/8551-7 Carbon/Epoxy Unidirectional Composite as a Function of Temperature.

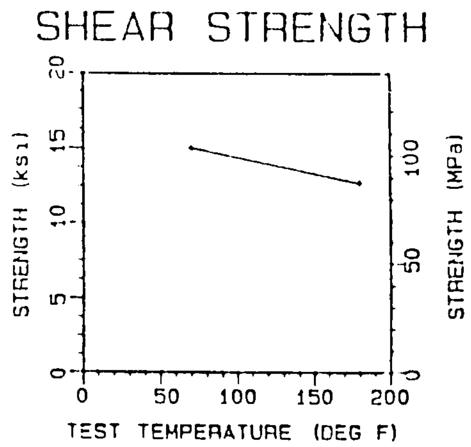

a) Static In-plane Iosipescu Shear Strength

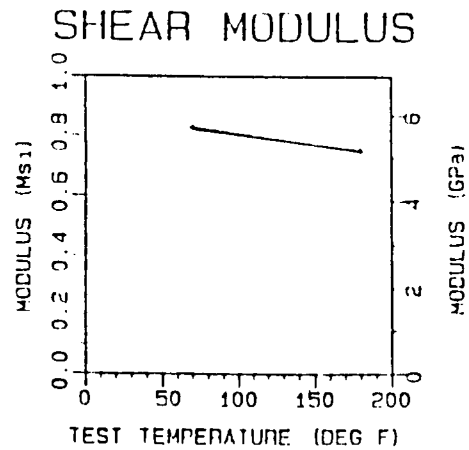

b) Static In-plane Iosipescu Shear Modulus

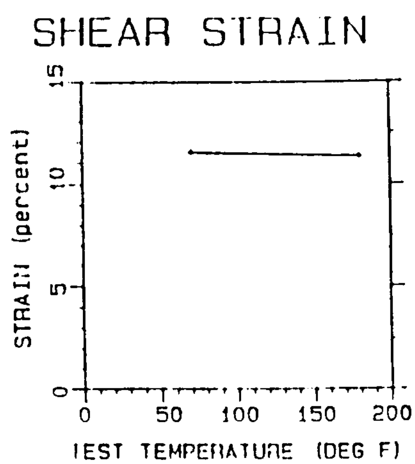

c. Static In-plane Iosipescu Shear Strain

Figure 4. Average In-plane Iosipescu Shear Results for IM7/8551-7 Carbon/Epoxy Unidirectional Composite as a Function of Temperature.

SECTION 3

SPECIMEN FABRICATION AND TEST PROCEDURES

3.1 Material

The material system chosen by NASA-Langley for this study was IM7/8551-7 carbon fiber-reinforced epoxy. It is a relatively new material system manufactured by Hercules Aerospace, Salt Lake City, Utah. The IM7 is a high strength, medium modulus carbon fiber (683 ksi (4.71 GPa), 41.0 Msi (283 GPa)) [4]. The 8551-7 is a rubber-toughened epoxy with good G_{IC} toughness properties (5.5 in-lb/in^2 (958 J/m^2)) [5]. All materials used in this program were supplied by NASA-Langley in flat plate form. Six inch (152.4 mm) square panels were supplied in the edge delamination test layup ($[\pm 35/0/90]_s$) and three different thickness unidirectional layups ($[0]_8$, $[0]_{12}$, and $[0]_{20}$). Enough material was supplied to complete six edge delamination fatigue curves and all required static tests.

3.2 Static Test Procedures

All specimens were cut from the supplied panels utilizing an abrasive cut-off wheel mounted on a surface grinder. Water cooling was used to ensure that the material did not overheat during the cutting process.

Acid digestion fiber volume determinations were performed on all panels. The procedure given in ASTM Standard Test Method D3171-76 was followed, where a 70% nitric acid was used to dissolve the matrix from the fibers using a hot plate to heat the samples to approximately 170°F (75°C) to speed up the reaction time [6]. The 8551-7 toughened epoxy dissolved at a slower rate than usually seen in this procedure on previously studied epoxies.

All static tests were conducted using a computer-controlled Instron Model 1125 electromechanical testing machine. A BEMCO Model FTU 3.0 environmental chamber was used to achieve the 180°F (82°C) test temperature. A crosshead rate of 0.08 in/min (2 mm/min) was used for all static testing except the edge delamination testing, which was performed at 0.04 in/min (1 mm/min).

3.2.1 Static Tension

Guidelines in ASTM Standard Test Procedure D3039-76 were followed for all static tension testing [7]. Conventional wedge action grips were utilized to load specimens for all static tension testing. Static axial tension test specimens were 6 in. (152 mm) long, 0.5 inch (12.7 mm) wide, and approximately 0.04 in. (1.0 mm) thick. Longer specimens are normally used for axial tension (9 in. (229 mm)) but the supplied panels limited the specimen length to the smaller dimension. Glass/epoxy circuit board material end tabs 1.5 in. (38 mm) long were bonded to each specimen using a two-part epoxy adhesive. The adhesive was Techkits A-12 (Techkits, Inc., Demarest, New Jersey). It is used extensively for bonding tabbing material to composite specimens and has good material properties up to 350°F (177°C). Axial strains were measured using a 2 inch (50.8 mm) gage length Instron extensometer, allowing complete stress-strain curves to be generated. Lateral strains were measured with a 0.5 inch (12.7 mm) gage length extensometer on the axial tension test specimens, allowing for the calculation of Poisson's ratio.

Transverse tension test specimens were 6 in. (152 mm) long, 0.75 in. (19 mm) wide, and 0.115 in. (2.9 mm) or 0.040 in. (1.0 mm) thick. Not all transverse tension specimens could be cut from the same thickness panel due to the small panel dimensions. None of the supplied panels were large enough to accommodate all the required ten transverse tension specimens. The five room temperature test specimens were cut from the 0.115 in. (2.9 mm) thick $[0]_{20}$ panel while the five elevated temperature test specimens were cut from a 0.04 inch (1.0 mm) thick $[0]_8$ panel. End tabs were not used with these specimens. Axial strains were measured using a 2 inch (50.8 mm) gage length Instron extensometer, allowing complete stress-strain curves to be generated. Transverse strains were not measured on the transverse tension specimens.

Edge delamination test (EDT) specimens were 6 in. (152 mm) long, 0.5 inch (12.7 mm) wide, and approximately 0.04 in. (1.0 mm) thick. This specimen geometry was used for previous edge delamination testing for NASA-Langley at the University of Wyoming [10]. Other geometries can be used for this test method as described by O'Brien and Carlsson and Pipes in references [3,14]. The smaller specimen configuration was used in this program to allow more specimens to be fabricated. Approximately 1.0 inch (25.4 mm) of each end of the EDT specimens was held in the grip area, leaving 4 in. (102 mm) between the grips. Axial strains were measured using a 2 inch (50.8 mm) gage length Instron extensometer, allowing complete stress-strain curves to be generated. Lateral strains were measured with a 0.5 inch (12.7 mm) gage length extensometer, allowing for the calculation of Poisson's ratio for the static EDT tests.

3.2.2 In-Plane Iosipescu Shear

In-plane Iosipescu shear test specimens were 3 in. (76.2 mm) long, 0.75 in. (19.1 mm) wide, and approximately 0.06 in. (1.6 mm) thick. Opposing 90° notches were cut on each edge of the specimens to a depth of 0.15 in. (3.8 mm). The notches were cut using a silicon-carbide grinding wheel dressed to the 90° angle with a 0.05 in. (1.3 mm) radius at the bottom of the notch.

Loads were applied to all in-plane shear specimens using a Wyoming Iosipescu shear test fixture. Shear strains were measured with a Measurements Group No. EP-13-062TH-120 two-element rosette strain gage mounted between the notches of the specimens. Complete shear stress-shear strain curves were generated for all Iosipescu shear specimens.

3.2.3 Transverse Coefficient of Thermal Expansion (CTE)

The transverse CTE test specimens were 5 in. (127 mm) long, 0.375 in. (9.5 mm) wide, and 0.115 in. (2.9 mm) thick. No axial coefficient of thermal expansion specimens were tested in this program.

Transverse CTE tests were performed using a microprocessor-controlled quartz-tube dilatometer in conjunction with a linear-variable differential transformer (LVDT). The specimens were exposed to thermal excursions between -40°F (-40°C) and 250°F (120°C). Data were acquired on the heat-up portion of the thermal cycles only. Two thermal cycles each were completed on the three specimens tested.

3.3 Tension-Tension Edge Delamination Fatigue Procedure

All fatigue tests were performed on an Instron Model 1321 biaxial servo-hydraulic testing machine using a 10 Hz sinusoidal excitation waveform and a load ratio R (ratio of minimum to maximum applied cyclic loading) approximately equal to 0.1. Axial strains were measured using a 2 inch (50.8 mm) gage length Instron extensometer. The extensometer knife edges were bonded to the EDT specimens using Devcon 5-minute two-part epoxy to ensure that the measured strains were not affected by slippage of the knife edges on the specimens' surface during the fatigue test.

Model 647.02S hydraulic grips manufactured by MTS, Inc., Minneapolis, Minnesota, were used to grip specimens for all edge delamination fatigue testing. The grips were equipped with special high temperature seals and actuating fluid system to allow usage up to 350°F (177°C). They have a load capacity of 5500 pounds (25 kN), which was sufficient to perform all EDT fatigue testing.

An Applied Test Systems, Inc. Series 2911 environmental chamber was used to achieve the required 180°F (82°C) test temperature. Chamber temperature was measured using a Type "E", Chromel-Constantan, thermocouple placed near the test specimen. Figure 5 shows the tension-tension fatigue test configuration used with the environmental chamber in place.

Six complete fatigue curves were generated using the EDT method while monitoring the dynamic modulus of the specimens. Three fatigue curves were generated at room temperature and three at elevated temperature, 180°F (82°C). The three fatigue curves at each temperature were generated using different preloading schemes prior to the normal sinusoidal fatigue test. One curve at each test temperature consisted of a normal sinusoidal loading to specimen delamination with no preload history (normal baseline curve). One curve at room temperature was

ORIGINAL PAGE IS
OF POOR QUALITY

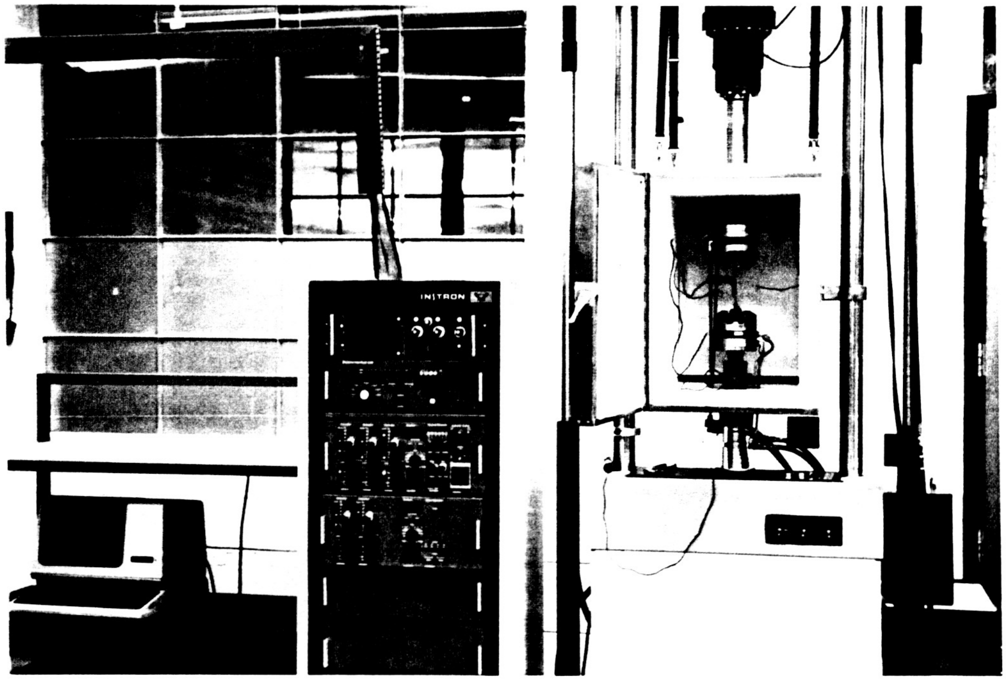

a) Overall View of EDT Fatigue Test Setup

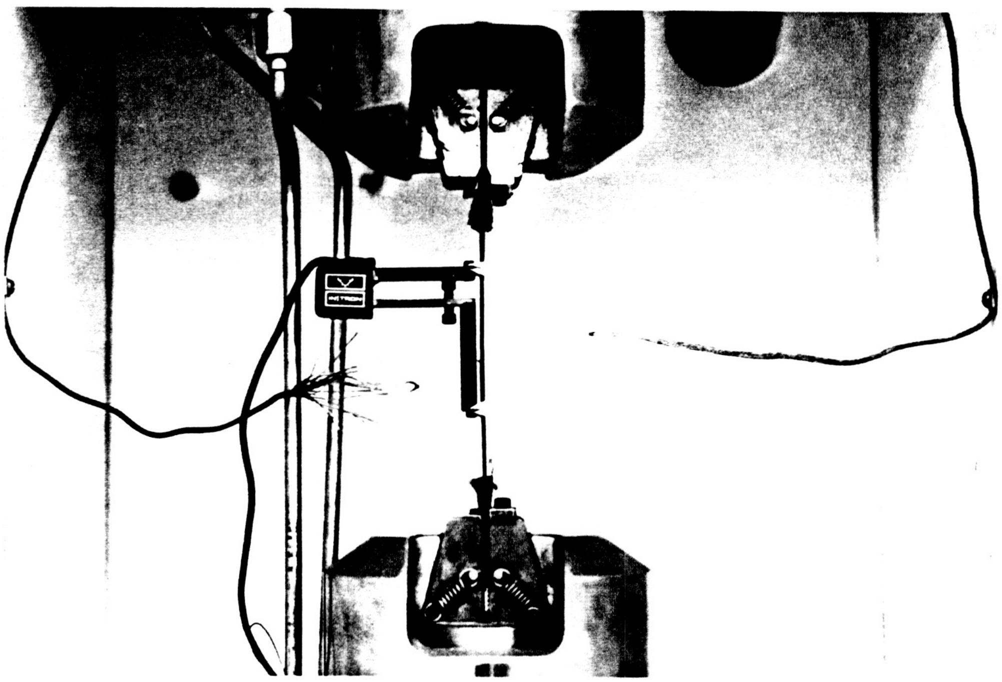

b) Close-up View of EDT Fatigue Test Setup

Figure 5. Edge Delamination Fatigue Test Configuration Showing Extensometer Mounted on EDT Specimen, Hydraulic Grips, Environmental Chamber, Instron Model 1321 Testing Machine, and Controls Cabinet.

generated with normal sinusoidal loading to delamination after the specimens had been subjected to a high cyclic load to 70 percent of ultimate load for 1000 cycles (high mean load curve). The elevated temperature fatigue curve with a high mean load for 1000 cycles was performed to only 60 percent of ultimate load because the EDT specimens delaminated before the 1000 cycles were completed at 70 percent of ultimate load. This precluded the possibility for further fatigue loading. The third fatigue curves at both test temperatures were generated after the EDT specimens had been subjected to a maximum load of 70 percent of ultimate load for one cycle (spike load curve).

The fatigue test procedure for all testing was quite complicated and required a great deal of time and effort to perfect. The application computer programs necessary to calibrate and perform the testing were written by the CMRG in Fortran 77 computer language on a PDP 11/24 minicomputer. The application programs interfaced with an Instron Machine Driver (IMD) to perform the required subroutine calls to control the test machine and to acquire the data during each fatigue test. The Instron Machine Driver is written in the Macro-11 computer language and is supported by Instron Corporation, Canton, Massachusetts. It consists of numerous machine control subroutines and data acquisition subroutines interfaced with the Instron testing machine hardware. Data recorded during each fatigue test were load, strain, stroke, and cycle count.

The application computer programs also performed many calculations and decisions based on the status of the fatigue test, such as to continue with the test if the specimen was intact, or stop the test if the specimen had delaminated causing a loss of stiffness. The decision to continue or suspend testing was based on the dynamic modulus calculated during the test. The dynamic modulus was calculated using a linear regression curve-fit technique. The lowest stress level during a cycle (σ_{min}) was found and the slope of the stress-strain curve was calculated over the next 20 data stress-strain pairs. If the calculated dynamic modulus had decreased by 5 percent or more from the initial calculated modulus, signifying delamination, then the computer would stop the fatigue test. Storage of data was accomplished using a logarithmic scheme similar to that used in previous modulus decay fatigue testing for NASA-Langley [8,9]. Table 5 gives the data storage progression used in this program.

There were five major steps required to prepare for and perform an EDT fatigue test. Step 1 was to calibrate the load, strain, and stroke

Table 5

DATA STORAGE PROGRESSION

Cycle Range	Cycle Increment Between Disk Storage
1 to 100	1
101 to 1000	10
1001 to 10,000	100
10,001 to 100,000	1,000
100,101 to 1,000,000	10,000
1,000,001 to 10,000,000	100,000

transducers to the appropriate values required. This step was performed periodically during the testing to verify that calibration values had not changed for the three transducers and their respective amplifiers.

Step 2 was to calibrate the computer with the three transducer outputs. This step was performed to ensure the computer had stored the current transducer calibrations before each fatigue test.

Step 3 was to perform a preliminary fatigue test using a square wave excitation on a specimen with similar stiffness to the actual test specimen. A square wave excitation was used to set the load transducer gain level for optimum control and response of the Instron test machine at each load level as described in the Instron Machine Operation Manual [11]. Step 3 was critical because of the limited load control response of the Instron 1321 at the 10 Hz cycling frequency. After setting the gain level to the optimum level, the computer program calculated the appropriate amount of computer control overprogramming necessary to ensure the loads transmitted to the specimen were close to the desired values. The mass of the torsional actuator below the linear actuator was very detrimental to the performance of the Instron Model 1321 test machine at the 10 Hz cycling frequency, but was fully compensated for by this load command overprogramming in the application computer program. The stiffness of the composite material specimens being tested was low enough and the inertia of the load frame actuator high enough to require a command overprogramming of 10 to 20 percent for all fatigue tests.

Step 4 was performed on only those specimens subjected to a pretest load history. The high mean load EDT specimens were tension-tension fatigue tested for 1000 cycles at a maximum peak load equal to 70 percent of ultimate load in the room temperature case, and 60 percent of ultimate load in the 180°F (82°C) case. The lower peak load precondition used for the elevated temperature specimens was necessary to prevent the delamination of the specimens prior to completing the full 1000 cycles. The spike load EDT specimens were cycled once to a peak load of 70 percent of ultimate prior to being subjected to the normal sinusoidal loading. It was not necessary to reduce the spike peak load level for the elevated temperature specimens because they did not delaminate during the one cycle at the 70 percent peak load level.

Performance of the actual tension-tension fatigue test on the edge delamination specimen at a particular stress level was Step 5. This step included performing the fatigue test between two predetermined stress values until delamination occurred and the specimen calculated dynamic modulus had decreased by at least 5 percent from the initial calculated value. Figure 6 shows a typical modulus decay curve. All modulus decay curves are included in Appendix B. When the dynamic modulus decreased to less than 95 percent of the original calculated value, the computer suspended the fatigue test and ramped to zero load. As Figure 6 shows, the drop in modulus was easily determined from the data. The critical strain value (ε_c) used in the G_C calculation was determined by looking at these curves and picking the location of the onset of delamination as the point where the modulus started to decrease to the minimum value for that test. At least one specimen for each fatigue curve was tested to 10^7 cycles to investigate material behavior at longer than normal fatigue test runout (typically 10^6 cycles). Optical inspection of test specimens, after the computer had suspended the tests, always revealed they had delaminated on one or both free edges.

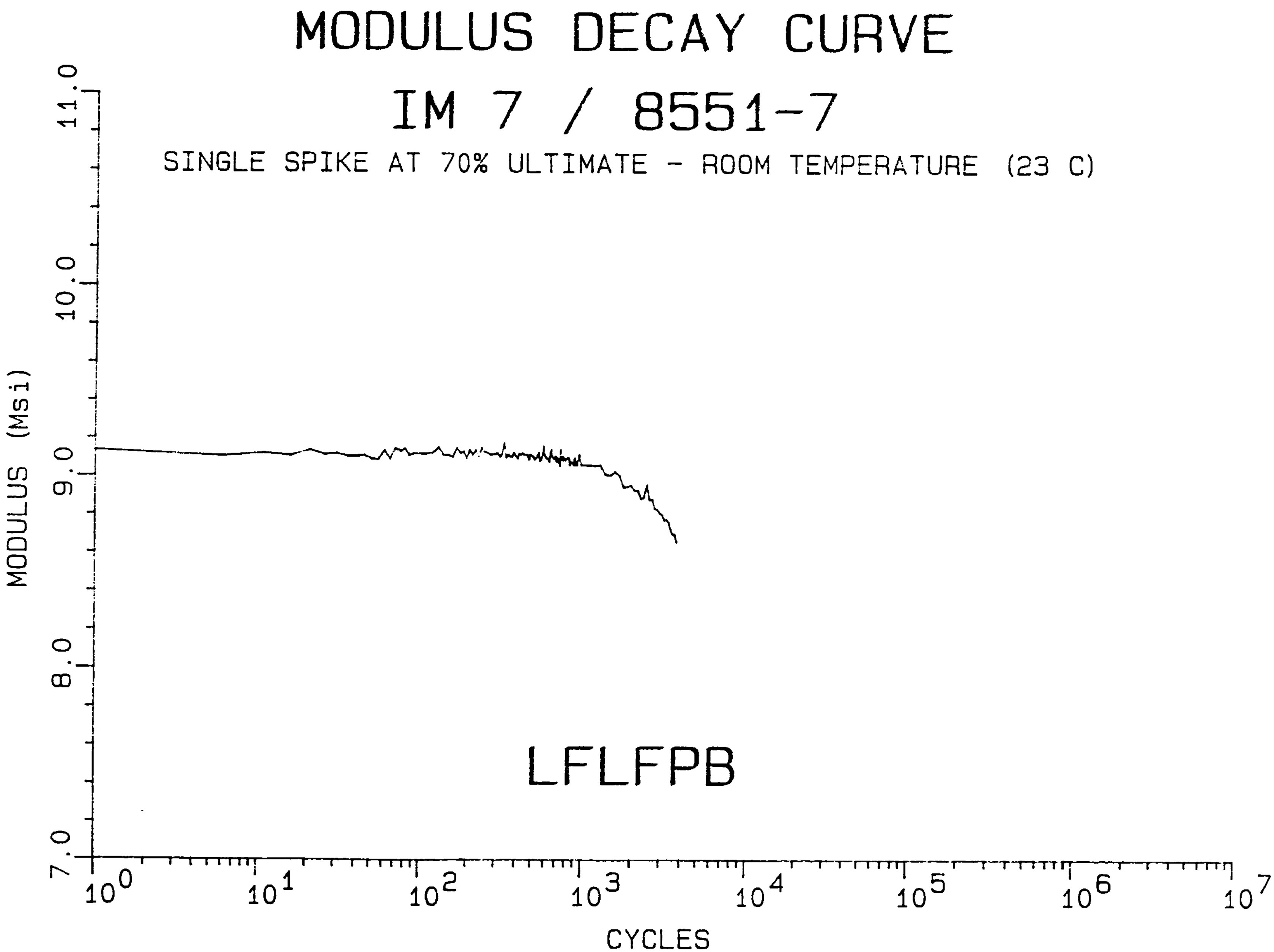

Figure 6. Typical Modulus Deday Curve Used to Determine Onset of Delamination.

Specimen data files were then transferred from the PDP11/24 to a VAX 11/750 minicomputer for reduction and plotting after test completion. Complete test results are presented in Section 4.

3.4 <u>Dye-Enhanced X-Ray and Optical Photography</u>

Dye-enhanced x-ray and optical photographs were taken of some of the specimens, to document the extent of the delaminations. A PANTEK Model HF75 Industrial X-ray unit was used to take all radiographs. This unit was designed especially for low density materials such as composites. The dye was the same used for previous work for NASA-Langley [10]. The mixture formula used is as follows:

60 gm	ZnI_2 (Zinc Iodide)
10 ml	Isopropyl Alcohol
10 ml	Deionized Water
1 ml	Kodak "Photo-Flo", Wetting Agent

Polaroid Type 55 sheet film was used for all x-ray photographs. Settings on the x-ray controls were adjusted to result in good contrast for better interpretation of the photographs. The control settings were 17 kilovolts (kV), 12 milliamps (mA), 20 seconds exposure time, and 17 inch (432 mm) film focal distance (FFD). Two specimens from each EDT fatigue curve were radiographed. These radiographs are presented in Section 4.

3.5 Temperature and Relative Humidity Measurement

Temperature and relative humidity measurements were recorded during most of the fatigue testing phase in the test laboratory using a Cole-Parmer Model 8368-50 hygrothermograph. Charts were changed periodically during the testing phase. Relative humidity ranged from 12 to 20 percent while laboratory temperature ranged from 68° to 86°F (20° to 30°C).

SECTION 4

TEST RESULTS

4.1 Fiber and Void Volume Results

All IM7/8551-7 panels supplied by NASA-Langley had a fiber volume of approximately 60 percent. The $[0]_8$ and $[\pm 35/0/90]_S$ panels had slightly higher fiber volumes than the $[0]_{12}$ and $[0]_{20}$ panels (62 percent versus 59 percent). Void volumes were typically less than 1 percent except for the EDT panels where 1.2 to 4.7 percent voids were measured. Individual tabulated fiber and void volume data are given in Appendix A.

4.2 Static Tension Test Results

All average static test results are given in Table 4. Individual static test results are given in Appendix A. Static tensile test results for the two test temperatures indicate the moderate elevated temperature, i.e., 180°F (82°C), had some effect on the material behavior.

A slight decrease in axial tensile strength, and axial Young's modulus, and an increase in ultimate axial tensile strain and major Poisson's ratio were measured at the elevated test temperature, possibly due to the higher test temperature causing slight softening of the matrix material.

Transverse tensile test results indicate that the IM7/8551-7 material had lower strength and stiffness properties at the elevated test temperature. Because the specimens tested at the two different

TABLE 4

Average Static Test Results for IM7/8551-7 Carbon Fiber-Reinforced Epoxy Composite Material

Test Method	Test Temperature (°F)	Ultimate Strength (ksi)	Ultimate Strength (MPa)	Modulus (Msi)	Modulus (GPa)	Ultimate Strain (percent)	Poisson's Ratio	Stress at Delamination (ksi)	Stress at Delamination (MPa)	Strain at Delamination (percent)	Strain Energy Release Rate $\frac{(in\text{-}lb)}{(in^2)}$	Strain Energy Release Rate $\frac{(J)}{(m^2)}$
Axial Tension	75	363	2505	23.3	160.7	1.19	0.18					
	180	359	2475	21.8	150.3	1.54	0.36					
Transverse Tension	75	7.3	51	1.20	8.2	0.62						
	180	5.9	41	1.08	7.4	0.56						
In-Plane Iosipescu Shear	75	15.0	104	0.83	5.7	>11.50						
	180	12.7	88	0.75	5.2	>11.30						
Edge Delamination $[\pm 35/0/90]_s$	75	106.6	735	9.85	67.9	1.16	0.20	81	559	0.85	2.84	497
	180	109.4	754	9.99	68.9	1.45	0.45	74	509	0.76	2.32	406

temperatures were cut from different panels and were of different thicknesses, an independent temperature effect could not be determined. The overall effect of specimen configuration and test temperature was seen as a decrease in transverse tensile strength and modulus and ultimate transverse tensile strain values at the higher test temperature.

Static EDT results indicate that the IM7/8551-7 material was almost 20 percent tougher at room temperature than at the elevated test temperature. Critical strain energy release rate (G_C) values were slightly lower at the elevated temperature due to the lower measured critical strain at delamination (ε_c) and the lower stiffness values for the laminates. Equation (1) was used to calculate G_C :

$$G_C = \tfrac{1}{2}\varepsilon_c^2 t \left(E_{lam} - E^*\right) \tag{1}$$

where G_C = critical strain energy release rate

ε_c = axial strain at delamination onset

t = laminate thickness

E_{lam} = initial laminate modulus

E^* = laminate modulus if completely delaminated along one or more interfaces

Strain at delamination onset (ε_c) was determined from the EDT stress-strain curves at the point where the curve began to deviate from linear behavior. E_{lam} was determined by calculating the initial tangent modulus for the static EDT specimens. Values for ε_c and E_{lam} are given in Table 4. The delaminated modulus (E^*) was calculated using Equation (2):

$$E^* = \frac{8E_{[\pm 35/0]s} + 2E_{22}}{8} \qquad (2)$$

No $[\pm 35/0]_S$ sub-laminate material was supplied to measure the stiffness values required to calculate the G_C values. Laminated Plate Theory Program AC3 was used to calculate the stiffness values for the sub-laminate used in the E^* calculations [12]. The E_{22} value was determined by calculating the initial tangent modulus from the transverse tensile tests. Appropriate values for each test temperature were used in all calculations.

4.3 In-Plane Iosipescu Shear Test Results

Average in-plane shear test results are presented in Table 4. Individual tabulated results and plotted results are given in Appendix A. Significant differences were seen in shear test results at the two test temperatures. Shear strength decreased by 25 percent and shear modulus decreased by 10 percent at the higher test temperature. Ultimate shear strains could not be determined due to saturation of the strain gage rosettes used to measure shear strain on the Iosipescu shear test specimens. Shear strains measured were quite nonlinear for this material system at both test temperatures.

4.4 Transverse Coefficient of Thermal Expansion (CTE) Results

Average transverse CTE results are presented here. Individual tabulated and plotted transverse CTE results are presented in Appendix A. The average transverse CTE value for the IM7/8551-7 material was 19.4 $\mu\varepsilon/°F$ (34.8 $\mu\varepsilon/°C$). This value is quite typical for most carbon fiber/epoxy material systems. No unusual behavior was seen in the thermal expansion testing results. No axial thermal expansion testing was conducted in this program due to the dilatometer equipment not being able to adequately measure the extremely small displacements in the axial direction for carbon fiber/epoxy composites.

4.5 **Tension-Tension Edge Delamination Fatigue Results**

Six complete fatigue curves were generated using the EDT method subjected to sinusoidal excitation loading at 10 Hz, R = 0.1, at various stress levels. Three of the fatigue curves were generated at room temperature and three at elevated temperature, 180°F (82°C). Three different specimen preconditioning methods were used to prepare the EDT test specimens for cyclic fatigue loading. One curve at each test temperature was generated using a normal sinusoidal loading to specimen delamination with no pretest load history (baseline curves). One curve at room temperature was generated with normal sinusoidal loading after the specimen had been subjected to a high cyclic load to 70 percent of ultimate load for 1000 cycles (high mean load curves). The elevated temperature precondition, with the high mean load for 1000 cycles, was performed to only 60 percent of ultimate load. The EDT specimens delaminated before the 1000 cycles were completed at 70 percent, precluding the need for further fatigue loading. The third fatigue curve at both test temperatures was generated after the EDT specimens had been subjected to 70 percent of ultimate load for one cycle only (spike load).

Figures 7 through 9 illustrate the temperature effect on G_C for each of the three load preconditions. Figure 7 shows the two normal fatigue curves generated at different temperatures. Figures 8 and 9

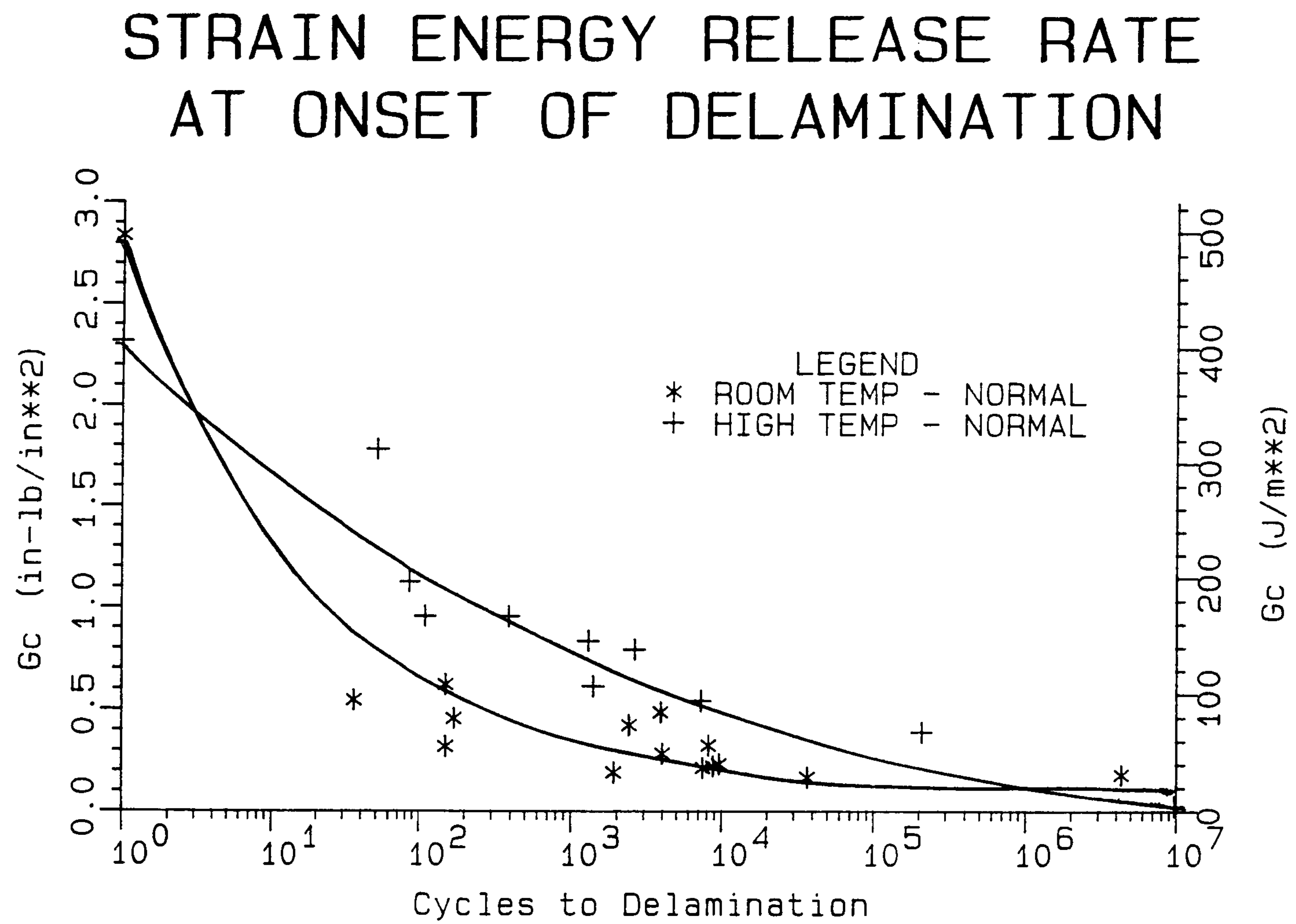

Figure 7. Critical Strain Energy Release Rate for IM7/8551-7 $[\underline{+}35/0/90]_s$ Laminates with No Precondition as a Function of Temperature.

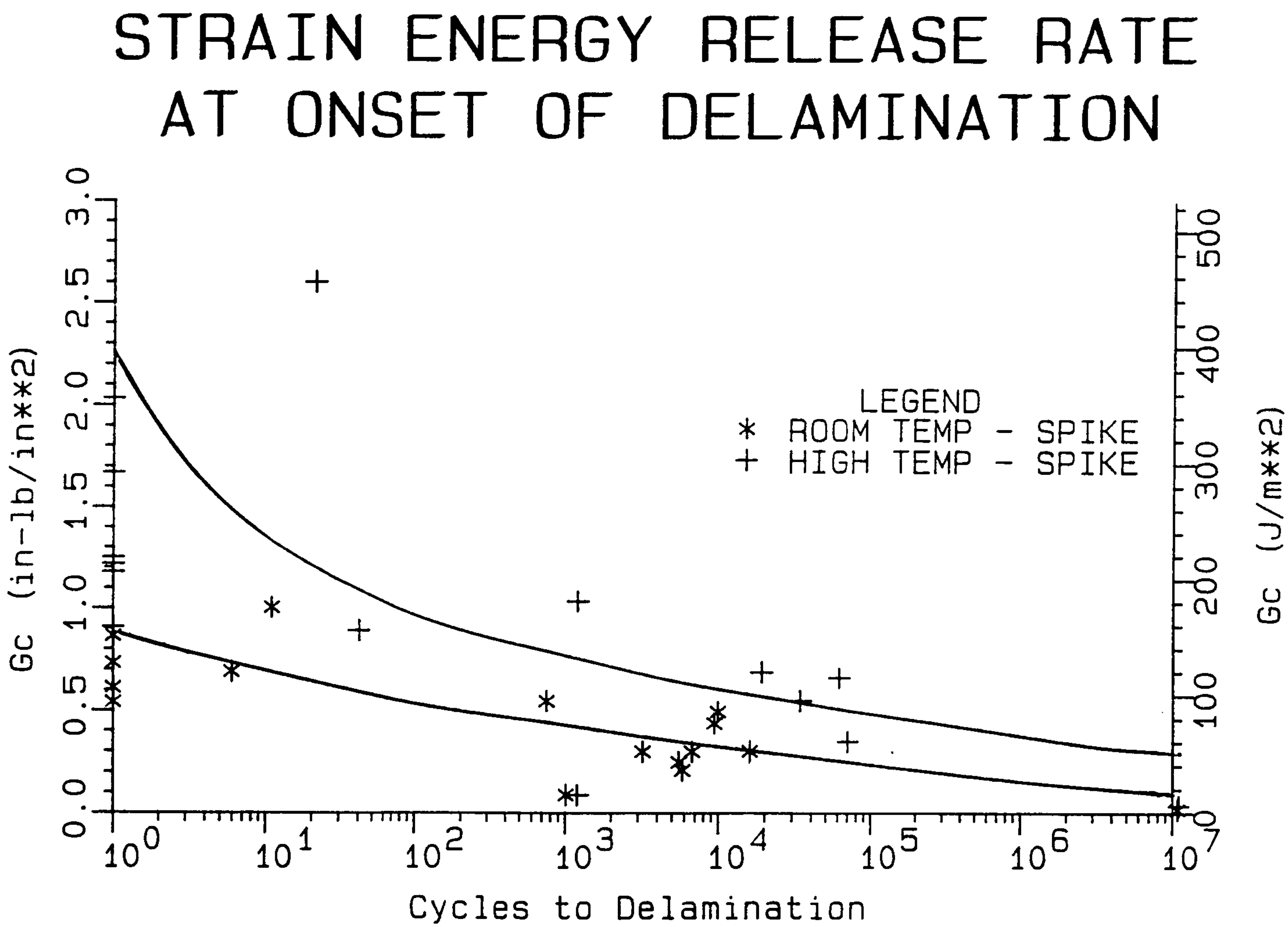

Figure 8. Critical Strain Energy Release Rate for IM7/8551-7 [±35/0/90]$_s$ Laminates with High Spike Load Precondition as a Function of Temperature.

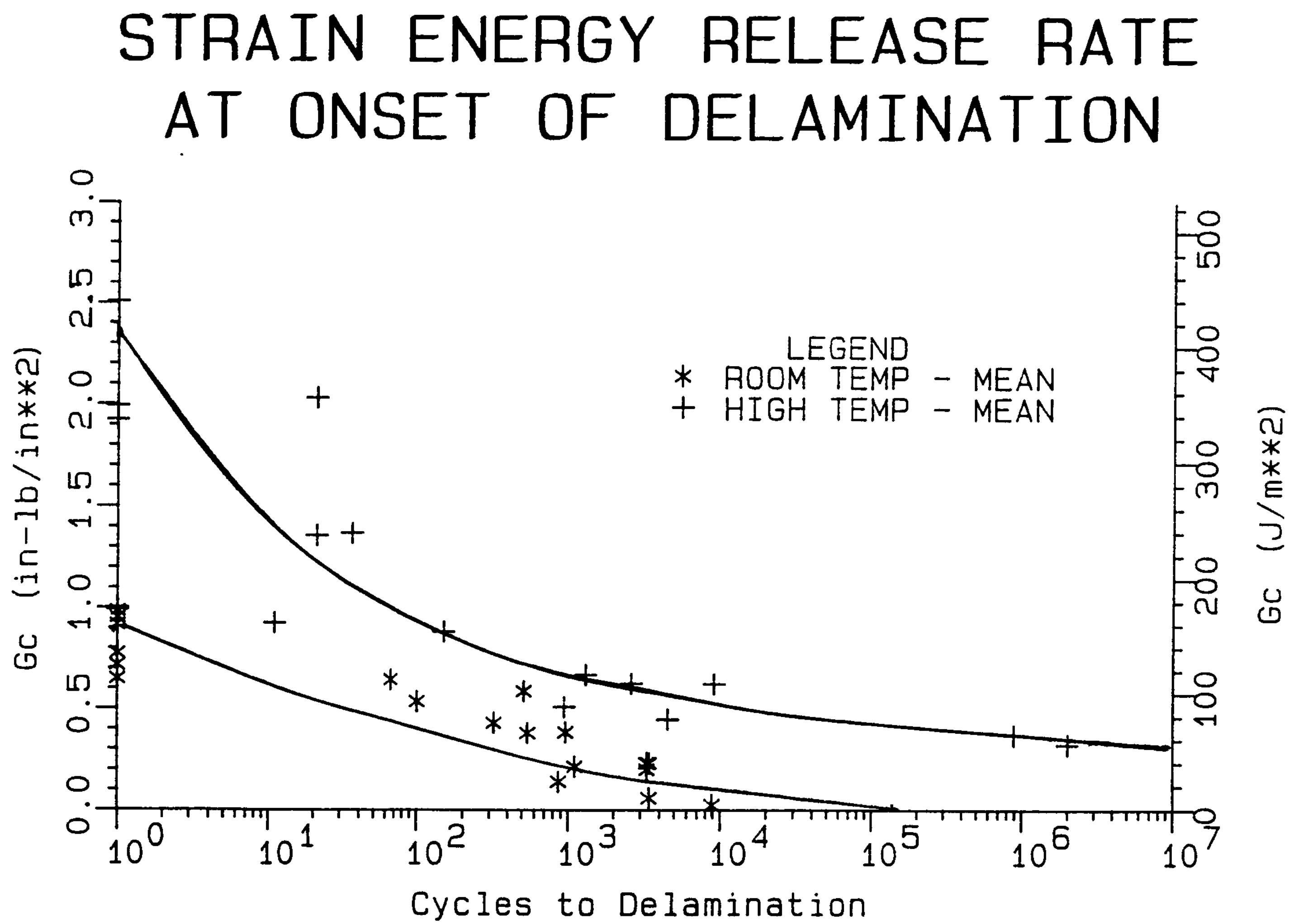

Figure 9. Critical Strain Energy Release Rate for IM7/8551-7 $[\pm 35/0/90]_s$ Laminates with High Mean Load for 1000 Cycles Precondition as a Function of Temperature.

show the high spike and high mean load precondition fatigue curves at the two test temperatures, respectively. The elevated temperature curve in all three of these figures indicates that higher dynamic G_C values were calculated independent of precondition method, for comparable cycles to delamination.

Comparisons of room temperature fatigue G_C values at low numbers of cycles with static G_C data (Table 4) indicate that the dynamic G_C values are much lower (a factor of two) than those generated under static loading at room temperature. Elevated temperature dynamic G_C values at a low number of cycles to delamination indicate much more consistent values compared with elevated temperature static G_C values.

The normal, high spike load, and high mean load curves at the room test temperature and elevated test temperature are plotted in Figures 10 and 11, respectively. Figure 10 indicates that there are significant effects due to the preloading history at room temperature. The two precondition loading curves indicate that damage incurred by the specimen is worse for the high mean load precondition than for the high spike precondition. At room temperature, nearly three decades fewer cycles were seen in the high mean precondition curve than the normal curve data. The spike precondition curve at room temperature indicates that approximately two decades fewer cycles to delamination were measured compared to the normal fatigue curve. Precondition comparisons in Figure 11 show that the effects were reduced significantly at the higher test temperature. Little difference could be seen between the three fatigue curves at the 180°F (82°C) test temperature after passing 10-100 cycles.

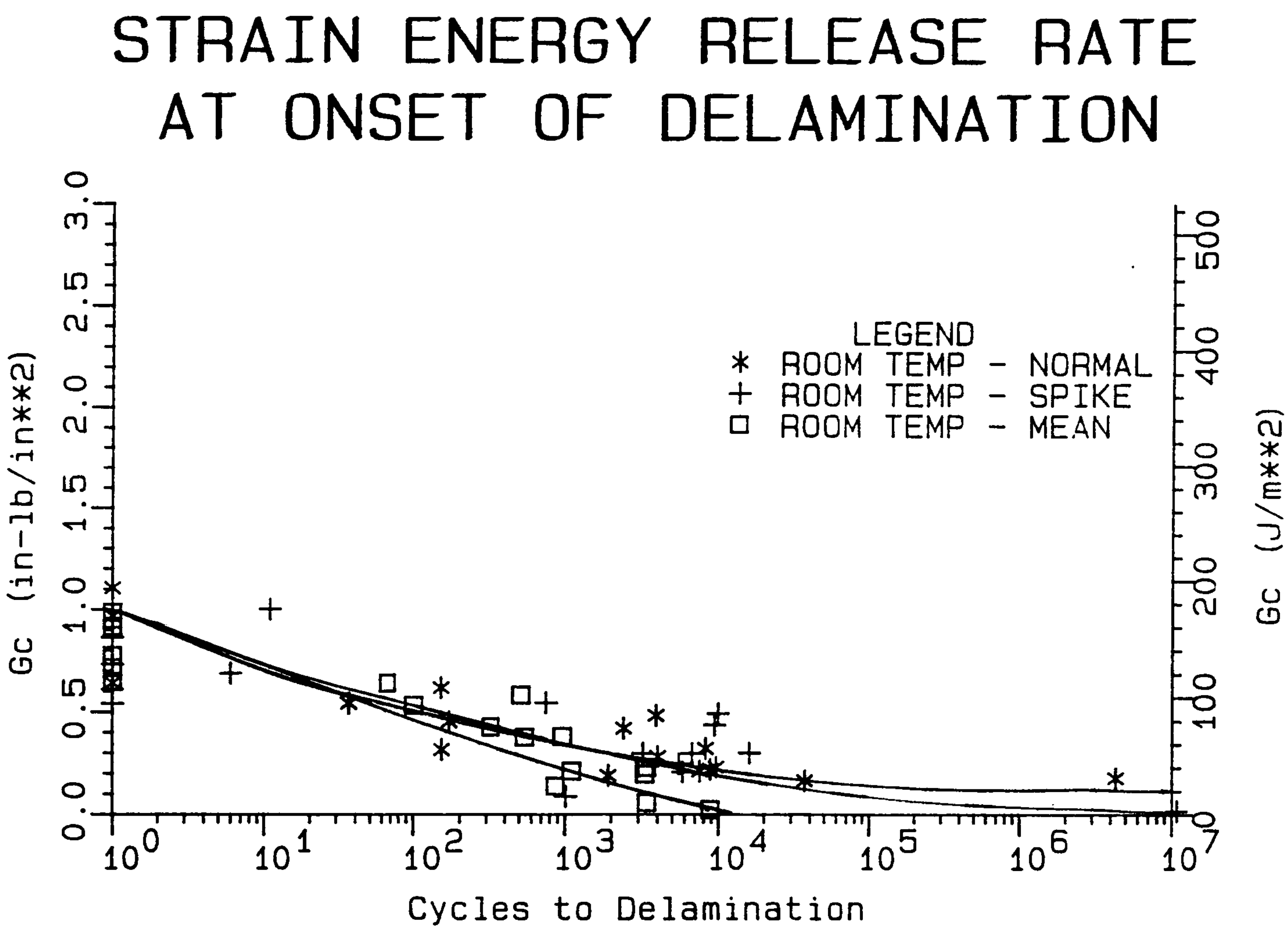

Figure 10. Critical Strain Energy Release Rate for IM7/8551-7 $[\underline{+}35/0/90]_s$ Laminates at Room Temperature as a Function of Precondition.

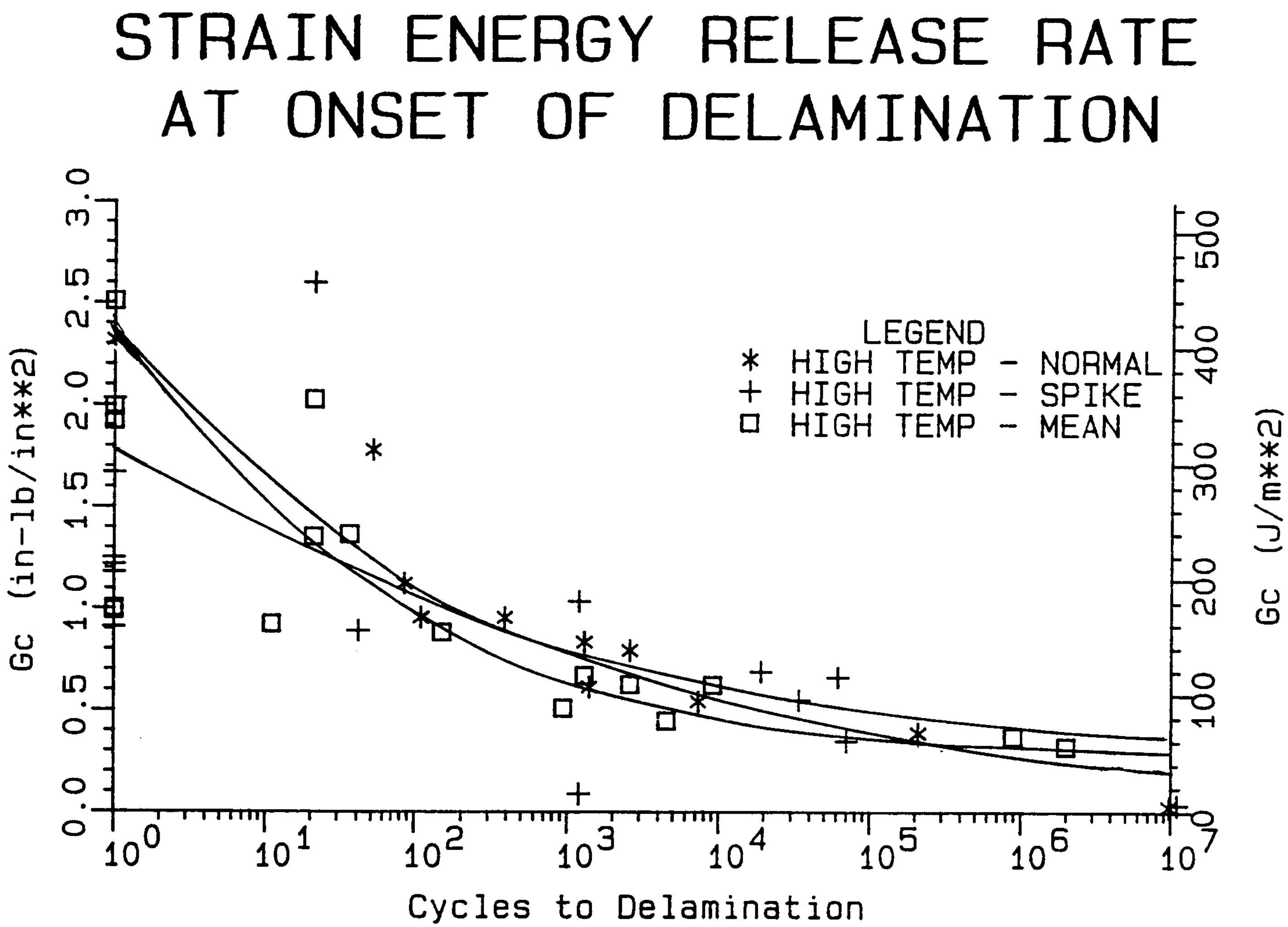

Figure 11. Critical Strain Energy Release Rate for IM7/8551-7 $[\pm 35/0/90]_s$ Laminates at Elevated Temperature (180°F (82°C)) as a Function of Precondition.

4.6 <u>X-ray and Optical Photograph Results</u>

Dye-penetrant enhanced x-rays and optical photographs were taken of some of the failed EDT specimens to document the extent of the delaminations. The x-ray opaque dye was composed of the materials listed in Section 3.5 at the given mixing ratios. Figures 12 through 17 are dye-penetrant enhanced x-rays of two specimens from each fatigue curve. At least two specimens from each fatigue curve were x-rayed to see if there were any differences in delamination zones due to temperature or the load history variations used for the fatigue testing. One specimen with less than 100 cycles and one with more than 10,000 cycles were x-rayed from each fatigue curve. The delamination zones appear as darkened areas in the radiographs. Number of cycles to delamination, temperature, and load precondition did not seem to affect the delamination zone size or appearance. Darkened areas at the points of extensometer attachment were due to the glue lines absorbing the dye and are not caused by actual damage to the specimens.

Optical photographs were taken of specimen edges to document the delamination crack at the free edge. Figures 18 and 19 are optical photographs of two specimen edges showing typical edge delamination cracks. The delamination occurred at the 0/90 interfaces in all cases, and wandered back and forth between the 0° plies within the 90° plies along the length of the specimens. This behavior was as expected for the $[\pm 35/0/90]_s$ layup used in this program. No variations in delaminations were seen between the different test temperatures or preloading history specimens to indicate any visible effect on the delamination crack path.

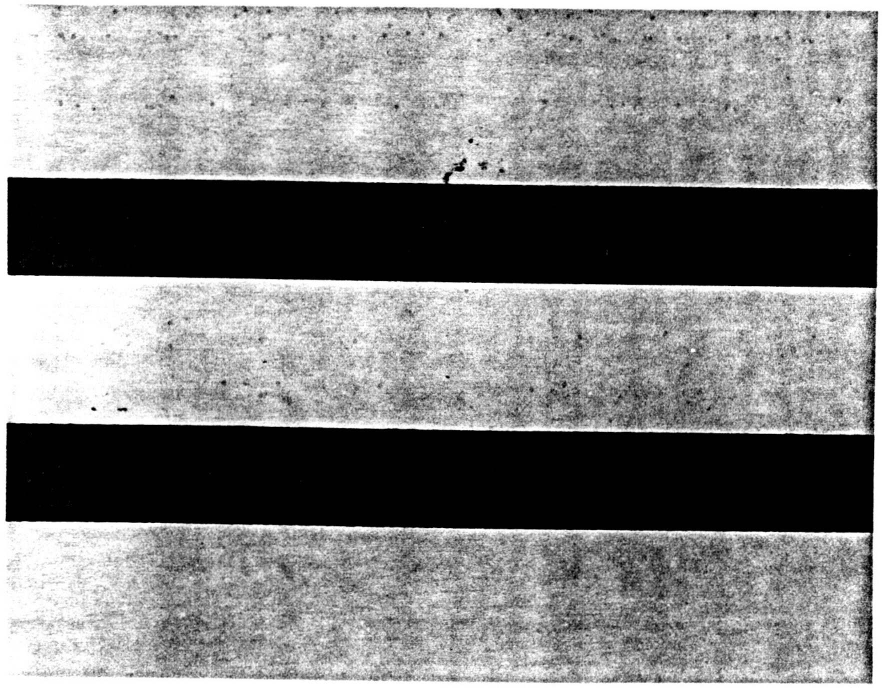

Figure 12. Dye-enhanced X-ray Photograph of Two EDT Fatigue Failed Specimens at Room Temperature, No Precondition.

Top: Specimen No. LFLESA - 36 Cycles to Delamination.
Bottom: Specimen No. LFLLSD - 950 Cycles to Delamination.

ORIGINAL PAGE IS
OF POOR QUALITY

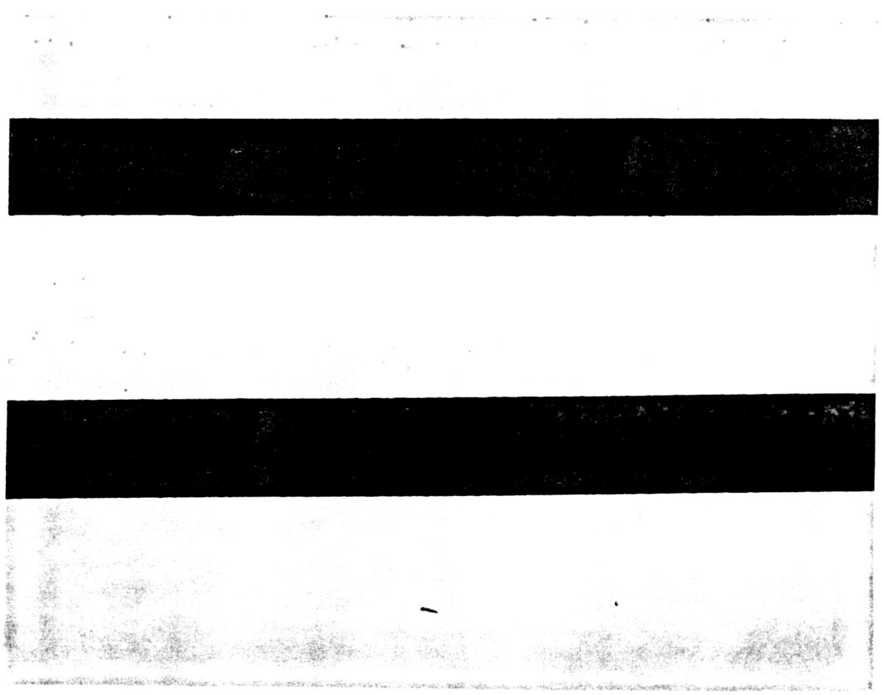

Figure 13. Dye-enhanced X-ray Photograph of Two EDT Fatigue Failed Specimens at Room Temperature, High Spike Load Precondition.

Top: Specimen No. LFLDPA - 1 Cycle to Delamination.
Bottom: Specimen No. LFLNPB - 1000 Cycles to Delamination.

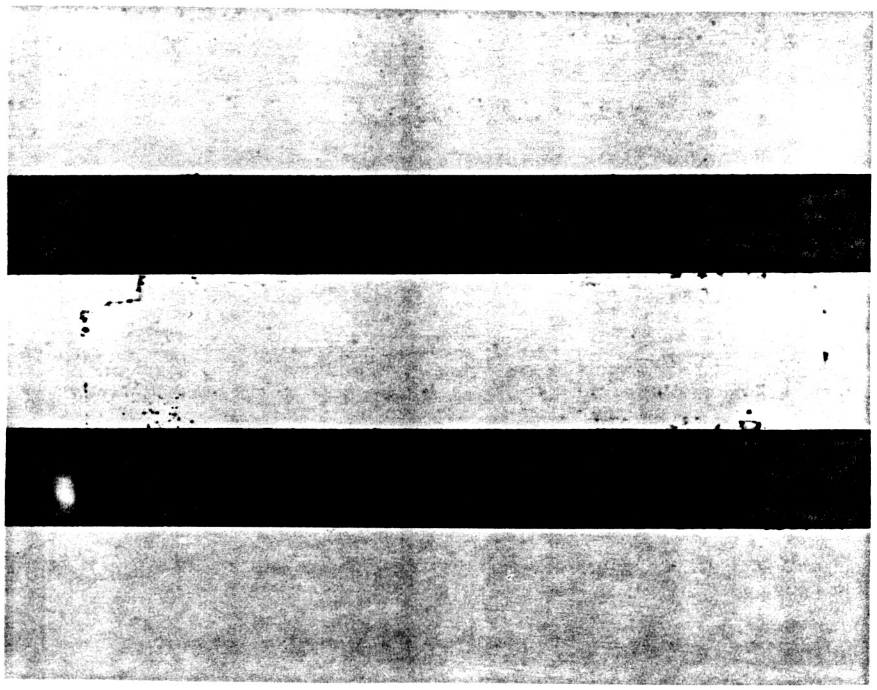

Figure 14. Dye-enhanced X-ray Photograph of Two EDT Fatigue Failed Specimens at Room Temperature, High Mean Load Precondition.

Top: Specimen No. LFLDMB - 66 Cycles to Delamination.
Bottom: Specimen No. LFLLMA - 3300 Cycles to Delamination.

ORIGINAL PAGE IS
OF POOR QUALITY

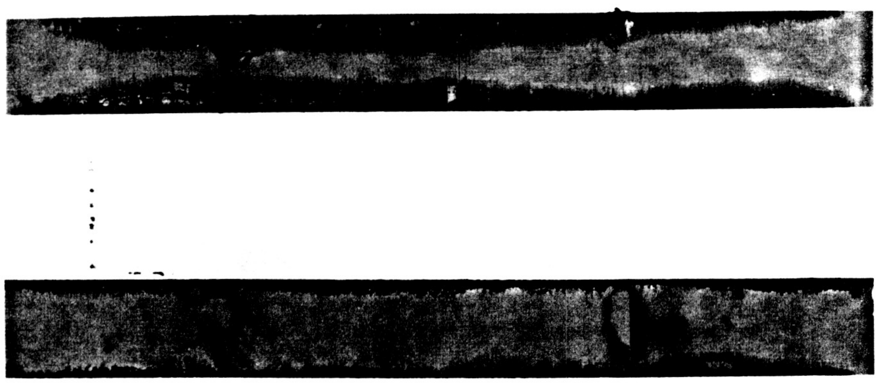

Figure 15. Dye-enhanced X-ray Photograph of Two EDT Fatigue Failed Specimens at 180°F (82°C), No Precondition.

Top: Specimen No. LFHESA - 51 Cycles to Delamination.
Bottom: Specimen No. LFHMSB - 210,000 Cycles to Delamination.

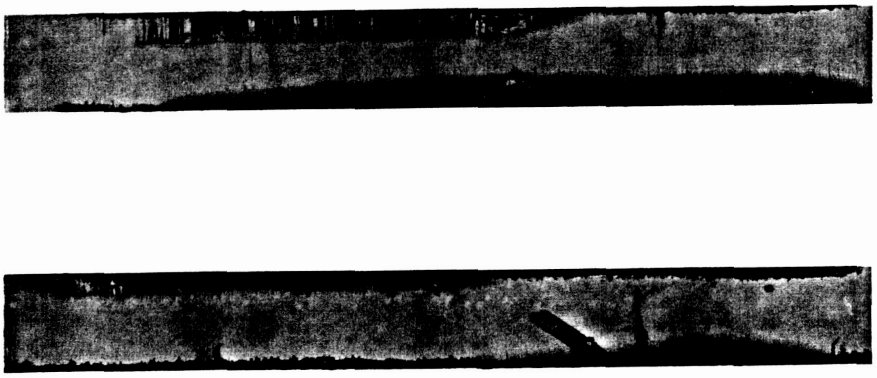

Figure 16. Dye-enhanced X-ray Photograph of Two EDT Fatigue Failed Specimens at 180°F (82°C), High Spike Load Precondition.

Top: Specimen No. LFHEPA - 1 Cycle to Delamination.
Bottom: Specimen No. LFHMPA - 70,000 Cycles to Delamination.

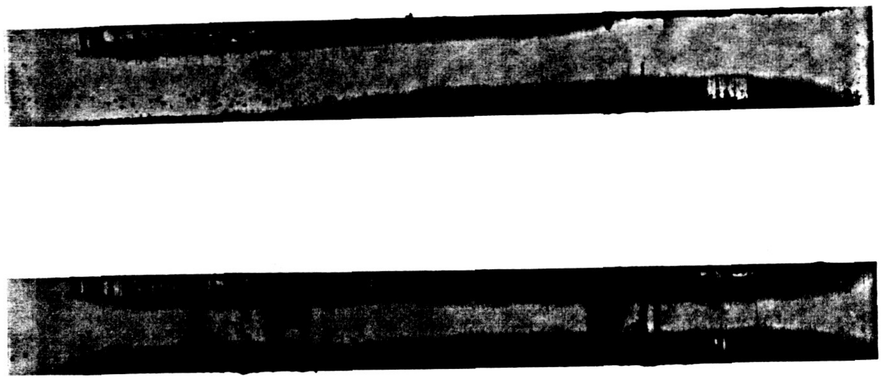

Figure 17. Dye-enhanced X-ray Photograph of Two EDT Fatigue Failed Specimens at 180°F (82°C), High Mean Load Precondition.

Top: Specimen No. LFHFMA - 1 Cycle to Delamination.
Bottom: Specimen No. LFHMMA - 890,000 Cycles to Delamination.

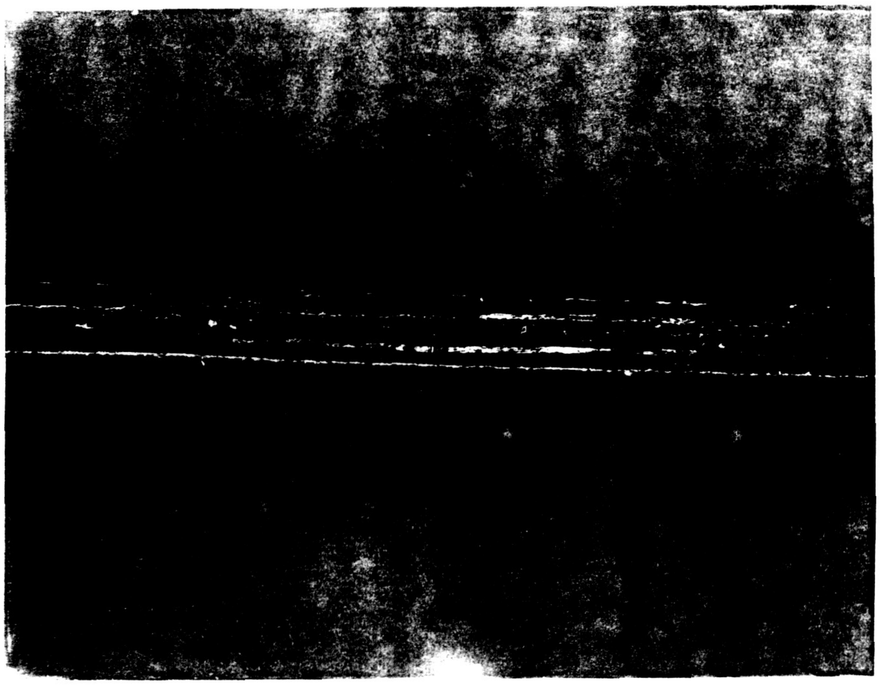

Figure 18. Optical Photograph of Failed EDT Fatigue Specimen Showing a Crack at the Free Edge in the 90° Plies.

Figure 19. Optical Photograph of Failed EDT Fatigue Specimen Showing a Crack on the Free Edge in the 90° Plies.

SECTION 5

CONCLUSIONS

Static lamina, static edge delamination, and tension-tension fatigue edge delamination testing was performed on IM7/8551-7 carbon fiber-reinforced/epoxy. Static lamina test results indicated some reduction in material properties from the elevated test temperature on this material system. Matrix-dependent material properties (shear, transverse tension, and EDT) measured at the elevated test temperature were typically lower than those measured at room temperature. Higher test temperatures could be used for future testing to identify an upper use temperature for this material system. The IM7/8551-7 performed well at the 180°F (82°C) test temperature. Static test results indicated that the G_C of this material system was quite good compared to other material systems previously tested [5,6]. Results from this test program should allow the finite element analysis used by O'Brien to predict the contributions of G_{Ic} and G_{IIc} to G_C for this material [3].

At room temperature, EDT fatigue results indicated lower G_C values (half of static values) were measured compared to static G_C values. All three preconditions resulted in lower G_C at room temperature. EDT fatigue testing at the 180°F (82°C) test temperature indicated that comparable values of G_C were measured compared to static EDT values.

Effects on G_C at elevated temperature due to preconditioning test specimens were minimal. Only at the high stress level/low number of cycles portion of the fatigue curves was there much variation in G_C between the different load preconditioning data. The high mean load and high spike load curves resulted in G_C values lower than the no precondition curve values up to about 100 cycles. Elevated temperature data from the three precondition curves approached the same G_C value at runout (10^7 cycles).

The room temperature G_C values at equal number of cycles from the three precondition curves were quite different after 10,000 cycles. The three room temperature curves showed a strong influence of the precondition method used with the high mean load having the lowest G_C values and the no precondition G_C values being the highest values at greater than 10,000 cycles. Number of cycles to delamination was reduced by three to four decades compared with the no precondition case after specimens had been preconditioned at room temperature by the high mean level method. Two to three fewer decades of cycles to delamination were measured after preconditioning with the single high spike loading compared with the no precondition case.

Optical photographs showed that the delamination crack on the free edge of specimens did not vary due to test temperature or precondition. Dye-enhanced radiographs taken of delaminated specimens showed that no discernible differences could be attributed to the two different test temperatures or three preconditions.

REFERENCES

1. R.B. Pipes and N.J. Pagano, "Interlaminar Stresses in Composite Laminates under Uniform Axial Extension," Journal of Composite Materials, Vol. 4, 1970, pp. 538-548.

2. N.J. Pagano and R.B. Pipes, "Some Observations on the Interlaminar Strength of Composite Laminates," International Journal of Mechanical Sciences, Vol. 15, 1973, pp. 679-688.

3. T.K. O'Brien, "Characterization of Delamination Onset and Growth in a Composite Laminate," Damage in Composite Materials, ASTM STP 775, American Society for Testing and Materials, Philadelphia, Pennsylvania, 1982, pp. 140-167.

4. T.K. O'Brien and N.J. Johnston, "A Simple Test for the Interlaminar Fracture Toughness of Graphite/Epoxy Laminates," Proceedings of the 27th National SAMPE Symposium, May 1982, Reno, Nevada, p. 401-415.

5. "Magnamite Graphite Fiber, Type IM7," Data Sheet 868, Hercules, Inc., Wilmington, Delaware, 1988.

6. "Hercules Prepreg Tape Materials Characterization Data Package," Hercules Composite Products Group, Magna, Utah, November 1988.

7. "Standard Test Method for Fiber Content of Resin-Matrix Composites by Matrix Digestion," ASTM Standard Test Method D-3171-76 (Reapproved 1982), 1988 ASTM Annual Book of Standards, Section 15, Volume 15.03, American Society for Testing and Materials, Philadelphia, Pennsylvania, 1988, pp. 122-124.

8. "Standard Test Method for Tensile Properties of Fiber-Reinforced Composites," ASTM Standard Test Method D-3039-76 (Reapproved 1982), 1988 ASTM Annual Book of Standards, Section 15, Volume 15.03, American Society for Testing and Materials, Philadelphia, Pennsylvania, 1988, pp. 117-121.

9. E.M. Odom and D.F. Adams, "Stiffness Reductions During Tensile Fatigue Testing of Graphite/Epoxy Angle-Ply Laminates," NASA Contractor Report 166019, National Aeronautics and Space Administration, Washington, D.C., November 1982.

10. R.S. Zimmerman, D.F. Adams, and E.M. Odom, "Load Ratio and Frequency Effects on Strain Energy Release Rate During Tensile Fatigue Testing Utilizing the Edge Delamination Test," Report UWME-DR-401-109-1, Department of Mechanical Engineering, University of Wyoming, December 1984.

11. Operation Manual for 2150 Controllers, Manual No. 11-1-12, Instron Corporation, Canton, Massachusetts, 1977, pp. 2.4-2.6.

12. Standard Tests for Toughened Resin Composites, NASA Reference Publication 1092, Revised Edition, Compiled by ACEE Composites Project Office, NASA-Langley Research Center, Hampton, Virginia, 1983, pp. 7-14.

13. Advanced Composites Design Guide, Vol. II-Analysis, Air Force Flight Dynamics Laboratory, Dayton, Ohio, January 1973, pp. 2.B.1.1-2.B.1.29.

14. L.A. Carlsson, and R.B. Pipes, Experimental Characterization of Advanced Composite Materials, Prentice-Hall, Inc., Englewood Cliffs, New Jersey, 1987.

APPENDIX A

INDIVIDUAL STATIC TEST RESULTS

Table A1

Individual Fiber and Void Volume Results for IM7/8551-7 Composites

Plate Layup	Fiber Volume (V_f) (Percent)	Void Volume (V_v) (Percent)
$[0]_8$	62.9	4.8
	64.1	1.7
	63.0	0.9
Average	63.4	2.5
Std. Dev.	0.6	2.1
$[0]_{12}$	59.6	0.7
	60.1	0.4
	59.8	0.6
Average	59.8	0.6
Std. Dev.	0.2	0.2
$[0]_{20}$	57.9	0.8
	57.8	1.0
	58.0	4.1
Average	57.9	2.0
Std. Dev.	0.1	1.8
$[\pm35/0/90]_S$	62.7	1.2
	61.8	2.8
	62.4	4.7
Average	62.3	2.9
Std. Dev.	0.5	1.8

Table A2

Individual Static Axial Tensile Results
for IM7/8551-7 Composites

Specimen Name	Test Temperature (°F)	Tensile Strength (ksi)	Tensile Strength (GPa)	Tensile Modulus (Msi)	Tensile Modulus (GPa)	Ultimate Strain (Percent)	Poisson's Ratio
NLOTD2	75	372	2.56	23.9	165	1.5	0.168
3		383	2.64	23.8	164	0.6*	0.186
4		341	2.35	21.7	150	1.9	0.174
5		231*	1.59*	24.7	170	0.8*	0.200
6		358	2.47	22.3	154	1.3	0.189
Average		364	2.51	23.3	161	1.5	0.183
Std. Dev.		18	0.12	1.2	8	0.3	0.013
NLFSH1	180	321	2.21	22.1	152	1.2*	0.419*
2		364	2.51	21.4	148	1.6	0.404
3		367	2.53	21.3	147	1.5	0.345
4		369	2.54	21.8	150	1.5	0.345
5		372	2.56	22.5	155	1.5	0.337
Average		359	2.47	21.8	150	1.5	0.358
Std. Dev.		21	0.15	0.5	3	0.1	0.031

*Not included in Average or Standard Deviation

Table A3

Individual Static Transverse Tensile Results
for IM7/8551-7 Composites

Specimen Name	Test Temperature (°F)	Tensile Strength (ksi)	Tensile Strength (GPa)	Tensile Modulus (Msi)	Tensile Modulus (GPa)	Ultimate Strain (Percent)
NLTTDO	75	6.84	47.8	1.19	8.2	0.58
1		7.56	52.1	1.15	7.9	0.67
2		7.61	52.5	1.21	8.3	0.64
3		2.80*	19.3*	1.15	7.9	0.22*
4		7.40	51.0	1.21	8.3	0.62
5		7.30	50.3	1.27	8.8	0.59
Average		7.34	50.7	1.20	8.2	0.62
Std. Dev.		0.03	1.86	0.05	0.3	0.04
NTTD21	180	3.84*	26.5*	1.07	7.4	0.37*
22		4.72	32.5	1.05	7.2	0.46
23		5.05	34.8	1.05	7.2	0.53
24		6.20	42.7	1.08	7.4	0.60
25		6.50	44.8	1.11	7.6	0.62
26		6.63	45.7	1.09	7.5	0.65*
27		6.19	42.7	1.09	7.5	0.60
Average		5.88	40.5	1.08	7.4	0.56
Std. Dev.		0.80	5.5	0.02	0.2	0.07

*Not included in Average and Standard Deviation

Table A4

Individual In-Plane Iosipescu Shear Results for IM7/8551-7 Composites

Specimen Name	Test Temperature	Shear Strength		Shear Modulus		Ultimate Strain
	(°F)	(ksi)	(GPa)	(Msi)	(GPa)	(Percent)
NFIRD1	75	16.1	111	0.86	6.0	11.9
2		14.9	103	0.87	6.0	11.9
3		15.8	109	0.83	5.7	11.9
4		15.5	107	0.83	5.7	10.3
5		12.8	88	0.76	5.2	5.4*
Average		15.0	104	0.83	5.7	11.5
Std. Dev.		1.3	9	0.05	0.3	0.8
NFIHD1	180	12.4	85	0.81	5.6	11.4
2		10.1*	70*	0.77	5.3	5.9*
3		13.3	91	0.76	5.3	11.3
4		13.1	90	0.78	5.4	11.3
5		12.3	85	0.62	4.2	11.3
Average		12.7	88	0.75	5.2	11.3
Std. Dev.		0.5	3	0.08	0.6	0.1

*Not included in Average or Standard Deviation

Table A5

Individual Static Edge Delamination Test Results
for IM7/8551-7 Composites

Specimen Name	Test Temperature	Thickness	Ultimate Strength		Modulus Strength		Strength Delamination		Critical Strain Energy Release Rate		Strain at Delamination	Poisson's Ratio
	(°F)	(in)	(ksi)	(MPa)	(Msi)	(MPa)	(ksi)	(MPa)	(in-lbf/in²)	(J/m²)	(percent)	
NLDTD1	75	0.042	108	745	9.0	62.0	93*	641*	3.95*	692*	0.99*	0.196
2		0.043	99	683	9.6	66.2	93*	641*	3.85*	675*	0.97	0.138*
3		0.044	99	683	9.7	66.9	79	545	2.62	459	0.79	0.168
4		0.044	120	827	10.1	69.6	92	634	3.59	628	0.93	0.211
5		0.044	94	648	10.2	70.3	81	558	2.91	509	0.83	0.183
6		0.042	115	793	9.6	66.2	75	517	2.37	416	0.77	0.258*
7		0.043	108	745	9.9	68.3	78	538	2.70	473	0.81	0.232
8		0.044	111	765	10.8	74.5	62*	428*	1.38*	241*	0.57*	0.267*
Average			107	736	9.9	68.0	81	558	2.84	497	0.85	0.198
Std. Dev.			9	61	0.5	3.7	7	45	0.46	80	0.08	0.025
NLTD21	180	0.045	112	772	9.9	68.3	72	496	2.32	406	0.73	0.388
22		0.044	109	751	10.8	74.5	70	483	1.94	339	0.67	0.564*
23		0.045	108	745	10.1	69.6	81	558	2.98	521	0.83	0.471
24		0.045	108	745	9.4	64.8	65	448	2.03	355	0.68	0.421
25		0.045	110	758	9.7	66.9	81	558	3.27*	573*	0.87	0.415
Average			109	754	10.0	68.8	74	509	2.32	405	0.76	0.424
Std. Dev.			2	11	0.5	3.6	7	48	0.47	82	0.09	0.035

*Not included in Average or Standard Deviation

TABLE A6

Lamina and Laminate Material Properties
for IM7/8551-7 Composites

		Test Temperature 75°F (25°C)	180°F (82°C)
$[0]_8$ (Input Properties From Static Tests Used in AC3)			
E_{11}	=	23.3 Msi (160.7 GPa)	21.1 Msi (145.5 GPa)
E_{22}	=	1.2 Msi (8.3 GPa)	1.1 Msi (7.6 GPa)
G_{12}	=	0.83 Msi (5.7 GPa)	0.75 Msi (5.2 GPa)
ν_{12}	=	0.180	0.370
$[\pm 35/0/90]_s$ (Predicted Properties From AC3)			
E_x	=	11.1 Msi (76.5 GPa)	10.3 Msi (71.0 GPa)
E_y	=	7.6 Msi (52.4 GPa)	7.1 Msi (49.0 GPa)
G_{xy}	=	3.1 Msi (21.4 GPa)	2.9 Msi (20.0 GPa)
ν_{xy}	=	0.311	0.332
$[\pm 35/0]_s$ (Predicted Properties From AC3)			
E_x	=	11.8 Msi (81.4 GPa)	10.9 Msi (75.2 GPa)
E_y	=	2.3 Msi (15.9 GPa)	2.1 Msi (14.5 GPa)
G_{xy}	=	3.9 Msi (26.9 GPa)	3.6 Msi (24.8 GPa)
ν_{xy}	=	1.093	1.140
E^*	=	9.18 Msi (63.3 GPa)	8.41 Msi (58.0 GPa)
(Calculated Using AC3 and Equation 2)			
E_{lam}	=	9.85 Msi (67.9 GPa)	9.99 Msi (68.9 GPa)
(Measured Static EDT Initial Tangent Modulus)			

AXIAL TENSION 23 DEG C

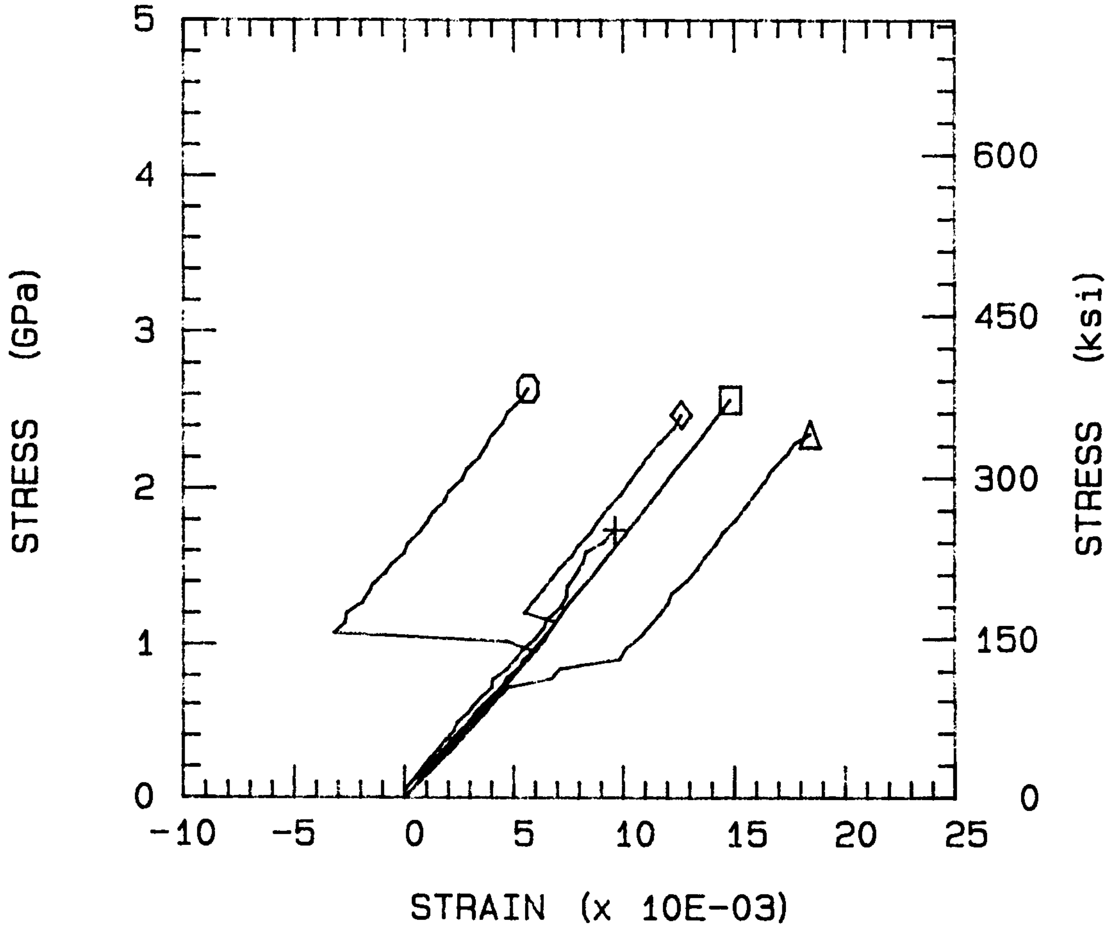

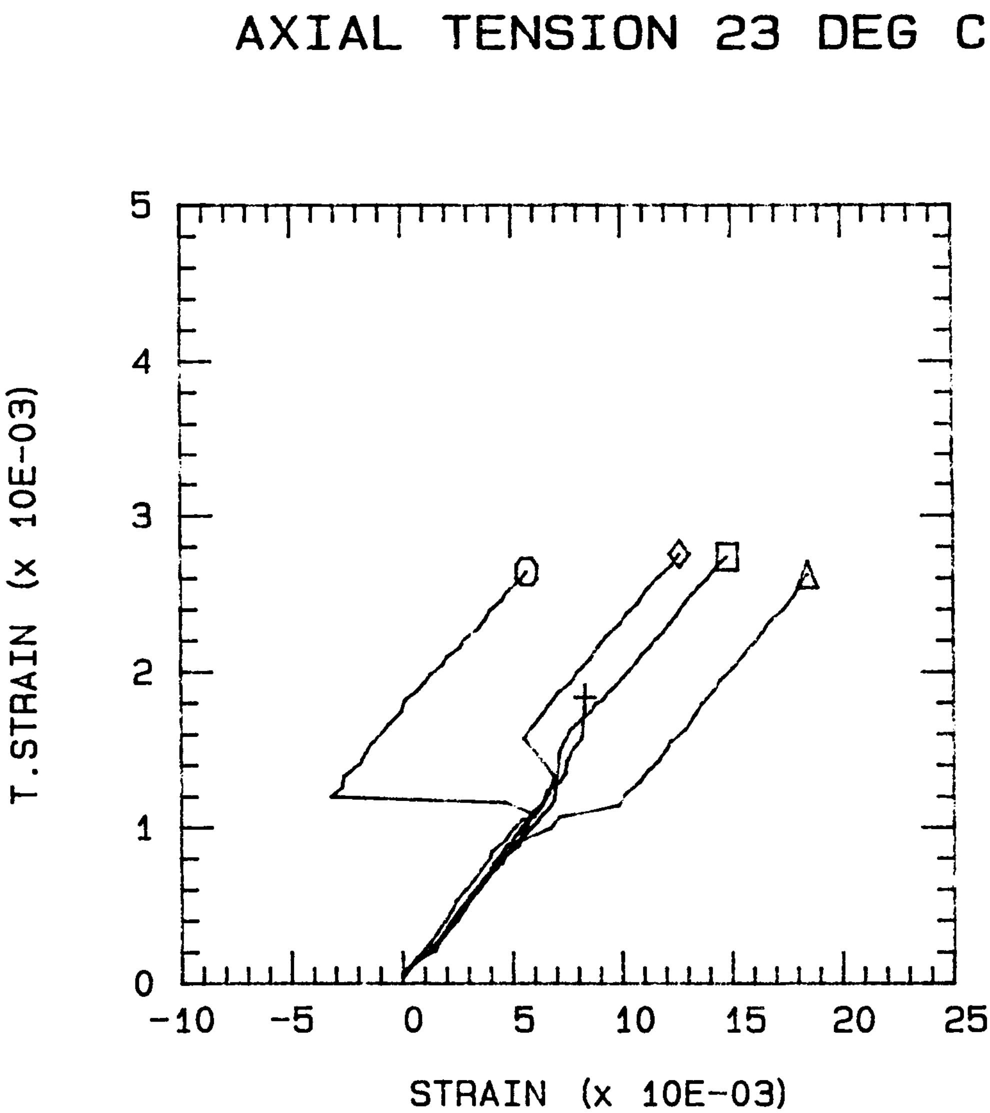

AXIAL TENSION 23 DEG C
T.STRAIN (x 10E-03)
STRAIN (x 10E-03)
0
1
2
3
4
5
-10
-5
0
5
10
15
20
25

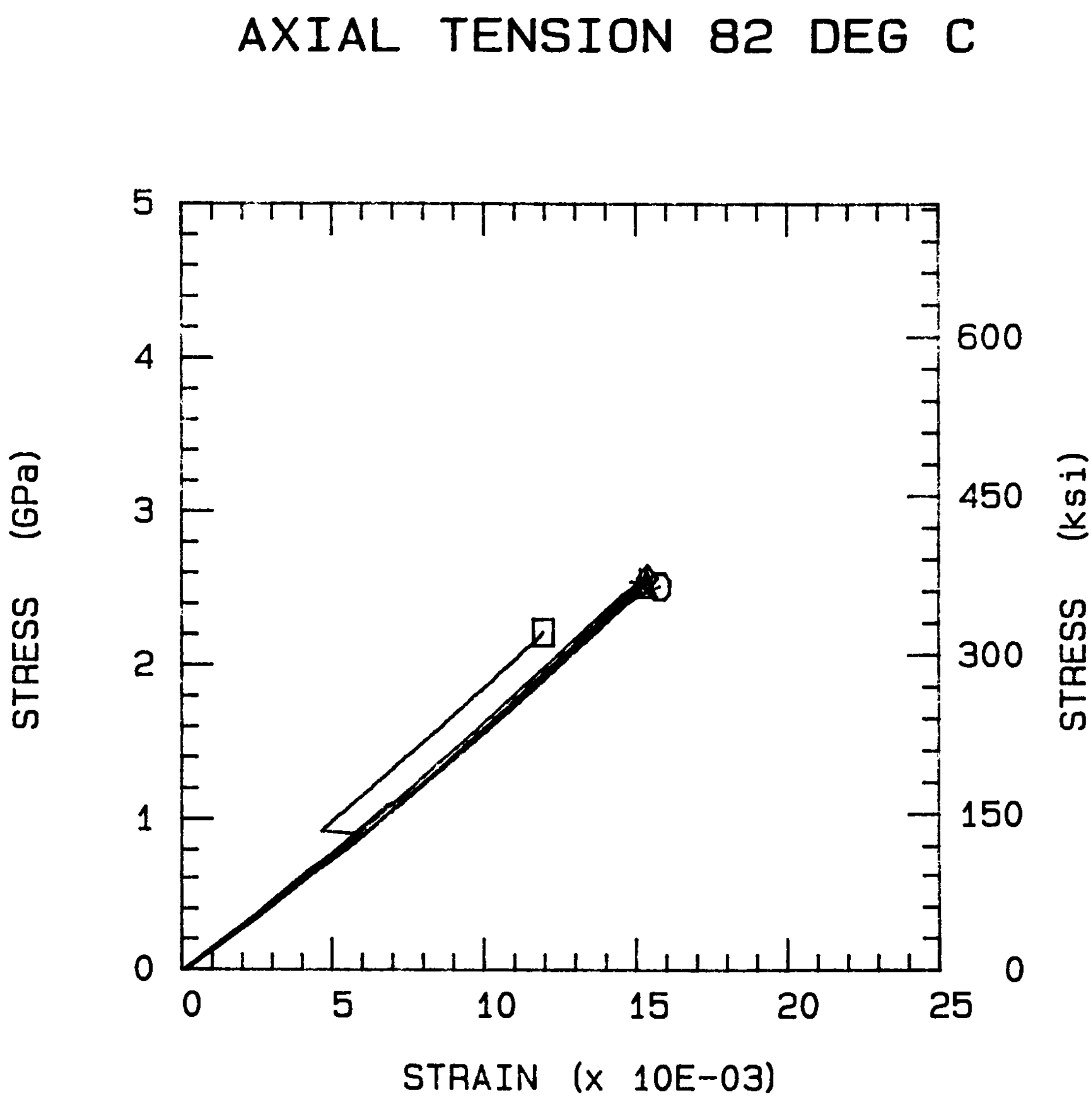

AXIAL TENSION 82 DEG C
STRESS (GPa)
STRESS (ksi)
STRAIN (x 10E-03)
0
1
2
3
4
5
0
150
300
450
600
0
5
10
15
20
25

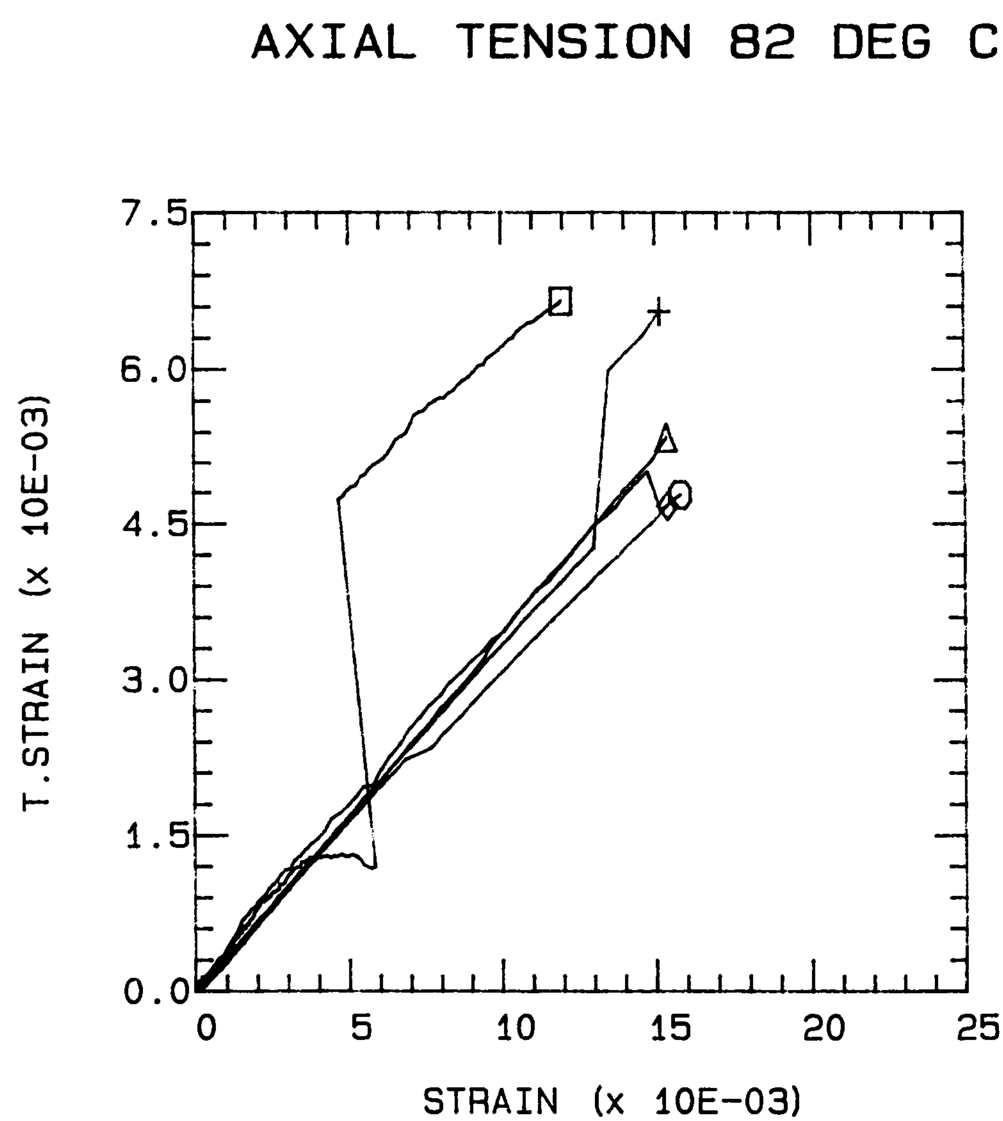
AXIAL TENSION 82 DEG C
T.STRAIN (x 10E-03)
7.5
6.0
4.5
3.0
1.5
0.0
0
5
10
15
20
25
STRAIN (x 10E-03)

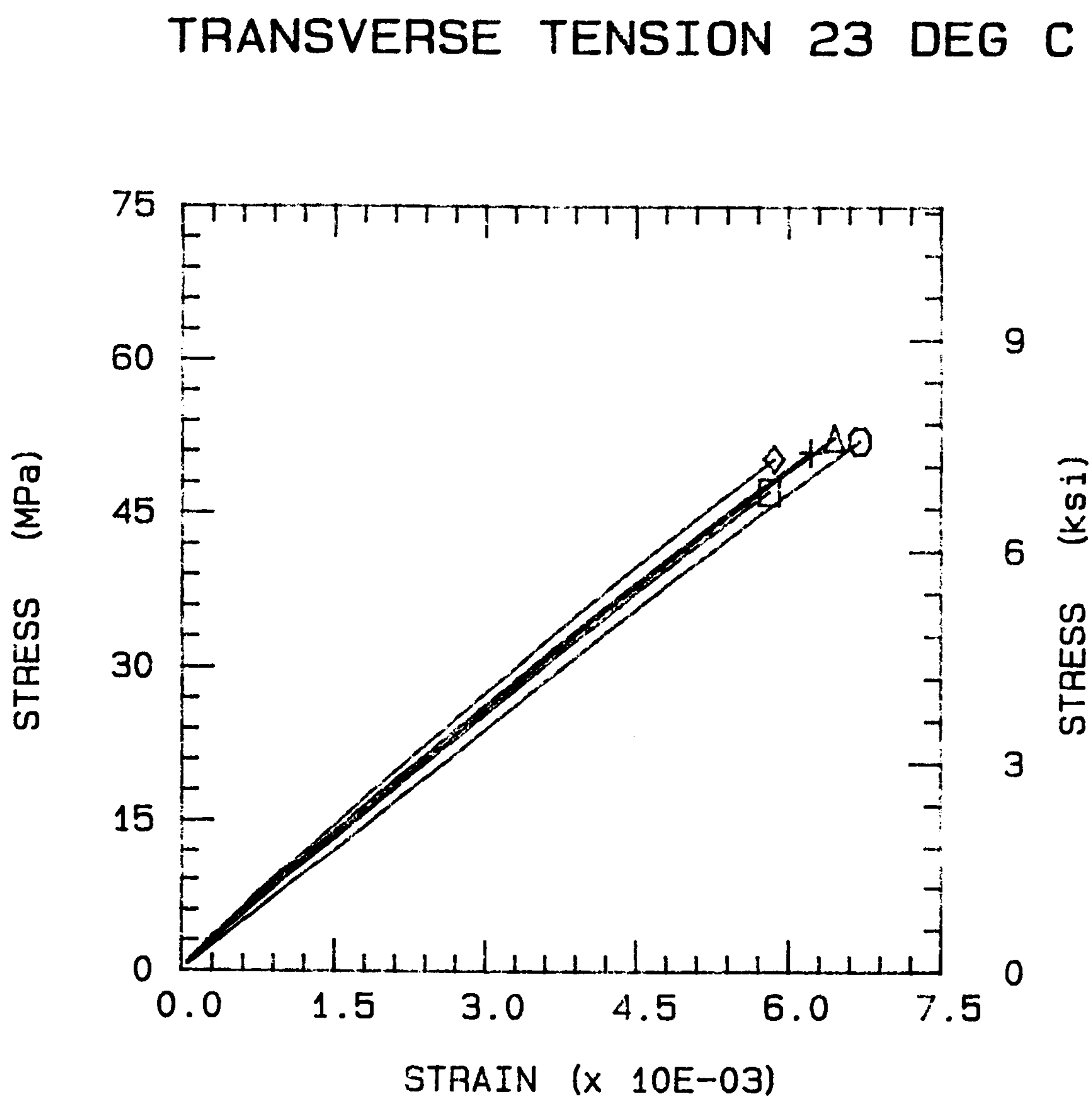
TRANSVERSE TENSION 23 DEG C
STRESS (MPa)
75
60
45
30
15
0
STRESS (ksi)
9
6
3
0
0.0
1.5
3.0
4.5
6.0
7.5
STRAIN (x 10E-03)

TRANSVERSE TENSION 82 DEG C

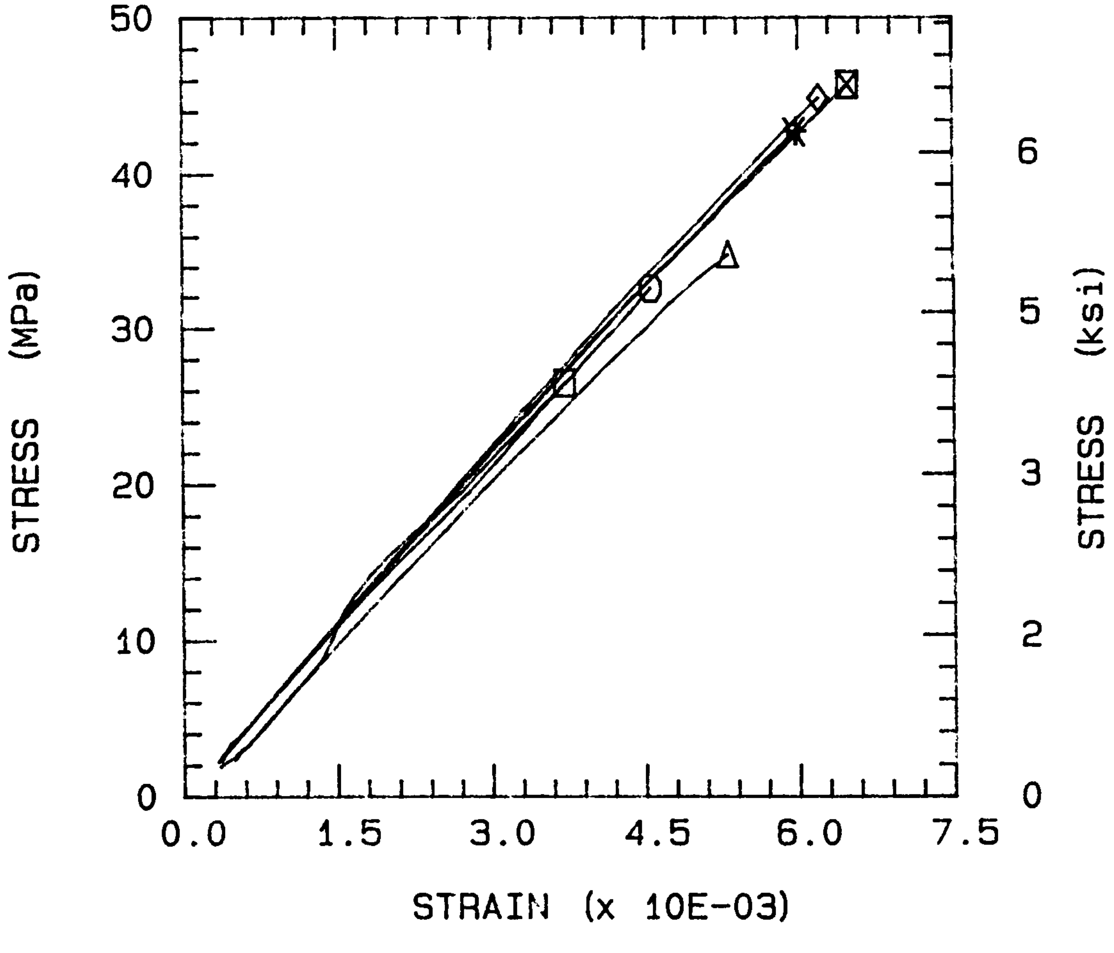

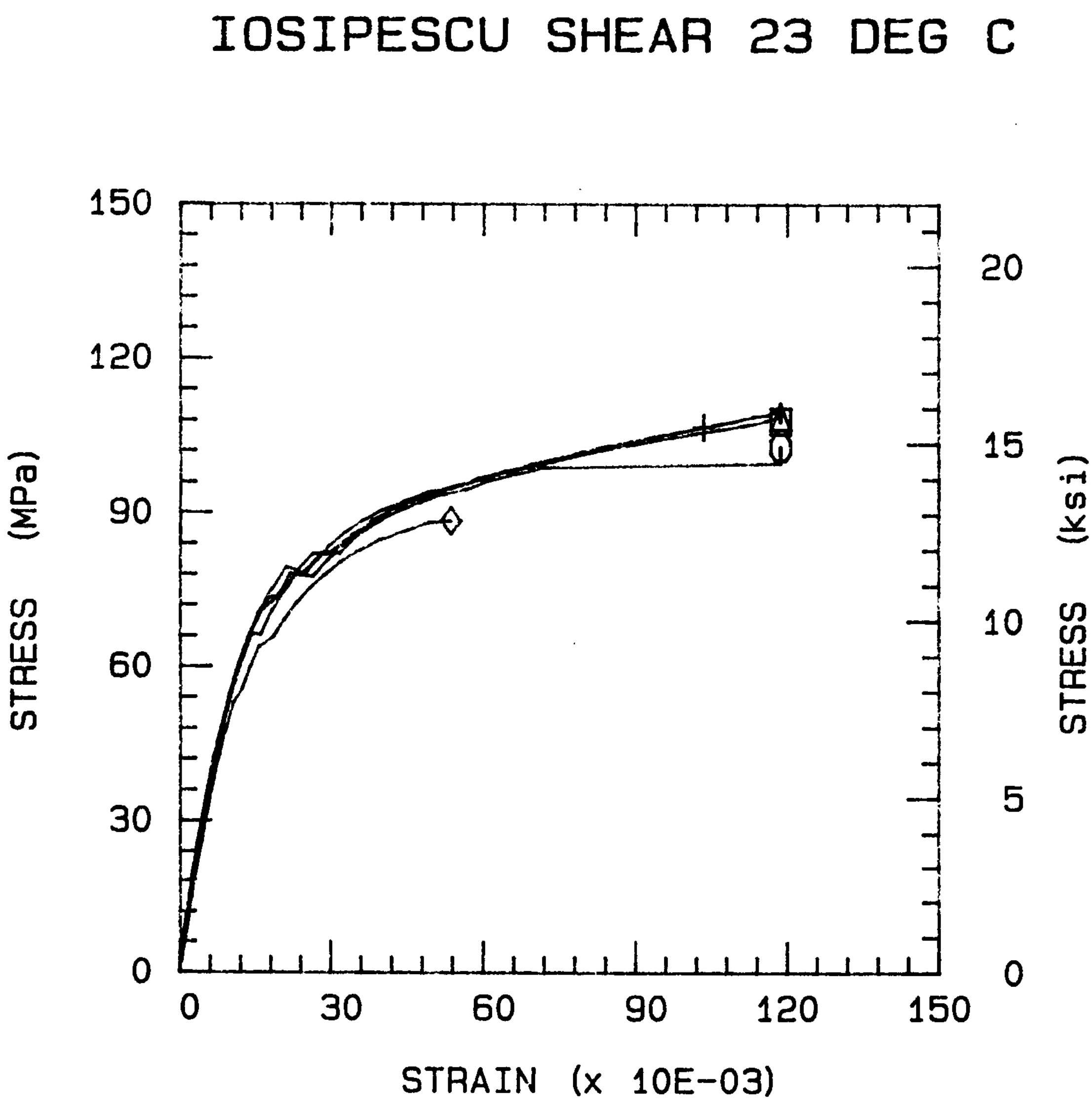
IOSIPESCU SHEAR 23 DEG C
150
120
90
60
30
0
STRESS (MPa)
20
15
10
5
0
STRESS (ksi)
0
30
60
90
120
150
STRAIN (x 10E-03)

IOSIPESCU SHEAR 23 DEG C

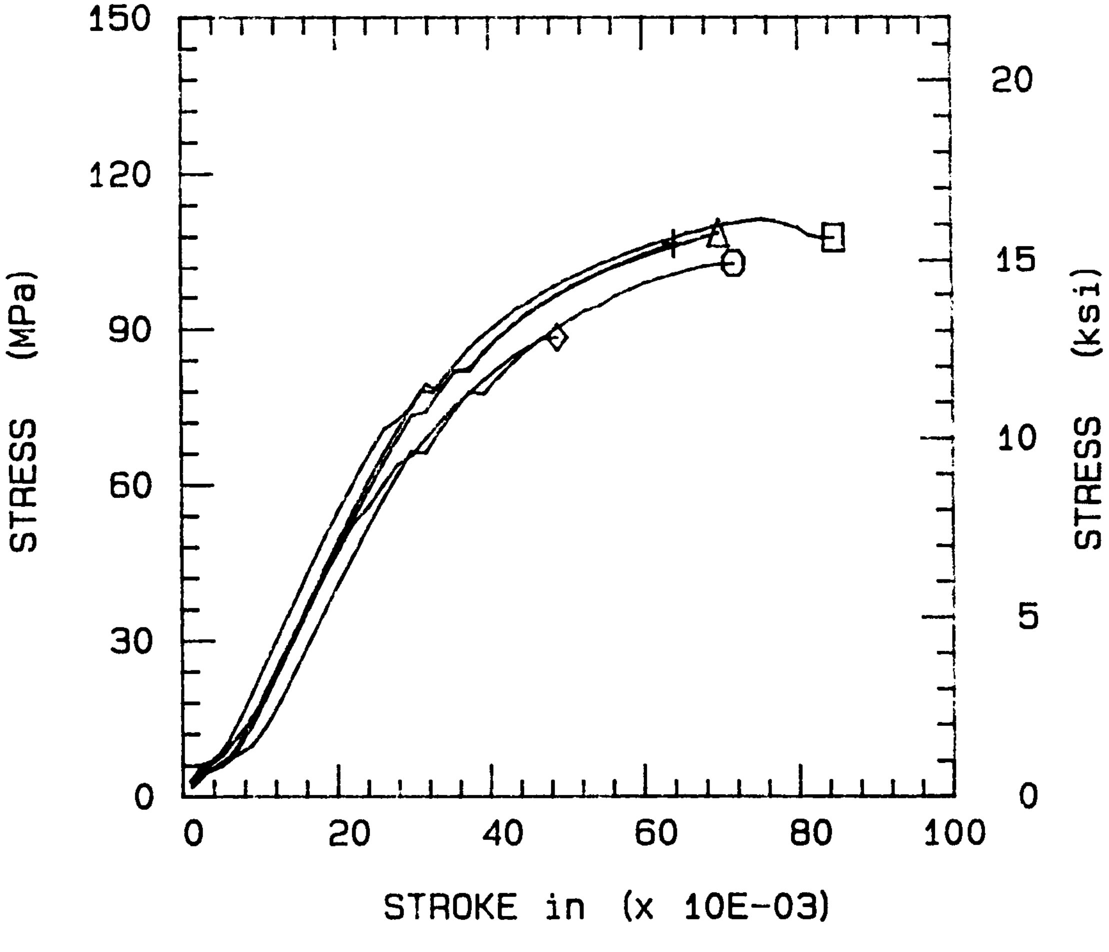

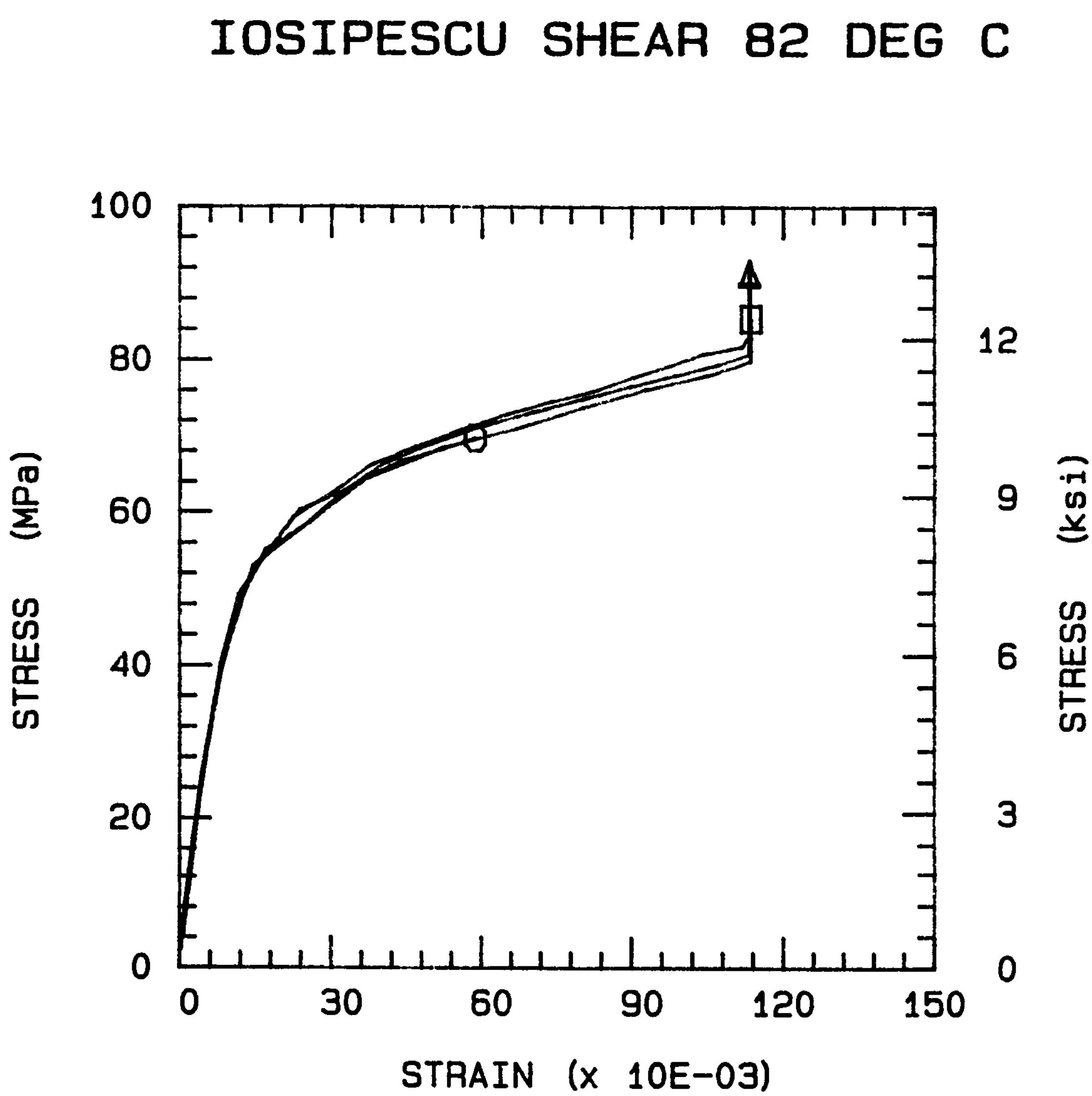
IOSIPESCU SHEAR 82 DEG C
STRESS (MPa)
STRESS (ksi)
STRAIN (x 10E-03)
0
20
40
60
80
100
0
3
6
9
12
0
30
60
90
120
150

IOSIPESCU SHEAR 82 DEG C

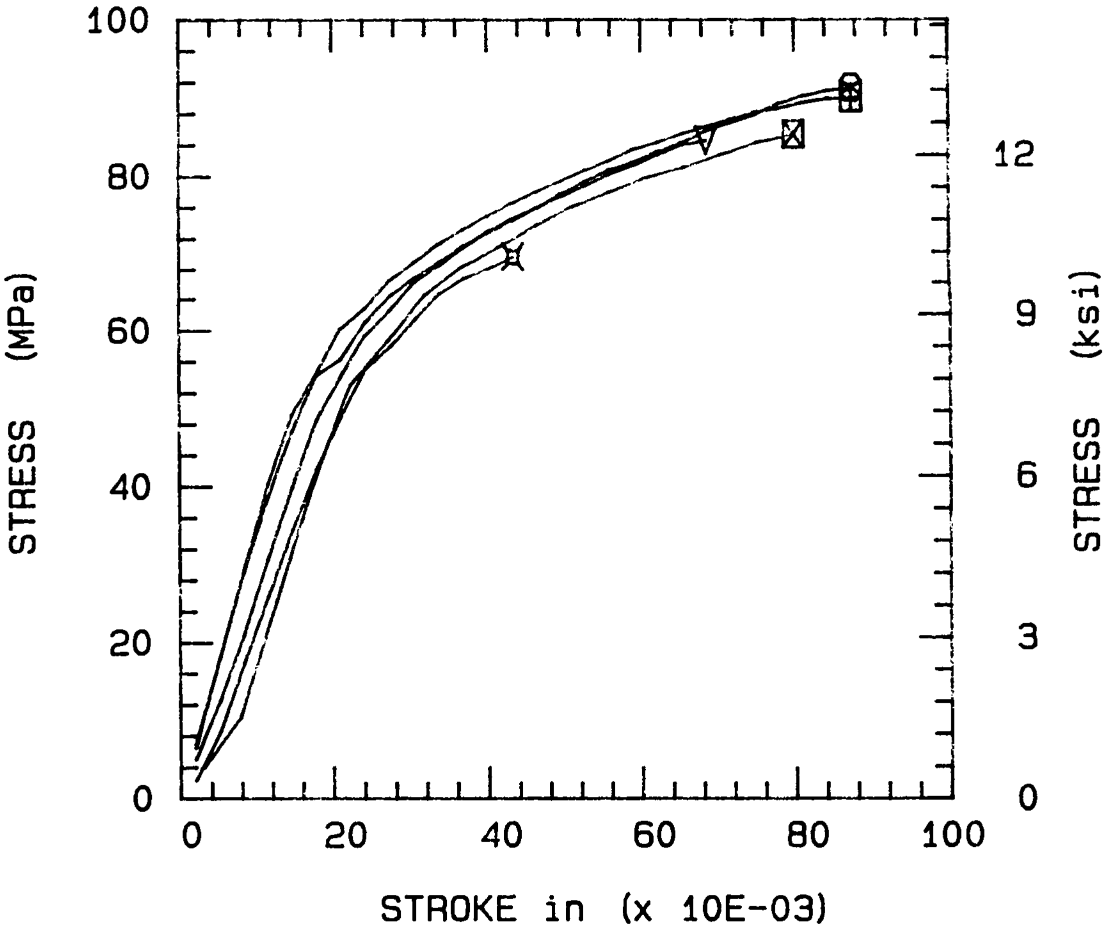

EDGE DELAMINATION 23 DEG C

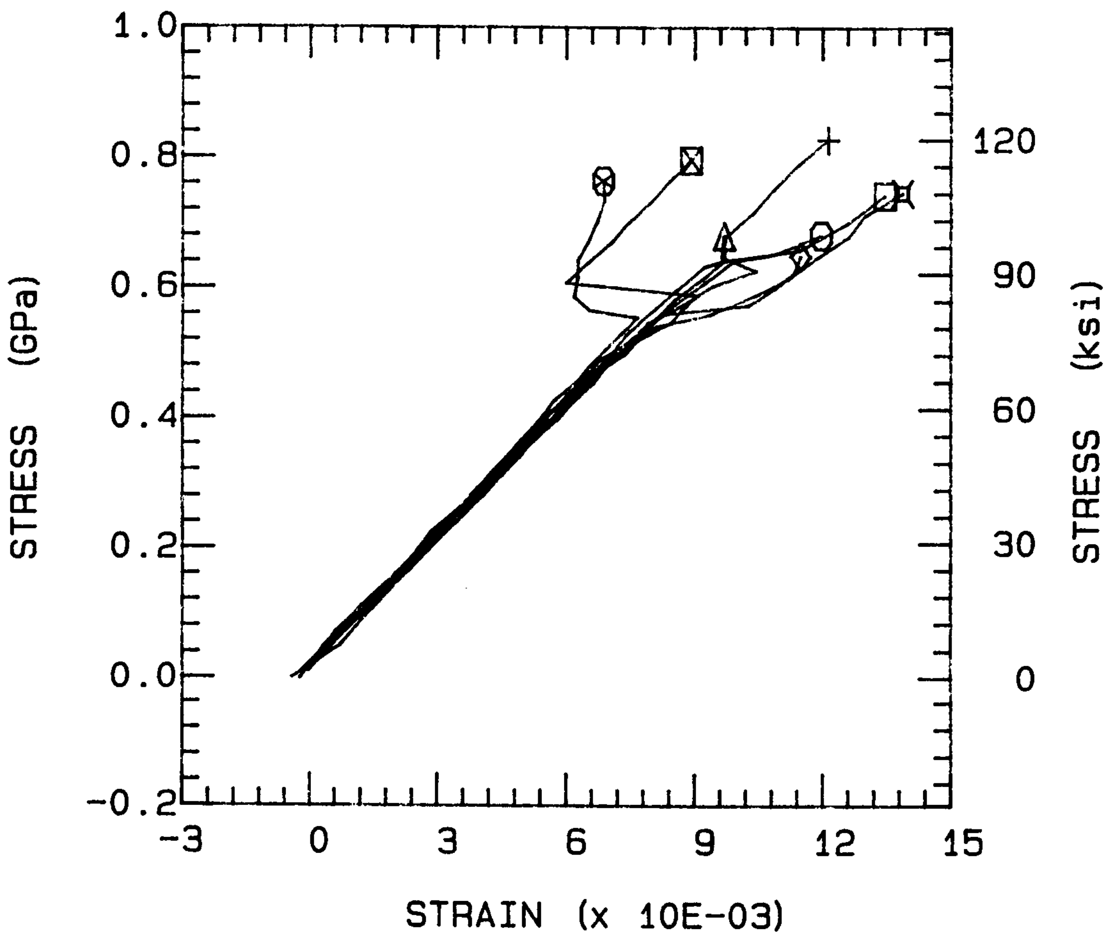

EDGE DELAMINATION 23 DEG C

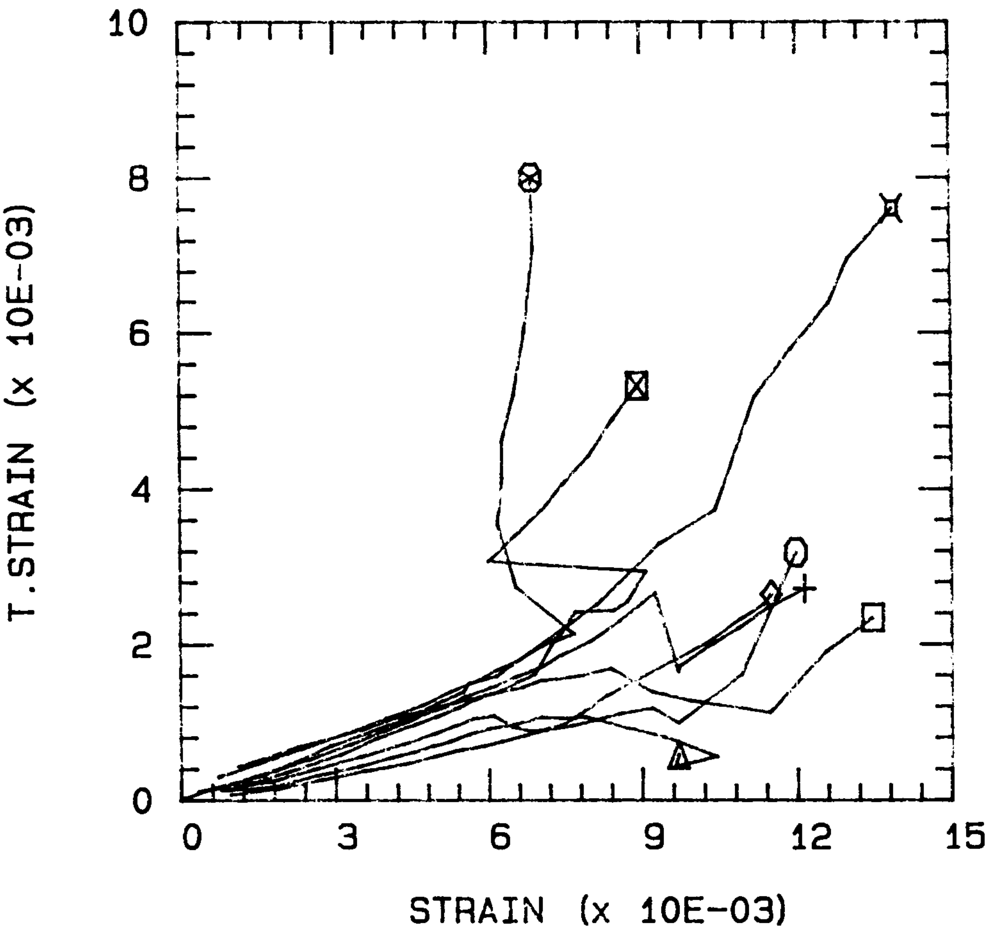

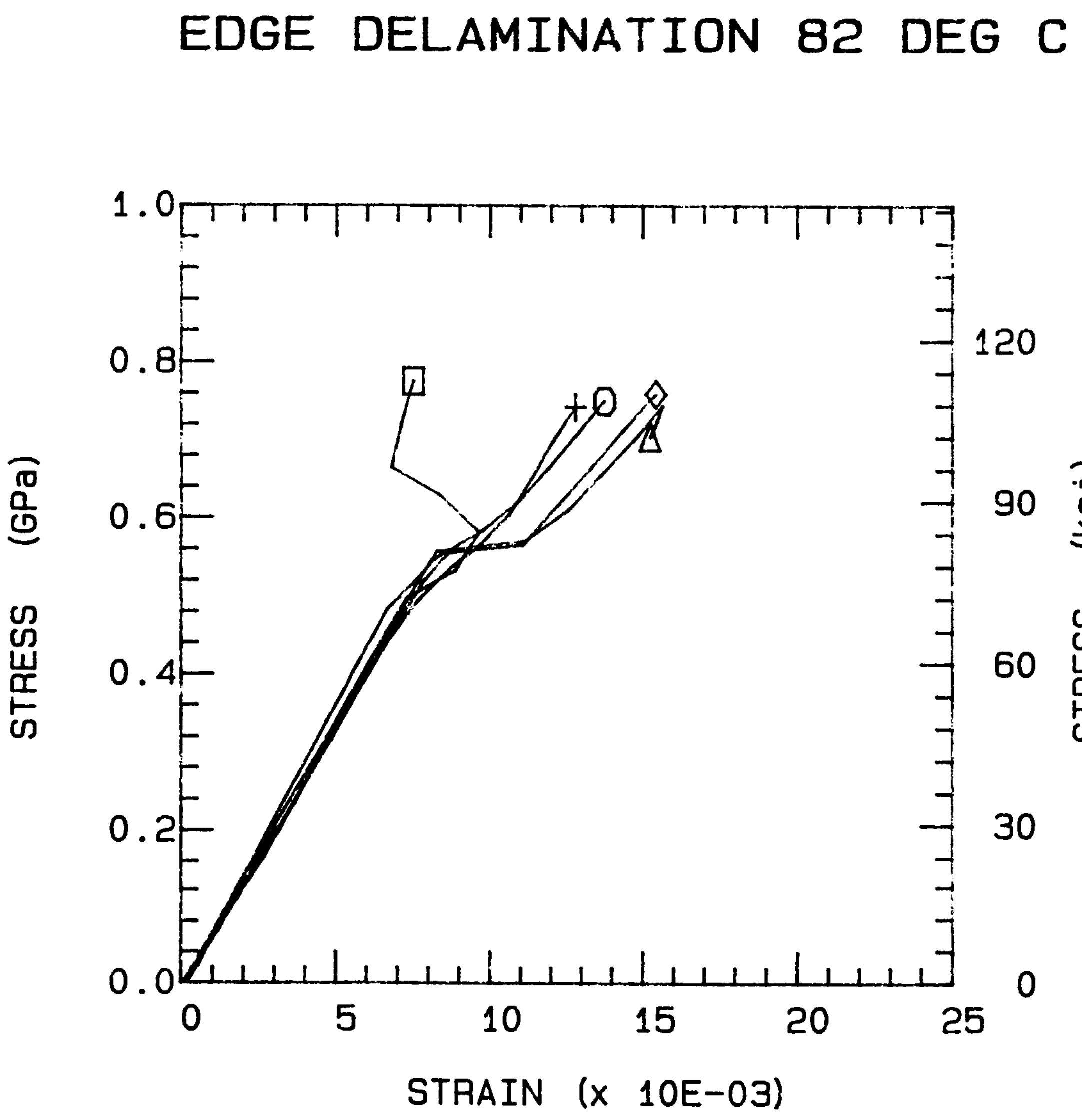

EDGE DELAMINATION 82 DEG C
1.0
0.8
0.6
0.4
0.2
0.0
STRESS (GPa)
120
90
60
30
0
STRESS (ksi)
0
5
10
15
20
25
STRAIN (x 10E-03)

EDGE DELAMINATION 82 DEG C

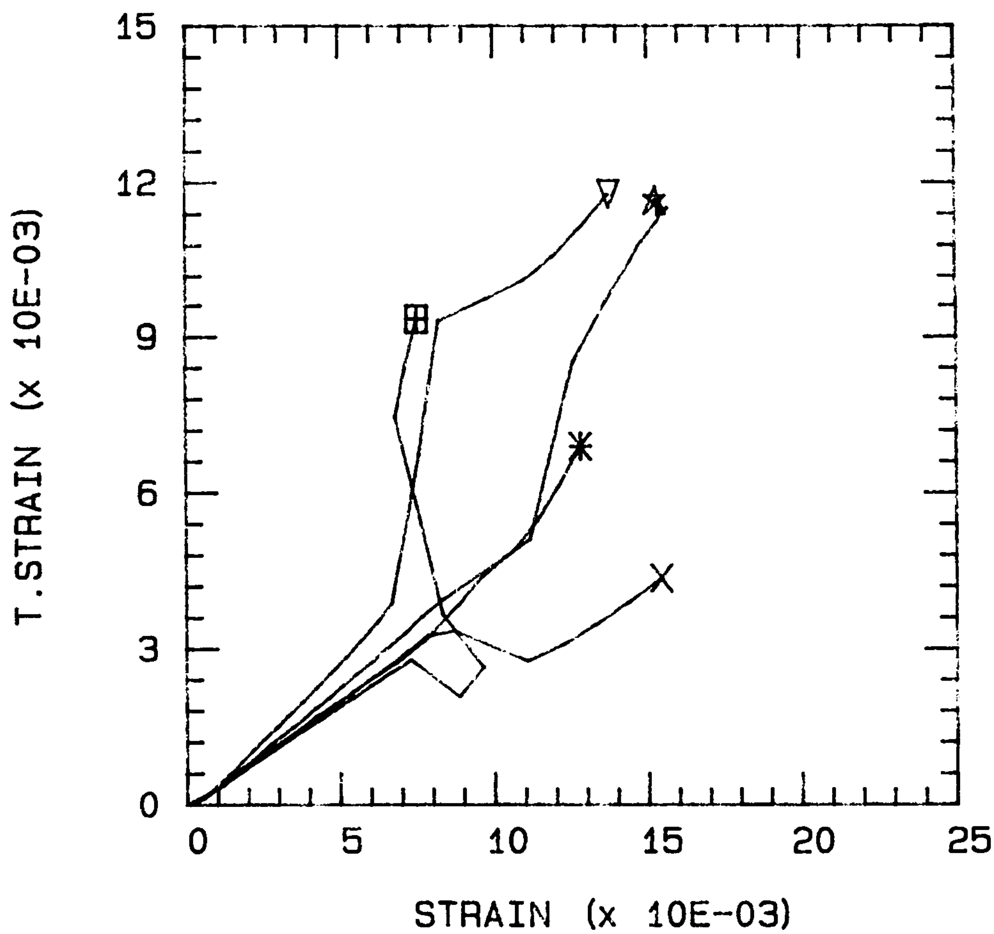

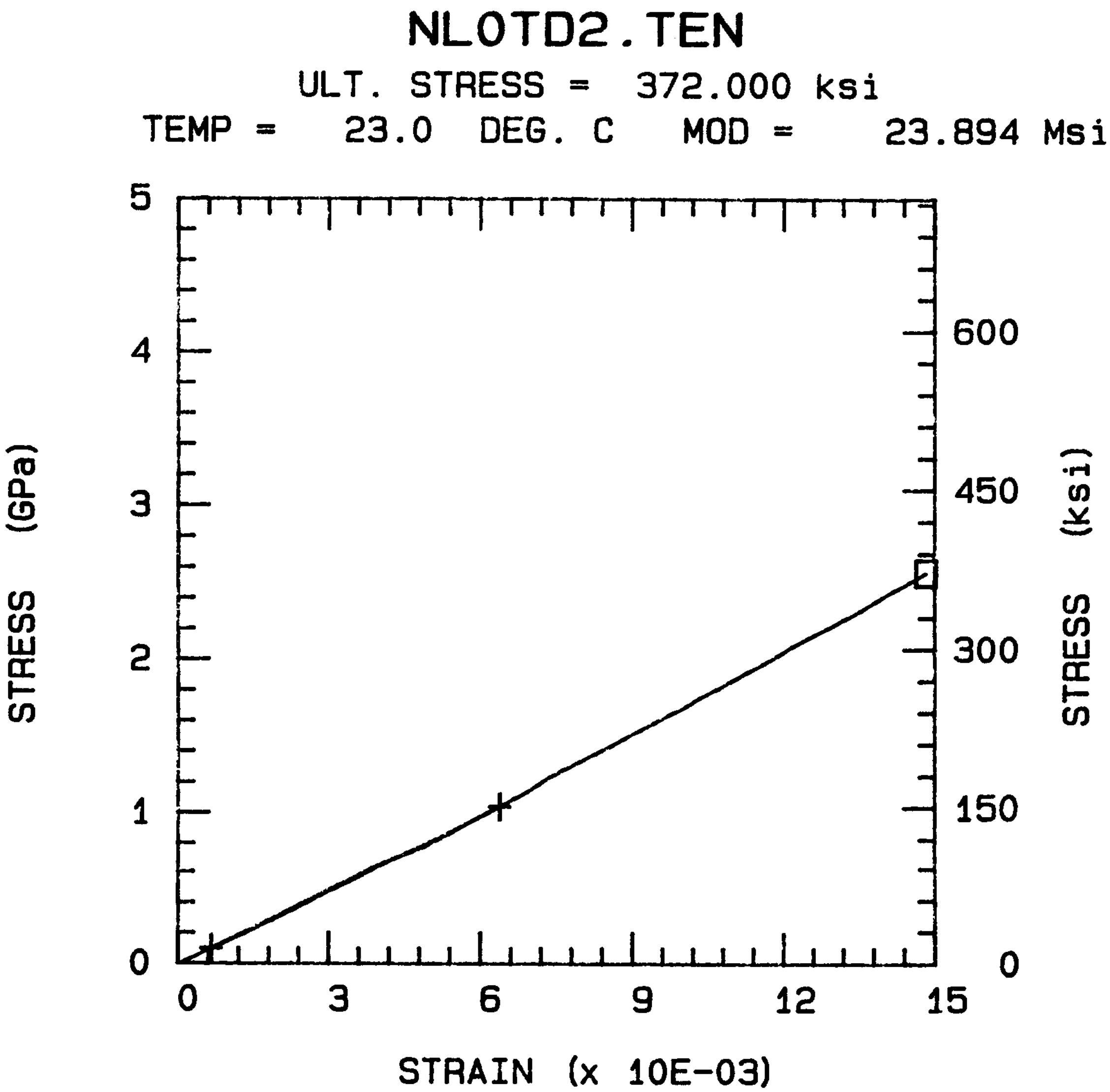
NLOTD2.TEN
ULT. STRESS = 372.000 ksi
TEMP = 23.0 DEG. C MOD = 23.894 Msi
STRESS (GPa)
STRESS (ksi)
STRAIN (x 10E-03)
0
1
2
3
4
5
150
300
450
600
3
6
9
12
15

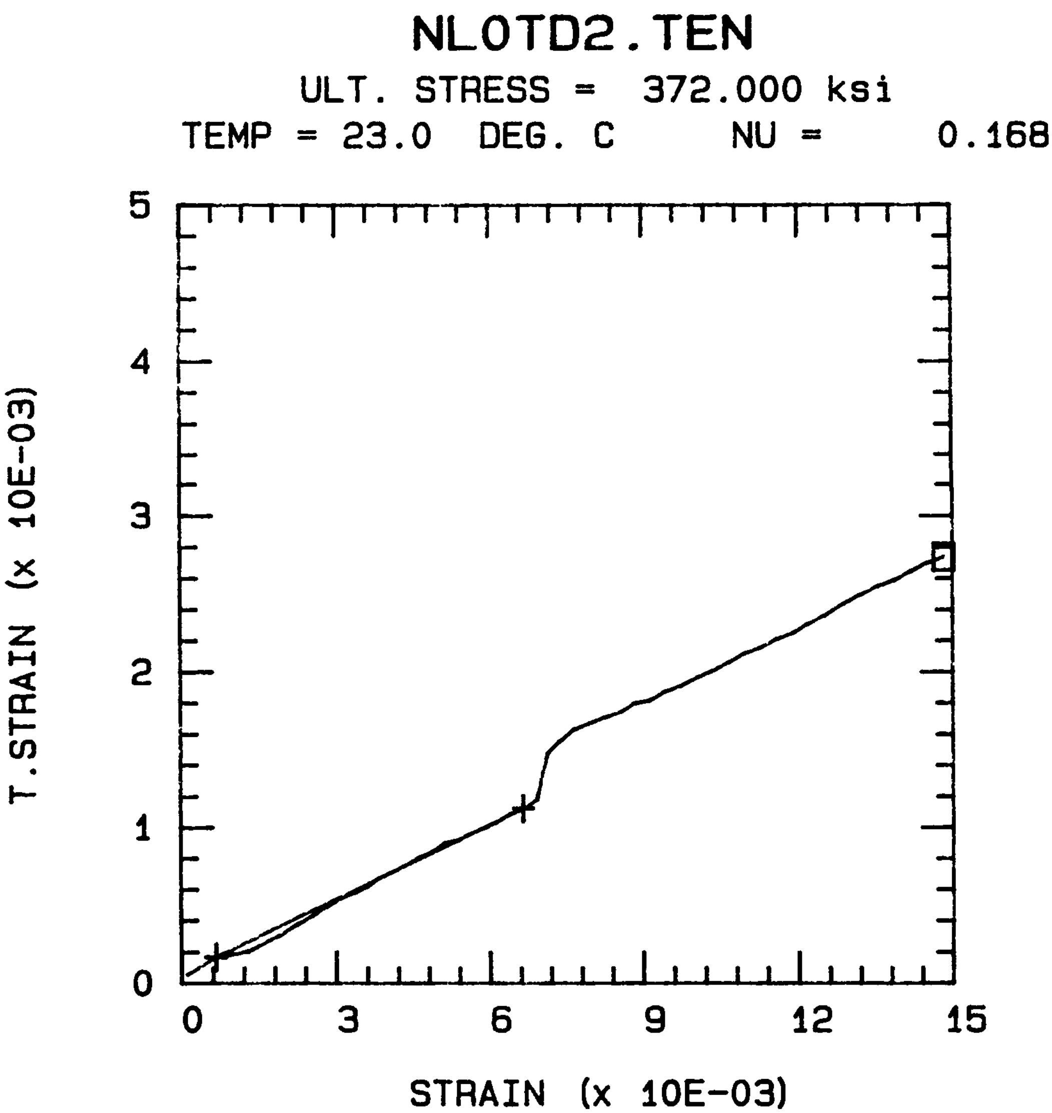

NLOTD2.TEN
ULT. STRESS = 372.000 ksi
TEMP = 23.0 DEG. C NU = 0.168
T.STRAIN (x 10E-03)
STRAIN (x 10E-03)
0
1
2
3
4
5
0
3
6
9
12
15

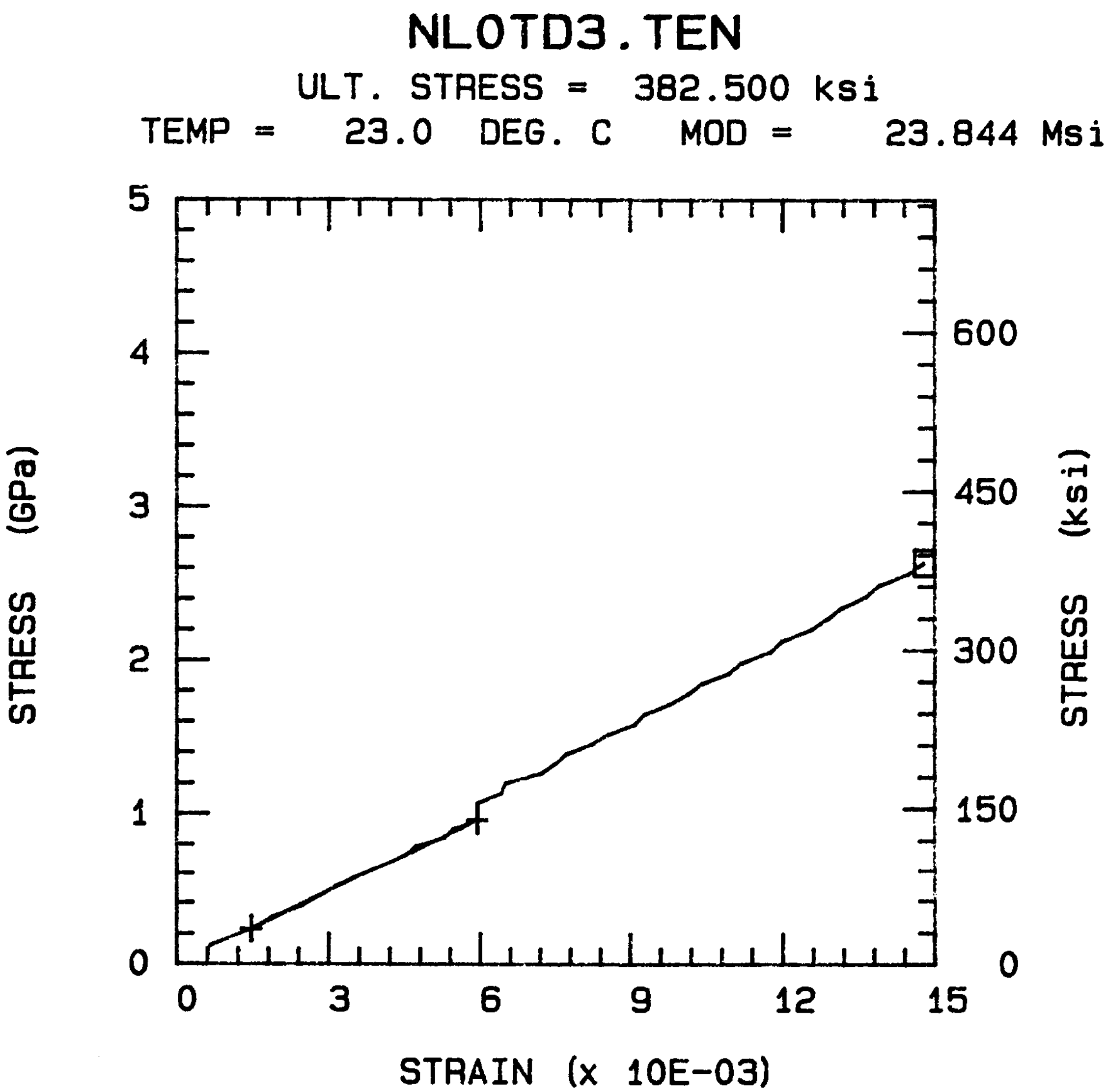

NLOTD3.TEN
ULT. STRESS = 382.500 ksi
TEMP = 23.0 DEG. C MOD = 23.844 Msi
STRESS (GPa)
STRESS (ksi)
STRAIN (x 10E-03)
0
1
2
3
4
5
0
150
300
450
600
0
3
6
9
12
15

NLOTD3.TEN

ULT. STRESS = 382.500 ksi

TEMP = 23.0 DEG. C NU = 0.186

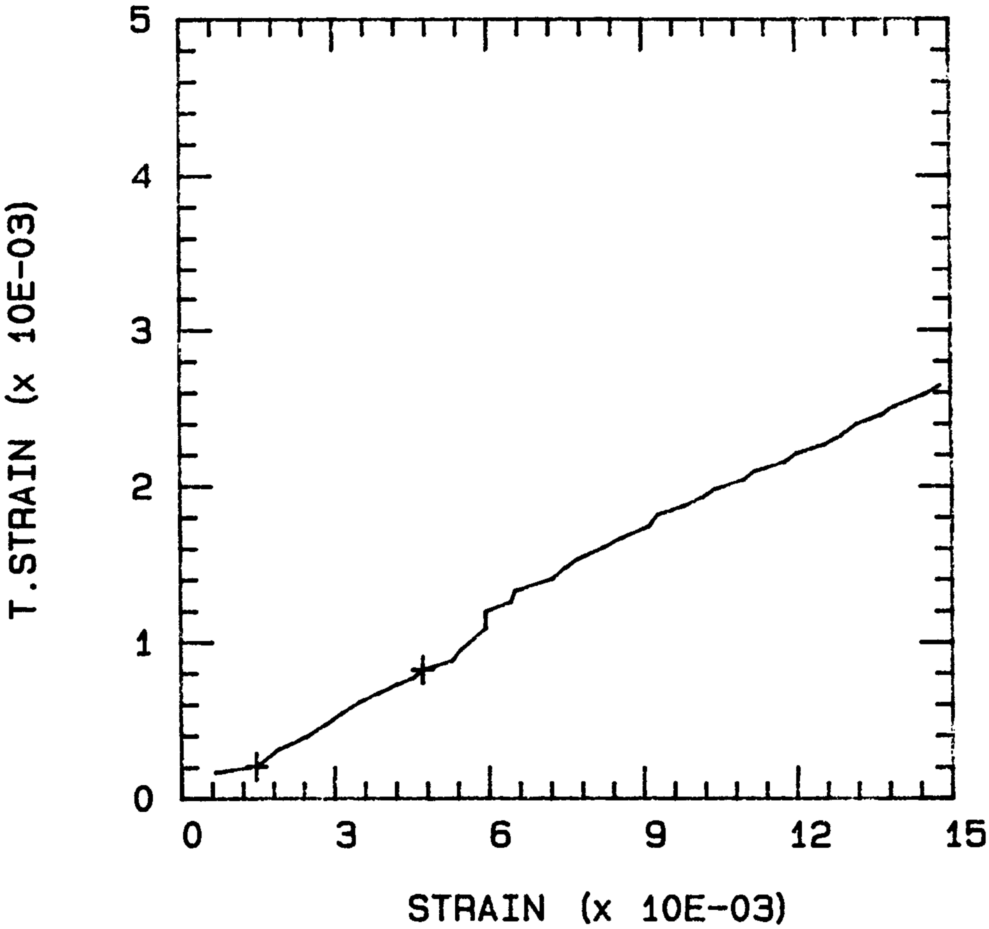

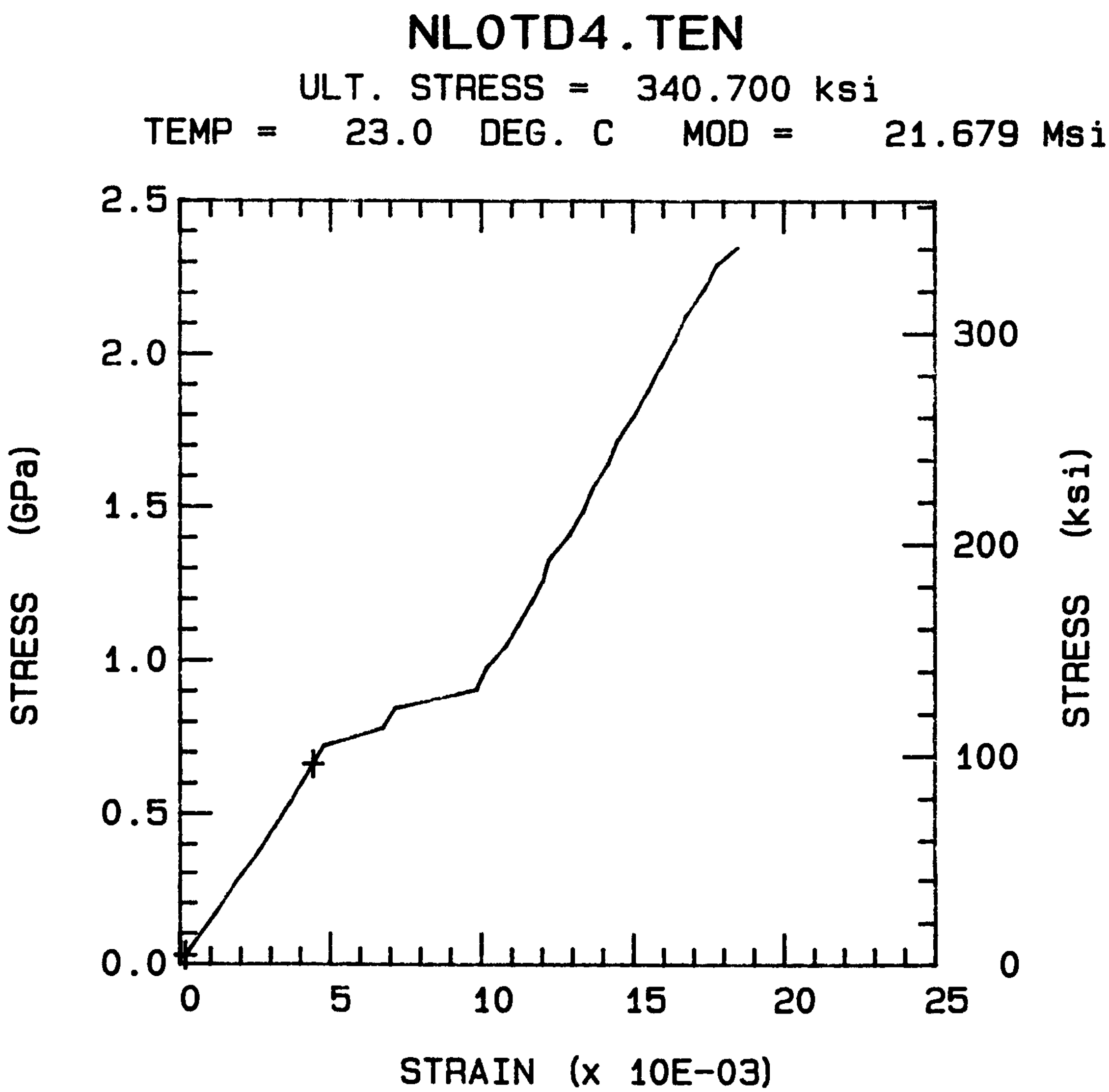
NLOTD4.TEN
ULT. STRESS = 340.700 ksi
TEMP = 23.0 DEG. C MOD = 21.679 Msi
STRESS (GPa)
2.5
2.0
1.5
1.0
0.5
0.0
0
5
10
15
20
25
STRAIN (x 10E-03)
STRESS (ksi)
300
200
100
0

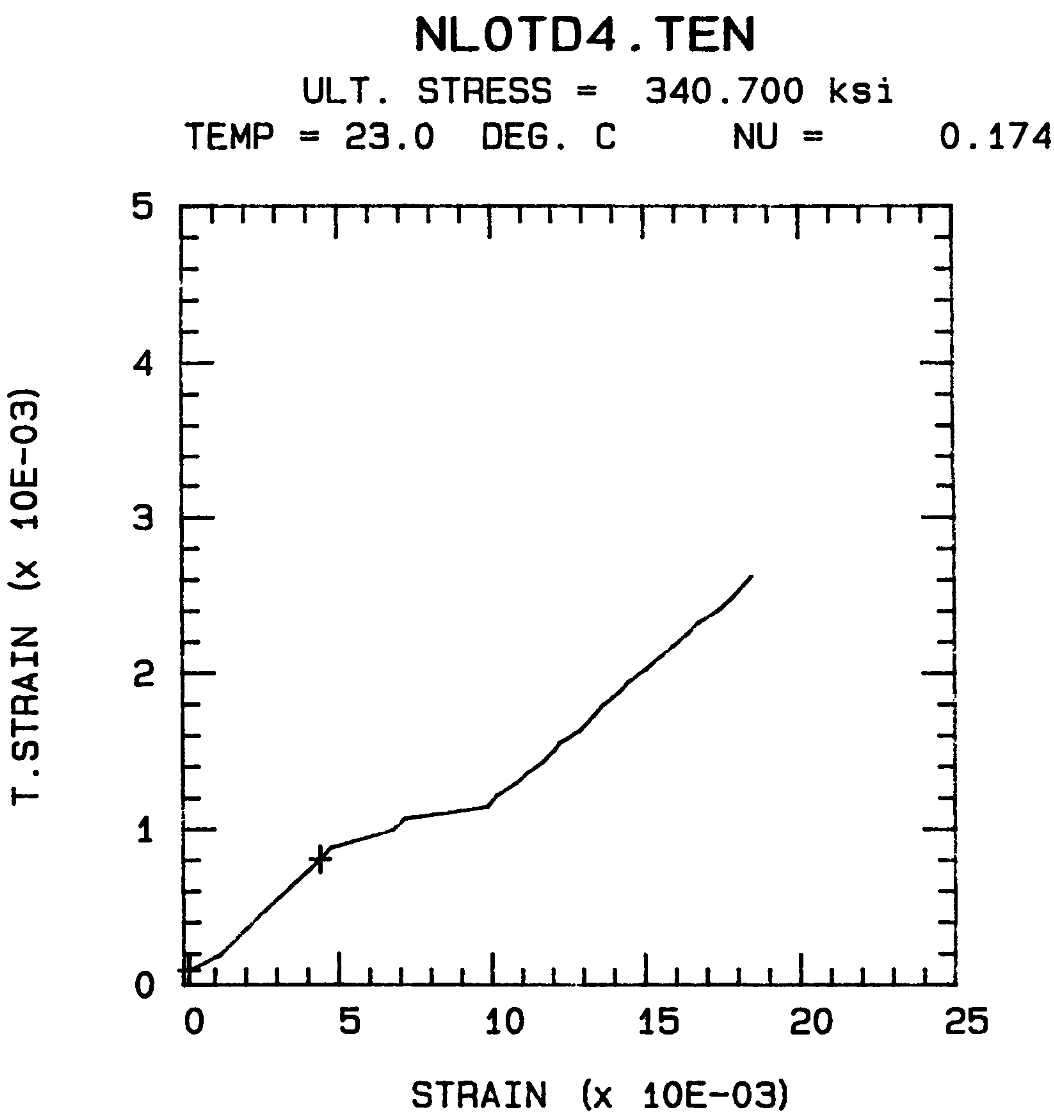
NLOTD4.TEN
ULT. STRESS = 340.700 ksi
TEMP = 23.0 DEG. C NU = 0.174
T.STRAIN (x 10E-03)
STRAIN (x 10E-03)
0
1
2
3
4
5
0
5
10
15
20
25

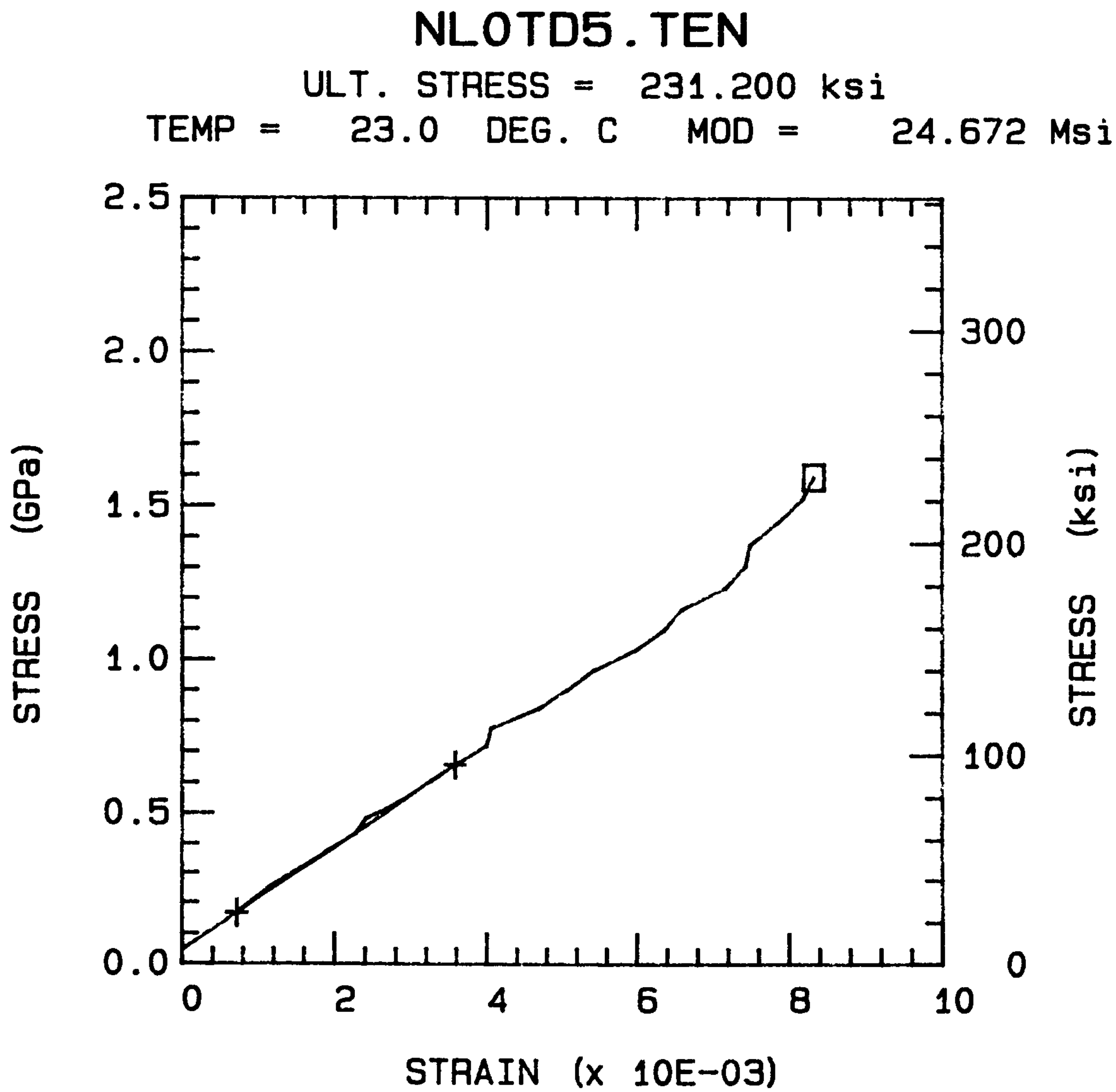
NLOTD5.TEN
ULT. STRESS = 231.200 ksi
TEMP = 23.0 DEG. C MOD = 24.672 Msi
2.5
2.0
1.5
1.0
0.5
0.0
STRESS (GPa)
300
200
100
0
STRESS (ksi)
0
2
4
6
8
10
STRAIN (x 10E-03)

NLOTD5.TEN

ULT. STRESS = 231.200 ksi
TEMP = 23.0 DEG. C NU = 0.200

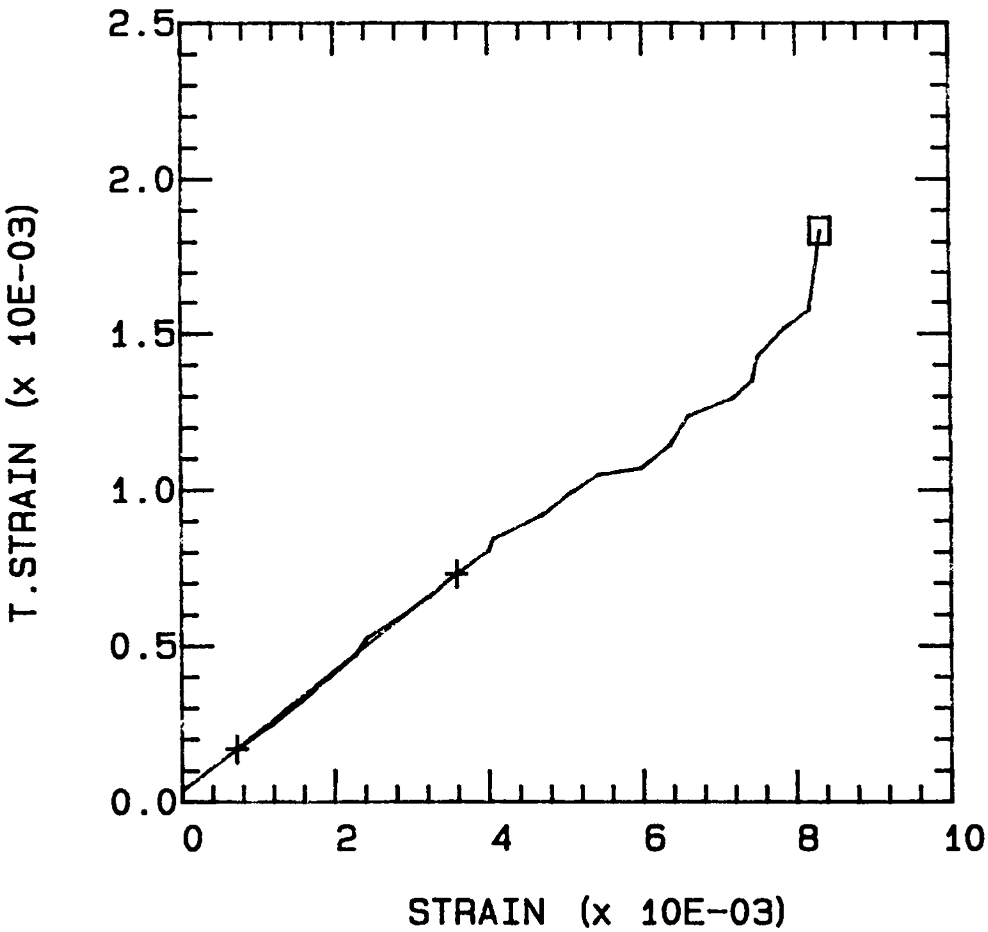

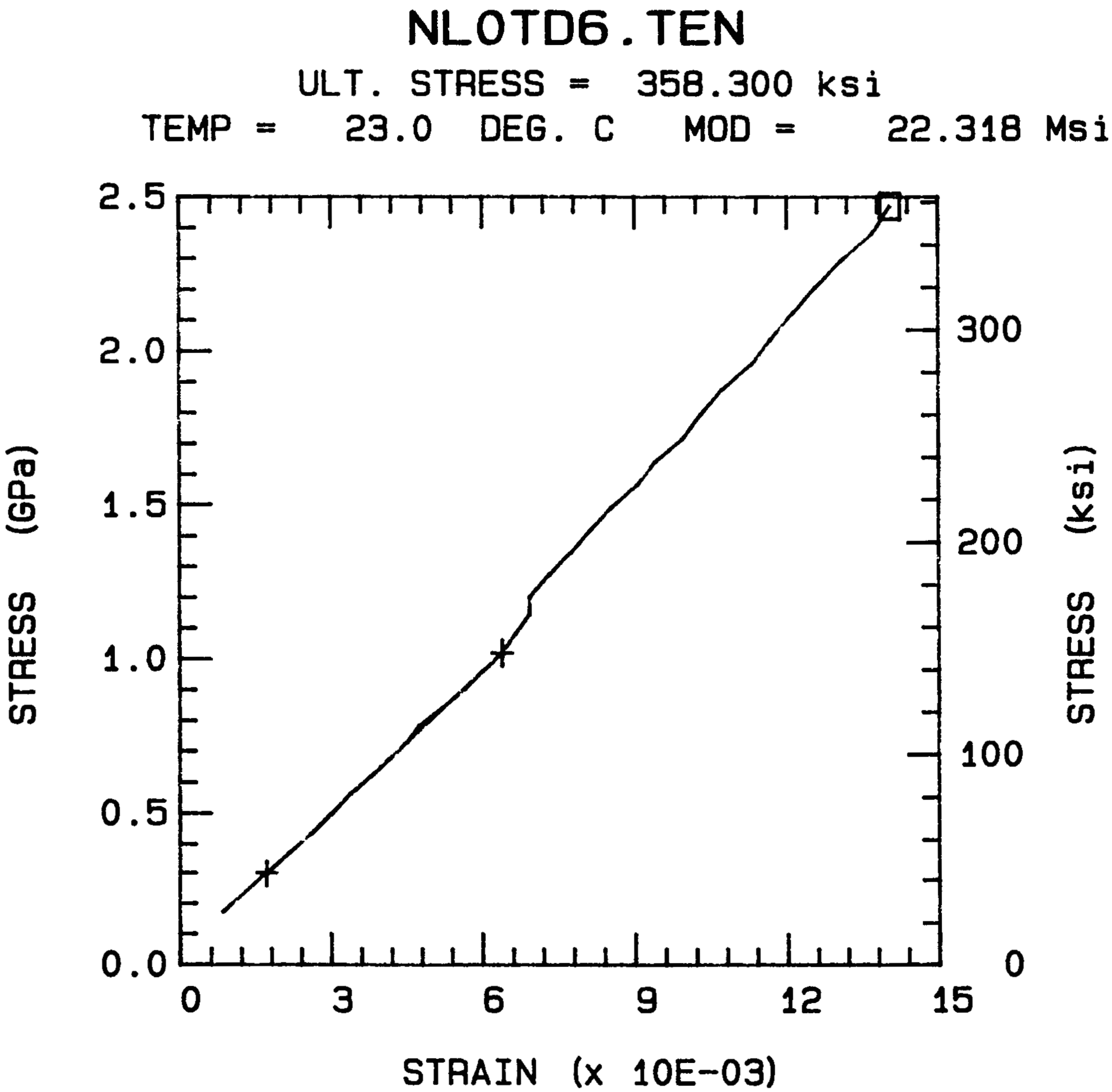

NLOTD6.TEN
ULT. STRESS = 358.300 ksi
TEMP = 23.0 DEG. C MOD = 22.318 Msi
STRESS (GPa)
STRESS (ksi)
STRAIN (x 10E-03)
0.0
0.5
1.0
1.5
2.0
2.5
0
100
200
300
0
3
6
9
12
15

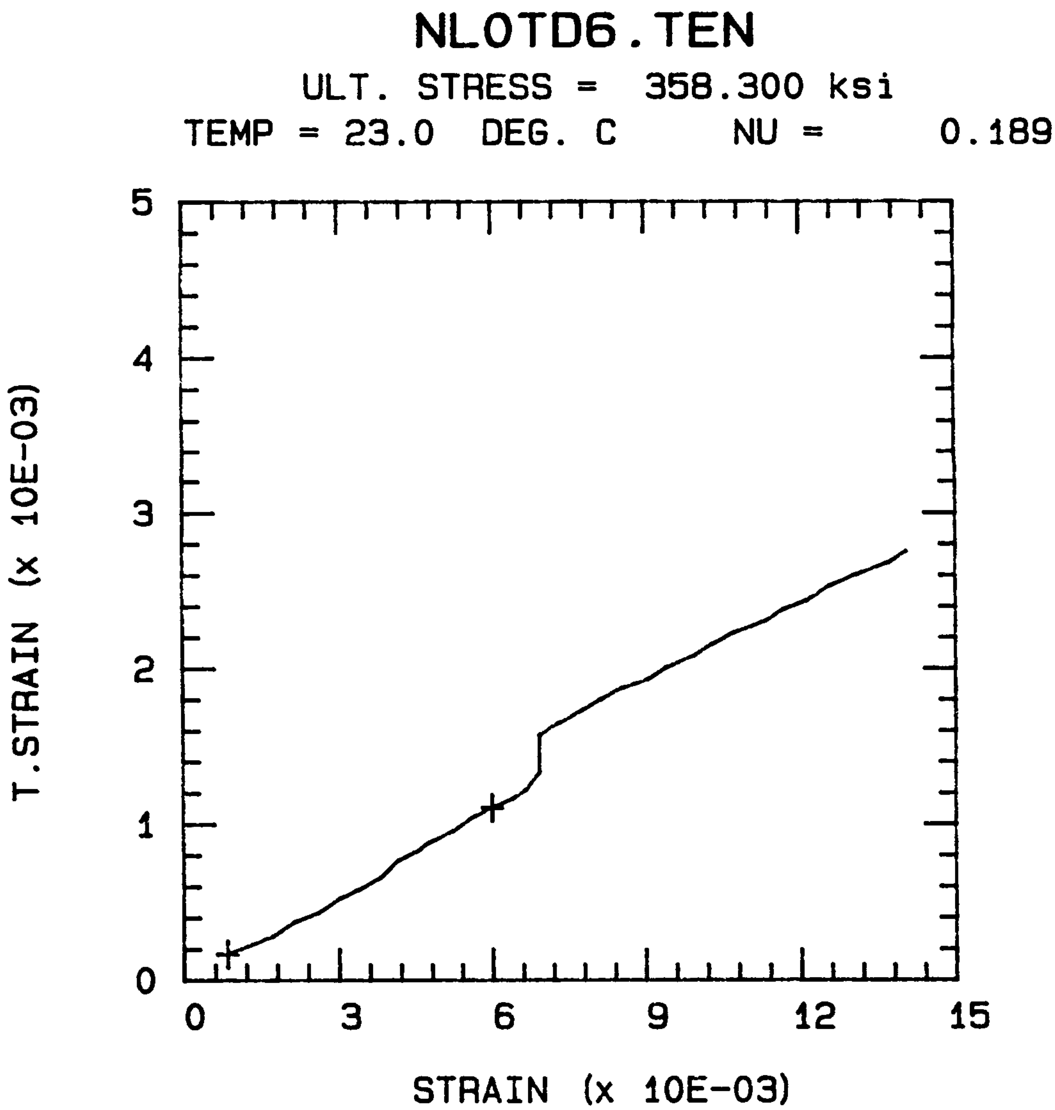
NLOTD6.TEN
ULT. STRESS = 358.300 ksi
TEMP = 23.0 DEG. C NU = 0.189
T.STRAIN (x 10E-03)
5
4
3
2
1
0
0
3
6
9
12
15
STRAIN (x 10E-03)

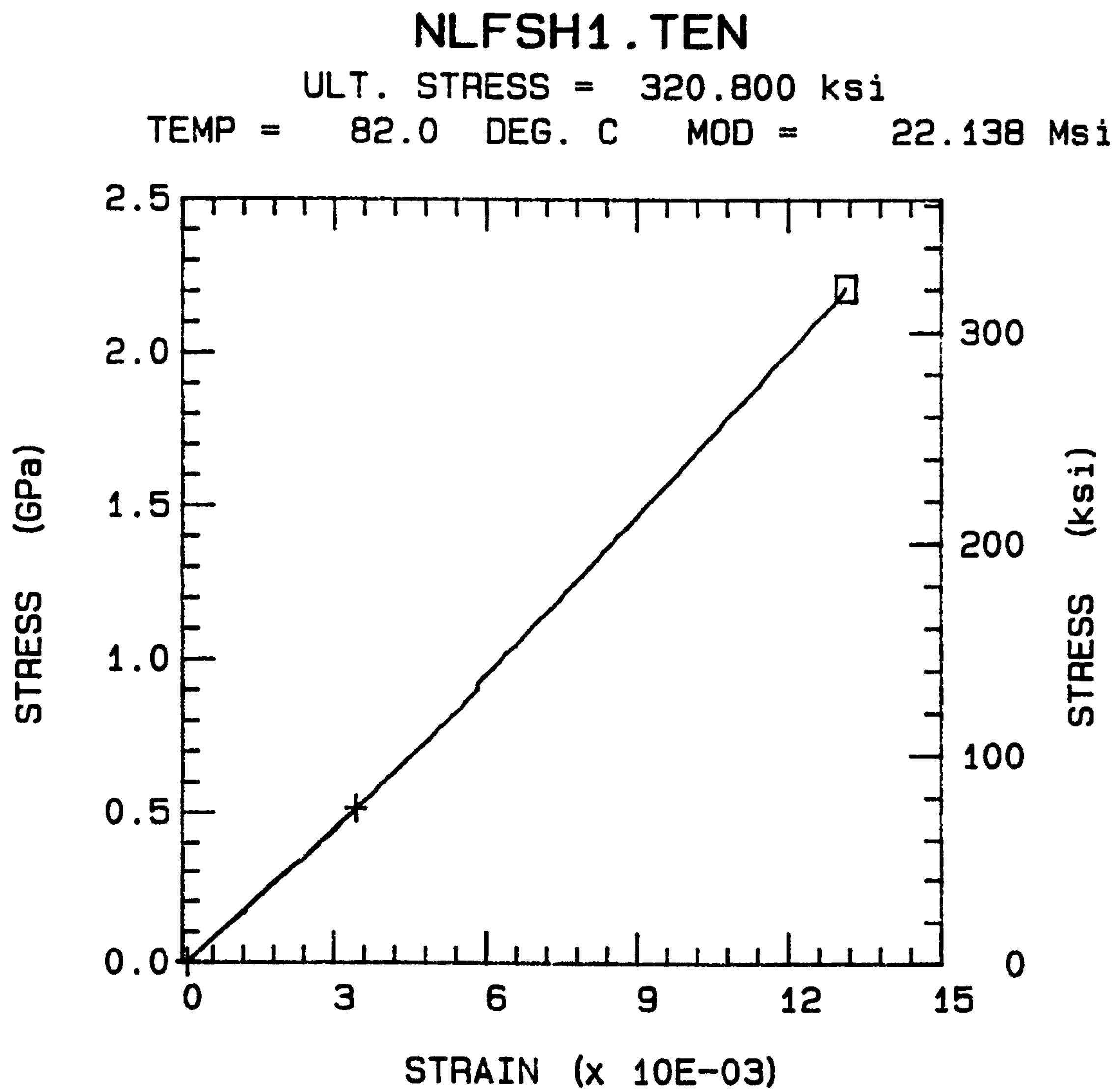
NLFSH1.TEN
ULT. STRESS = 320.800 ksi
TEMP = 82.0 DEG. C MOD = 22.138 Msi
STRESS (GPa)
2.5
2.0
1.5
1.0
0.5
0.0
STRESS (ksi)
300
200
100
0
0
3
6
9
12
15
STRAIN (x 10E-03)

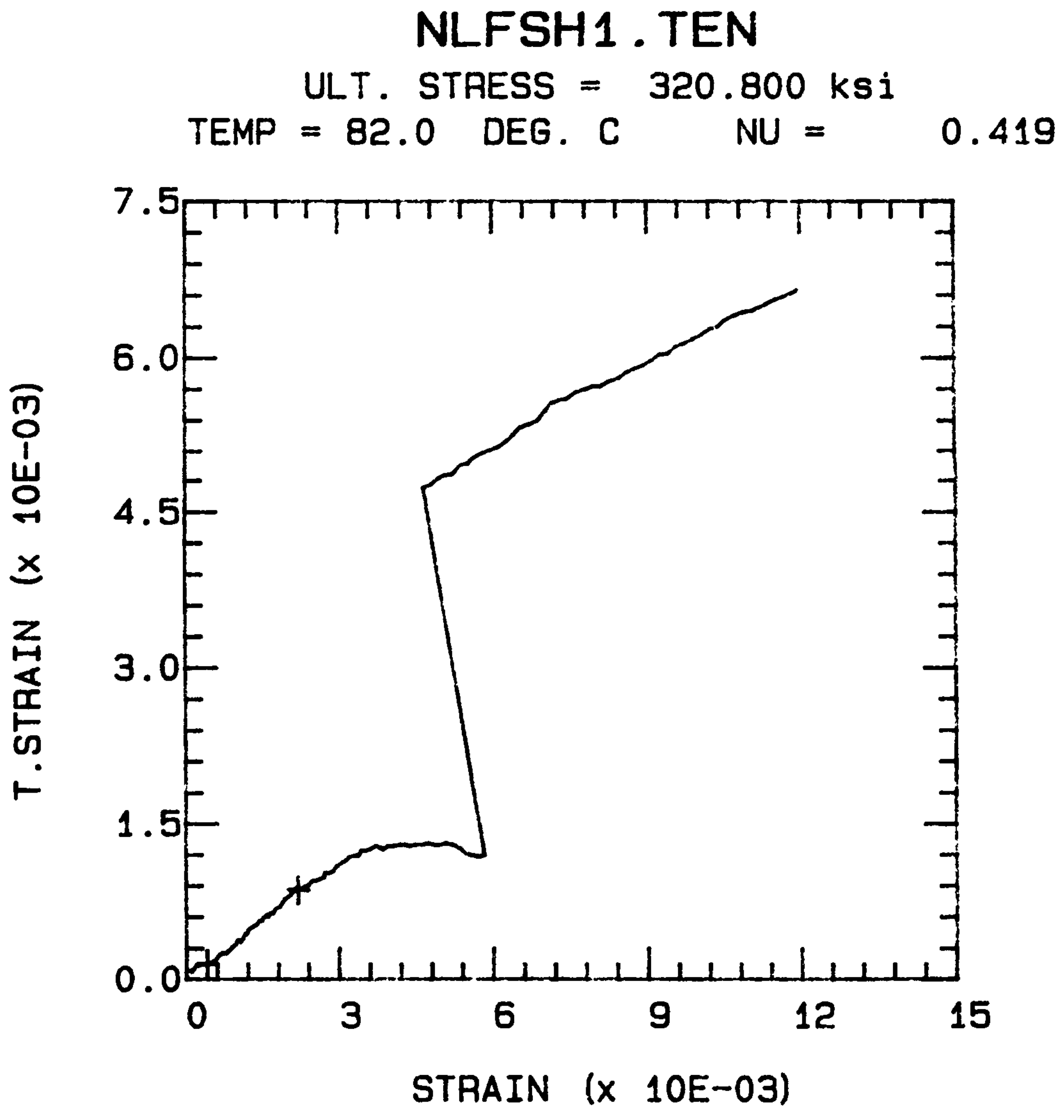
NLFSH1.TEN
ULT. STRESS = 320.800 ksi
TEMP = 82.0 DEG. C NU = 0.419
7.5
6.0
4.5
3.0
1.5
0.0
T.STRAIN (x 10E-03)
0
3
6
9
12
15
STRAIN (x 10E-03)

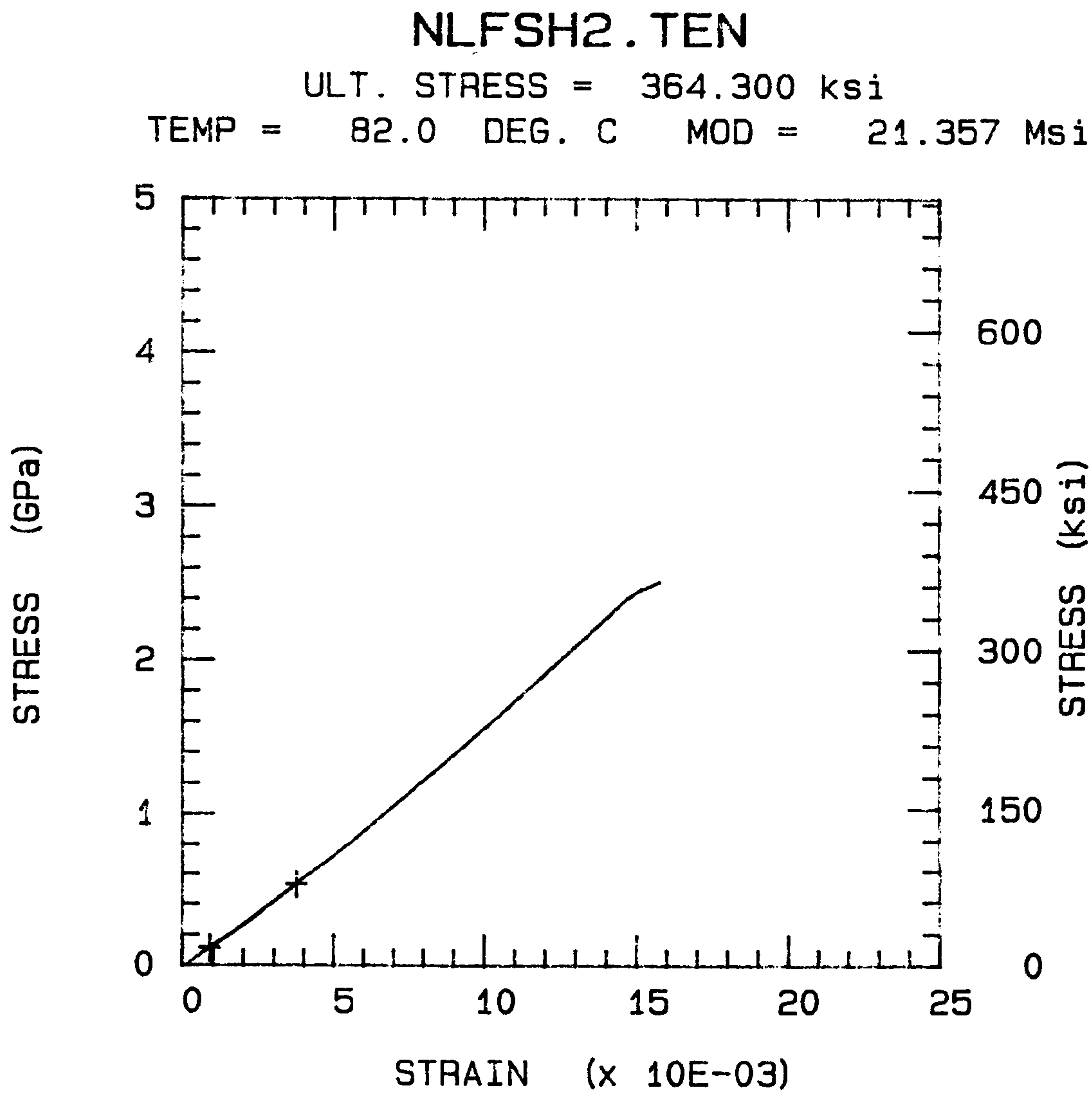
NLFSH2.TEN
ULT. STRESS = 364.300 ksi
TEMP = 82.0 DEG. C MOD = 21.357 Msi
STRESS (GPa)
STRESS (ksi)
STRAIN (x 10E-03)
0
1
2
3
4
5
150
300
450
600
10
15
20
25

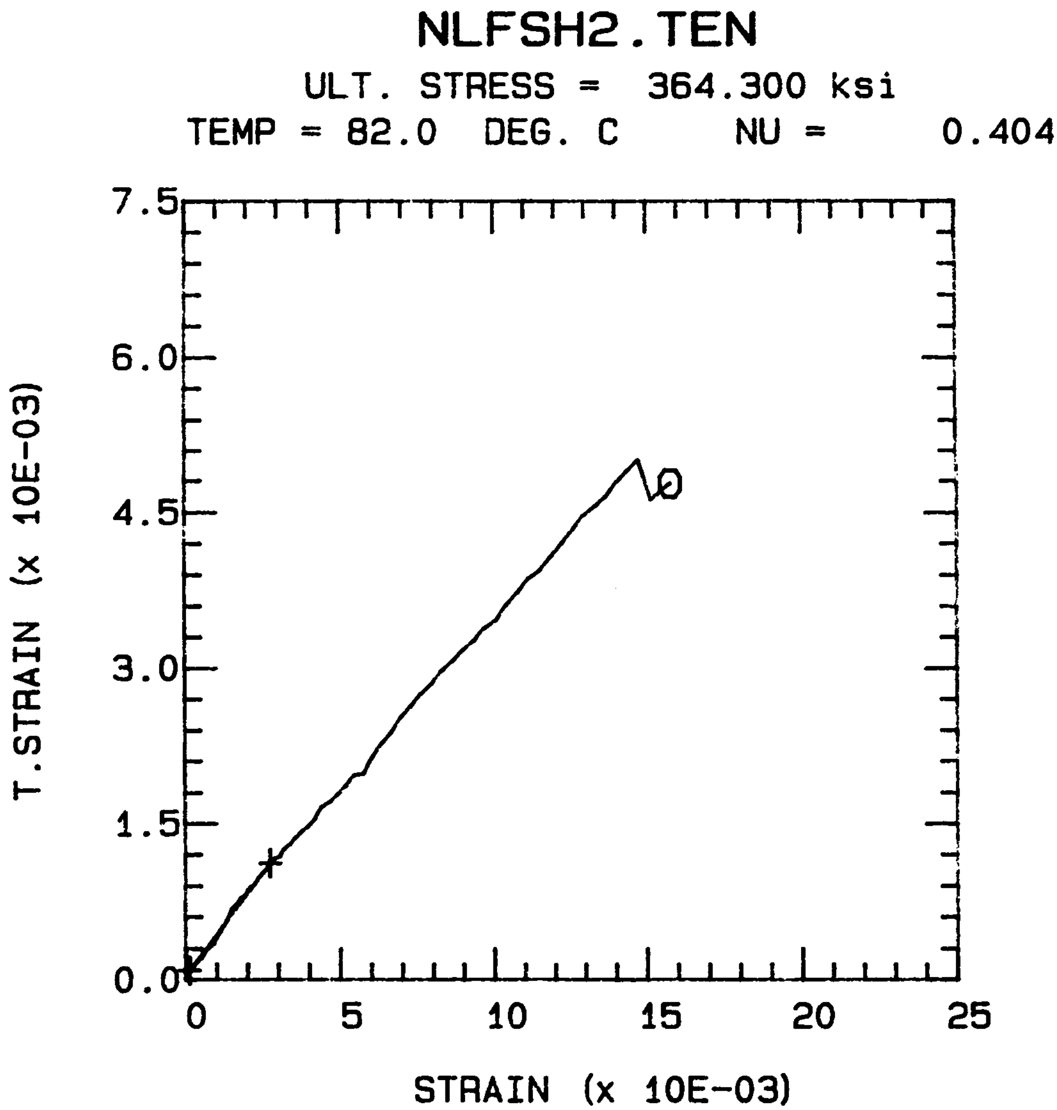
NLFSH2.TEN
ULT. STRESS = 364.300 ksi
TEMP = 82.0 DEG. C NU = 0.404
7.5
6.0
4.5
3.0
1.5
0.0
0
5
10
15
20
25
T.STRAIN (x 10E-03)
STRAIN (x 10E-03)

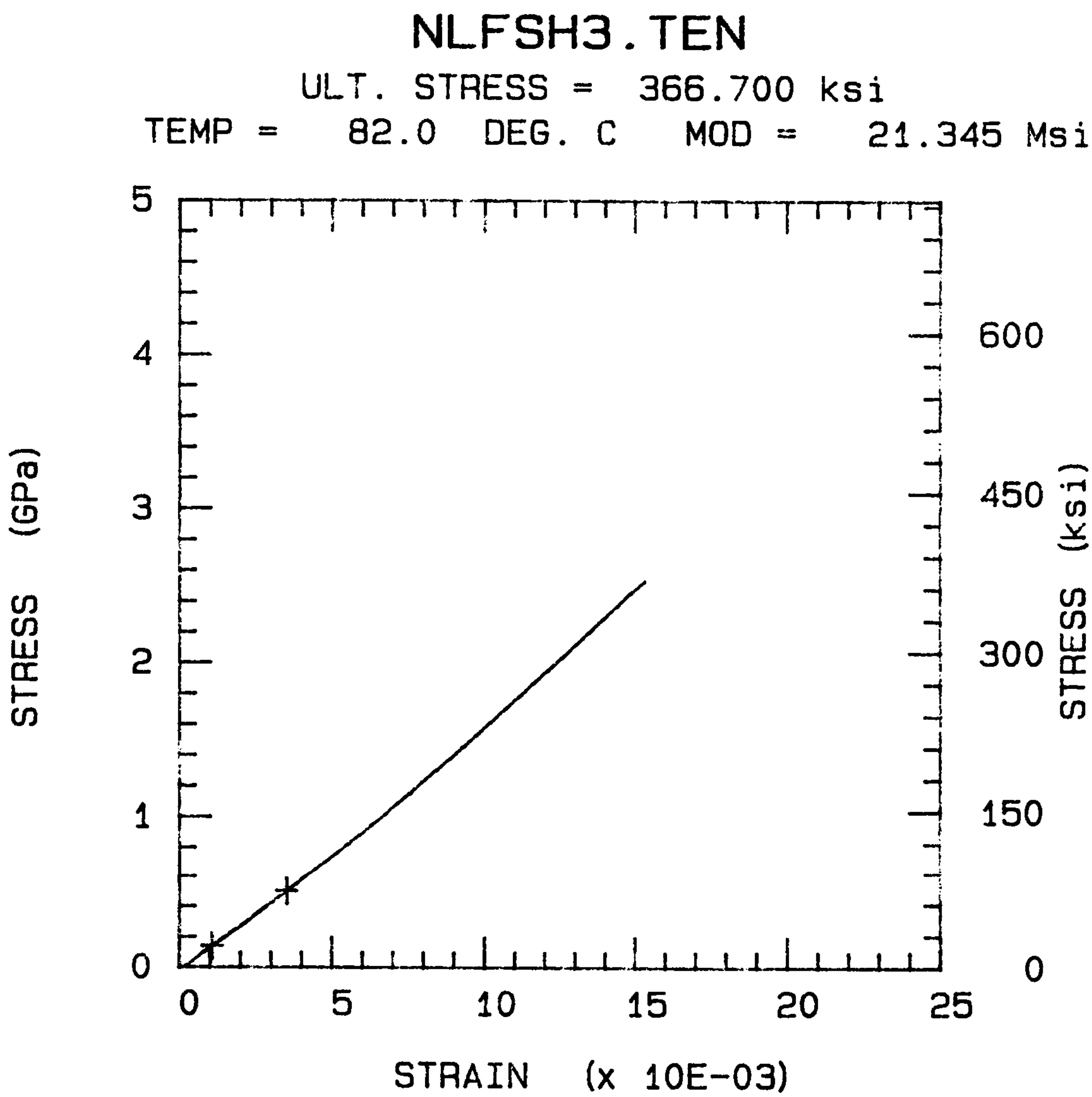
NLFSH3.TEN
ULT. STRESS = 366.700 ksi
TEMP = 82.0 DEG. C MOD = 21.345 Msi
STRESS (GPa)
0
1
2
3
4
5
STRESS (ksi)
0
150
300
450
600
0
5
10
15
20
25
STRAIN (x 10E-03)

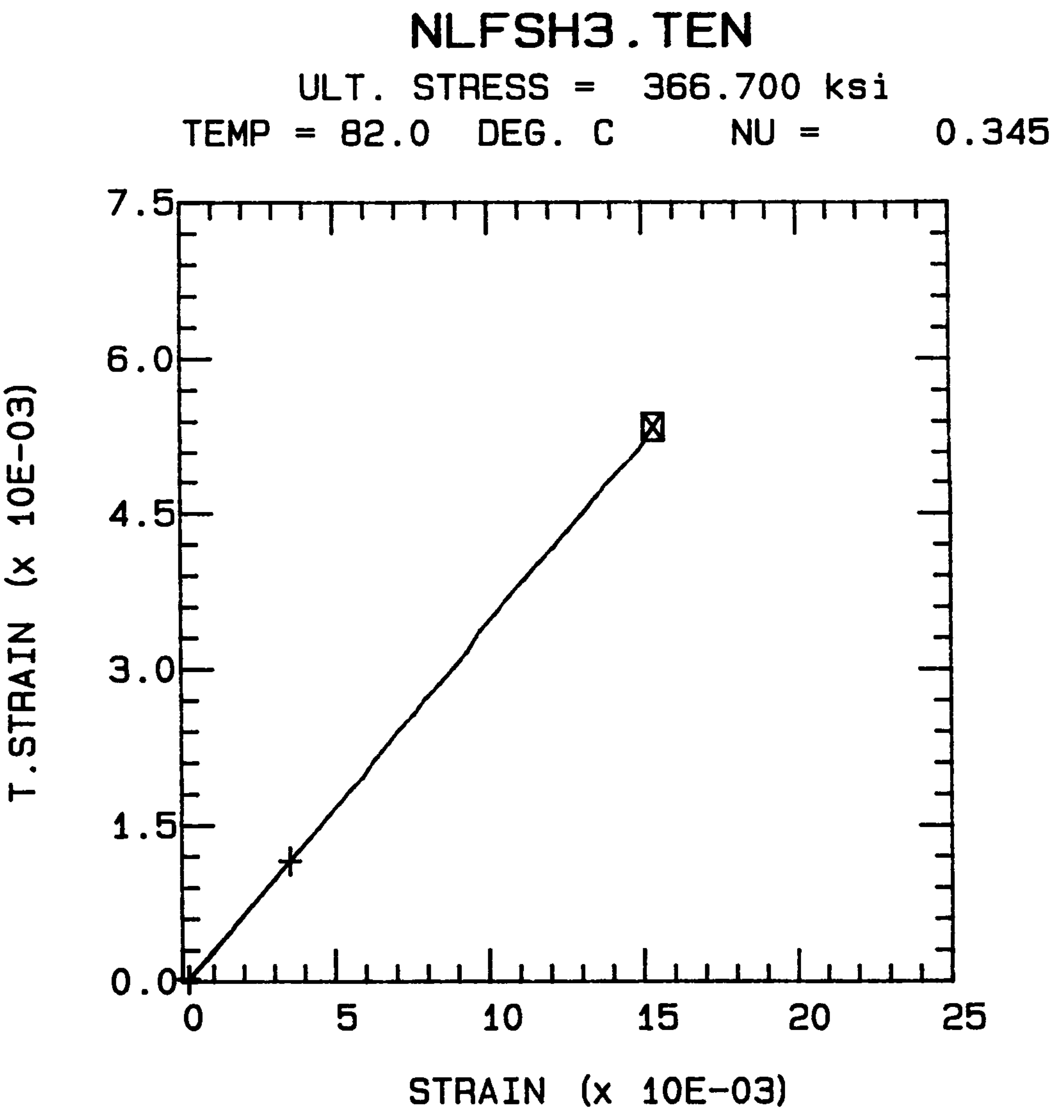

NLFSH3.TEN
ULT. STRESS = 366.700 ksi
TEMP = 82.0 DEG. C NU = 0.345
7.5
6.0
4.5
3.0
1.5
0.0
T.STRAIN (x 10E-03)
0
5
10
15
20
25
STRAIN (x 10E-03)

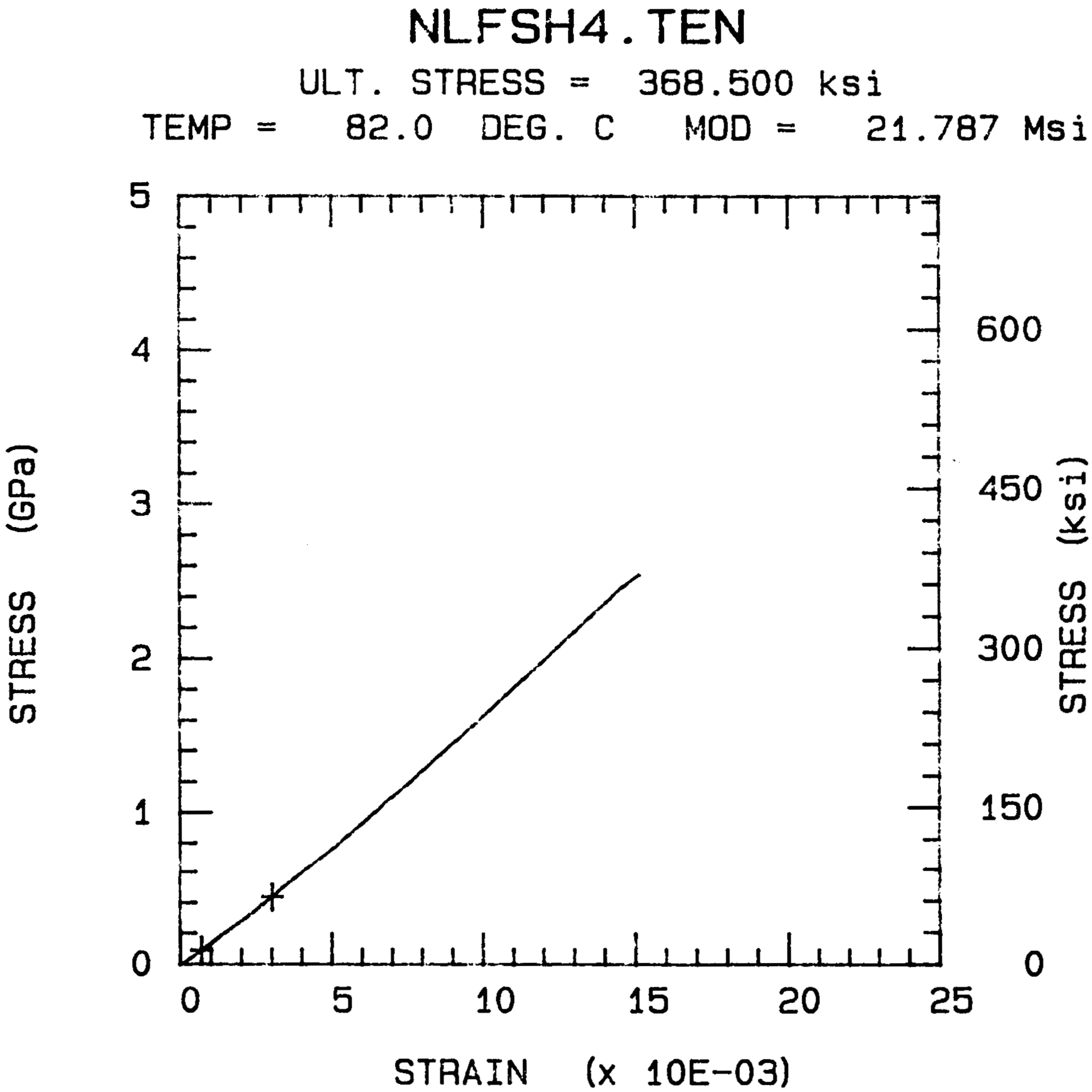

NLFSH4.TEN
ULT. STRESS = 368.500 ksi
TEMP = 82.0 DEG. C MOD = 21.787 Msi
STRESS (GPa)
0
1
2
3
4
5
STRESS (ksi)
0
150
300
450
600
STRAIN (x 10E-03)
0
5
10
15
20
25

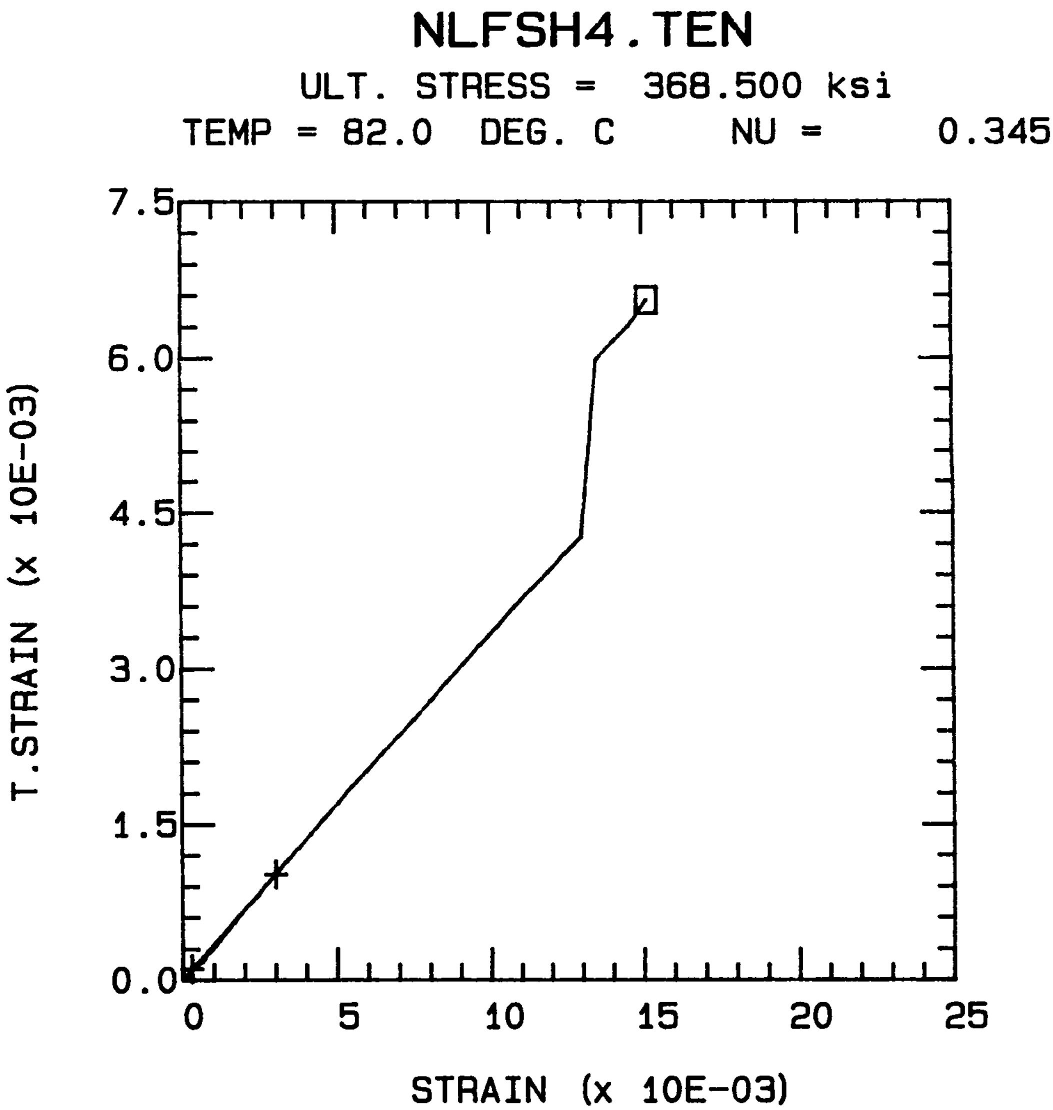
NLFSH4.TEN
ULT. STRESS = 368.500 ksi
TEMP = 82.0 DEG. C NU = 0.345
7.5
6.0
4.5
3.0
1.5
0.0
T.STRAIN (x 10E-03)
0
5
10
15
20
25
STRAIN (x 10E-03)

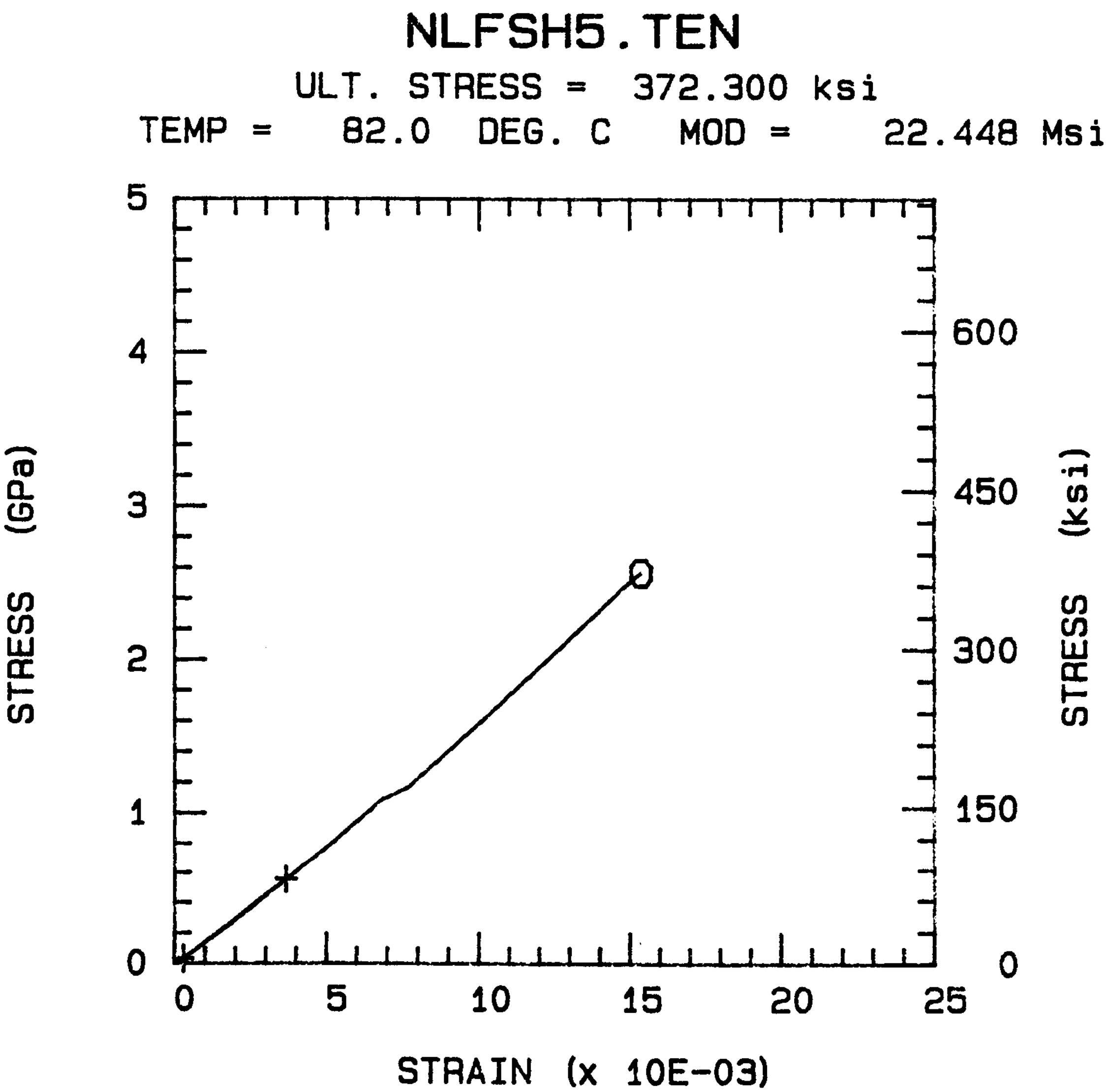
NLFSH5.TEN
ULT. STRESS = 372.300 ksi
TEMP = 82.0 DEG. C MOD = 22.448 Msi
STRESS (GPa)
STRESS (ksi)
STRAIN (x 10E-03)
0
1
2
3
4
5
0
150
300
450
600
0
5
10
15
20
25

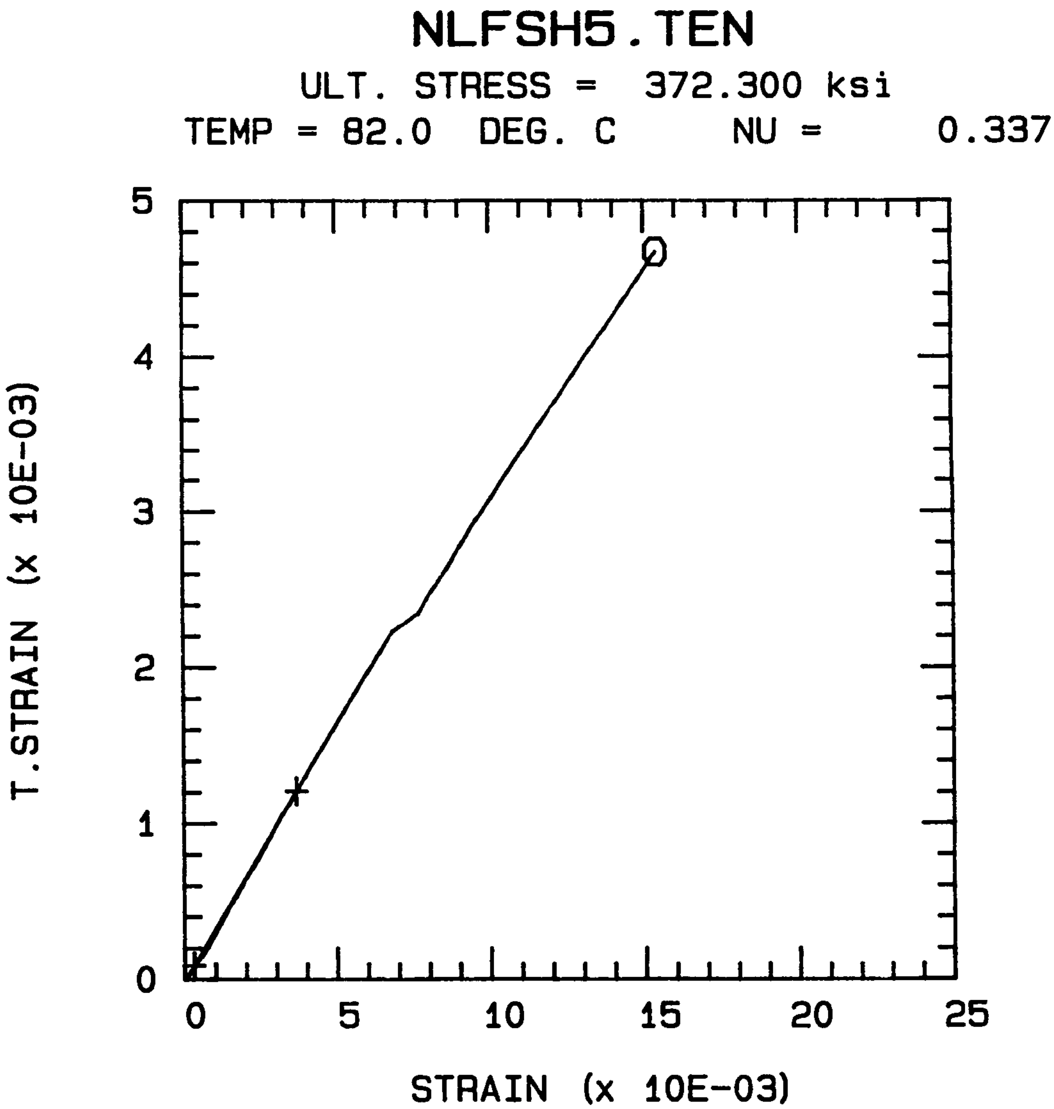
NLFSH5.TEN
ULT. STRESS = 372.300 ksi
TEMP = 82.0 DEG. C NU = 0.337
T.STRAIN (x 10E-03)
STRAIN (x 10E-03)
0
1
2
3
4
5
0
5
10
15
20
25

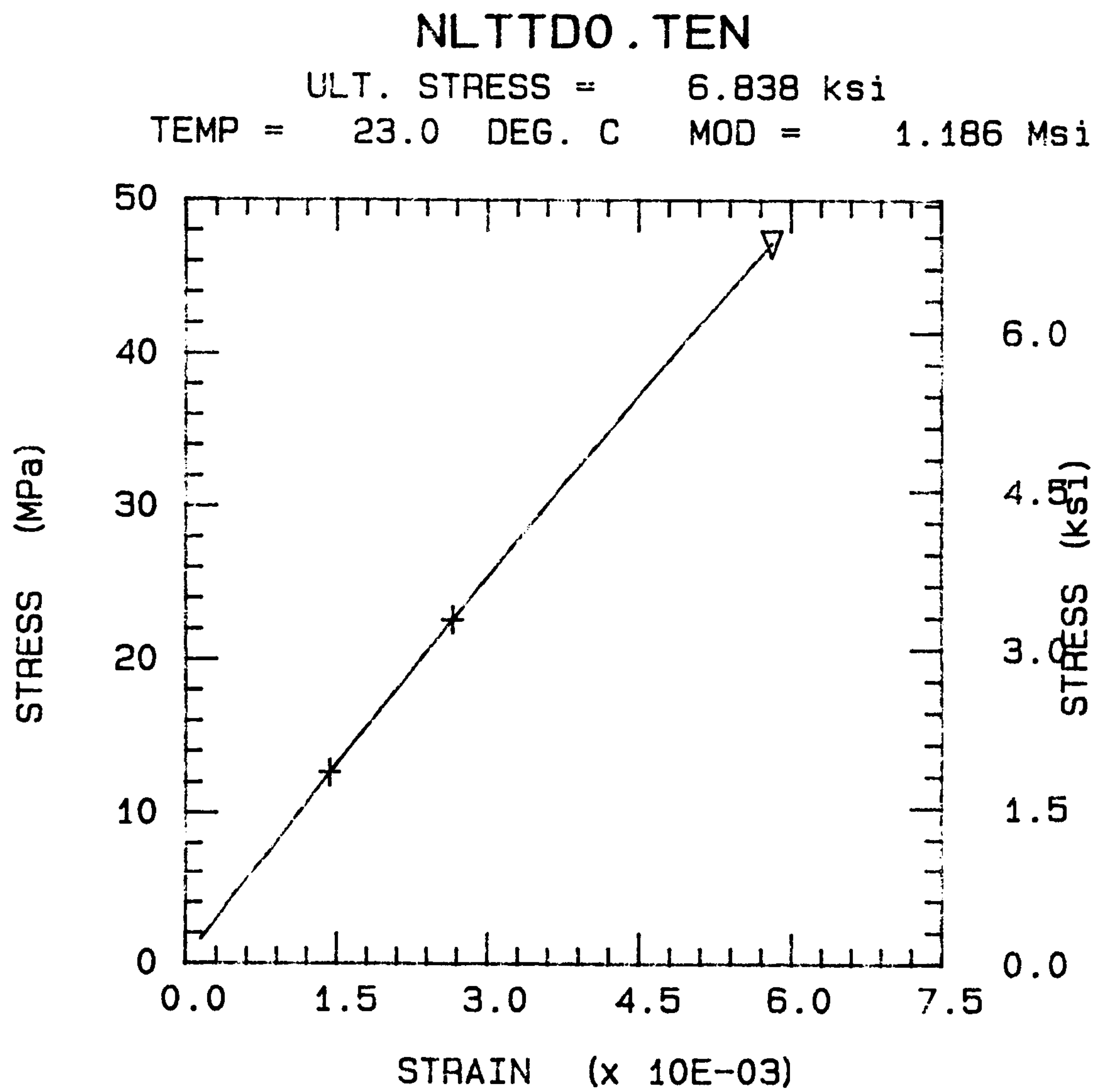
NLTTDO.TEN
ULT. STRESS = 6.838 ksi
TEMP = 23.0 DEG. C MOD = 1.186 Msi
STRESS (MPa)
0
10
20
30
40
50
STRESS (ksi)
0.0
1.5
3.0
4.5
6.0
0.0
1.5
3.0
4.5
6.0
7.5
STRAIN (x 10E-03)

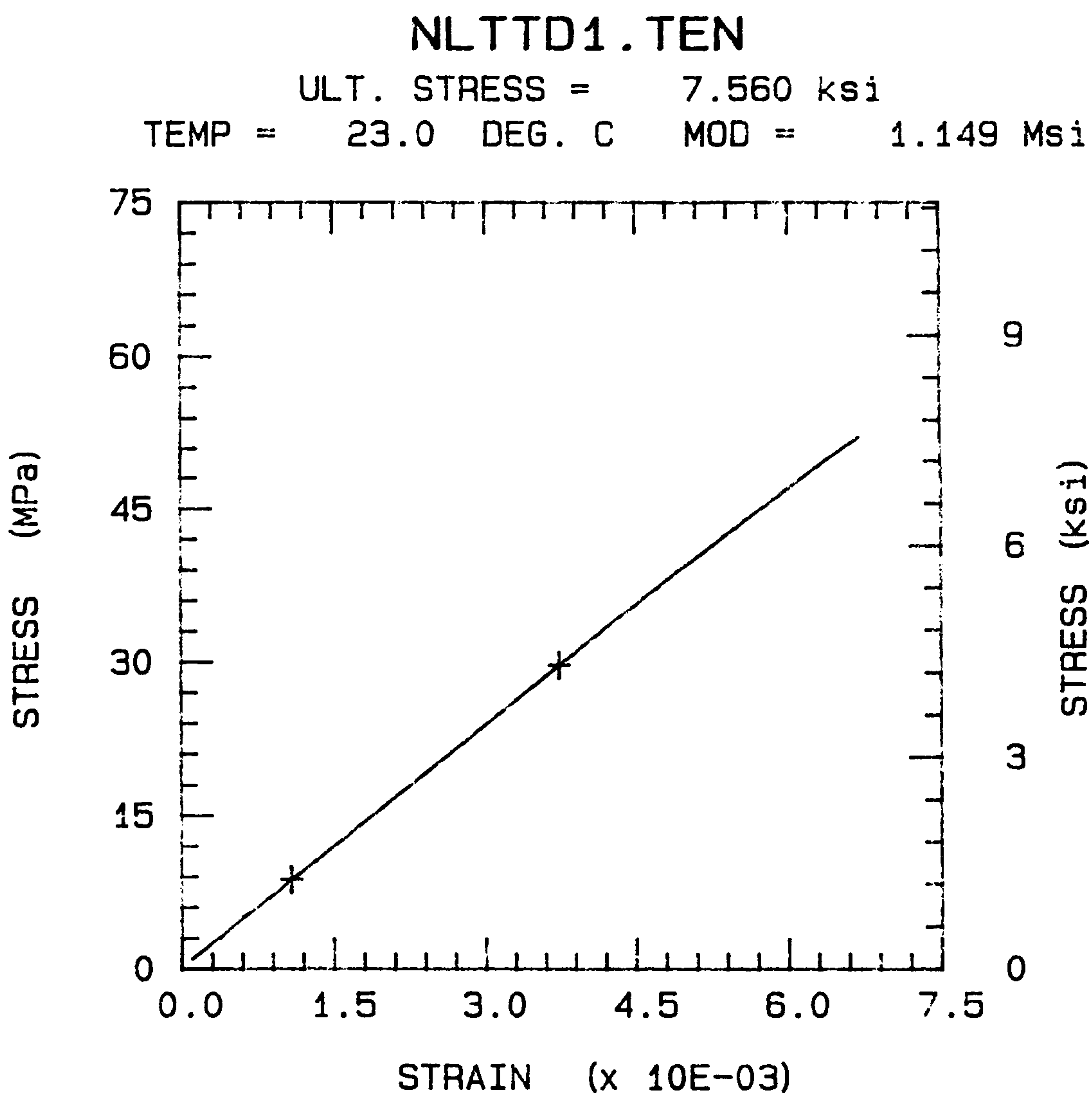
NLTTD1.TEN
ULT. STRESS = 7.560 ksi
TEMP = 23.0 DEG. C MOD = 1.149 Msi
75
60
45
30
15
0
9
6
3
0
STRESS (MPa)
STRESS (ksi)
0.0
1.5
3.0
4.5
6.0
7.5
STRAIN (x 10E-03)

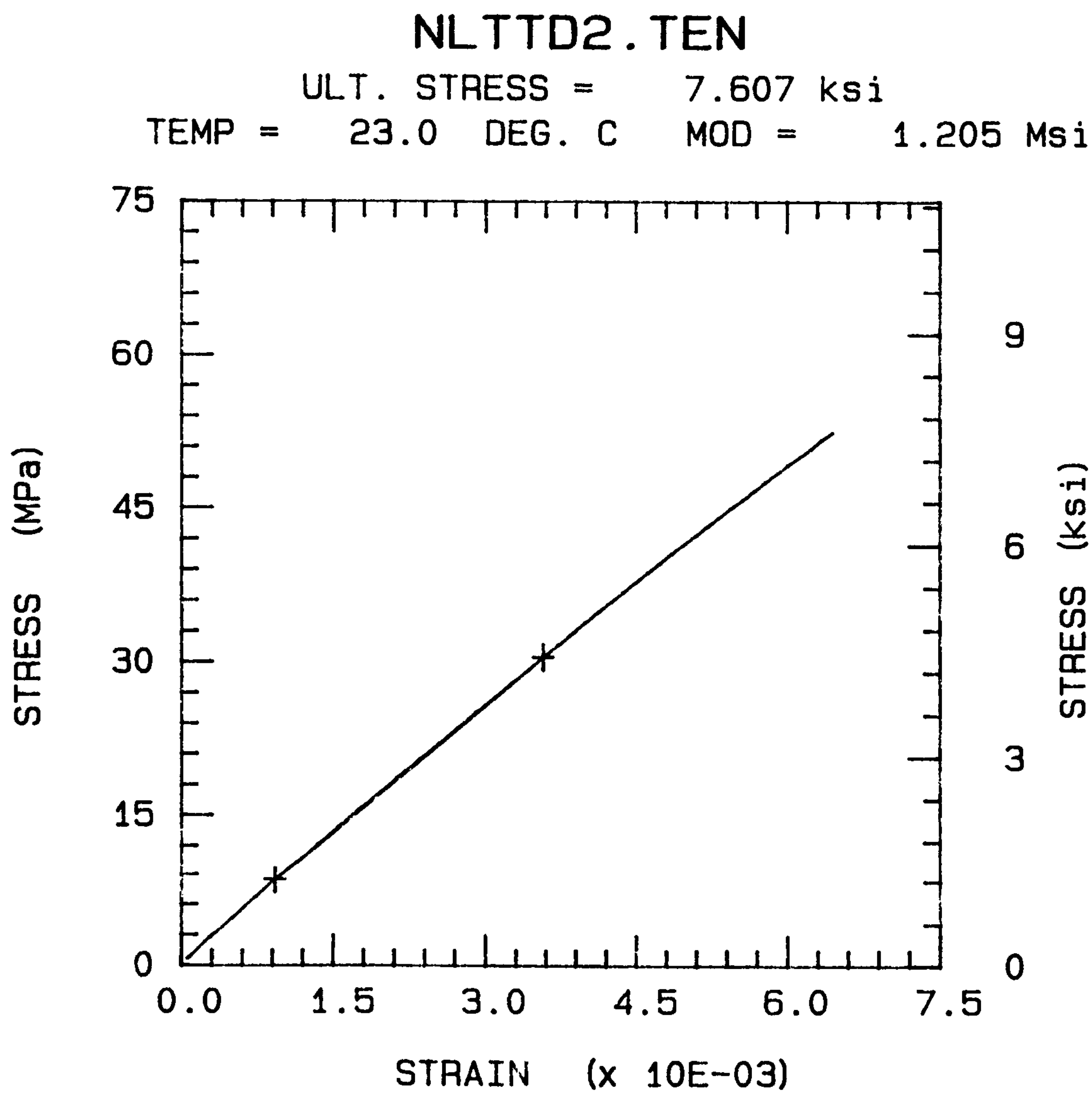
NLTTD2.TEN
ULT. STRESS = 7.607 ksi
TEMP = 23.0 DEG. C MOD = 1.205 Msi
STRESS (MPa)
0
15
30
45
60
75
STRESS (ksi)
0
3
6
9
0.0
1.5
3.0
4.5
6.0
7.5
STRAIN (x 10E-03)

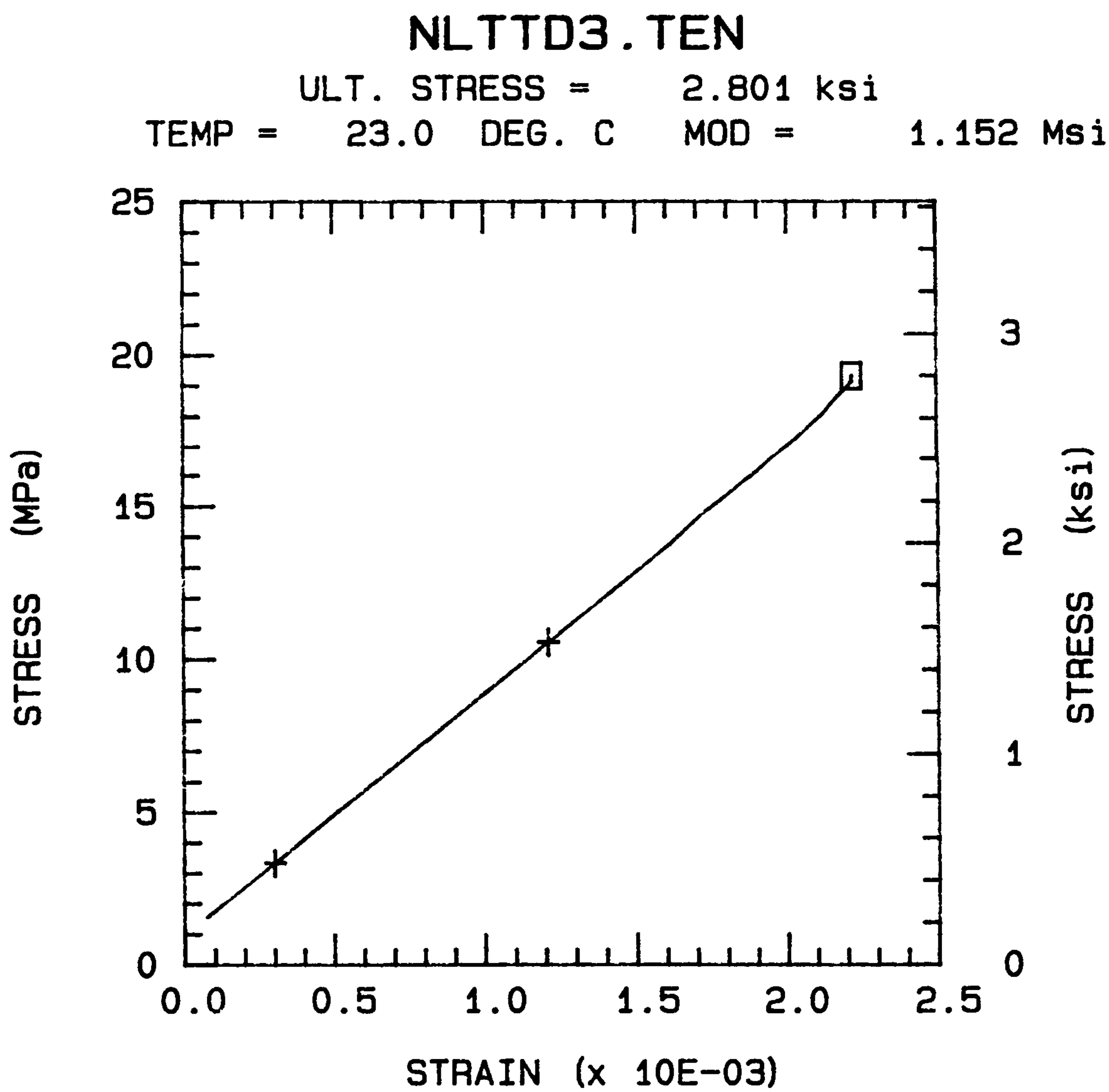
NLTTD3.TEN
ULT. STRESS = 2.801 ksi
TEMP = 23.0 DEG. C MOD = 1.152 Msi
STRESS (MPa)
STRESS (ksi)
STRAIN (x 10E-03)
0
5
10
15
20
25
0
1
2
3
0.0
0.5
1.0
1.5
2.0
2.5

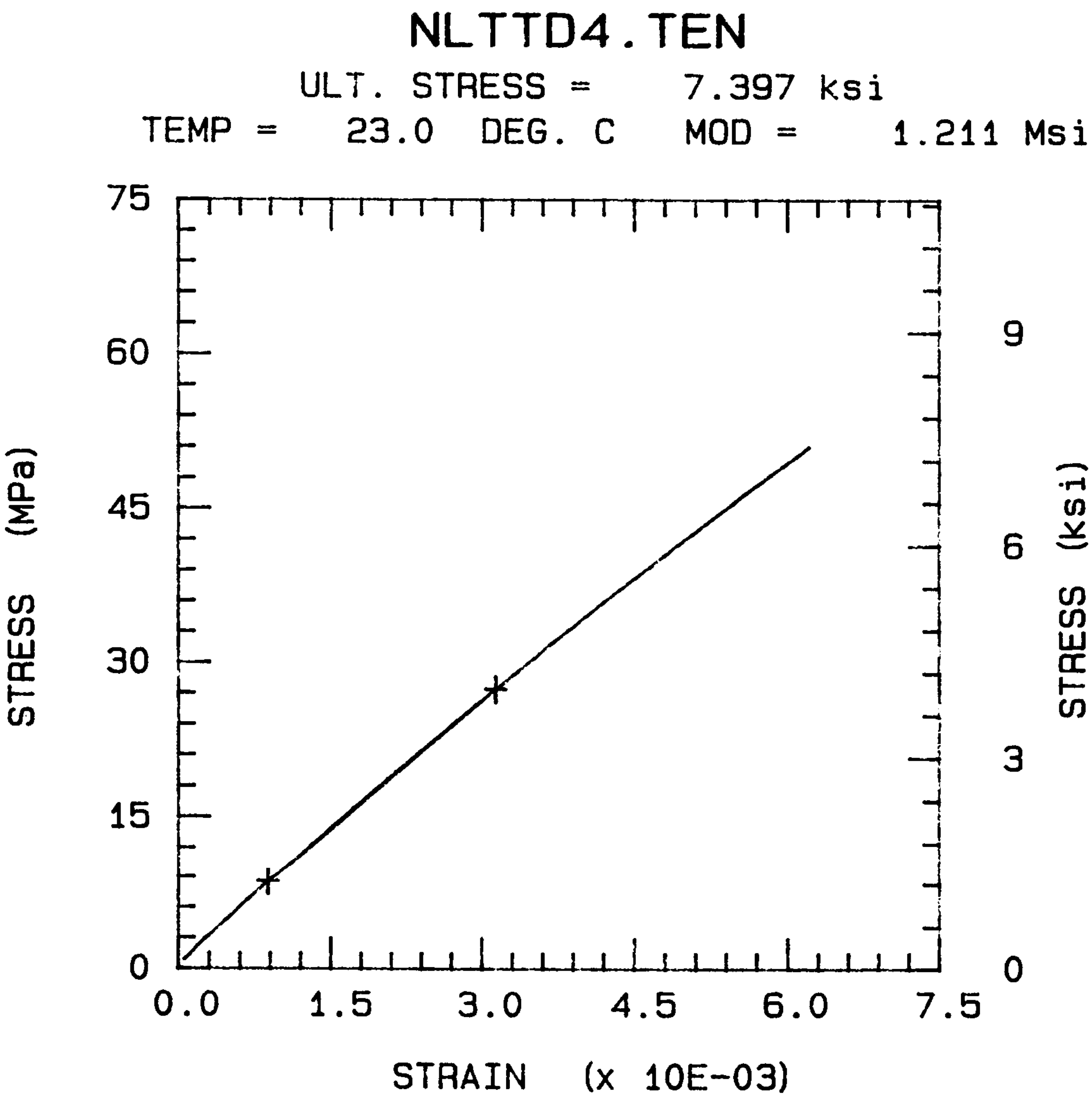

NLTTD4.TEN
ULT. STRESS = 7.397 ksi
TEMP = 23.0 DEG. C MOD = 1.211 Msi
STRESS (MPa)
75
60
45
30
15
0
STRESS (ksi)
9
6
3
0
0.0
1.5
3.0
4.5
6.0
7.5
STRAIN (x 10E-03)

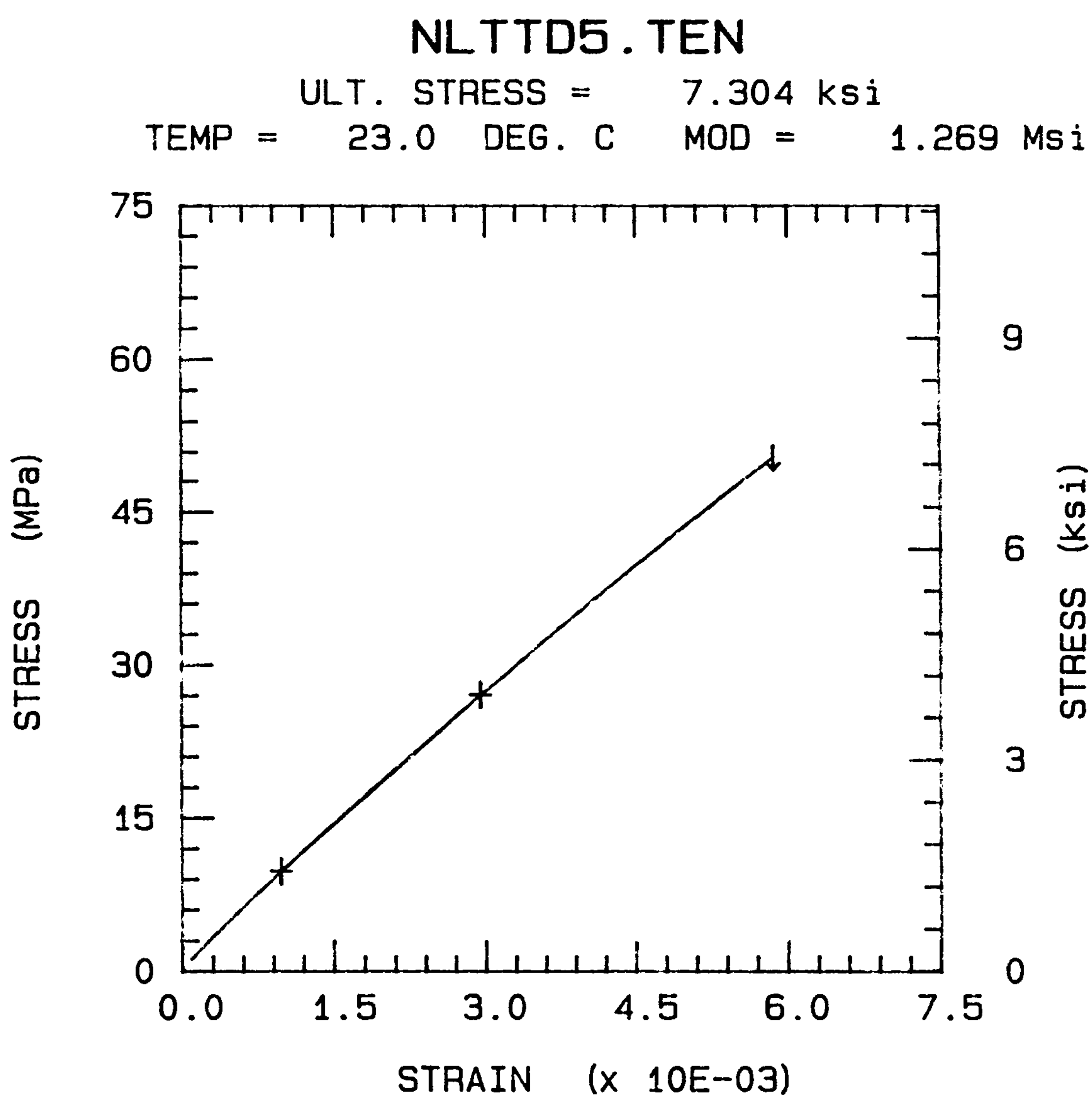

NLTTD5.TEN
ULT. STRESS = 7.304 ksi
TEMP = 23.0 DEG. C MOD = 1.269 Msi
75
60
45
30
15
0
STRESS (MPa)
9
6
3
0
STRESS (ksi)
0.0
1.5
3.0
4.5
6.0
7.5
STRAIN (x 10E-03)

C-2

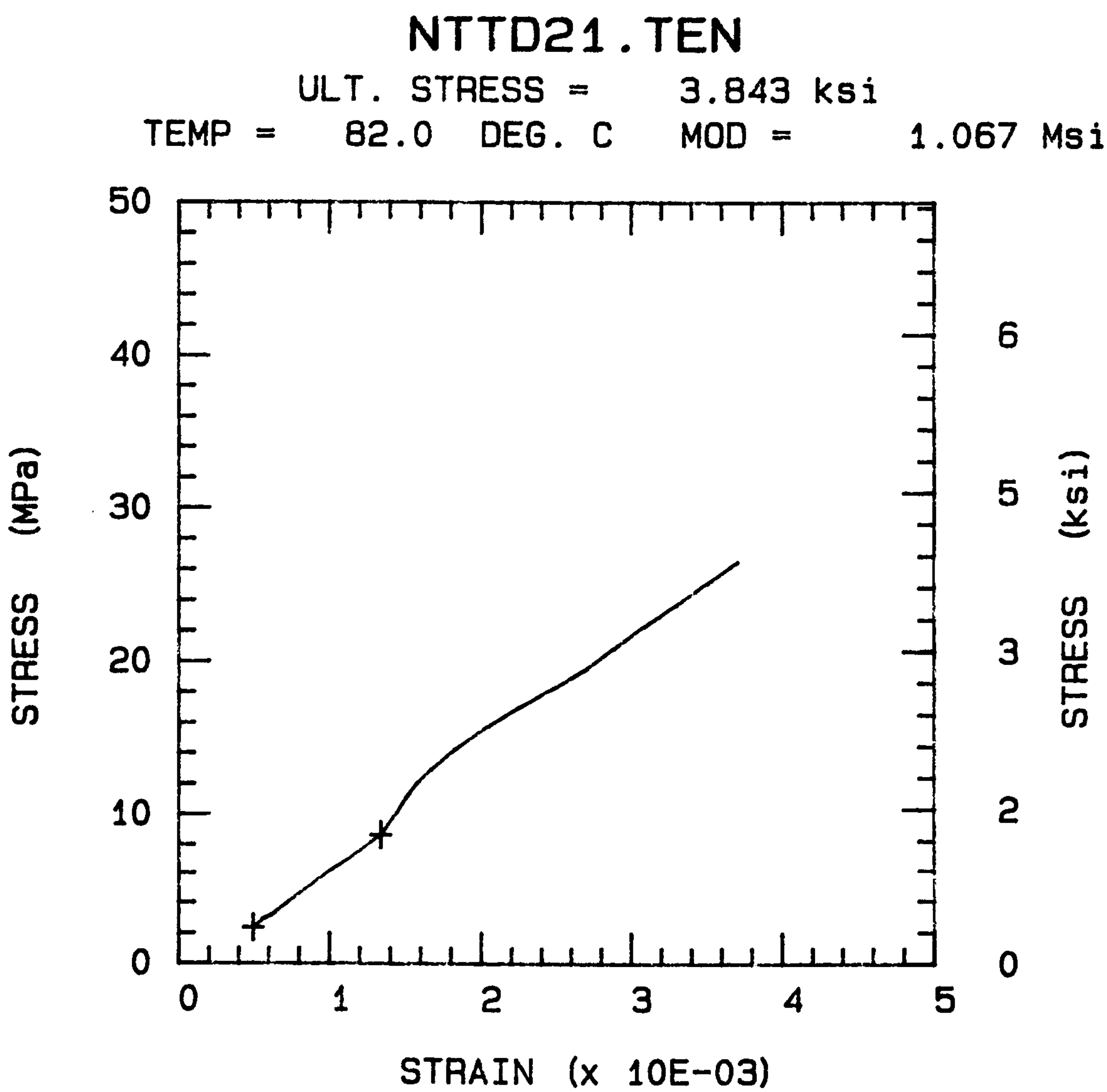
NTTD21.TEN
ULT. STRESS = 3.843 ksi
TEMP = 82.0 DEG. C MOD = 1.067 Msi
STRESS (MPa)
STRESS (ksi)
STRAIN (x 10E-03)
0
10
20
30
40
50
0
1
2
3
4
5
0
2
3
5
6

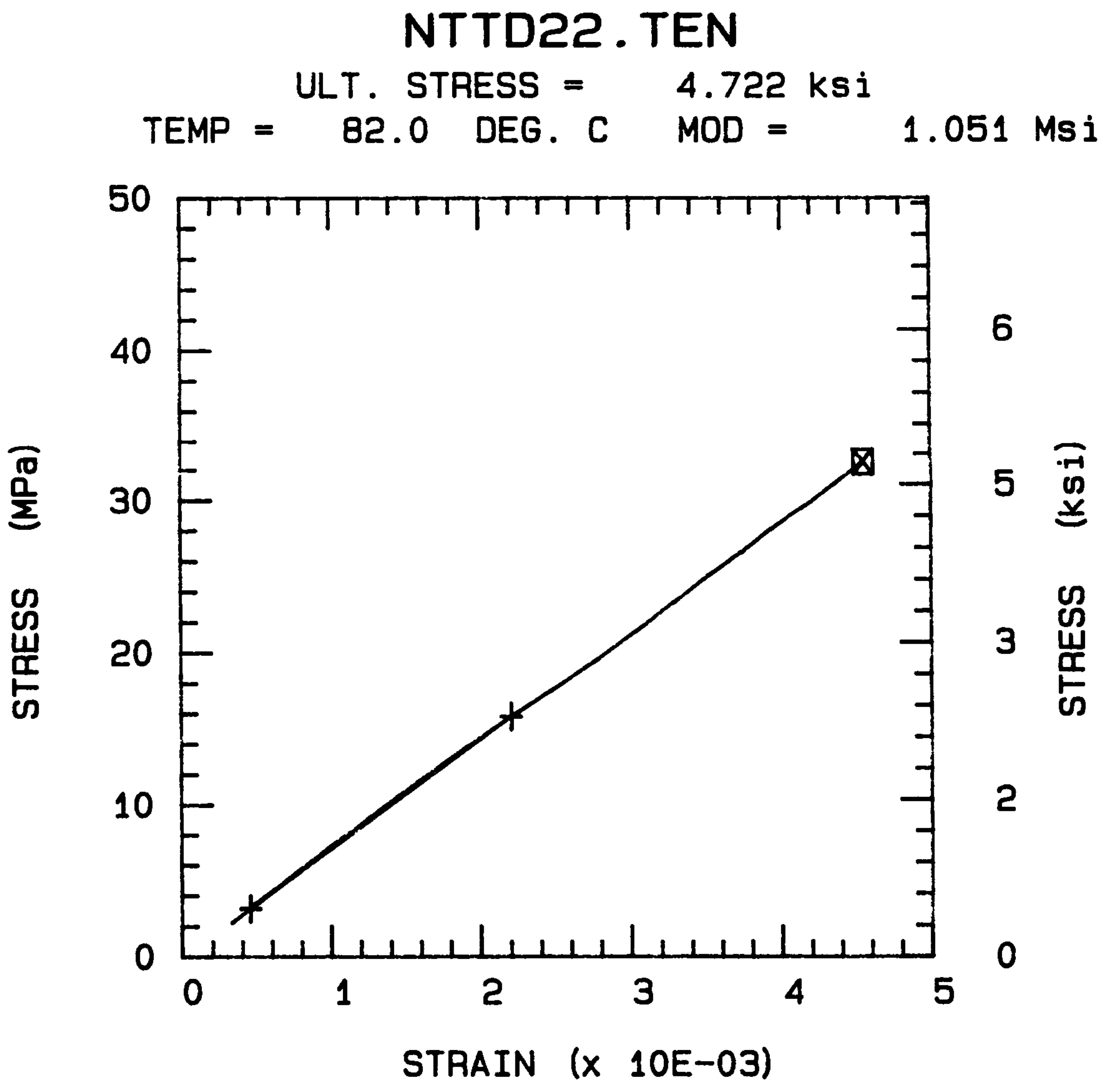
NTTD22.TEN
ULT. STRESS = 4.722 ksi
TEMP = 82.0 DEG. C MOD = 1.051 Msi
STRESS (MPa)
STRESS (ksi)
STRAIN (x 10E-03)
50
40
30
20
10
0
6
5
3
2
0
0
1
2
3
4
5

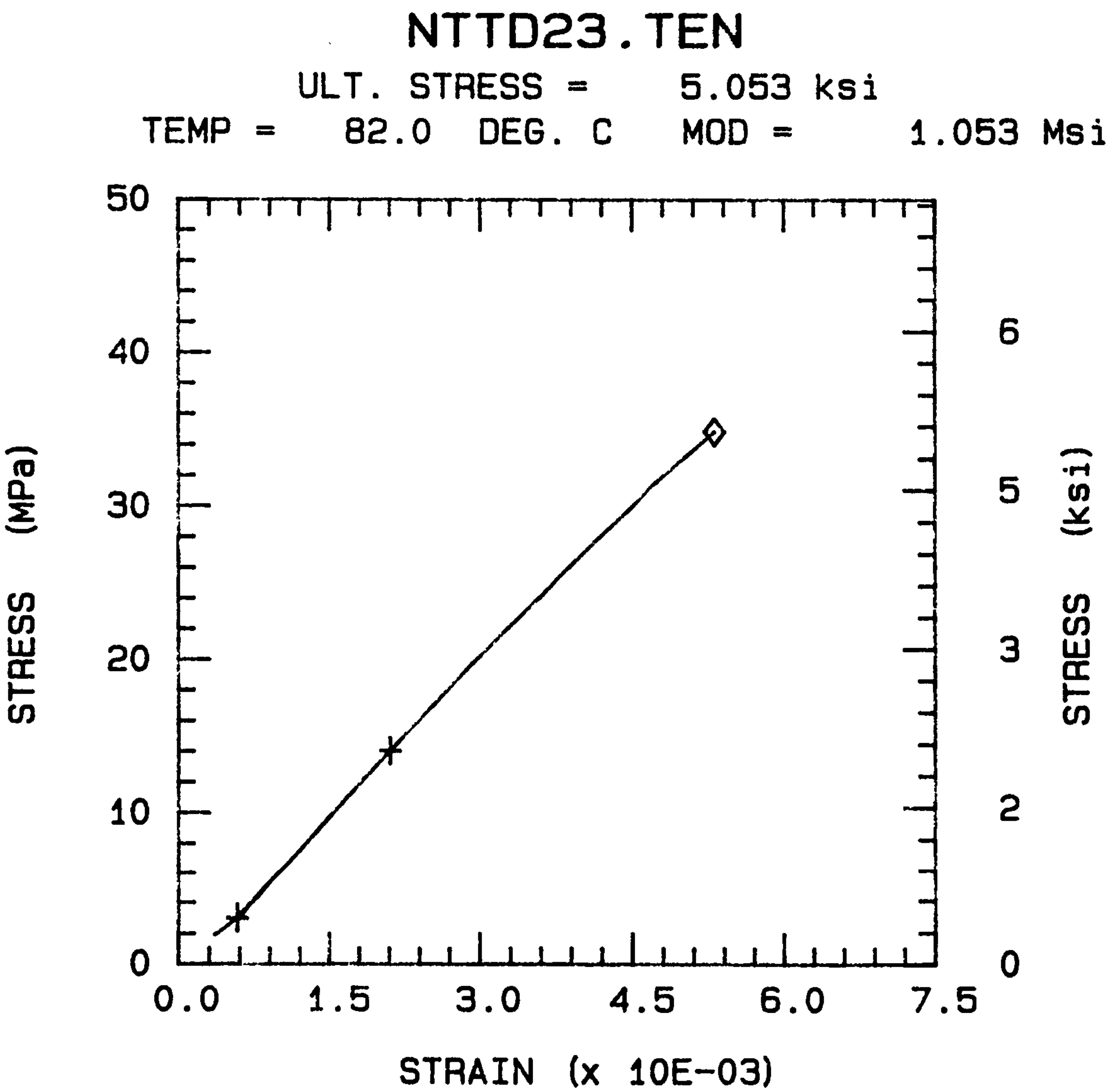
NTTD23.TEN
ULT. STRESS = 5.053 ksi
TEMP = 82.0 DEG. C MOD = 1.053 Msi
STRESS (MPa)
STRESS (ksi)
STRAIN (x 10E-03)
0
10
20
30
40
50
0.0
1.5
3.0
4.5
6.0
7.5
2
3
5
6

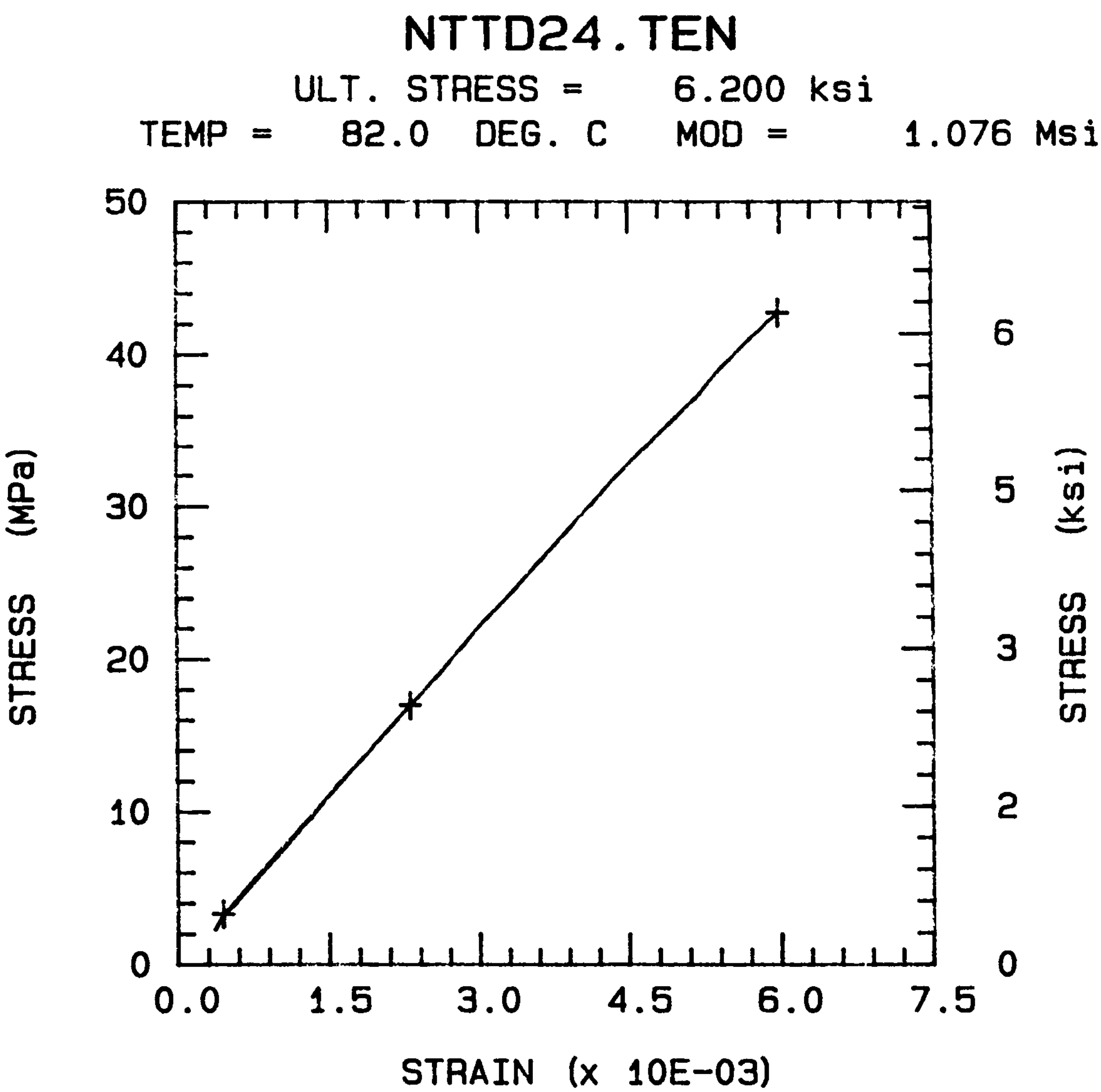
NTTD24.TEN
ULT. STRESS = 6.200 ksi
TEMP = 82.0 DEG. C MOD = 1.076 Msi
50
40
30
20
10
0
STRESS (MPa)
6
5
3
2
0
STRESS (ksi)
0.0
1.5
3.0
4.5
6.0
7.5
STRAIN (x 10E-03)

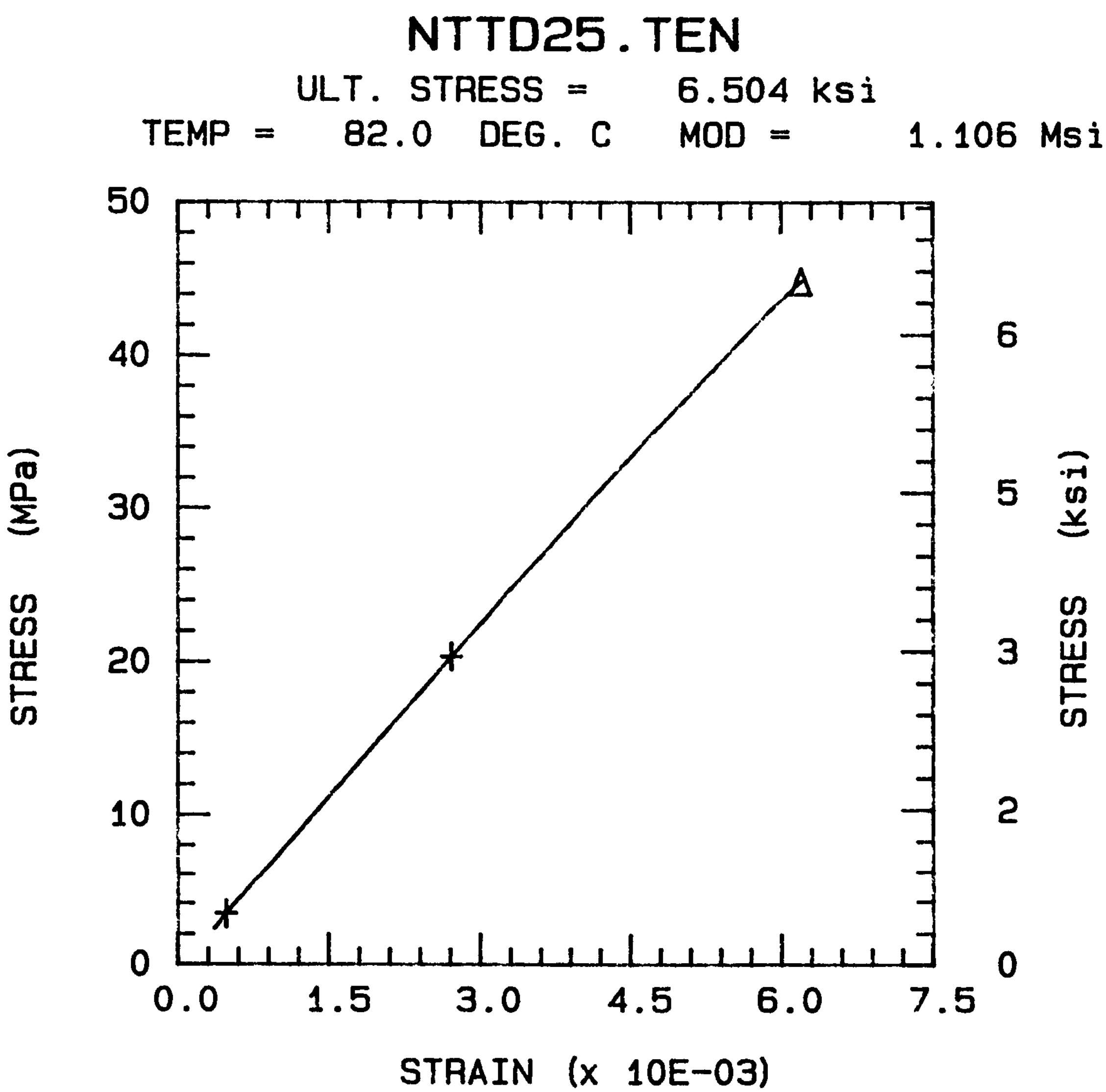

NTTD25.TEN
ULT. STRESS = 6.504 ksi
TEMP = 82.0 DEG. C MOD = 1.106 Msi
STRESS (MPa)
STRESS (ksi)
STRAIN (x 10E-03)
0
10
20
30
40
50
0.0
1.5
3.0
4.5
6.0
7.5
2
3
5
6

NTTD26.TEN

ULT. STRESS = 6.631 ksi

TEMP = 82.0 DEG. C MOD = 1.094 Msi

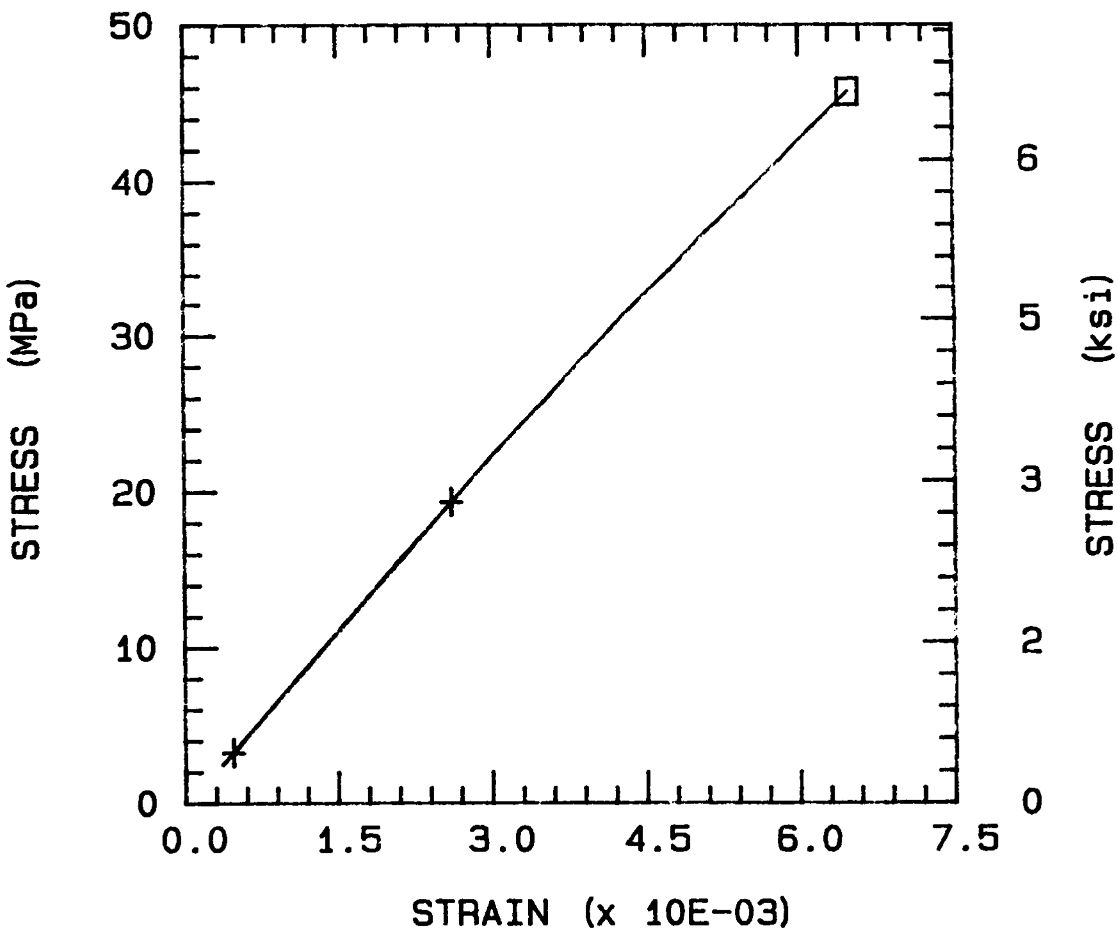

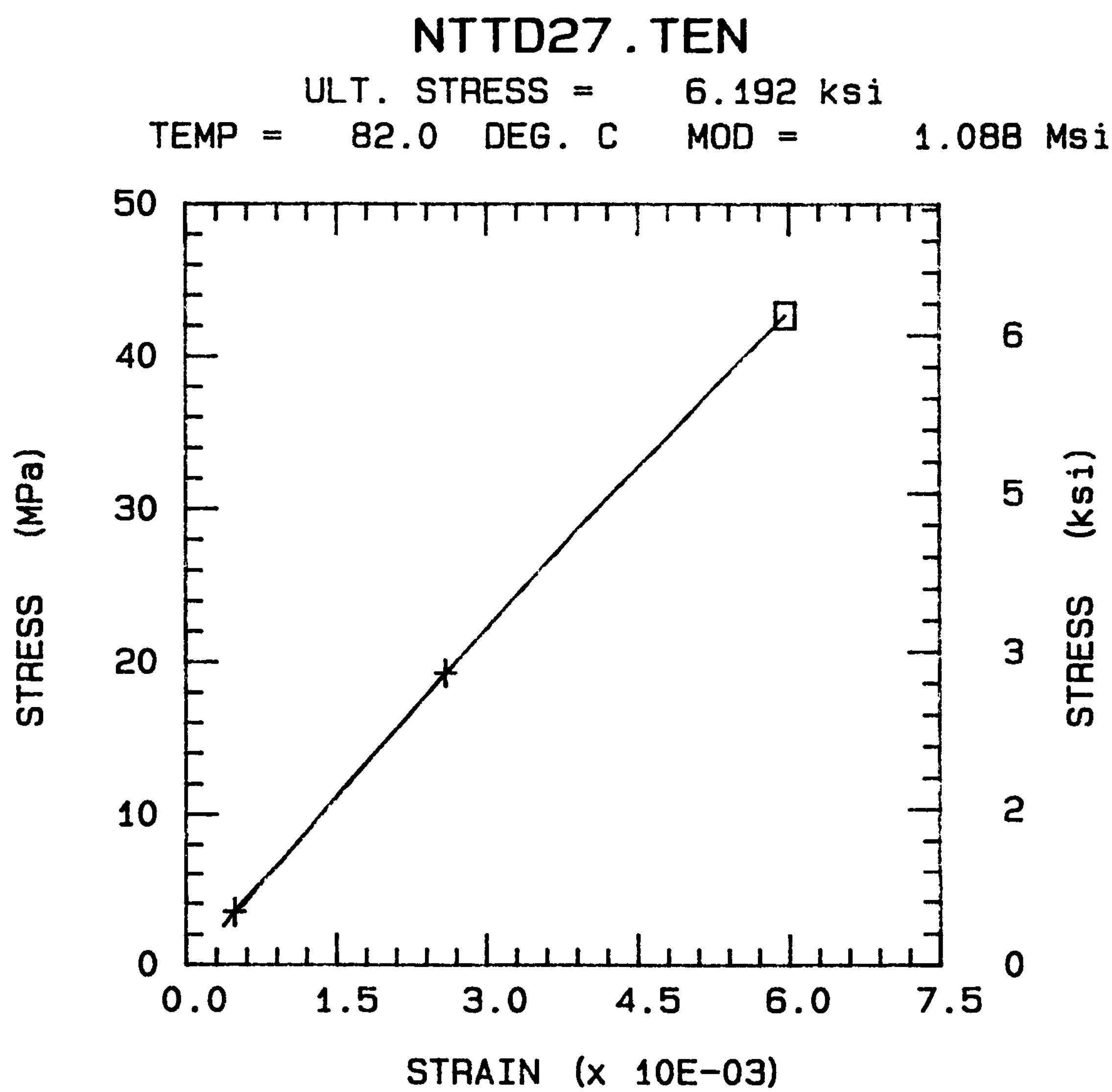
NTTD27.TEN
ULT. STRESS = 6.192 ksi
TEMP = 82.0 DEG. C MOD = 1.088 Msi
STRESS (MPa)
STRESS (ksi)
STRAIN (x 10E-03)
0
10
20
30
40
50
0
2
3
5
6
0.0
1.5
3.0
4.5
6.0
7.5

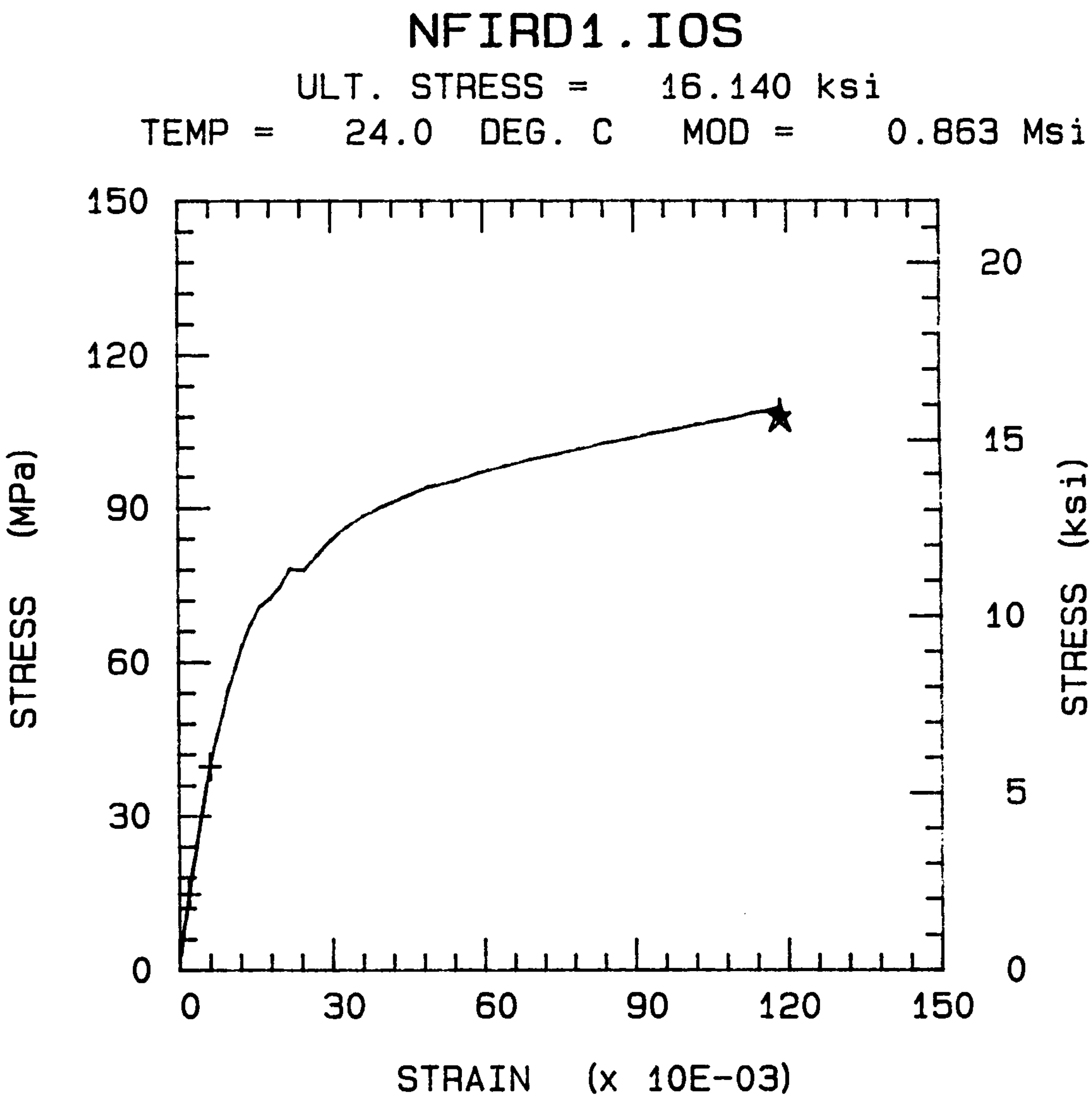
NFIRD1.IOS
ULT. STRESS = 16.140 ksi
TEMP = 24.0 DEG. C MOD = 0.863 Msi
STRESS (MPa)
STRESS (ksi)
STRAIN (x 10E-03)
0
30
60
90
120
150
0
5
10
15
20

NFIRD1.IOS

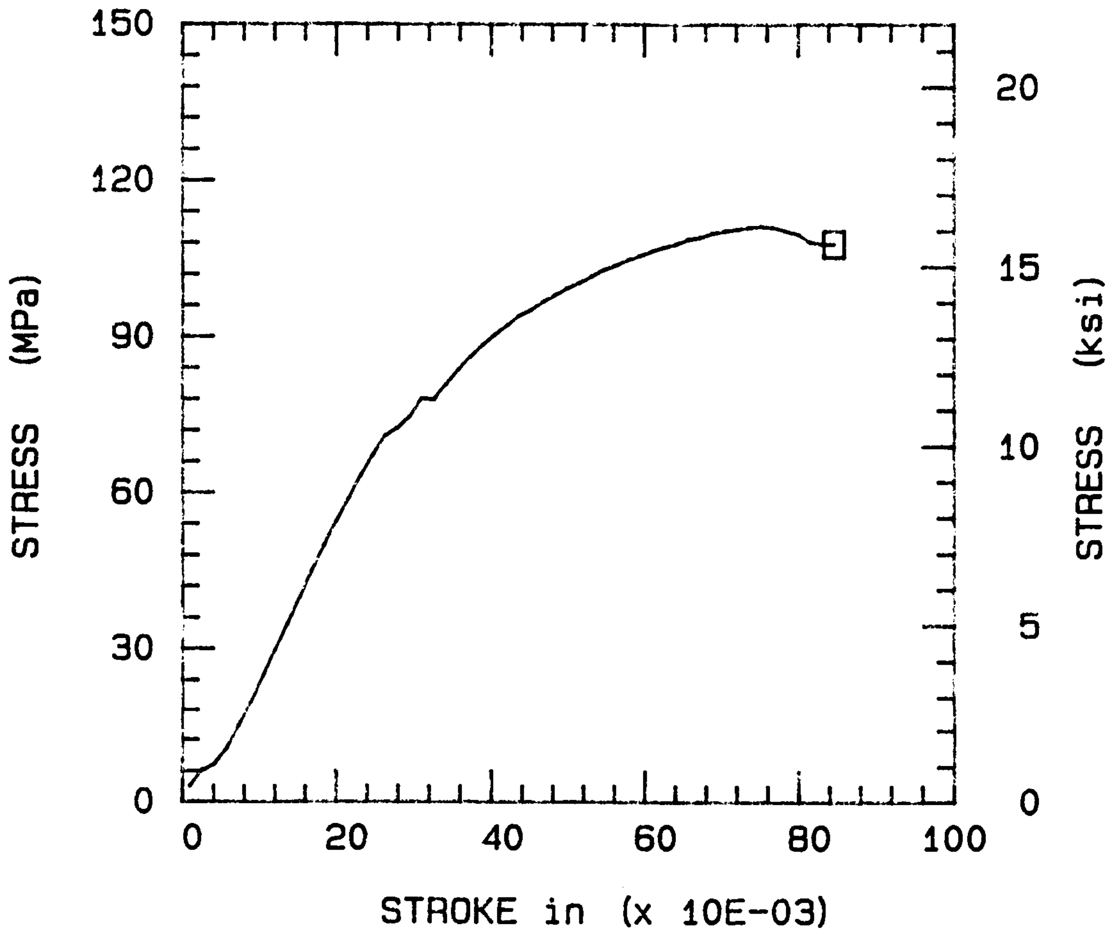

150
120
90
60
30
0
20
15
10
5
0
0
20
40
60
80
100
STRESS (MPa)
STRESS (ksi)
STROKE in (x 10E-03)

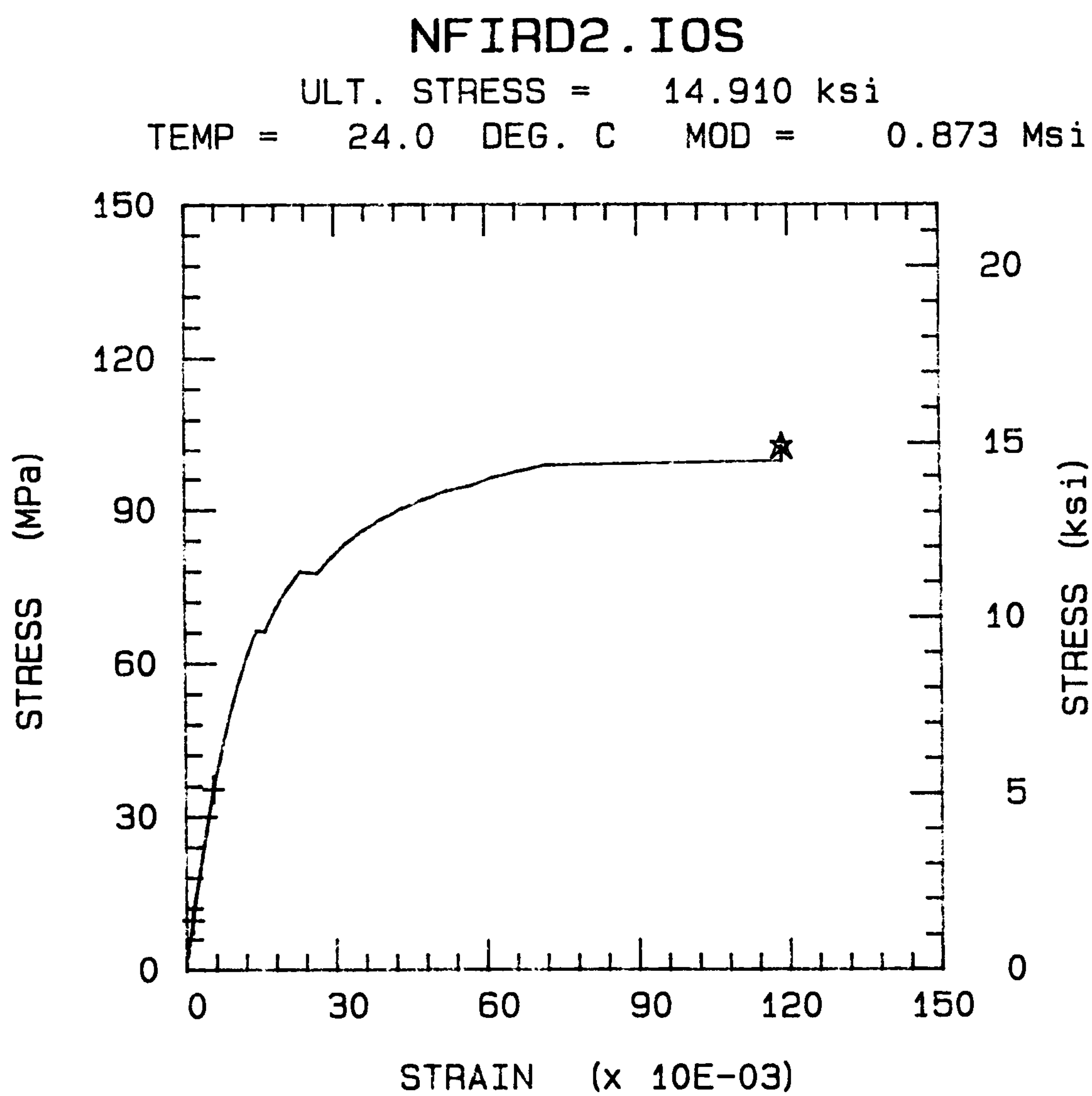
NFIRD2.IOS
ULT. STRESS = 14.910 ksi
TEMP = 24.0 DEG. C MOD = 0.873 Msi
150
120
90
60
30
0
20
15
10
5
0
0
30
60
90
120
150
STRESS (MPa)
STRESS (ksi)
STRAIN (x 10E-03)

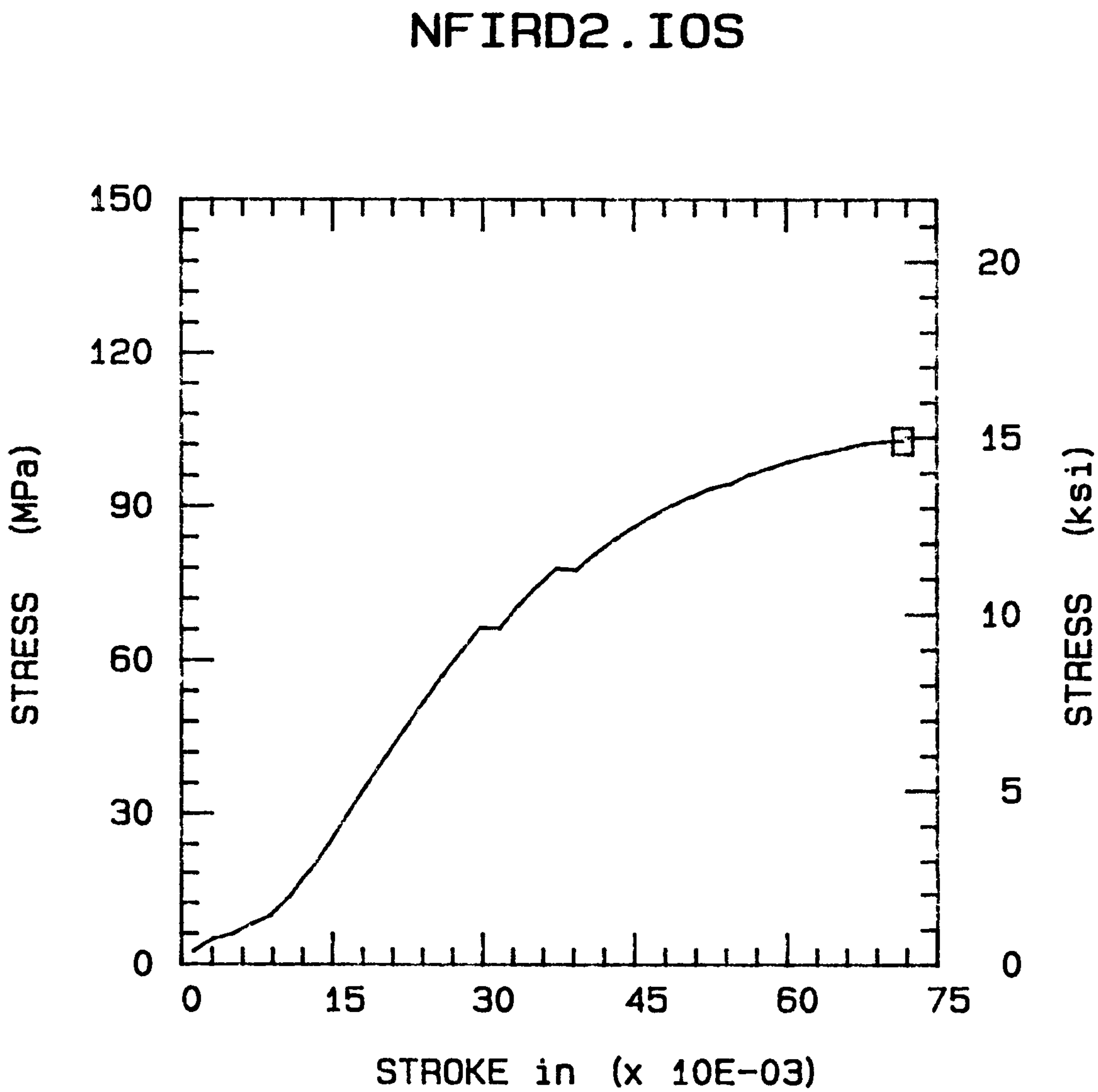
NFIRD2.IOS
150
120
90
60
30
0
STRESS (MPa)
20
15
10
5
0
STRESS (ksi)
0
15
30
45
60
75
STROKE in (x 10E-03)

NFIRD3.IOS

ULT. STRESS = 15.770 ksi

TEMP = 24.0 DEG. C MOD = 0.828 Msi

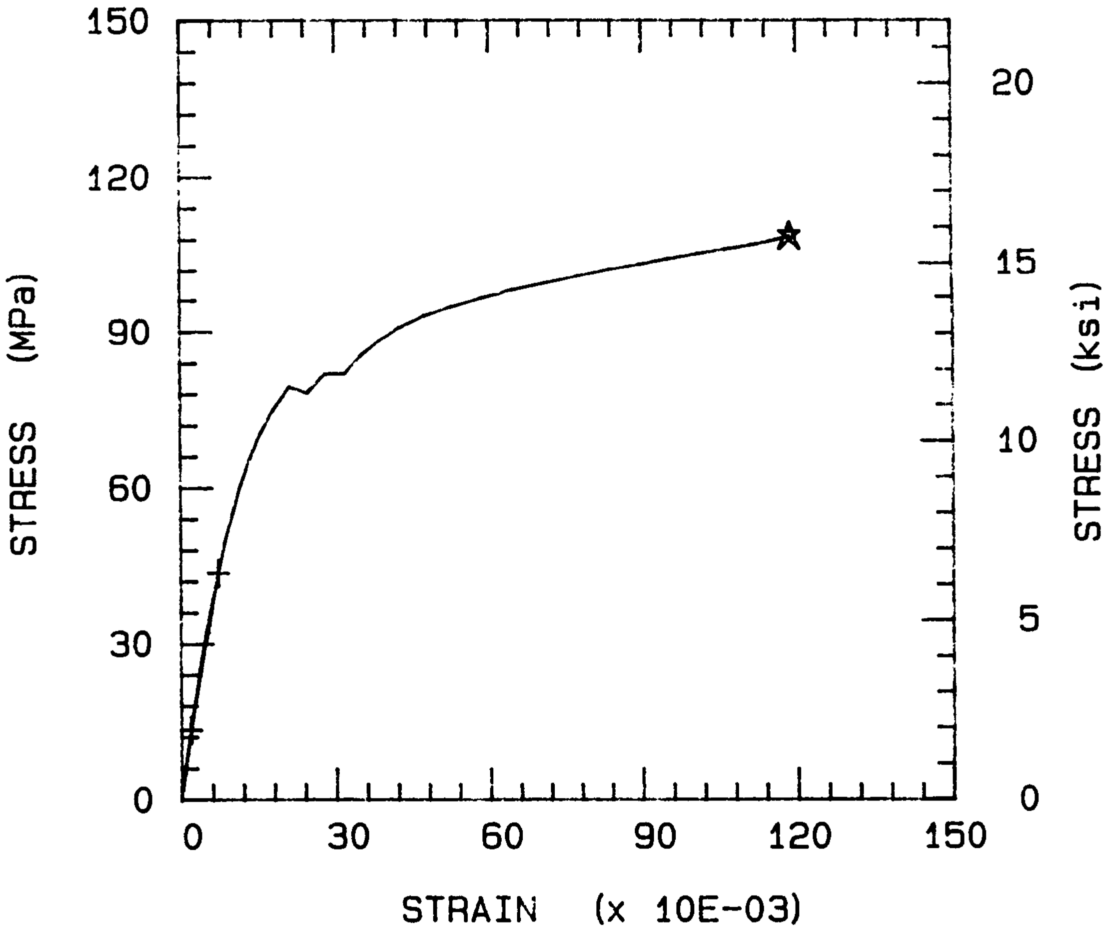

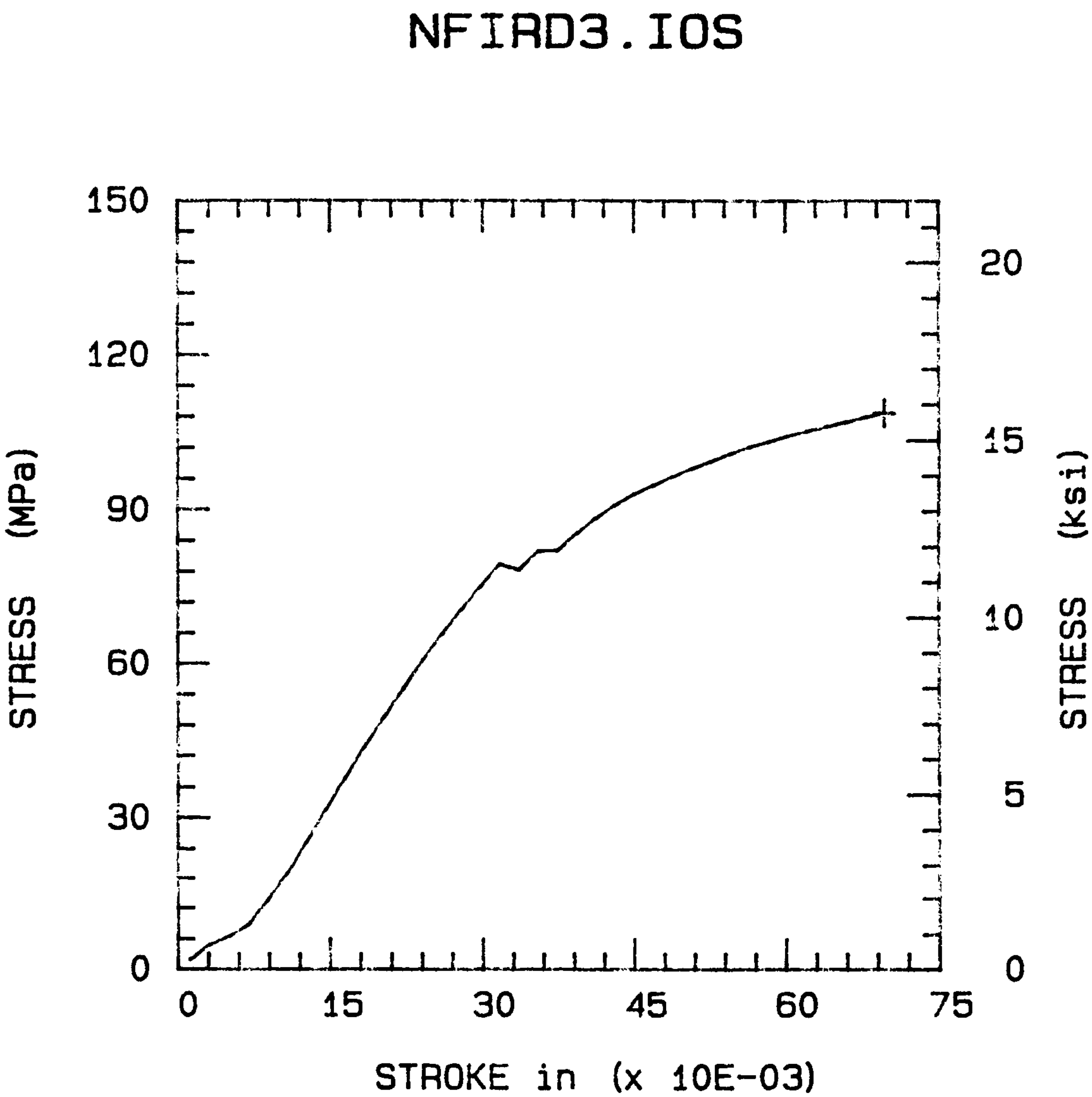
NFIRD3.IOS
150
120
90
60
30
0
STRESS (MPa)
20
15
10
5
0
STRESS (ksi)
0
15
30
45
60
75
STROKE in (x 10E-03)

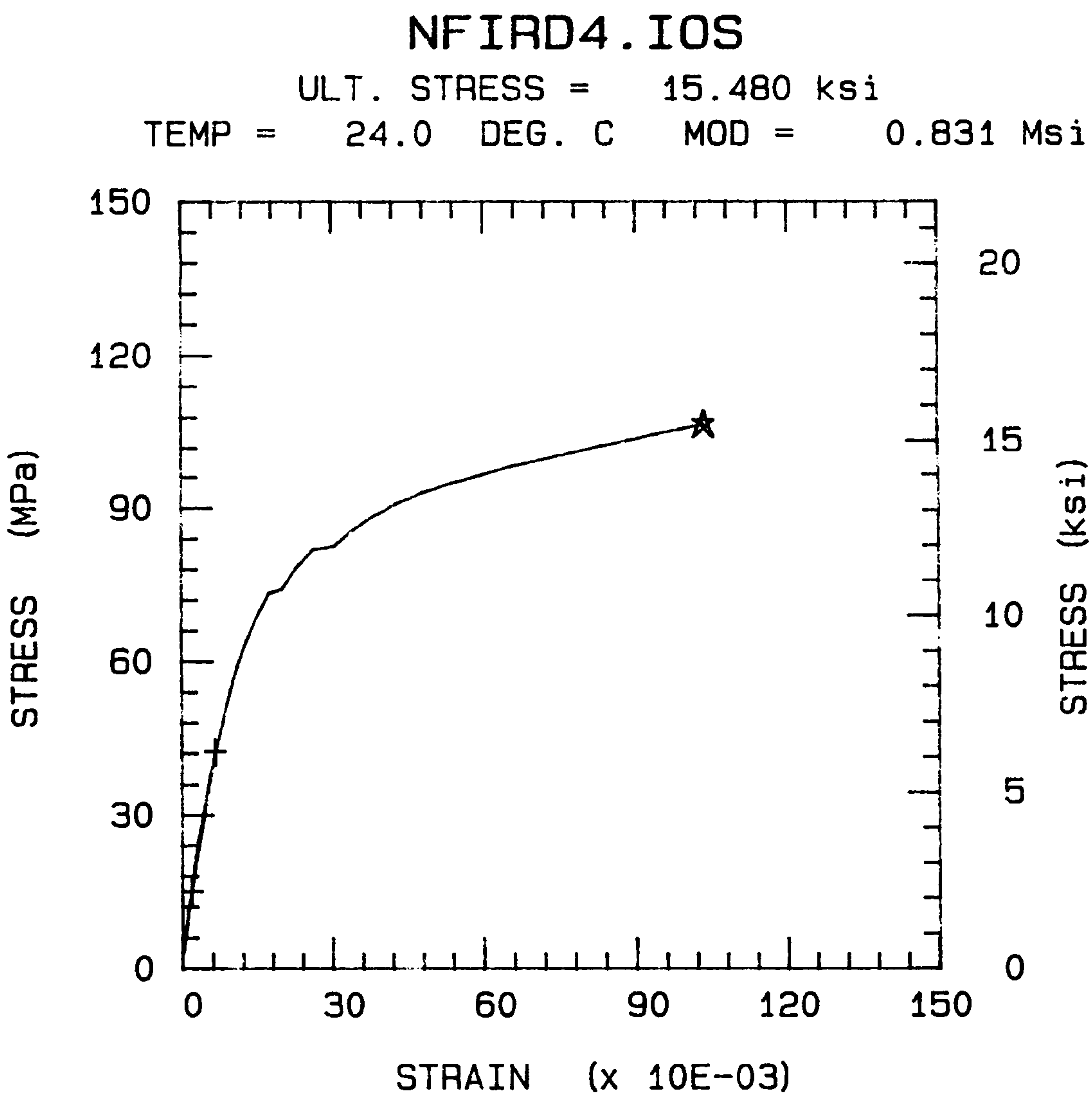
NFIRD4.IOS
ULT. STRESS = 15.480 ksi
TEMP = 24.0 DEG. C MOD = 0.831 Msi
STRESS (MPa)
STRESS (ksi)
STRAIN (x 10E-03)
0
30
60
90
120
150
0
5
10
15
20

NFIRD4.IOS

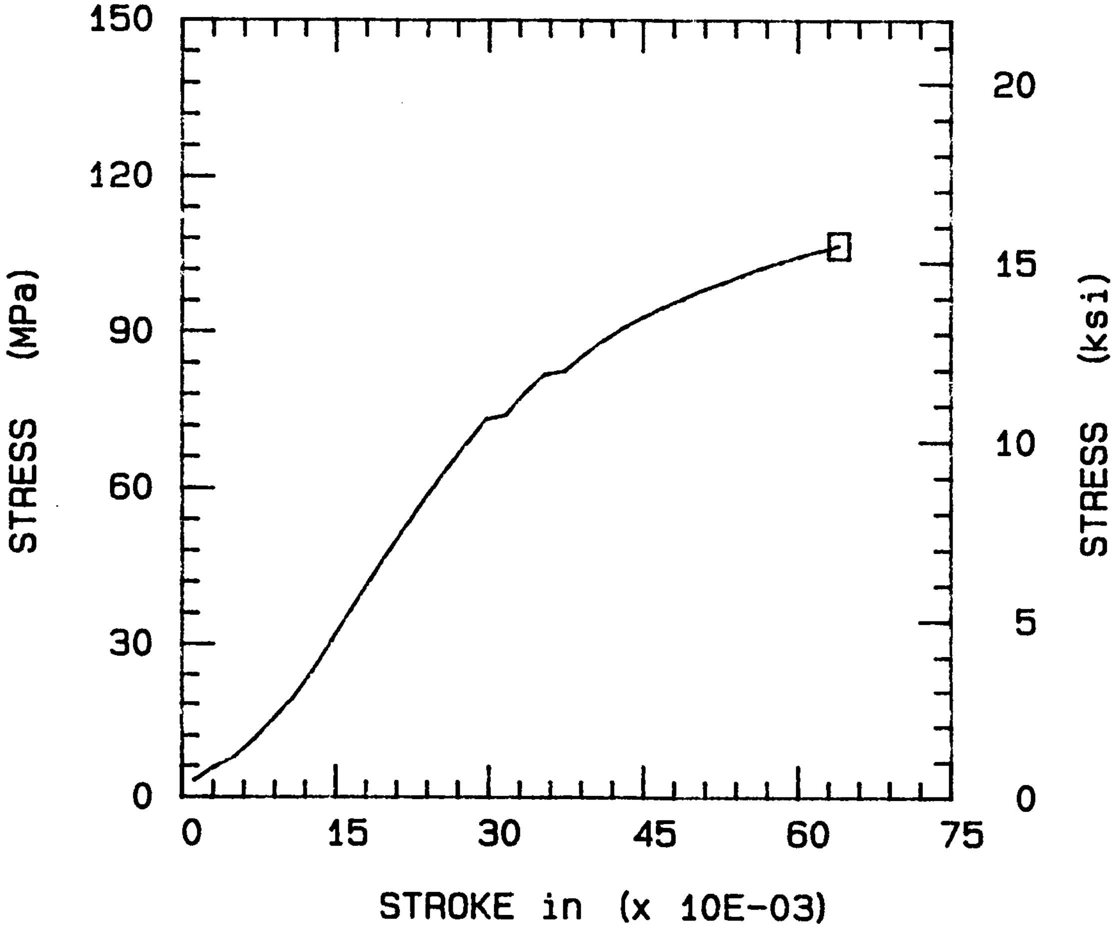

150
120
90
60
30
0
STRESS (MPa)
20
15
10
5
0
STRESS (ksi)
0
15
30
45
60
75
STROKE in (x 10E-03)

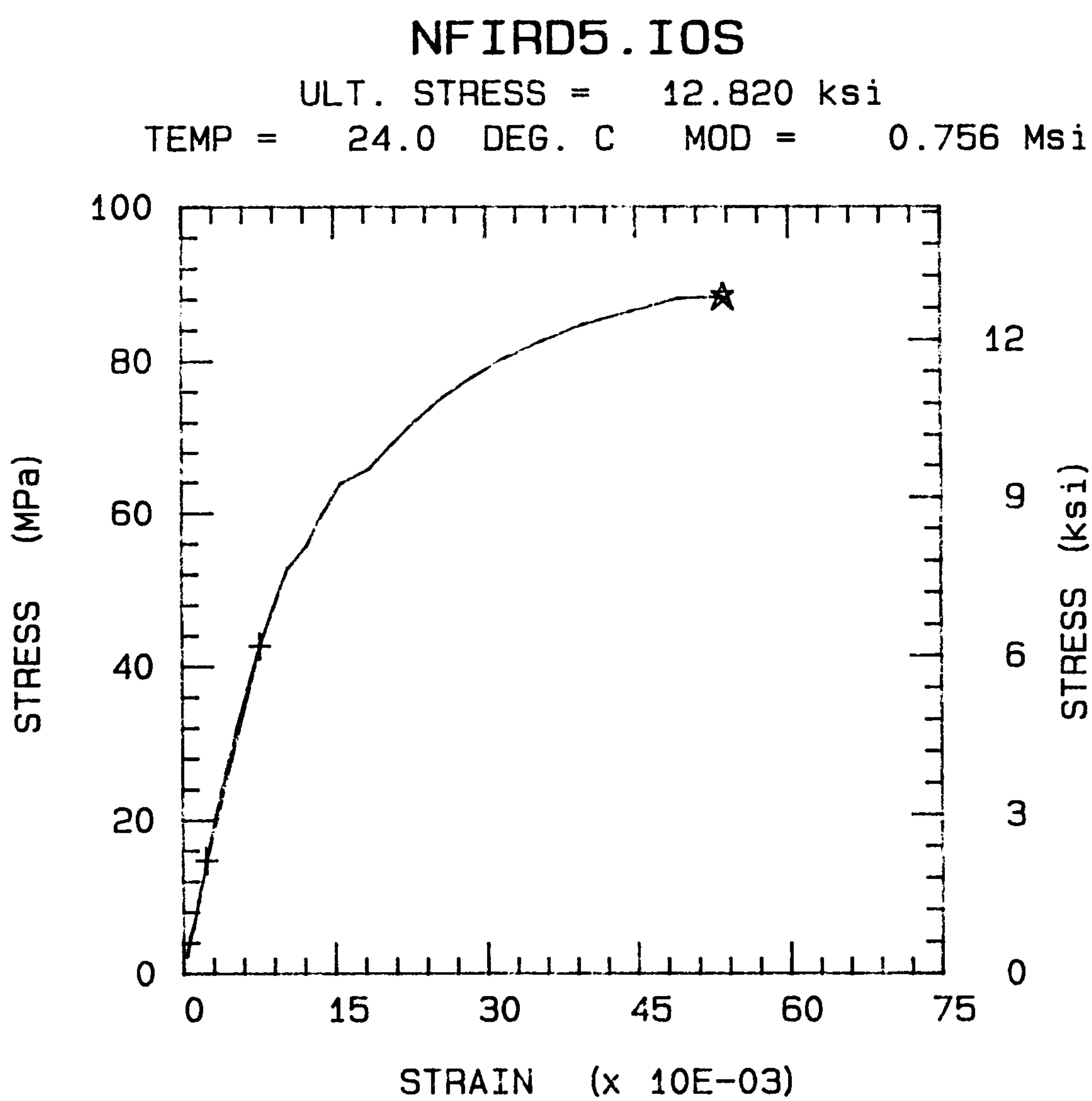

NFIRD5.IOS
ULT. STRESS = 12.820 ksi
TEMP = 24.0 DEG. C MOD = 0.756 Msi
100
80
60
40
20
0
STRESS (MPa)
12
9
6
3
0
STRESS (ksi)
0
15
30
45
60
75
STRAIN (x 10E-03)

NFIRD5.IOS

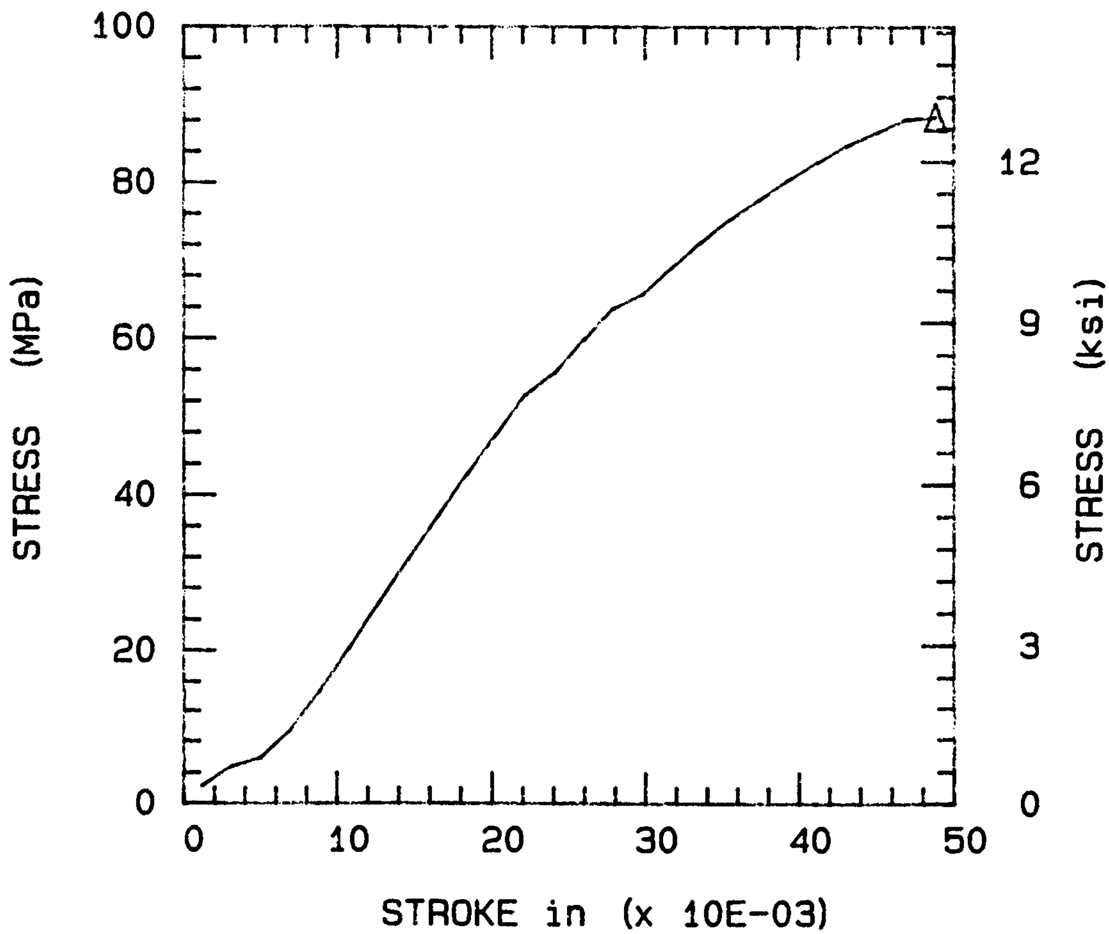

100
80
60
40
20
0
STRESS (MPa)
12
9
6
3
0
STRESS (ksi)
0
10
20
30
40
50
STROKE in (x 10E-03)

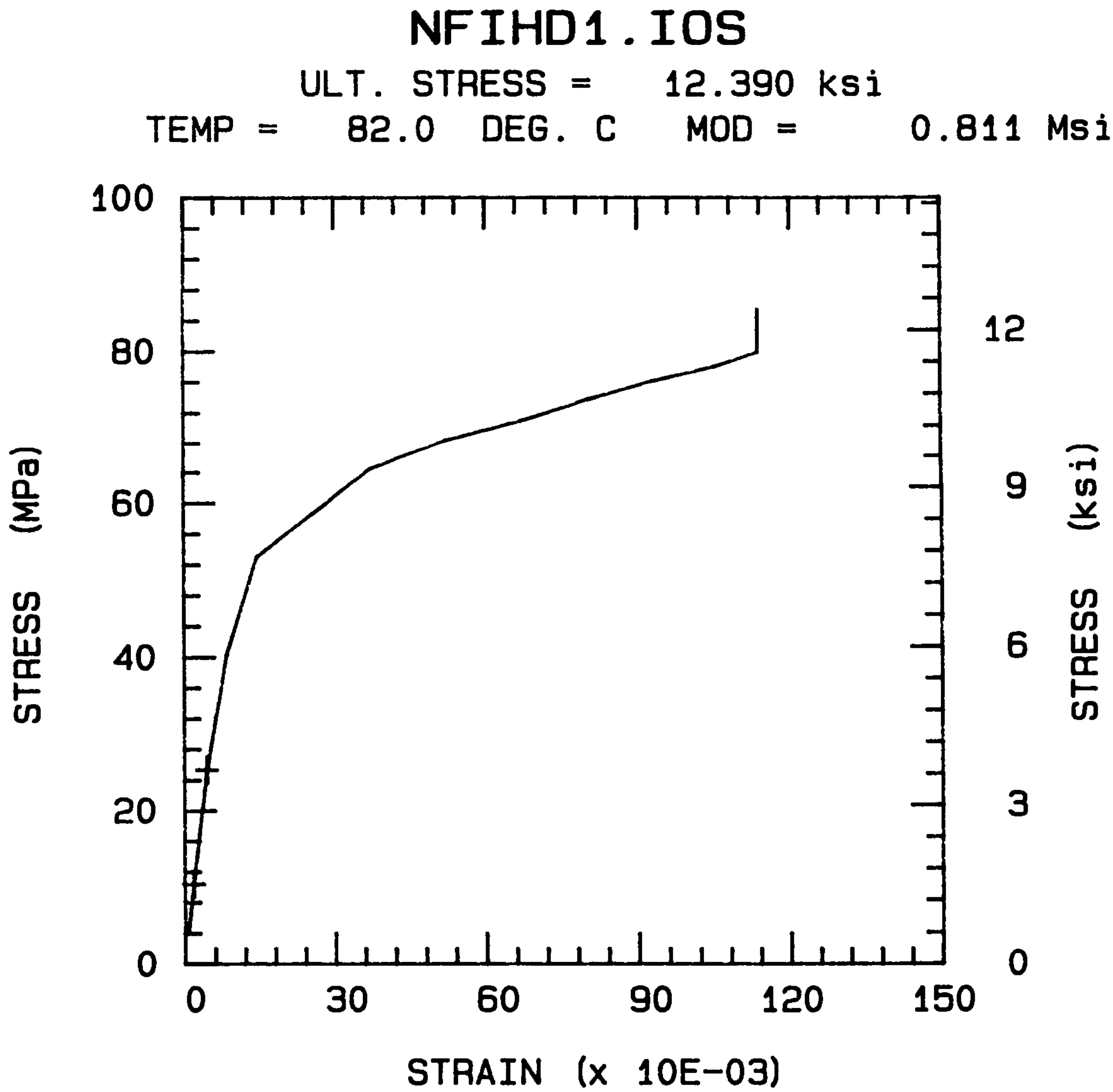
NFIHD1.IOS
ULT. STRESS = 12.390 ksi
TEMP = 82.0 DEG. C MOD = 0.811 Msi
100
80
60
40
20
0
STRESS (MPa)
12
9
6
3
0
STRESS (ksi)
0
30
60
90
120
150
STRAIN (x 10E-03)

NFIHD1.IOS

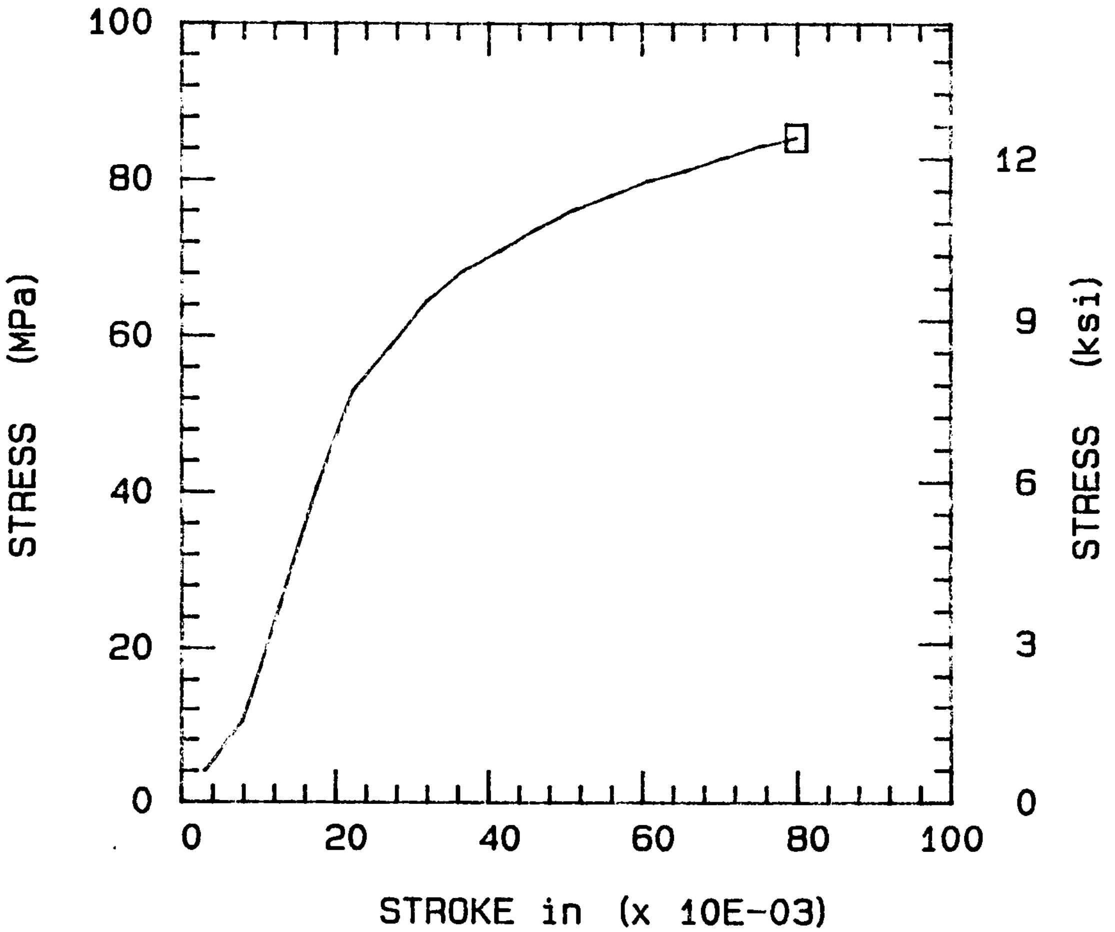

100
80
60
40
20
0
STRESS (MPa)
12
9
6
3
0
STRESS (ksi)
0
20
40
60
80
100
STROKE in (x 10E-03)

NFIHD2.IOS

ULT. STRESS = 10.110 ksi

TEMP = 82.0 DEG. C MOD = 0.772 Msi

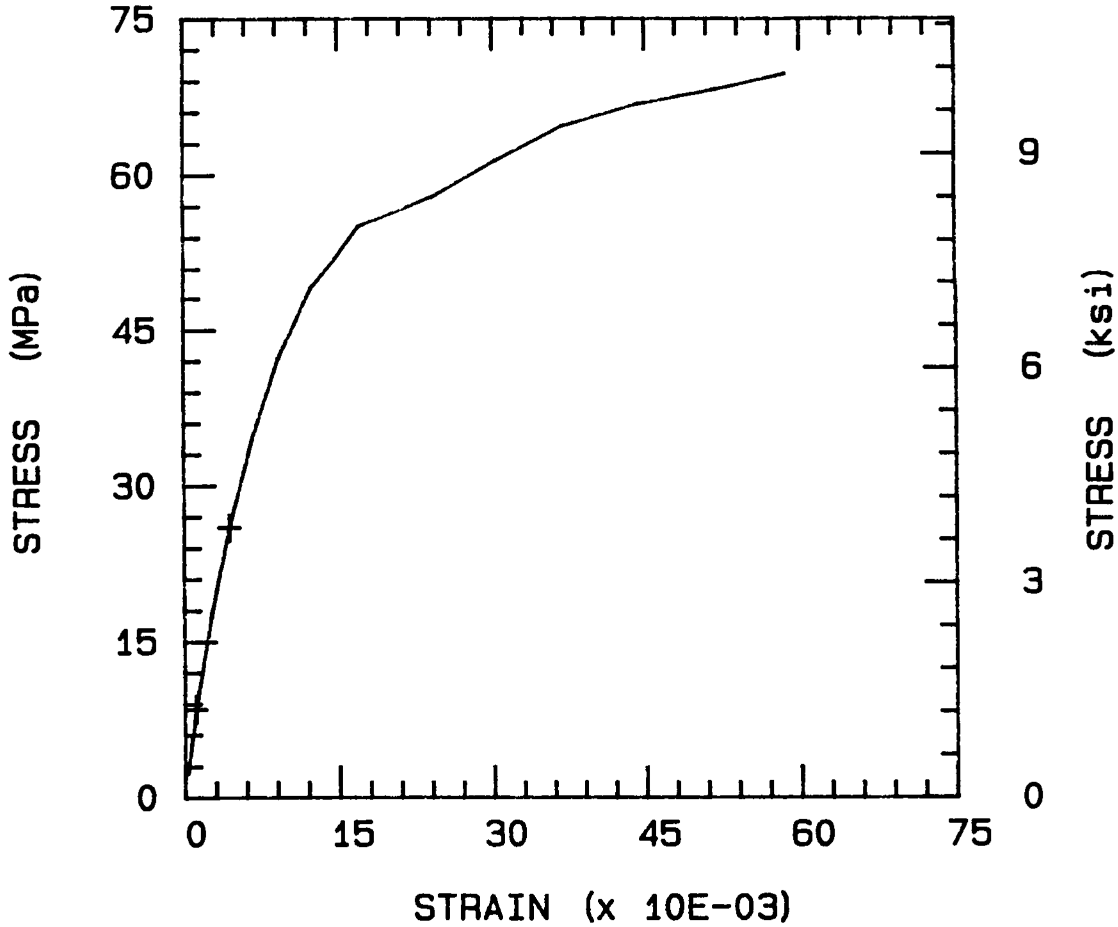

NFIHD2.IOS

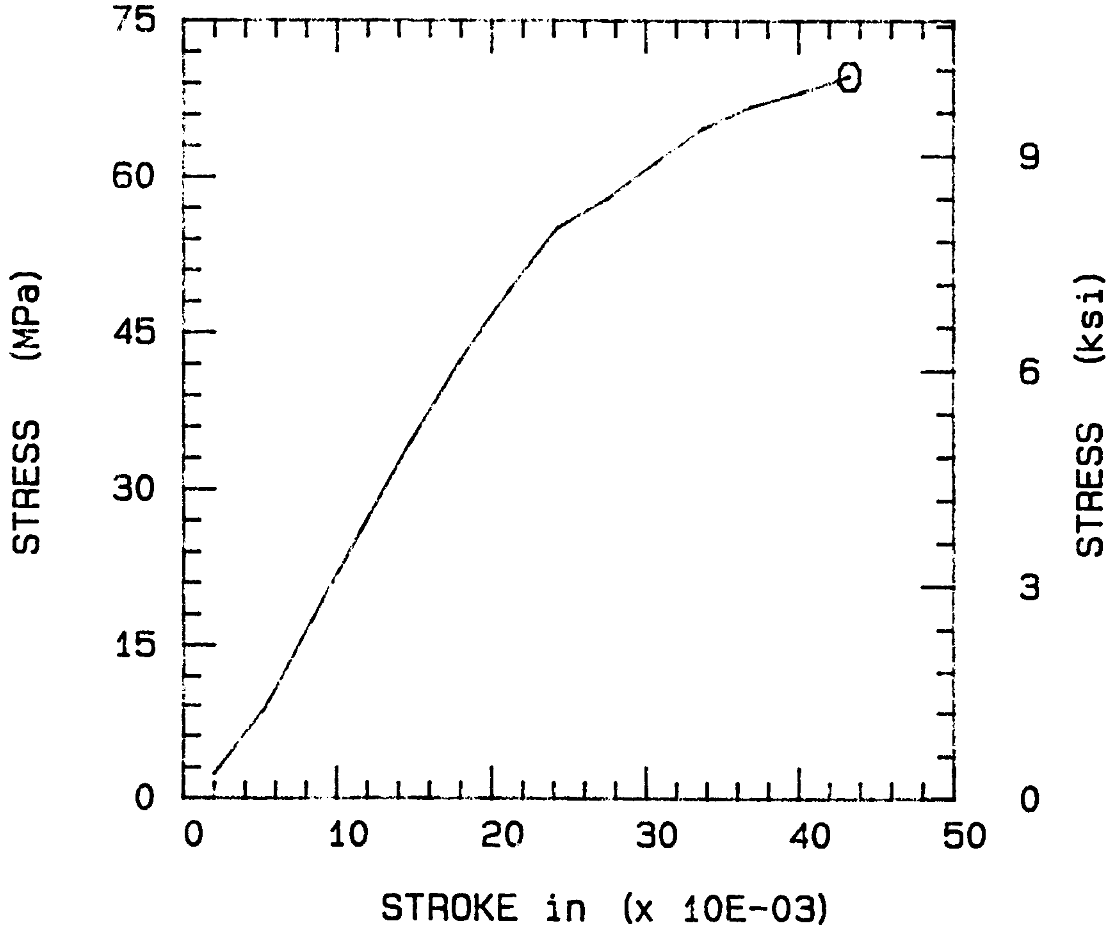

75
60
45
30
15
0
STRESS (MPa)
9
6
3
0
STRESS (ksi)
0
10
20
30
40
50
STROKE in (x 10E-03)

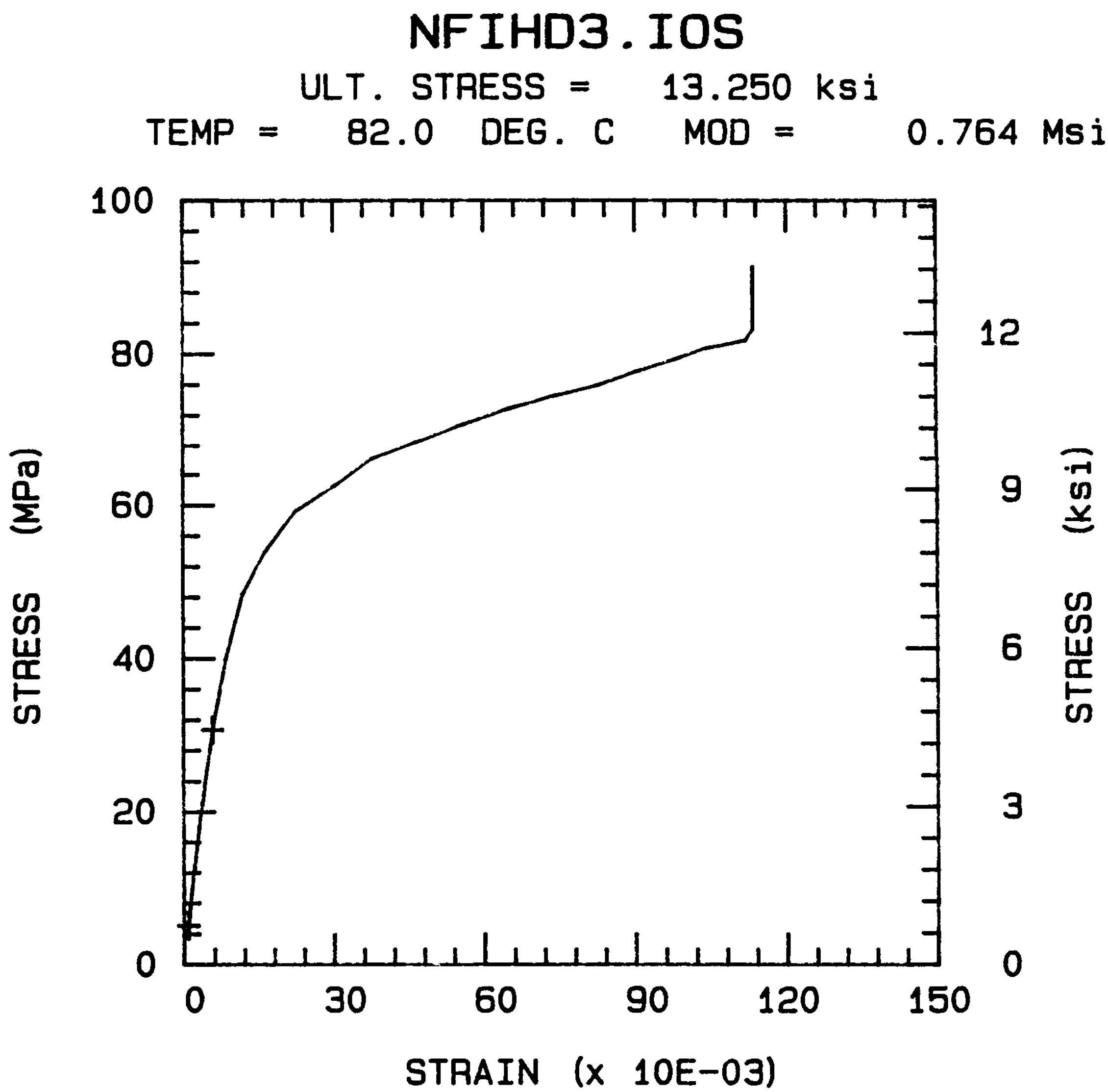

NFIHD3.IOS
ULT. STRESS = 13.250 ksi
TEMP = 82.0 DEG. C MOD = 0.764 Msi
STRESS (MPa)
100
80
60
40
20
0
STRESS (ksi)
12
9
6
3
0
0
30
60
90
120
150
STRAIN (x 10E-03)

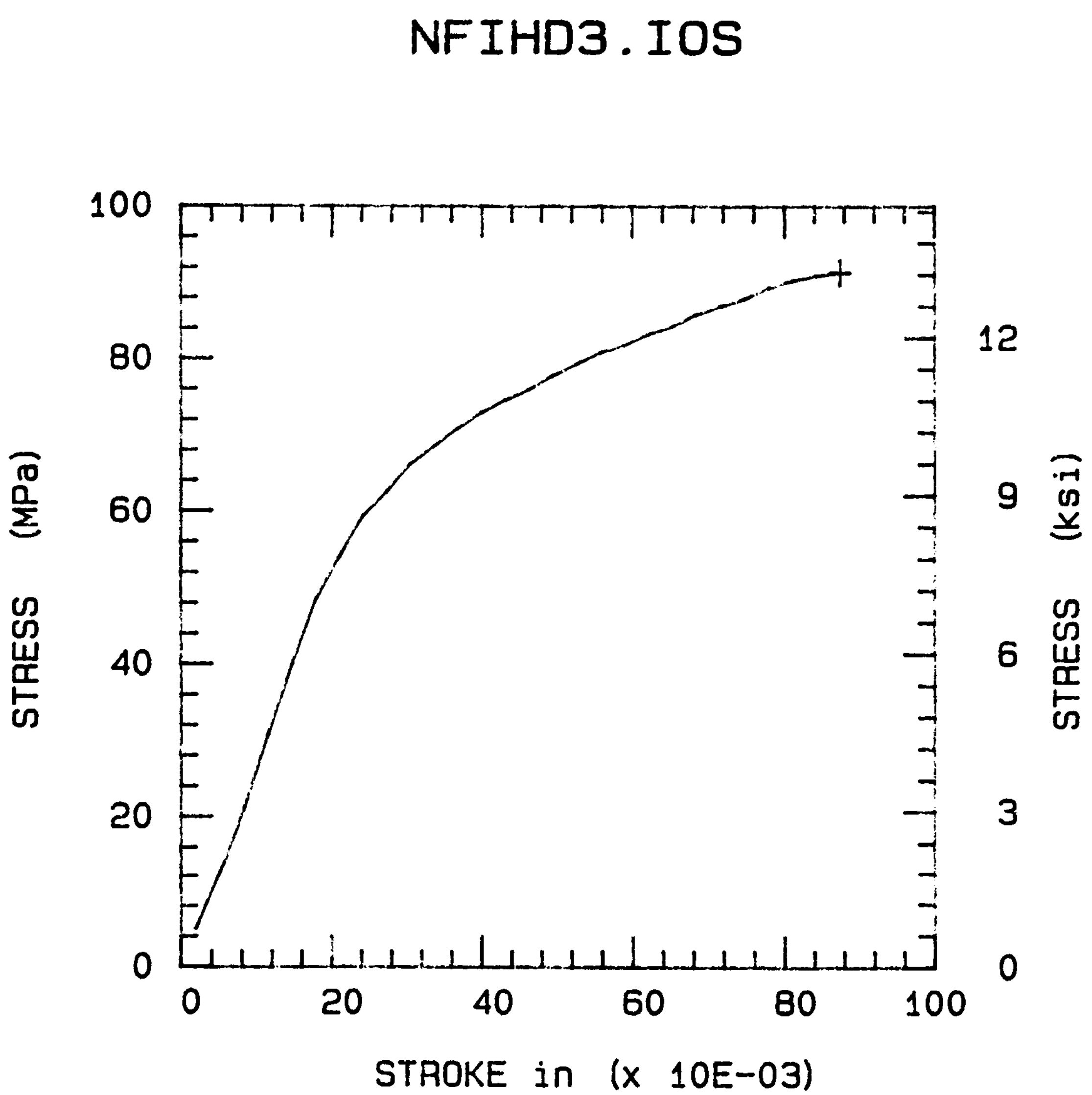
NFIHD3.IOS
STRESS (MPa)
STRESS (ksi)
STROKE in (x 10E-03)
0
20
40
60
80
100
0
3
6
9
12

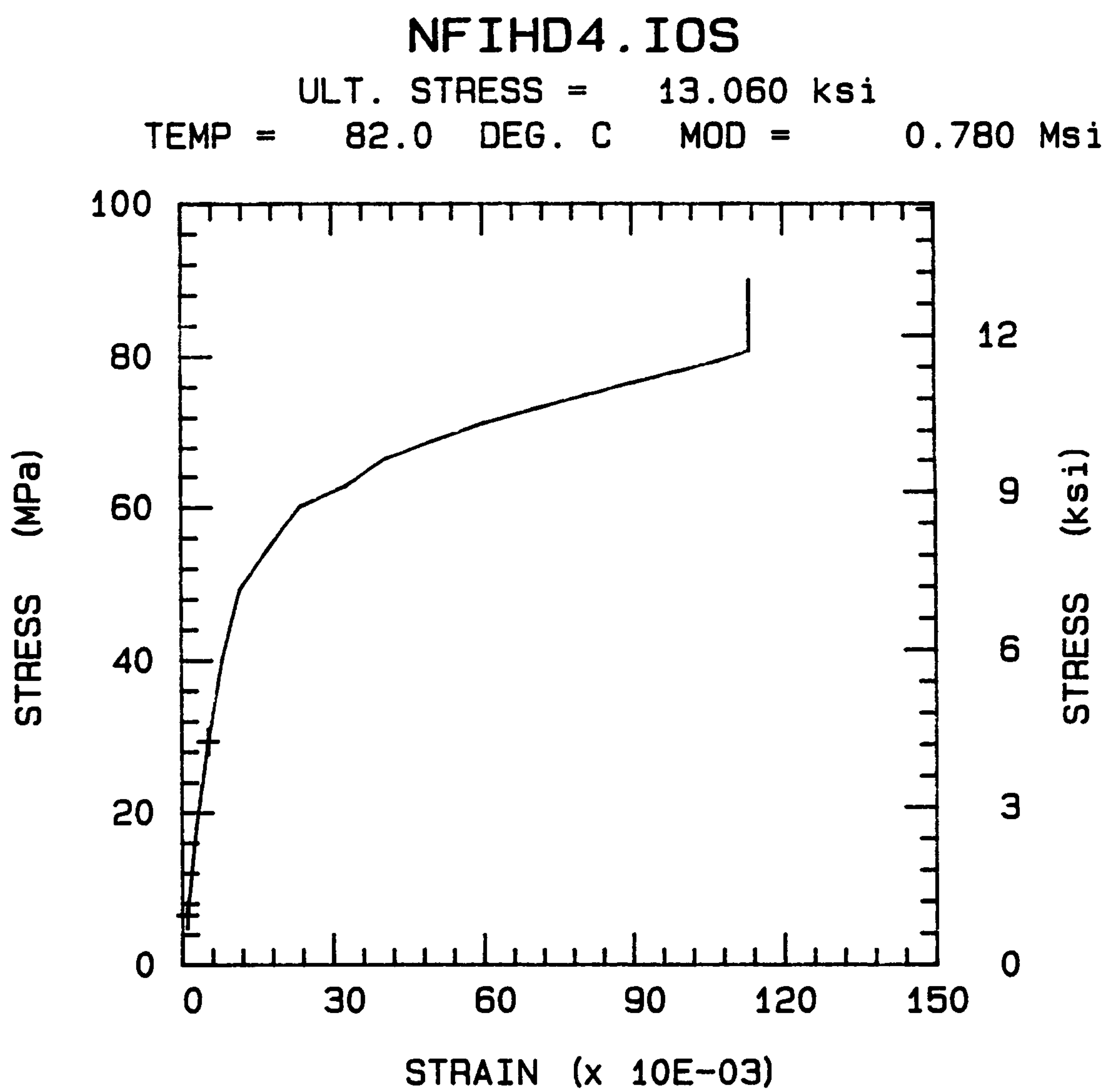
NFIHD4.IOS
ULT. STRESS = 13.060 ksi
TEMP = 82.0 DEG. C MOD = 0.780 Msi
STRESS (MPa)
STRESS (ksi)
STRAIN (x 10E-03)
100
80
60
40
20
0
12
9
6
3
0
0
30
60
90
120
150

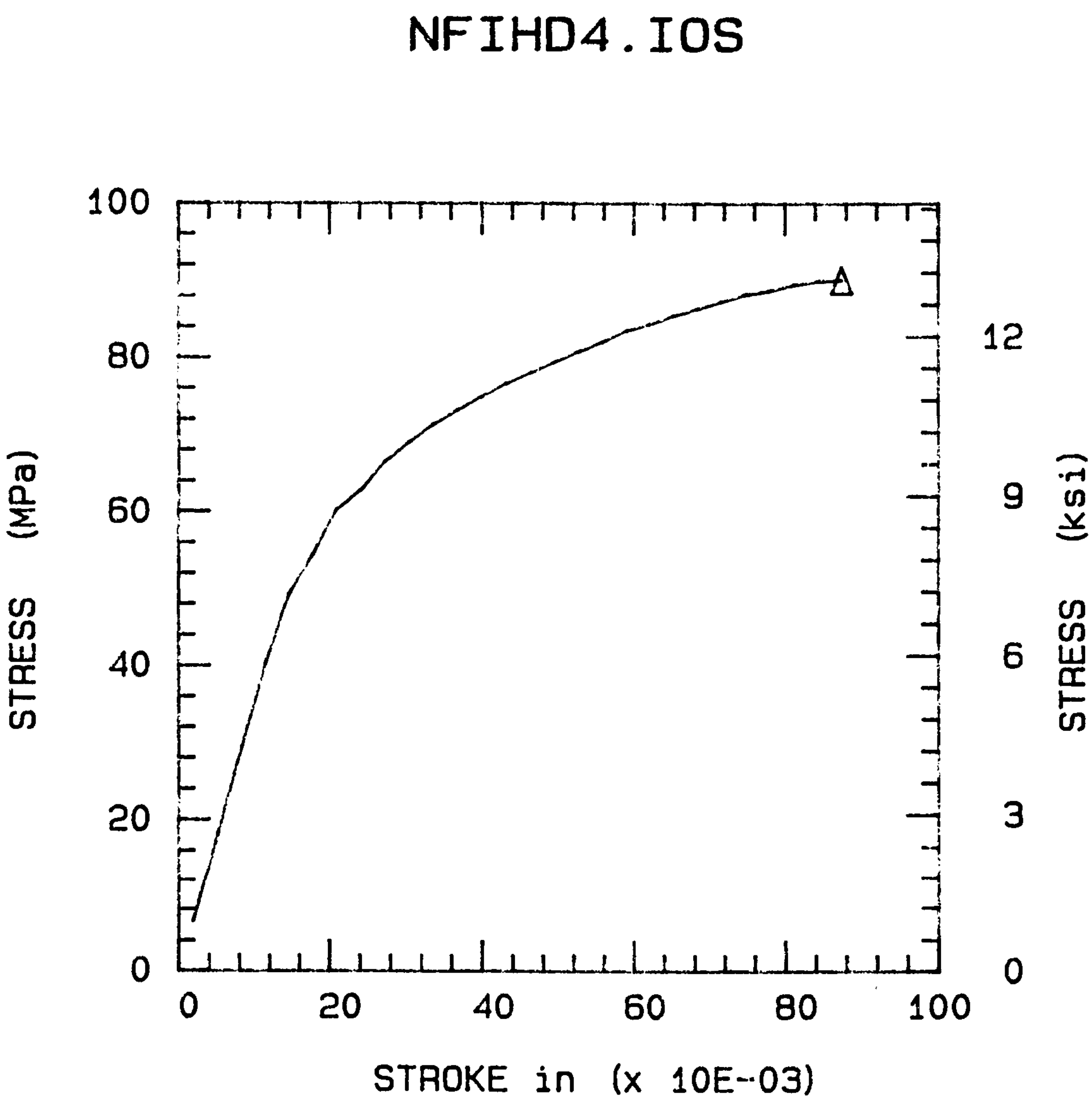
NFIHD4.IOS
STRESS (MPa)
STRESS (ksi)
STROKE in (x 10E-03)
0
20
40
60
80
100
3
6
9
12

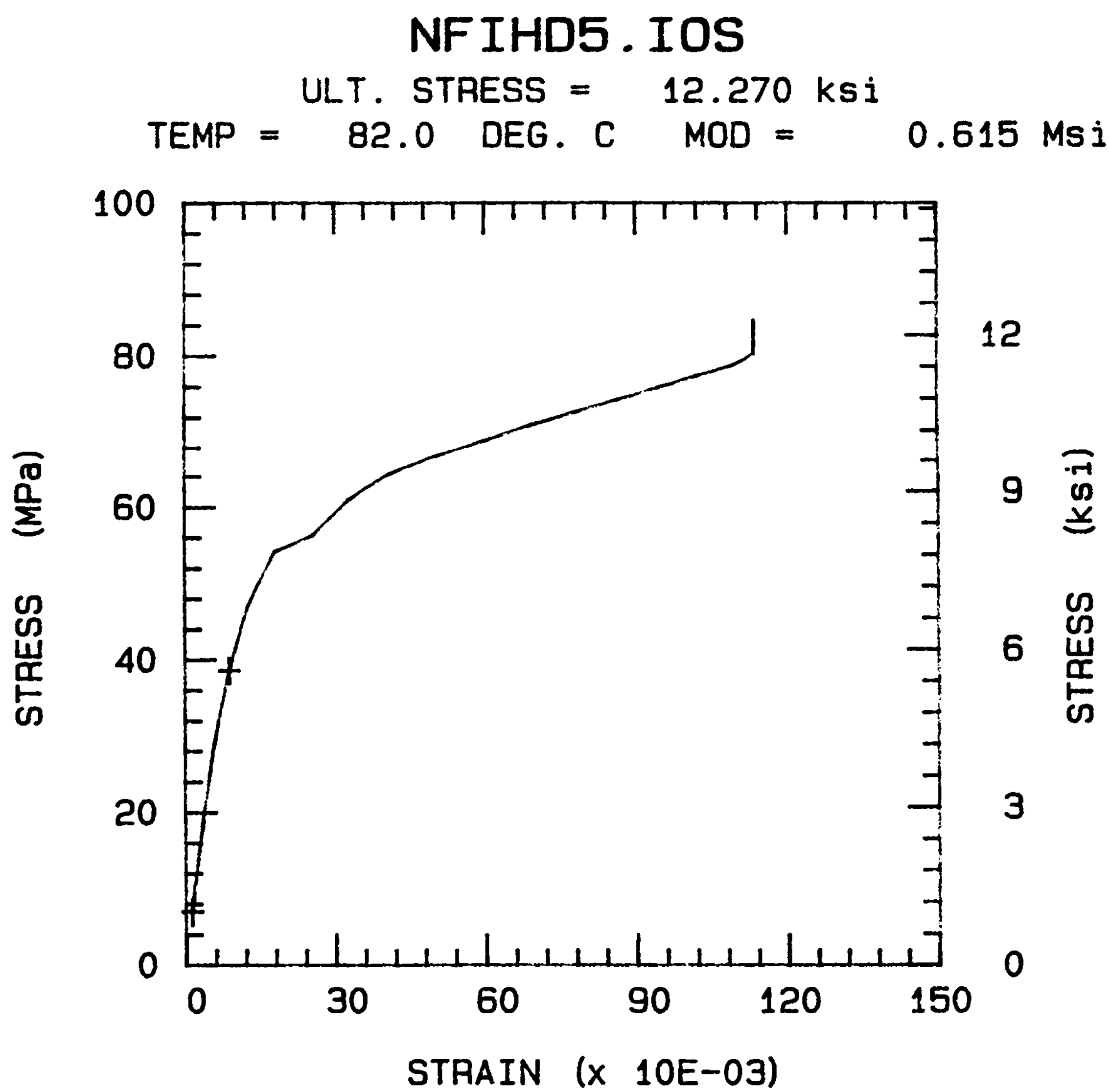

NFIHD5.IOS
ULT. STRESS = 12.270 ksi
TEMP = 82.0 DEG. C MOD = 0.615 Msi
STRESS (MPa)
STRESS (ksi)
STRAIN (x 10E-03)
100
80
60
40
20
0
12
9
6
3
0
0
30
60
90
120
150

NFIHD5.IOS

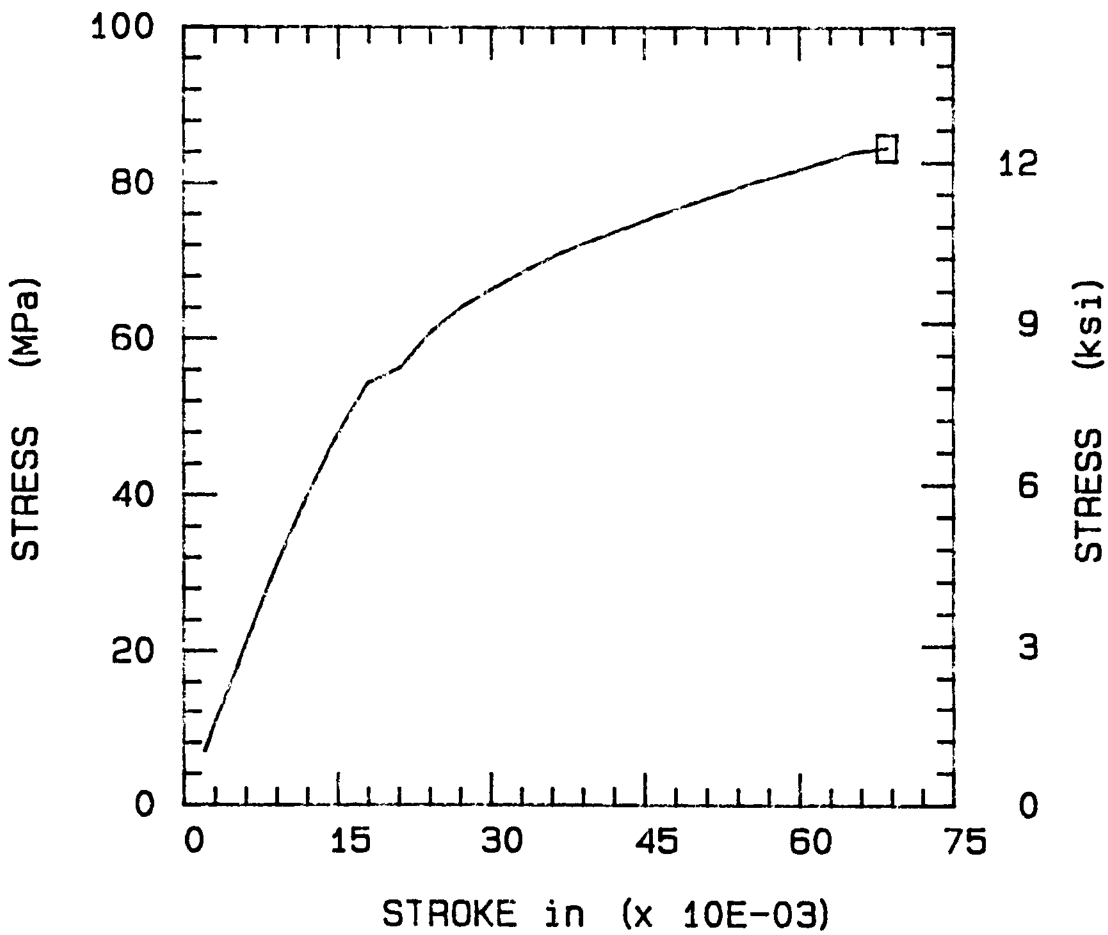

100
80
60
40
20
0
STRESS (MPa)
12
9
6
3
0
STRESS (ksi)
0
15
30
45
60
75
STROKE in (x 10E-03)

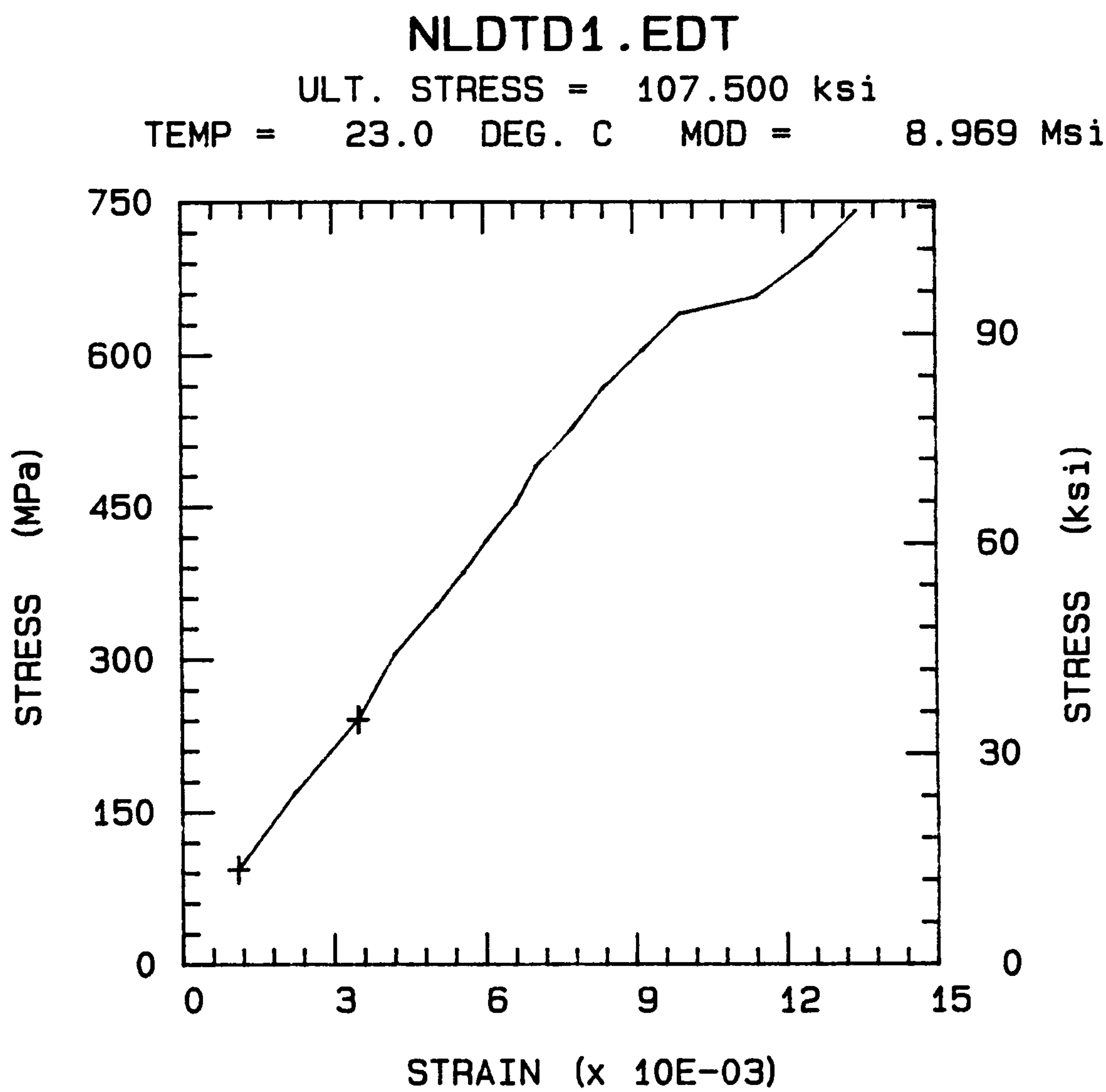

NLDTD1.EDT
ULT. STRESS = 107.500 ksi
TEMP = 23.0 DEG. C MOD = 8.969 Msi
750
600
450
300
150
0
STRESS (MPa)
90
60
30
0
STRESS (ksi)
0
3
6
9
12
15
STRAIN (x 10E-03)

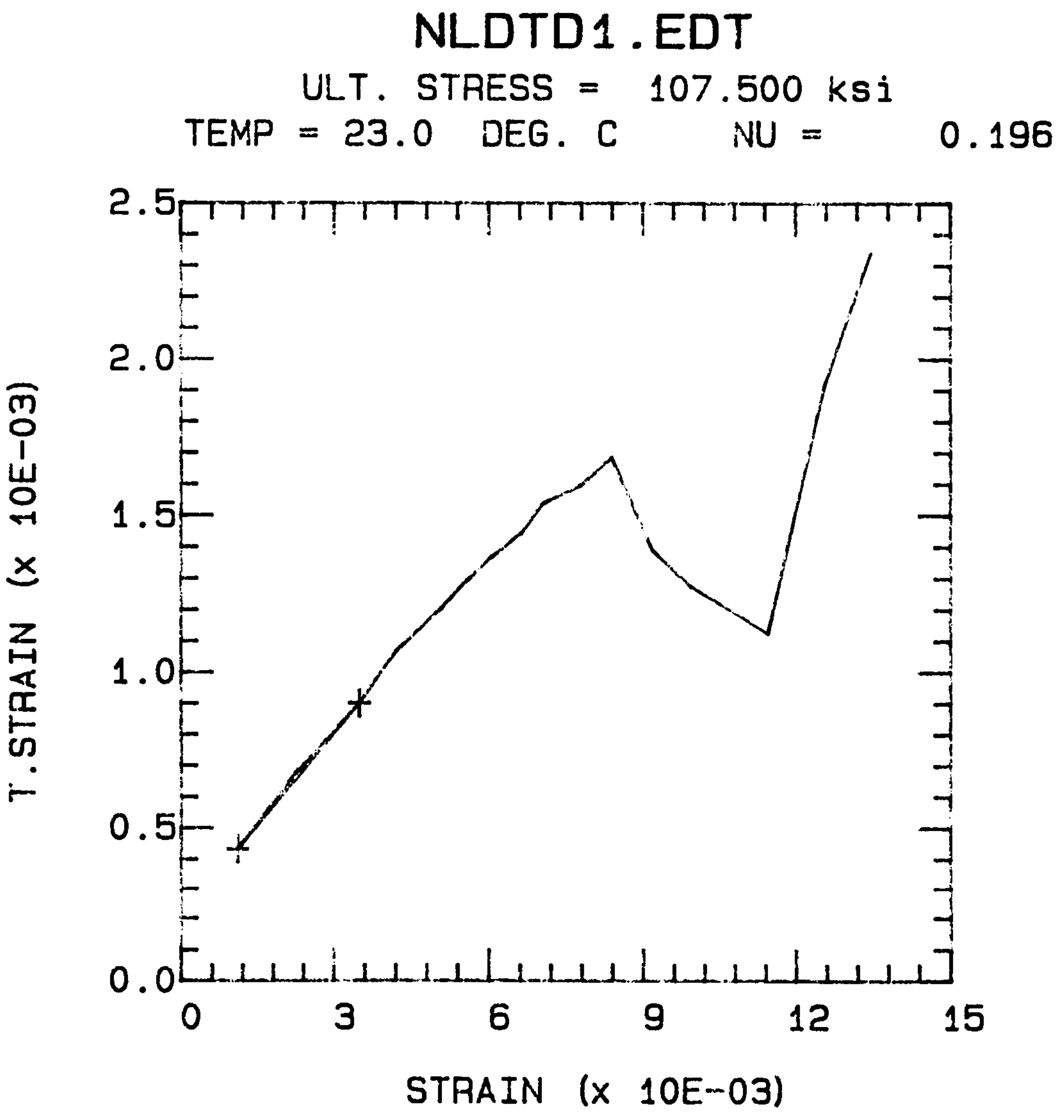

NLDTD1.EDT
ULT. STRESS = 107.500 ksi
TEMP = 23.0 DEG. C NU = 0.196
2.5
2.0
1.5
1.0
0.5
0.0
T.STRAIN (x 10E-03)
0
3
6
9
12
15
STRAIN (x 10E-03)

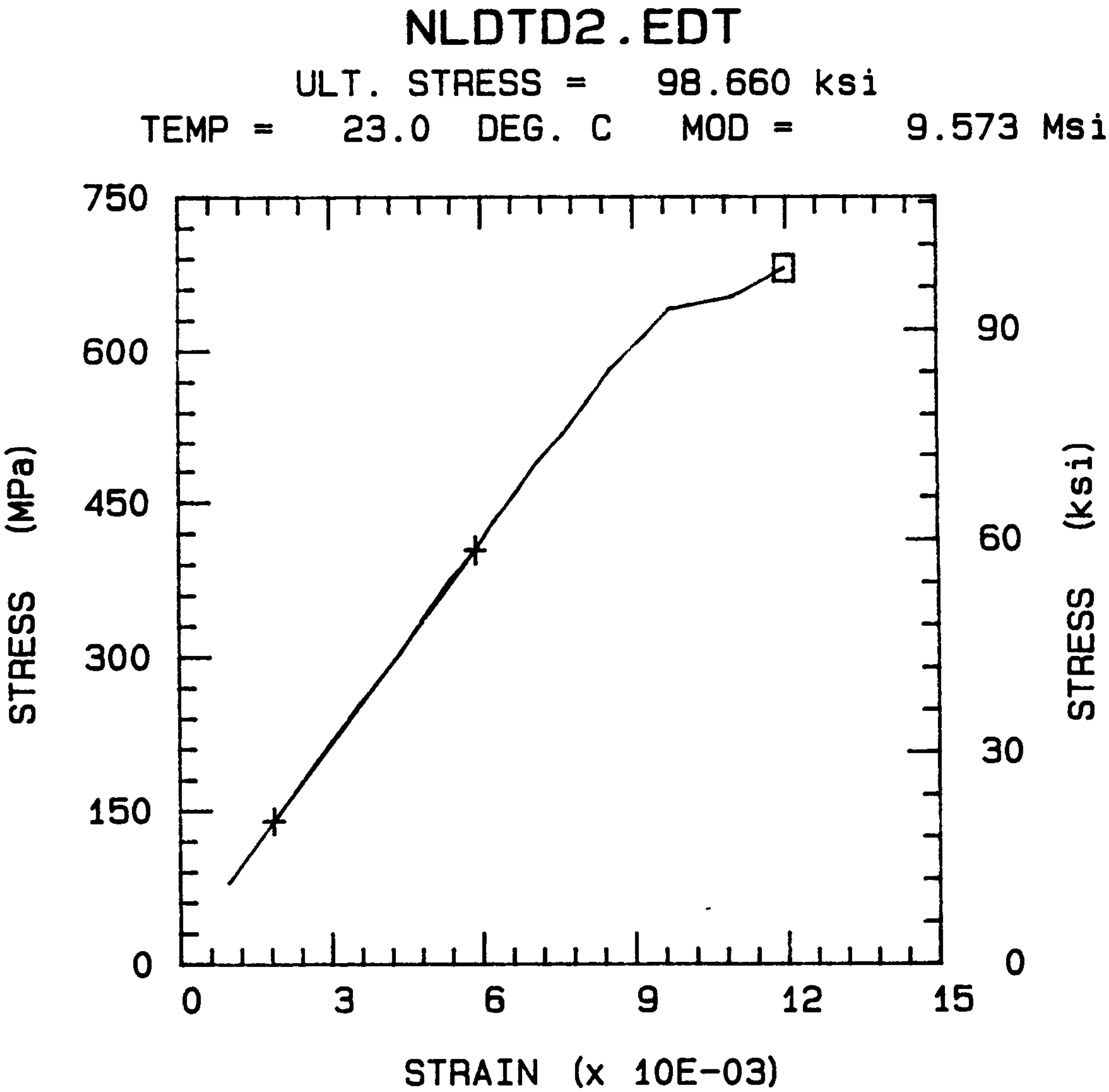
NLDTD2.EDT
ULT. STRESS = 98.660 ksi
TEMP = 23.0 DEG. C MOD = 9.573 Msi
750
600
450
300
150
0
STRESS (MPa)
90
60
30
0
STRESS (ksi)
0
3
6
9
12
15
STRAIN (x 10E-03)

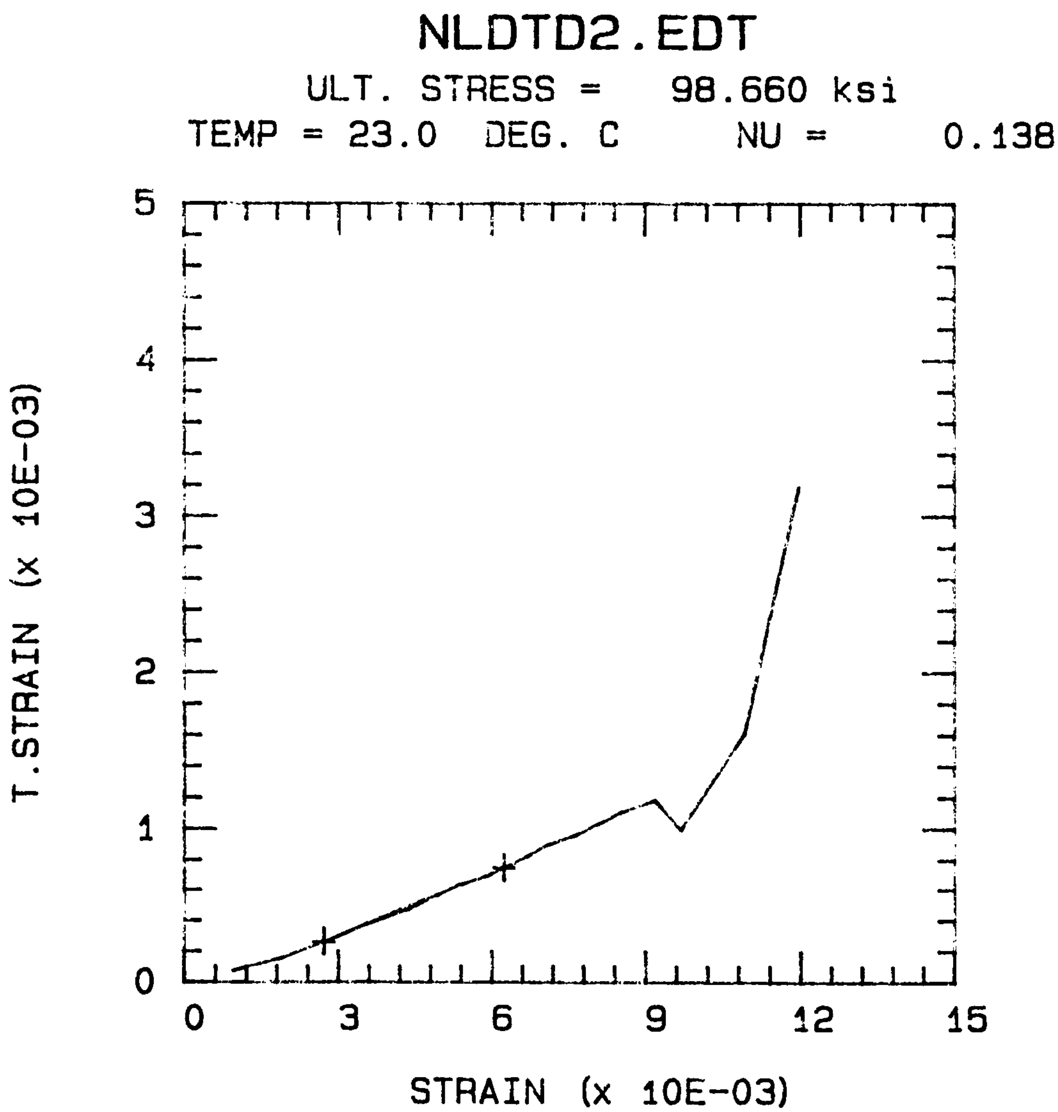
NLDTD2.EDT
ULT. STRESS = 98.660 ksi
TEMP = 23.0 DEG. C NU = 0.138
T.STRAIN (x 10E-03)
0
1
2
3
4
5
0
3
6
9
12
15
STRAIN (x 10E-03)

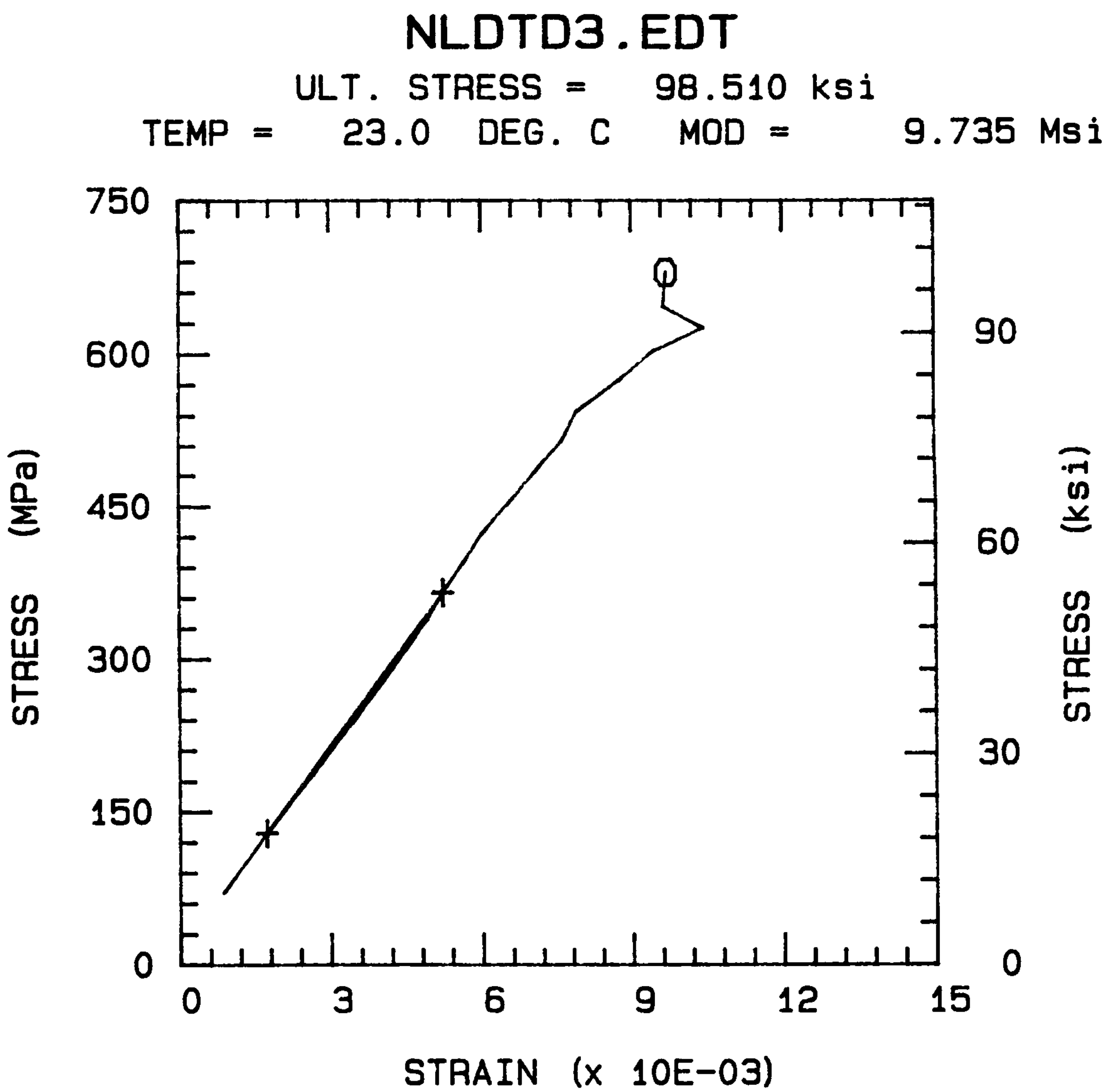

NLDTD3.EDT
ULT. STRESS = 98.510 ksi
TEMP = 23.0 DEG. C MOD = 9.735 Msi
750
600
450
300
150
0
STRESS (MPa)
90
60
30
0
STRESS (ksi)
0
3
6
9
12
15
STRAIN (x 10E-03)

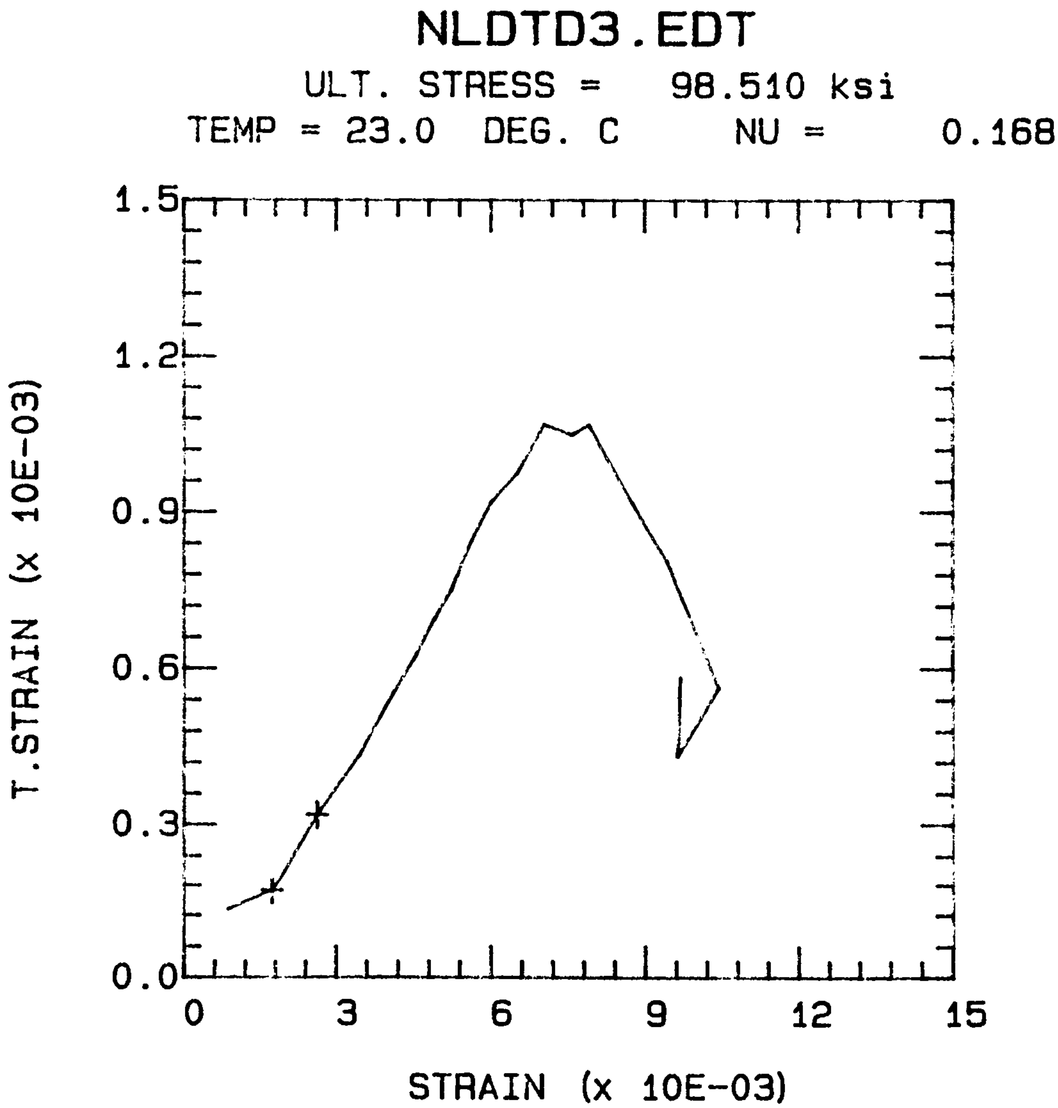
NLDTD3.EDT
ULT. STRESS = 98.510 ksi
TEMP = 23.0 DEG. C NU = 0.168
1.5
1.2
0.9
0.6
0.3
0.0
0
3
6
9
12
15
T.STRAIN (x 10E-03)
STRAIN (x 10E-03)

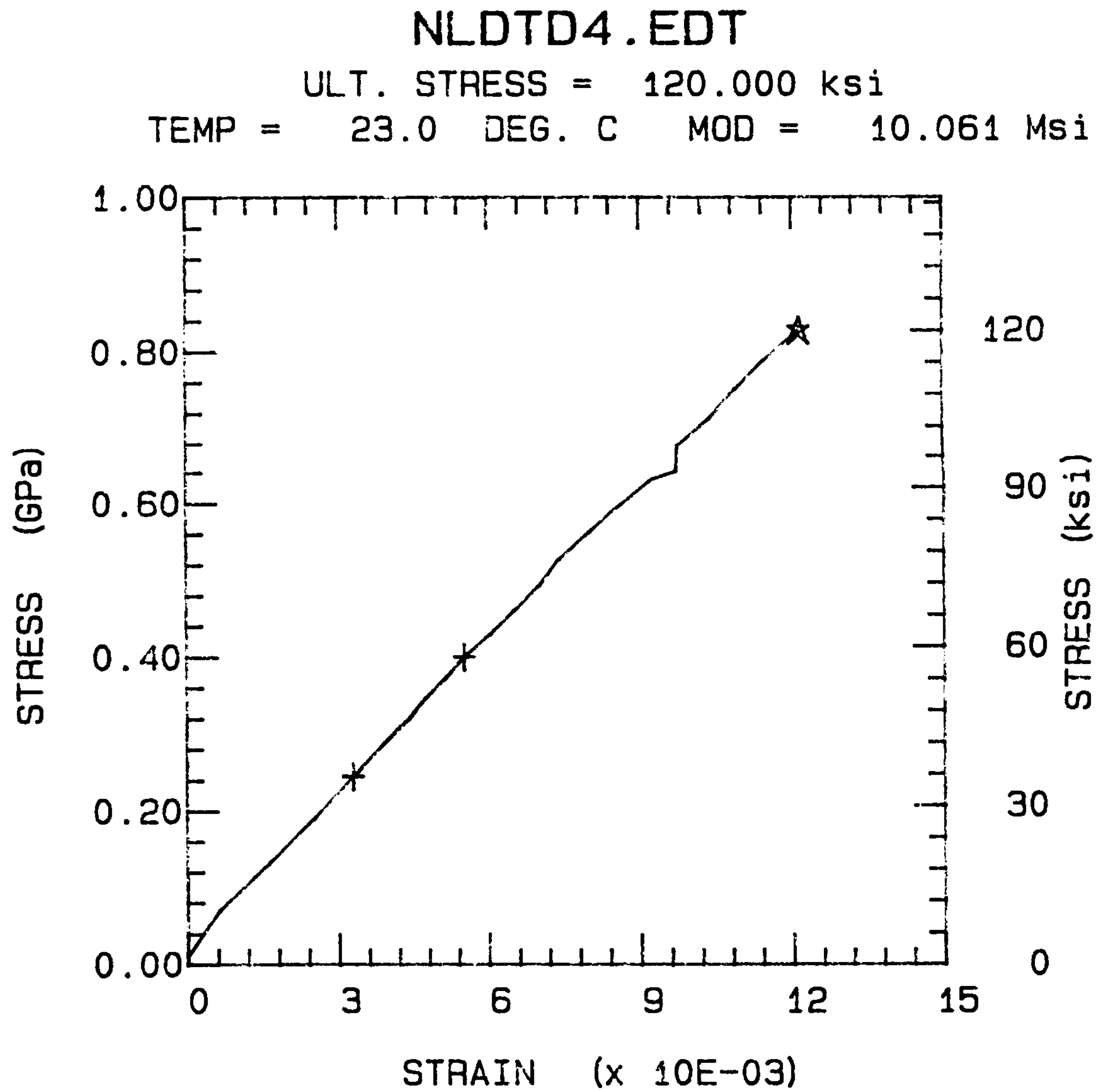
NLDTD4.EDT
ULT. STRESS = 120.000 ksi
TEMP = 23.0 DEG. C MOD = 10.061 Msi
1.00
0.80
0.60
0.40
0.20
0.00
STRESS (GPa)
120
90
60
30
0
STRESS (ksi)
0
3
6
9
12
15
STRAIN (x 10E-03)

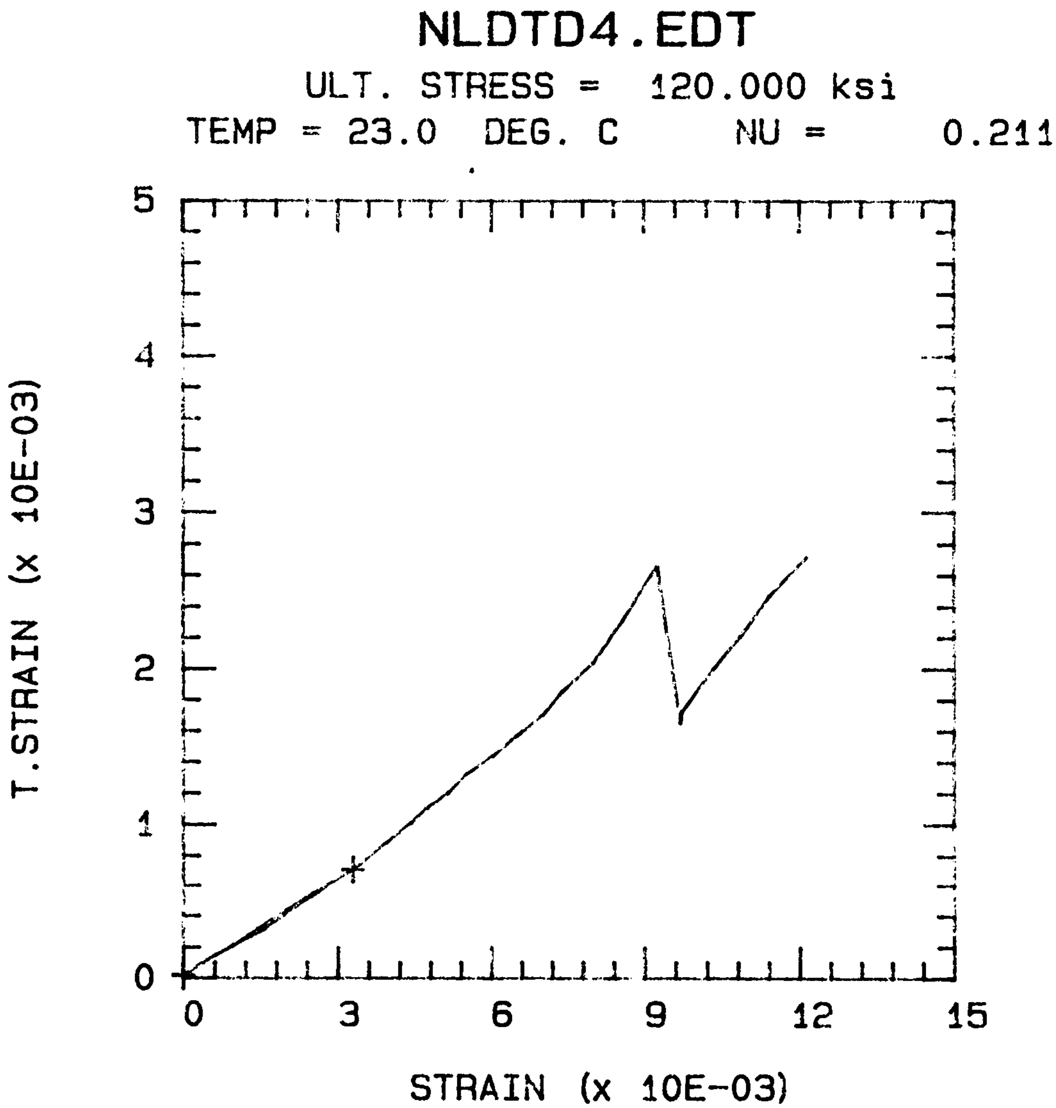
NLDTD4.EDT
ULT. STRESS = 120.000 ksi
TEMP = 23.0 DEG. C NU = 0.211
T.STRAIN (x 10E-03)
STRAIN (x 10E-03)
0
1
2
3
4
5
0
3
6
9
12
15

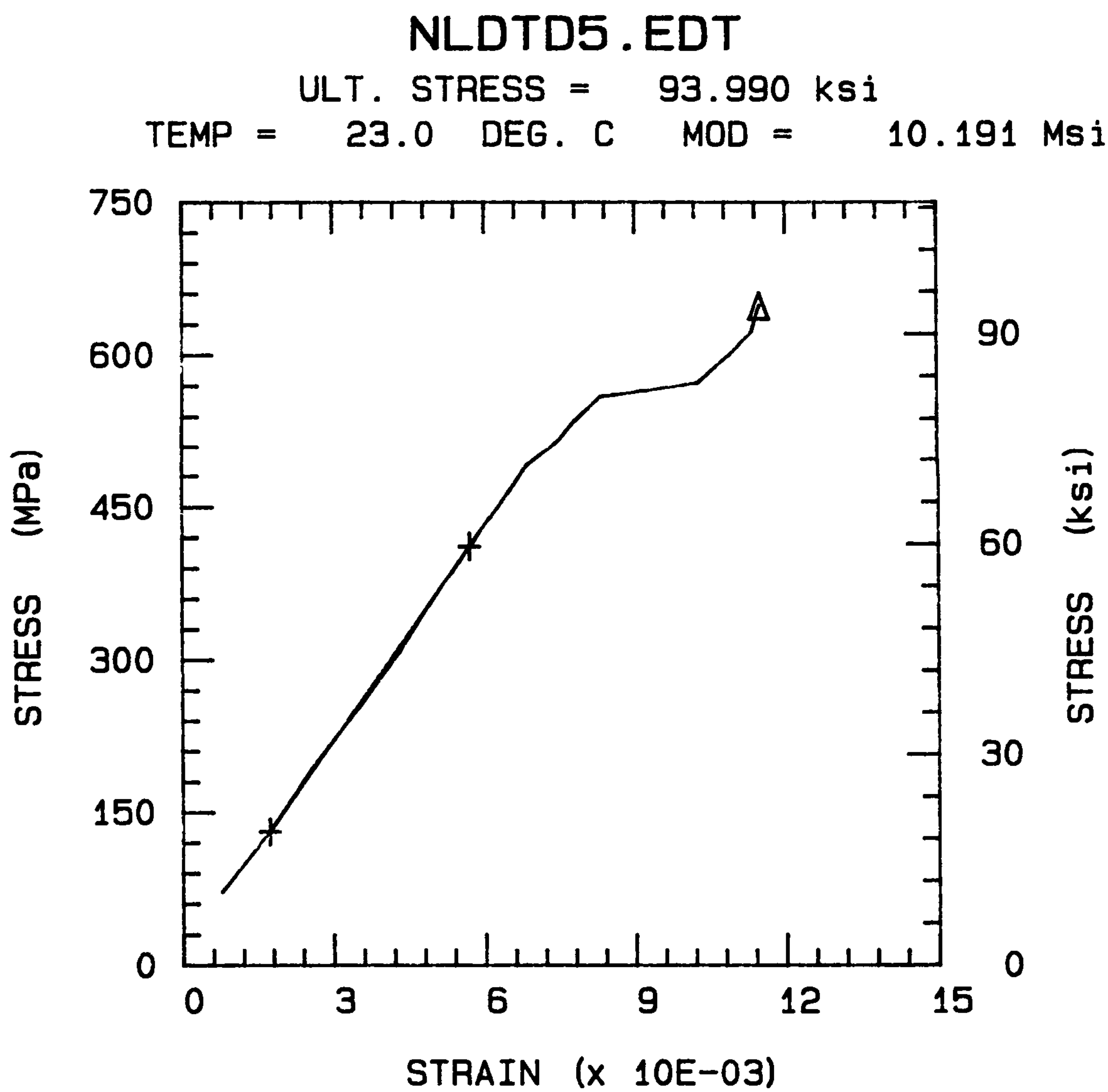
NLDTD5.EDT
ULT. STRESS = 93.990 ksi
TEMP = 23.0 DEG. C MOD = 10.191 Msi
STRESS (MPa)
STRESS (ksi)
STRAIN (x 10E-03)
750
600
450
300
150
0
90
60
30
0
0
3
6
9
12
15

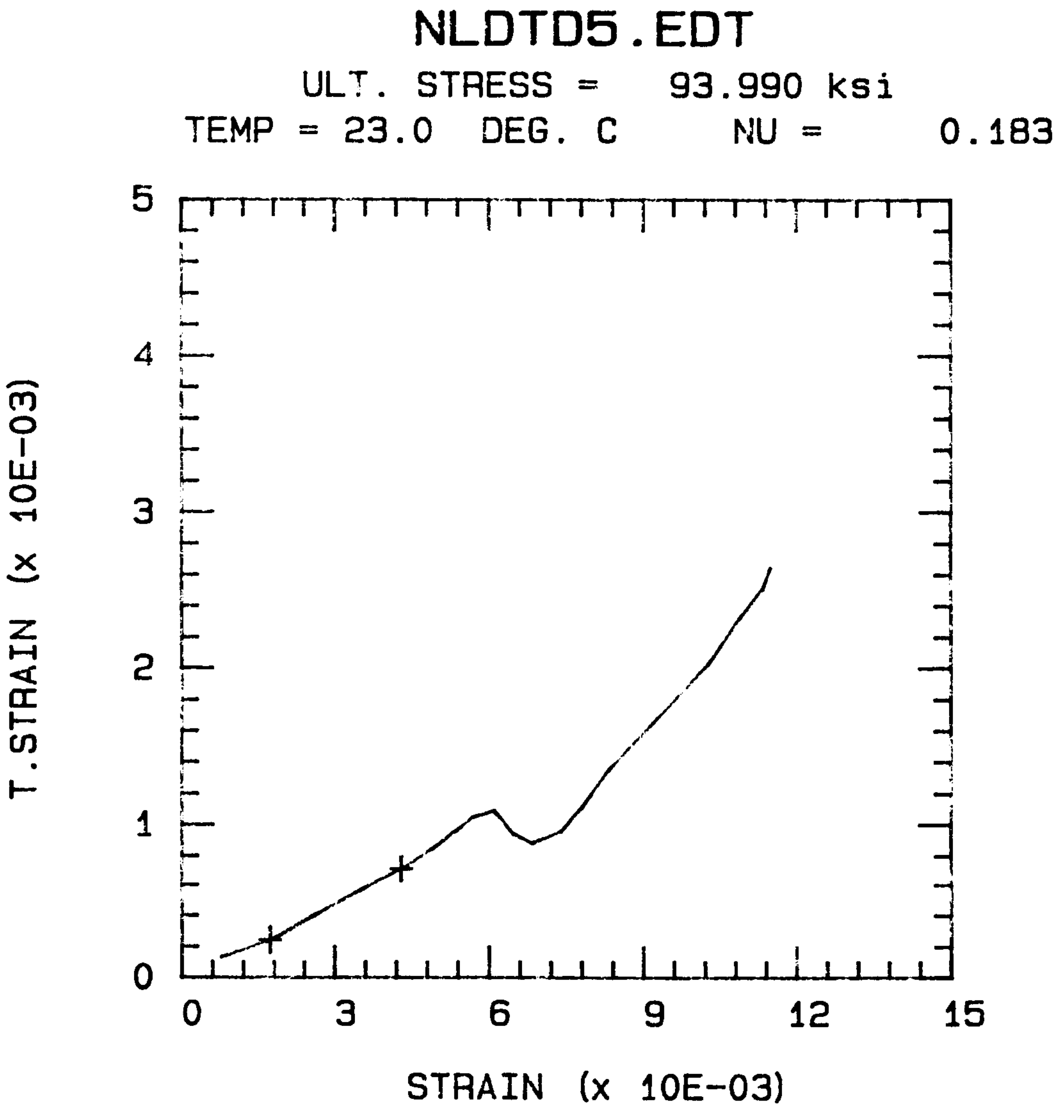
NLDTD5.EDT
ULT. STRESS = 93.990 ksi
TEMP = 23.0 DEG. C NU = 0.183
T.STRAIN (x 10E-03)
5
4
3
2
1
0
0
3
6
9
12
15
STRAIN (x 10E-03)

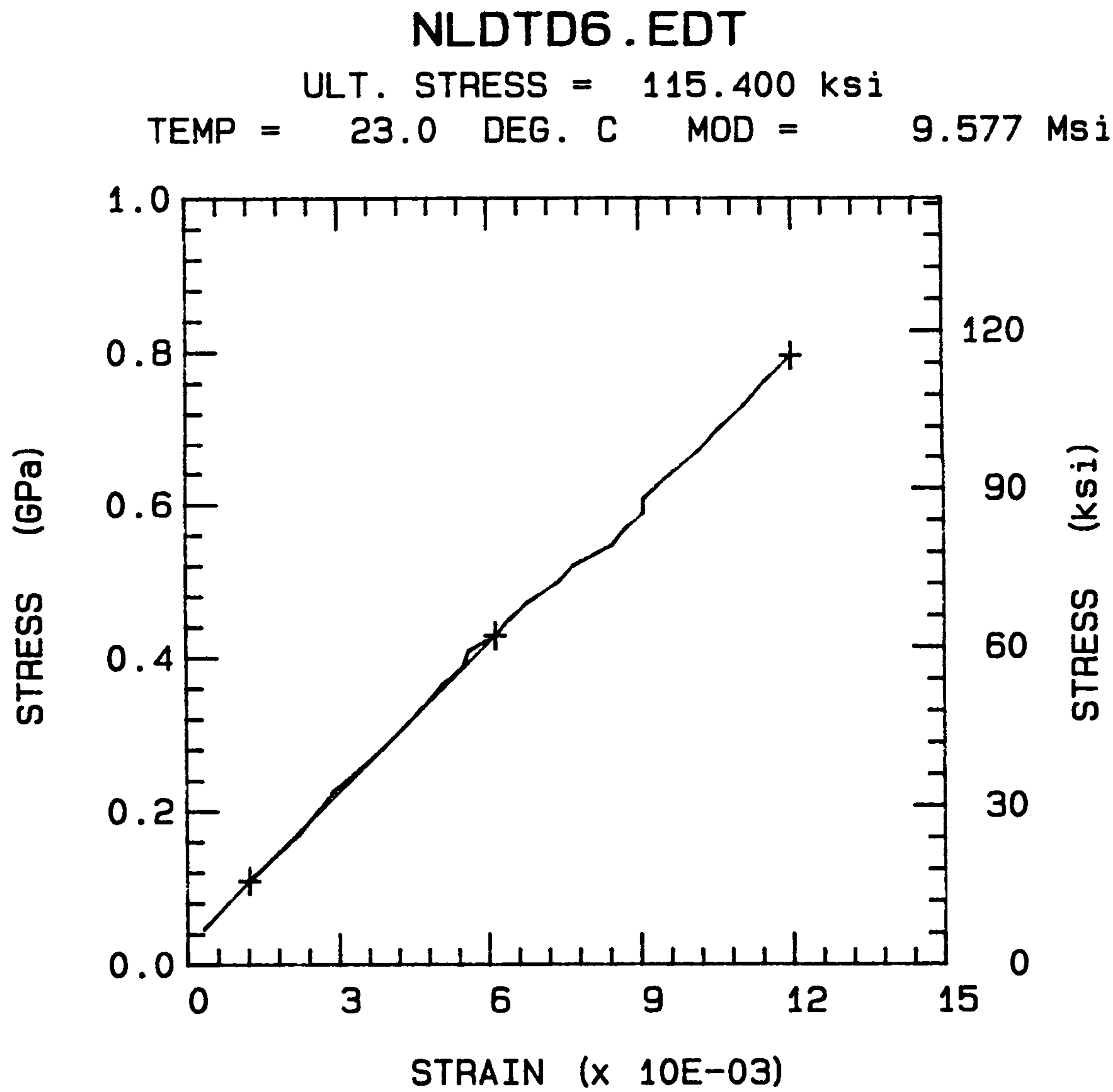
NLDTD6.EDT
ULT. STRESS = 115.400 ksi
TEMP = 23.0 DEG. C MOD = 9.577 Msi
STRESS (GPa)
STRESS (ksi)
STRAIN (x 10E-03)
1.0
0.8
0.6
0.4
0.2
0.0
120
90
60
30
0
0
3
6
9
12
15

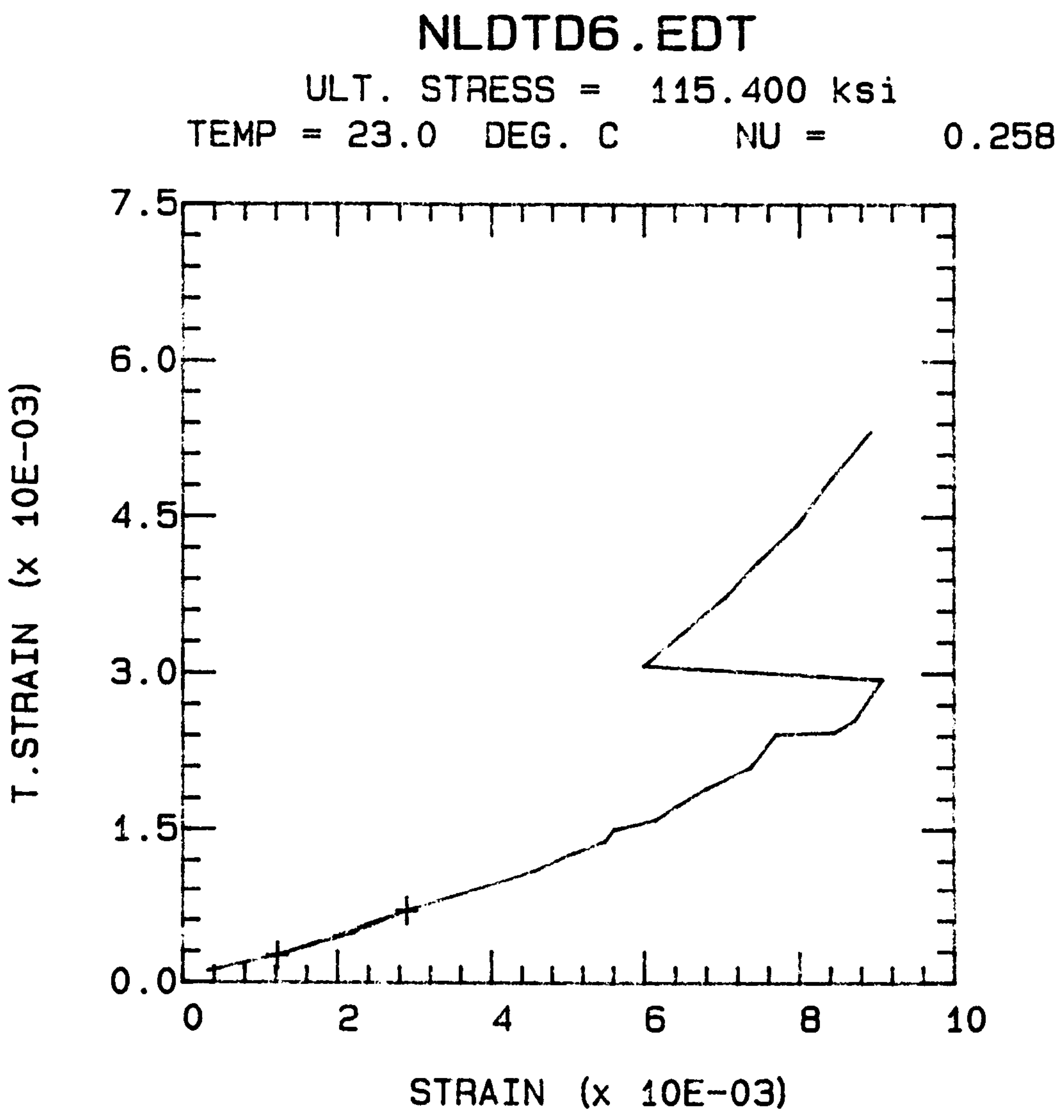
NLDTD6.EDT
ULT. STRESS = 115.400 ksi
TEMP = 23.0 DEG. C NU = 0.258
7.5
6.0
4.5
3.0
1.5
0.0
0
2
4
6
8
10
T.STRAIN (x 10E-03)
STRAIN (x 10E-03)

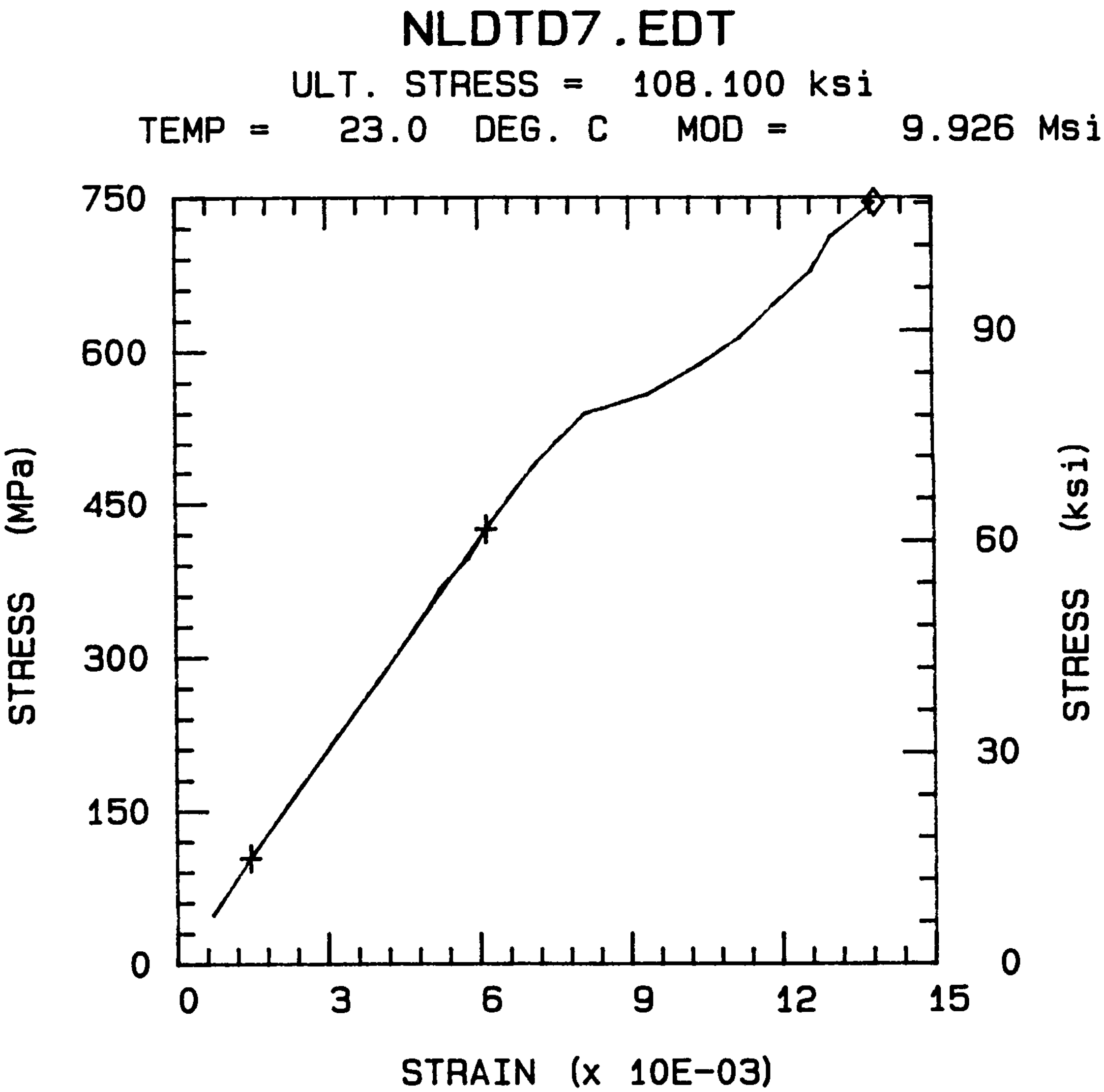

NLDTD7.EDT
ULT. STRESS = 108.100 ksi
TEMP = 23.0 DEG. C MOD = 9.926 Msi
750
600
450
300
150
0
90
60
30
0
STRESS (MPa)
STRESS (ksi)
0
3
6
9
12
15
STRAIN (x 10E-03)

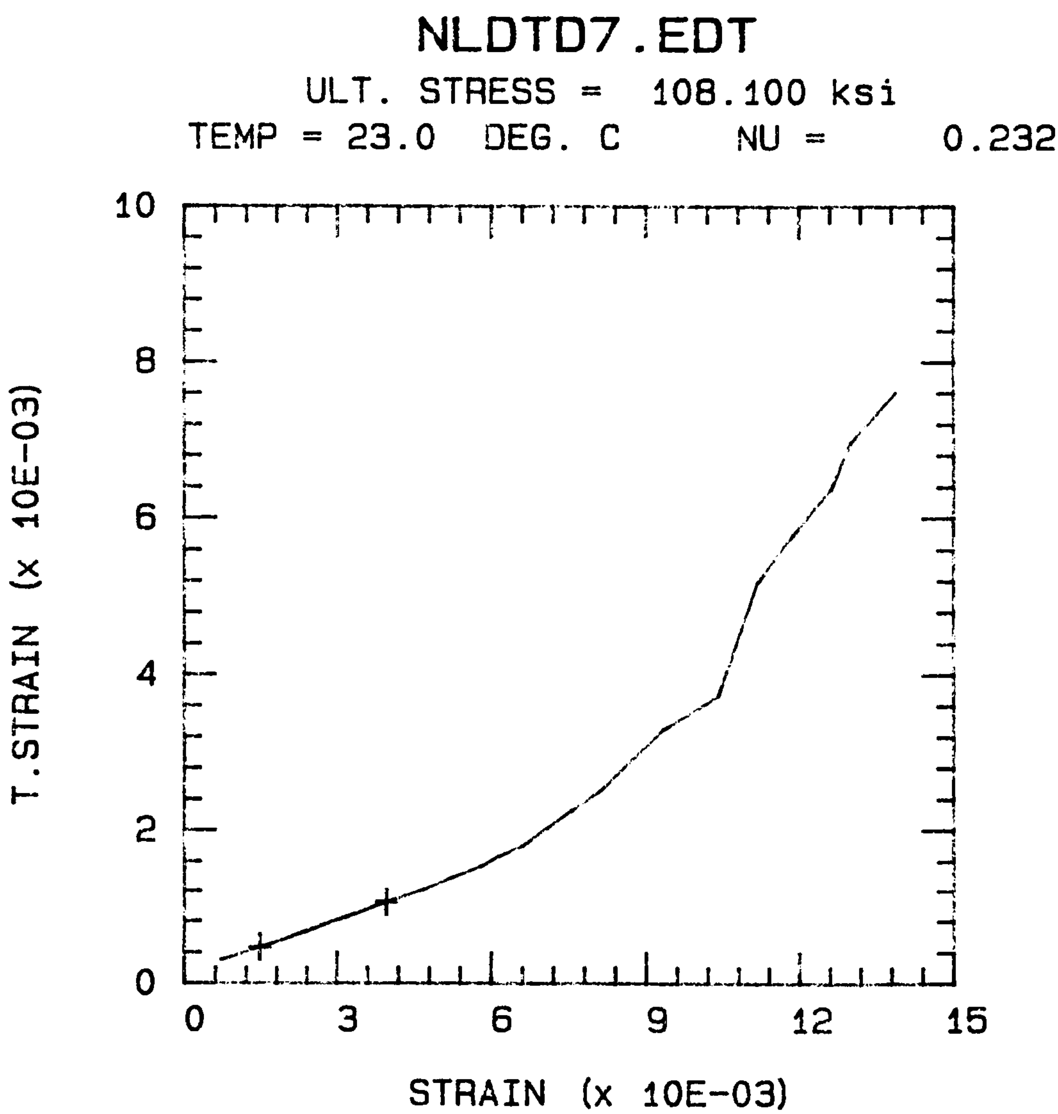

NLDTD7.EDT
ULT. STRESS = 108.100 ksi
TEMP = 23.0 DEG. C NU = 0.232
T.STRAIN (x 10E-03)
0
2
4
6
8
10
0
3
6
9
12
15
STRAIN (x 10E-03)

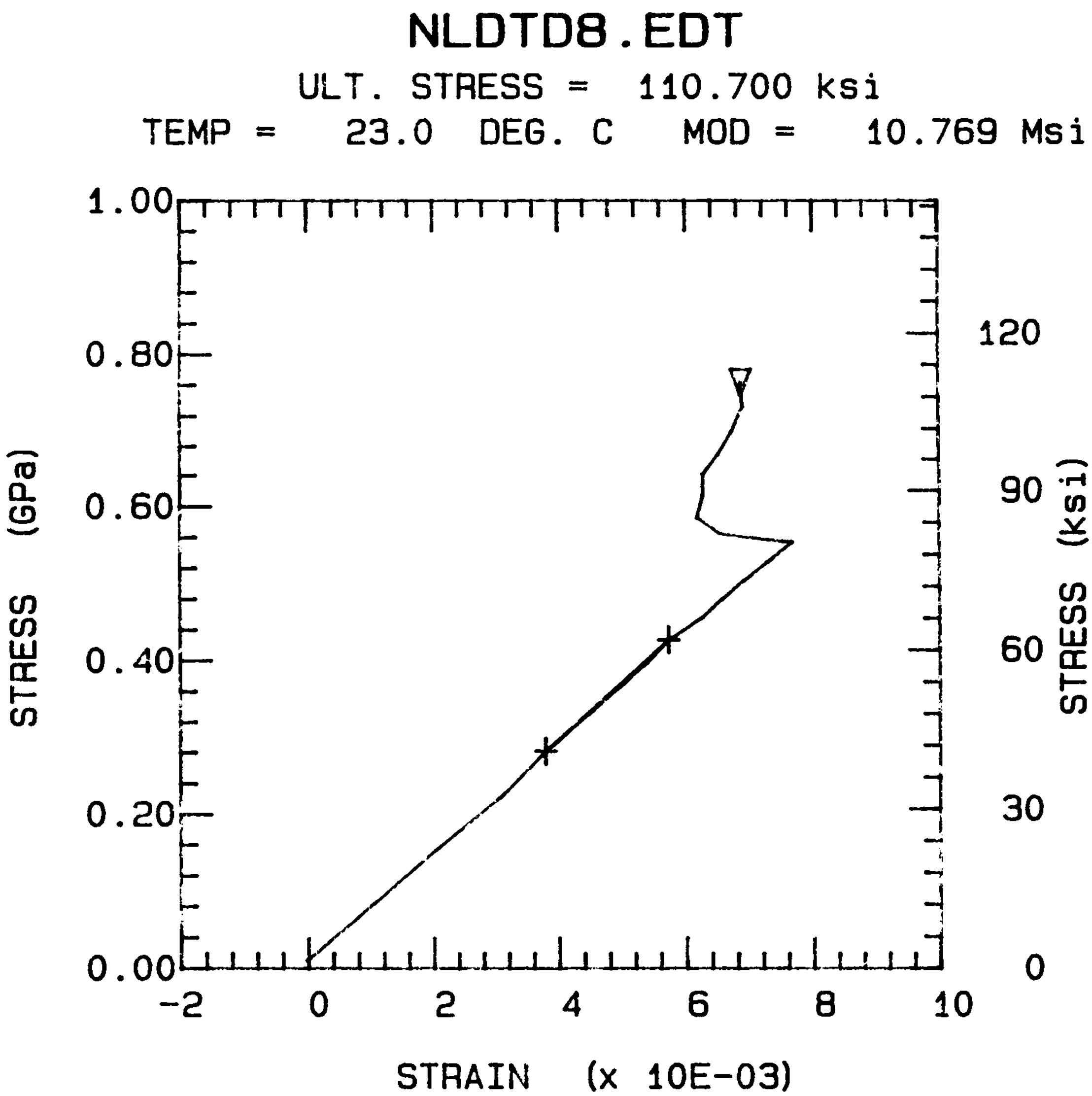
NLDTD8.EDT
ULT. STRESS = 110.700 ksi
TEMP = 23.0 DEG. C MOD = 10.769 Msi
1.00
0.80
0.60
0.40
0.20
0.00
STRESS (GPa)
120
90
60
30
0
STRESS (ksi)
-2
0
2
4
6
8
10
STRAIN (x 10E-03)

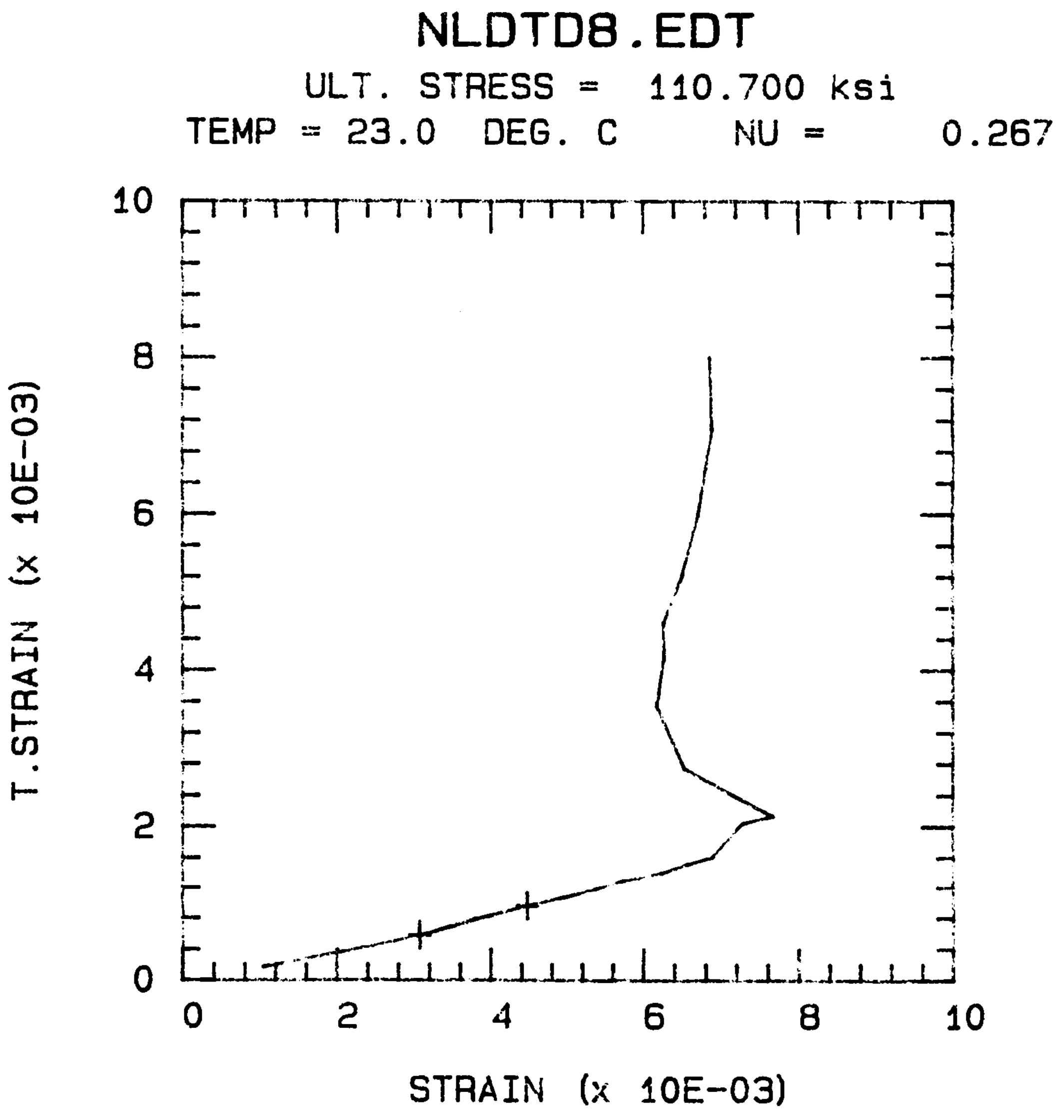
NLDTD8.EDT
ULT. STRESS = 110.700 ksi
TEMP = 23.0 DEG. C NU = 0.267
T.STRAIN (x 10E-03)
STRAIN (x 10E-03)
0
2
4
6
8
10

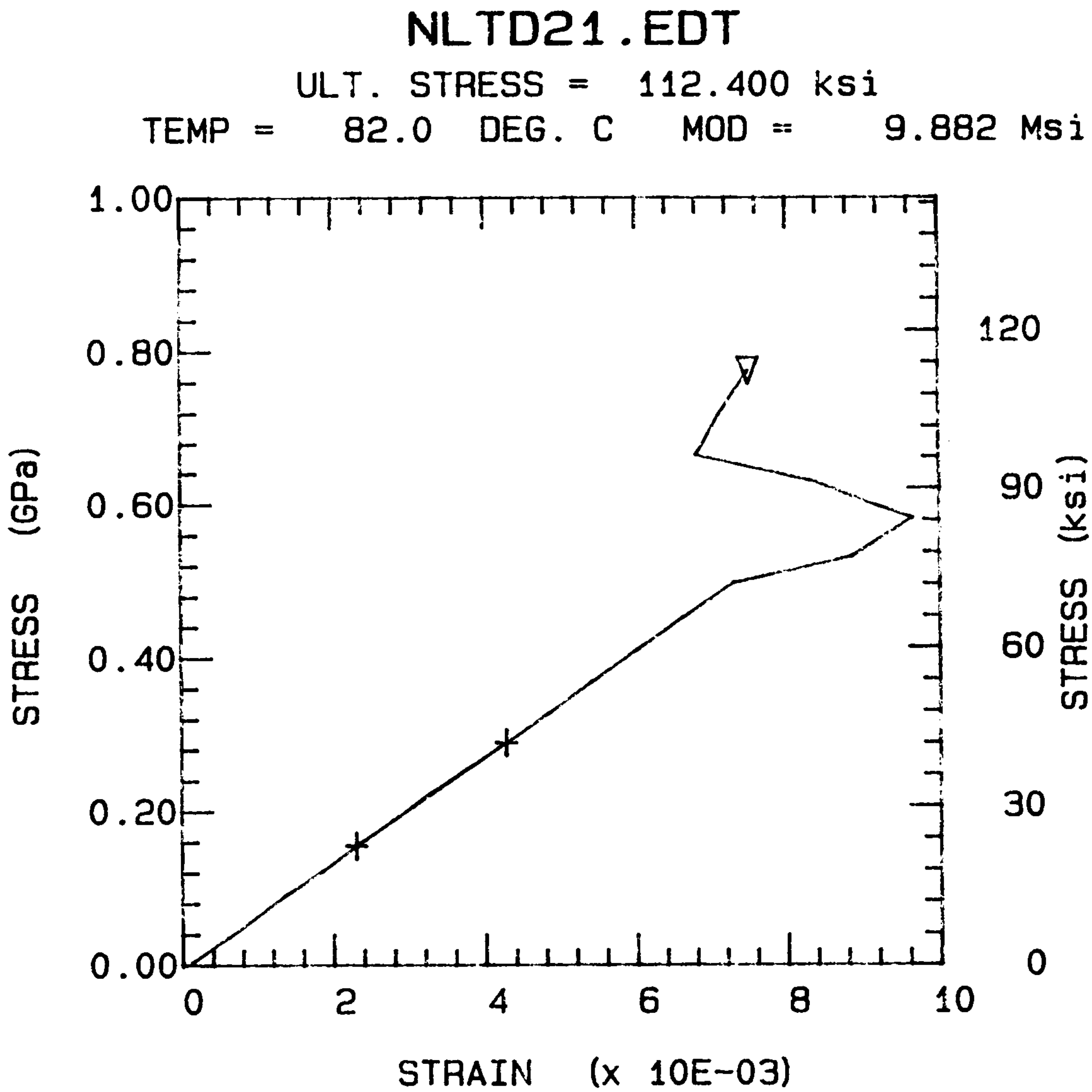
NLTD21.EDT
ULT. STRESS = 112.400 ksi
TEMP = 82.0 DEG. C MOD = 9.882 Msi
STRESS (GPa)
1.00
0.80
0.60
0.40
0.20
0.00
0
2
4
6
8
10
STRAIN (x 10E-03)
120
90
60
30
0
STRESS (ksi)

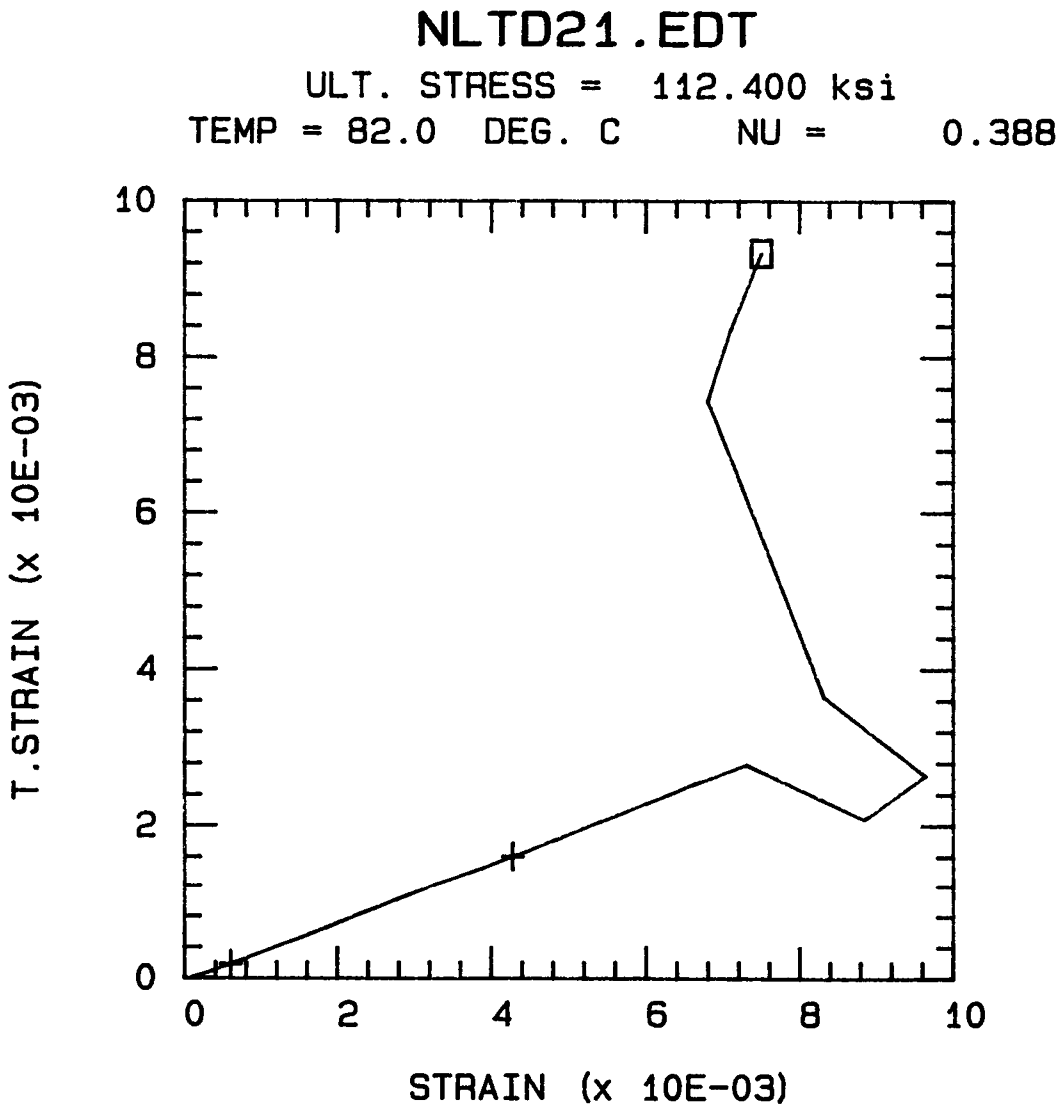
NLTD21.EDT
ULT. STRESS = 112.400 ksi
TEMP = 82.0 DEG. C NU = 0.388
T.STRAIN (x 10E-03)
STRAIN (x 10E-03)
0
2
4
6
8
10

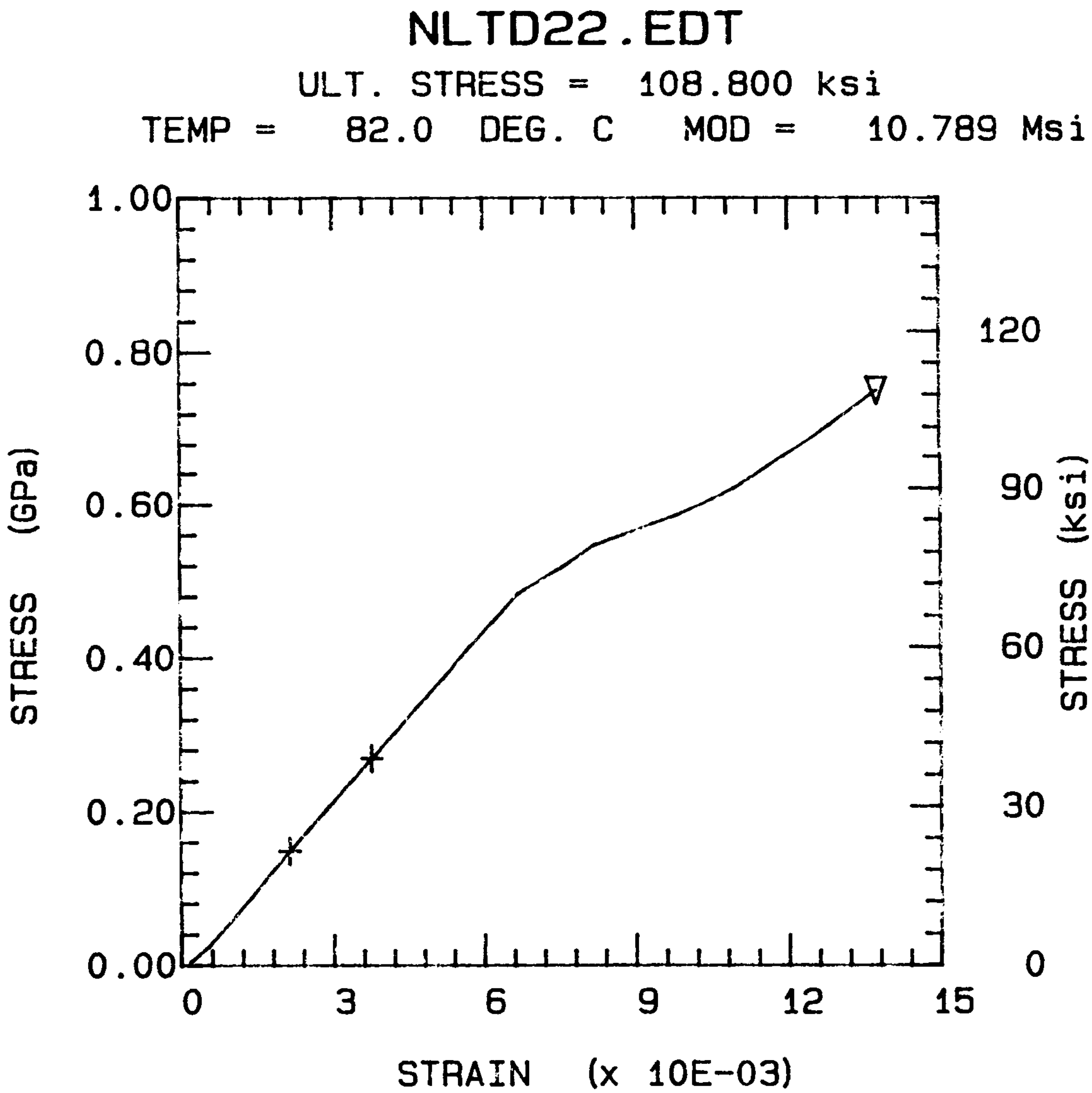
NLTD22.EDT
ULT. STRESS = 108.800 ksi
TEMP = 82.0 DEG. C MOD = 10.789 Msi
1.00
0.80
0.60
0.40
0.20
0.00
STRESS (GPa)
120
90
60
30
0
STRESS (ksi)
0
3
6
9
12
15
STRAIN (x 10E-03)

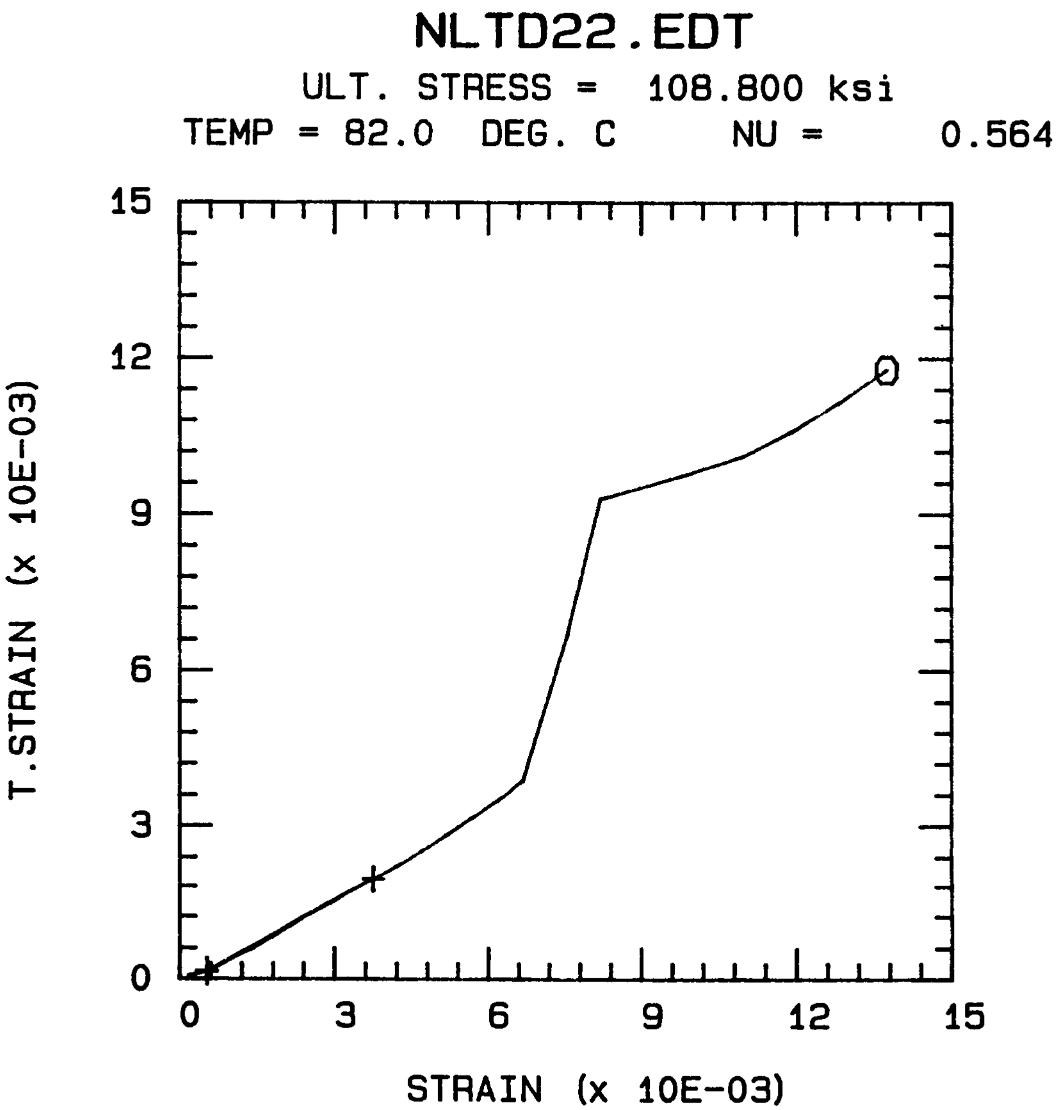
NLTD22.EDT
ULT. STRESS = 108.800 ksi
TEMP = 82.0 DEG. C NU = 0.564
T.STRAIN (x 10E-03)
STRAIN (x 10E-03)
0
3
6
9
12
15

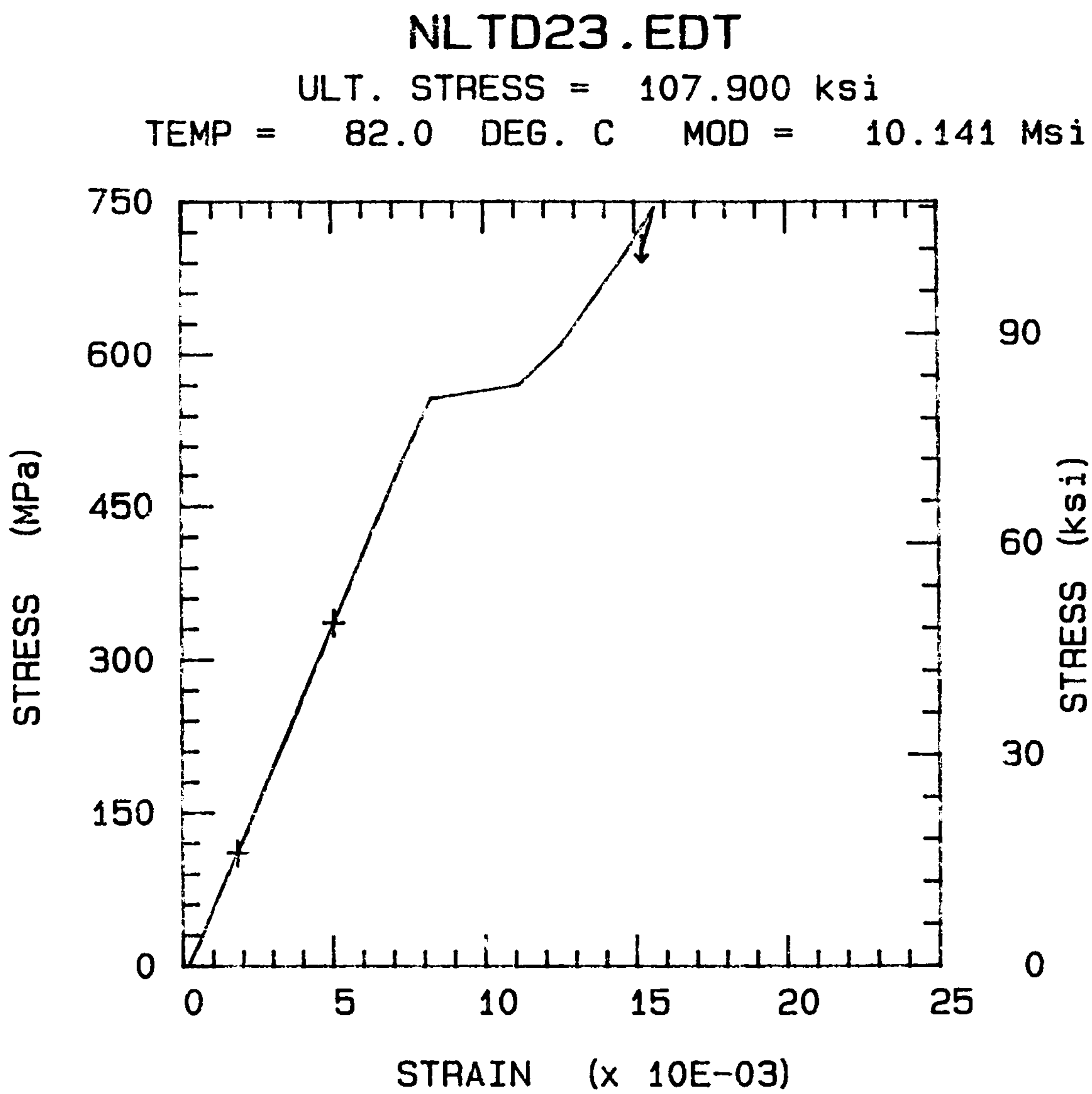
NLTD23.EDT
ULT. STRESS = 107.900 ksi
TEMP = 82.0 DEG. C MOD = 10.141 Msi
STRESS (MPa)
STRESS (ksi)
STRAIN (x 10E-03)
0
150
300
450
600
750
0
30
60
90
0
5
10
15
20
25

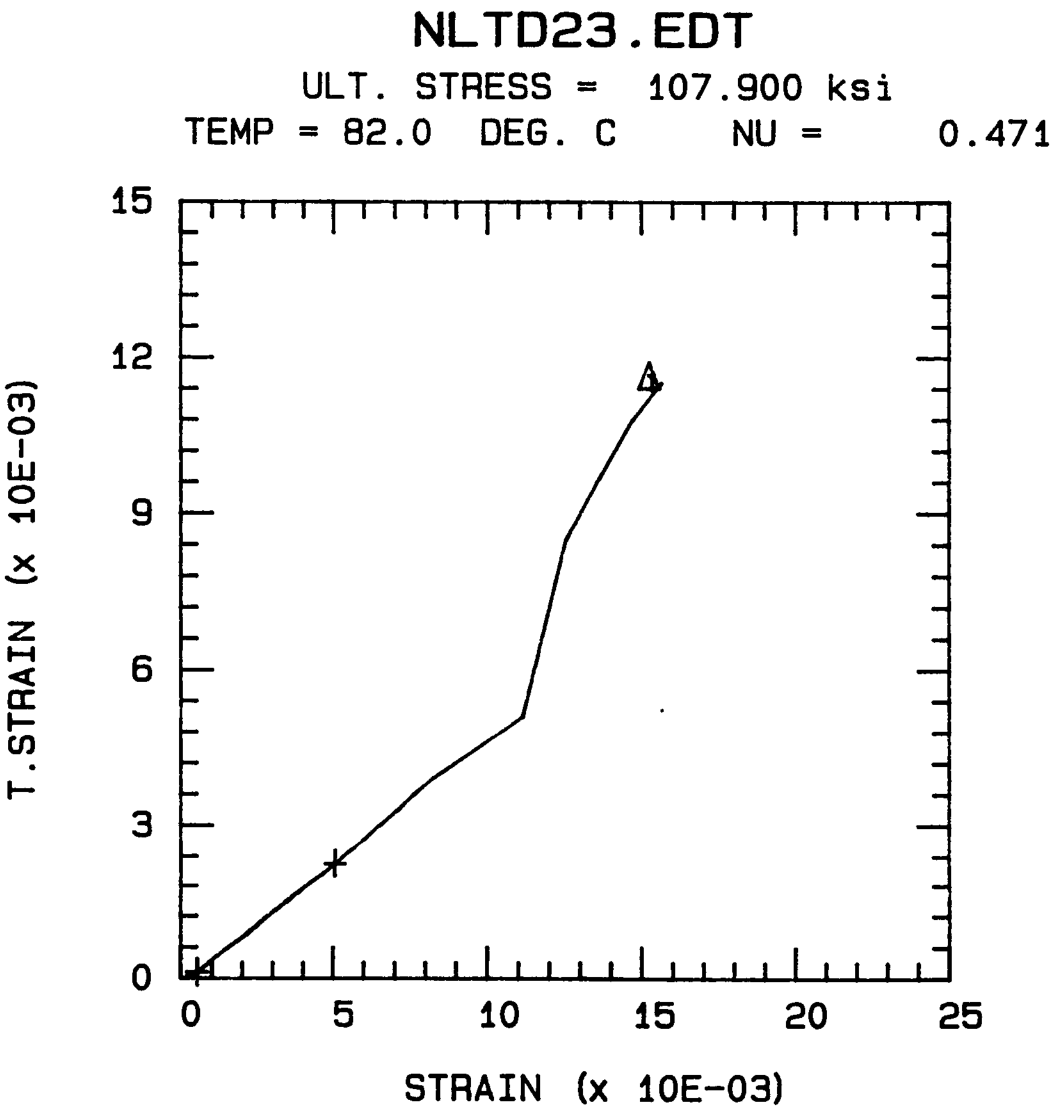
NLTD23.EDT
ULT. STRESS = 107.900 ksi
TEMP = 82.0 DEG. C NU = 0.471
T.STRAIN (x 10E-03)
15
12
9
6
3
0
0
5
10
15
20
25
STRAIN (x 10E-03)

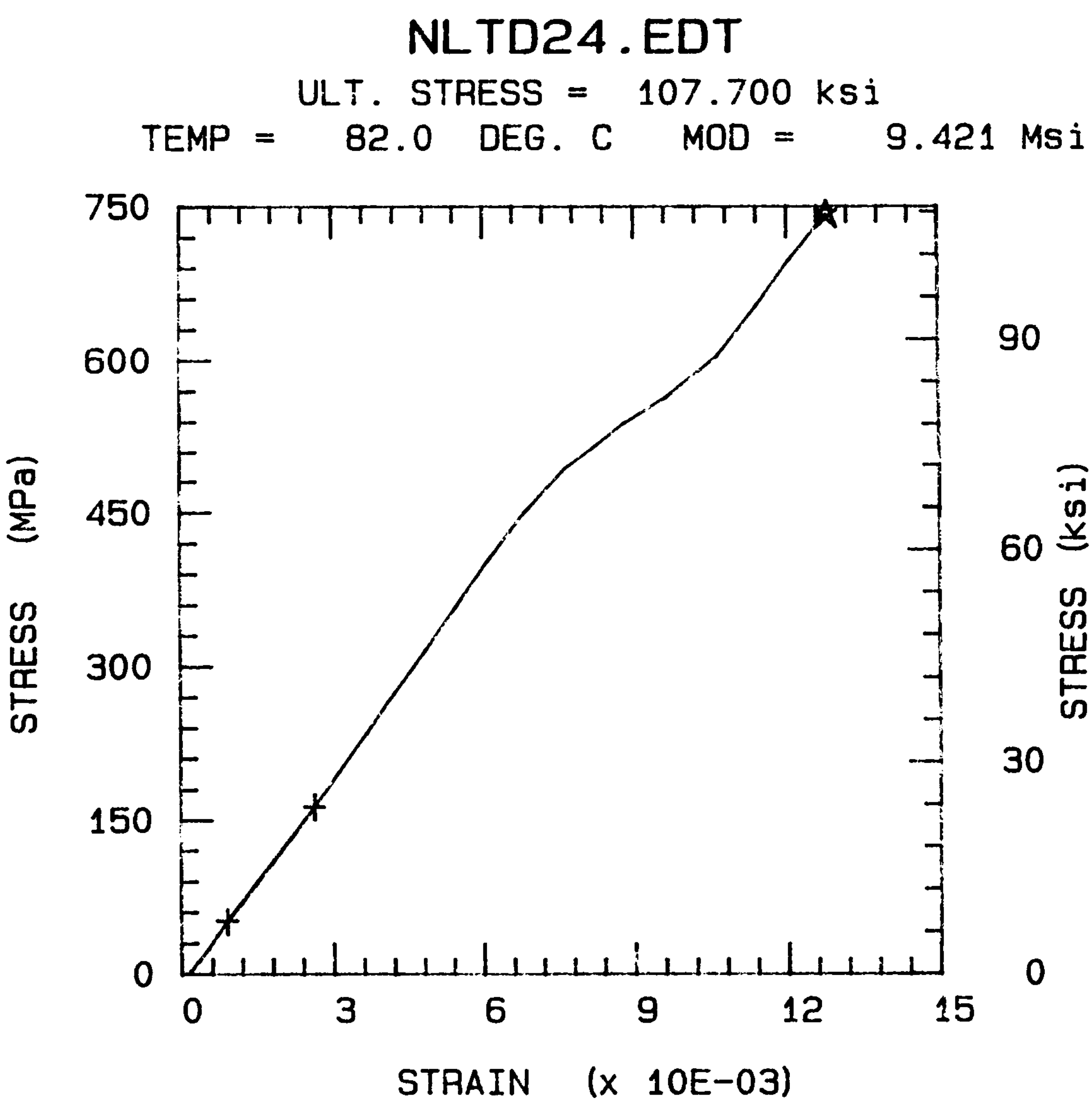
NLTD24.EDT
ULT. STRESS = 107.700 ksi
TEMP = 82.0 DEG. C MOD = 9.421 Msi
750
600
450
300
150
0
STRESS (MPa)
90
60
30
0
STRESS (ksi)
0
3
6
9
12
15
STRAIN (x 10E-03)

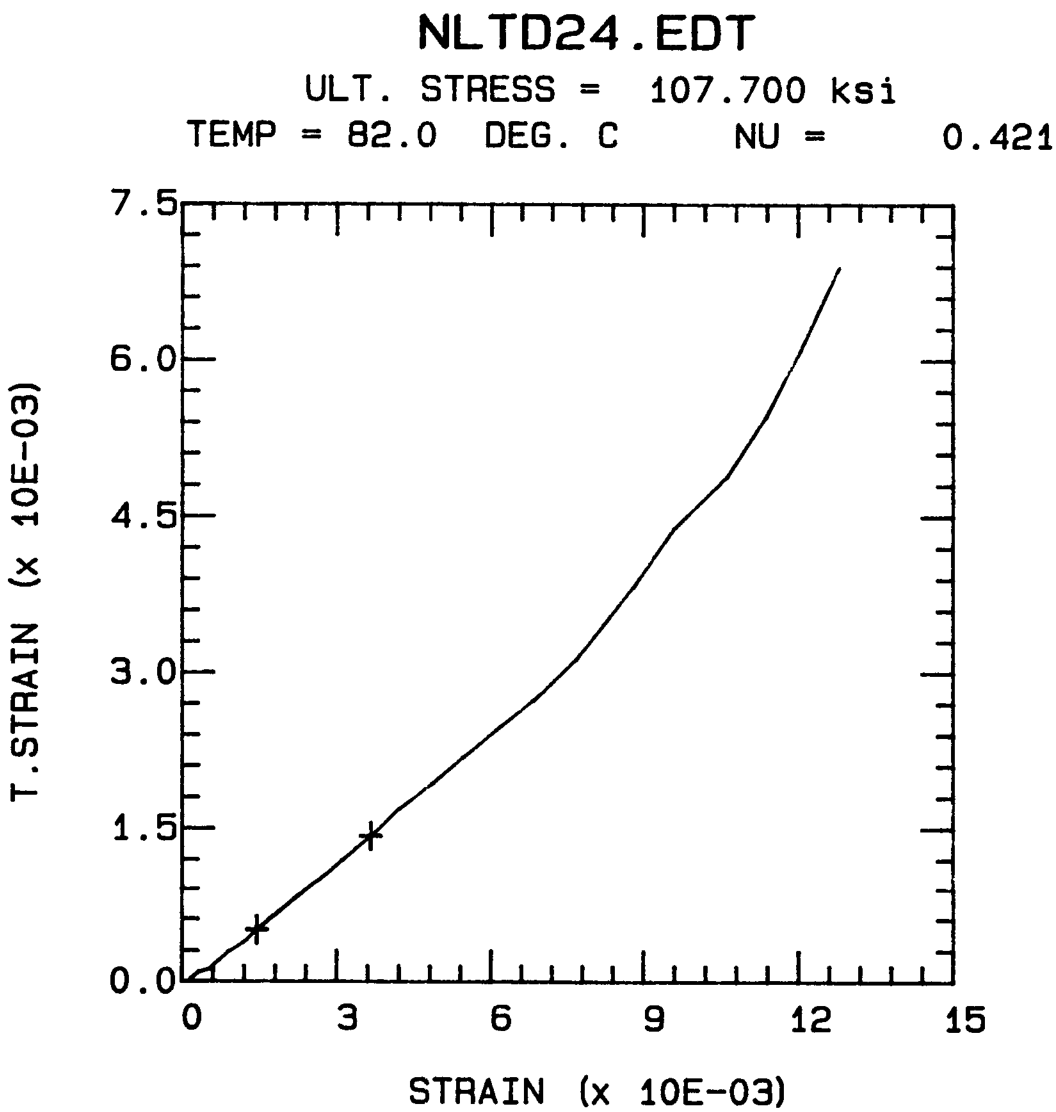

NLTD24.EDT
ULT. STRESS = 107.700 ksi
TEMP = 82.0 DEG. C NU = 0.421
7.5
6.0
4.5
3.0
1.5
0.0
0
3
6
9
12
15
T.STRAIN (x 10E-03)
STRAIN (x 10E-03)

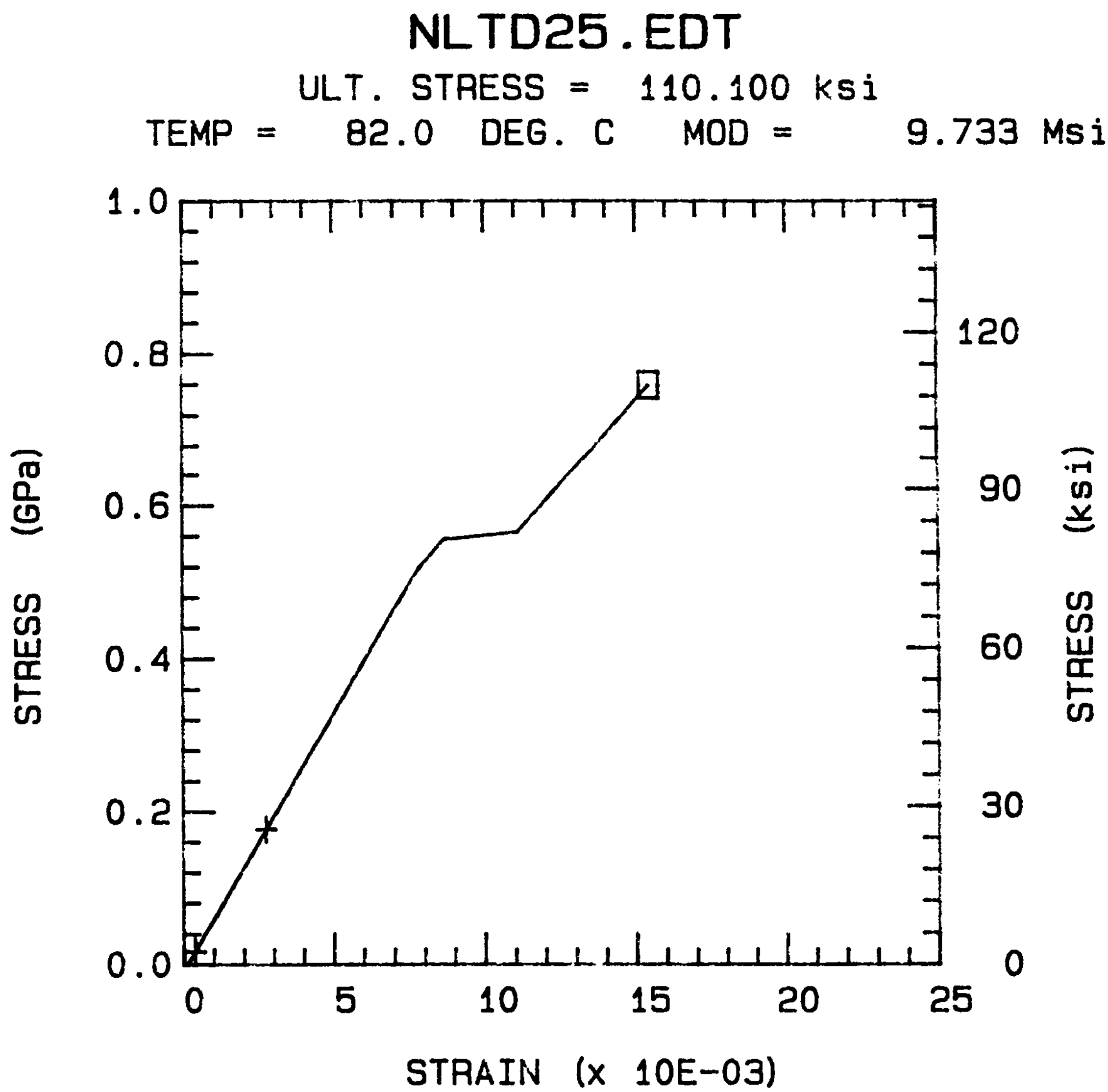
NLTD25.EDT
ULT. STRESS = 110.100 ksi
TEMP = 82.0 DEG. C MOD = 9.733 Msi
STRESS (GPa)
1.0
0.8
0.6
0.4
0.2
0.0
STRESS (ksi)
120
90
60
30
0
0
5
10
15
20
25
STRAIN (x 10E-03)

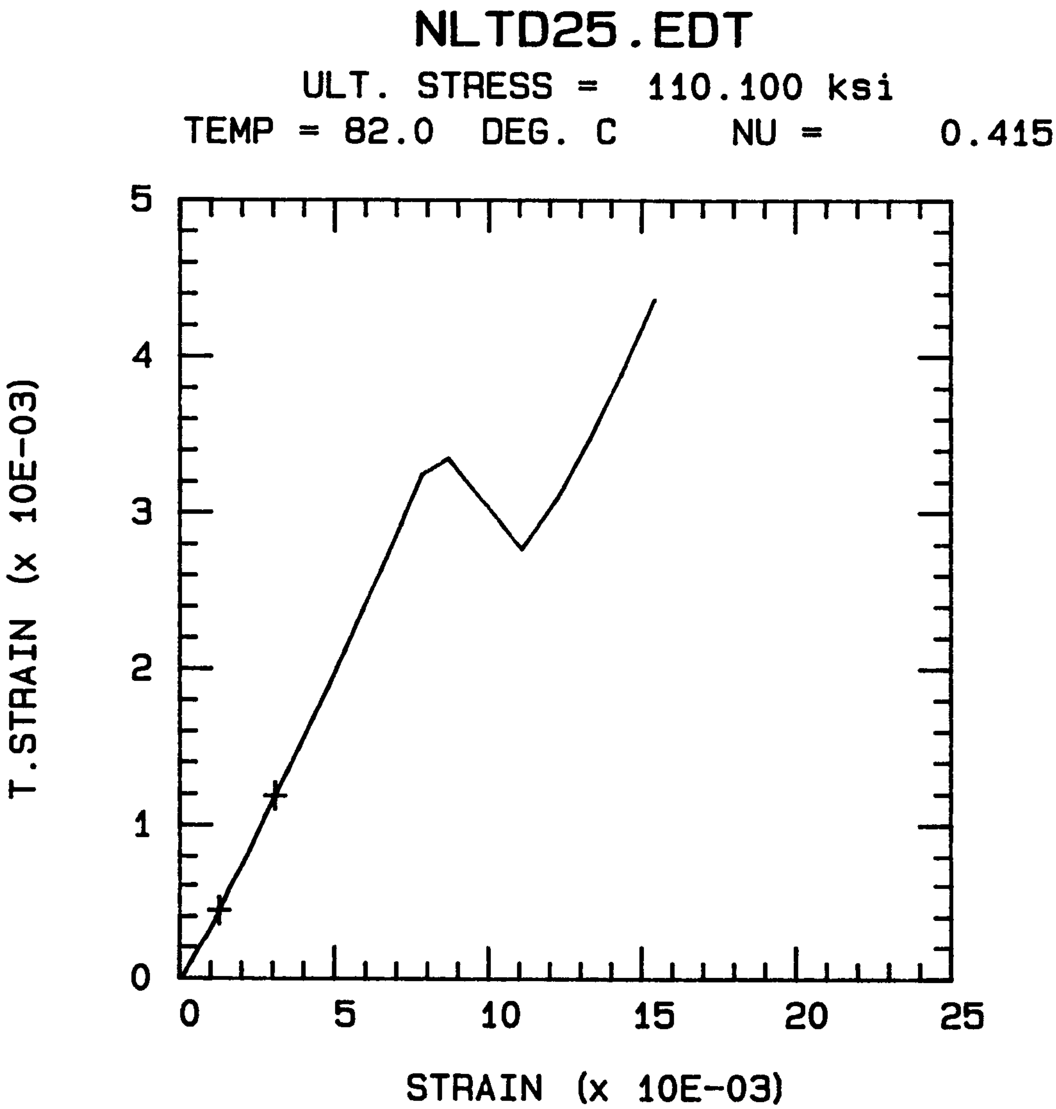
NLTD25.EDT
ULT. STRESS = 110.100 ksi
TEMP = 82.0 DEG. C NU = 0.415
T.STRAIN (x 10E-03)
0
1
2
3
4
5
0
5
10
15
20
25
STRAIN (x 10E-03)

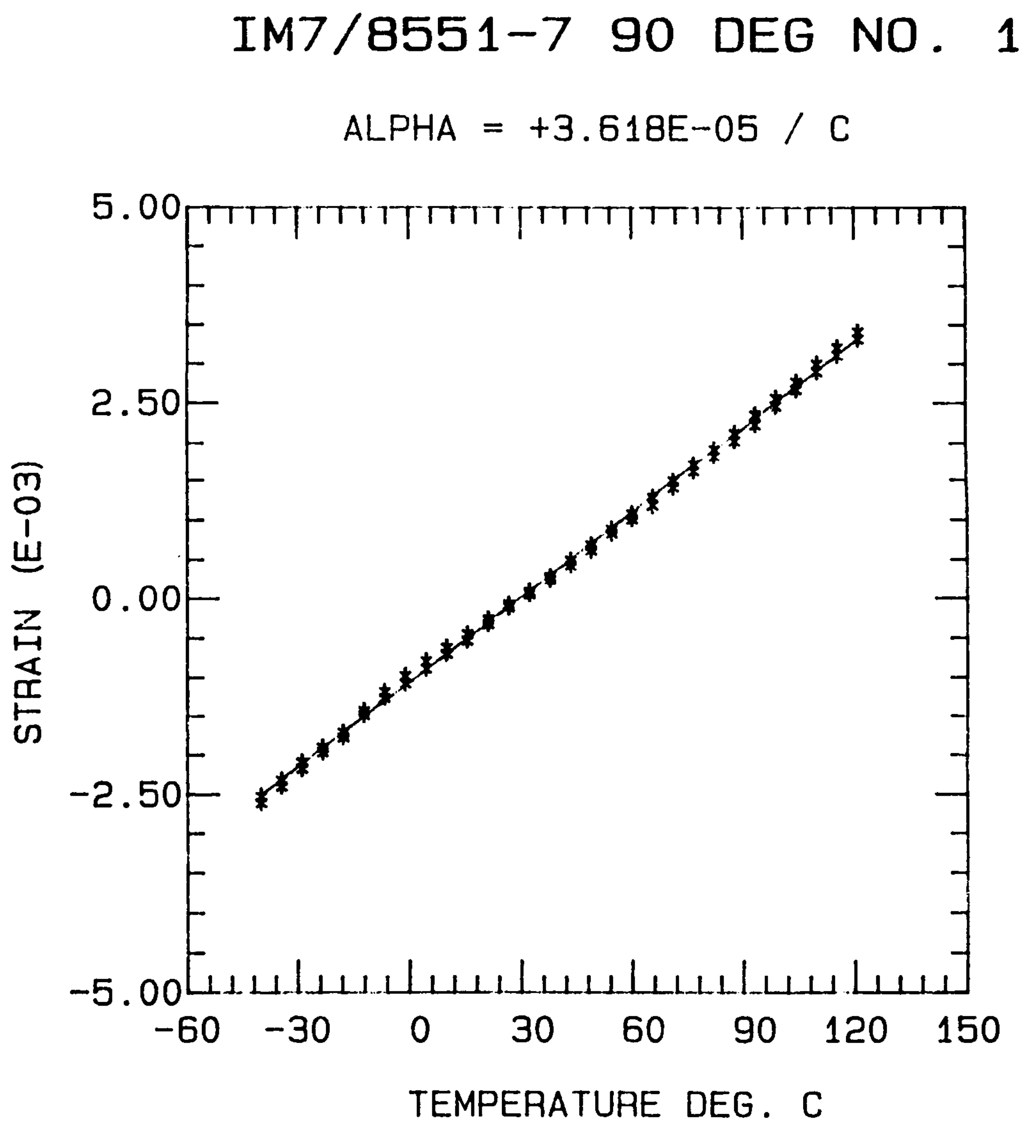
IM7/8551-7 90 DEG NO. 1
ALPHA = +3.618E-05 / C
5.00
2.50
0.00
-2.50
-5.00
STRAIN (E-03)
-60
-30
0
30
60
90
120
150
TEMPERATURE DEG. C

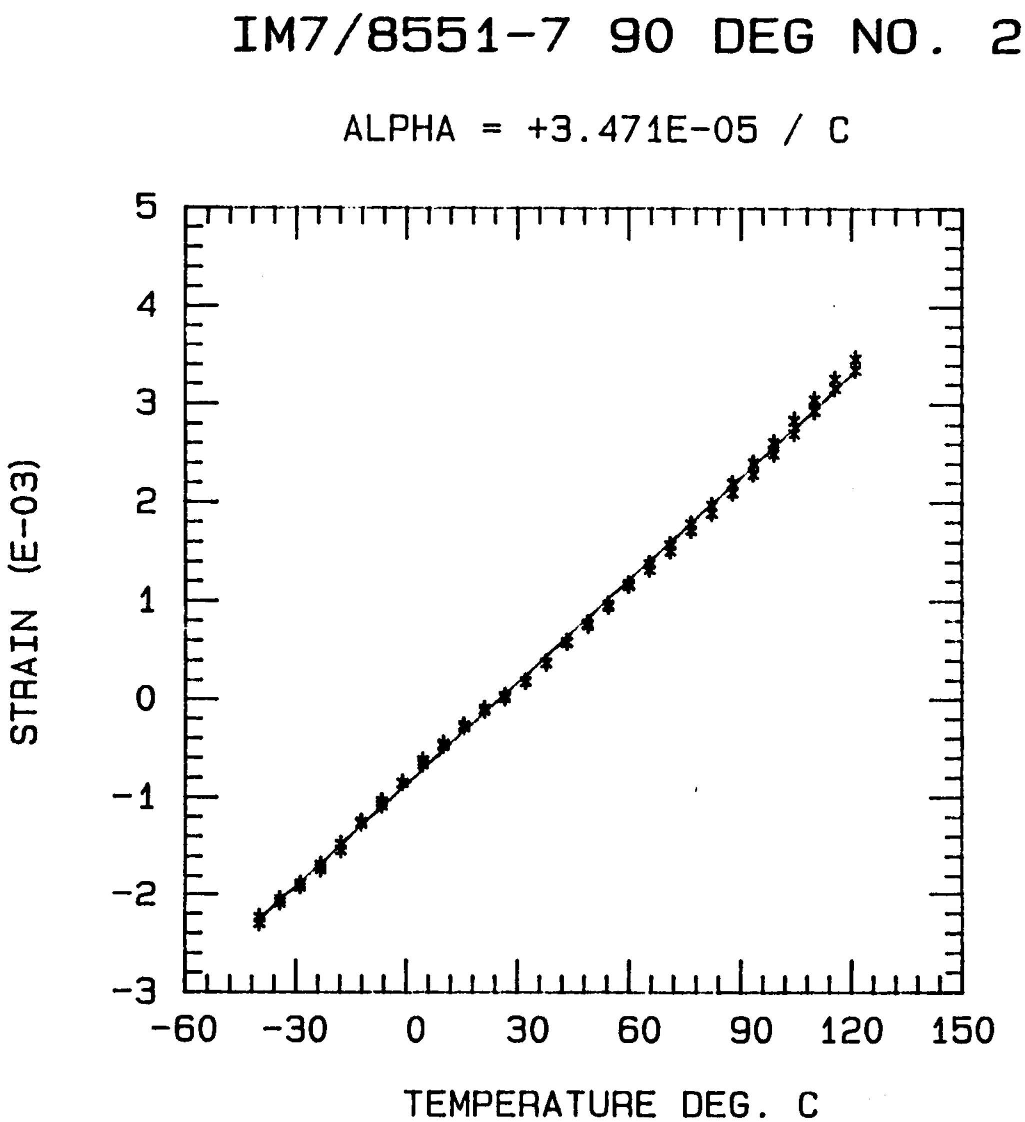
IM7/8551-7 90 DEG NO. 2
ALPHA = +3.471E-05 / C
STRAIN (E-03)
5
4
3
2
1
0
-1
-2
-3
-60
-30
0
30
60
90
120
150
TEMPERATURE DEG. C

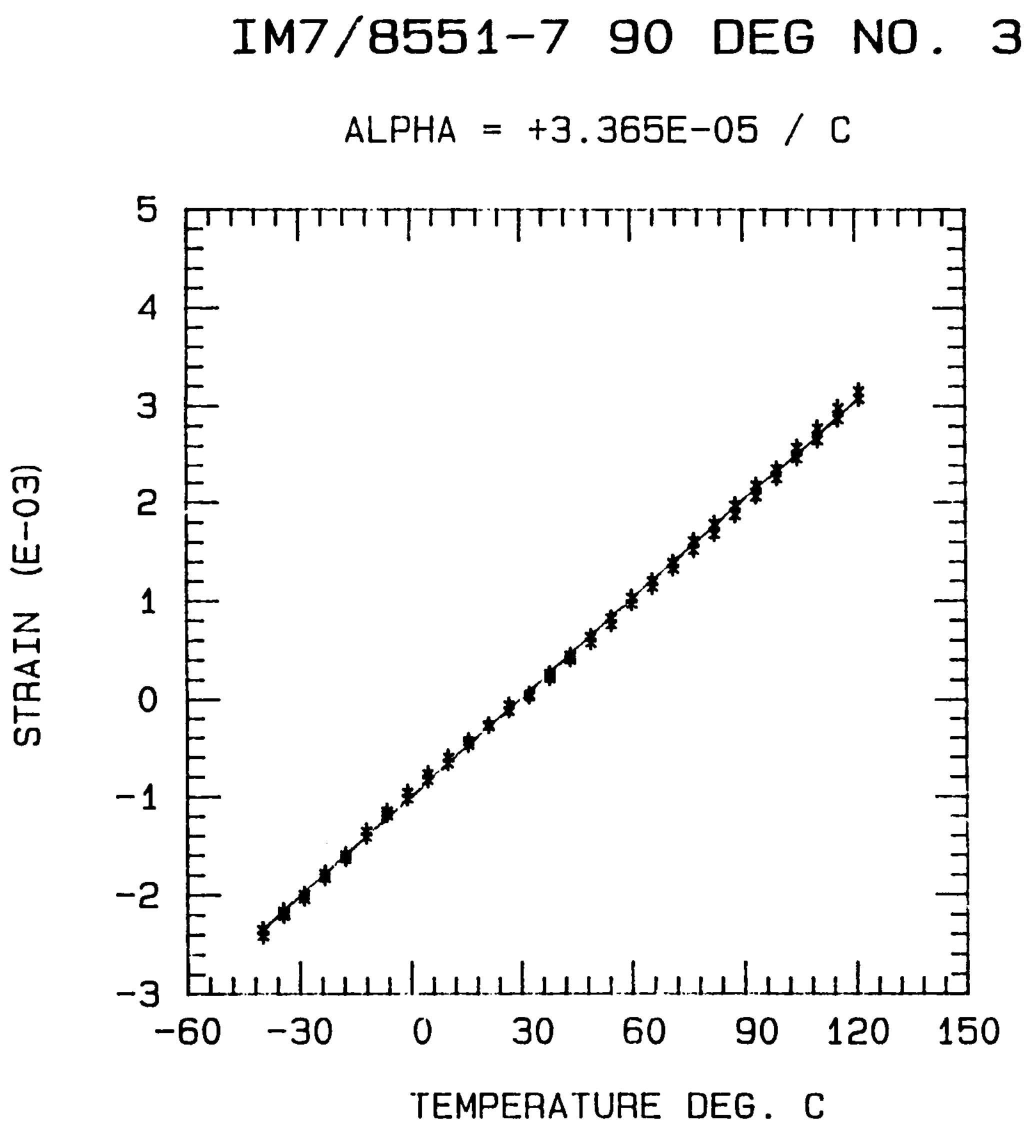
IM7/8551-7 90 DEG NO. 3
ALPHA = +3.365E-05 / C
STRAIN (E-03)
5
4
3
2
1
0
-1
-2
-3
-60
-30
0
30
60
90
120
150
TEMPERATURE DEG. C

APPENDIX B

INDIVIDUAL TENSION-TENSION FATIGUE RESULTS

Naming Convention for Edge Delamination Fatigue Specimens

Specimen name = 123456.FTG - six characters with .FTG extension

Character Meaning:

1. L - NASA-Langley

2. F - Fatigue Specimen

3. L or H - Test Temperature
   L = Low 75°F (25°C)
   H = High 180°F (82°C)

4. Maximum Load Value where:

A = 95% of Ultimate Load	J = 50% of Ultimate Load
B = 90%	K = 45%
C = 85%	L = 40%
D = 80%	M = 35%
E = 75%	N = 30%
F = 70%	O = 25%
G = 65%	P = 20%
H = 60%	Q = 15%
I = 55%	R = 10%

5. - Precondition Type
   S = No precondition (Normal)
   M = High Mean Load (1000 cycles)
   P = Spike Load (One cycle)

6. - Specimen Number 0-9, A-Z

Example - LFLESA.FTG

Explanation -
LF = NASA-Langley Fatigue Program
L = Low temperature 75°F (25°C)
E = 75% of Ultimate Load
S = No Precondition
A = Specimen No. A

PRECEDING PAGE BLANK NOT FILMED

Table B1

Individual Tension-Tension Edge Delamination Fatigue Results for
IM7/8551-7 Composites at Room Temperature No Precondition

Specimen Name	Thickness		Peak Stress		Initial Modulus		Final Modulus		R Ratio	Cycles to 5% Modulus Decay	Cycles to Delami-nation	Delami-nation Strain	Gc $(\frac{lb_f\ in}{in^2})$	Gc
	(in)	(mm)	(ksi)	(MPa)	(Msi)	(GPa)	(Msi)	(GPa)				(percent)		(J/m²)
LFSASA 95%	0.044	1.12	79.1	545	9.34	64.35	8.86	61.05	0.113	66	1	0.87	1.11	193.58
LFLASC 95%	0.044	1.12	81.8	564	9.37	64.56	8.26	56.91	0.151	6	1	0.81	0.970	169.77
LFLCSA 85%	0.044	1.12	73.6	507	10.12	69.73	9.55	65.80	0.139	56	1	0.66	0.642	112.44
LFLDSB 80%	0.044	1.12	70.8	488	9.82	67.66	9.31	64.15	0.119	390	170	0.56	0.454	79.51
LFLESA 75%	0.044	1.12	62.5	431	10.16	70.00	9.65	66.49	0.112	950	36	0.61	0.545	95.42
LFLFSA 70%	0.045	1.14	55.2	380	8.96	61.73	8.51	58.63	0.110	3,700	150	0.64	0.619	108.47
LFLGSA 65%	0.044	1.12	50.8	350	9.30	64.08	8.83	60.84	0.087	37,000	3,900	0.57	0.484	84.75
LFLISC 55%	0.043	1.09	42.6	294	9.27	63.87	8.87	61.11	0.127	240,000	8,200	0.47	0.322	56.44
LFLISH 55%	0.045	1.14	47.4	327	8.82	60.77	8.37	57.67	0.124	31,000	2,400	0.53	0.422	73.88
LFLISK 55%	0.047	1.19	38.5	265	8.23	56.70	7.79	53.67	0.112	240,000	150	0.45	0.317	55.59
LFLJSE 50%	0.044	1.12	39.7	274	9.01	62.08	8.56	58.98	0.087	52,000	4,000	0.44	0.283	49.52
LFLKSA 45%	0.044	1.12	34.3	236	8.93	61.53	8.48	58.43	0.099	300,000	9,600	0.40	0.231	40.48
LFLKSE 45%	0.044	1.12	35.2	243	9.41	64.83	8.88	61.18	0.107	370,000	8,800	0.39	0.220	38.46
LFLLSA 40%	0.044	1.12	33.7	232	9.52	65.59	8.99	61.94	0.112	8,600	1,900	0.36	0.190	33.27
LFLLSB 40%	0.043	1.09	32.9	227	9.68	66.70	9.17	63.18	0.096	39,000	37,000	0.34	0.166	28.99
LFLLSD 40%	0.045	1.14	30.2	208	9.10	62.70	8.63	59.46	0.126	480,000	7,500	0.38	0.212	37.12
LFLMSA 35%	0.045	1.14	30.2	208	9.03	62.22	8.65	59.60	0.116	9,500,000	4,300,000	0.34	0.179	31.42

Table B2

Individual Tension-Tension Edge Delamination Fatigue Results for IM7/8551-7 Composites at High Temperature No Precondition

Specimen Name	Thickness		Peak Stress		Initial Modulus		Final Modulus		R Ratio	Cycles to 5% Modulus Decay	Cycles to Delamination	Delamination Strain	Gc	Gc
	(in)	(mm)	(ksi)	(MPa)	(Msi)	(GPa)	(Msi)	(GPa)				(percent)	$(\frac{lb_f\ in}{in^2})$	(J/m^2)
LFLBPA 90%	0.044	1.12	74.2	511	9.14	62.97	8.68	59.81	0.138	330	11	0.82	1.00	175.69
LFLBPB 90%	0.045	1.14	73.9	509	9.50	65.46	9.01	62.08	0.109	36	1	0.76	0.864	151.28
LFLCPA 85%	0.044	1.12	70.6	486	10.22	70.42	9.71	66.90	0.144	86	6	0.68	0.690	120.76
LFLDPA 80%	0.044	1.12	65.6	452	9.04	62.29	8.57	59.05	0.133	490	1	0.70	0.733	128.29
LFLEPA 75%	0.043	1.09	66.0	455	10.23	70.48	9.71	66.90	0.105	320	1	0.61	0.541	94.79
LFLFPA 70%	0.045	1.14	59.1	407	9.07	62.49	8.59	59.19	0.103	490	1	0.64	0.612	107.12
LFLFPB 70%	0.045	1.14	54.7	377	9.13	62.91	8.66	59.67	0.109	3,800	750	0.60	0.546	95.67
LFLGPA 65%	0.045	1.14	53.7	370	8.87	61.11	8.37	57.67	0.118	15,000	9,900	0.57	0.493	86.37
LFLHPA 60%	0.043	1.09	50.9	351	9.16	63.11	8.70	59.94	0.104	5,800	9,400	0.55	0.437	76.59
LFLIPA 55%	0.045	1.14	42.0	289	8.91	61.39	8.45	58.22	0.114	200,000	160,000	0.45	0.301	52.75
LFLIPB 55%	0.044	1.12	46.9	323	10.18	70.14	9.63	66.35	0.099	24,000	3,200	0.45	0.299	52.27
LFLJPA 50%	0.044	1.12	41.7	287	8.97	61.80	8.52	58.70	0.106	140,000	6,700	0.45	0.299	52.27
LFLKPA 45%	0.044	1.12	36.2	249	8.88	61.18	8.42	58.01	0.118	41,000	5,500	0.41	0.247	43.18
LFLLPA 40%	0.044	1.12	31.8	219	9.90	68.21	9.40	64.77	0.104	7,900	1	0.31	0.145	25.45
LFLLPC 40%	0.045	1.14	32.8	226	8.96	61.73	8.51	58.63	0.118	960,000	5,800	0.37	0.208	36.34
LFLNPB 30%	0.044	1.12	24.5	169	8.86	61.05	8.40	57.88	0.110	19,000	1,000	0.24	0.088	15.49
LFLQPB 15%	0.044	1.12	12.9	89	9.55	65.80	9.45	65.11	0.119	*11,700,000	10,788,200	0.11	0.018	3.18

Table B3

Individual Tension-Tension Edge Delamination Fatigue Results for IM7/8551-7 Composites at Room Temperature High Spike

Specimen Name	Thickness		Peak Stress		Initial Modulus		Final Modulus		R Ratio	Cycles to 5% Modulus Decay	Cycles to Delamination	Delamination Strain	Gc	Gc
	(in)	(mm)	(ksi)	(MPa)	(Msi)	(GPa)	(Msi)	(GPa)				(percent)	($\frac{lb_f\ in}{in^2}$)	(J/m^2)
LFLAMB 95%	0.043	1.09	80.1	552	9.40	64.77	8.91	61.39	0.102	170	1	0.83	0.985	172.53
LFLAMC 95%	0.044	1.12	77.1	531	9.14	62.97	8.65	59.60	0.122	190	1	0.80	0.953	166.86
LFLBMA 90%	0.043	1.09	77.0	531	9.80	67.52	9.25	63.73	1.177	11	1	0.80	0.917	160.64
LFLBM[redacted] 90%	0.044	1.12	75.3	519	10.22	70.42	9.65	66.49	0.091	31	1	0.70	0.716	125.40
LFLBMC 90%	0.045	1.14	73.4	506	9.76	67.25	9.26	63.80	0.114	6	1	0.72	0.775	135.71
LFLDMA 80%	0.043	1.09	68.1	469	9.78	67.38	9.29	64.01	0.111	250	1	0.67	0.649	113.58
LFLDMB 80%	0.044	1.12	66.3	457	9.73	67.04	9.23	63.59	0.119	460	66	0.69	0.700	122.54
LFLFMA 70%	0.045	1.14	57.9	399	9.66	66.56	9.16	63.11	0.099	4,800	510	0.62	0.585	102.46
LFLFMB 70%	0.045	1.14	58.6	404	9.48	65.32	8.99	61.94	0.101	900	100	0.60	0.534	93.46
LFLHMA 60%	0.045	1.12	50.2	346	9.60	66.14	9.10	62.70	0.102	27,000	320	0.53	0.428	75.00
LFLHMB 60%	0.044	1.14	51.0	351	9.62	66.28	9.13	62.91	0.101	8,400	960	0.51	0.382	66.88
LFLJMB 50%	0.045	1.12	43.5	300	8.49	58.50	8.06	55.53	0.089	74,000	540	0.50	0.378	66.26
LFLKMA 45%	0.044	1.12	37.3	257	9.40	64.77	8.92	61.46	0.107	20,000	3,300	0.40	0.230	40.27
LFLKMB 45%	0.044	1.14	37.5	258	9.85	67.87	9.32	64.21	0.092	25,000	1,100	0.38	0.213	37.27
LFLKMC 45%	0.045	1.12	37.2	256	9.44	65.04	8.94	61.60	0.097	98,000	3,400	0.39	0.229	40.15
LFLLMA 40%	0.044	1.09	33.0	227	8.81	60.70	8.35	57.53	0.132	36,000	3,300	0.37	0.197	34.58
LFLMMA	0.043	1.09	29.6	204	9.02	62.15	8.55	58.91	0.090	290,000	860	0.31	0.138	24.24
LFLOMA	0.043	1.09	21.4	147	9.71	66.90	9.21	63.46	0.096	13,000	3,400	0.20	0.058	10.19
LFLQMA	0.044	1.12	12.6	87	9.57	65.94	9.12	62.84	0.102	2,000,000	8,800	0.13	0.025	4.30

Table B4

Individual Tension-Tension Edge Delamination Fatigue Results for IM7/8551-7 Composites at High Temperature High Spike

Specimen Name	Thickness		Peak Stress		Initial Modulus		Final Modulus		R Ratio	Cycles to 5% Modulus Decay	Cycles to Delamination	Delamination Strain	Gc	Gc
	(in)	(mm)	(ksi)	(MPa)	(Msi)	(GPa)	(Msi)	(GPa)				(percent)	$\left(\frac{lb_f\ in}{in^2}\right)$	(J/m^2)
LFHASC 95%	0.049	1.24	77.8	535	7.60	52.36	7.21	49.68	0.102	320	1	0.98	3.74	655.03
LFHASD 95%	0.044	1.12	78.8	543	8.97	61.80	7.94	54.71	0.113	6	1	0.87	2.64	462.85
LFHCSA 85%	0.044	1.12	71.5	493	8.82	60.77	8.23	56.70	0.123	16	1	0.82	2.31	404.32
LFHCSB 85%	0.045	1.14	71.4	492	9.80	67.52	9.30	64.08	0.103	26	1	0.72	1.83	320.04
LFHDSA 80%	0.049	1.24	67.5	465	8.18	56.36	7.73	53.26	0.125	31	1	0.83	2.69	471.50
LFHESA 75%	0.044	1.12	64.4	444	9.15	63.04	8.66	59.67	0.106	590	51	0.72	1.78	312.06
LFHFSA 70%	0.051	1.30	59.0	407	8.09	55.74	7.66	52.78	0.116	220	1	0.71	2.03	354.67
LFHFSB 70%	0.043	1.09	59.1	407	10.37	71.45	9.84	67.80	0.101	690	86	0.58	1.12	196.68
LFHGSA 65%	0.043	1.09	55.1	380	10.41	71.72	9.87	68.00	0.100	1,400	110	0.53	0.954	167.10
LFHHSB 60%	0.042	1.07	50.3	347	9.32	64.21	8.83	60.84	0.107	6,300	390	0.54	0.953	166.93
LFHISA 55%	0.043	1.09	46.8	322	9.25	63.73	8.72	60.08	0.102	6,800	1,300	0.50	0.832	145.76
LFHJSA 50%	0.043	1.09	42.3	291	9.57	65.94	9.08	62.56	0.145	50,000	1,400	0.42	0.611	106.94
LFHJSB 50%	0.044	1.12	42.4	292	8.92	61.46	8.48	58.43	0.125	23,000	2,600	0.48	0.791	138.50
LFHKSA 45%	0.044	1.12	37.8	260	9.73	67.04	9.23	63.59	0.106	48,000	7,300	0.39	0.540	94.49
LFHMSB 35%	0.044	1.12	29.2	201	9.09	62.63	8.36	57.60	0.111	1,150,000	210,000	0.33	0.388	67.91
LFHQSB 15%	0.045	1.14	11.8	81	8.88	61.18	8.81	60.70	0.106	10,000,000	9,700,000	0.08	0.026	4.50

ORIGINAL PAGE IS OF POOR QUALITY

ORIGINAL PAGE IS
OF POOR QUALITY

Table B5

Individual Tension-Tension Edge Delamination Fatigue Results for
IM7/8551-7 Composites at Room Temperature High Mean

Specimen Name	Thickness		Peak Stress		Initial Modulus		Final Modulus		R Ratio	Cycles to 5% Modulus Decay	Cycles to Delami-nation	Delami-nation Strain	Gc	Gc
	(in)	(mm)	(ksi)	(MPa)	(Msi)	(GPa)	(Msi)	(GPa)				(percent)	($\frac{lb_f\ in}{in^2}$)	(J/m^2)
LFHAPB 95%	0.044	1.12	79.5	548	9.15	63.04	8.64	59.53	0.143	140	21	0.86	2.60	455.45
LFHBPA 90%	0.043	1.09	75.6	521	10.28	70.83	9.73	67.04	0.128	11	1	0.70	1.67	292.32
LFHCPA 85%	0.045	1.14	72.8	502	8.91	61.39	8.39	57.81	0.091	16	1	0.76	2.03	355.81
LFHDPA 80%	0.043	1.09	67.7	466	10.33	71.17	9.79	67.45	0.119	170	1	0.61	1.25	219.18
LFHEPA 75%	0.043	1.09	64.6	445	10.46	72.07	9.94	68.49	0.115	520	1	0.59	1.18	206.37
LFHFPA 70%	0.044	1.12	60.7	418	9.87	68.00	9.34	64.35	0.090	500	1	0.59	1.22	213.33
LFHGPA 65%	0.043	1.09	54.3	374	10.21	70.35	9.70	66.83	0.125	2,600	41	0.51	0.891	155.94
LFHHPA 60%	0.044	1.12	52.6	362	9.91	68.28	9.37	64.56	0.111	480	1	0.51	0.908	158.95
LFHHPB 60%	0.043	1.09	52.1	359	9.40	64.77	8.92	61.46	0.106	9,900	1,200	0.55	1.04	181.26
LFHIPA 55%	0.044	1.12	47.9	330	9.45	65.11	8.96	61.73	0.097	7,500	1,200	0.50	0.859	150.36
LFHJPA 50%	0.045	1.14	42.8	295	9.69	66.76	9.17	63.18	0.090	41,000	61,400	0.43	0.660	115.64
LFHKPA 45%	0.043	1.09	39.4	271	8.90	61.32	8.40	57.88	0.097	130,000	19,000	0.45	0.688	120.46
LFHLPA 40%	0.044	1.12	33.6	232	8.86	61.04	8.37	57.67	0.107	150,000	34,000	0.40	0.548	95.94
LFHMPA 35%	0.044	1.12	30.0	207	9.55	65.80	9.05	62.35	0.099	370,000	70,000	0.32	0.347	60.78
LFHQPB 15%	0.043	1.09	11.9	82	10.11	69.66	10.48	72.21	0.093	*11,000,000	11,000,000	0.10	0.035	6.19

ORIGINAL PAGE IS
OF POOR QUALITY

Table B6

Individual Tension-Tension Edge Delamination Fatigue Results for
IM7/8551-7 Composites at High Temperature High Mean

Specimen Name	Thickness		Peak Stress		Initial Modulus		Final Modulus		R Ratio	Cycles to 5% Modulus Decay	Cycles to Delamination	Delamination Strain	Gc	Gc
	(in)	(mm)	(ksi)	(MPa)	(Msi)	(GPa)	(Msi)	(GPa)				(percent)	($\frac{lb_f\ in}{in^2}$)	(J/m^2)
LFHAMB 95%	0.045	1.14	81.7	563	9.02	62.15	8.50	58.57	0.089	41	1	0.84	2.51	439.27
LFHBMA 90%	0.044	1.12	76.2	525	9.31	64.21	8.66	59.67	0.089	16	1	0.76	1.99	348.82
LFHCMA 85%	0.044	1.12	72.7	501	9.07	62.49	8.60	59.25	0.093	140	1	0.74	1.92	336.94
LFHDMA 80%	0.044	1.12	69.5	479	9.07	62.49	8.61	59.32	0.081	130	21	0.76	2.03	355.30
LFHEMA 75%	0.042	1.07	63.1	435	9.77	67.32	9.28	63.94	0.134	390	21	0.64	1.36	237.25
LFHFMA 70%	0.044	1.12	58.7	404	10.01	68.97	9.50	65.46	0.117	340	1	0.54	1.00	175.53
LFHFMB 70%	0.044	1.12	58.9	406	9.51	65.52	9.01	62.08	0.130	790	36	0.63	1.37	239.30
LFHGMA 65%	0.045	1.14	54.4	375	9.30	64.08	8.81	60.70	0.120	1,700	1	0.53	0.991	173.56
LFHHMA 60%	0.045	1.14	50.9	351	9.52	65.59	9.03	62.22	0.144	2,700	11	0.51	0.925	161.92
LFHIMA 55%	0.045	1.14	47.1	325	9.17	63.18	8.69	59.87	0.134	2,600	150	0.50	0.882	154.39
LFHIMC 55%	0.044	1.12	46.8	322	9.83	67.73	9.27	63.87	0.127	9,800	1,300	0.44	0.667	116.78
LFHJMA 50%	0.044	1.12	42.5	293	9.80	67.52	9.28	63.94	0.120	17,000	940	0.38	0.507	88.83
LFHJMB 50%	0.042	1.07	41.7	287	9.63	66.35	9.04	62.29	0.111	180,000	2,600	0.44	0.628	109.95
LFHKMA 45%	0.045	1.14	38.2	263	9.28	63.94	8.81	60.70	0.142	44,000	9,100	0.42	0.621	108.77
LFHLMA 40%	0.044	1.12	32.9	227	8.89	61.25	8.45	58.22	0.139	160,000	4,500	0.36	0.446	78.01
LFHMMA 35%	0.044	1.12	29.5	203	9.15	63.04	8.87	61.11	0.119	2,370,000	890,000	0.33	0.369	64.69
LFHMMC 35%	0.042	1.07	27.5	189	8.88	61.18	8.34	57.46	0.142	7,400,000	2,000,000	0.31	0.321	56.20

STRAIN ENERGY RELEASE RATE AT ONSET OF DELAMINATION

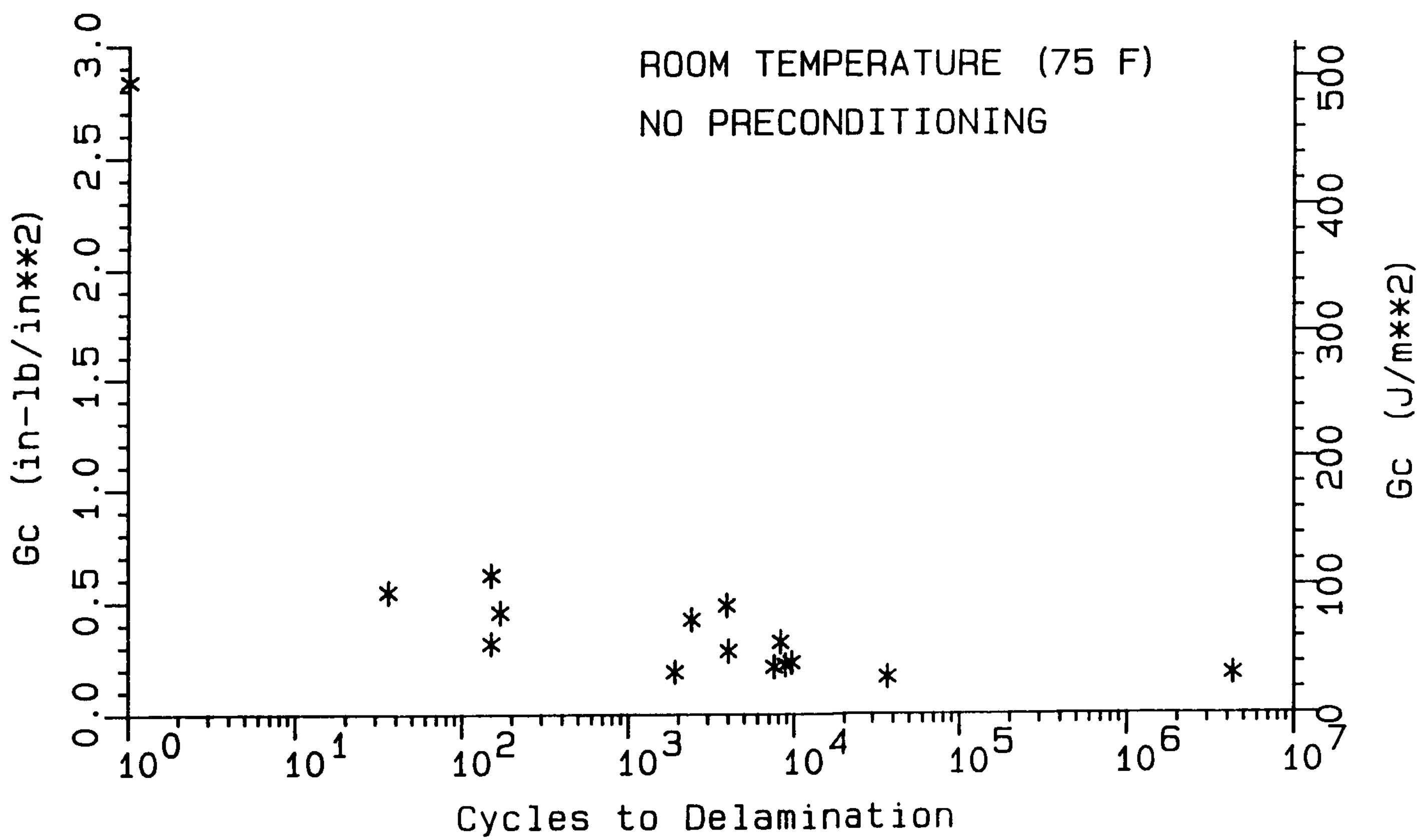

STRAIN ENERGY RELEASE RATE AT ONSET OF DELAMINATION

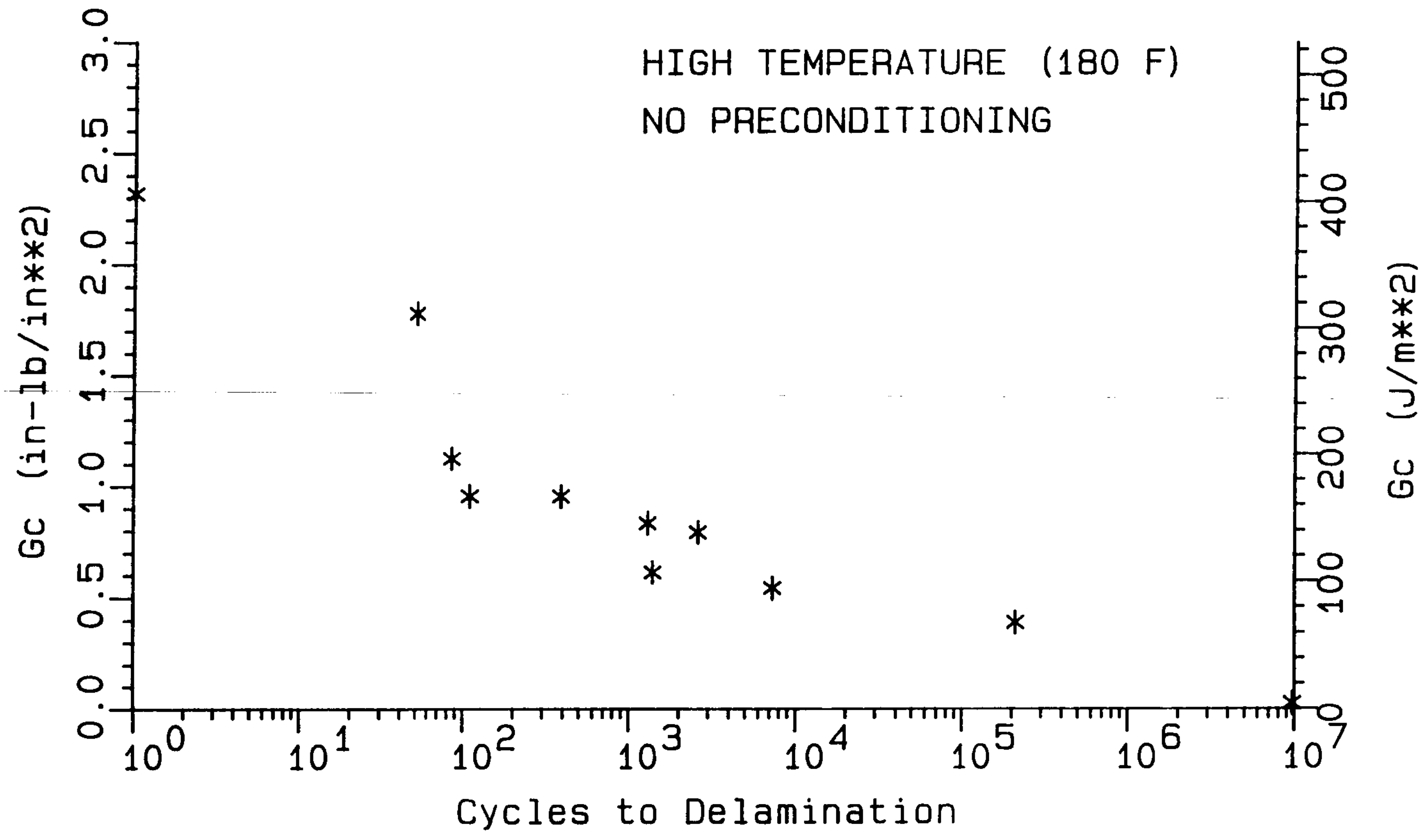

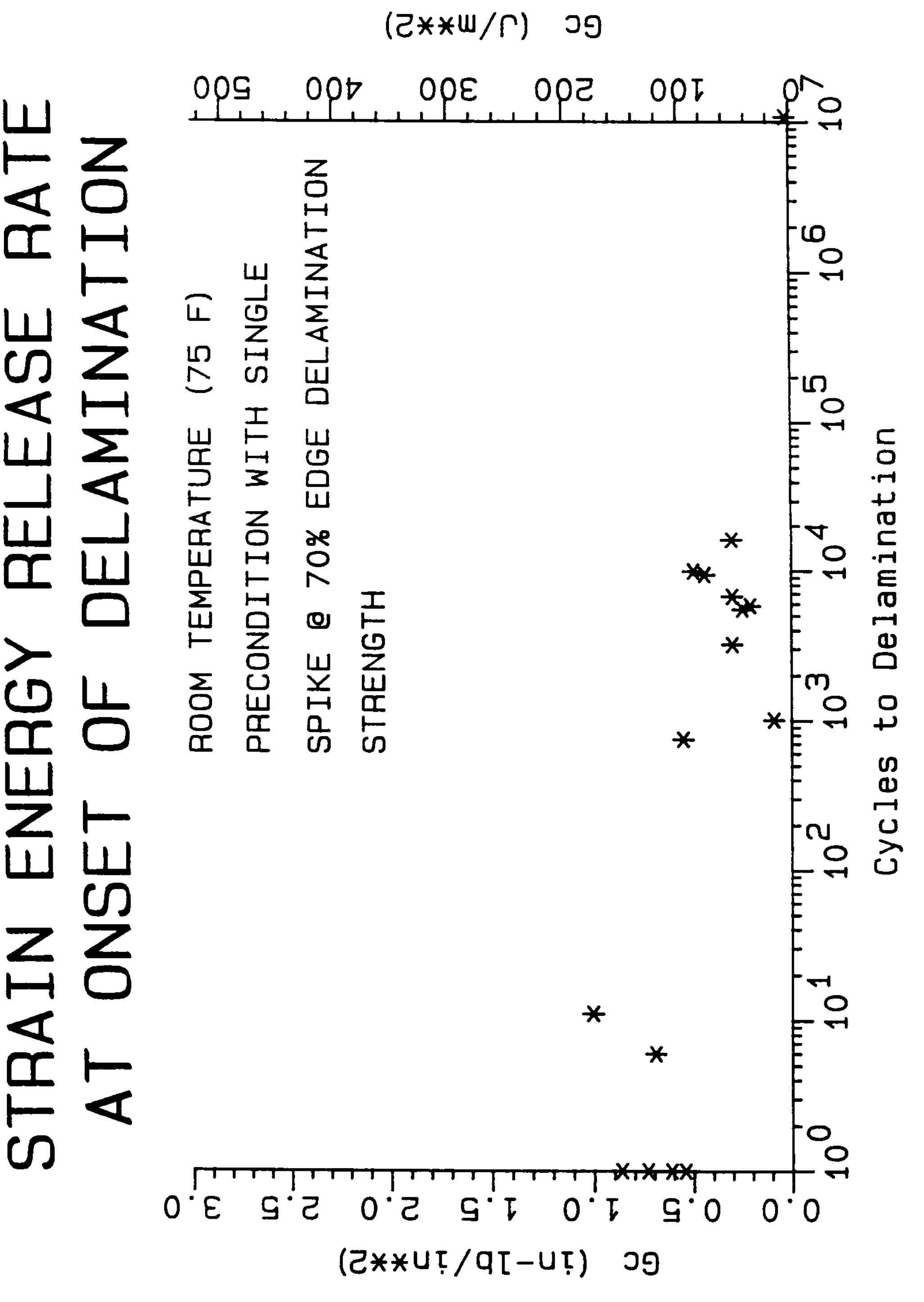
STRAIN ENERGY RELEASE RATE
AT ONSET OF DELAMINATION
ROOM TEMPERATURE (75 F)
PRECONDITION WITH SINGLE
SPIKE @ 70% EDGE DELAMINATION
STRENGTH
Gc (in-lb/in**2)
0.0
0.5
1.0
1.5
2.0
2.5
3.0
Gc (J/m**2)
100
200
300
400
500
10^0
10^1
10^2
10^3
10^4
10^5
10^6
10^7
Cycles to Delamination

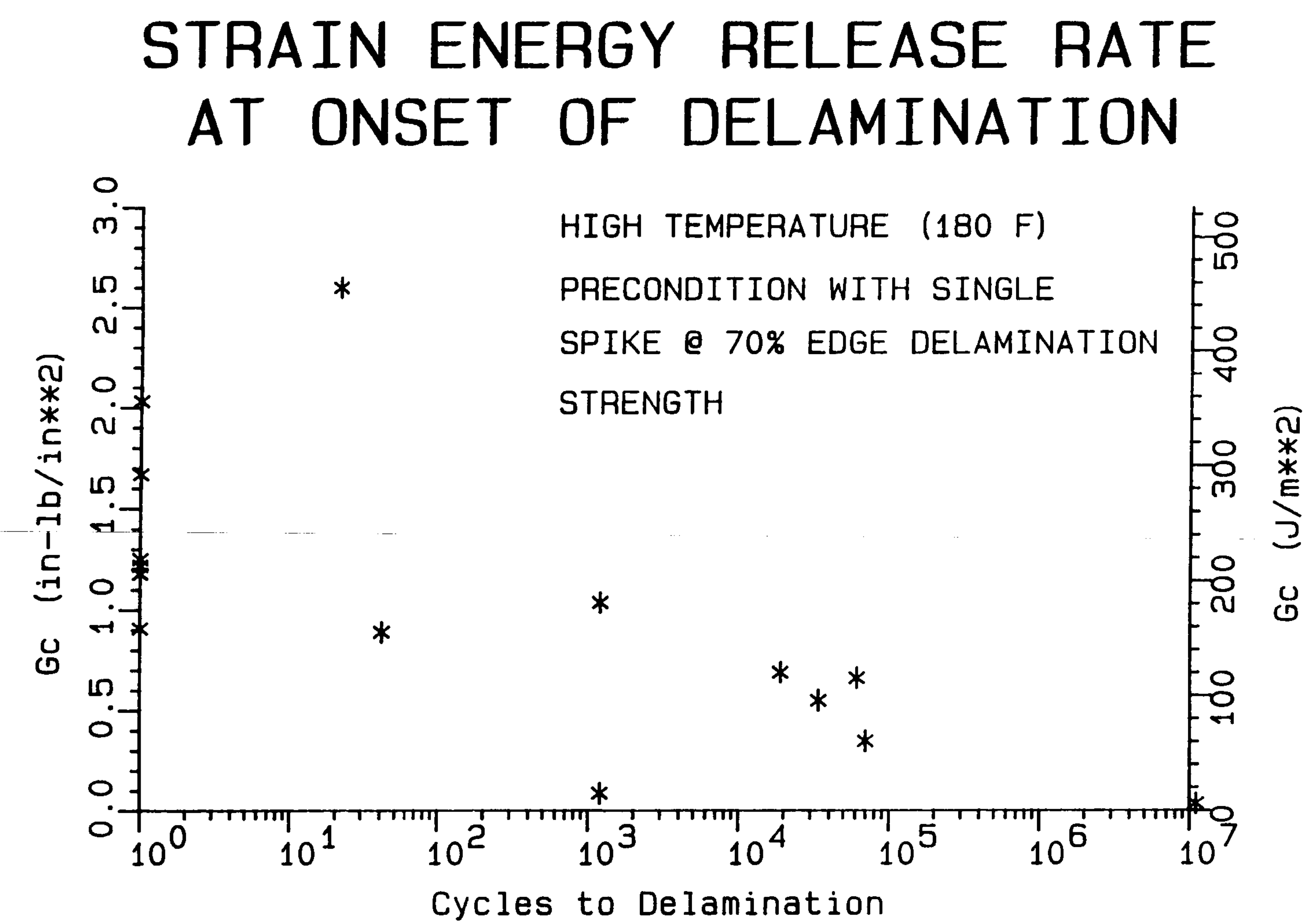
STRAIN ENERGY RELEASE RATE
AT ONSET OF DELAMINATION
HIGH TEMPERATURE (180 F)
PRECONDITION WITH SINGLE
SPIKE @ 70% EDGE DELAMINATION
STRENGTH
Gc (in-lb/in**2)
0.0
0.5
1.0
1.5
2.0
2.5
3.0
Gc (J/m**2)
0
100
200
300
400
500
10^0
10^1
10^2
10^3
10^4
10^5
10^6
10^7
Cycles to Delamination

STRAIN ENERGY RELEASE RATE AT ONSET OF DELAMINATION

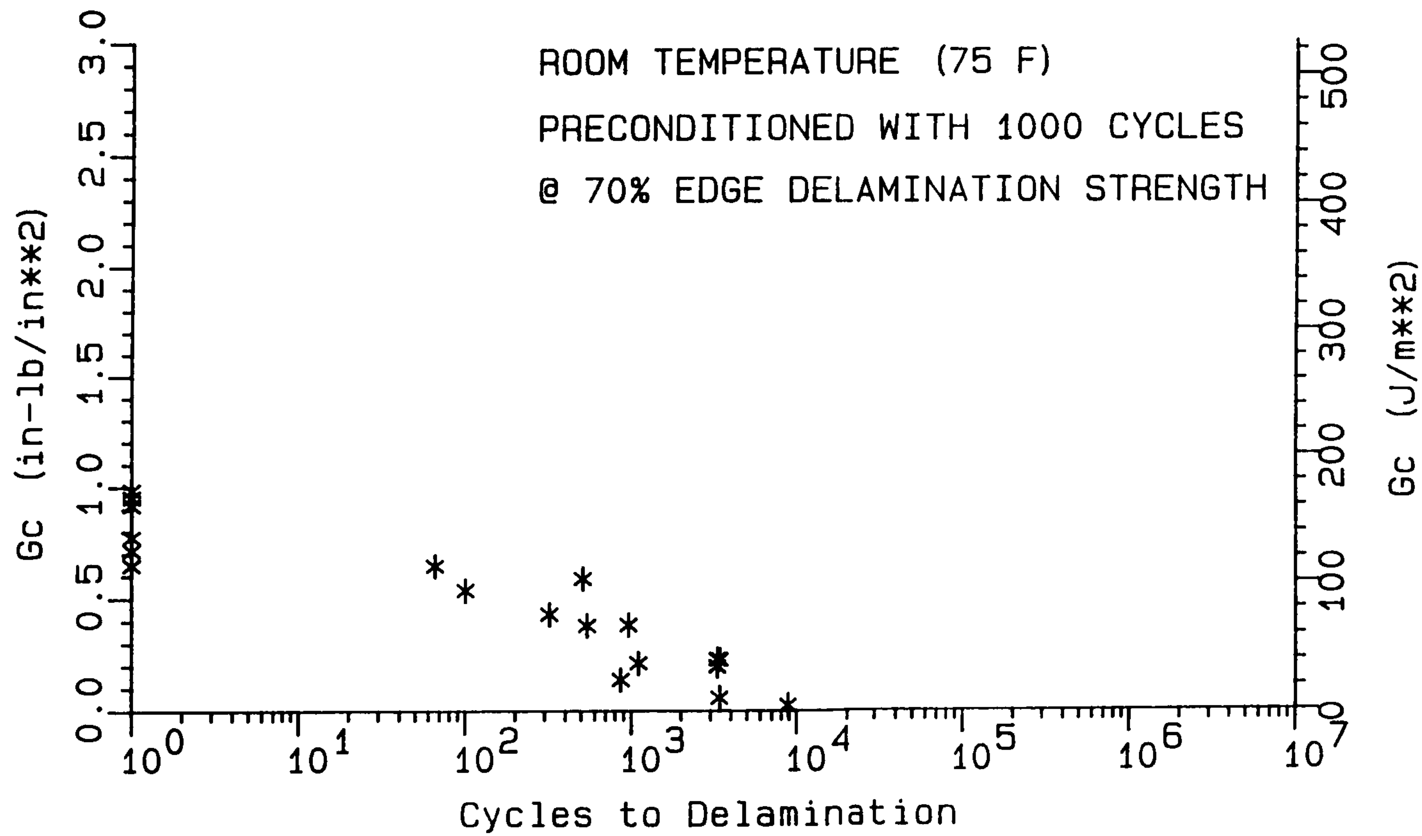

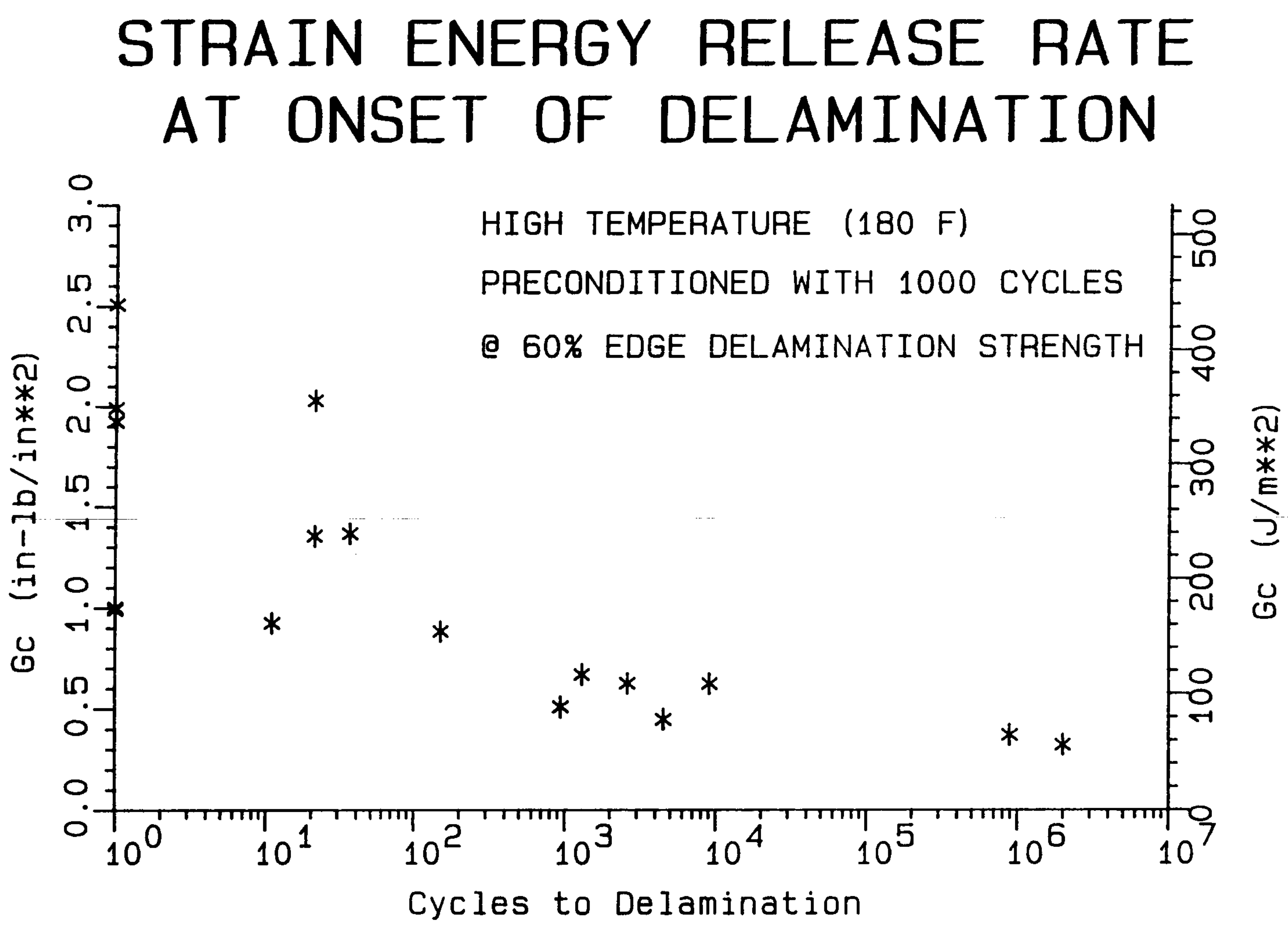
STRAIN ENERGY RELEASE RATE
AT ONSET OF DELAMINATION
HIGH TEMPERATURE (180 F)
PRECONDITIONED WITH 1000 CYCLES
@ 60% EDGE DELAMINATION STRENGTH
Gc (in-lb/in**2)
0.0
0.5
1.0
1.5
2.0
2.5
3.0
Gc (J/m**2)
0
100
200
300
400
500
10^0
10^1
10^2
10^3
10^4
10^5
10^6
10^7
Cycles to Delamination

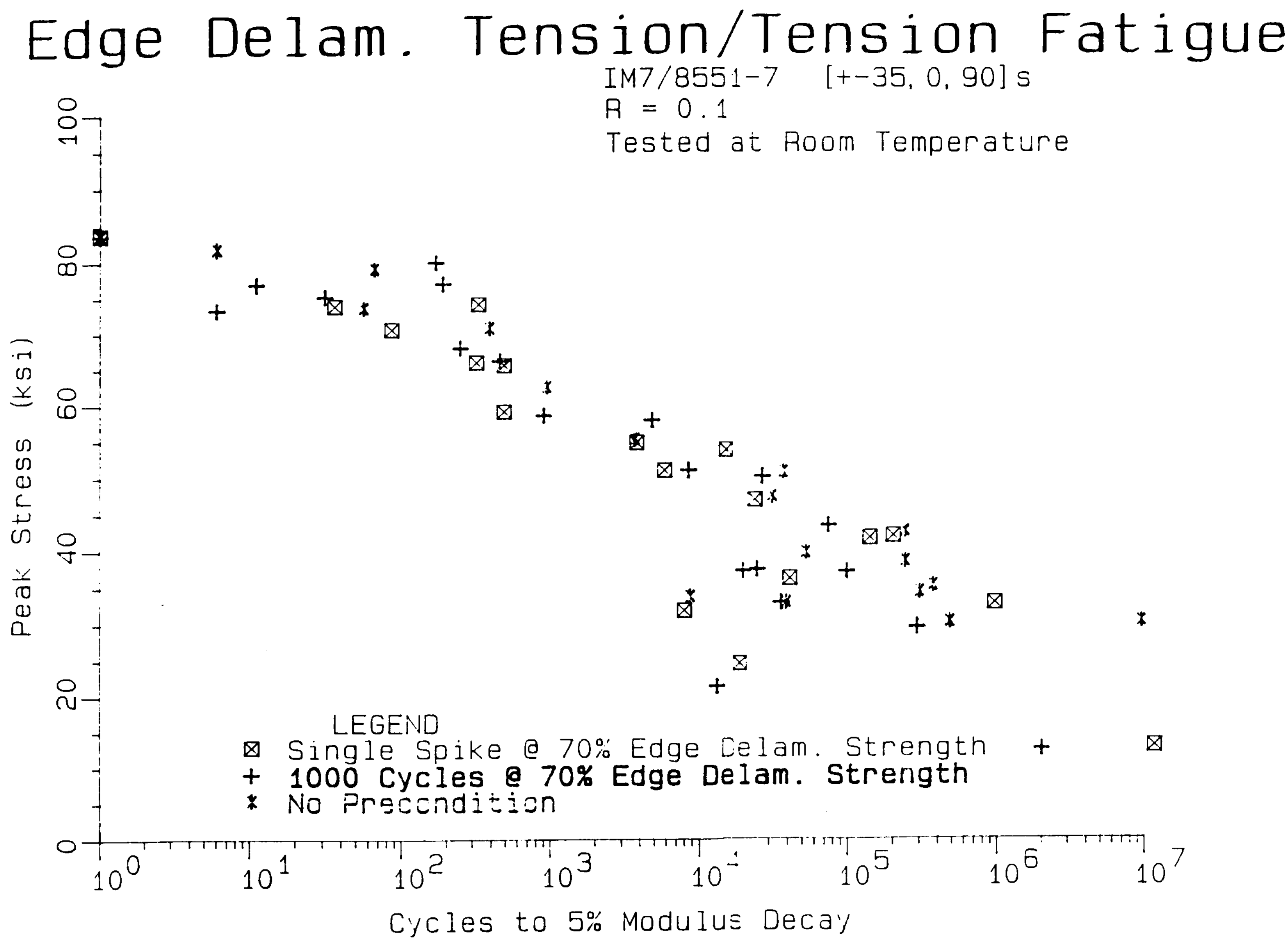

Edge Delam. Tension/Tension Fatigue
IM7/8551-7 [+-35, 0, 90]s
R = 0.1
Tested at Room Temperature
Peak Stress (ksi)
0
20
40
60
80
100
10^0
10^1
10^2
10^3
10^5
10^6
10^7
Cycles to 5% Modulus Decay
LEGEND
Single Spike @ 70% Edge Delam. Strength
1000 Cycles @ 70% Edge Delam. Strength
No Precondition

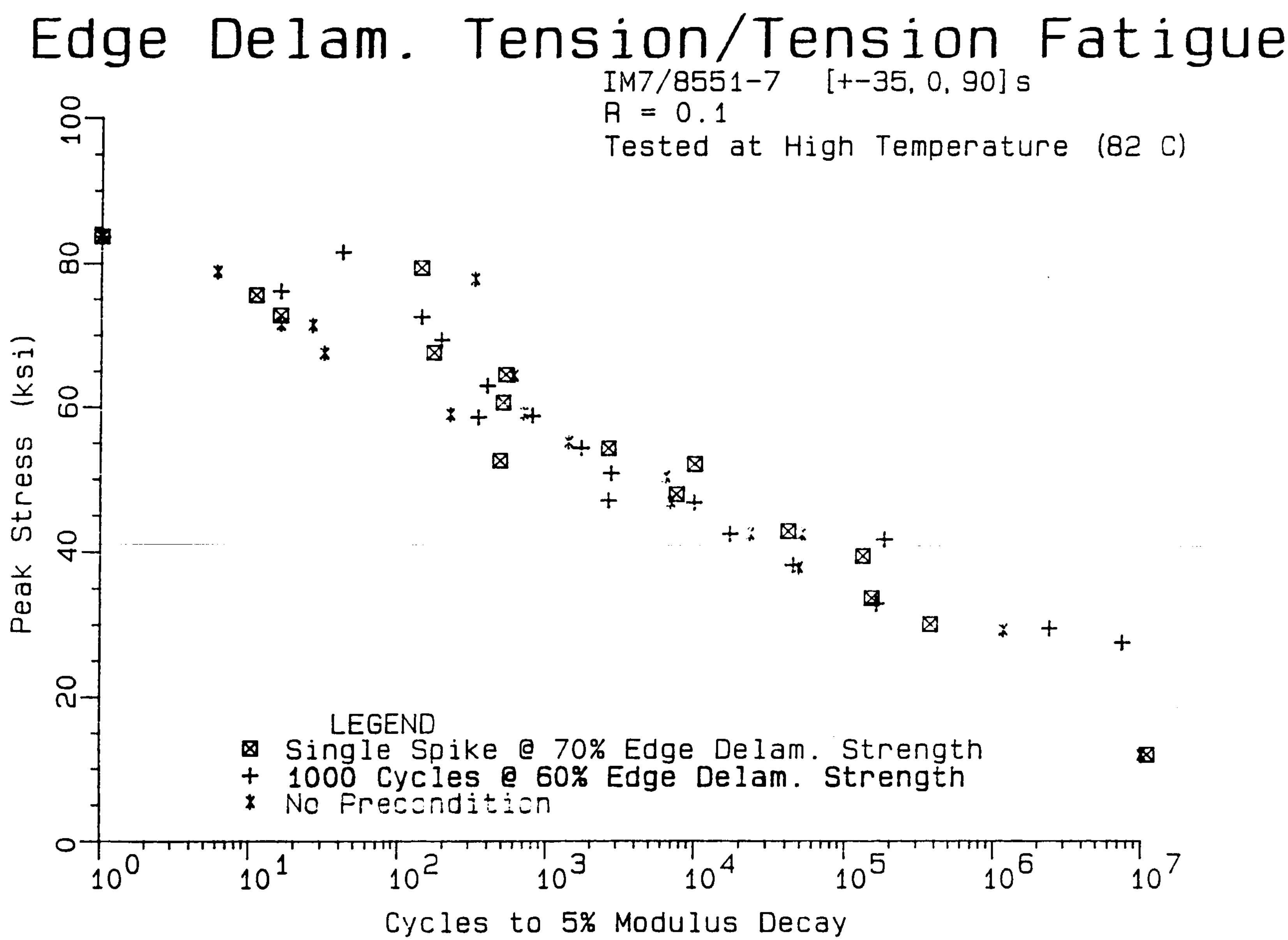

Edge Delam. Tension/Tension Fatigue
IM7/8551-7 [+-35, 0, 90]s
R = 0.1
Tested at High Temperature (82 C)
Peak Stress (ksi)
0
20
40
60
80
100
10^0
10^1
10^2
10^3
10^4
10^5
10^6
10^7
Cycles to 5% Modulus Decay
LEGEND
Single Spike @ 70% Edge Delam. Strength
1000 Cycles @ 60% Edge Delam. Strength
No Precondition

Edge Delam. Tension/Tension Fatigue

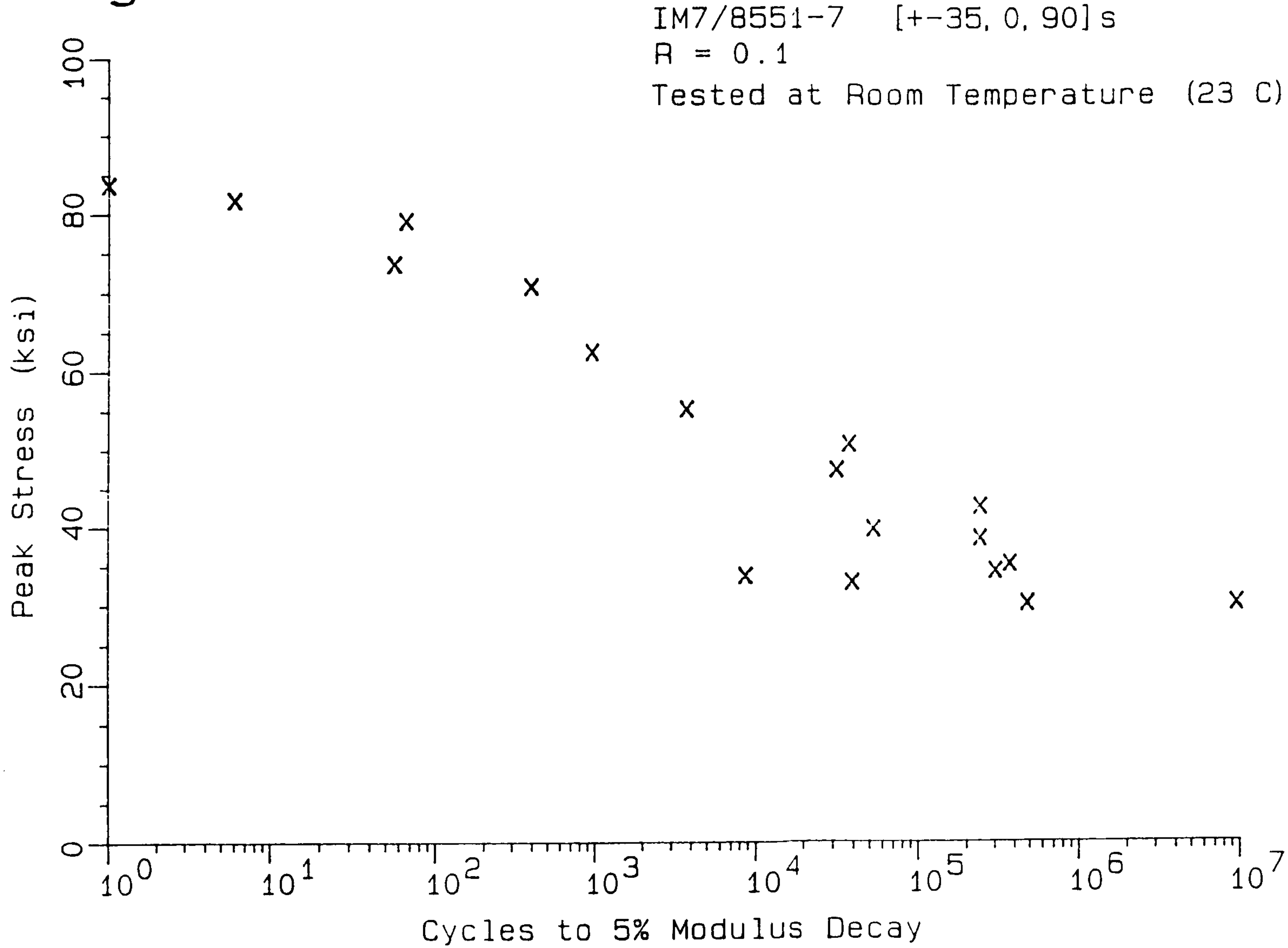

Edge Delam. Tension/Tension Fatigue

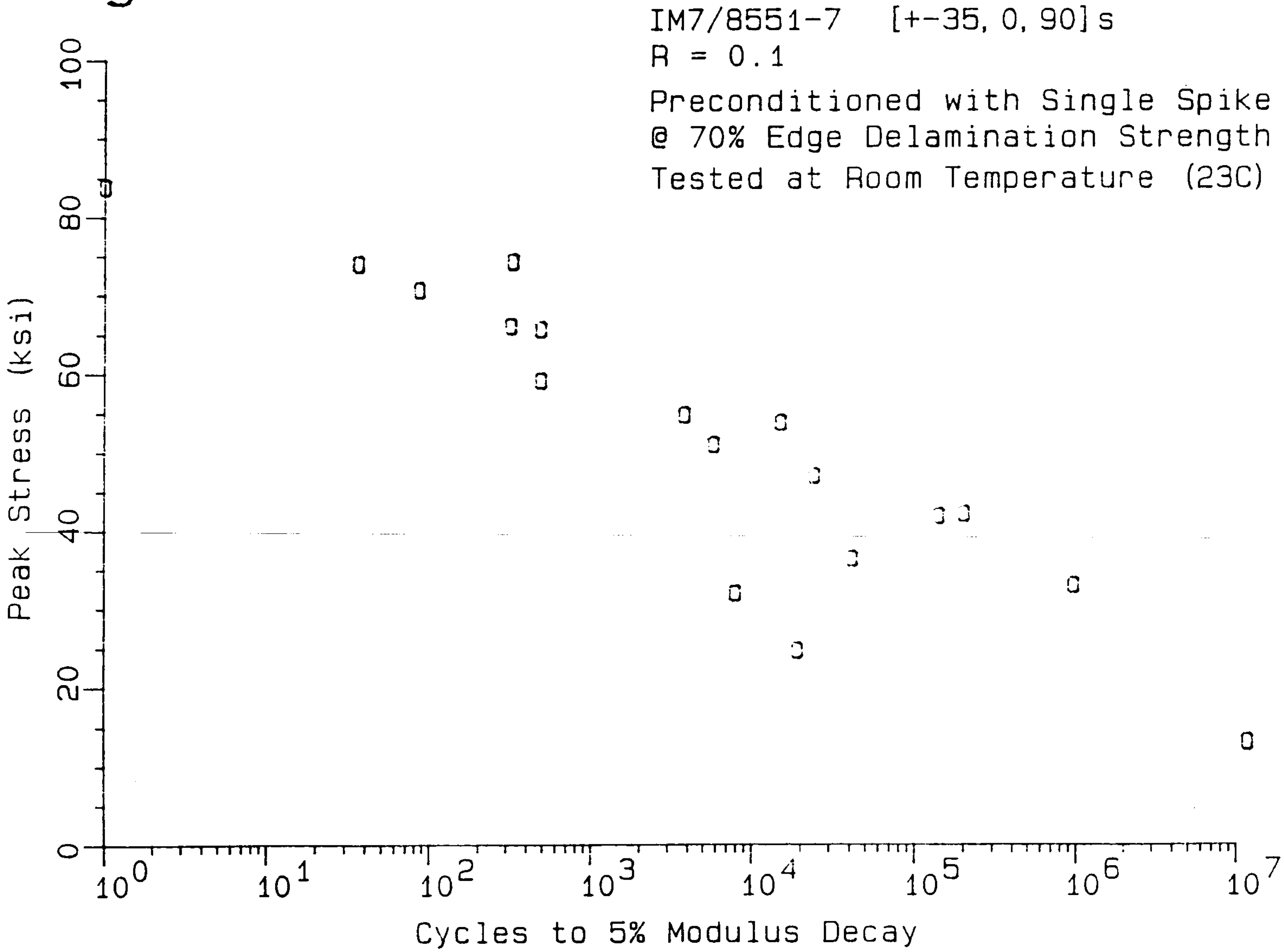

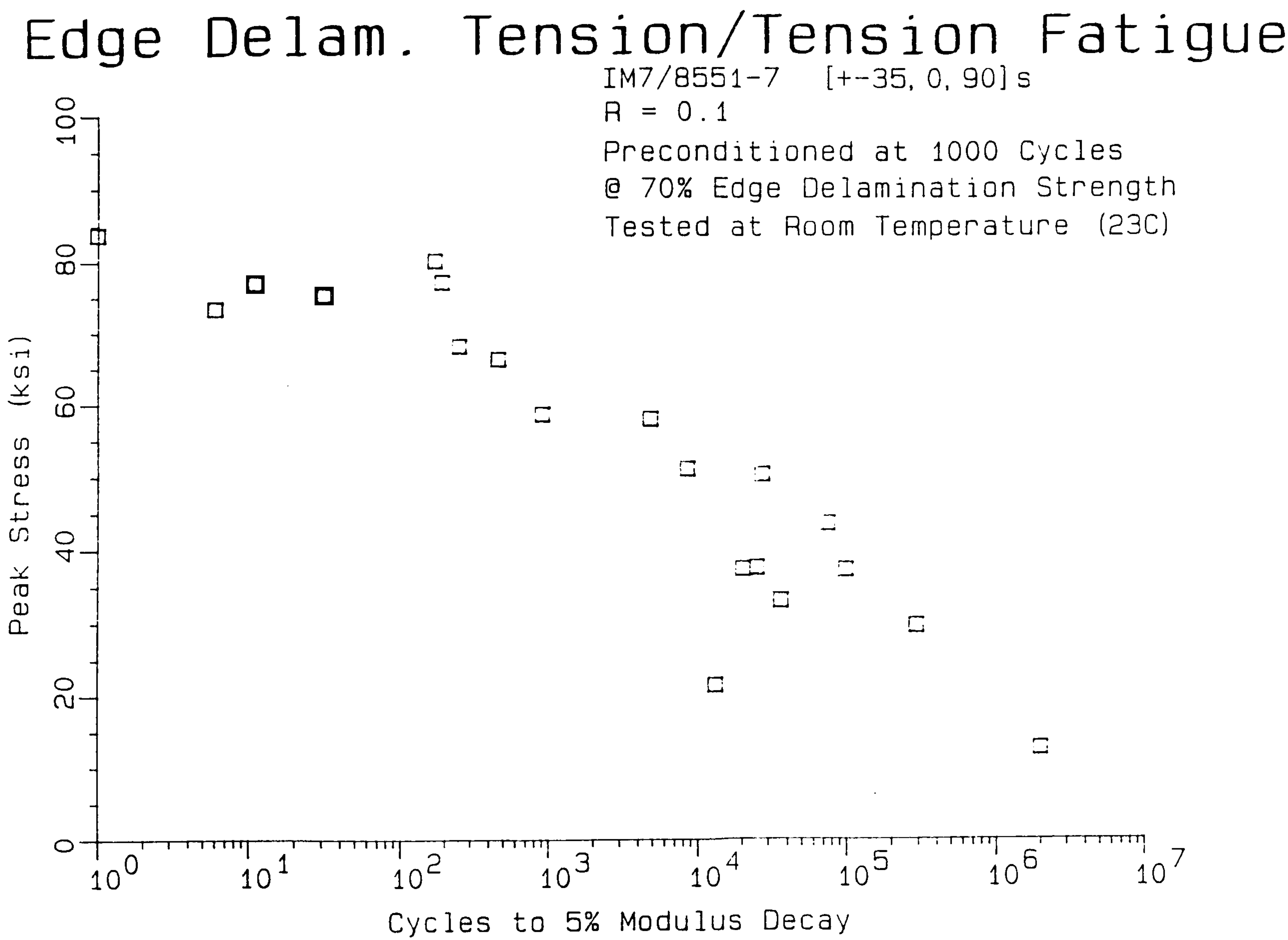
Edge Delam. Tension/Tension Fatigue
IM7/8551-7 [+-35, 0, 90]s
R = 0.1
Preconditioned at 1000 Cycles
@ 70% Edge Delamination Strength
Tested at Room Temperature (23C)
Peak Stress (ksi)
0
20
40
60
80
100
10^0
10^1
10^2
10^3
10^4
10^5
10^6
10^7
Cycles to 5% Modulus Decay

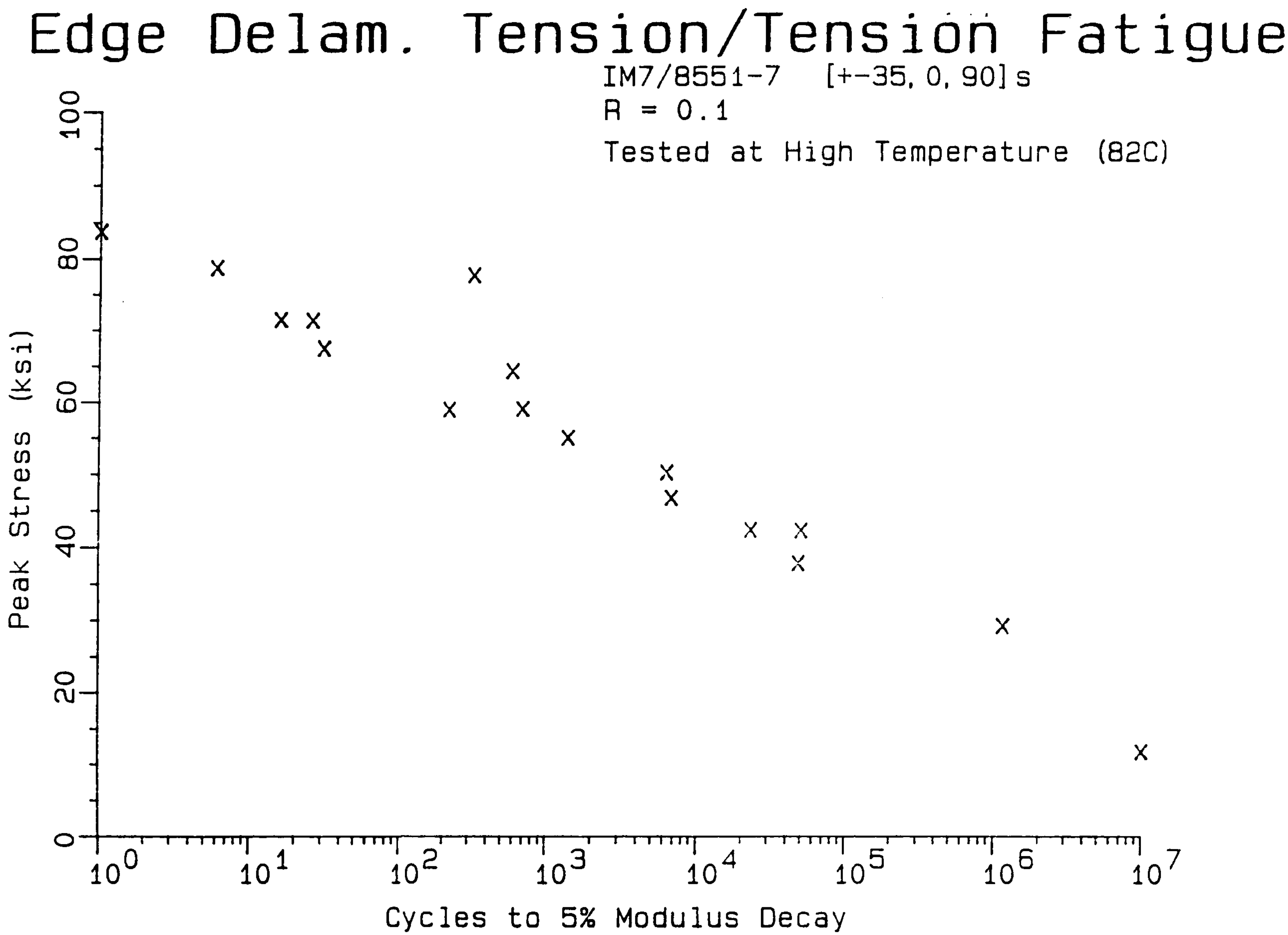
Edge Delam. Tension/Tension Fatigue
IM7/8551-7 [+-35, 0, 90]s
R = 0.1
Tested at High Temperature (82C)
Peak Stress (ksi)
Cycles to 5% Modulus Decay
0
20
40
60
80
100
10^0
10^1
10^2
10^3
10^4
10^5
10^6
10^7

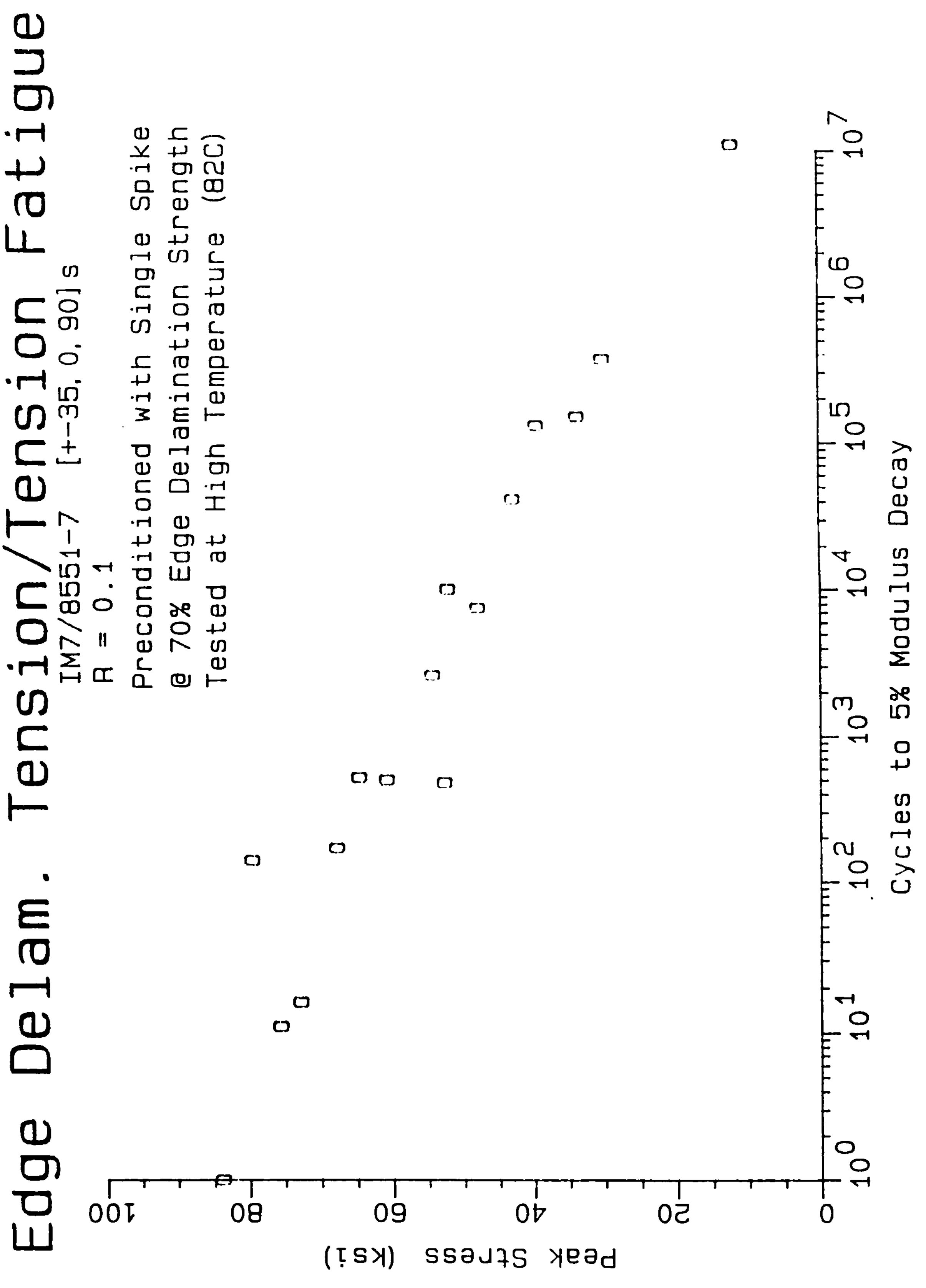
Edge Delam. Tension/Tension Fatigue
IM7/8551-7 [+-35, 0, 90]s
R = 0.1
Preconditioned with Single Spike
@ 70% Edge Delamination Strength
Tested at High Temperature (82C)
Peak Stress (ksi)
0
20
40
60
80
100
10^0
10^1
10^2
10^3
10^4
10^5
10^6
10^7
Cycles to 5% Modulus Decay

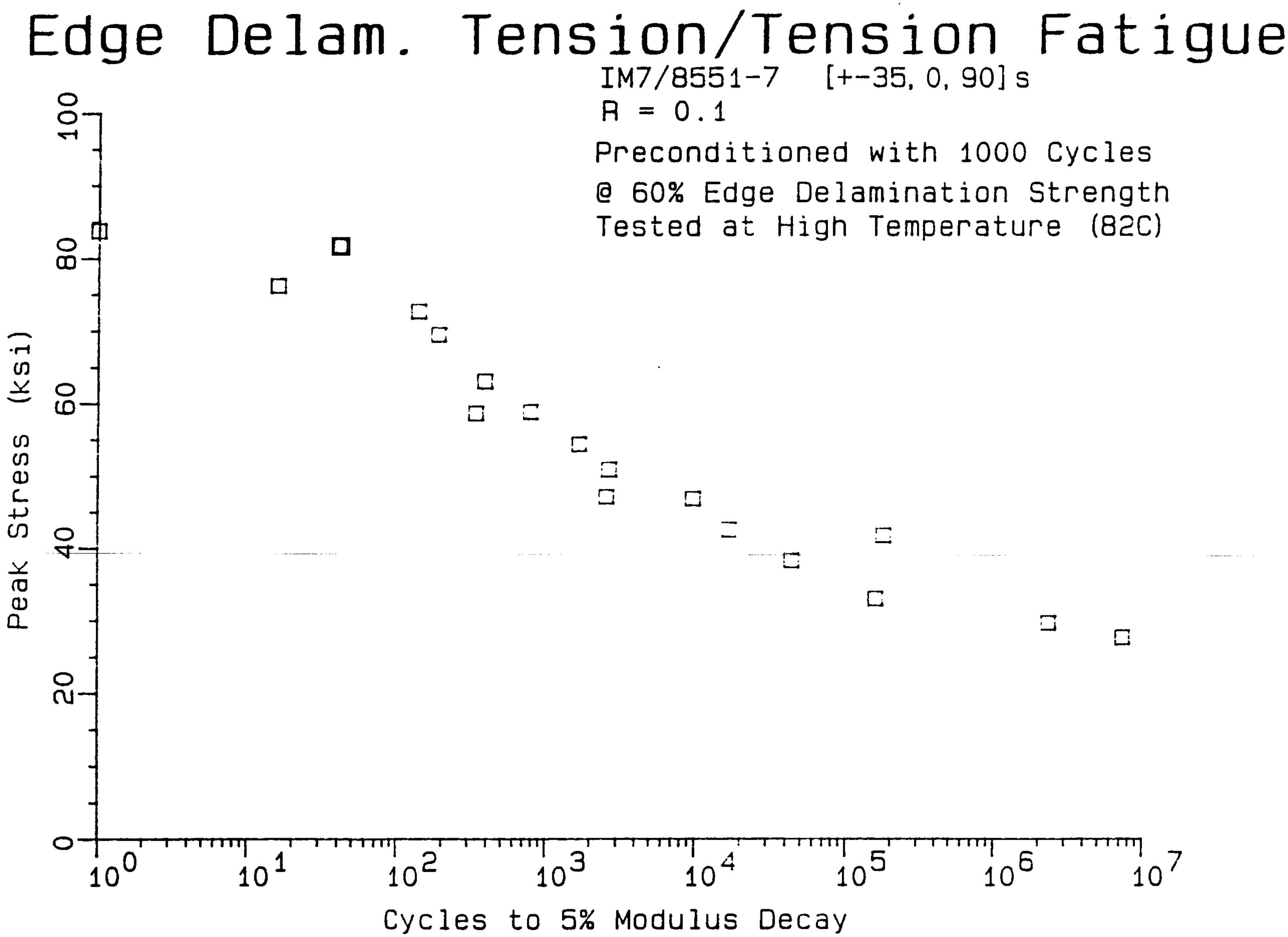
Edge Delam. Tension/Tension Fatigue
IM7/8551-7 [+-35, 0, 90]s
R = 0.1
Preconditioned with 1000 Cycles
@ 60% Edge Delamination Strength
Tested at High Temperature (82C)
Peak Stress (ksi)
0
20
40
60
80
100
10^0
10^1
10^2
10^3
10^4
10^5
10^6
10^7
Cycles to 5% Modulus Decay

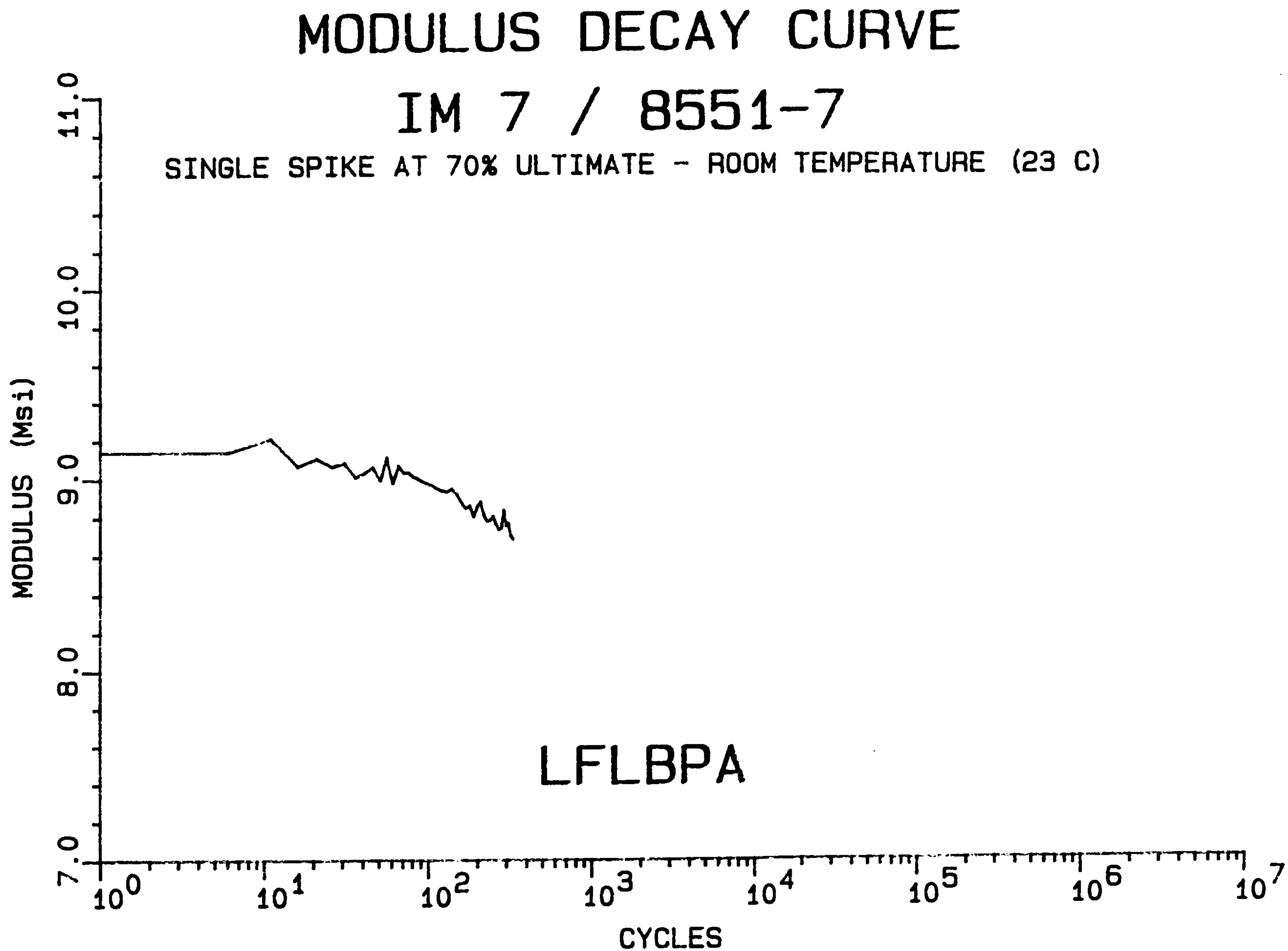
MODULUS DECAY CURVE
IM 7 / 8551-7
SINGLE SPIKE AT 70% ULTIMATE - ROOM TEMPERATURE (23 C)
MODULUS (Msi)
11.0
10.0
9.0
8.0
7.0
LFLBPA
10^0
10^1
10^2
10^3
10^4
10^5
10^6
10^7
CYCLES

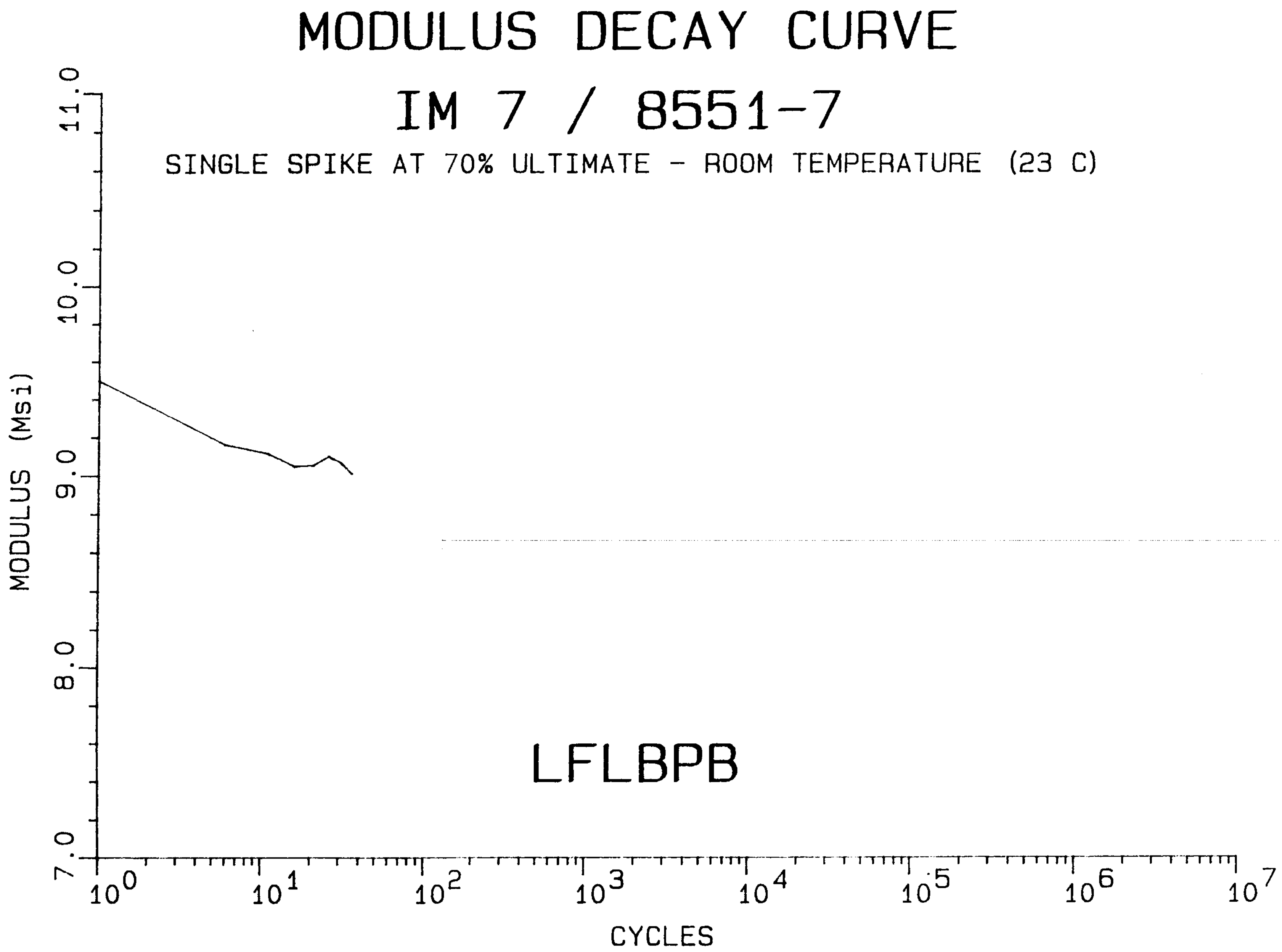
MODULUS DECAY CURVE
IM 7 / 8551-7
SINGLE SPIKE AT 70% ULTIMATE - ROOM TEMPERATURE (23 C)
MODULUS (Msi)
11.0
10.0
9.0
8.0
7.0
LFLBPB
10^0
10^1
10^2
10^3
10^4
10^5
10^6
10^7
CYCLES

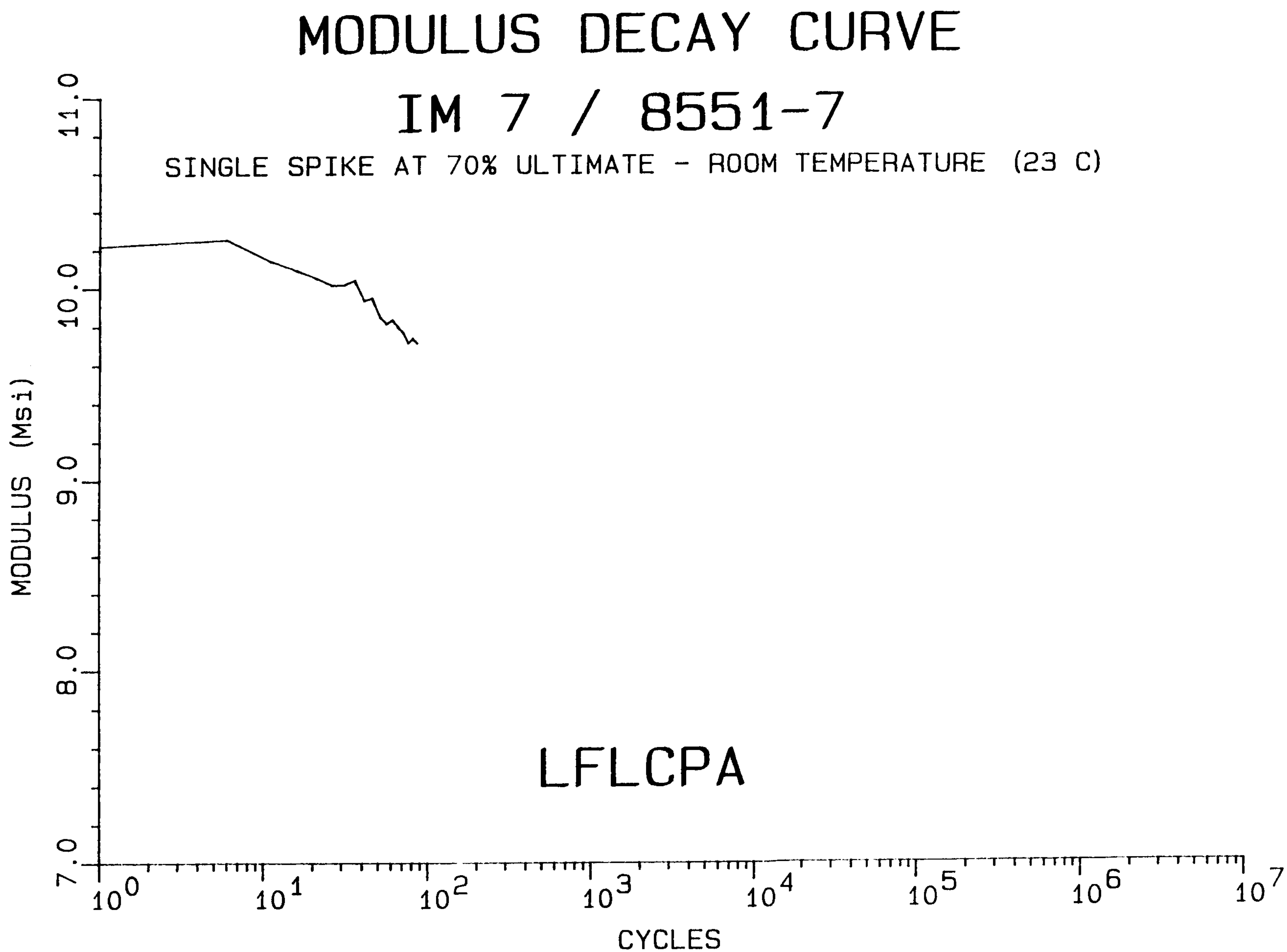

MODULUS DECAY CURVE
IM 7 / 8551-7
SINGLE SPIKE AT 70% ULTIMATE - ROOM TEMPERATURE (23 C)
LFLCPA
MODULUS (Msi)
11.0
10.0
9.0
8.0
7.0
CYCLES
10^0
10^1
10^2
10^3
10^4
10^5
10^6
10^7

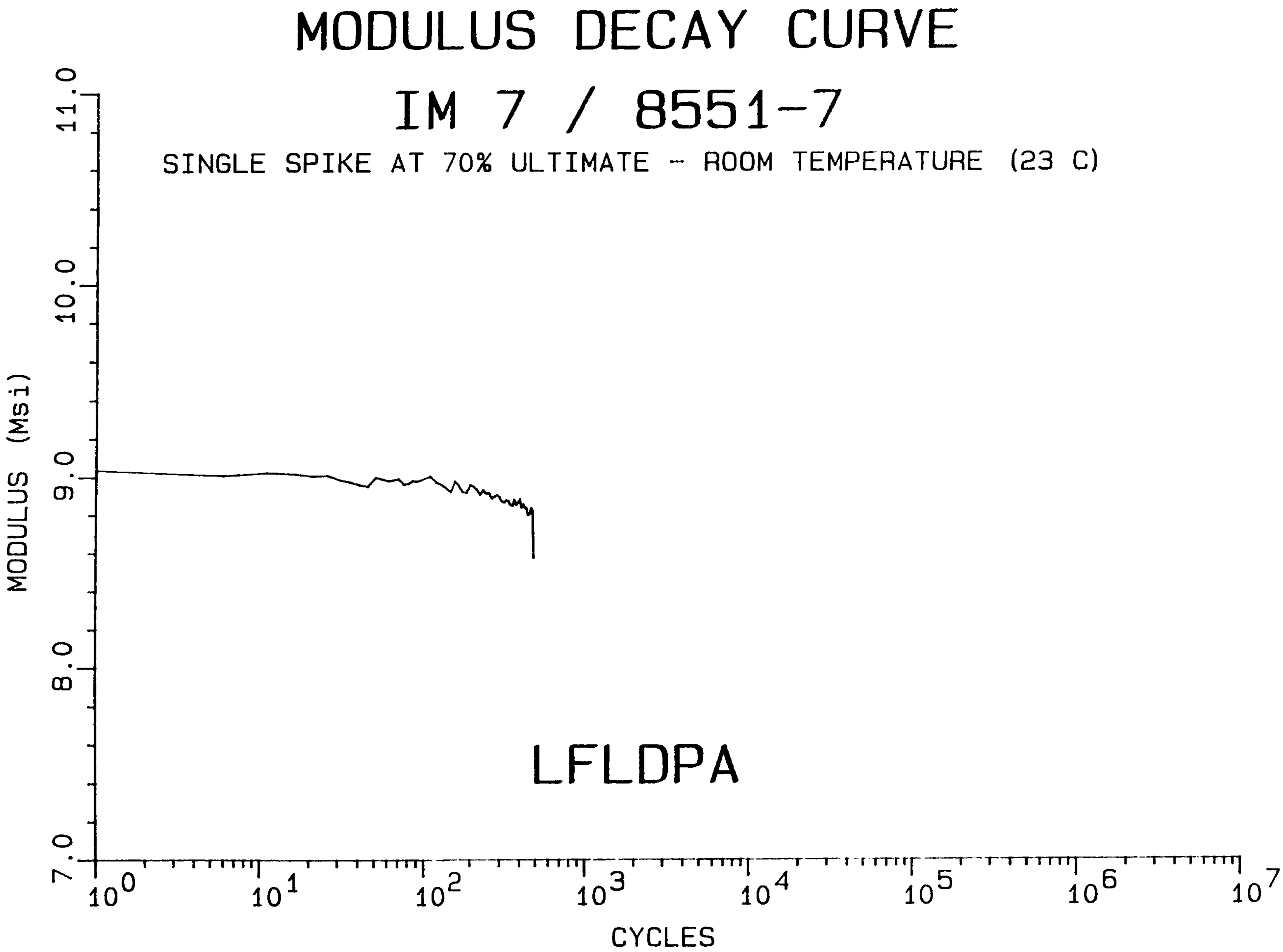
MODULUS DECAY CURVE
IM 7 / 8551-7
SINGLE SPIKE AT 70% ULTIMATE - ROOM TEMPERATURE (23 C)
LFLDPA
MODULUS (Msi)
CYCLES
11.0
10.0
9.0
8.0
7.0
10^0
10^1
10^2
10^3
10^4
10^5
10^6
10^7

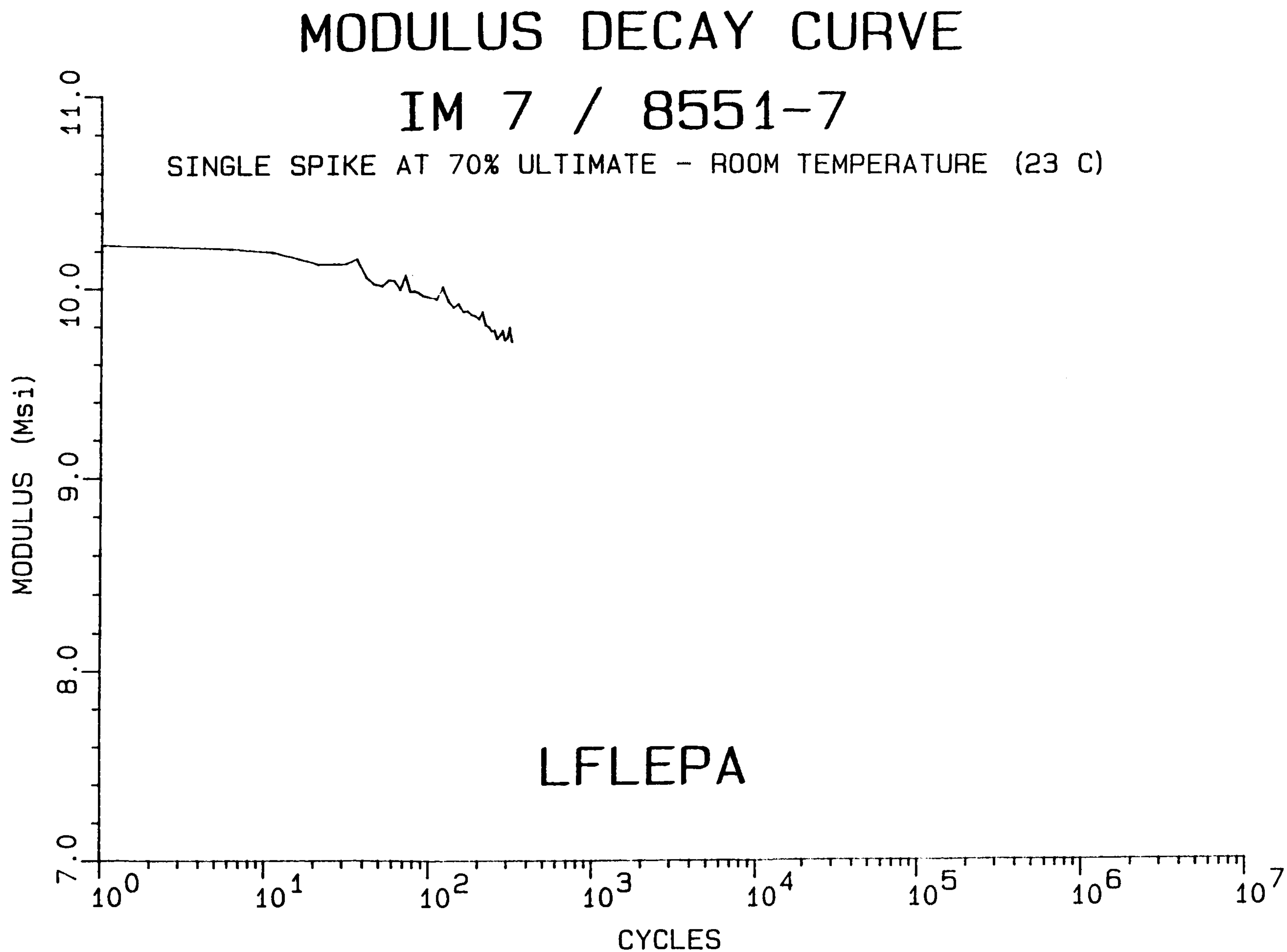
MODULUS DECAY CURVE
IM 7 / 8551-7
SINGLE SPIKE AT 70% ULTIMATE - ROOM TEMPERATURE (23 C)
MODULUS (Msi)
11.0
10.0
9.0
8.0
7.0
LFLEPA
10^0
10^1
10^2
10^3
10^4
10^5
10^6
10^7
CYCLES

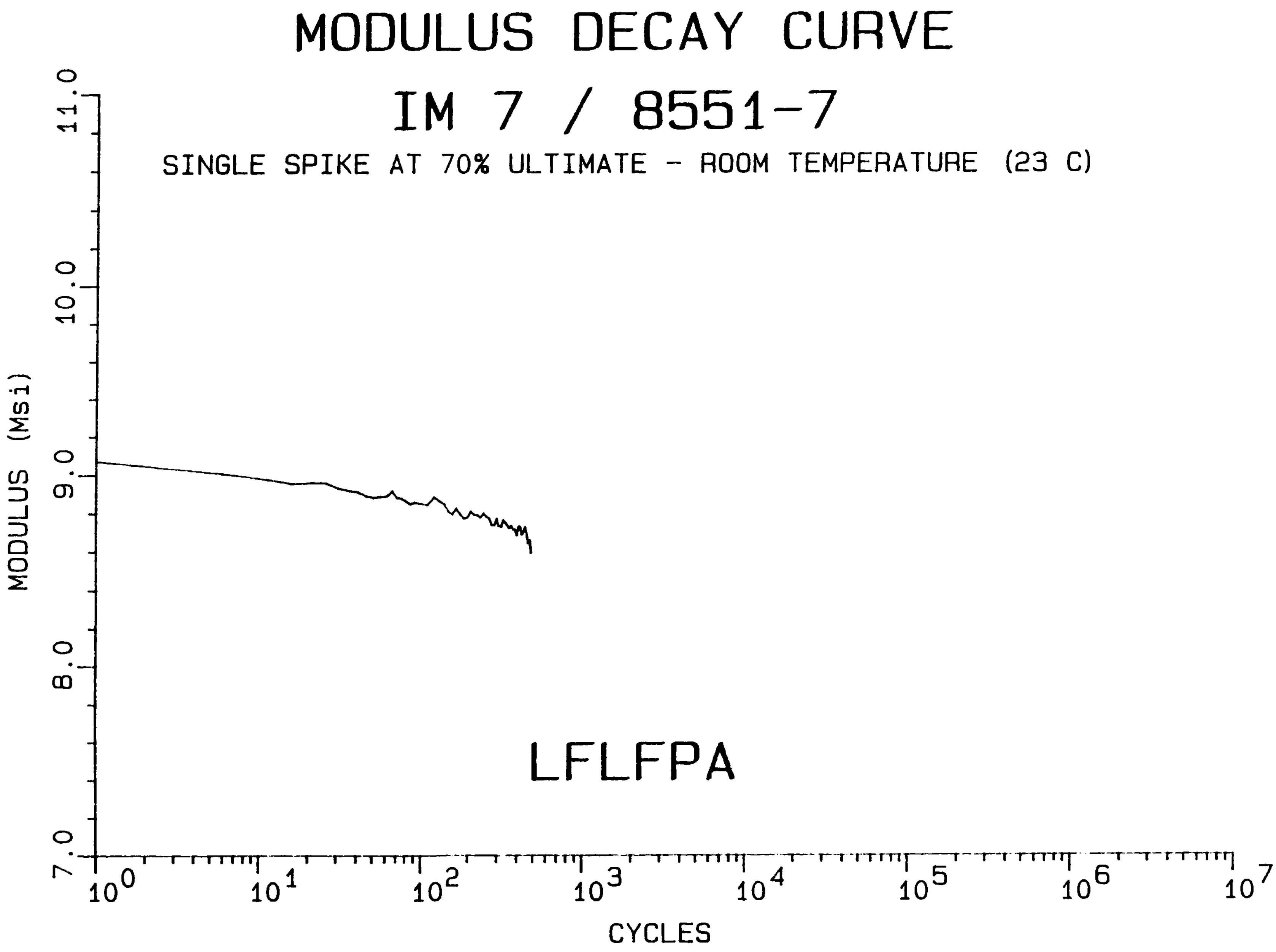
MODULUS DECAY CURVE
IM 7 / 8551-7
SINGLE SPIKE AT 70% ULTIMATE - ROOM TEMPERATURE (23 C)
MODULUS (Msi)
11.0
10.0
9.0
8.0
7.0
CYCLES
10^0
10^1
10^2
10^3
10^4
10^5
10^6
10^7
LFLFPA

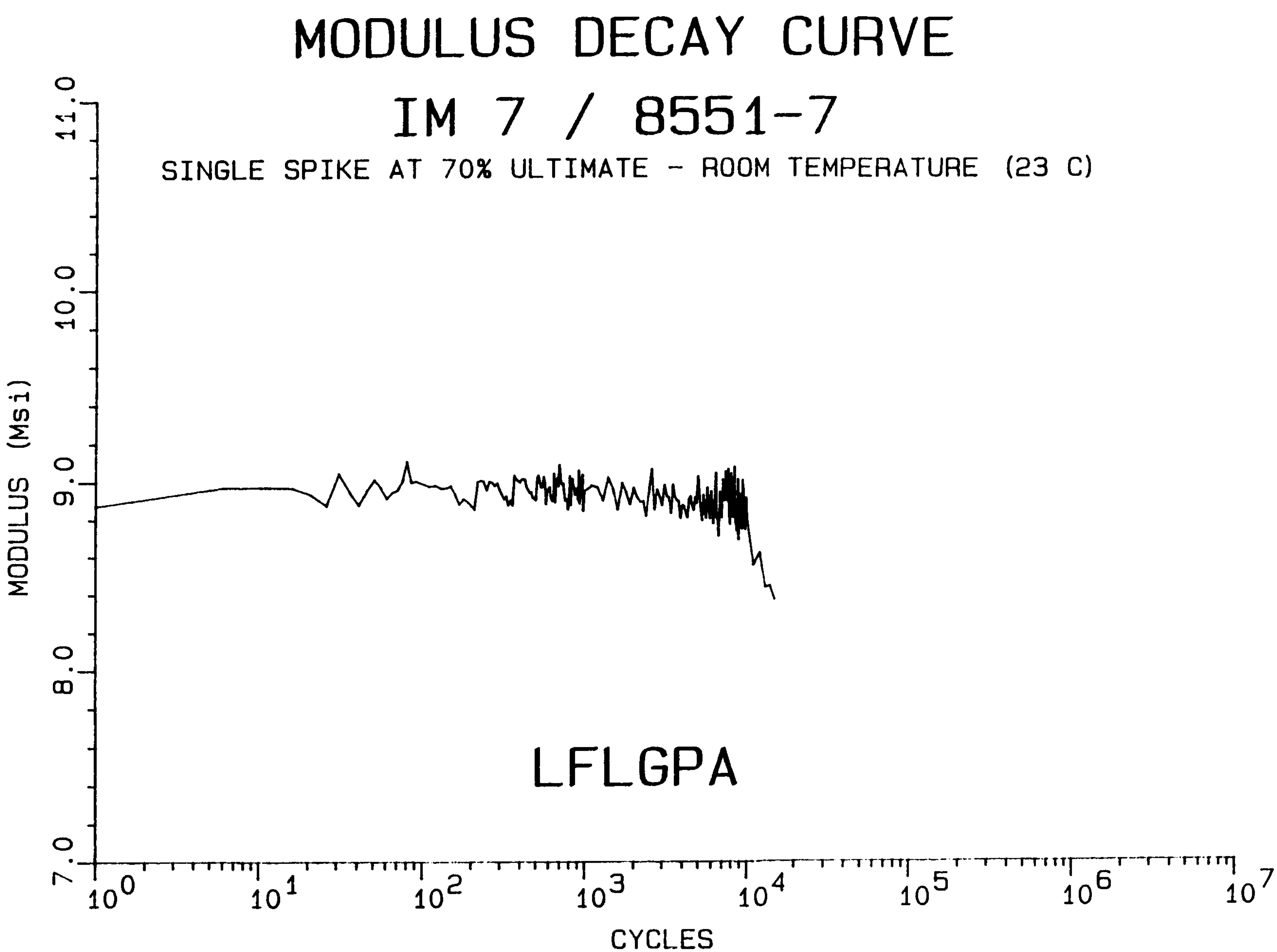
MODULUS DECAY CURVE
IM 7 / 8551-7
SINGLE SPIKE AT 70% ULTIMATE - ROOM TEMPERATURE (23 C)
MODULUS (Msi)
11.0
10.0
9.0
8.0
7.0
LFLGPA
10^0
10^1
10^2
10^3
10^4
10^5
10^6
10^7
CYCLES

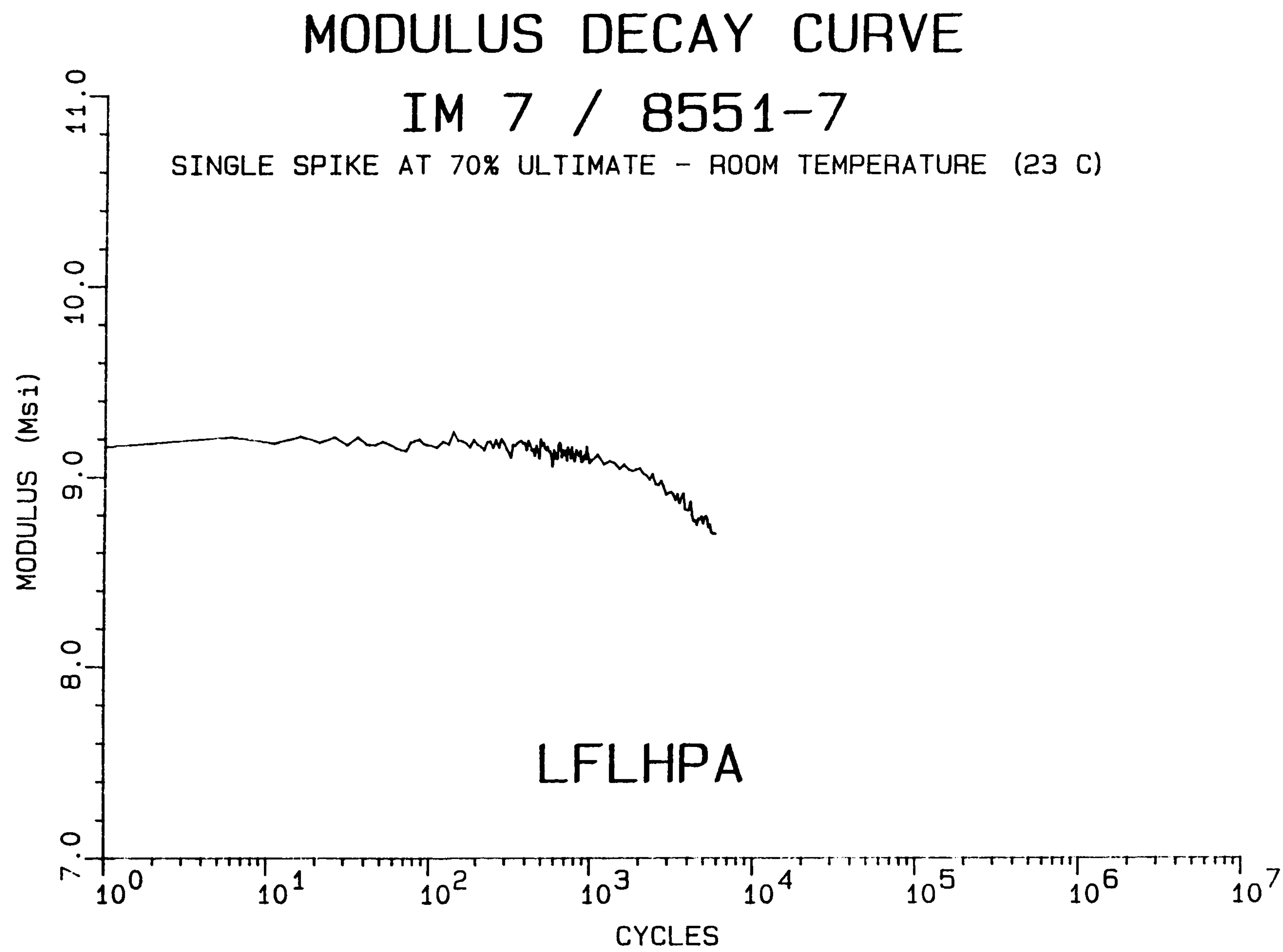
MODULUS DECAY CURVE
IM 7 / 8551-7
SINGLE SPIKE AT 70% ULTIMATE - ROOM TEMPERATURE (23 C)
MODULUS (Msi)
11.0
10.0
9.0
8.0
7.0
LFLHPA
10^0
10^1
10^2
10^3
10^4
10^5
10^6
10^7
CYCLES

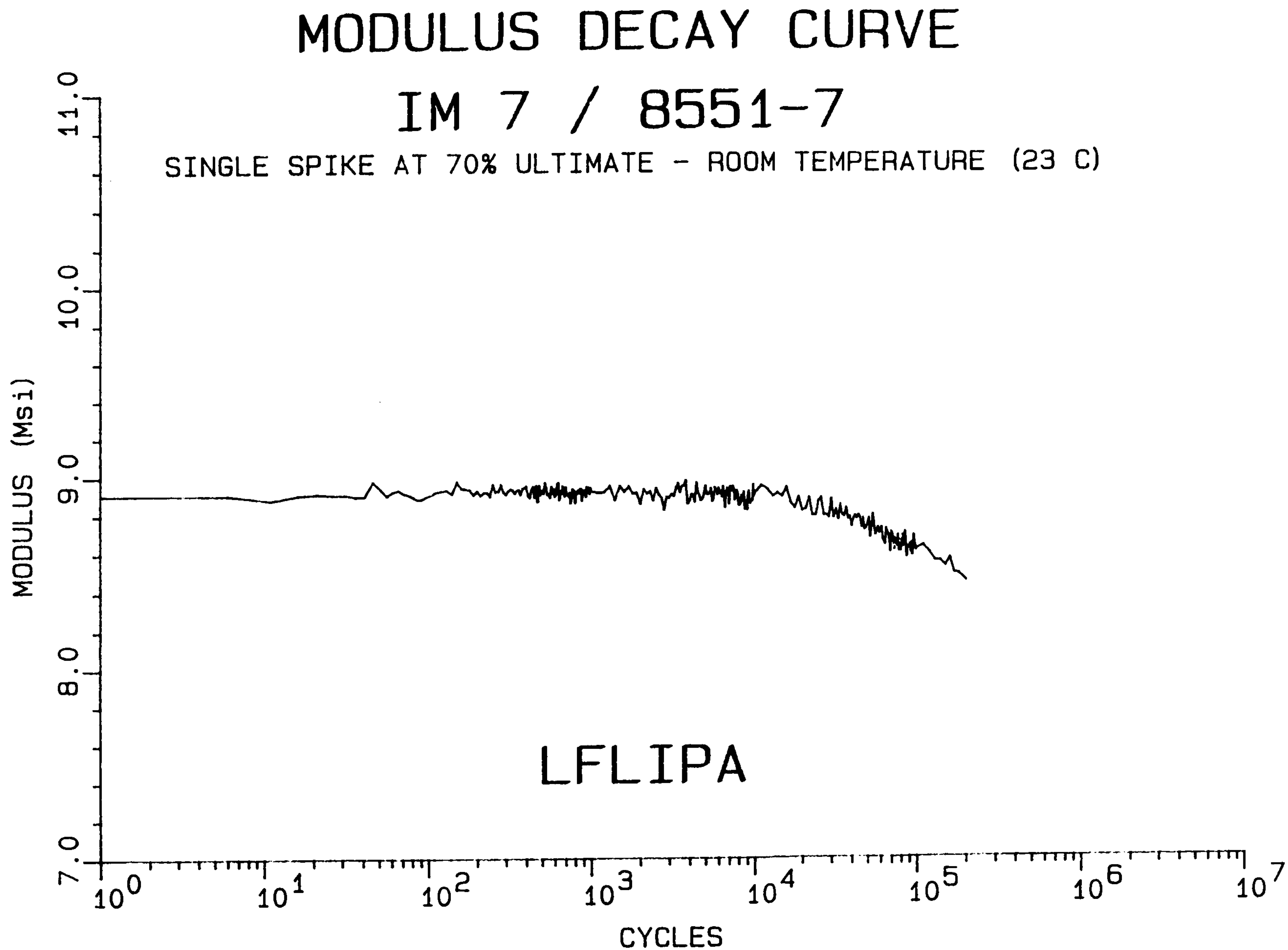

MODULUS DECAY CURVE
IM 7 / 8551-7
SINGLE SPIKE AT 70% ULTIMATE - ROOM TEMPERATURE (23 C)
LFLIPA
MODULUS (Msi)
11.0
10.0
9.0
8.0
7.0
CYCLES
10^0
10^1
10^2
10^3
10^4
10^5
10^6
10^7

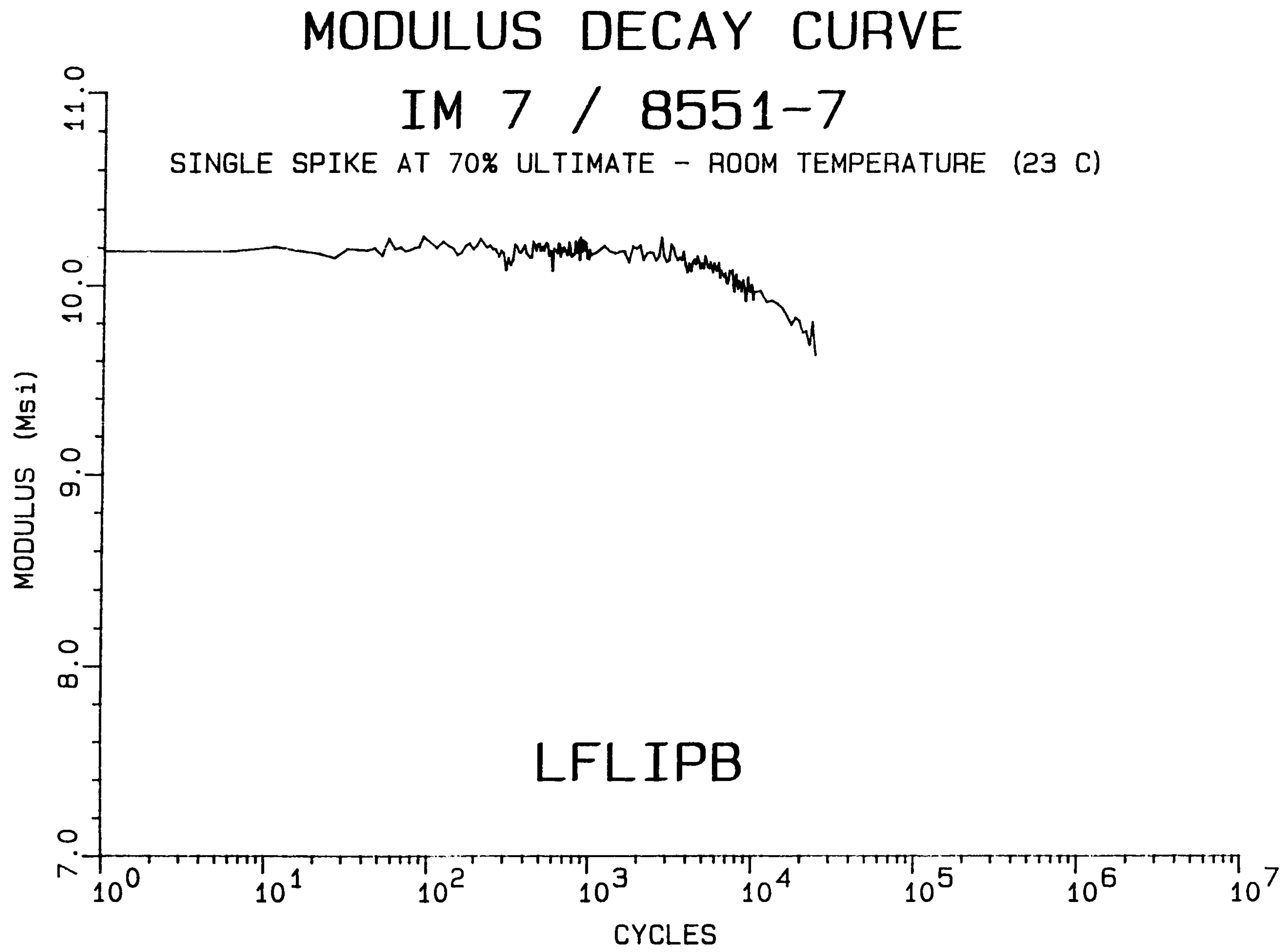
MODULUS DECAY CURVE
IM 7 / 8551-7
SINGLE SPIKE AT 70% ULTIMATE - ROOM TEMPERATURE (23 C)
11.0
10.0
9.0
8.0
7.0
MODULUS (Msi)
LFLIPB
10^0
10^1
10^2
10^3
10^4
10^5
10^6
10^7
CYCLES

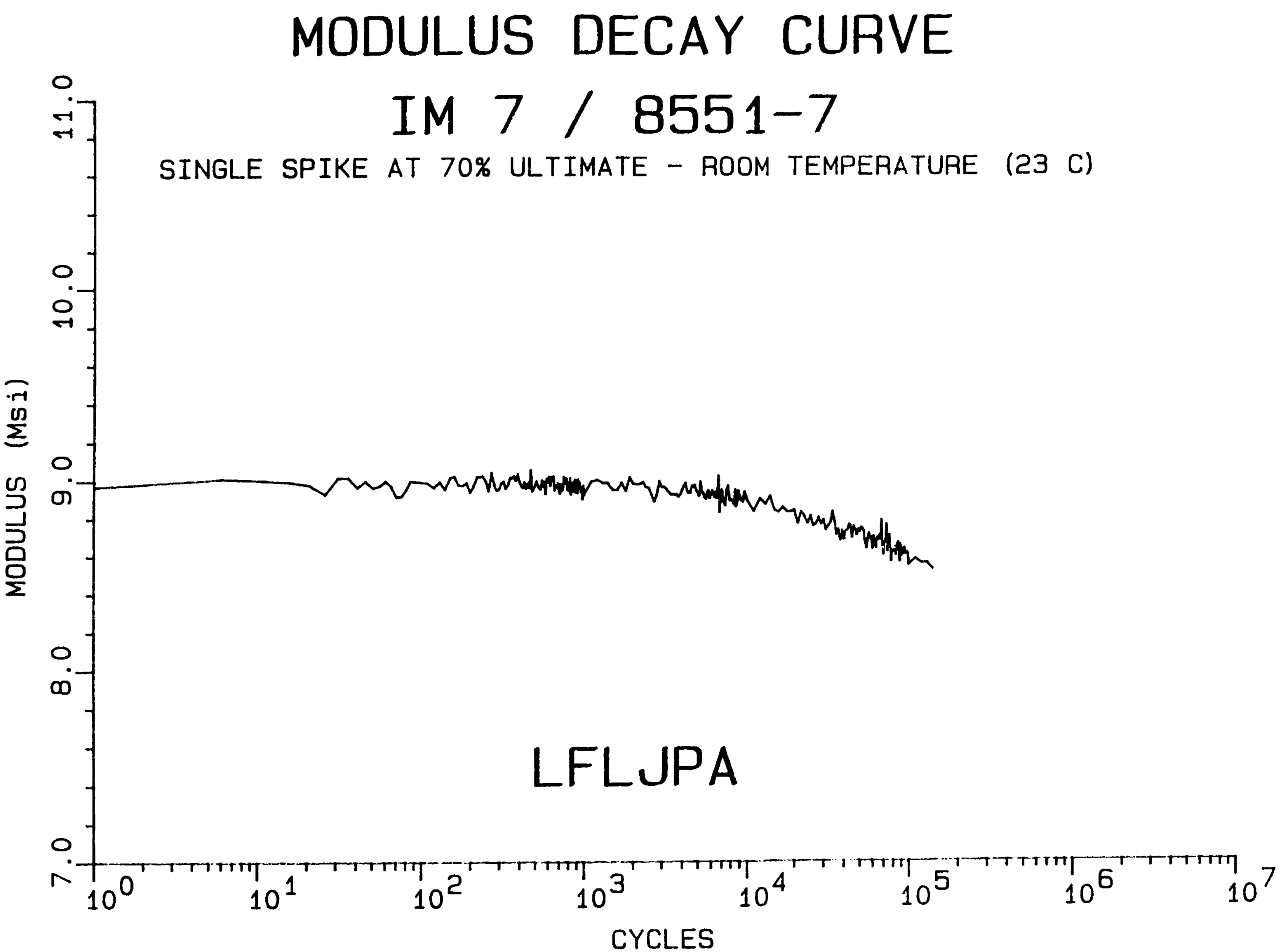
MODULUS DECAY CURVE
IM 7 / 8551-7
SINGLE SPIKE AT 70% ULTIMATE - ROOM TEMPERATURE (23 C)
LFLJPA
MODULUS (Msi)
7.0
8.0
9.0
10.0
11.0
CYCLES
10^0
10^1
10^2
10^3
10^4
10^5
10^6
10^7

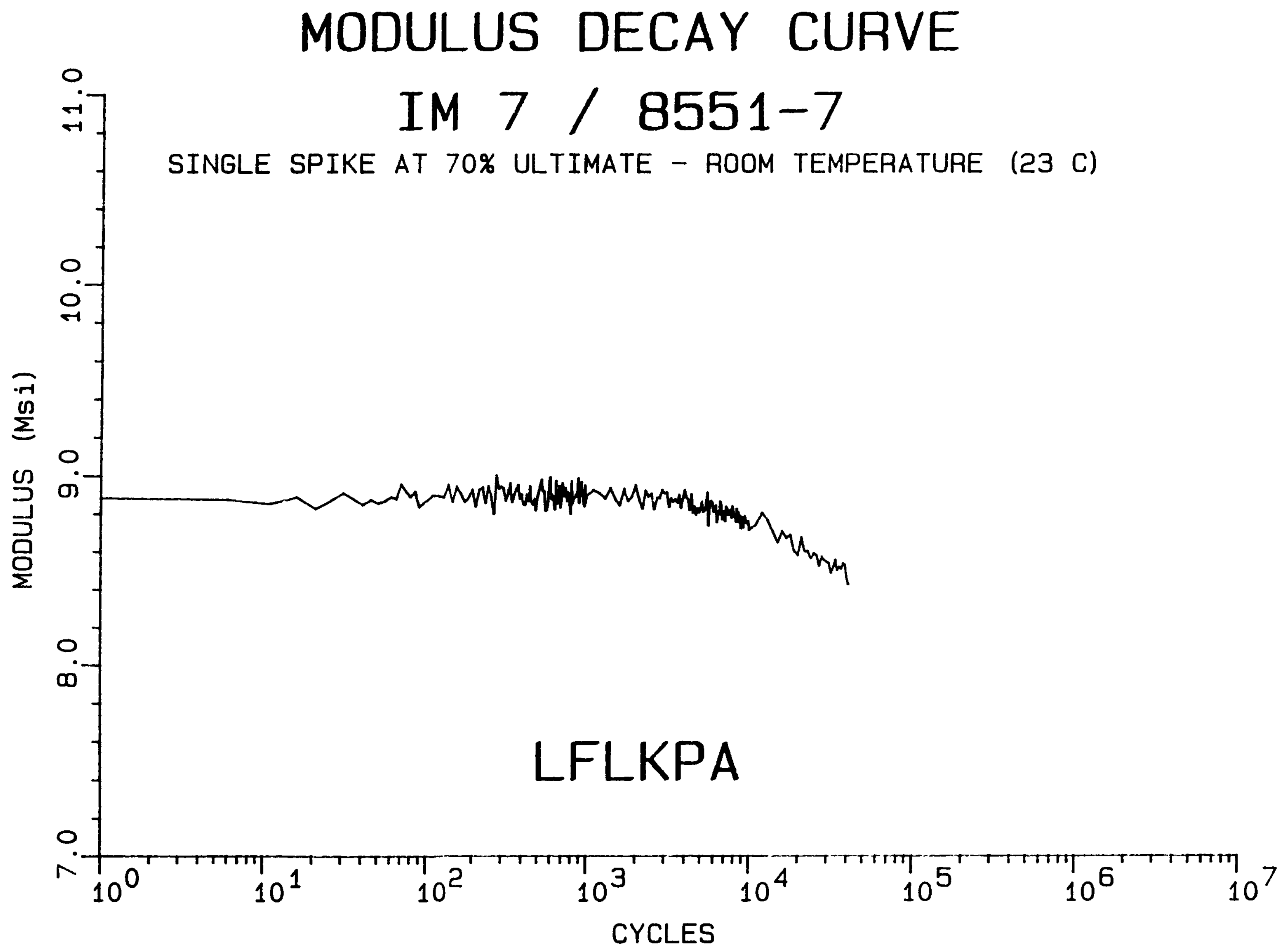
MODULUS DECAY CURVE
IM 7 / 8551-7
SINGLE SPIKE AT 70% ULTIMATE - ROOM TEMPERATURE (23 C)
LFLKPA
MODULUS (Msi)
7.0
8.0
9.0
10.0
11.0
CYCLES
10^0
10^1
10^2
10^3
10^4
10^5
10^6
10^7

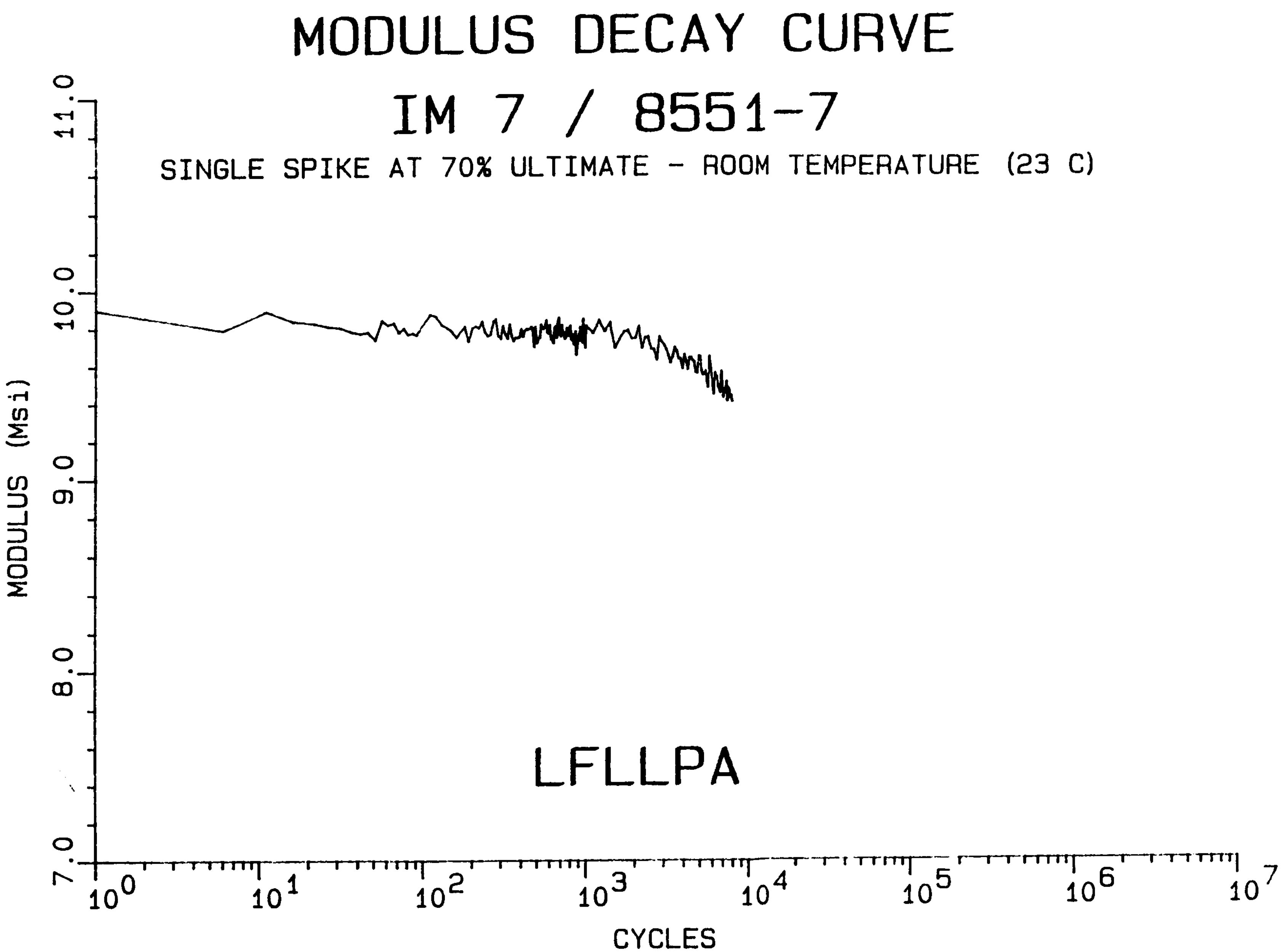
MODULUS DECAY CURVE
IM 7 / 8551-7
SINGLE SPIKE AT 70% ULTIMATE - ROOM TEMPERATURE (23 C)
MODULUS (Msi)
11.0
10.0
9.0
8.0
7.0
10^0
10^1
10^2
10^3
10^4
10^5
10^6
10^7
CYCLES
LFLLPA

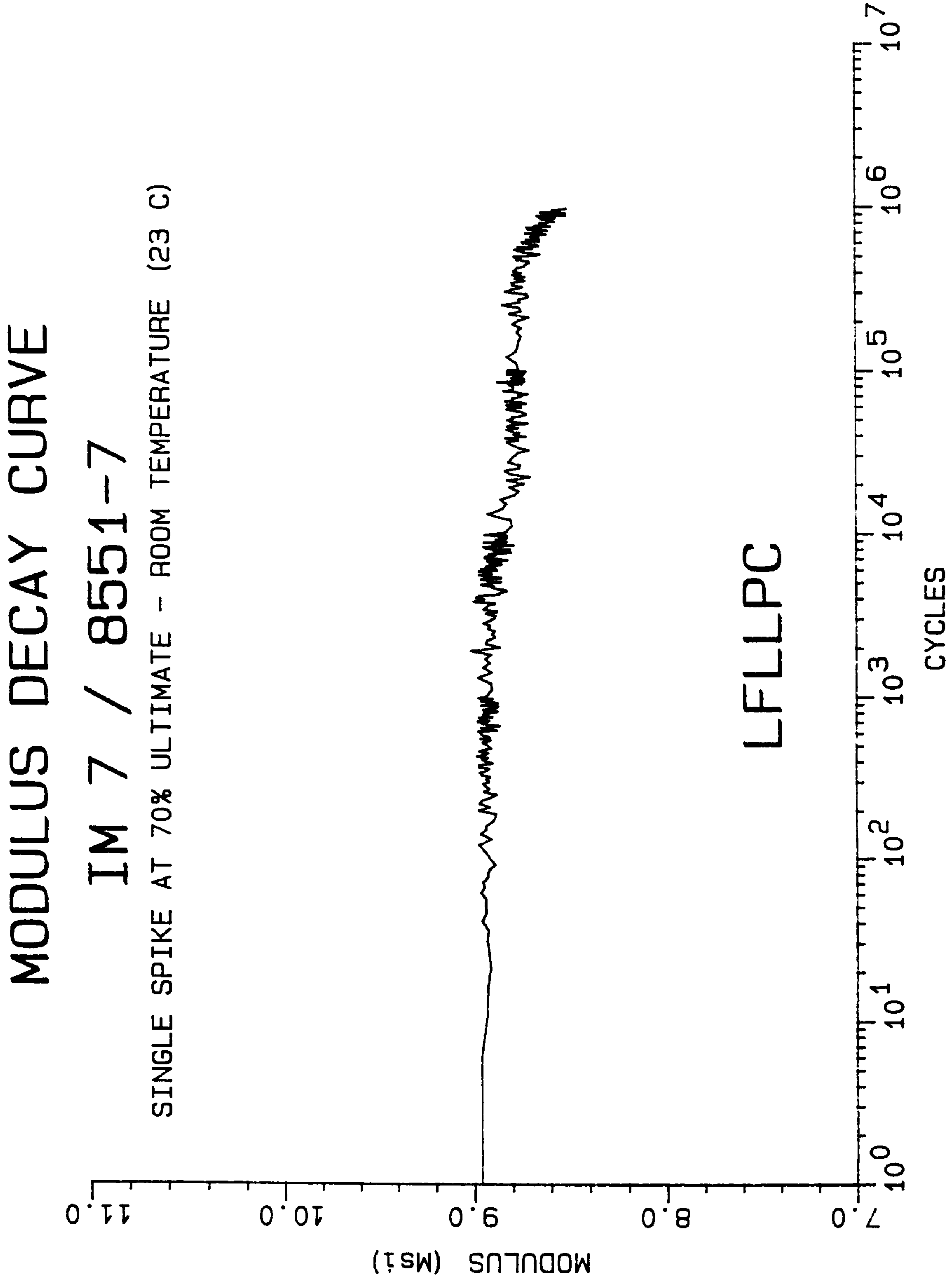
MODULUS DECAY CURVE
IM 7 / 8551-7
SINGLE SPIKE AT 70% ULTIMATE - ROOM TEMPERATURE (23 C)
LFLLPC
MODULUS (Msi)
7.0
8.0
9.0
10.0
11.0
CYCLES
10^0
10^1
10^2
10^3
10^4
10^5
10^6
10^7

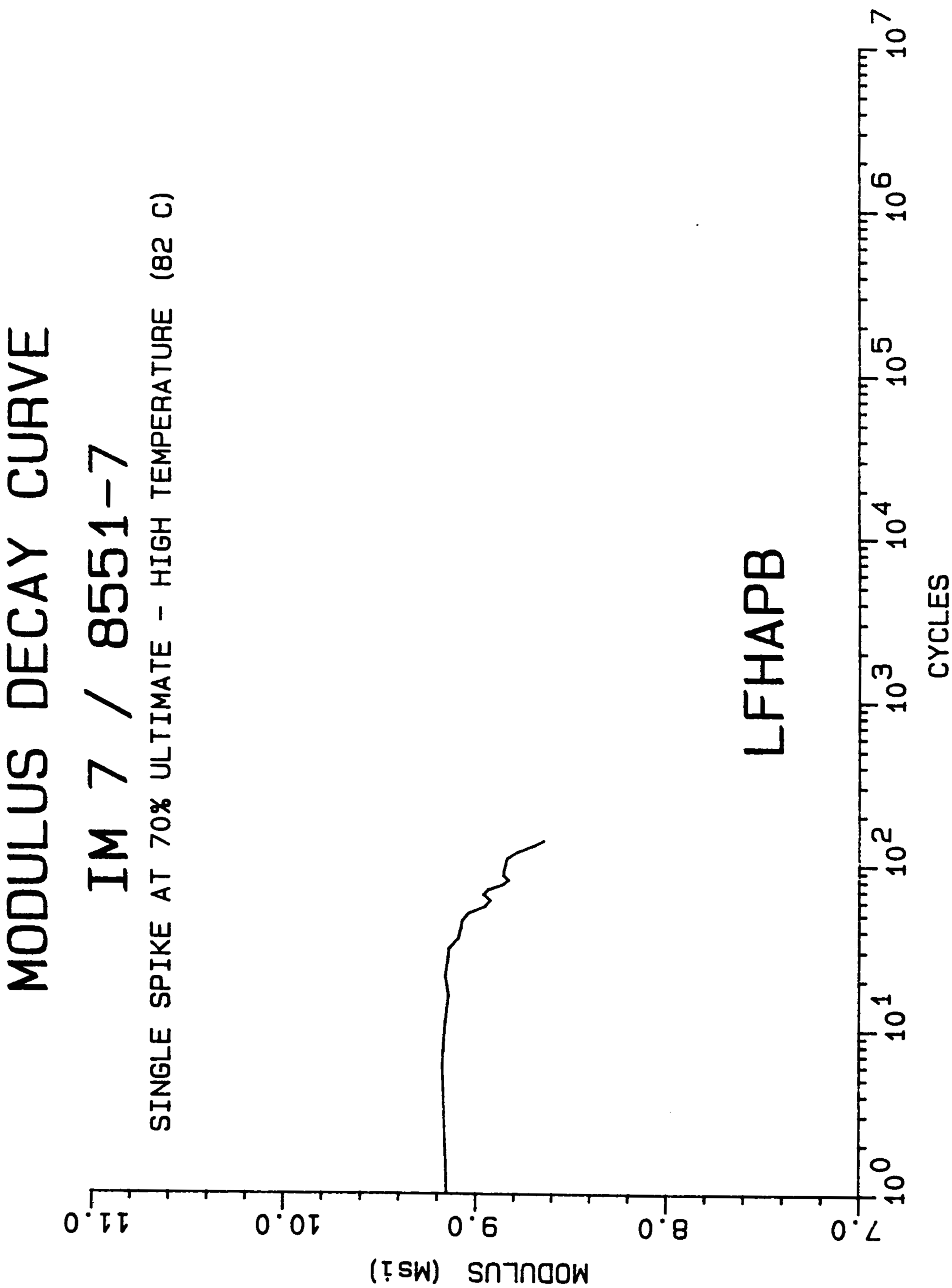
MODULUS DECAY CURVE
IM 7 / 8551-7
SINGLE SPIKE AT 70% ULTIMATE - HIGH TEMPERATURE (82 C)
LFHAPB
MODULUS (Msi)
7.0
8.0
9.0
10.0
11.0
CYCLES
10^0
10^1
10^2
10^3
10^4
10^5
10^6
10^7

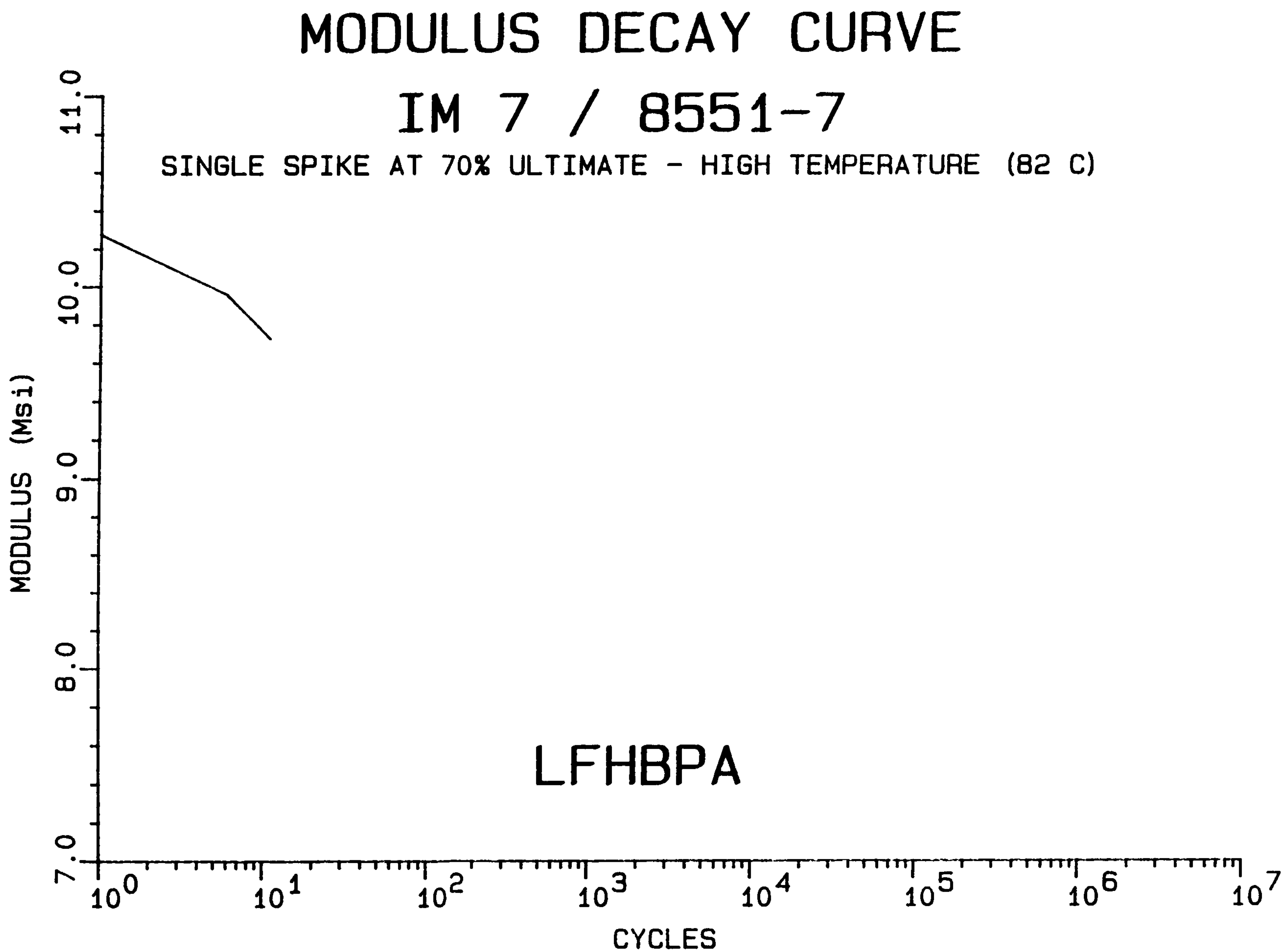
MODULUS DECAY CURVE
IM 7 / 8551-7
SINGLE SPIKE AT 70% ULTIMATE - HIGH TEMPERATURE (82 C)
LFHBPA
MODULUS (Msi)
7.0
8.0
9.0
10.0
11.0
CYCLES
10^0
10^1
10^2
10^3
10^4
10^5
10^6
10^7

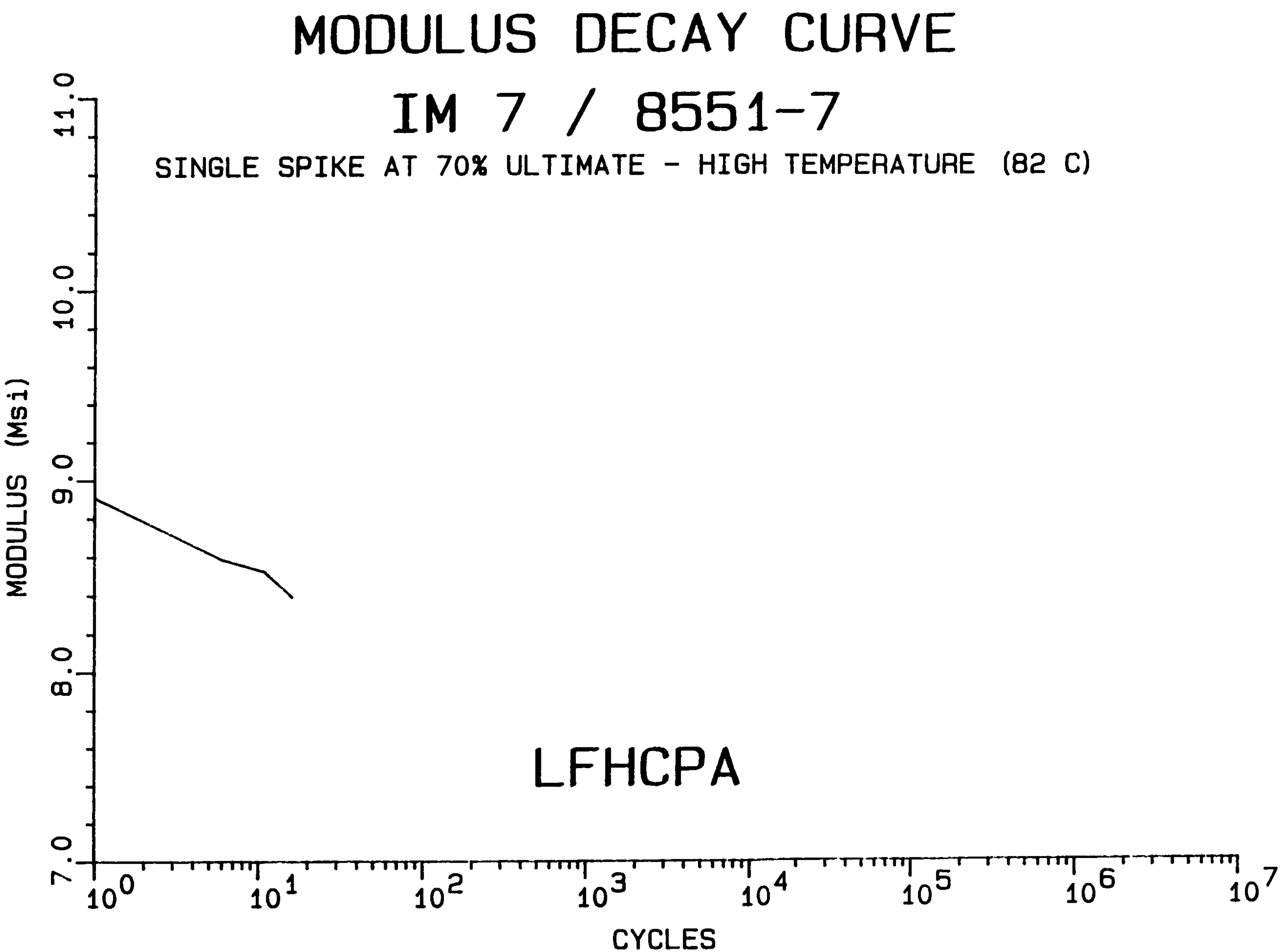
MODULUS DECAY CURVE
IM 7 / 8551-7
SINGLE SPIKE AT 70% ULTIMATE - HIGH TEMPERATURE (82 C)
MODULUS (Msi)
7.0
8.0
9.0
10.0
11.0
10^0
10^1
10^2
10^3
10^4
10^5
10^6
10^7
CYCLES
LFHCPA

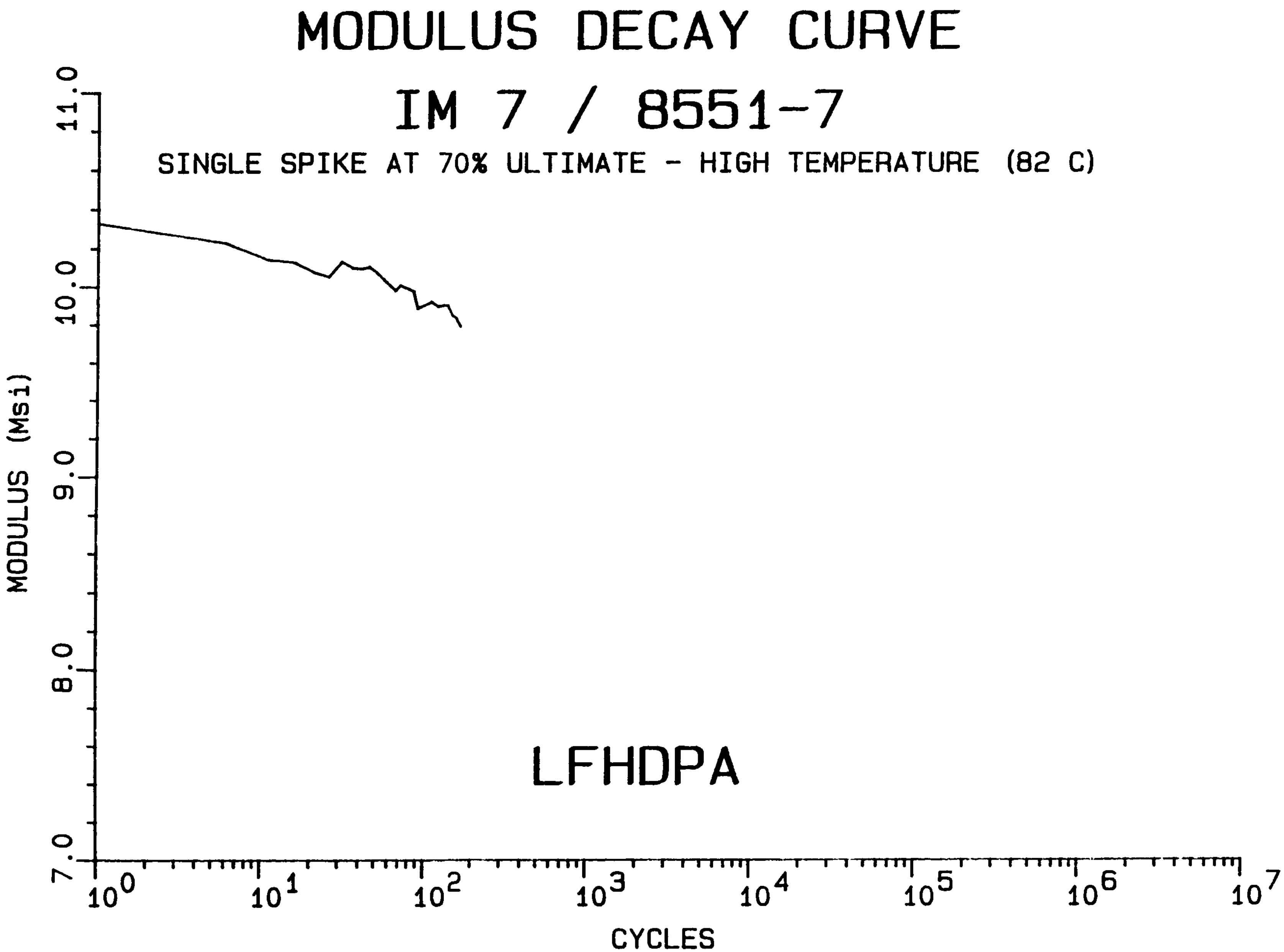
MODULUS DECAY CURVE
IM 7 / 8551-7
SINGLE SPIKE AT 70% ULTIMATE - HIGH TEMPERATURE (82 C)
MODULUS (Msi)
11.0
10.0
9.0
8.0
7.0
10^0
10^1
10^2
10^3
10^4
10^5
10^6
10^7
CYCLES
LFHDPA

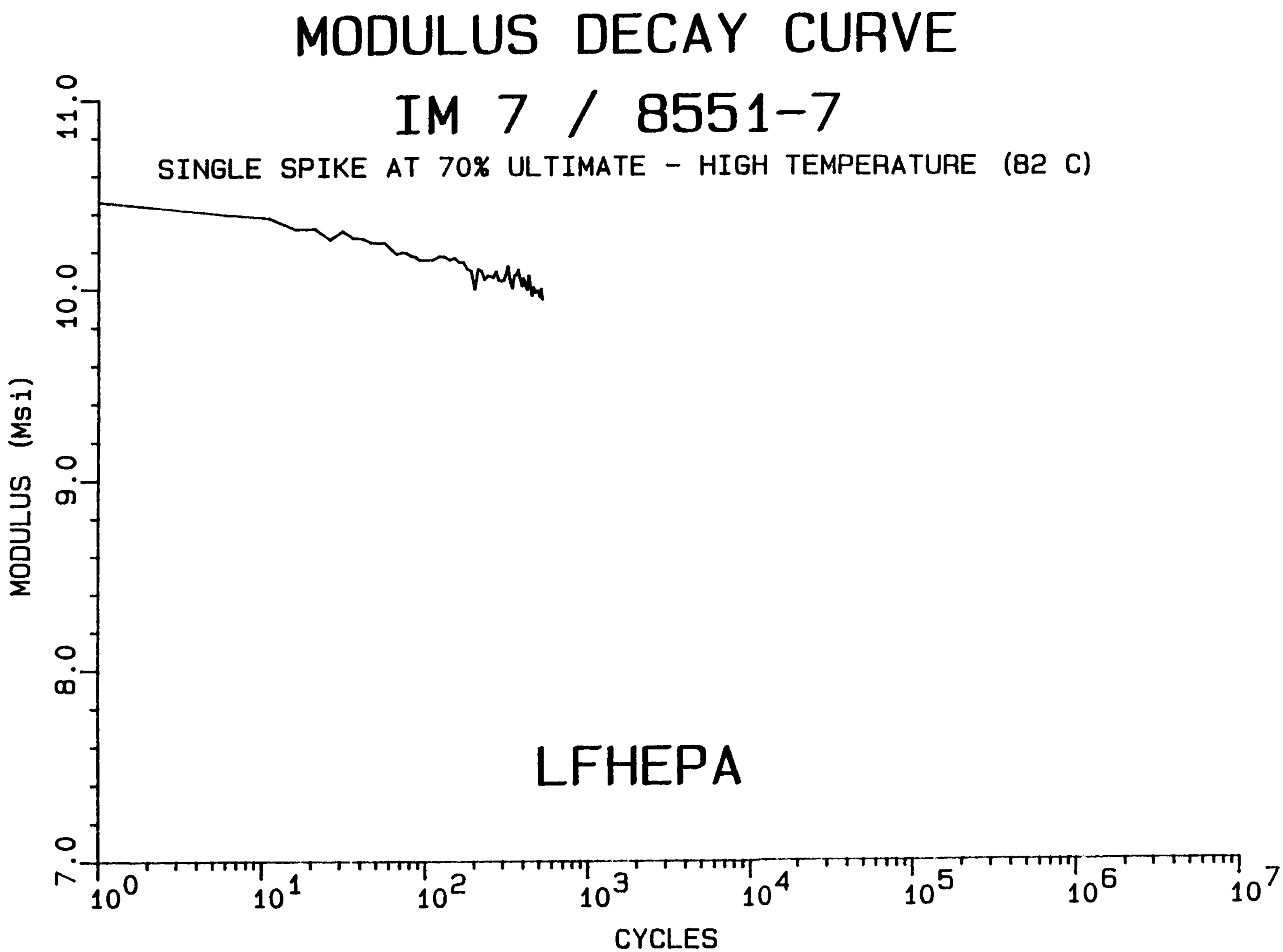
MODULUS DECAY CURVE
IM 7 / 8551-7
SINGLE SPIKE AT 70% ULTIMATE - HIGH TEMPERATURE (82 C)
MODULUS (Msi)
11.0
10.0
9.0
8.0
7.0
10^0
10^1
10^2
10^3
10^4
10^5
10^6
10^7
CYCLES
LFHEPA

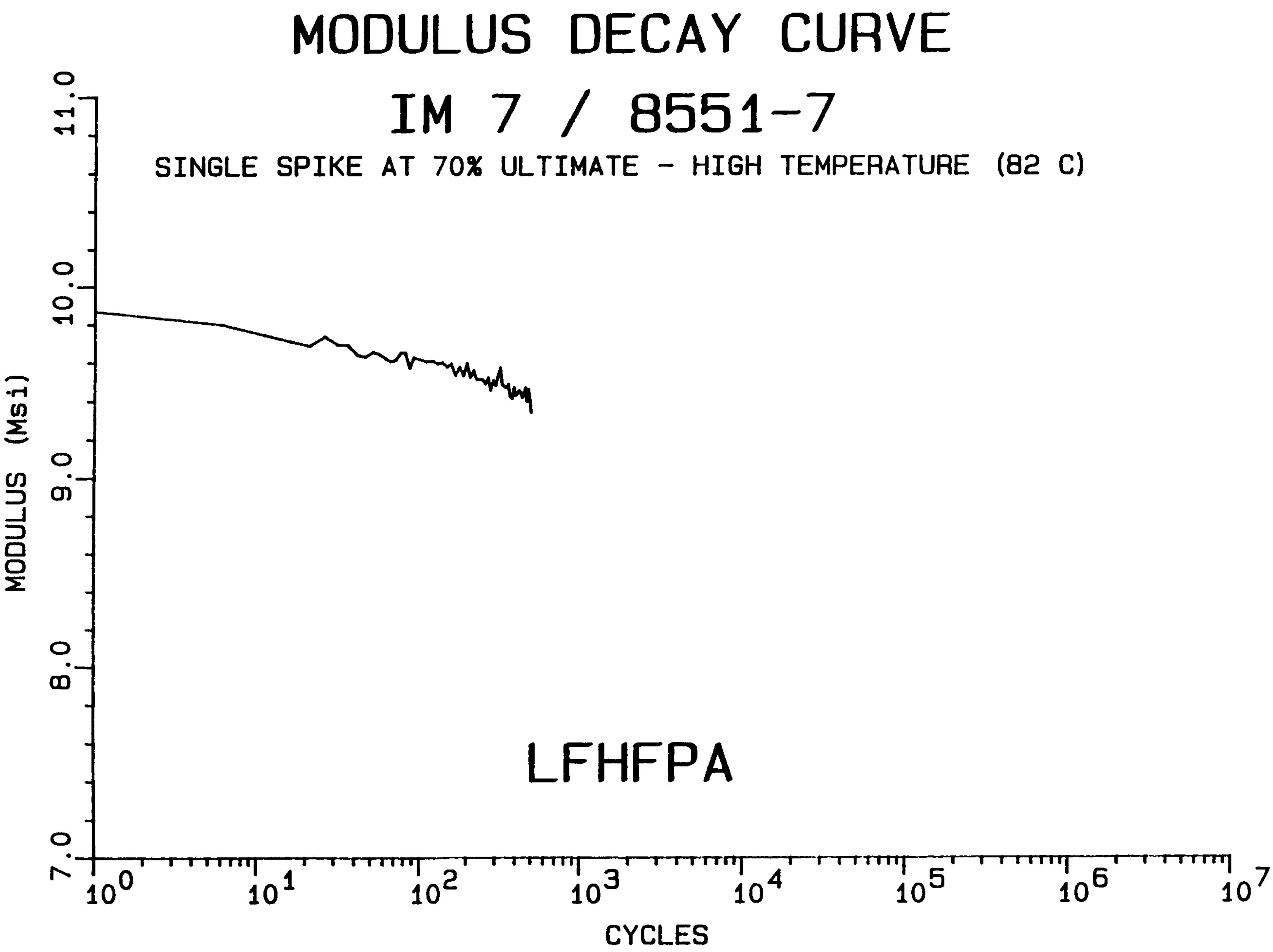
MODULUS DECAY CURVE
IM 7 / 8551-7
SINGLE SPIKE AT 70% ULTIMATE - HIGH TEMPERATURE (82 C)
LFHFPA
MODULUS (Msi)
11.0
10.0
9.0
8.0
7.0
CYCLES
10^0
10^1
10^2
10^3
10^4
10^5
10^6
10^7

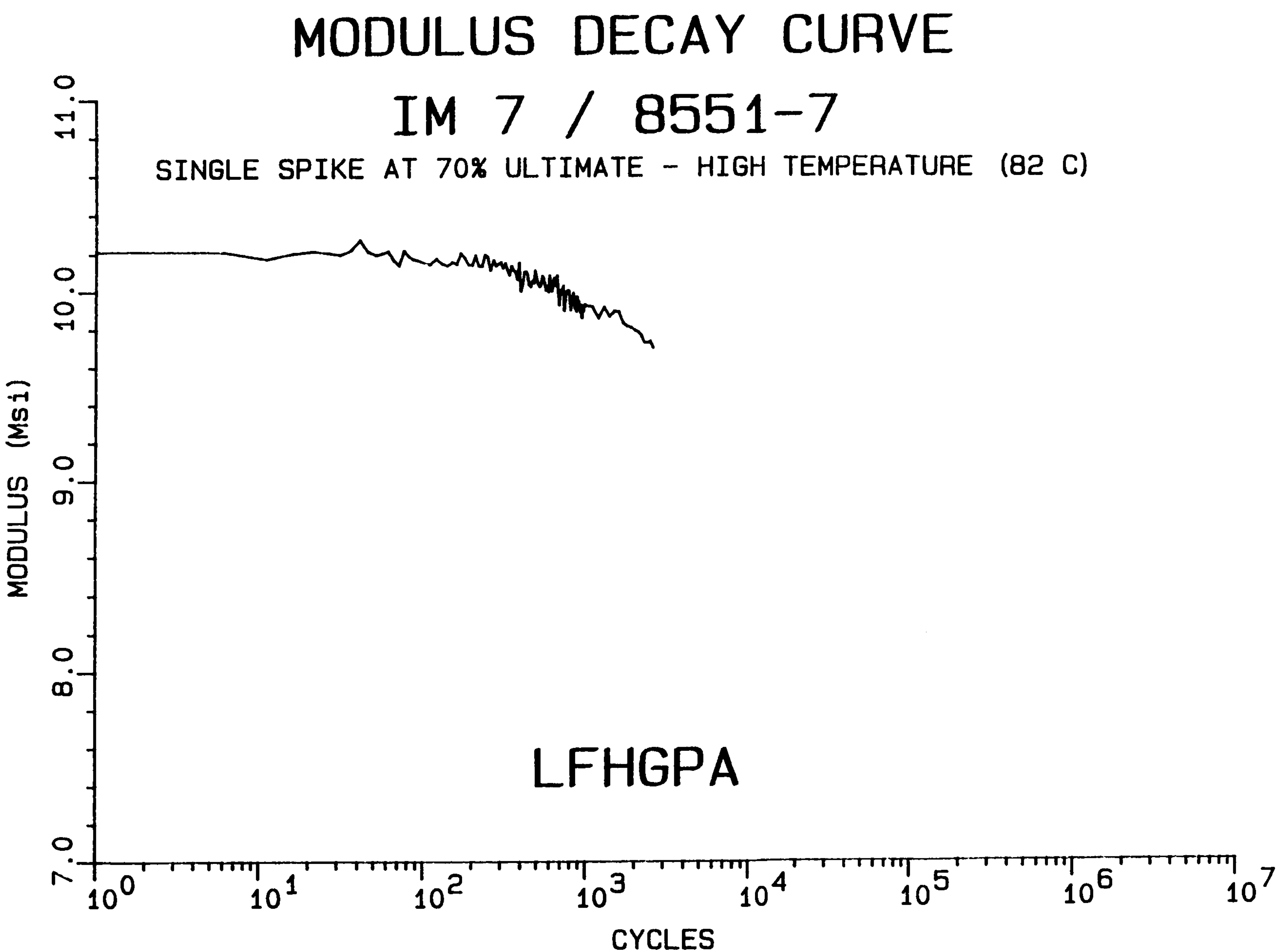

MODULUS DECAY CURVE
IM 7 / 8551-7
SINGLE SPIKE AT 70% ULTIMATE - HIGH TEMPERATURE (82 C)
LFHGPA
MODULUS (Msi)
11.0
10.0
9.0
8.0
7.0
10^0
10^1
10^2
10^3
10^4
10^5
10^6
10^7
CYCLES

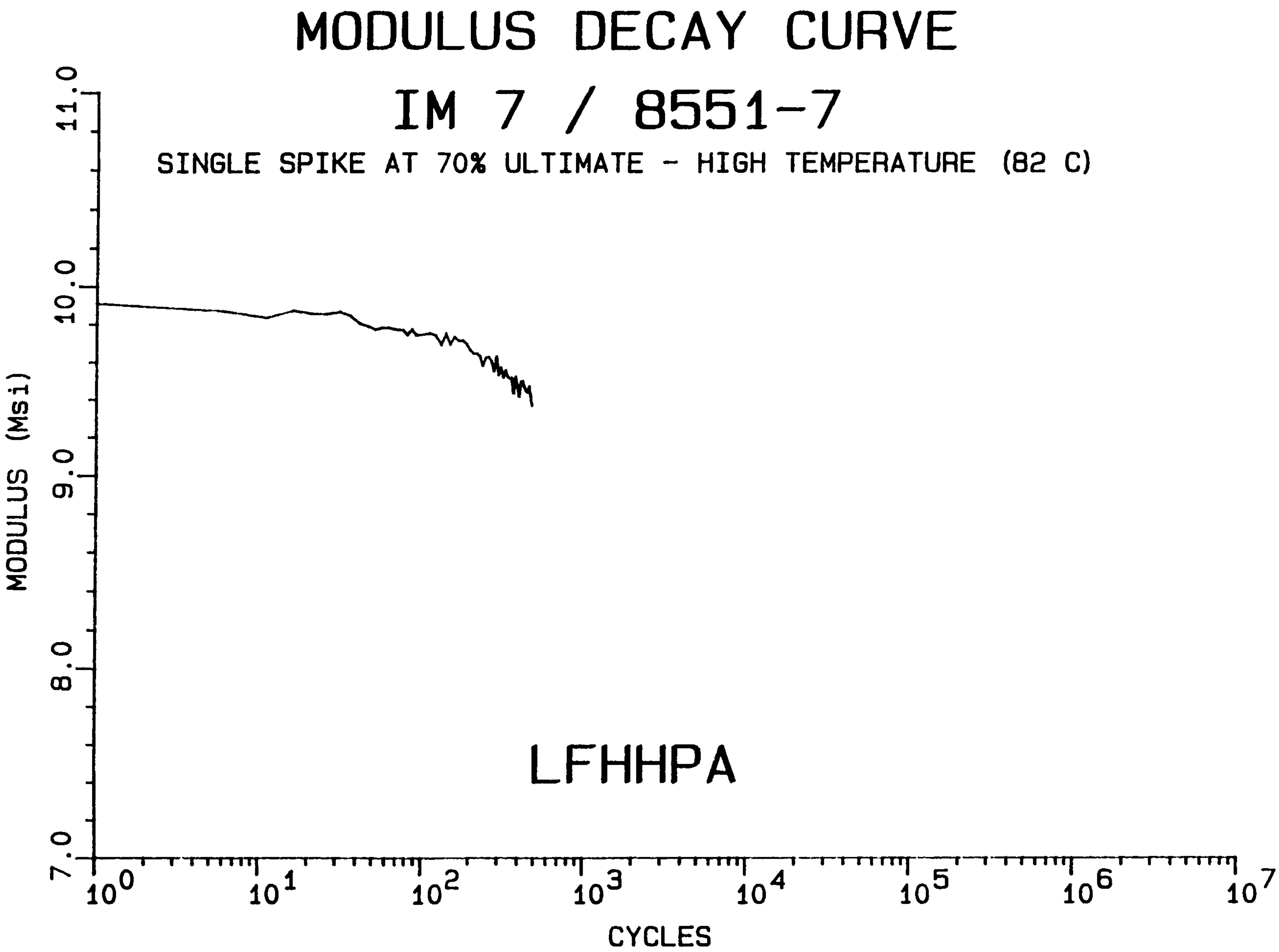
MODULUS DECAY CURVE
IM 7 / 8551-7
SINGLE SPIKE AT 70% ULTIMATE - HIGH TEMPERATURE (82 C)
MODULUS (Msi)
11.0
10.0
9.0
8.0
7.0
LFHHPA
10^0
10^1
10^2
10^3
10^4
10^5
10^6
10^7
CYCLES

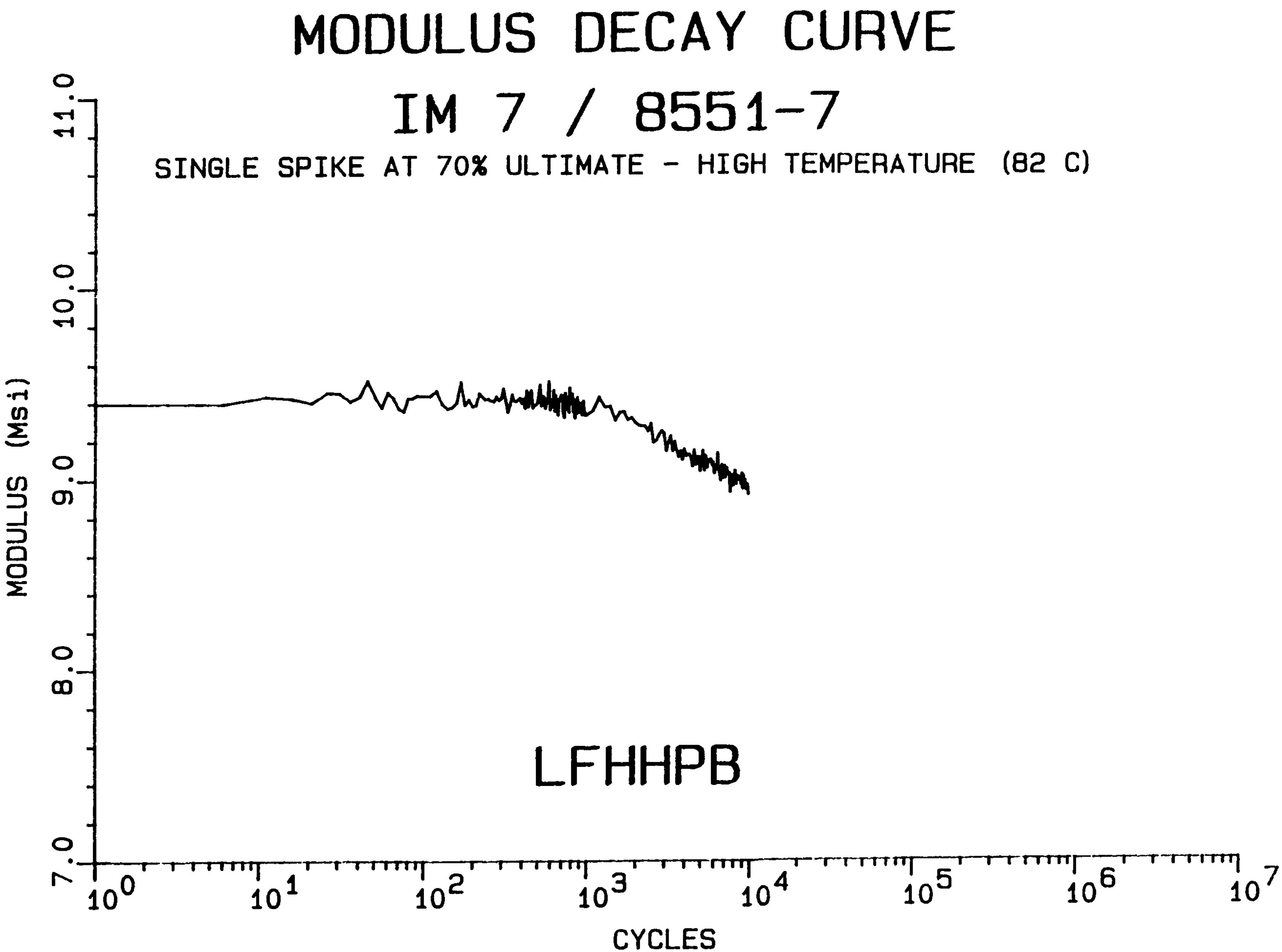

MODULUS DECAY CURVE
IM 7 / 8551-7
SINGLE SPIKE AT 70% ULTIMATE - HIGH TEMPERATURE (82 C)
MODULUS (Msi)
11.0
10.0
9.0
8.0
7.0
LFHHPB
10^0
10^1
10^2
10^3
10^4
10^5
10^6
10^7
CYCLES

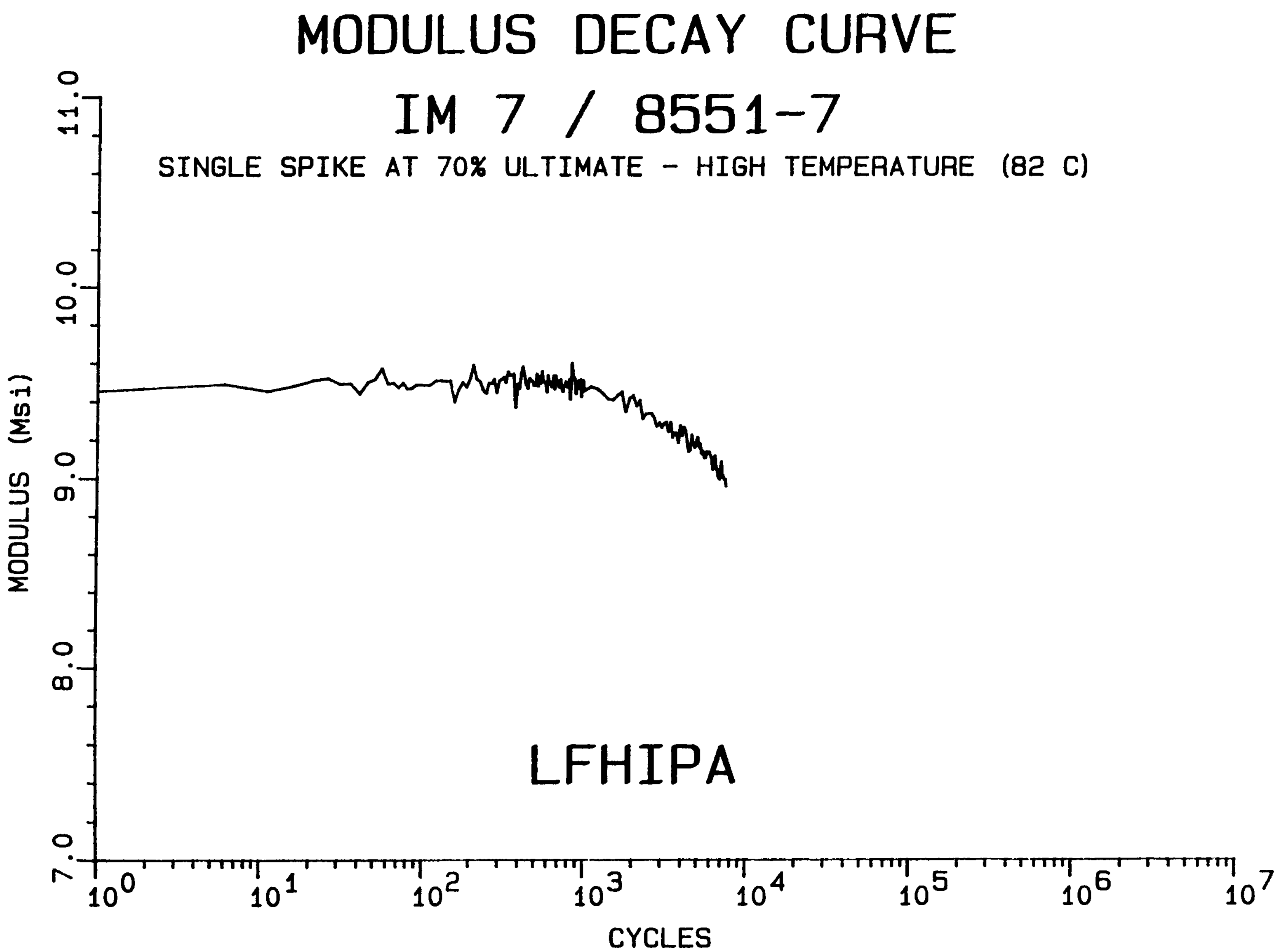
MODULUS DECAY CURVE
IM 7 / 8551-7
SINGLE SPIKE AT 70% ULTIMATE - HIGH TEMPERATURE (82 C)
MODULUS (Msi)
11.0
10.0
9.0
8.0
7.0
10^0
10^1
10^2
10^3
10^4
10^5
10^6
10^7
CYCLES
LFHIPA

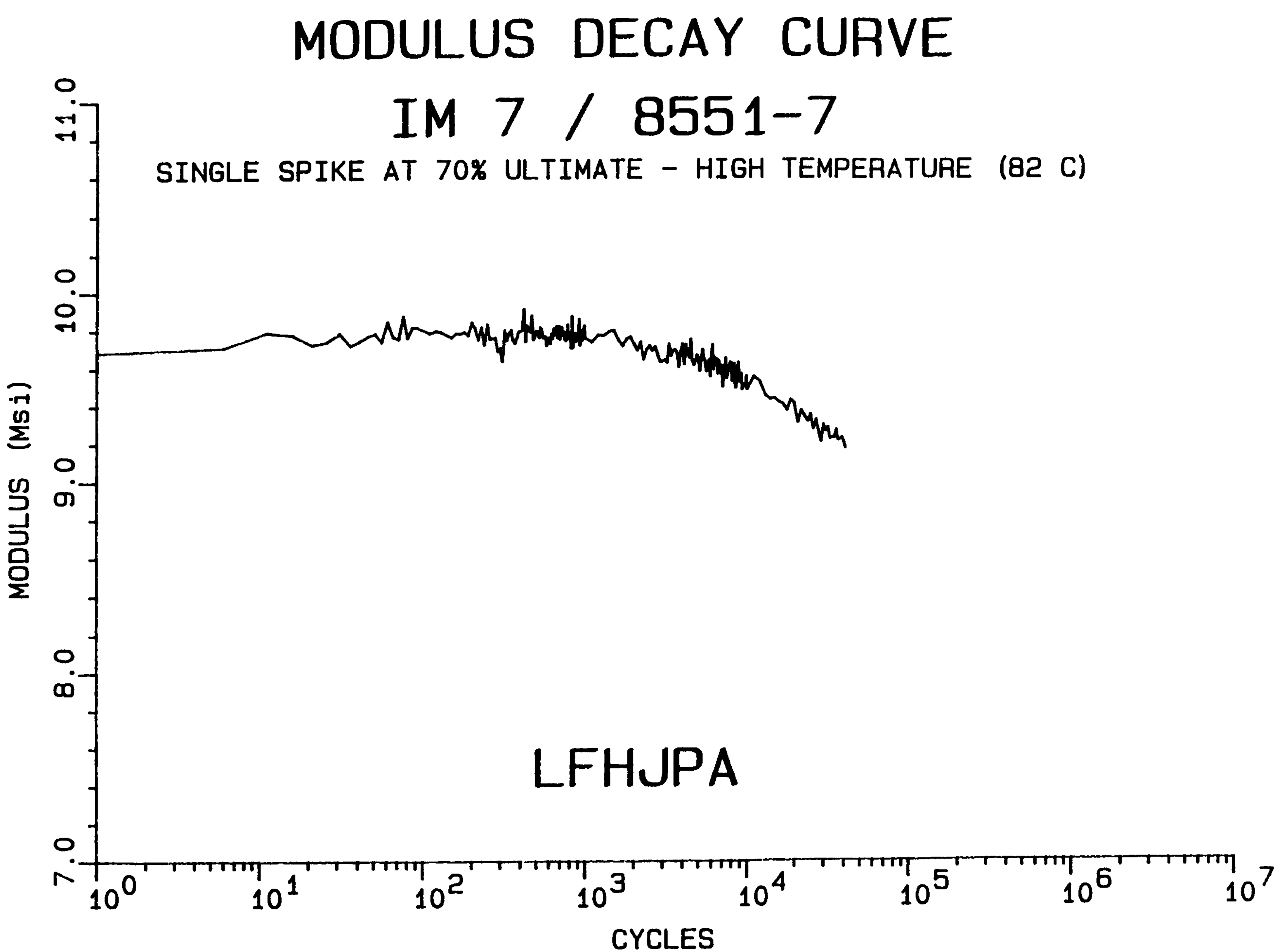
MODULUS DECAY CURVE
IM 7 / 8551-7
SINGLE SPIKE AT 70% ULTIMATE - HIGH TEMPERATURE (82 C)
MODULUS (Msi)
11.0
10.0
9.0
8.0
7.0
LFHJPA
10^0
10^1
10^2
10^3
10^4
10^5
10^6
10^7
CYCLES

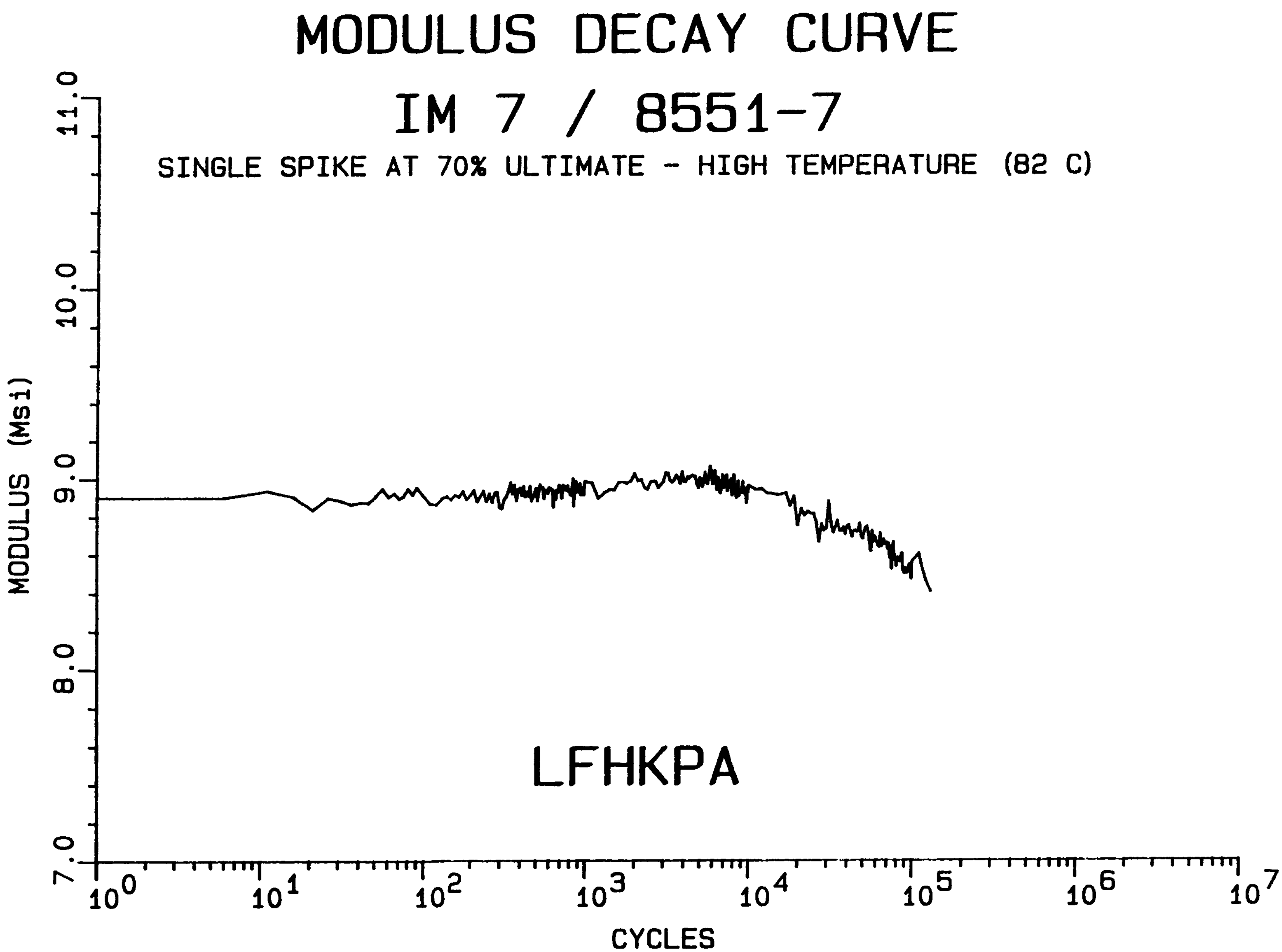
MODULUS DECAY CURVE
IM 7 / 8551-7
SINGLE SPIKE AT 70% ULTIMATE - HIGH TEMPERATURE (82 C)
LFHKPA
MODULUS (Msi)
CYCLES
7.0
8.0
9.0
10.0
11.0
10^0
10^1
10^2
10^3
10^4
10^5
10^6
10^7

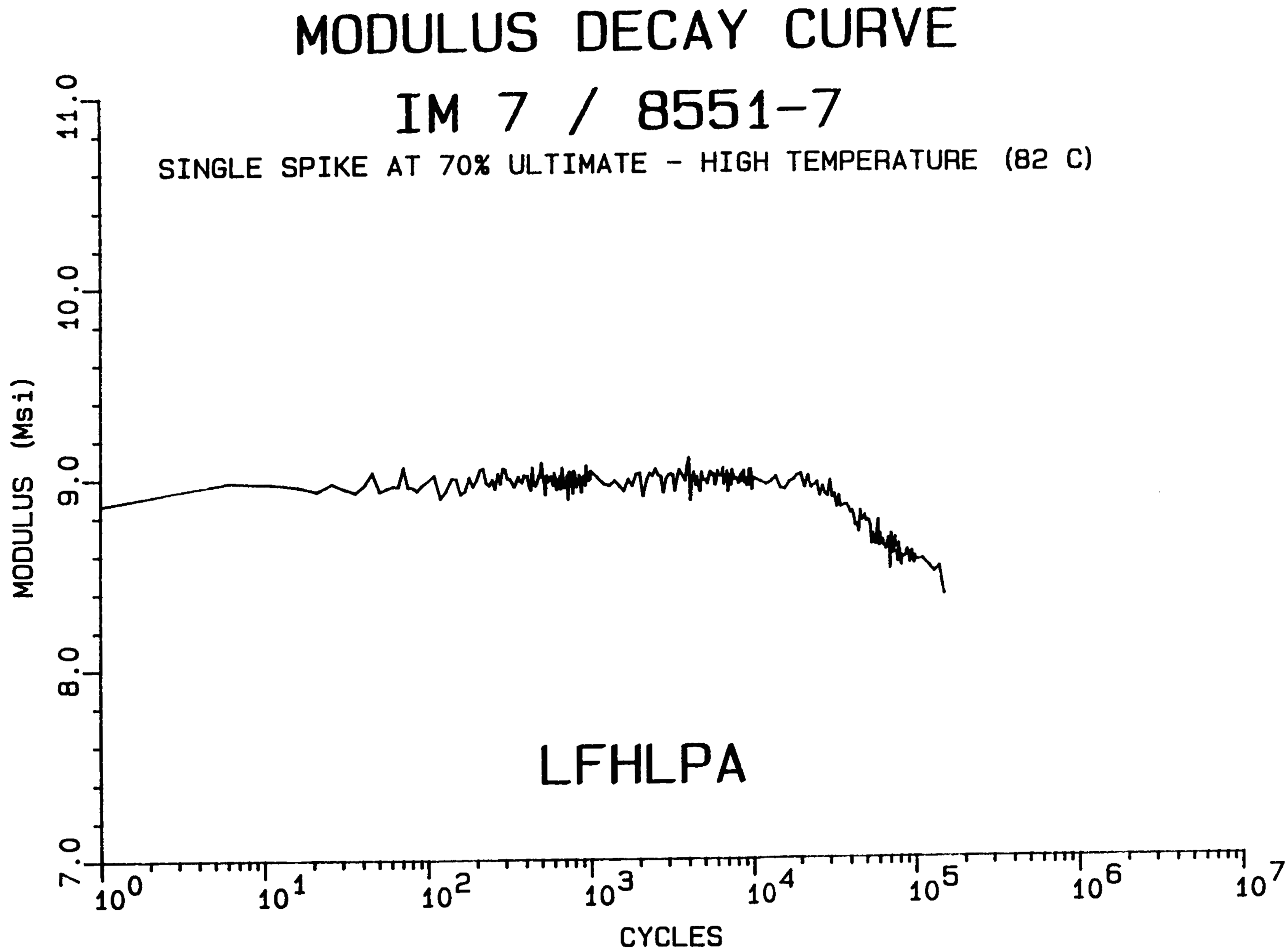
MODULUS DECAY CURVE
IM 7 / 8551-7
SINGLE SPIKE AT 70% ULTIMATE - HIGH TEMPERATURE (82 C)
MODULUS (Msi)
11.0
10.0
9.0
8.0
7.0
LFHLPA
10^0
10^1
10^2
10^3
10^4
10^5
10^6
10^7
CYCLES

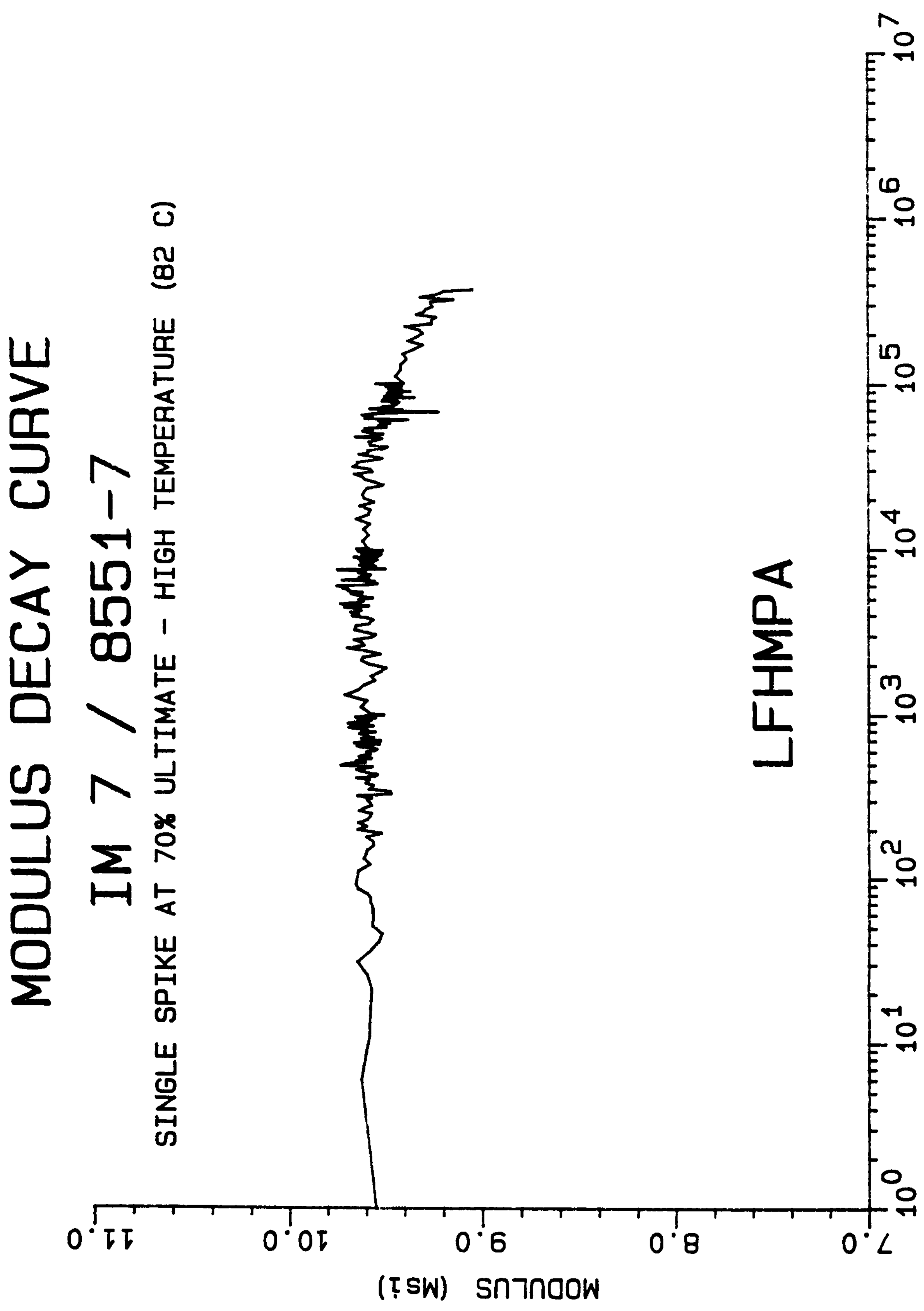
MODULUS DECAY CURVE
IM 7 / 8551-7
SINGLE SPIKE AT 70% ULTIMATE - HIGH TEMPERATURE (82 C)
LFHMPA
MODULUS (Msi)
11.0
10.0
9.0
8.0
7.0
CYCLES
10^0
10^1
10^2
10^3
10^4
10^5
10^6
10^7

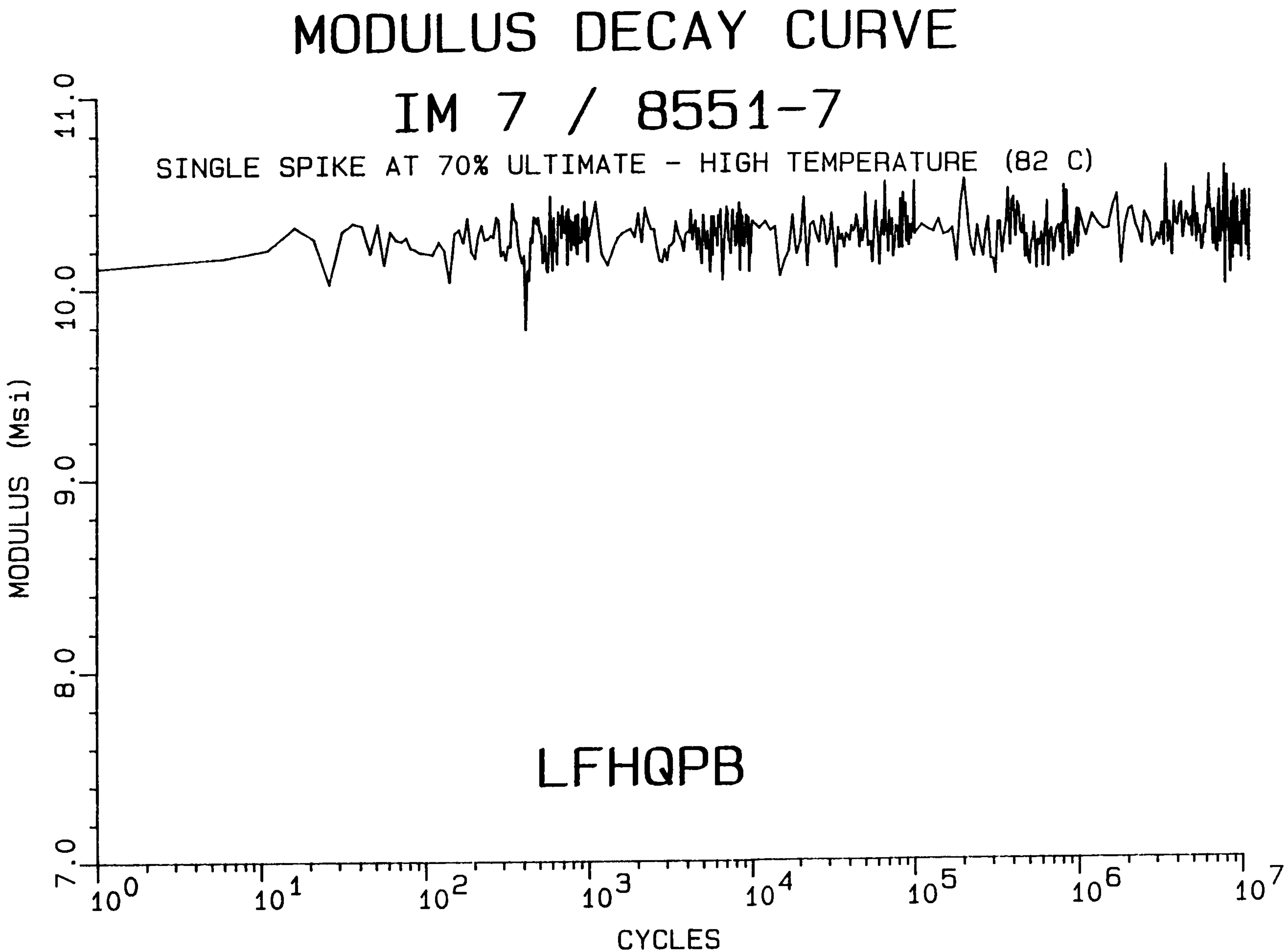
MODULUS DECAY CURVE
IM 7 / 8551-7
SINGLE SPIKE AT 70% ULTIMATE - HIGH TEMPERATURE (82 C)
LFHQPB
MODULUS (Msi)
7.0
8.0
9.0
10.0
11.0
CYCLES
10^0
10^1
10^2
10^3
10^4
10^5
10^6
10^7

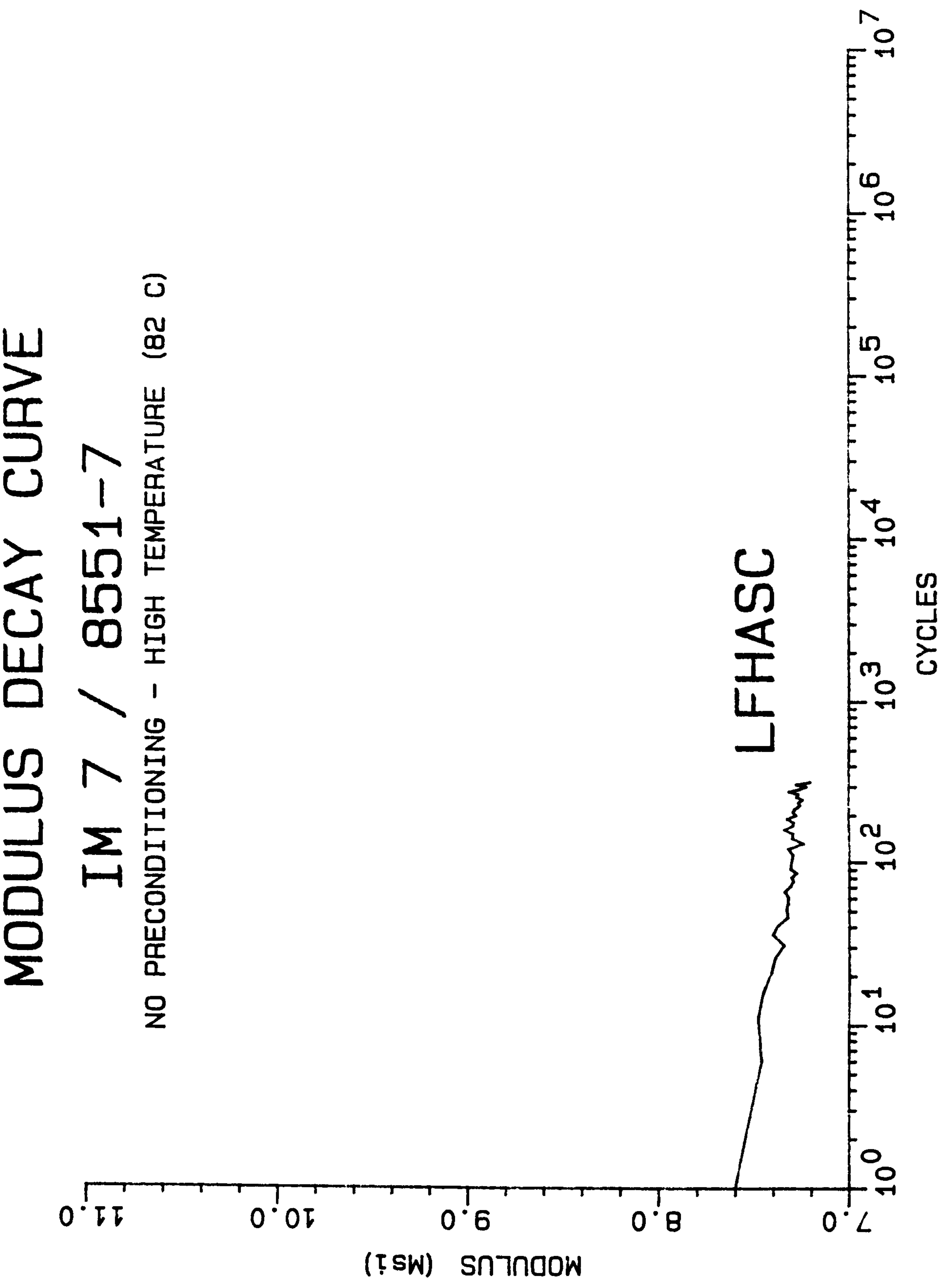
MODULUS DECAY CURVE
IM 7 / 8551-7
NO PRECONDITIONING - HIGH TEMPERATURE (82 C)
LFHASC
CYCLES
MODULUS (Msi)
7.0
8.0
9.0
10.0
11.0
10^0
10^1
10^2
10^3
10^4
10^5
10^6
10^7

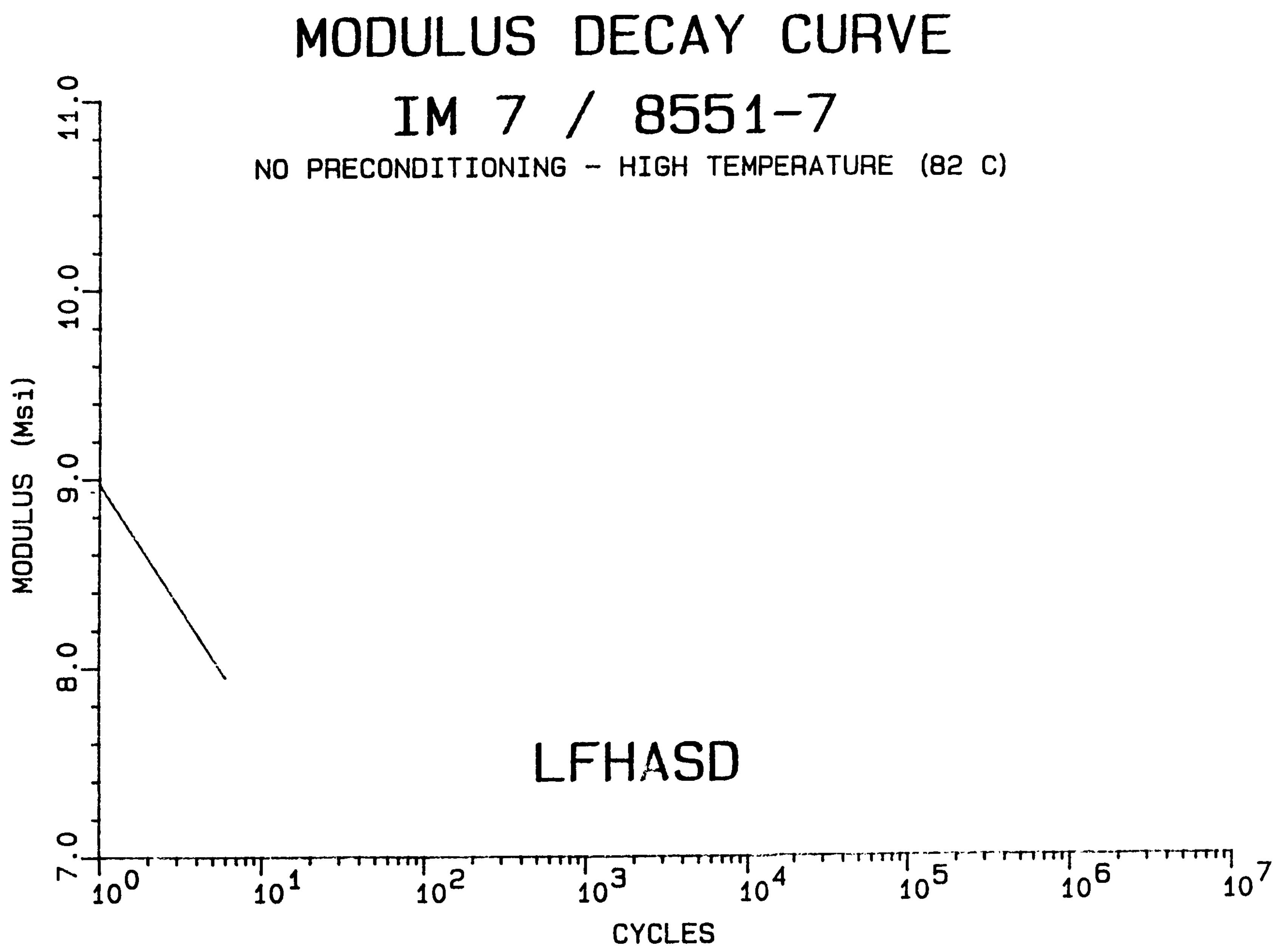
MODULUS DECAY CURVE
IM 7 / 8551-7
NO PRECONDITIONING - HIGH TEMPERATURE (82 C)
LFHASD
MODULUS (Msi)
7.0
8.0
9.0
10.0
11.0
CYCLES
10^0
10^1
10^2
10^3
10^4
10^5
10^6
10^7

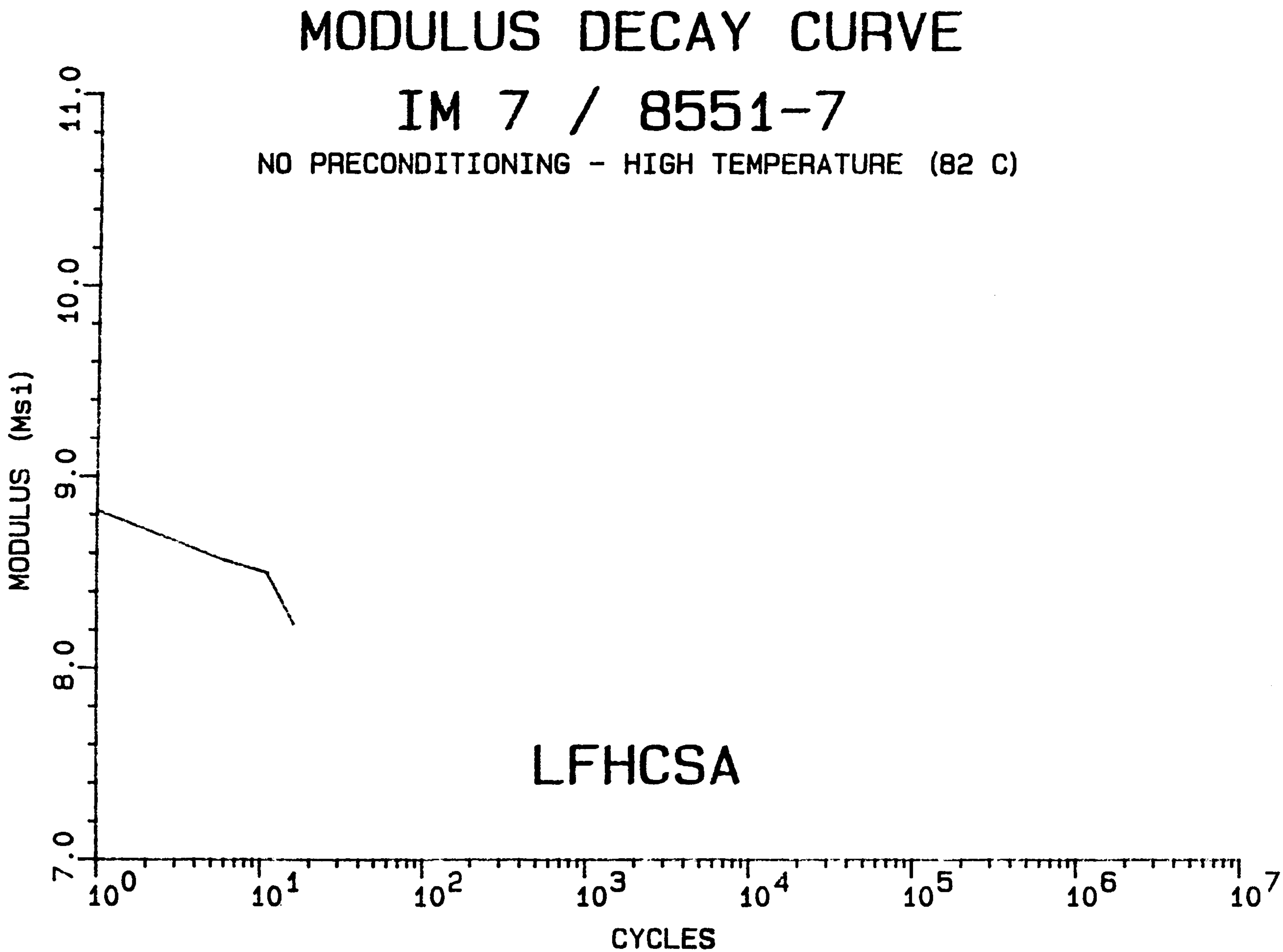
MODULUS DECAY CURVE
IM 7 / 8551-7
NO PRECONDITIONING - HIGH TEMPERATURE (82 C)
LFHCSA
MODULUS (Msi)
7.0
8.0
9.0
10.0
11.0
CYCLES
10^0
10^1
10^2
10^3
10^4
10^5
10^6
10^7

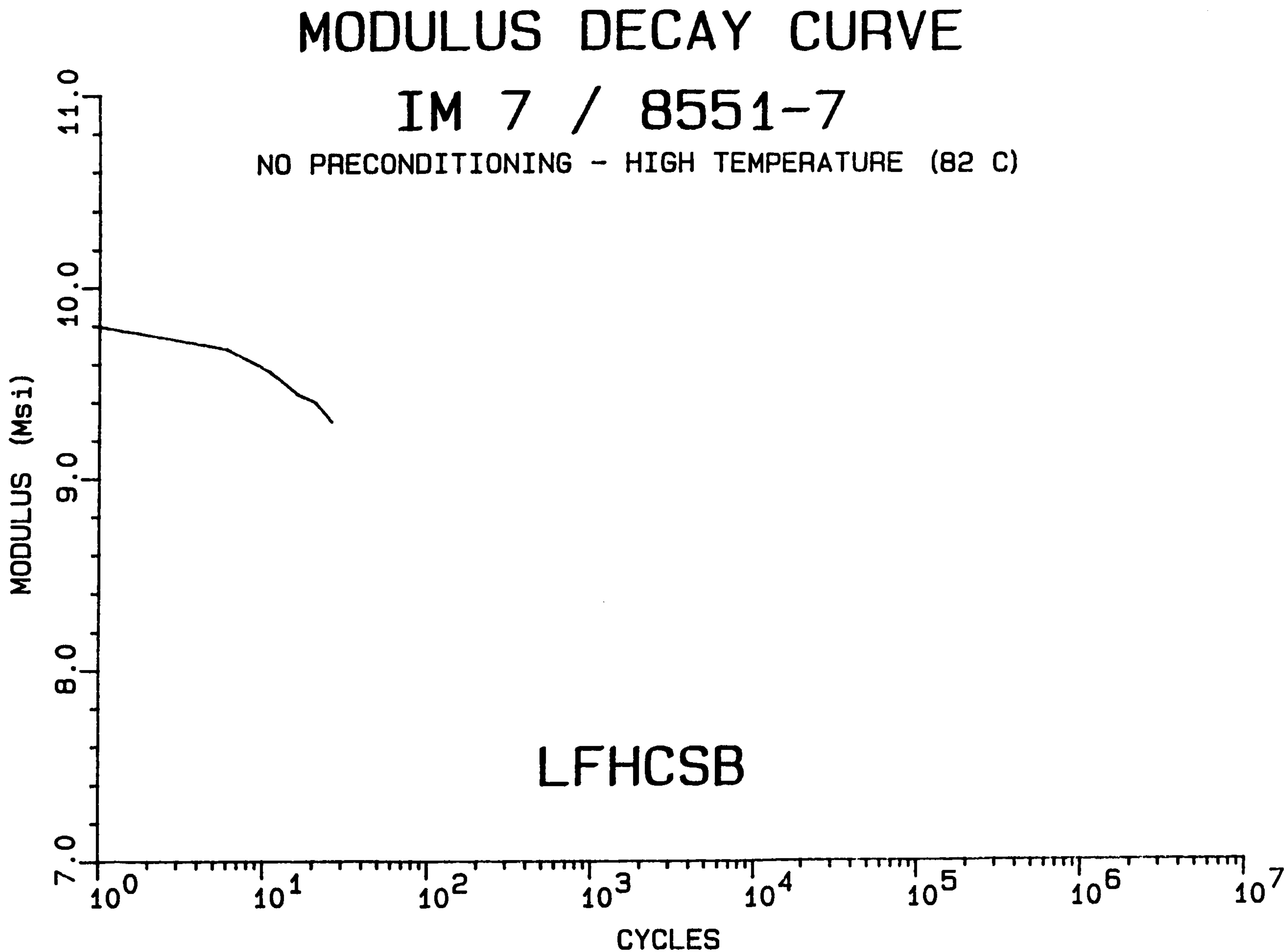
MODULUS DECAY CURVE
IM 7 / 8551-7
NO PRECONDITIONING - HIGH TEMPERATURE (82 C)
LFHCSB
MODULUS (Msi)
7.0
8.0
9.0
10.0
11.0
CYCLES
10^0
10^1
10^2
10^3
10^4
10^5
10^6
10^7

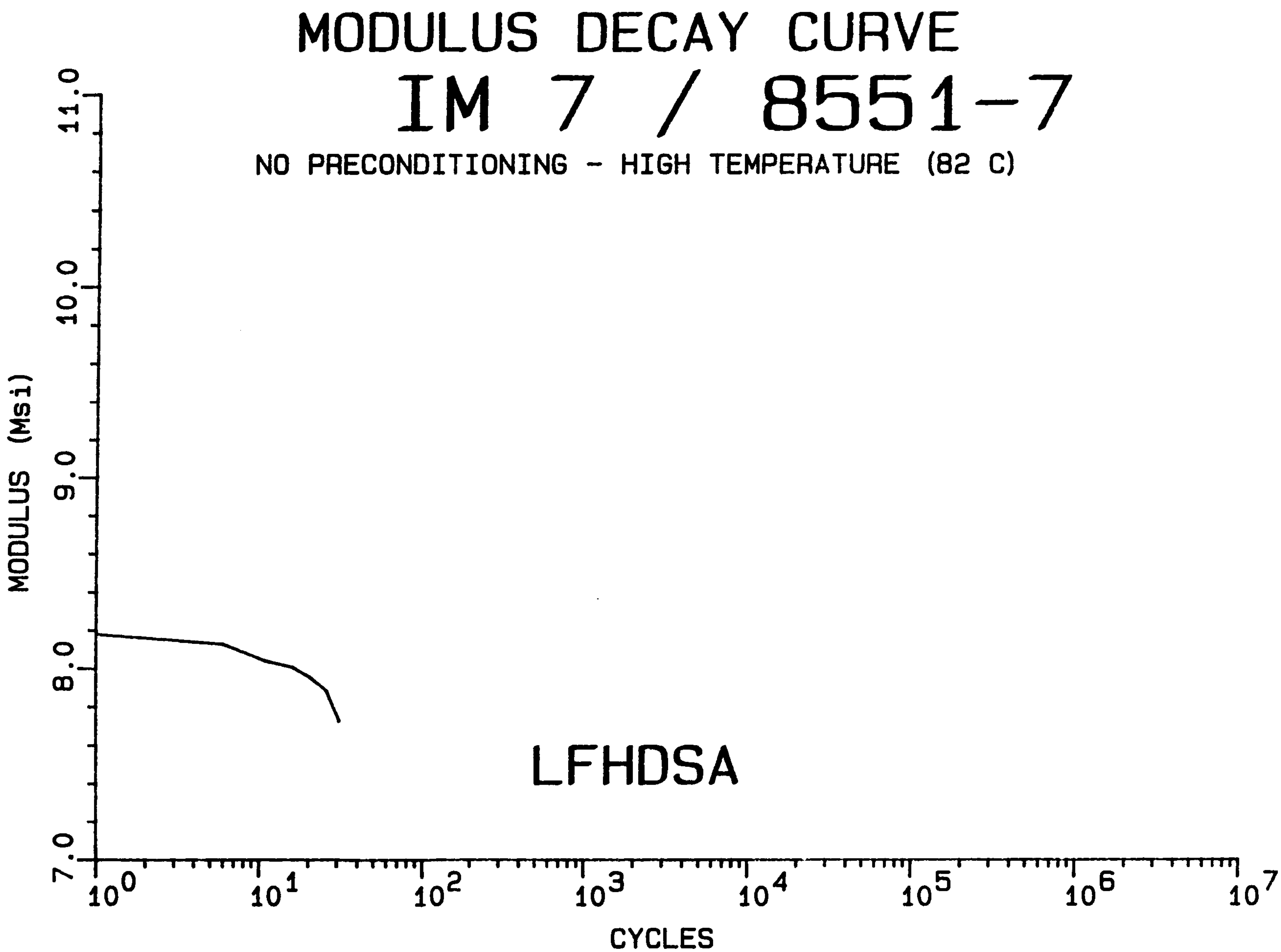
MODULUS DECAY CURVE
IM 7 / 8551-7
NO PRECONDITIONING - HIGH TEMPERATURE (82 C)
MODULUS (Msi)
11.0
10.0
9.0
8.0
7.0
LFHDSA
10^0
10^1
10^2
10^3
10^4
10^5
10^6
10^7
CYCLES

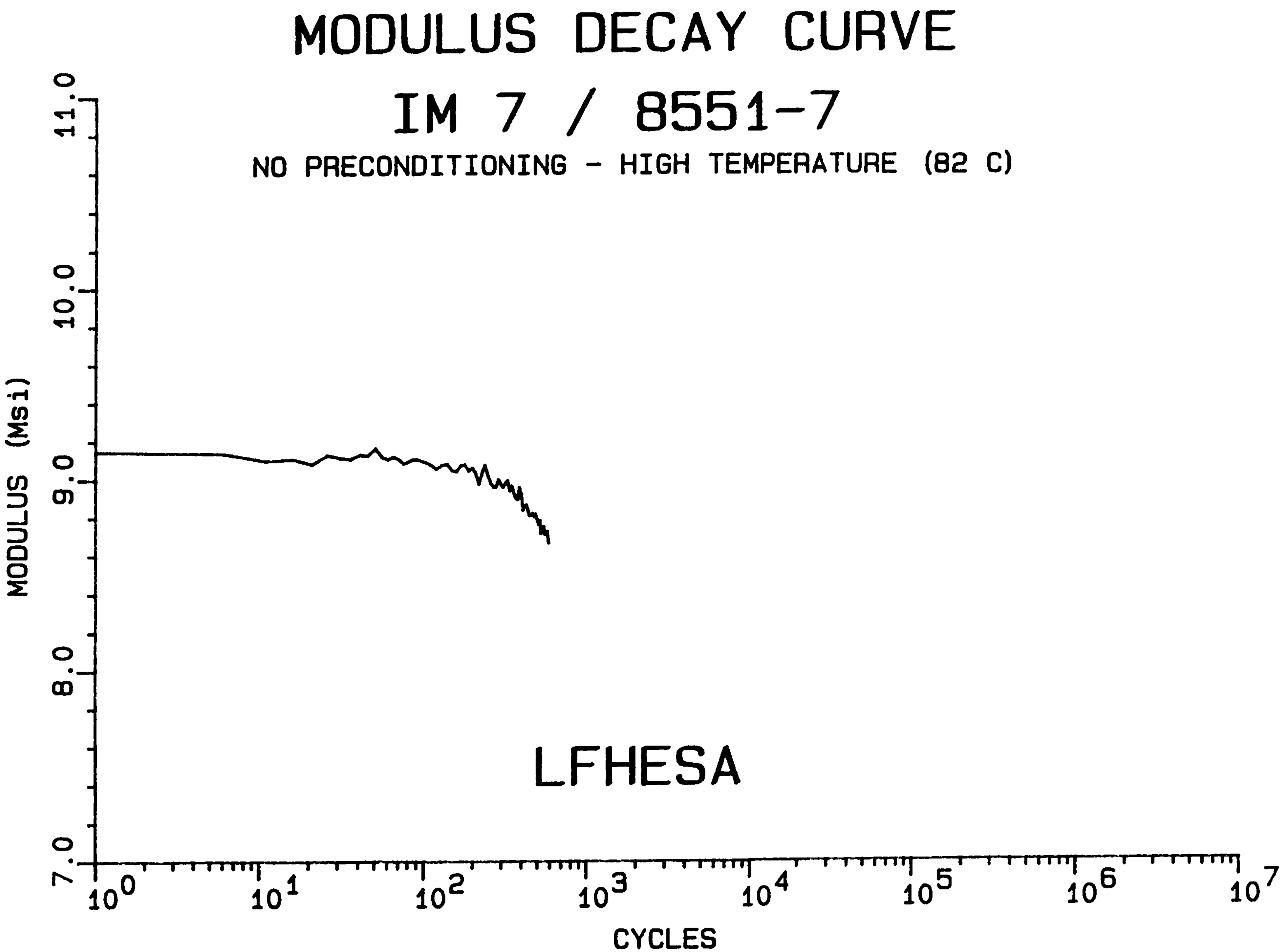
MODULUS DECAY CURVE
IM 7 / 8551-7
NO PRECONDITIONING - HIGH TEMPERATURE (82 C)
MODULUS (Msi)
11.0
10.0
9.0
8.0
7.0
LFHESA
10^0
10^1
10^2
10^3
10^4
10^5
10^6
10^7
CYCLES

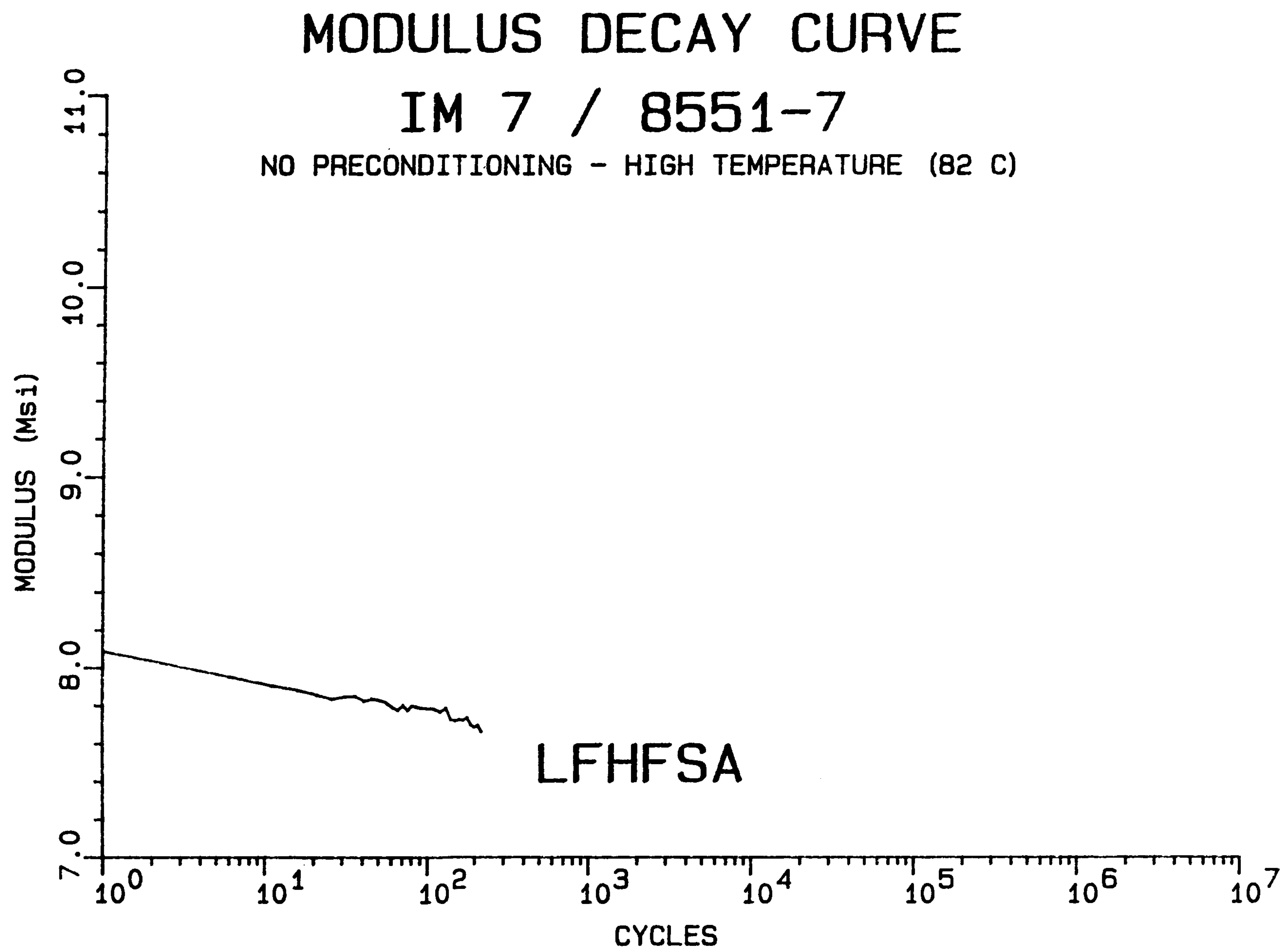
MODULUS DECAY CURVE
IM 7 / 8551-7
NO PRECONDITIONING - HIGH TEMPERATURE (82 C)
LFHFSA
MODULUS (Msi)
CYCLES
7.0
8.0
9.0
10.0
11.0
10^0
10^1
10^2
10^3
10^4
10^5
10^6
10^7

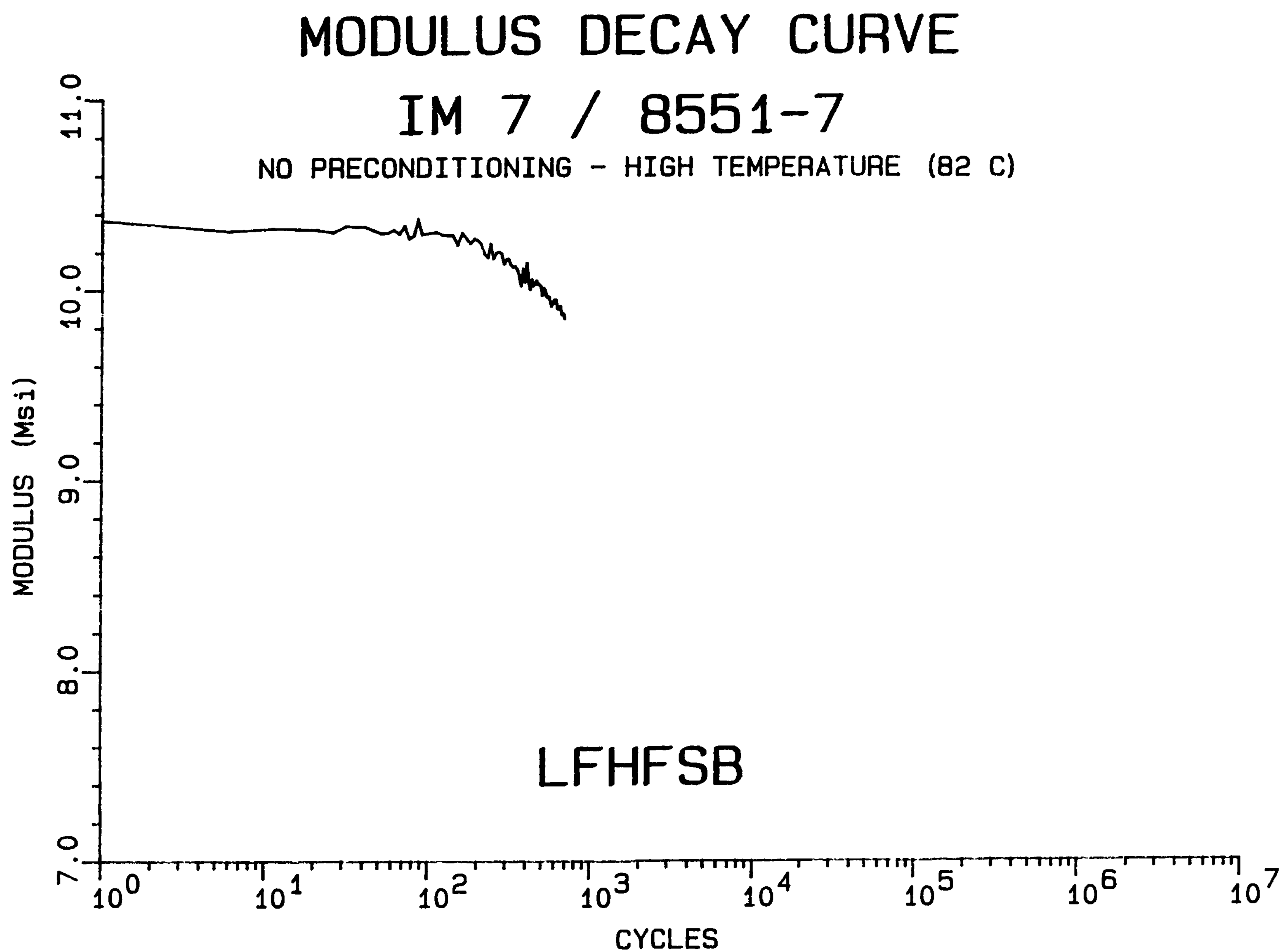
MODULUS DECAY CURVE
IM 7 / 8551-7
NO PRECONDITIONING - HIGH TEMPERATURE (82 C)
MODULUS (Msi)
11.0
10.0
9.0
8.0
7.0
10^0 10^1 10^2 10^3 10^4 10^5 10^6 10^7
CYCLES
LFHFSB

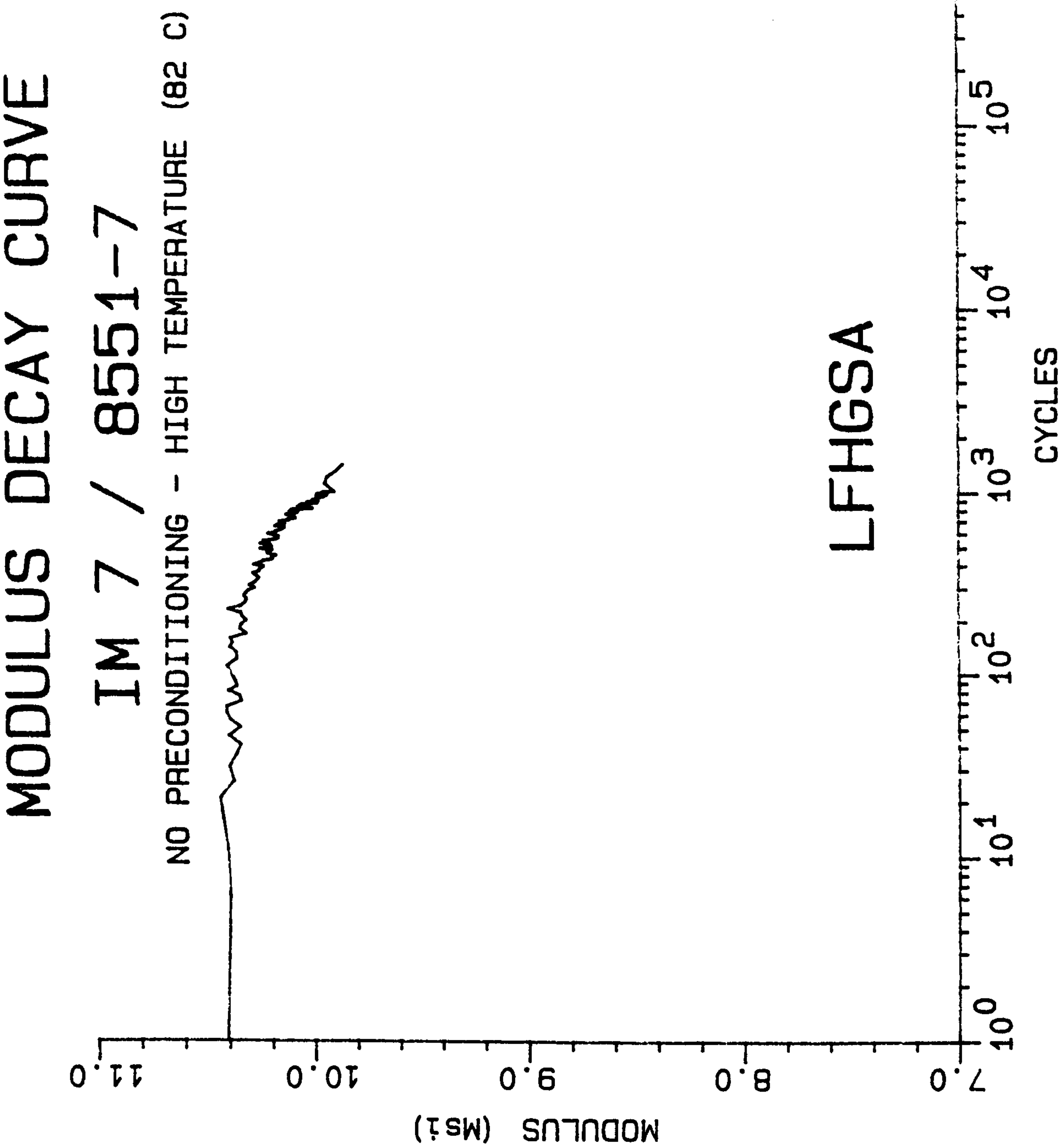
MODULUS DECAY CURVE
IM 7 / 8551-7
NO PRECONDITIONING - HIGH TEMPERATURE (82 C)
LFHGSA
MODULUS (Msi)
7.0
8.0
9.0
10.0
11.0
CYCLES
10^0
10^1
10^2
10^3
10^4
10^5
10^6
10^7

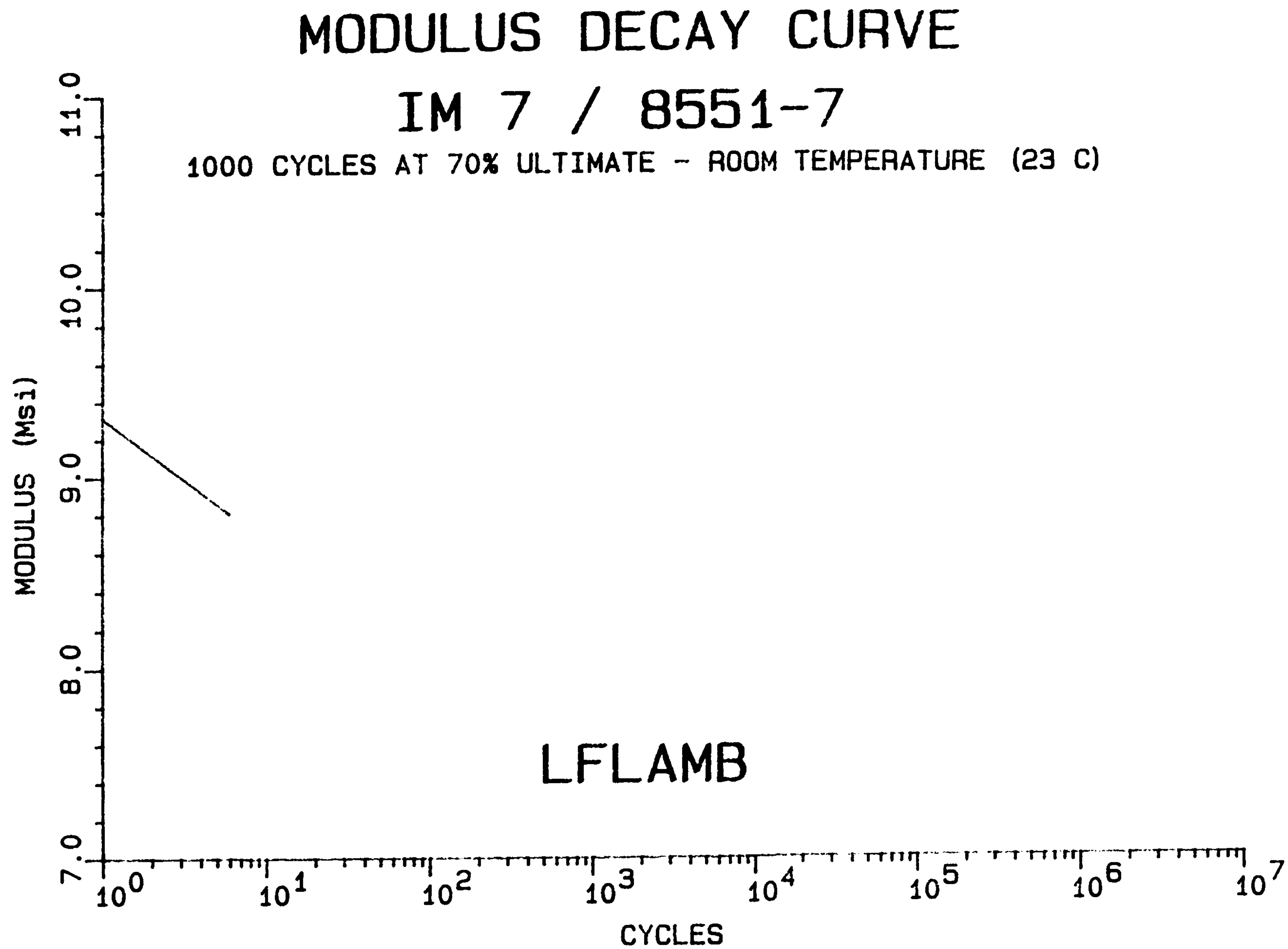
MODULUS DECAY CURVE
IM 7 / 8551-7
1000 CYCLES AT 70% ULTIMATE - ROOM TEMPERATURE (23 C)
LFLAMB
MODULUS (Msi)
7.0
8.0
9.0
10.0
11.0
CYCLES
10^0
10^1
10^2
10^3
10^4
10^5
10^6
10^7

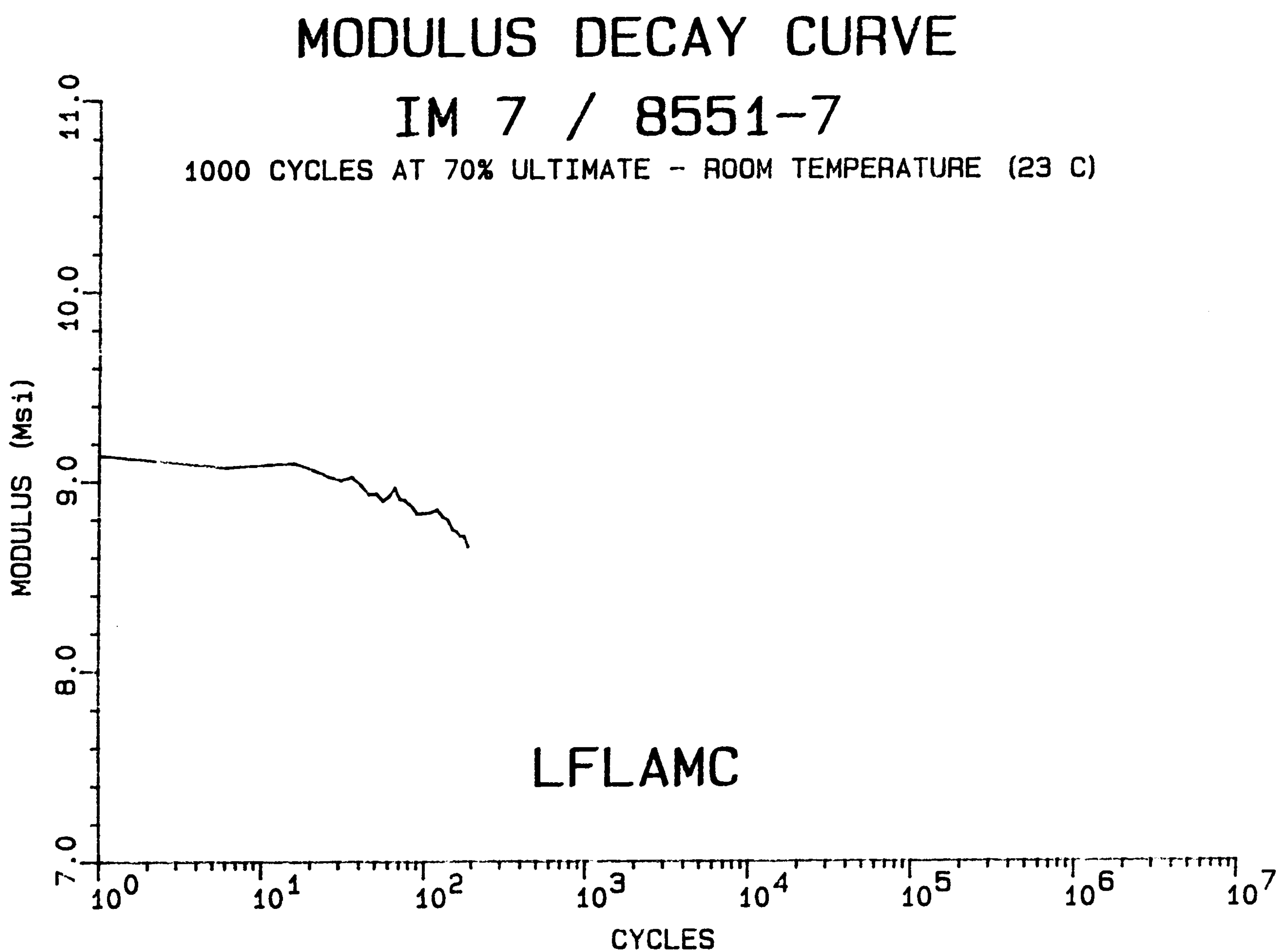
MODULUS DECAY CURVE
IM 7 / 8551-7
1000 CYCLES AT 70% ULTIMATE - ROOM TEMPERATURE (23 C)
LFLAMC
MODULUS (Msi)
7.0
8.0
9.0
10.0
11.0
CYCLES
10^0
10^1
10^2
10^3
10^4
10^5
10^6
10^7

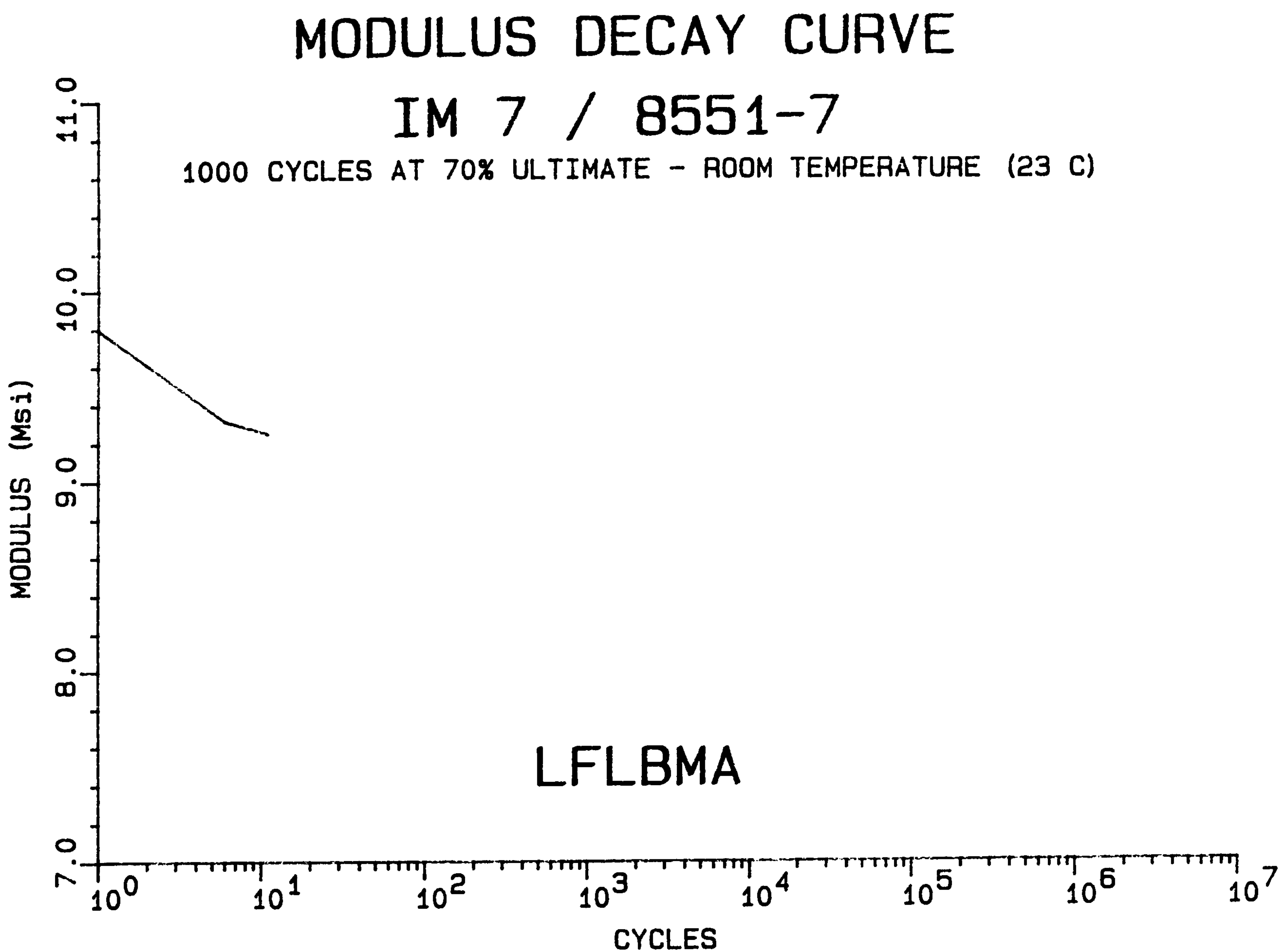
MODULUS DECAY CURVE
IM 7 / 8551-7
1000 CYCLES AT 70% ULTIMATE - ROOM TEMPERATURE (23 C)
LFLBMA
MODULUS (Msi)
11.0
10.0
9.0
8.0
7.0
CYCLES
10^0
10^1
10^2
10^3
10^4
10^5
10^6
10^7

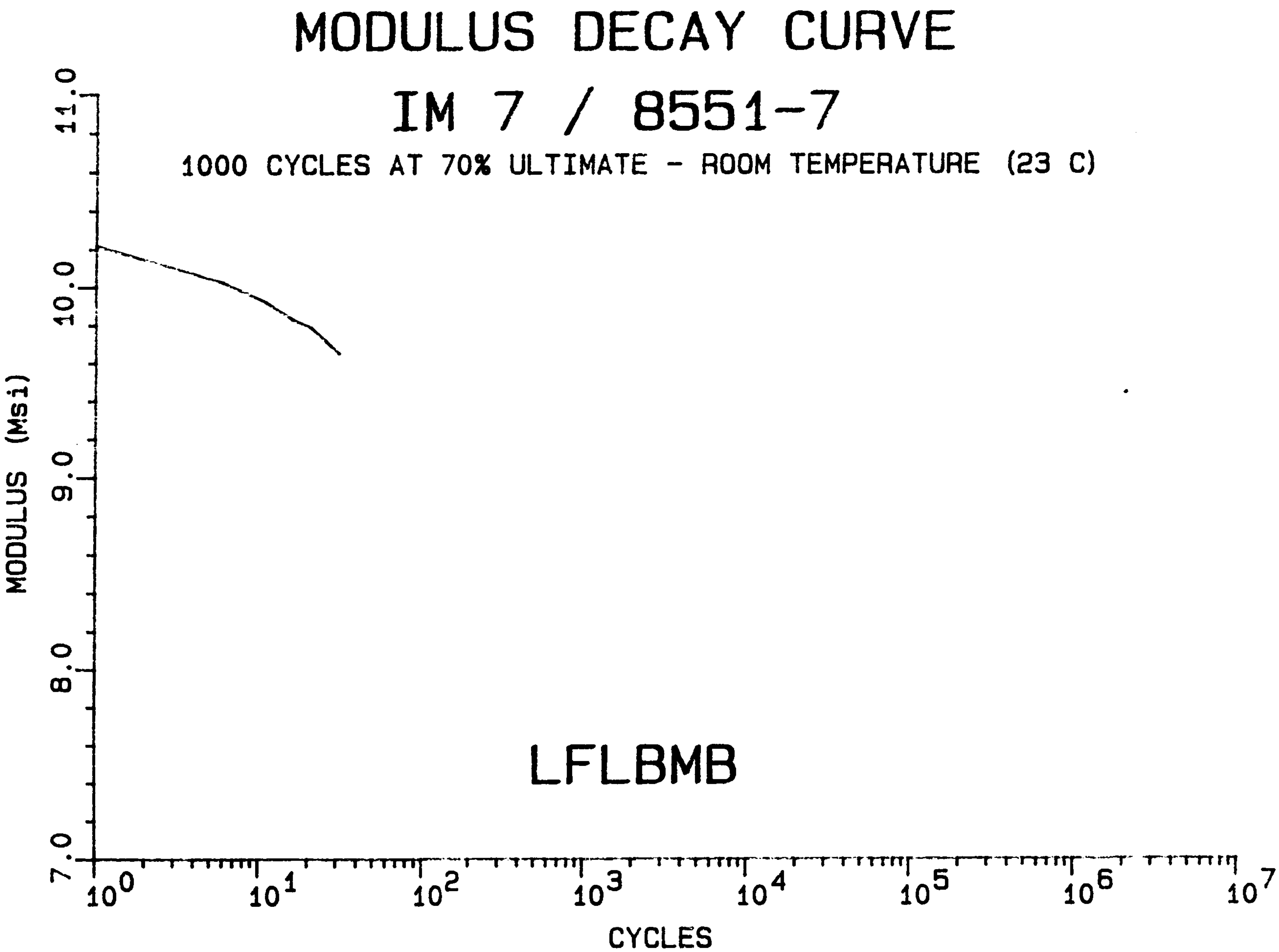

MODULUS DECAY CURVE
IM 7 / 8551-7
1000 CYCLES AT 70% ULTIMATE - ROOM TEMPERATURE (23 C)
LFLBMB
MODULUS (Msi)
11.0
10.0
9.0
8.0
7.0
10^0
10^1
10^2
10^3
10^4
10^5
10^6
10^7
CYCLES

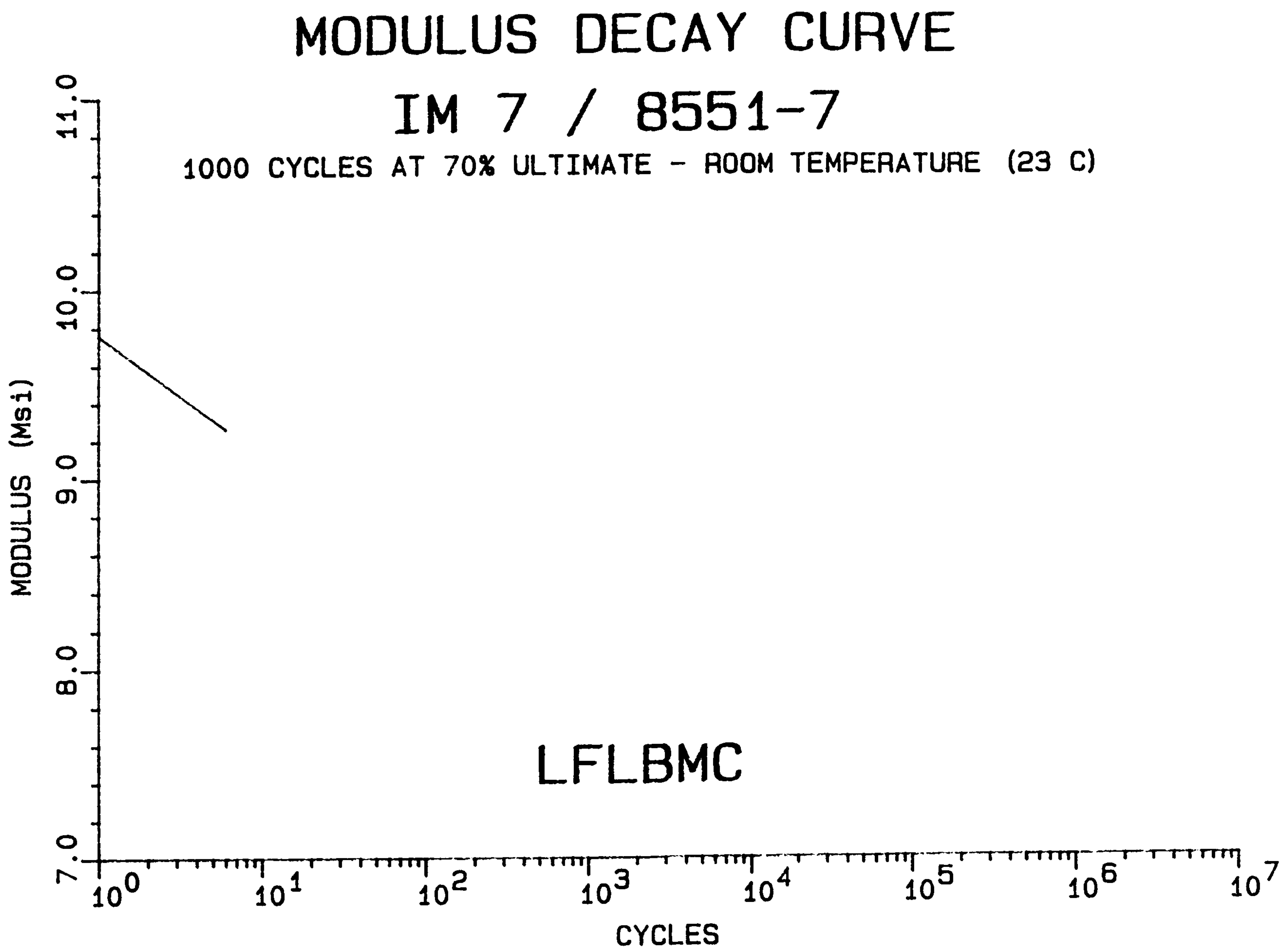
MODULUS DECAY CURVE
IM 7 / 8551-7
1000 CYCLES AT 70% ULTIMATE - ROOM TEMPERATURE (23 C)
MODULUS (Msi)
11.0
10.0
9.0
8.0
7.0
10^0
10^1
10^2
10^3
10^4
10^5
10^6
10^7
CYCLES
LFLBMC

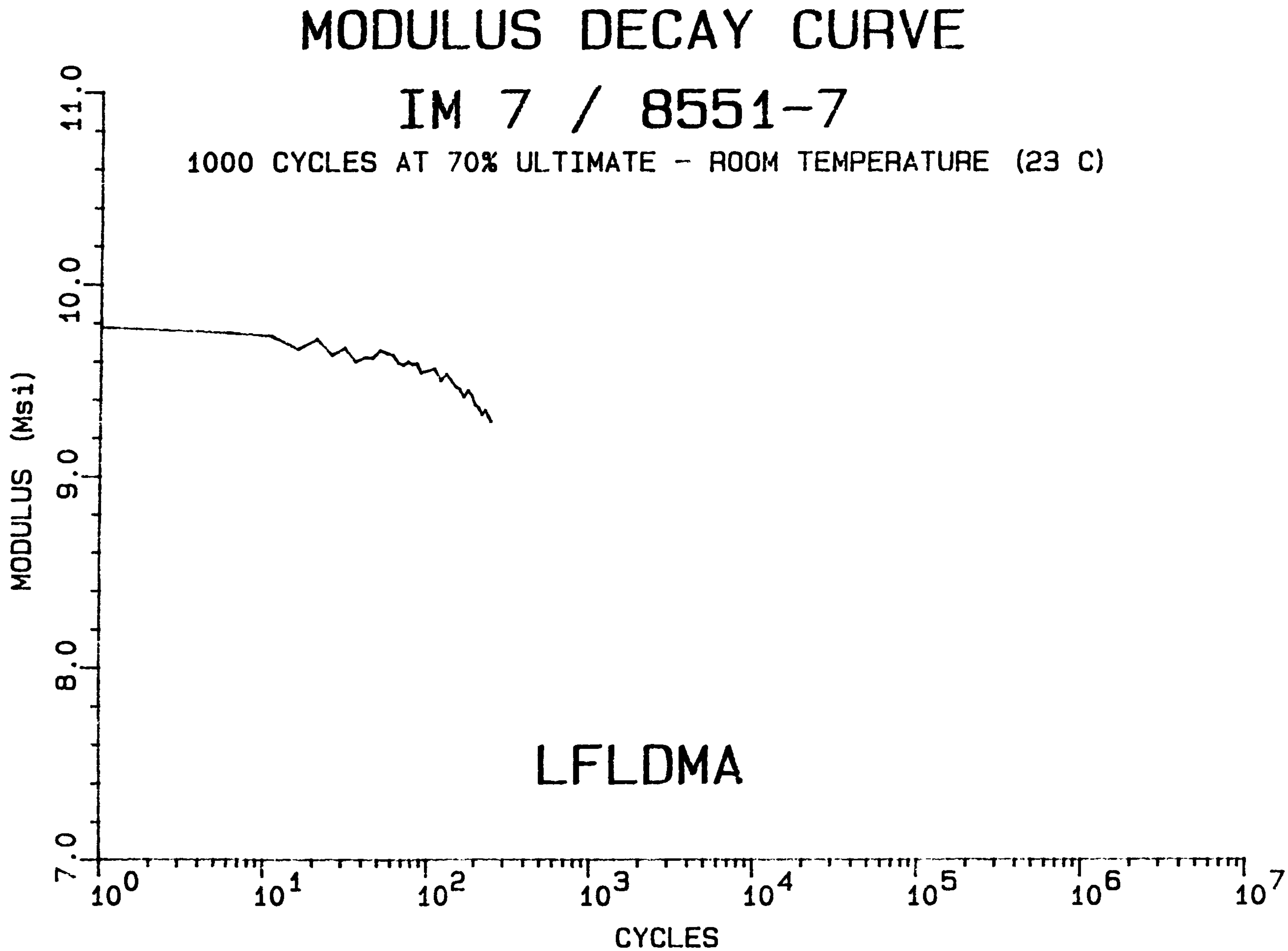

MODULUS DECAY CURVE
IM 7 / 8551-7
1000 CYCLES AT 70% ULTIMATE - ROOM TEMPERATURE (23 C)
LFLDMA
MODULUS (Msi)
7.0
8.0
9.0
10.0
11.0
CYCLES
10^0
10^1
10^2
10^3
10^4
10^5
10^6
10^7

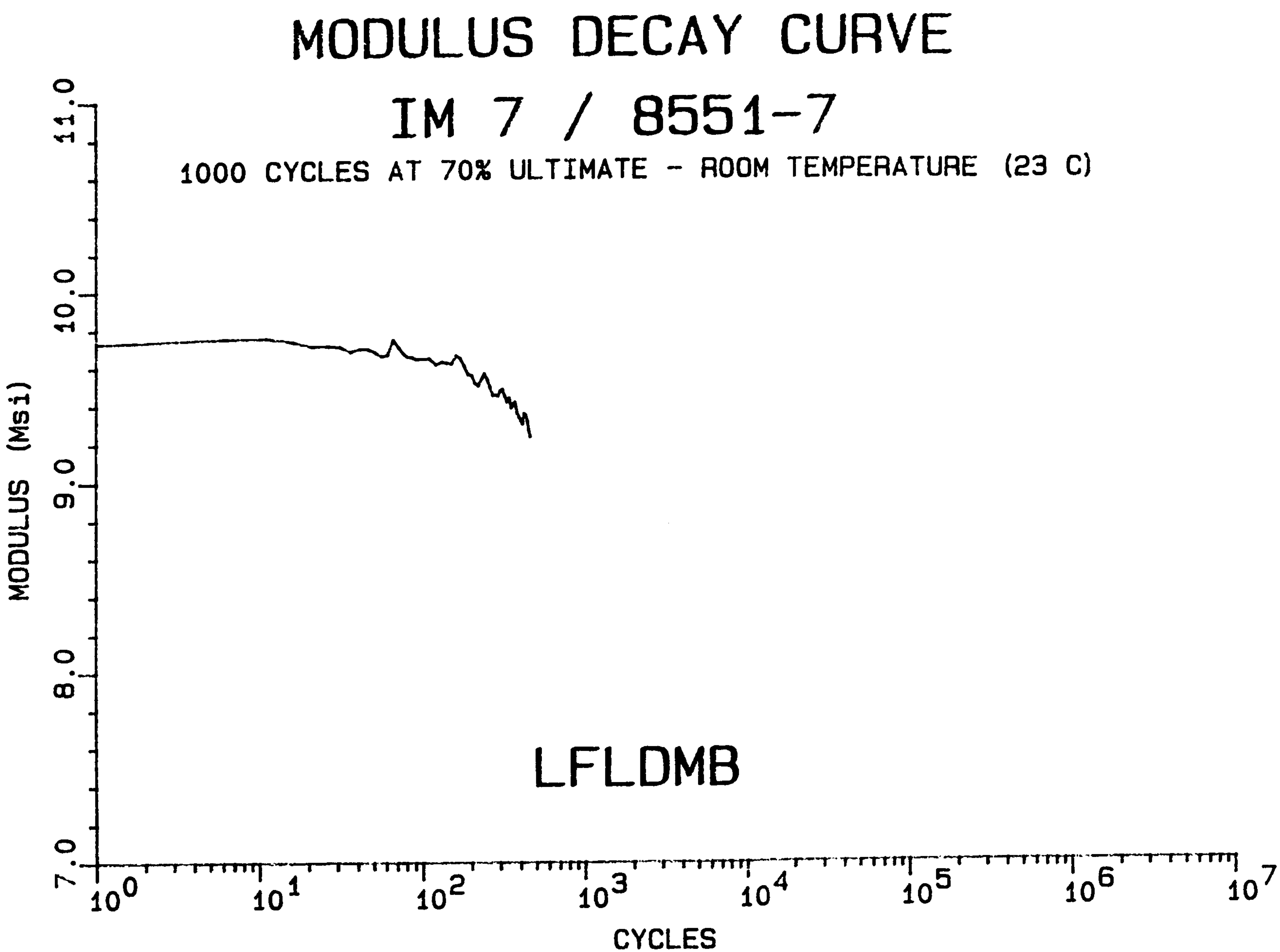
MODULUS DECAY CURVE
IM 7 / 8551-7
1000 CYCLES AT 70% ULTIMATE - ROOM TEMPERATURE (23 C)
MODULUS (Msi)
11.0
10.0
9.0
8.0
7.0
10^0
10^1
10^2
10^3
10^4
10^5
10^6
10^7
CYCLES
LFLDMB

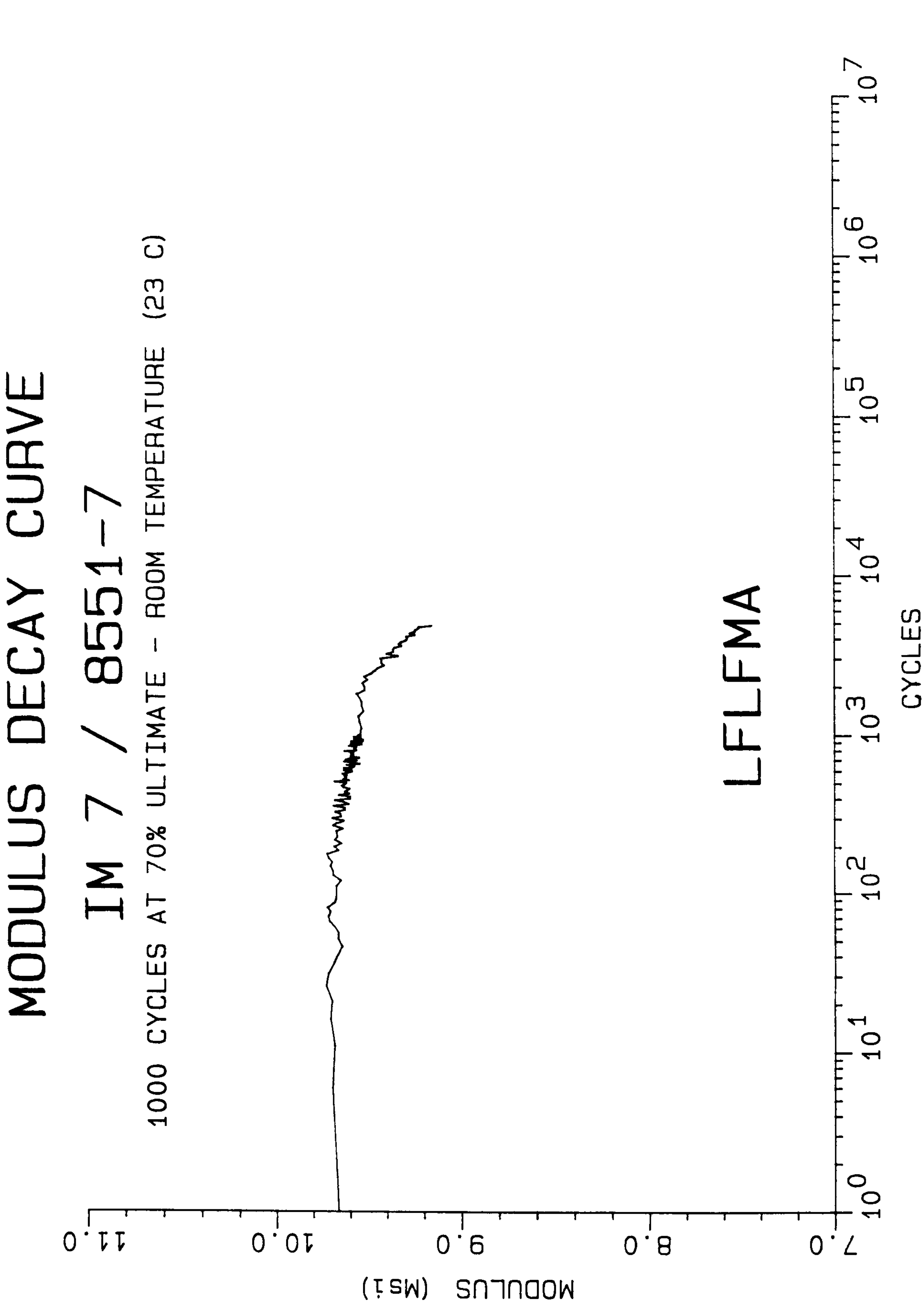
MODULUS DECAY CURVE
IM 7 / 8551-7
1000 CYCLES AT 70% ULTIMATE - ROOM TEMPERATURE (23 C)
LFLFMA
MODULUS (Msi)
CYCLES
7.0
8.0
9.0
10.0
11.0
10^0
10^1
10^2
10^3
10^4
10^5
10^6
10^7

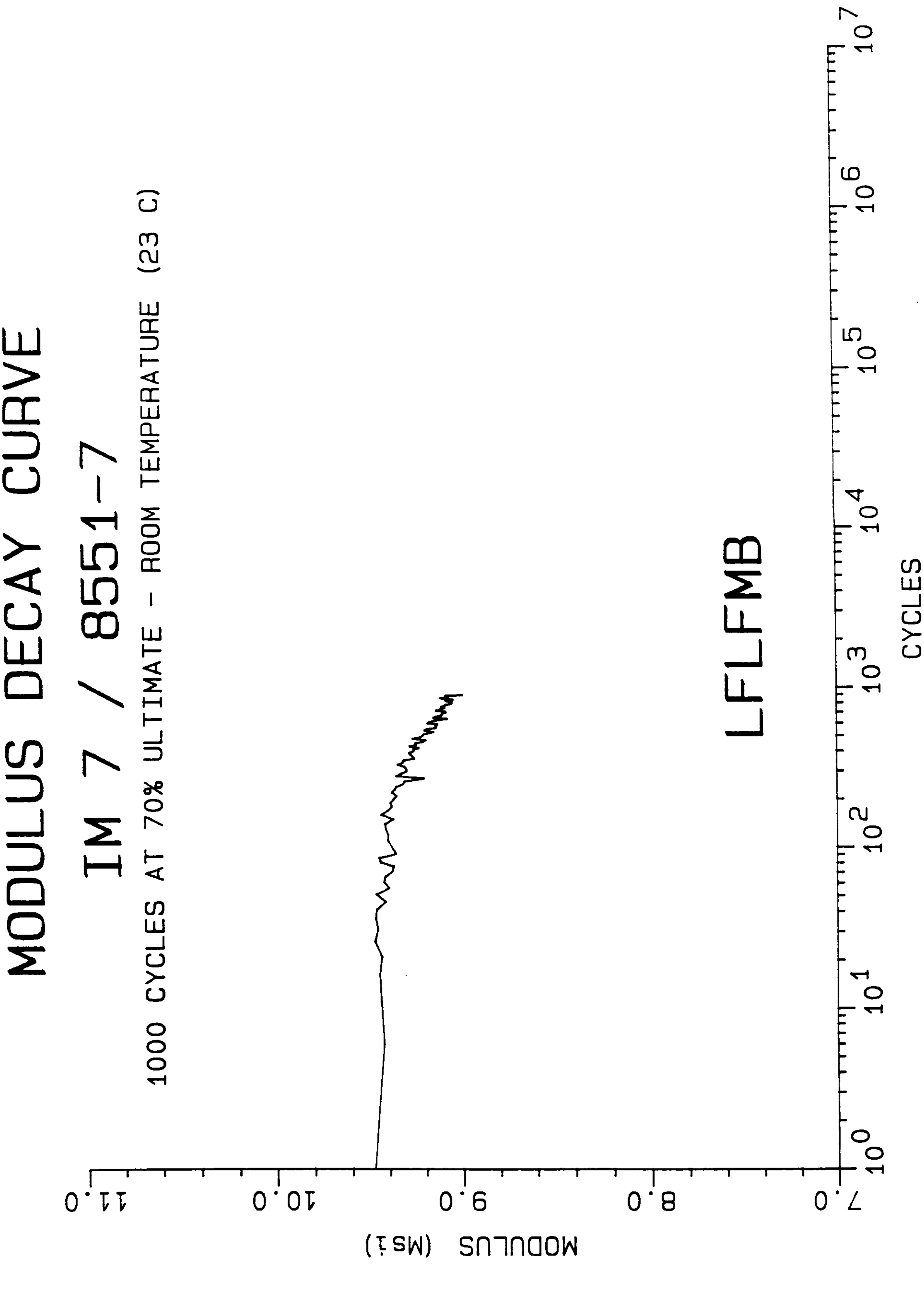
MODULUS DECAY CURVE
IM 7 / 8551-7
1000 CYCLES AT 70% ULTIMATE - ROOM TEMPERATURE (23 C)
LFLFMB
MODULUS (Msi)
7.0
8.0
9.0
10.0
11.0
CYCLES
10^0
10^1
10^2
10^3
10^4
10^5
10^6
10^7

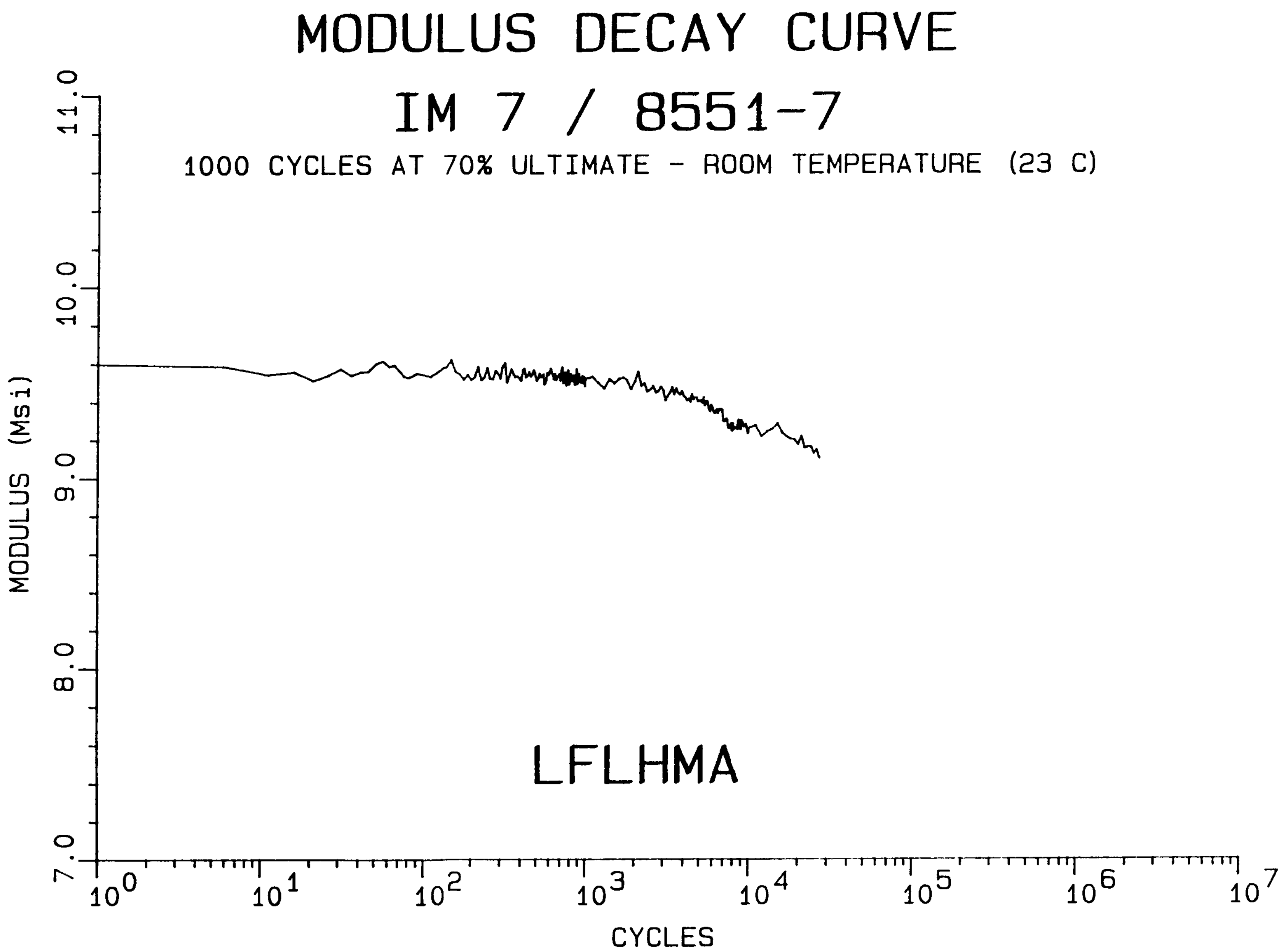

MODULUS DECAY CURVE
IM 7 / 8551-7
1000 CYCLES AT 70% ULTIMATE - ROOM TEMPERATURE (23 C)
MODULUS (Msi)
11.0
10.0
9.0
8.0
7.0
LFLHMA
10^0
10^1
10^2
10^3
10^4
10^5
10^6
10^7
CYCLES

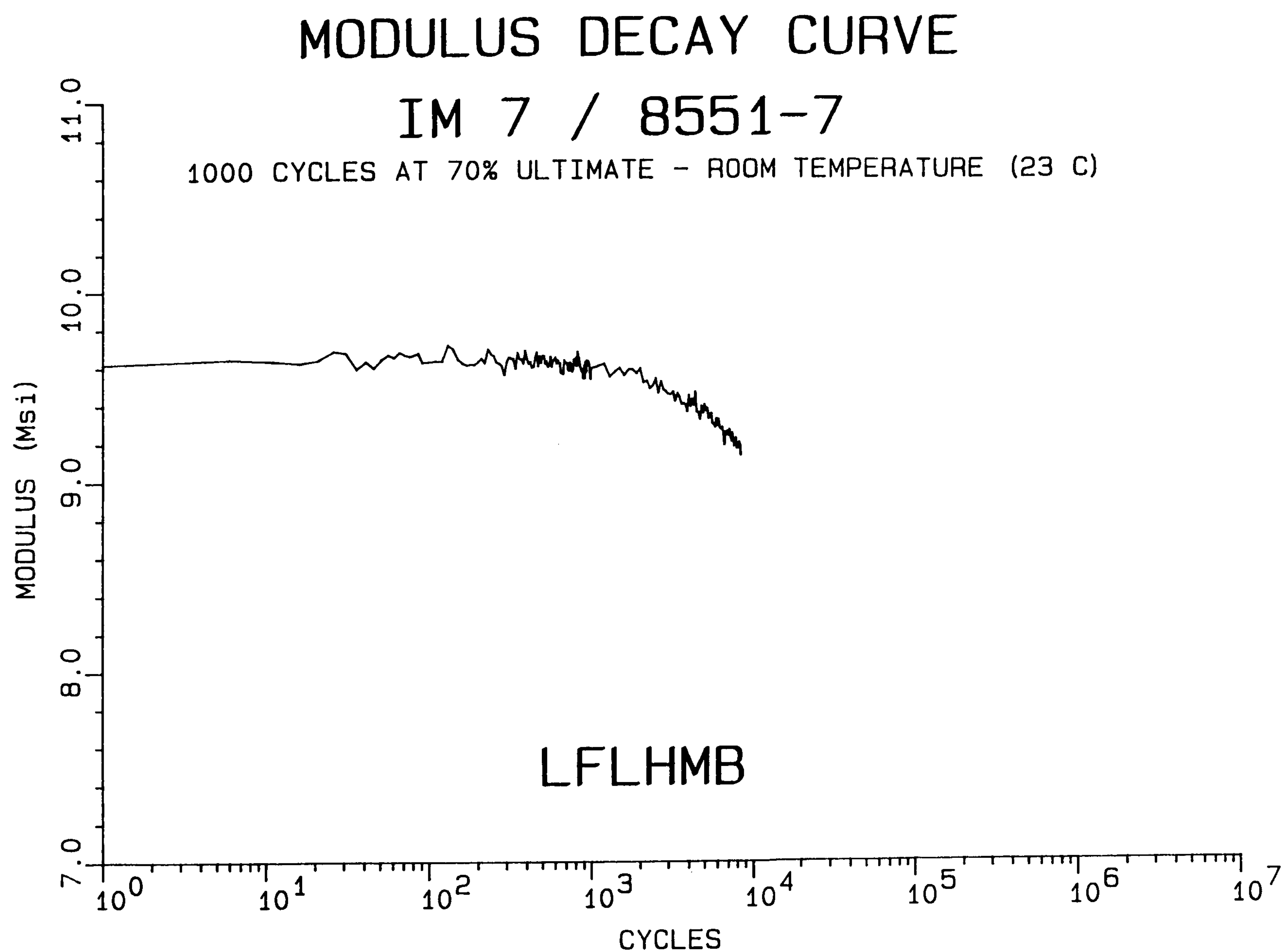
MODULUS DECAY CURVE
IM 7 / 8551-7
1000 CYCLES AT 70% ULTIMATE - ROOM TEMPERATURE (23 C)
MODULUS (Msi)
11.0
10.0
9.0
8.0
7.0
LFLHMB
10^0
10^1
10^2
10^3
10^4
10^5
10^6
10^7
CYCLES

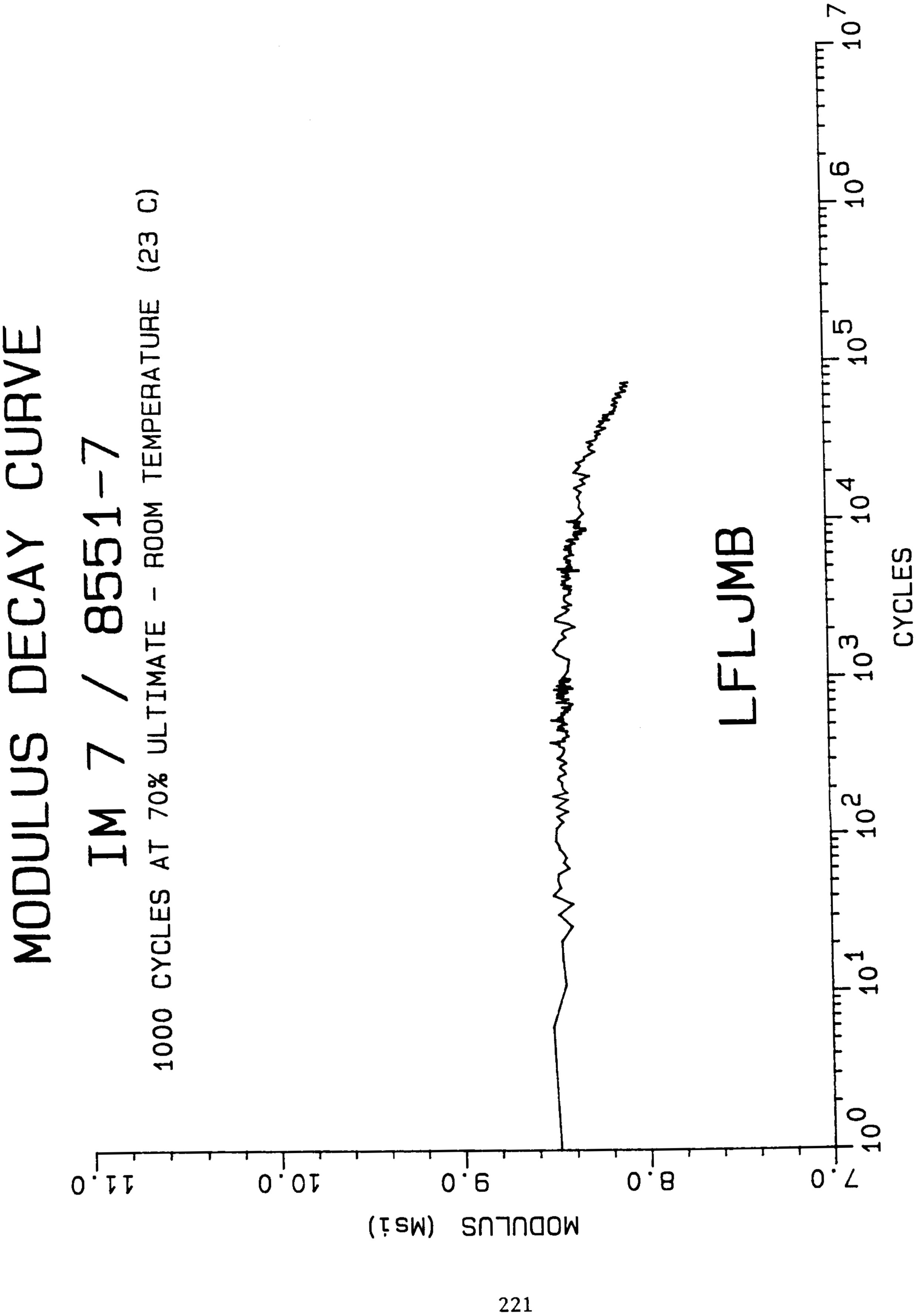
MODULUS DECAY CURVE
IM 7 / 8551-7
1000 CYCLES AT 70% ULTIMATE - ROOM TEMPERATURE (23 C)
LFLJMB
MODULUS (Msi)
7.0
8.0
9.0
10.0
11.0
CYCLES
10^0
10^1
10^2
10^3
10^4
10^5
10^6
10^7

MODULUS DECAY CURVE

IM 7 / 8551-7

1000 CYCLES AT 70% ULTIMATE - ROOM TEMPERATURE (23 C)

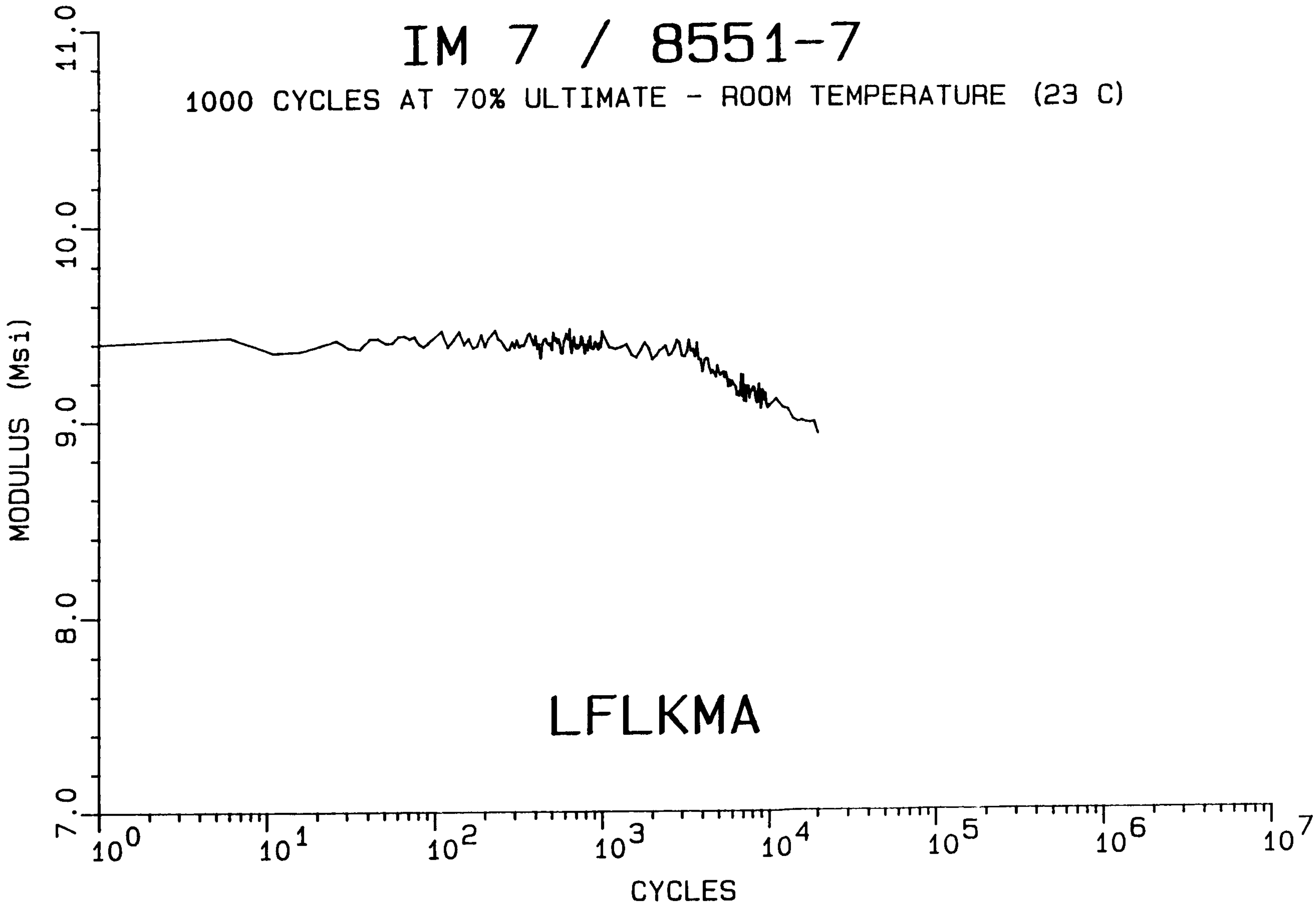

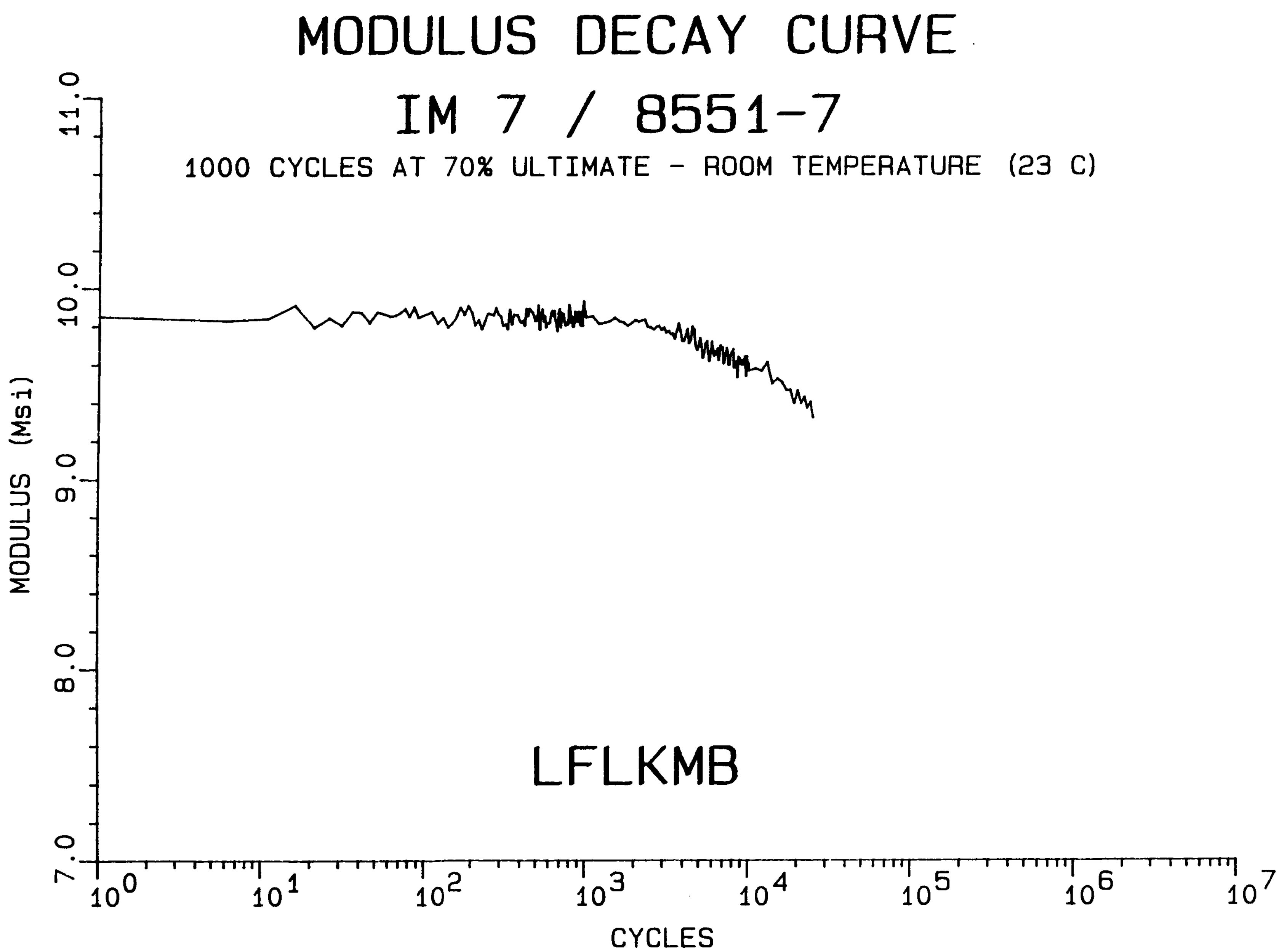
MODULUS DECAY CURVE
IM 7 / 8551-7
1000 CYCLES AT 70% ULTIMATE - ROOM TEMPERATURE (23 C)
LFLKMB
MODULUS (Msi)
11.0
10.0
9.0
8.0
7.0
10^0
10^1
10^2
10^3
10^4
10^5
10^6
10^7
CYCLES

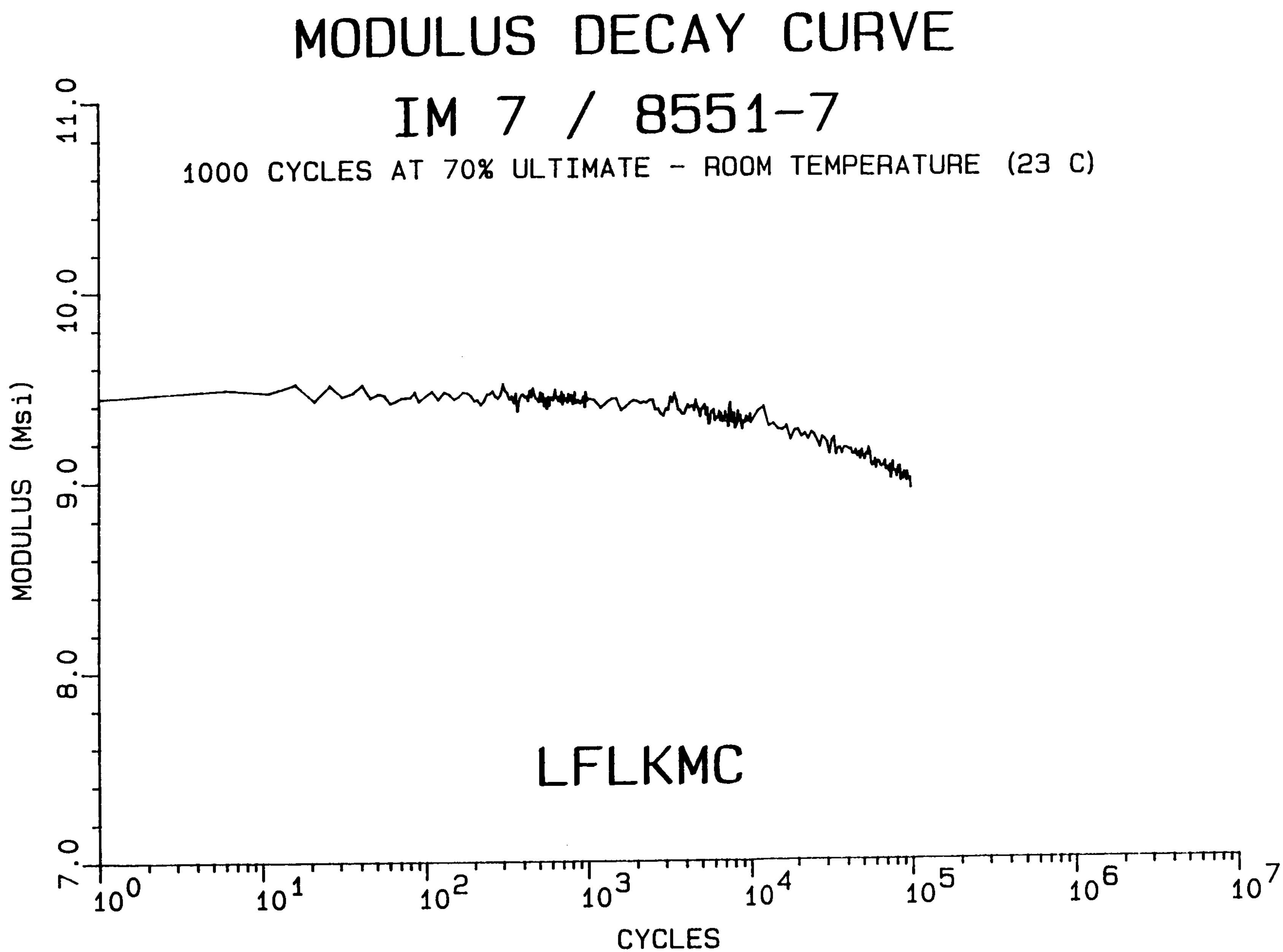

MODULUS DECAY CURVE
IM 7 / 8551-7
1000 CYCLES AT 70% ULTIMATE - ROOM TEMPERATURE (23 C)
MODULUS (Msi)
11.0
10.0
9.0
8.0
7.0
10^0
10^1
10^2
10^3
10^4
10^5
10^6
10^7
CYCLES
LFLKMC

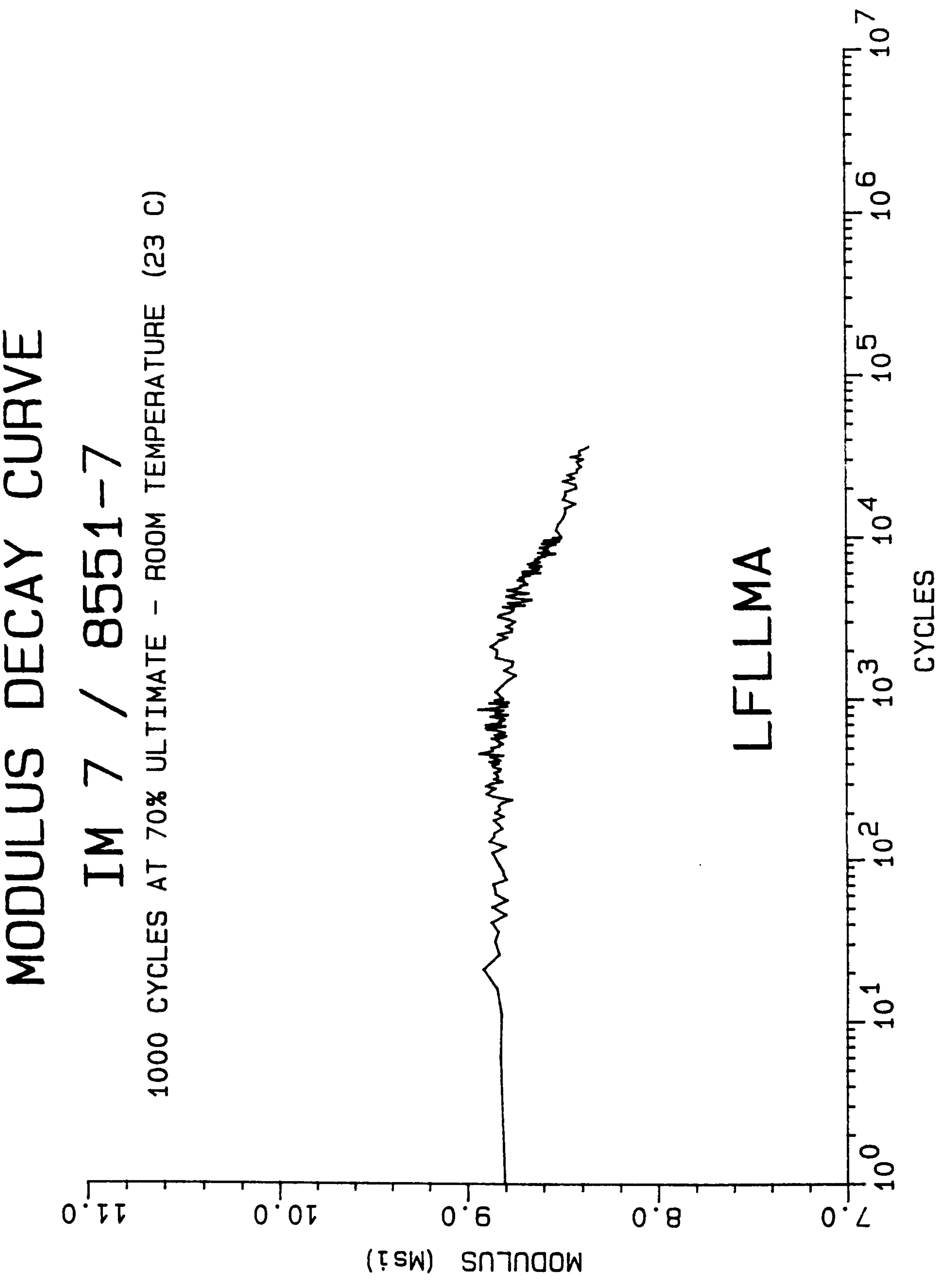
MODULUS DECAY CURVE
IM 7 / 8551-7
1000 CYCLES AT 70% ULTIMATE - ROOM TEMPERATURE (23 C)
LFLLMA
MODULUS (Msi)
7.0
8.0
9.0
10.0
11.0
CYCLES
10^0
10^1
10^2
10^3
10^4
10^5
10^6
10^7

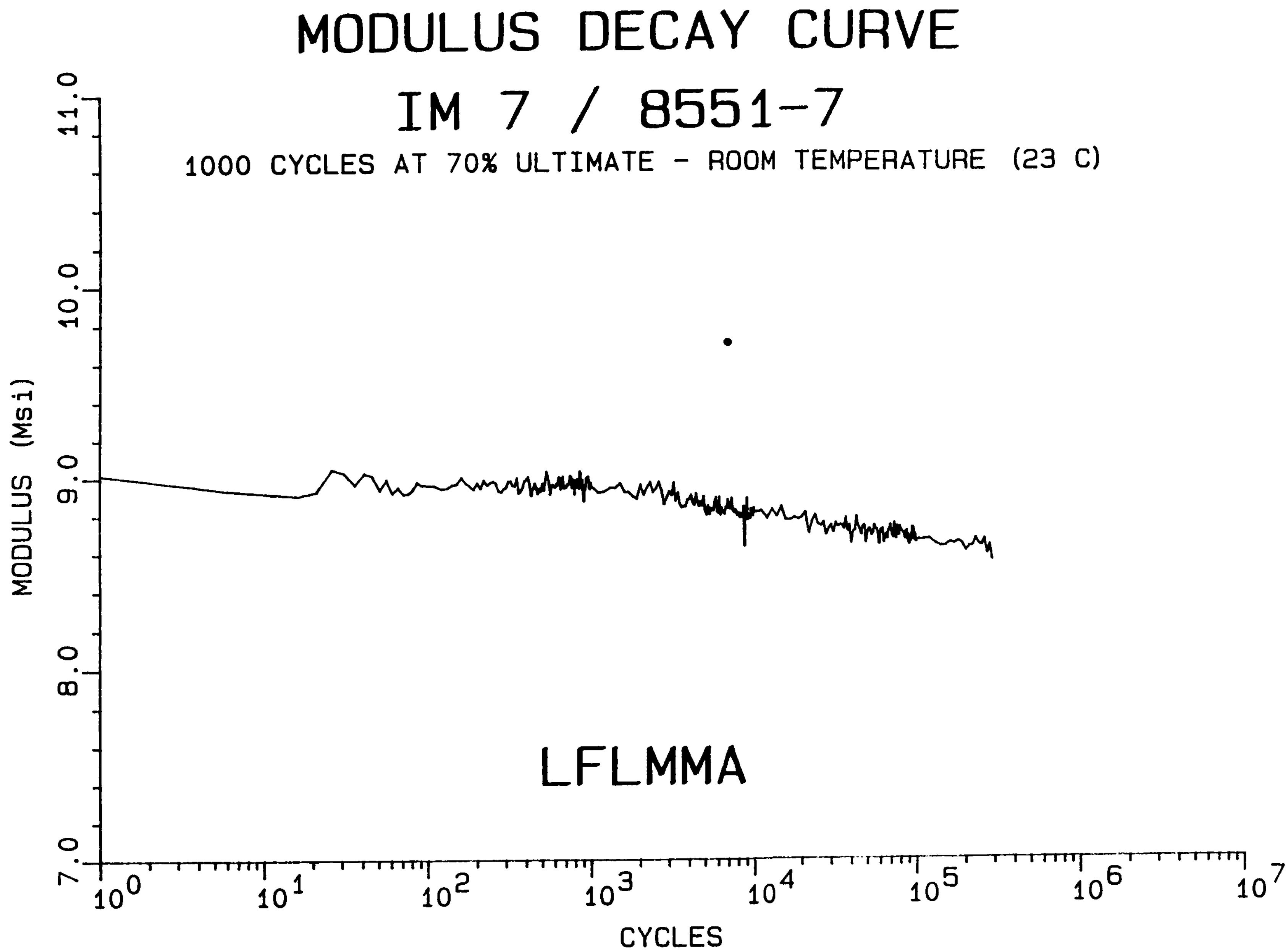
MODULUS DECAY CURVE
IM 7 / 8551-7
1000 CYCLES AT 70% ULTIMATE - ROOM TEMPERATURE (23 C)
MODULUS (Msi)
11.0
10.0
9.0
8.0
7.0
LFLMMA
CYCLES
10^0
10^1
10^2
10^3
10^4
10^5
10^6
10^7

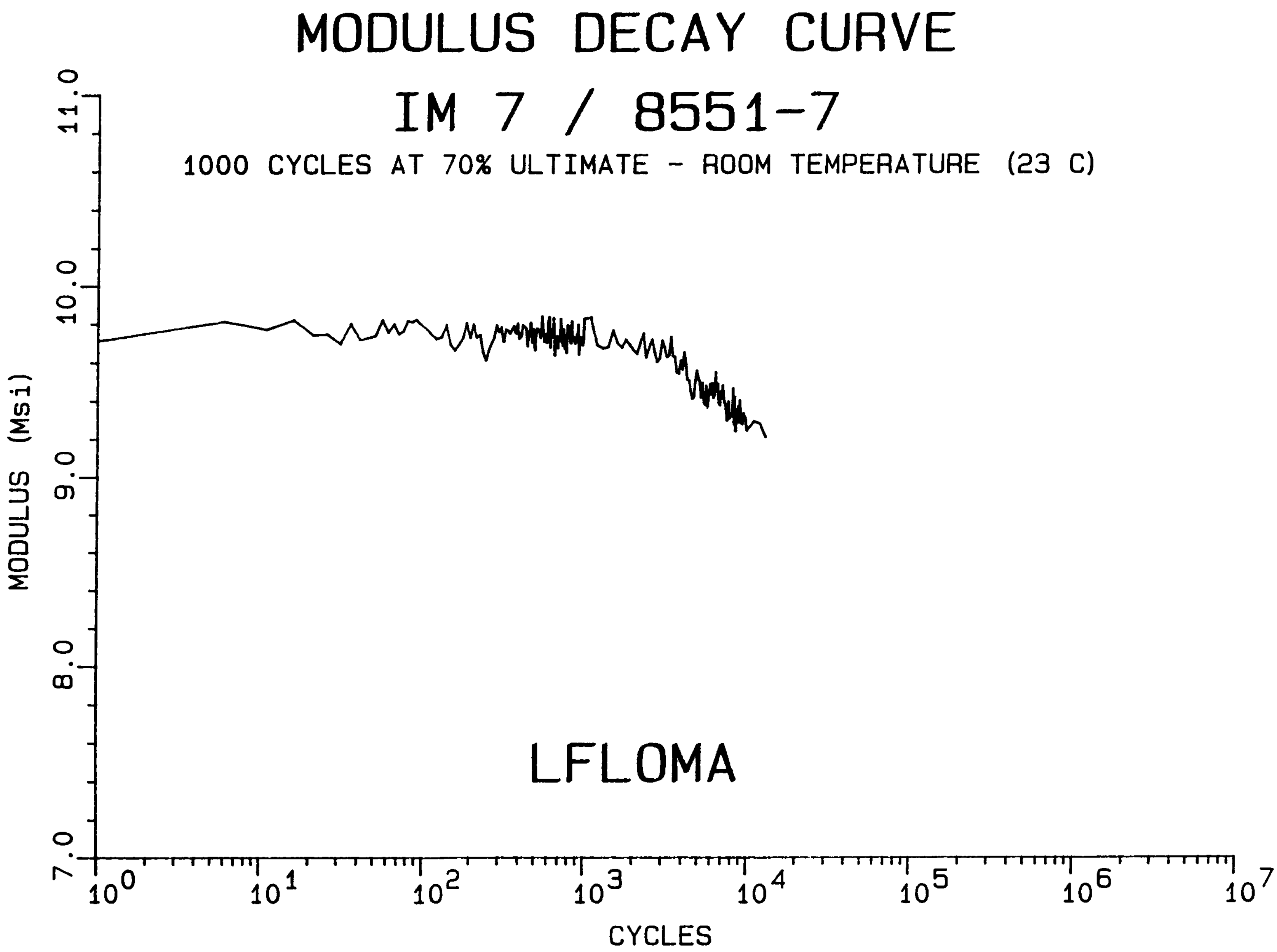
MODULUS DECAY CURVE
IM 7 / 8551-7
1000 CYCLES AT 70% ULTIMATE - ROOM TEMPERATURE (23 C)
MODULUS (Msi)
11.0
10.0
9.0
8.0
7.0
LFLOMA
10^0
10^1
10^2
10^3
10^4
10^5
10^6
10^7
CYCLES

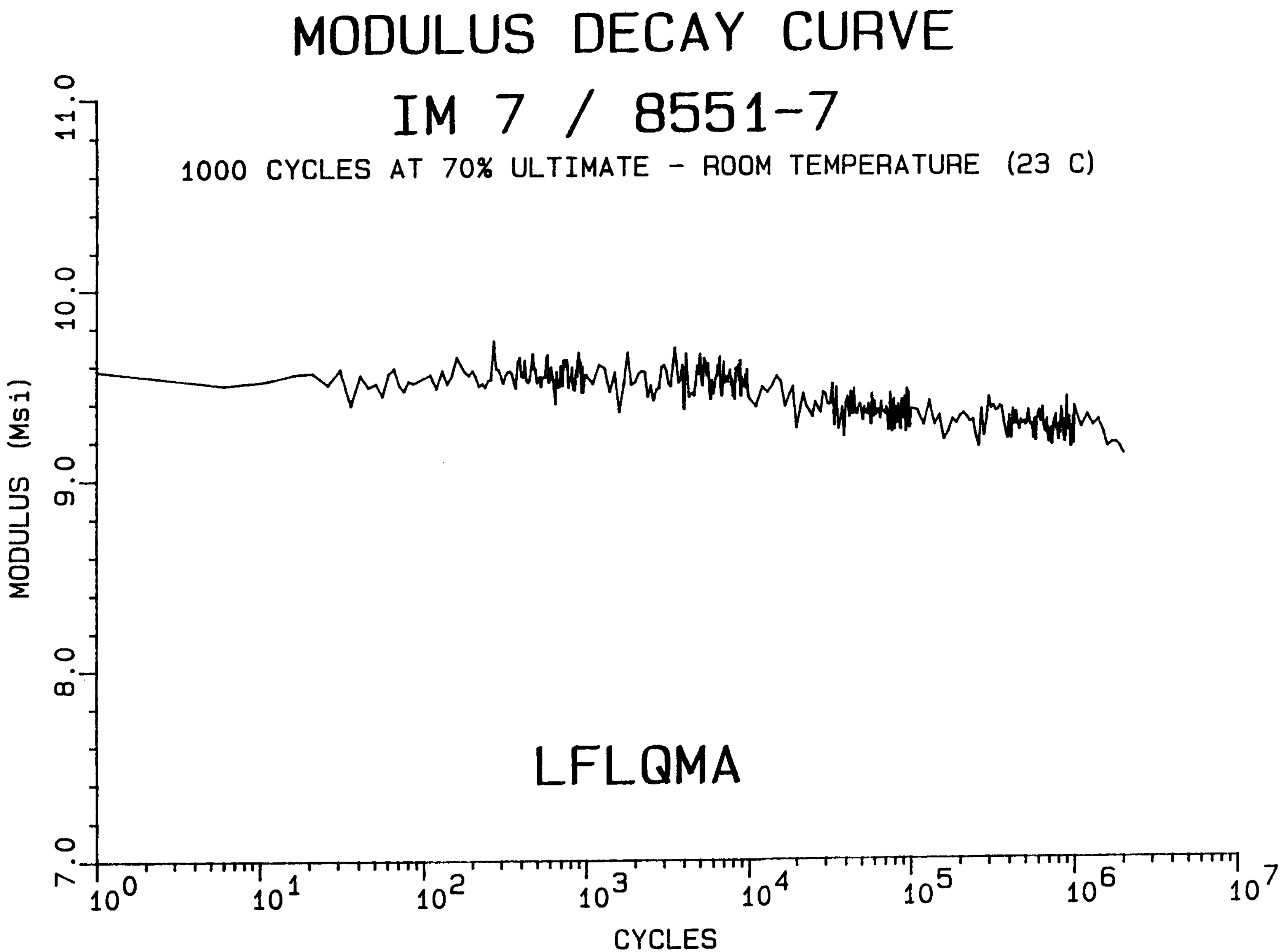
MODULUS DECAY CURVE
IM 7 / 8551-7
1000 CYCLES AT 70% ULTIMATE - ROOM TEMPERATURE (23 C)
LFLQMA
MODULUS (Msi)
11.0
10.0
9.0
8.0
7.0
CYCLES
10^0
10^1
10^2
10^3
10^4
10^5
10^6
10^7

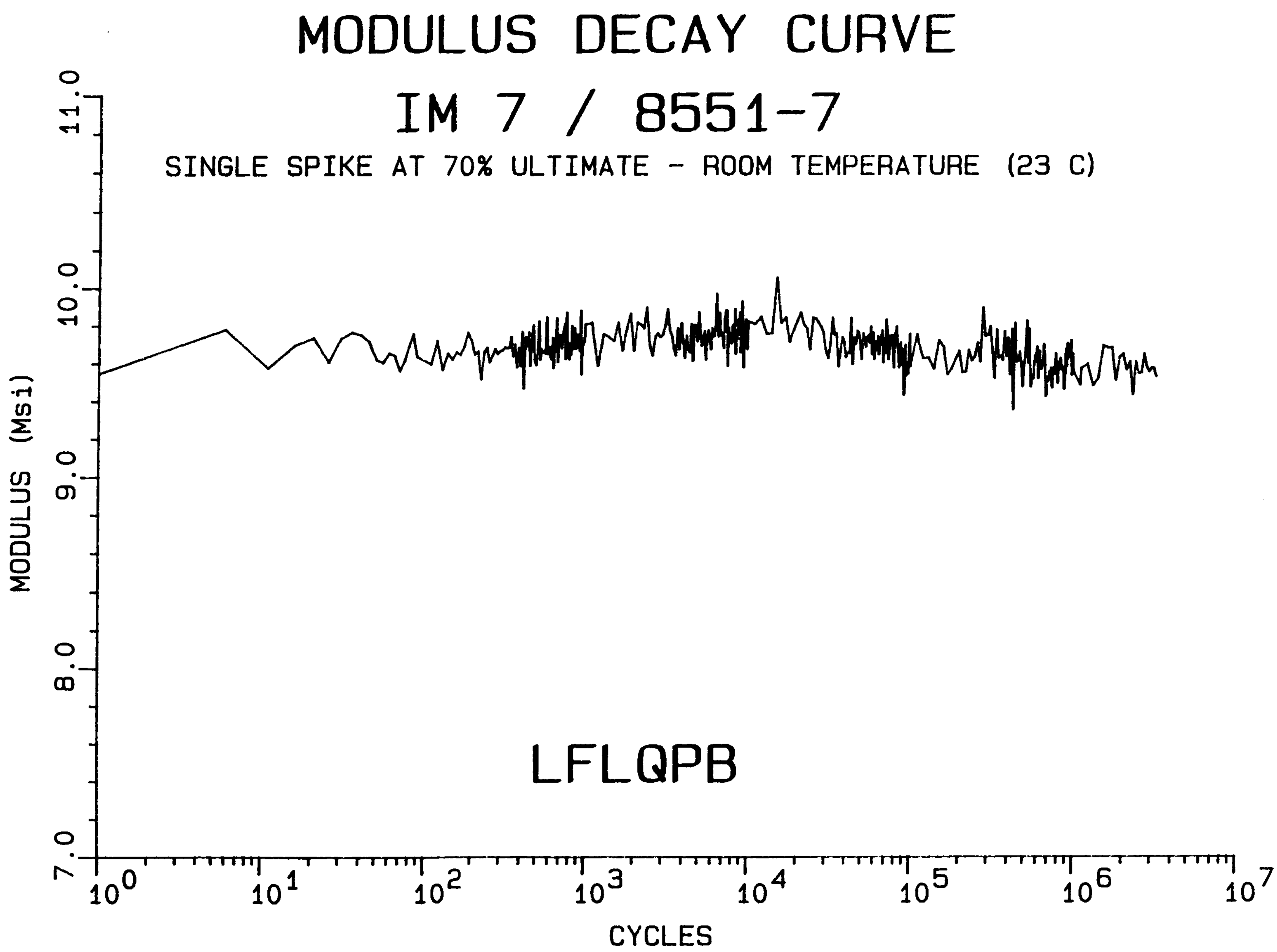

MODULUS DECAY CURVE
IM 7 / 8551-7
SINGLE SPIKE AT 70% ULTIMATE - ROOM TEMPERATURE (23 C)
MODULUS (Msi)
11.0
10.0
9.0
8.0
7.0
10^0
10^1
10^2
10^3
10^4
10^5
10^6
10^7
CYCLES
LFLQPB

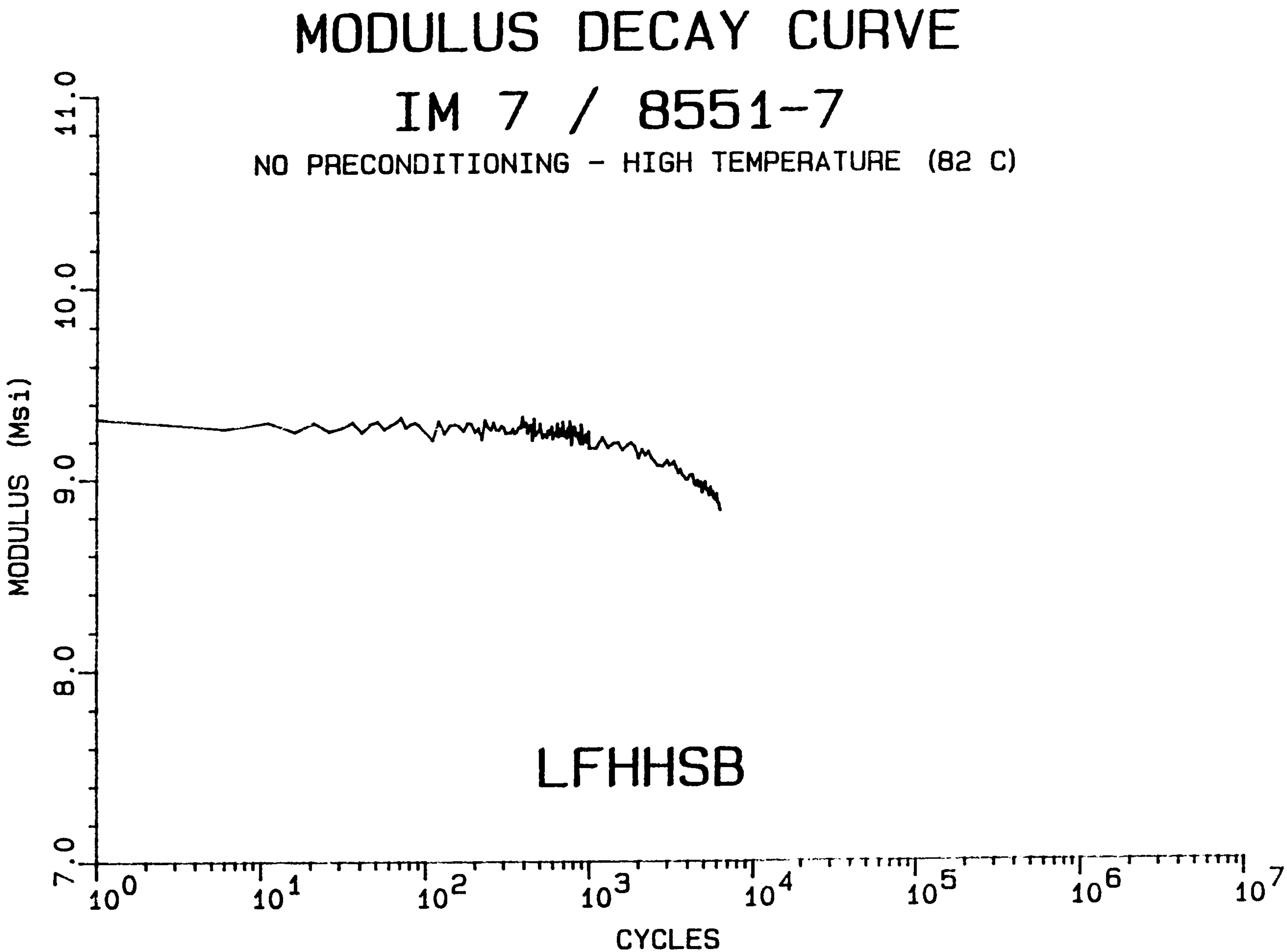

MODULUS DECAY CURVE
IM 7 / 8551-7
NO PRECONDITIONING - HIGH TEMPERATURE (82 C)
MODULUS (Msi)
11.0
10.0
9.0
8.0
7.0
LFHHSB
10^0
10^1
10^2
10^3
10^4
10^5
10^6
10^7
CYCLES

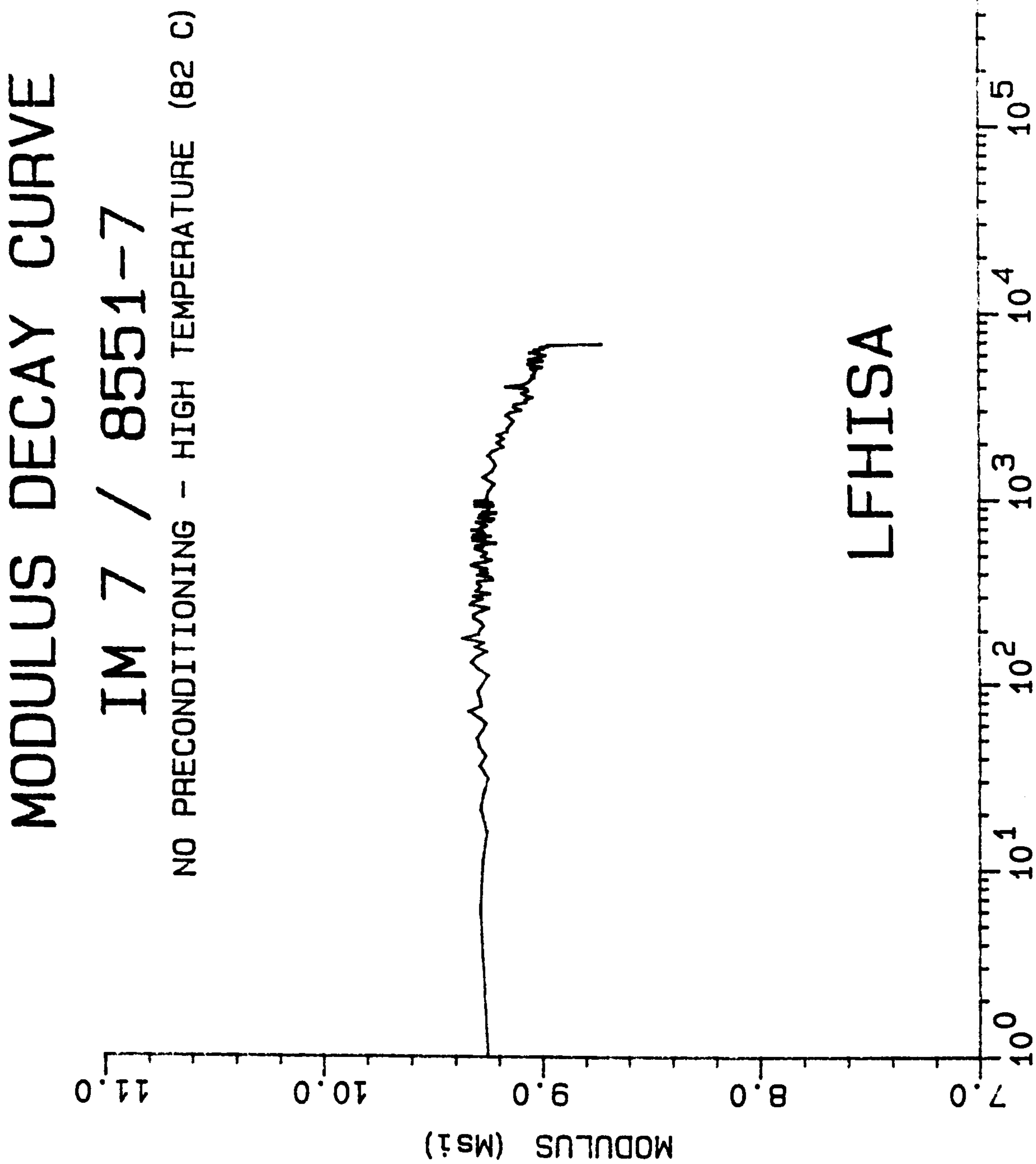
MODULUS DECAY CURVE
IM 7 / 8551-7
NO PRECONDITIONING - HIGH TEMPERATURE (82 C)
LFHISA
CYCLES
MODULUS (Msi)
7.0
8.0
9.0
10.0
11.0
10^0
10^1
10^2
10^3
10^4
10^5
10^6
10^7

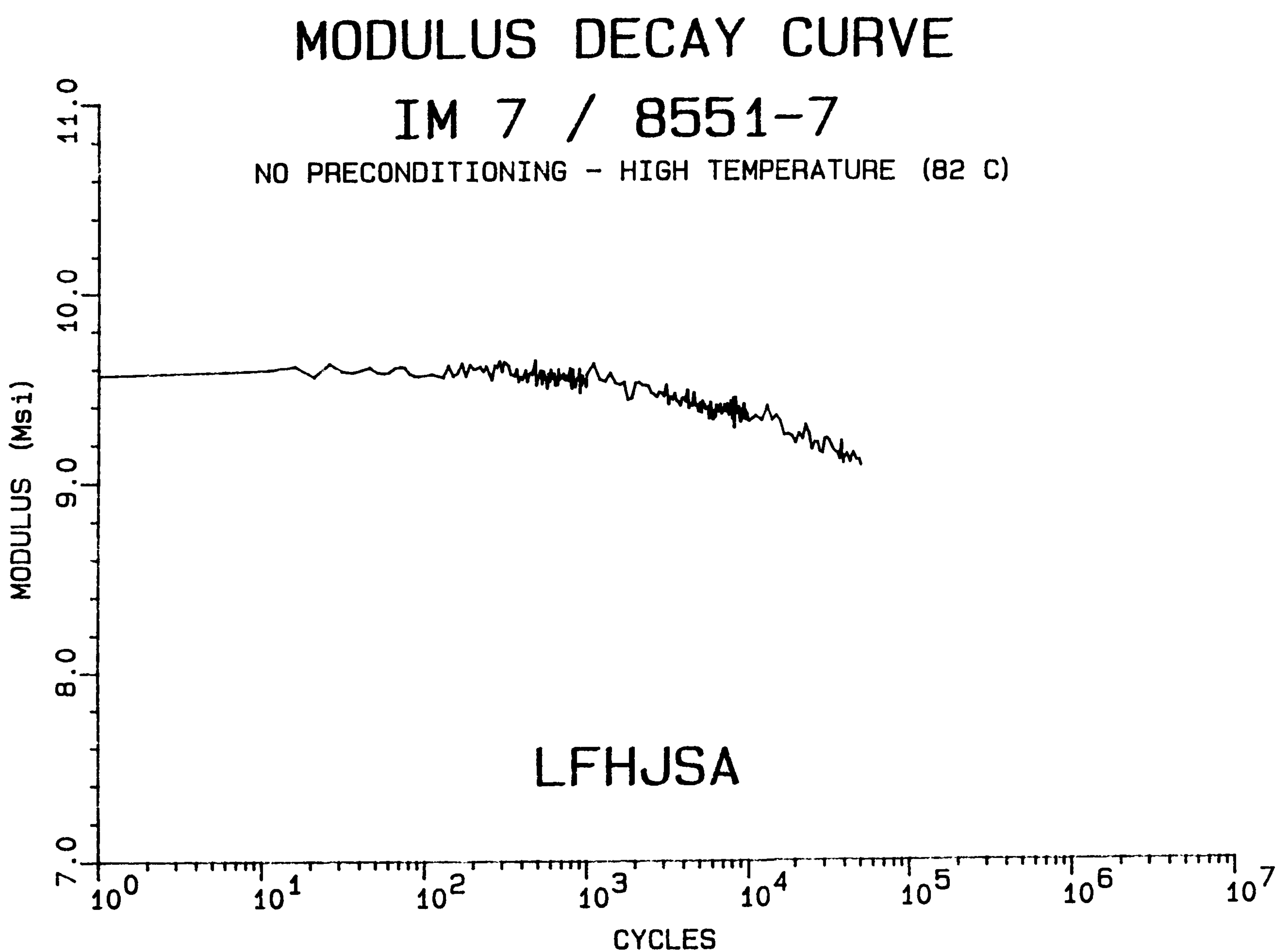

MODULUS DECAY CURVE
IM 7 / 8551-7
NO PRECONDITIONING - HIGH TEMPERATURE (82 C)
MODULUS (Msi)
11.0
10.0
9.0
8.0
7.0
LFHJSA
10^0
10^1
10^2
10^3
10^4
10^5
10^6
10^7
CYCLES

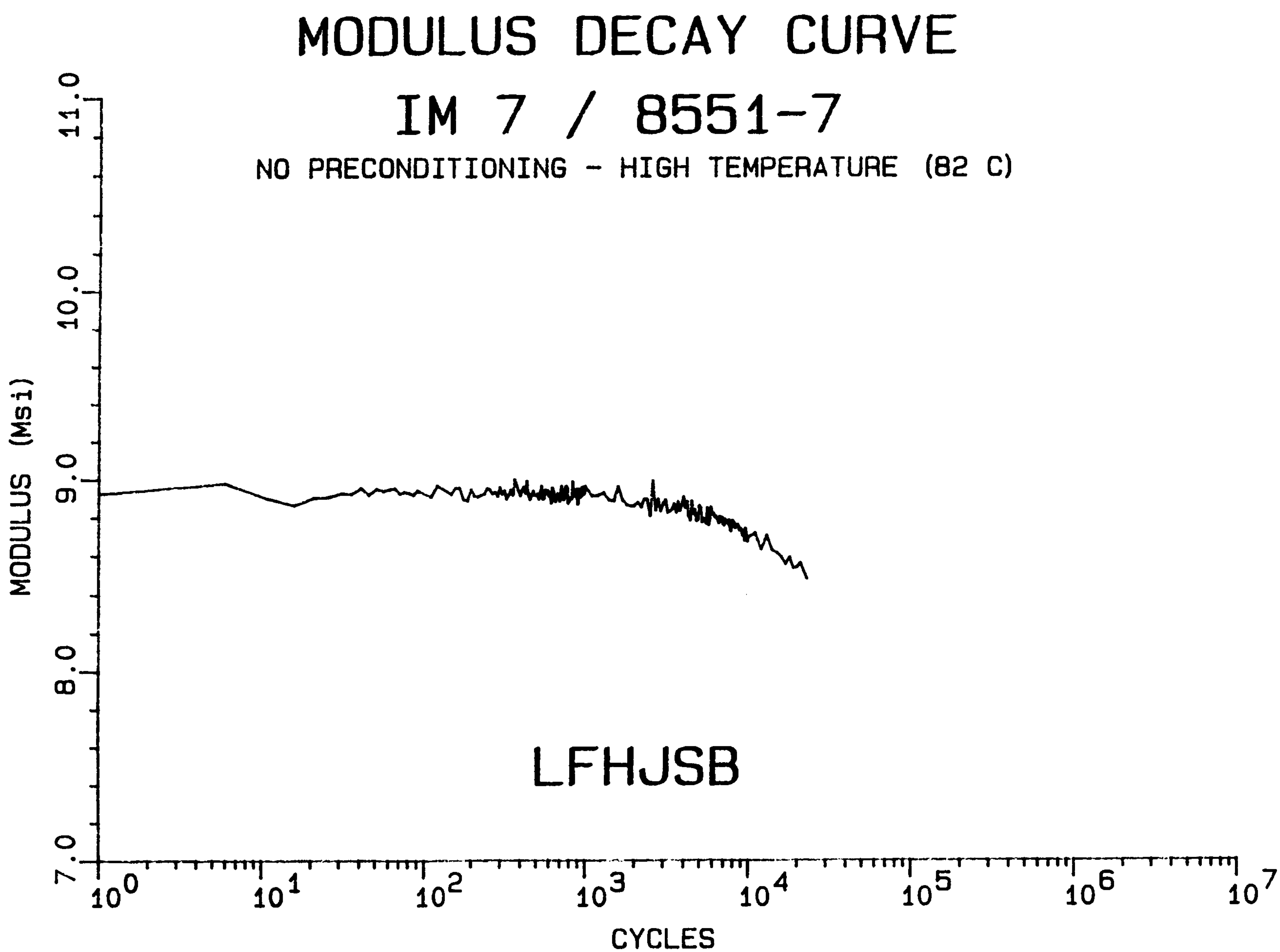
MODULUS DECAY CURVE
IM 7 / 8551-7
NO PRECONDITIONING - HIGH TEMPERATURE (82 C)
MODULUS (Msi)
11.0
10.0
9.0
8.0
7.0
LFHJSB
10^0
10^1
10^2
10^3
10^4
10^5
10^6
10^7
CYCLES

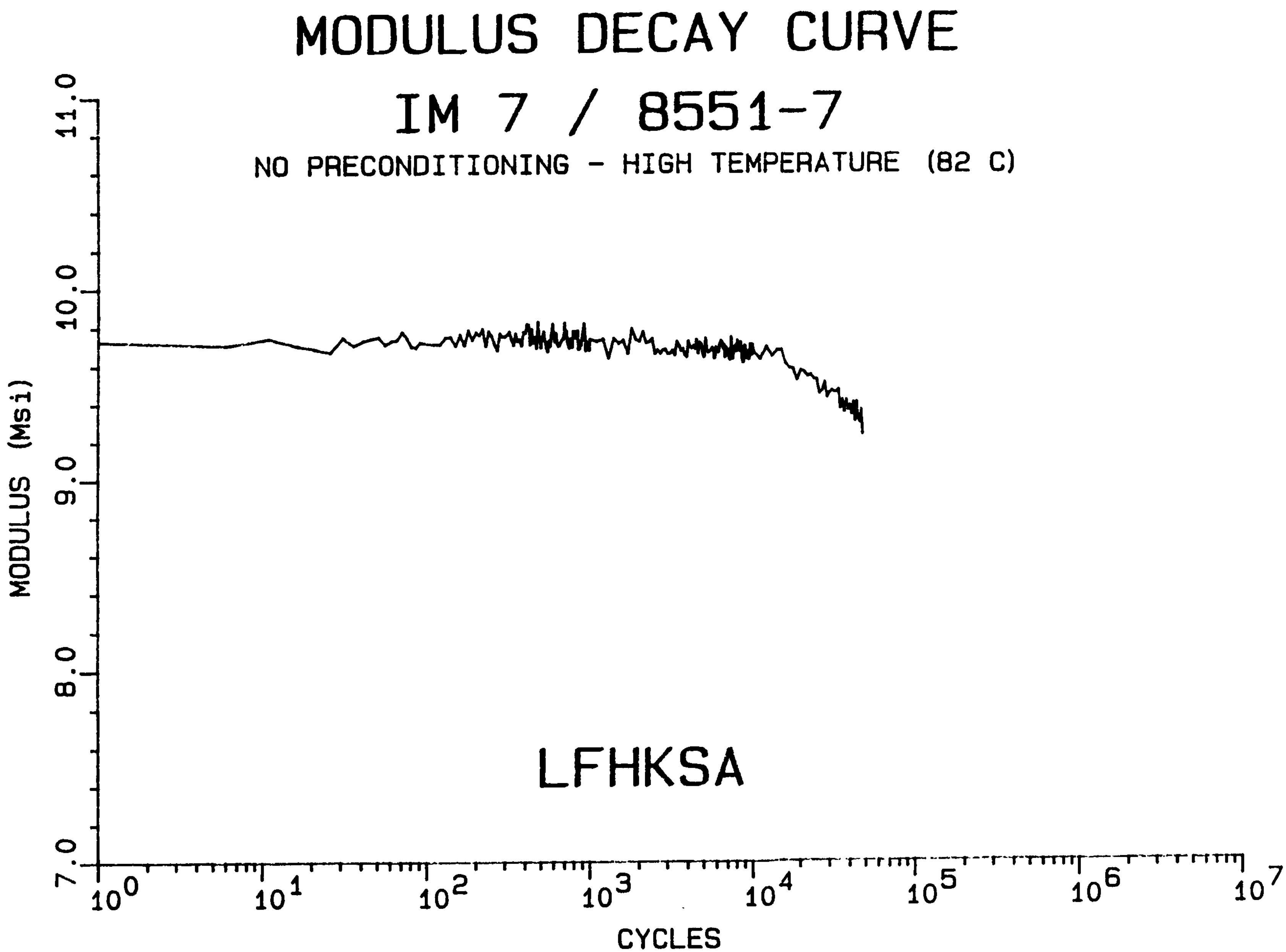
MODULUS DECAY CURVE
IM 7 / 8551-7
NO PRECONDITIONING - HIGH TEMPERATURE (82 C)
LFHKSA
MODULUS (Msi)
CYCLES
11.0
10.0
9.0
8.0
7.0
10^0
10^1
10^2
10^3
10^4
10^5
10^6
10^7

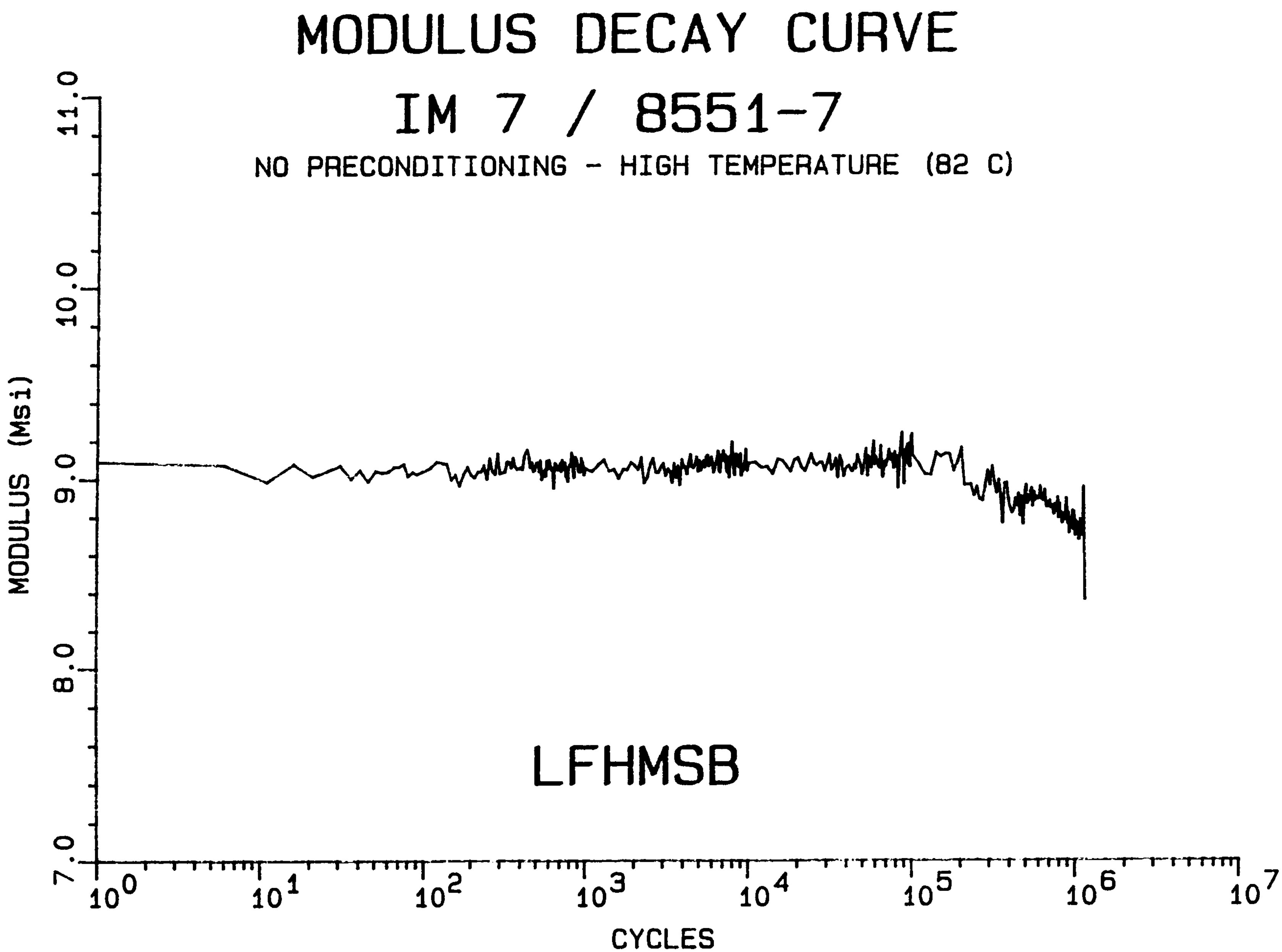
MODULUS DECAY CURVE
IM 7 / 8551-7
NO PRECONDITIONING - HIGH TEMPERATURE (82 C)
MODULUS (Msi)
11.0
10.0
9.0
8.0
7.0
LFHMSB
10^0
10^1
10^2
10^3
10^4
10^5
10^6
10^7
CYCLES

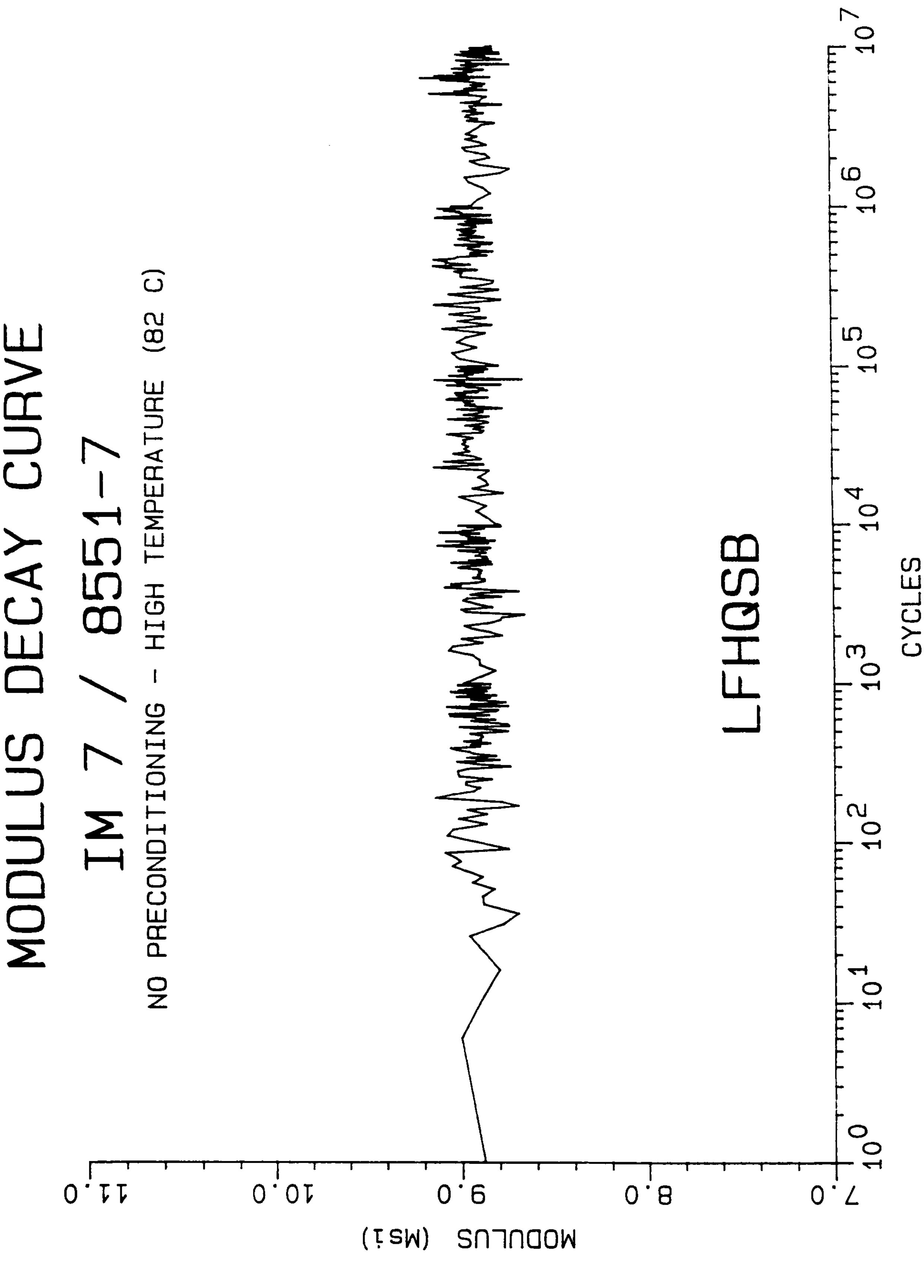
MODULUS DECAY CURVE
IM 7 / 8551-7
NO PRECONDITIONING - HIGH TEMPERATURE (82 C)
LFHQSB
MODULUS (Msi)
7.0
8.0
9.0
10.0
11.0
CYCLES
10^0
10^1
10^2
10^3
10^4
10^5
10^6
10^7

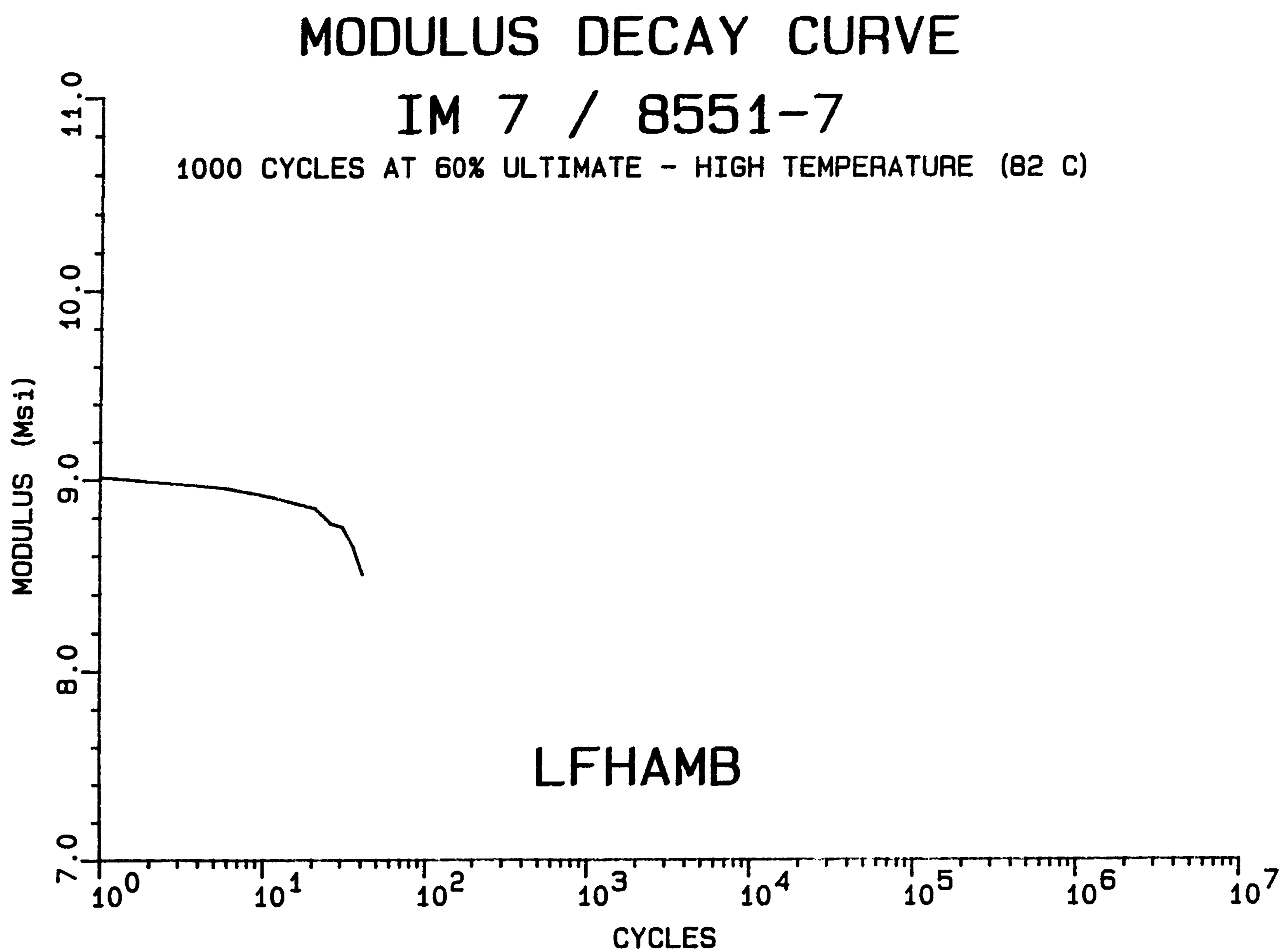
MODULUS DECAY CURVE
IM 7 / 8551-7
1000 CYCLES AT 60% ULTIMATE - HIGH TEMPERATURE (82 C)
MODULUS (Msi)
11.0
10.0
9.0
8.0
7.0
LFHAMB
10^0
10^1
10^2
10^3
10^4
10^5
10^6
10^7
CYCLES

MODULUS DECAY CURVE

IM 7 / 8551-7

1000 CYCLES AT 60% ULTIMATE - HIGH TEMPERATURE (82 C)

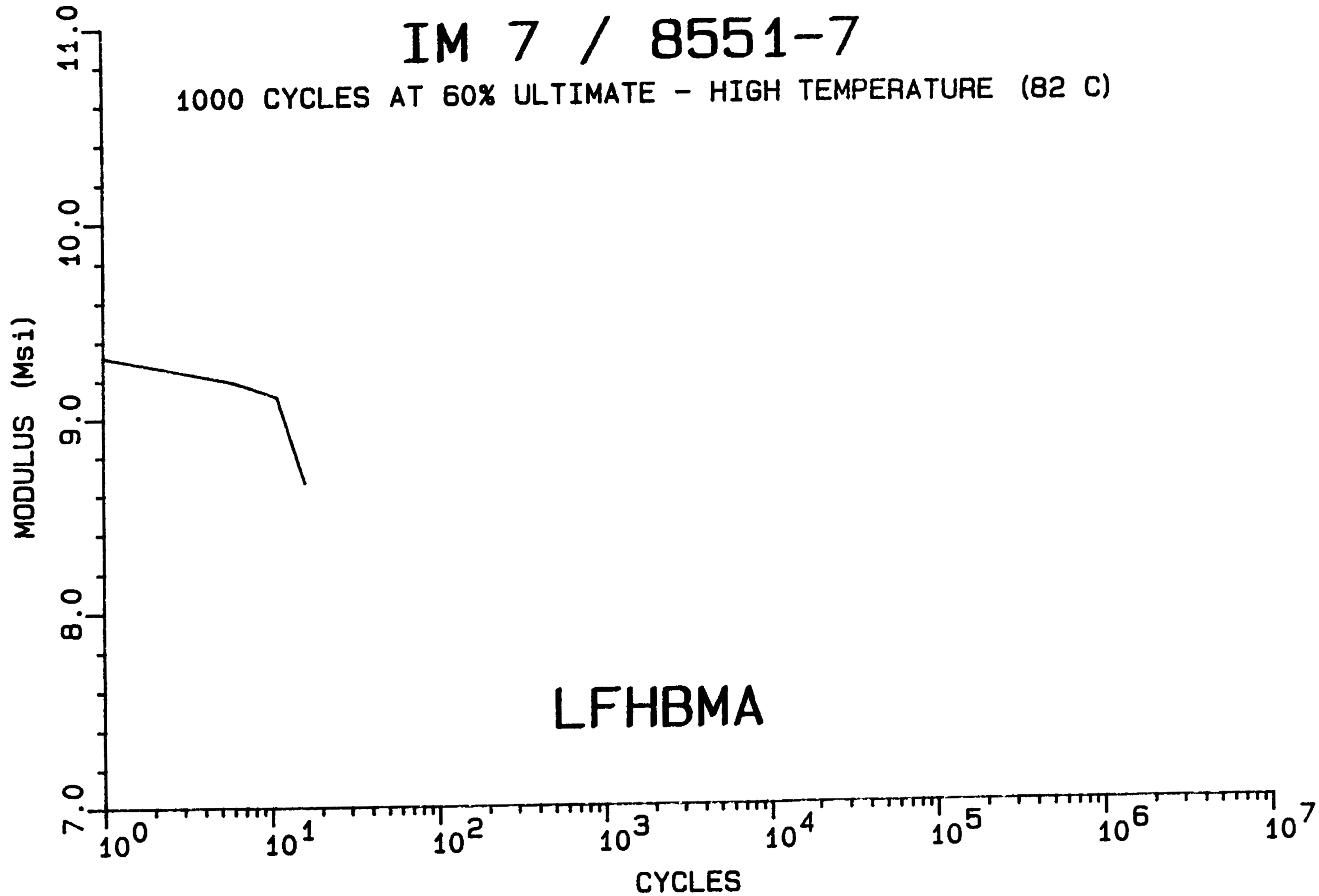

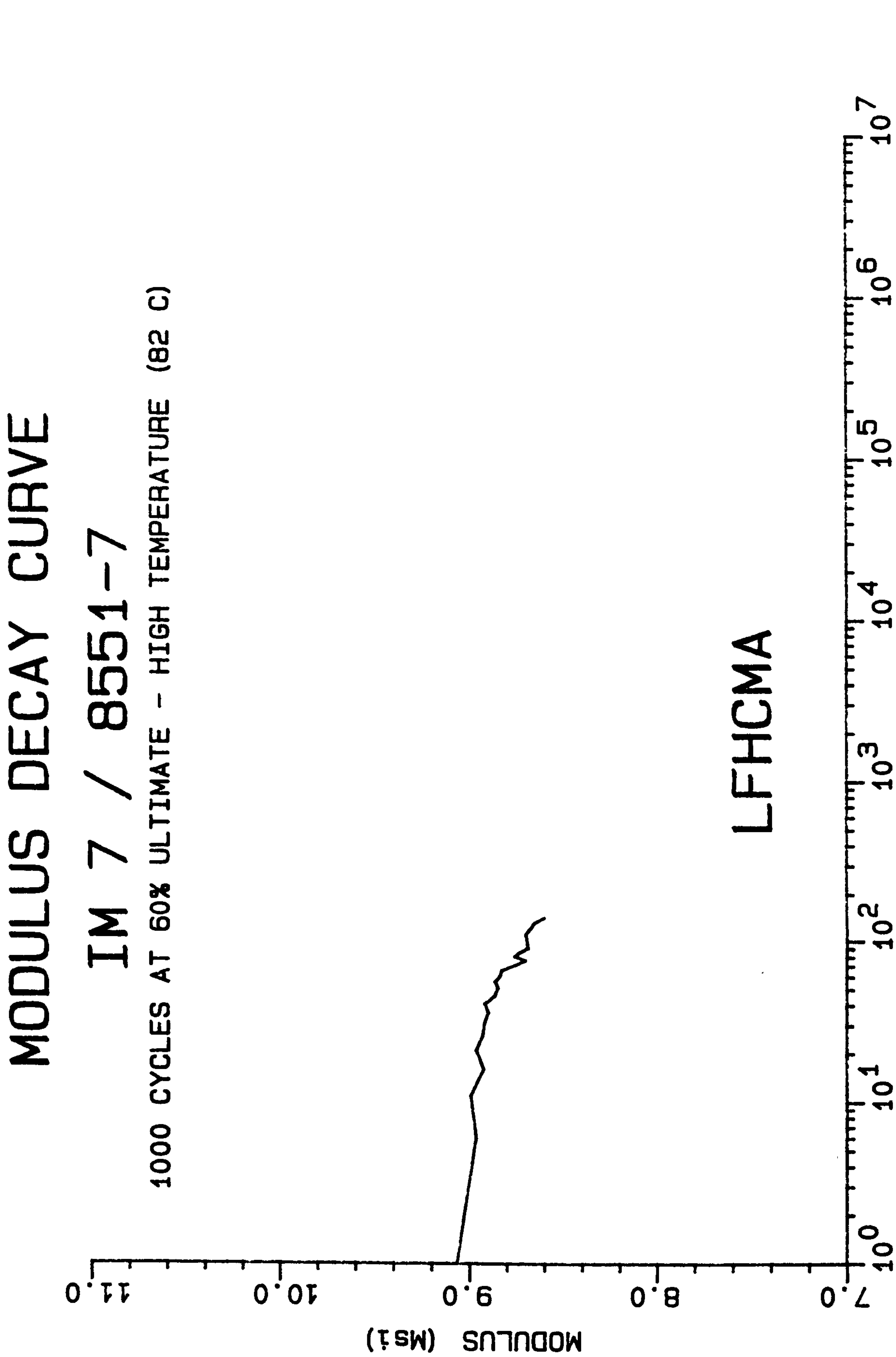

MODULUS DECAY CURVE
IM 7 / 8551-7
1000 CYCLES AT 60% ULTIMATE - HIGH TEMPERATURE (82 C)
LFHCMA
CYCLES
MODULUS (Msi)
7.0
8.0
9.0
10.0
11.0
10^0
10^1
10^2
10^3
10^4
10^5
10^6
10^7

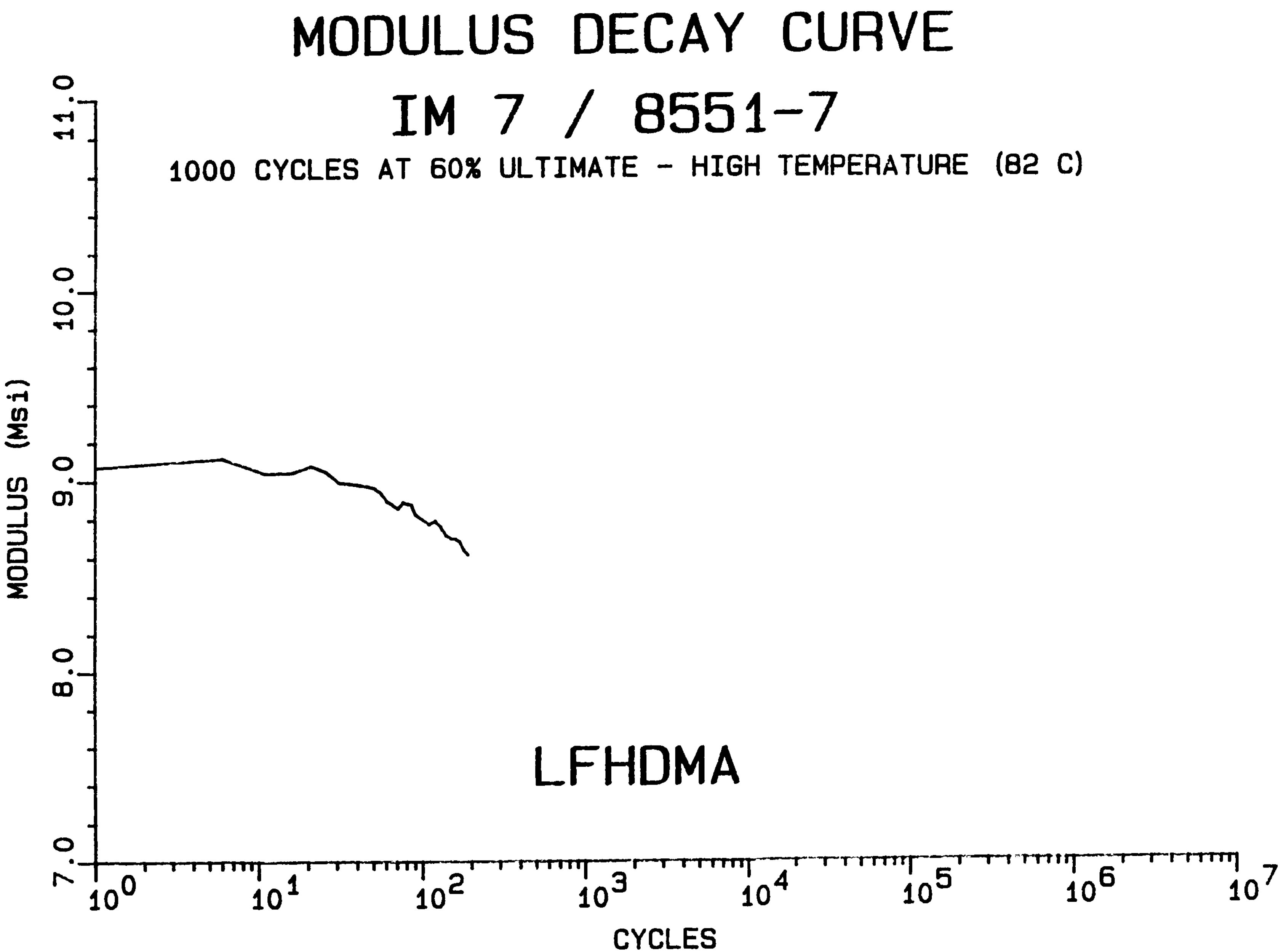
MODULUS DECAY CURVE
IM 7 / 8551-7
1000 CYCLES AT 60% ULTIMATE - HIGH TEMPERATURE (82 C)
MODULUS (Msi)
11.0
10.0
9.0
8.0
7.0
LFHDMA
10^0
10^1
10^2
10^3
10^4
10^5
10^6
10^7
CYCLES

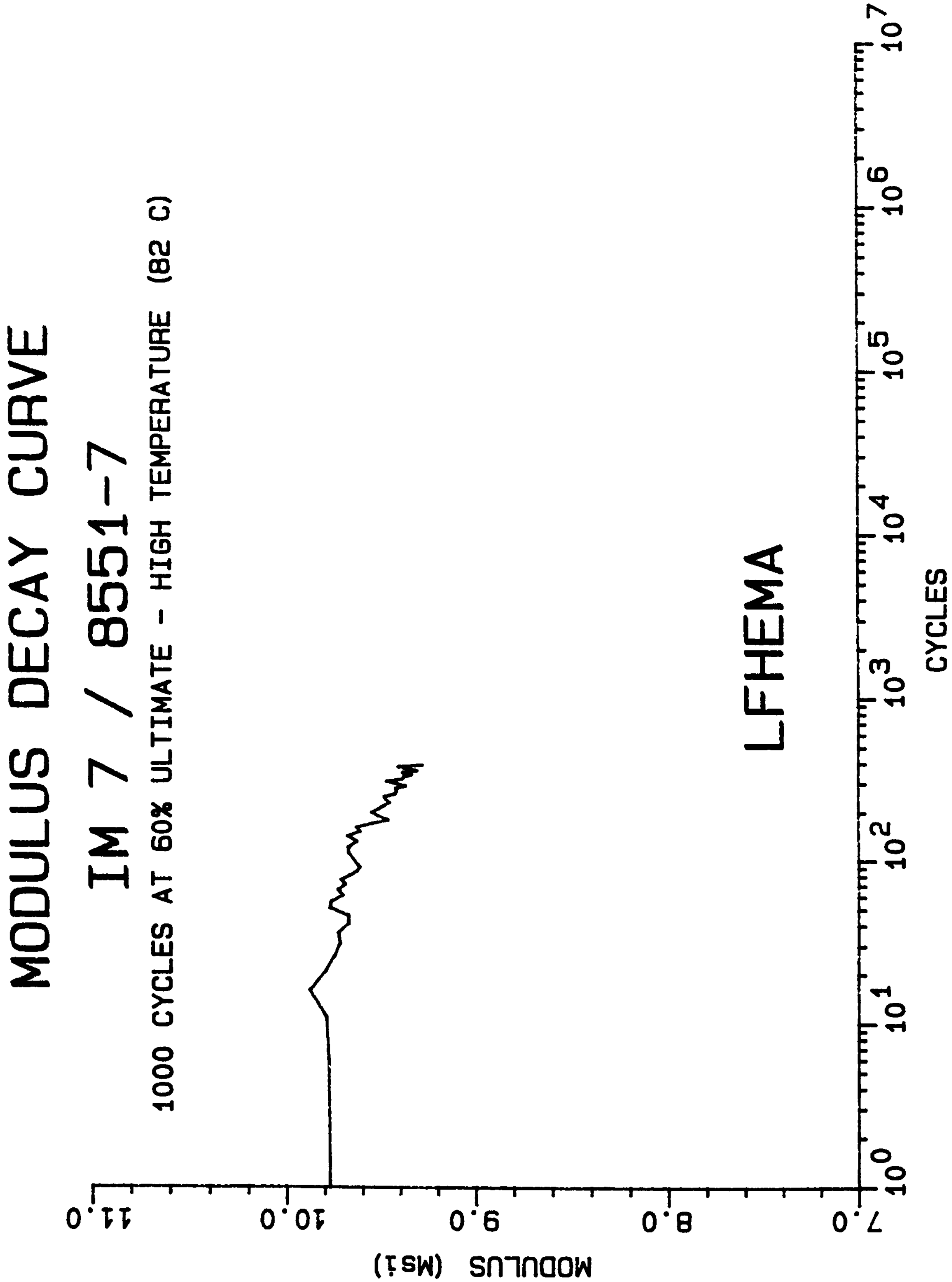

MODULUS DECAY CURVE
IM 7 / 8551-7
1000 CYCLES AT 60% ULTIMATE - HIGH TEMPERATURE (82 C)
LFHEMA
MODULUS (Msi)
7.0
8.0
9.0
10.0
11.0
CYCLES
10^0
10^1
10^2
10^3
10^4
10^5
10^6
10^7

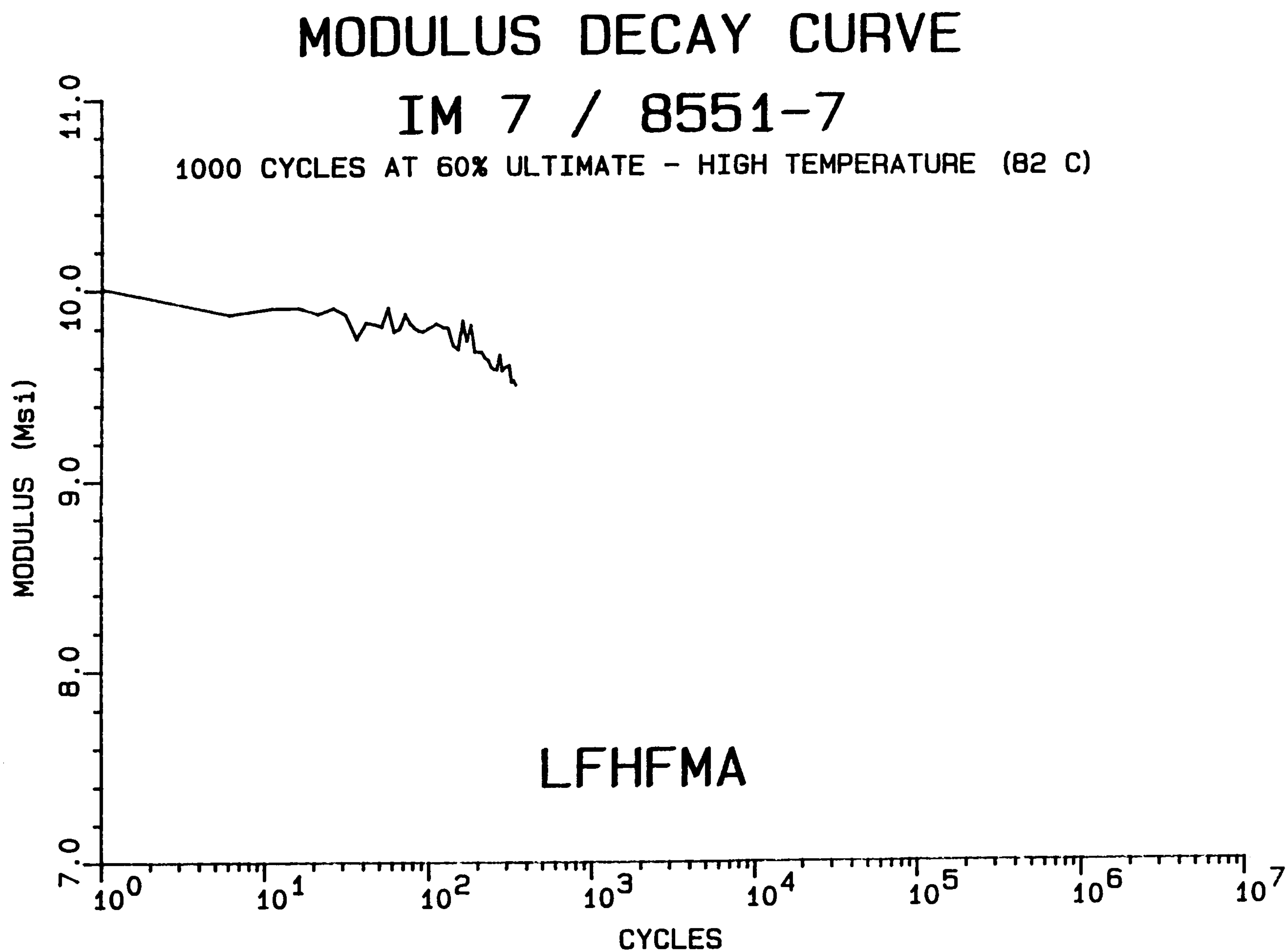
MODULUS DECAY CURVE
IM 7 / 8551-7
1000 CYCLES AT 60% ULTIMATE - HIGH TEMPERATURE (82 C)
MODULUS (Msi)
11.0
10.0
9.0
8.0
7.0
LFHFMA
10^0
10^1
10^2
10^3
10^4
10^5
10^6
10^7
CYCLES

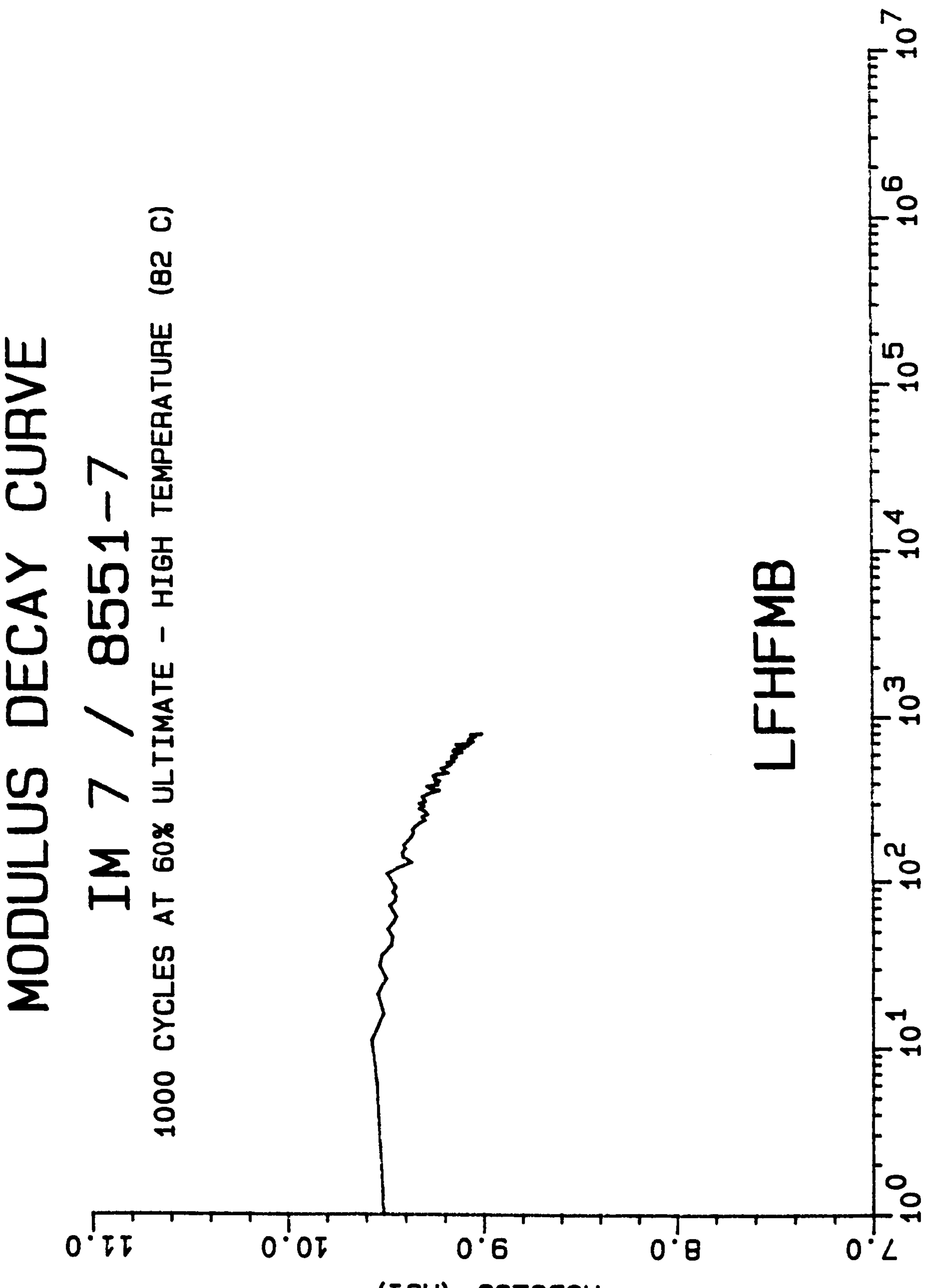
MODULUS DECAY CURVE
IM 7 / 8551-7
1000 CYCLES AT 60% ULTIMATE - HIGH TEMPERATURE (82 C)
LFHFMB
MODULUS (Msi)
7.0
8.0
9.0
10.0
11.0
CYCLES
10^0
10^1
10^2
10^3
10^4
10^5
10^6
10^7

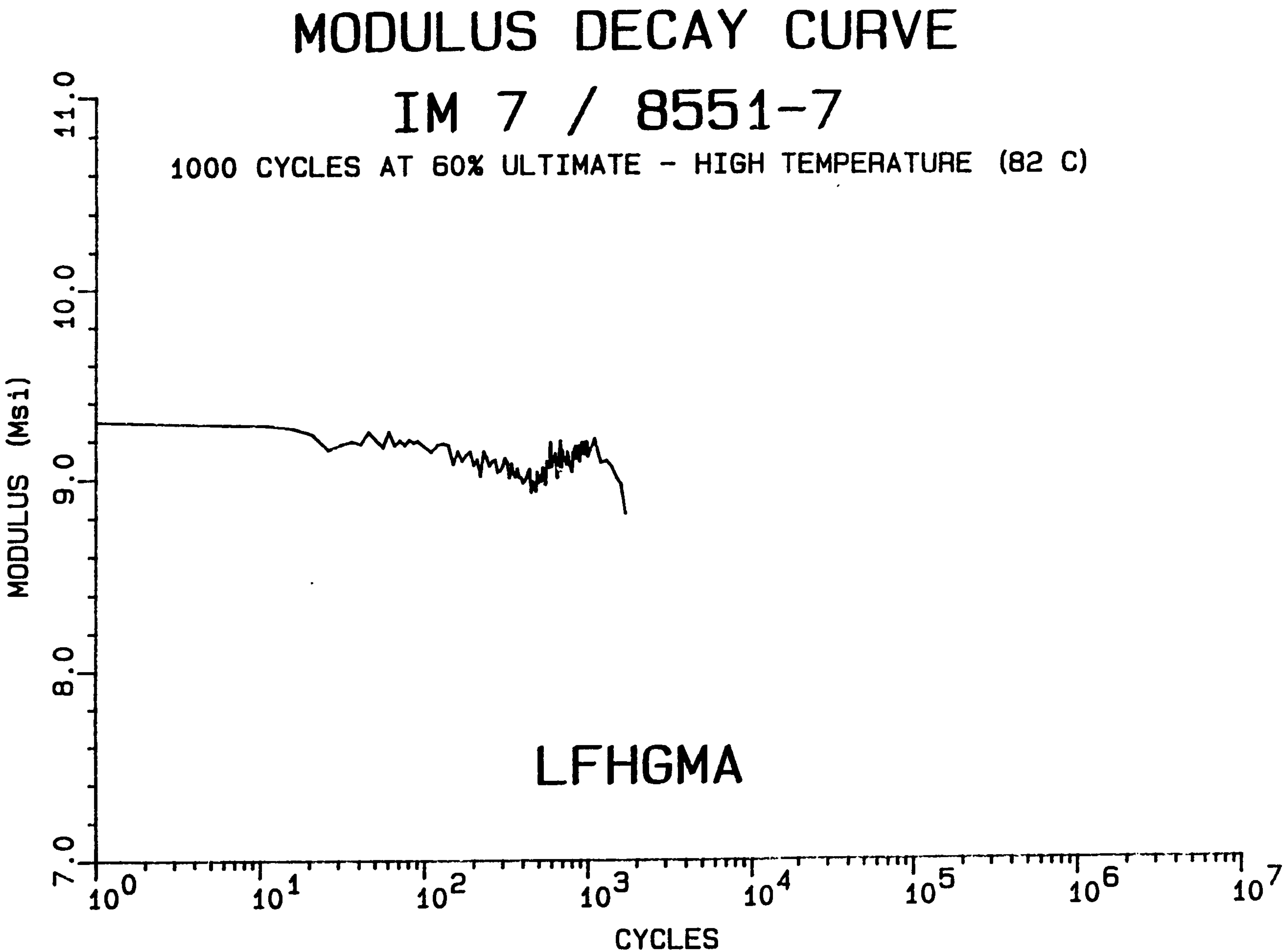

MODULUS DECAY CURVE
IM 7 / 8551-7
1000 CYCLES AT 60% ULTIMATE - HIGH TEMPERATURE (82 C)
LFHGMA
MODULUS (Msi)
7.0
8.0
9.0
10.0
11.0
CYCLES
10^0
10^1
10^2
10^3
10^4
10^5
10^6
10^7

MODULUS DECAY CURVE

IM 7 / 8551-7

1000 CYCLES AT 60% ULTIMATE - HIGH TEMPERATURE (82 C)

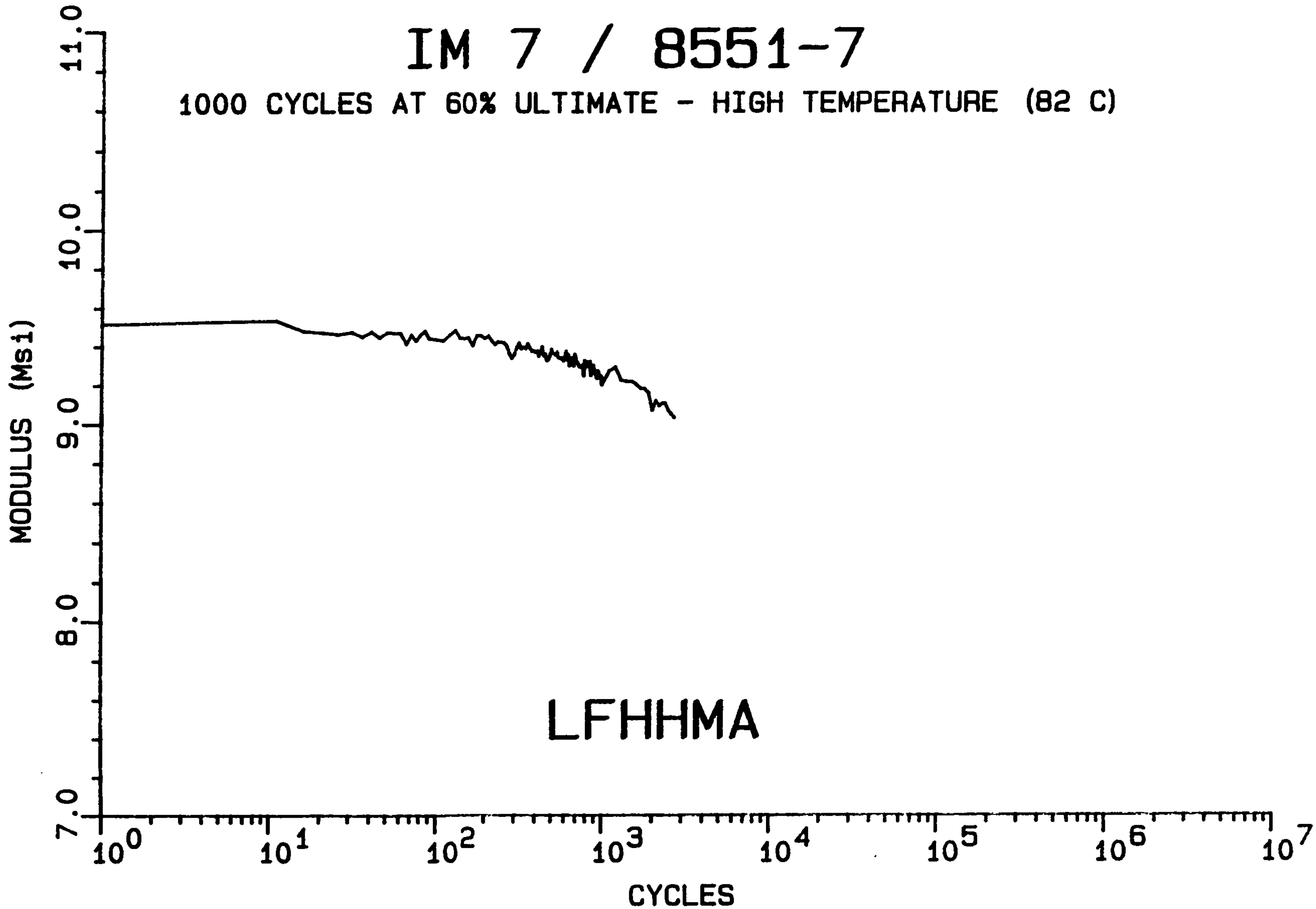

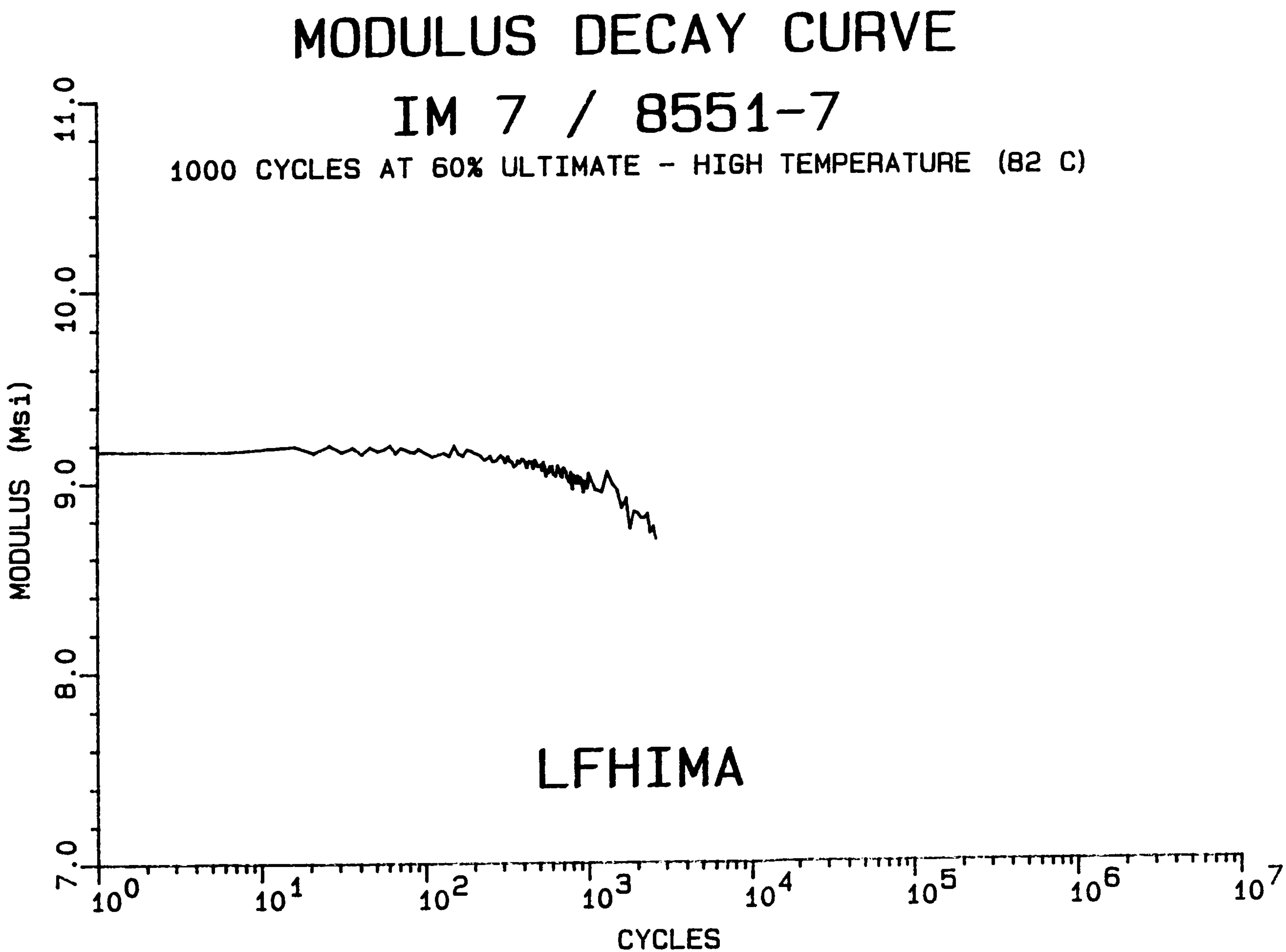
MODULUS DECAY CURVE
IM 7 / 8551-7
1000 CYCLES AT 60% ULTIMATE - HIGH TEMPERATURE (82 C)
MODULUS (Msi)
11.0
10.0
9.0
8.0
7.0
10^0
10^1
10^2
10^3
10^4
10^5
10^6
10^7
CYCLES
LFHIMA

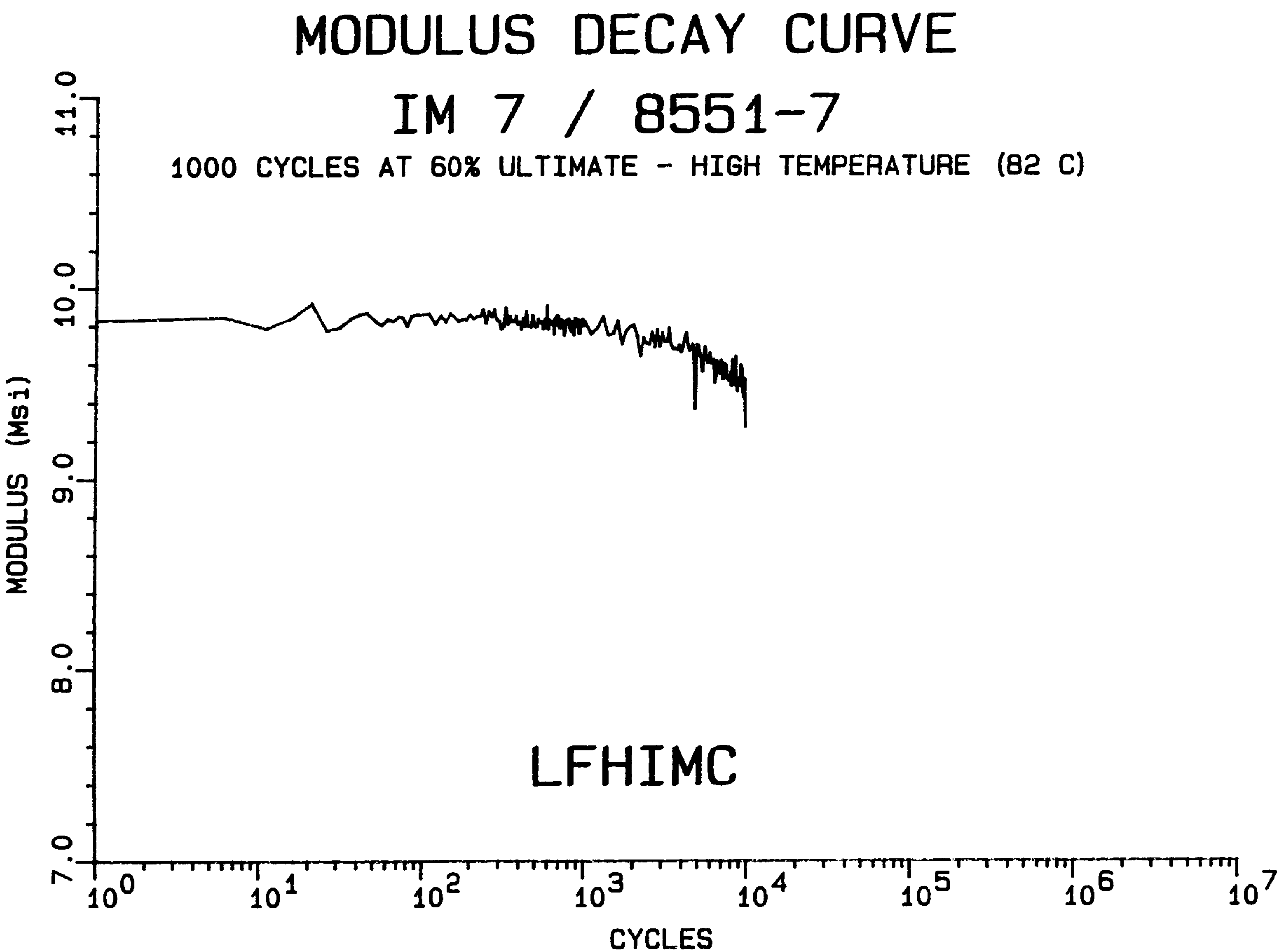

MODULUS DECAY CURVE
IM 7 / 8551-7
1000 CYCLES AT 60% ULTIMATE - HIGH TEMPERATURE (82 C)
MODULUS (Msi)
11.0
10.0
9.0
8.0
7.0
LFHIMC
10^0
10^1
10^2
10^3
10^4
10^5
10^6
10^7
CYCLES

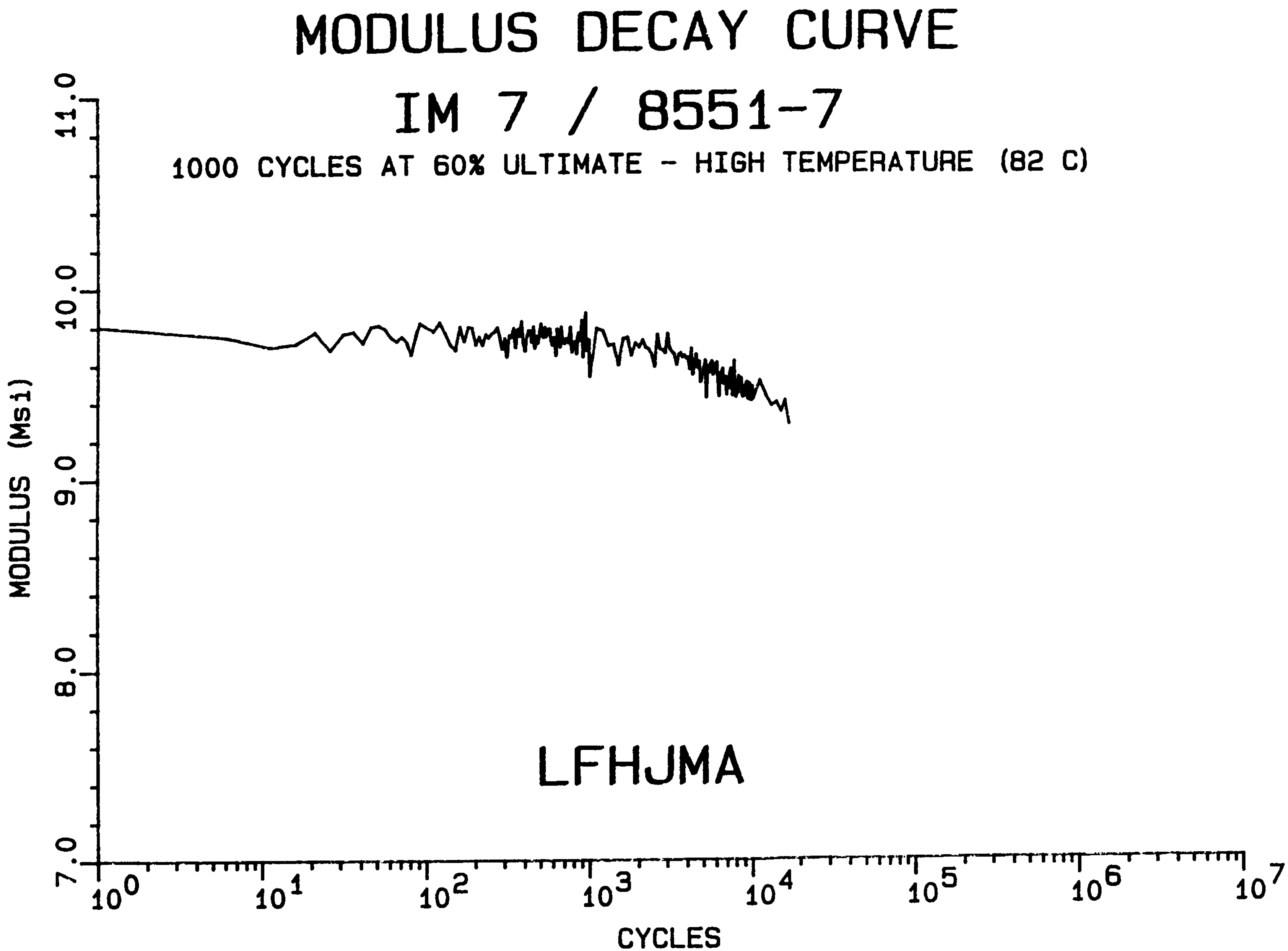
MODULUS DECAY CURVE
IM 7 / 8551-7
1000 CYCLES AT 60% ULTIMATE - HIGH TEMPERATURE (82 C)
MODULUS (Msi)
11.0
10.0
9.0
8.0
7.0
LFHJMA
10^0
10^1
10^2
10^3
10^4
10^5
10^6
10^7
CYCLES

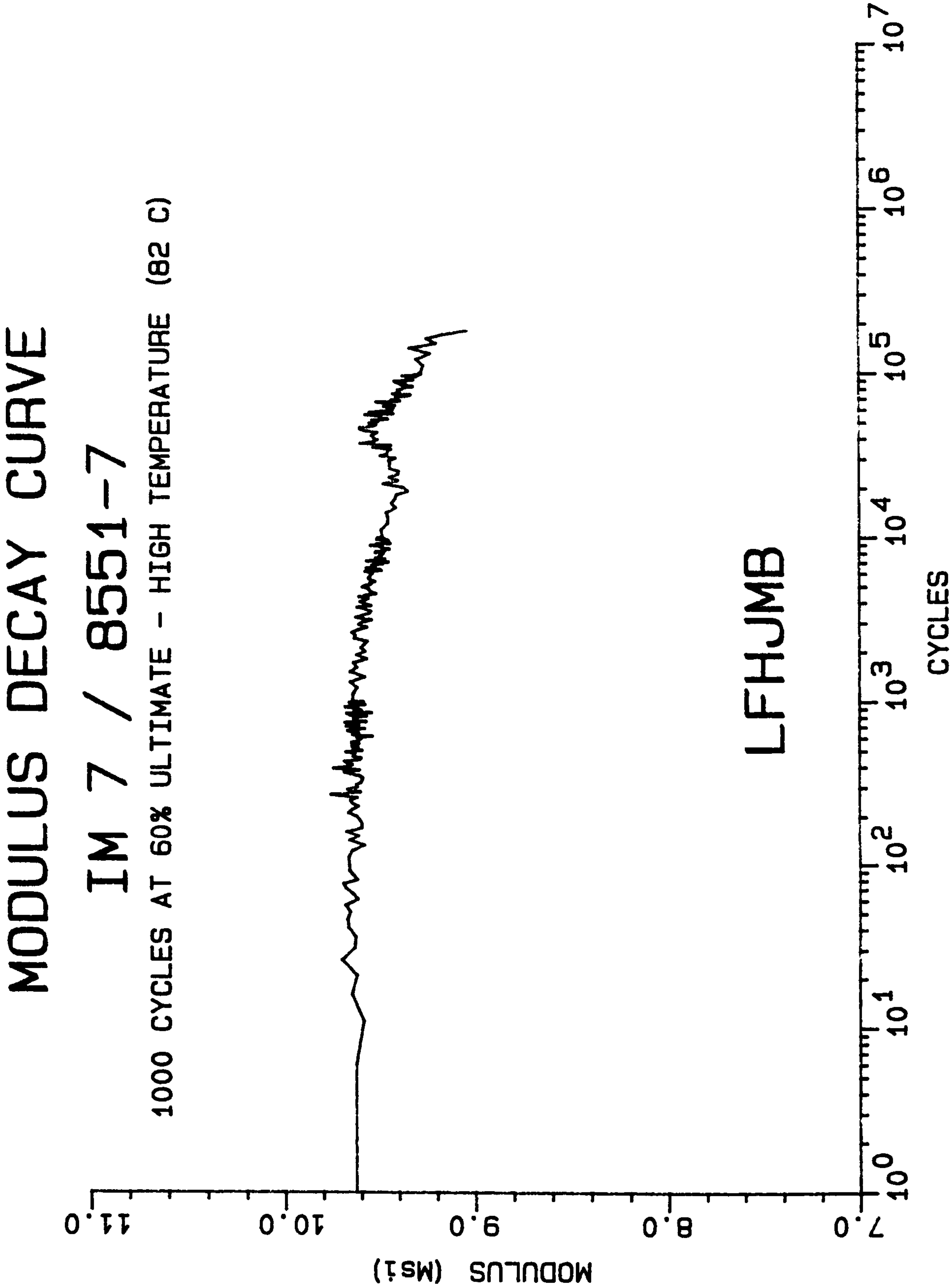

MODULUS DECAY CURVE
IM 7 / 8551-7
1000 CYCLES AT 60% ULTIMATE - HIGH TEMPERATURE (82 C)
LFHJMB
MODULUS (Msi)
7.0
8.0
9.0
10.0
11.0
CYCLES
10^0
10^1
10^2
10^3
10^4
10^5
10^6
10^7

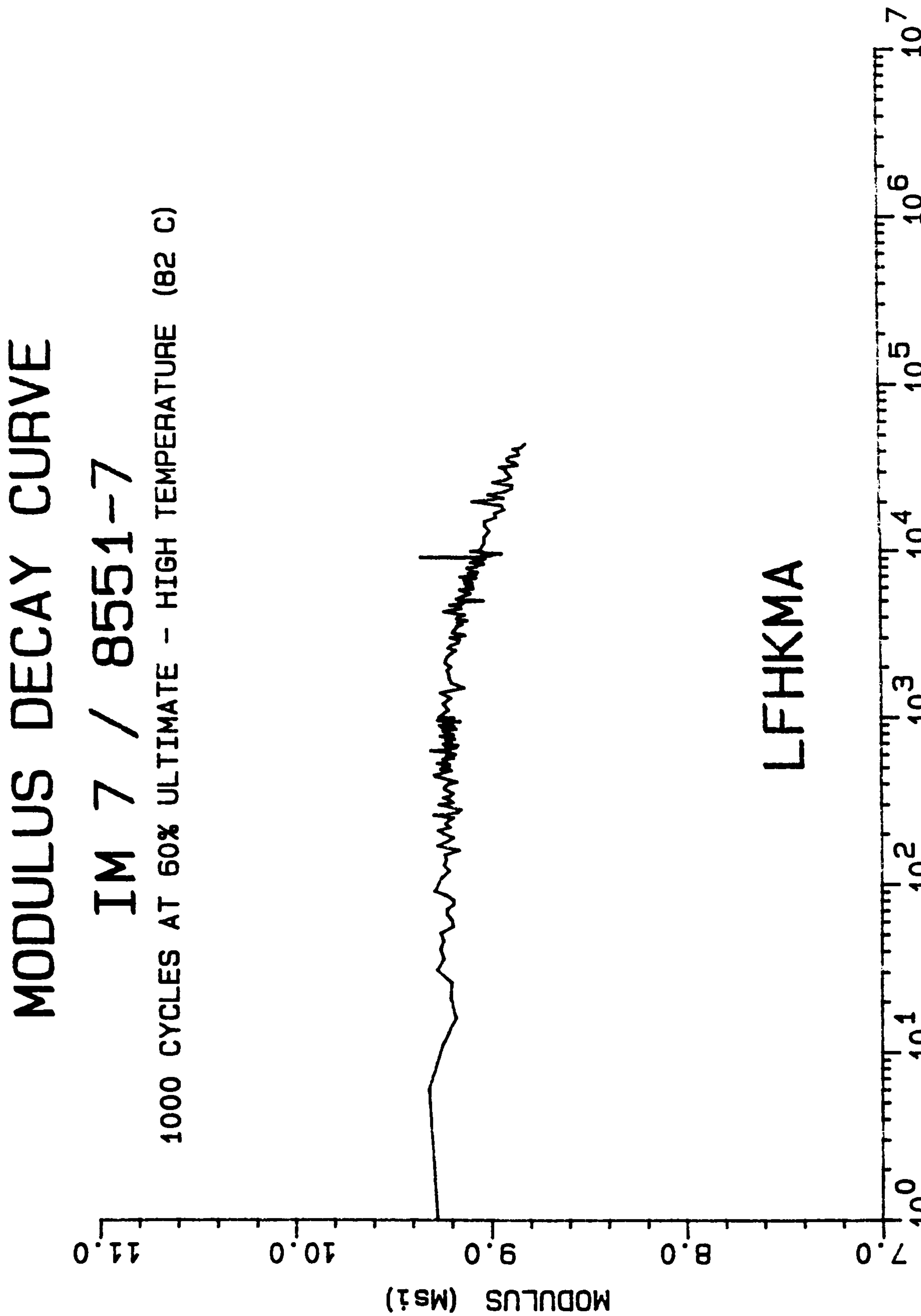
MODULUS DECAY CURVE
IM 7 / 8551-7
1000 CYCLES AT 60% ULTIMATE - HIGH TEMPERATURE (82 C)
LFHKMA
MODULUS (Msi)
7.0
8.0
9.0
10.0
11.0
CYCLES
10^0
10^1
10^2
10^3
10^4
10^5
10^6
10^7

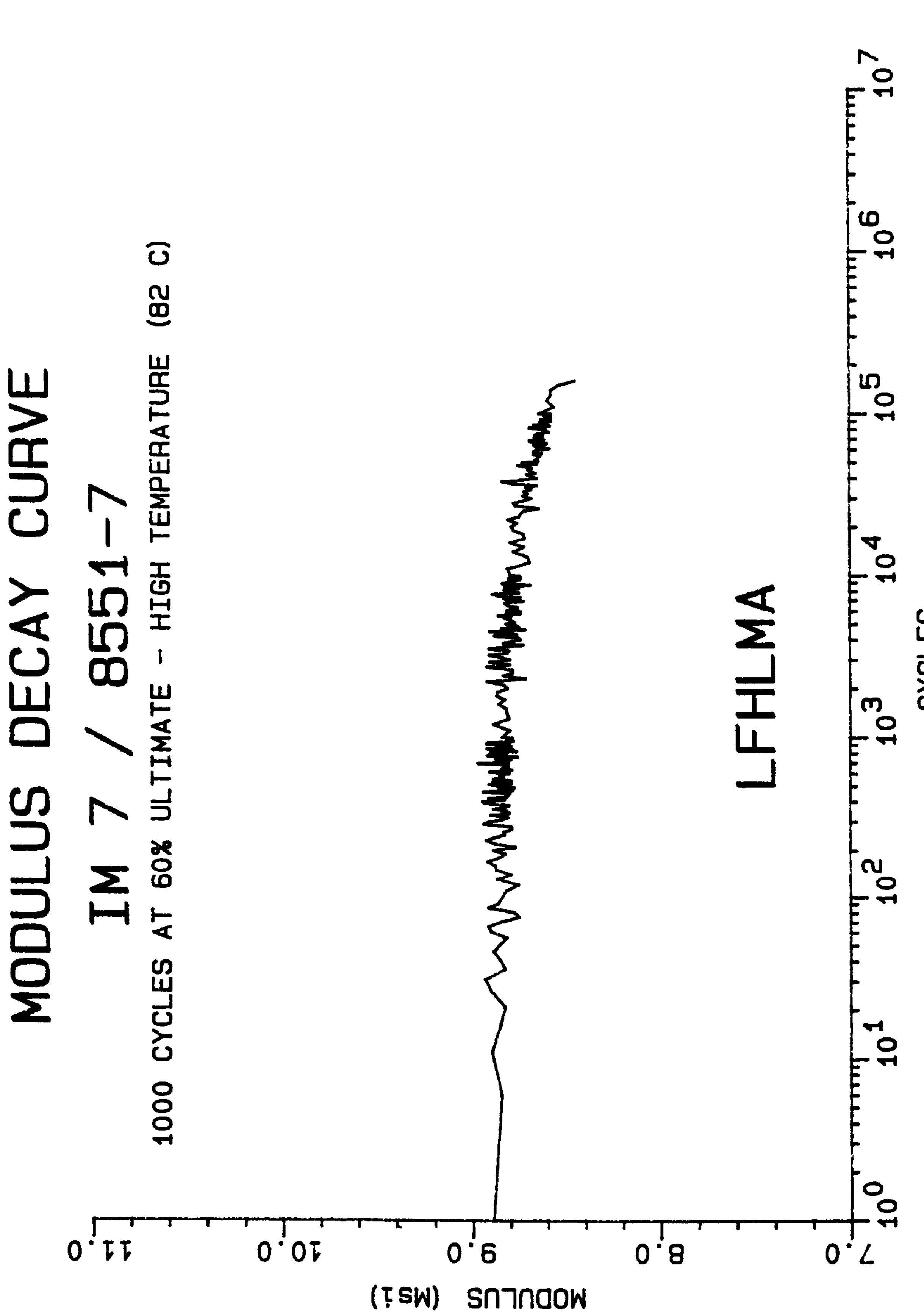
MODULUS DECAY CURVE
IM 7 / 8551-7
1000 CYCLES AT 60% ULTIMATE - HIGH TEMPERATURE (82 C)
LFHLMA
MODULUS (Msi)
7.0
8.0
9.0
10.0
11.0
CYCLES
10^0
10^1
10^2
10^3
10^4
10^5
10^6
10^7

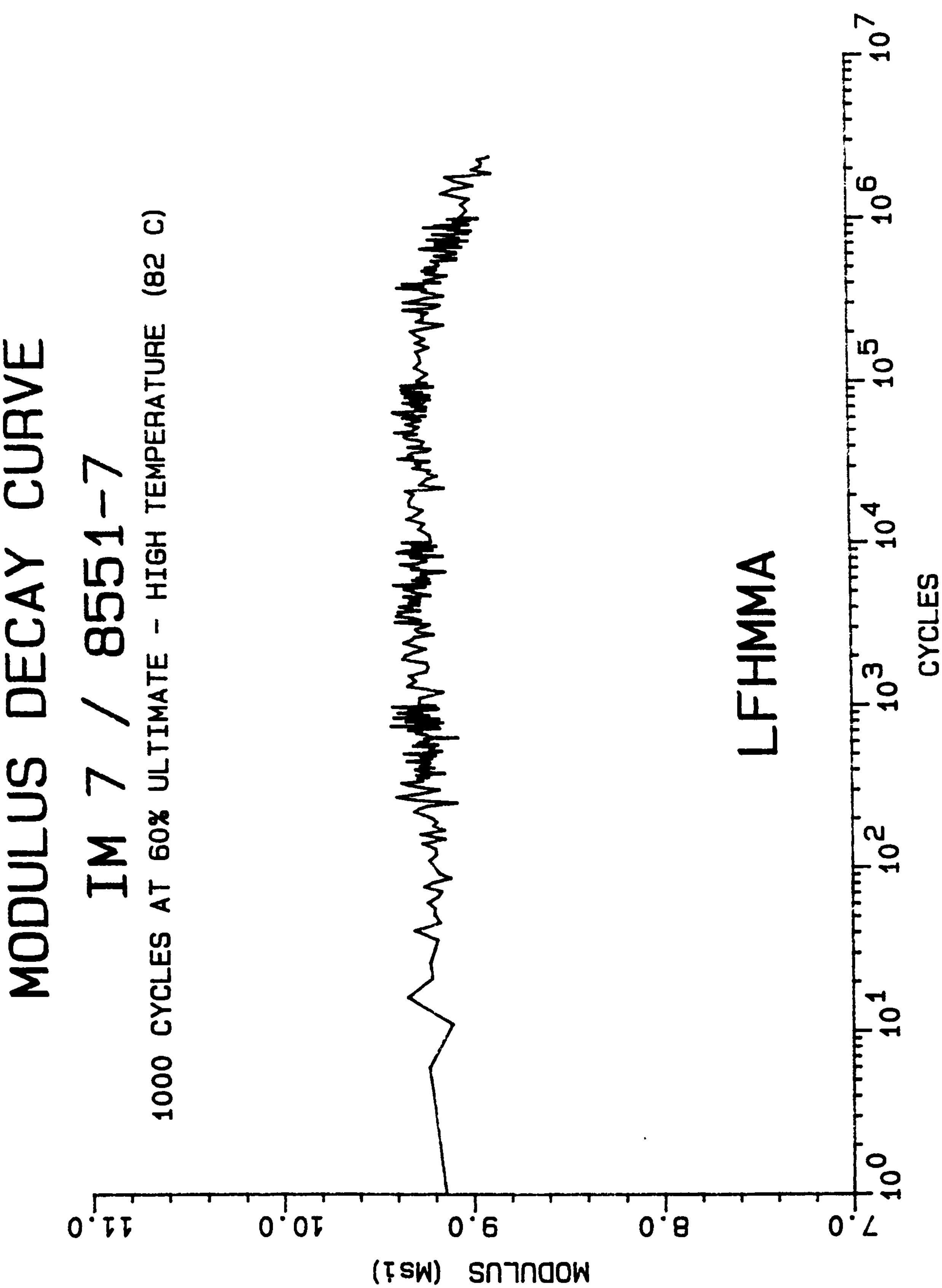
MODULUS DECAY CURVE
IM 7 / 8551-7
1000 CYCLES AT 60% ULTIMATE - HIGH TEMPERATURE (82 C)
LFHMMA
MODULUS (Msi)
7.0
8.0
9.0
10.0
11.0
CYCLES
10^0
10^1
10^2
10^3
10^4
10^5
10^6
10^7

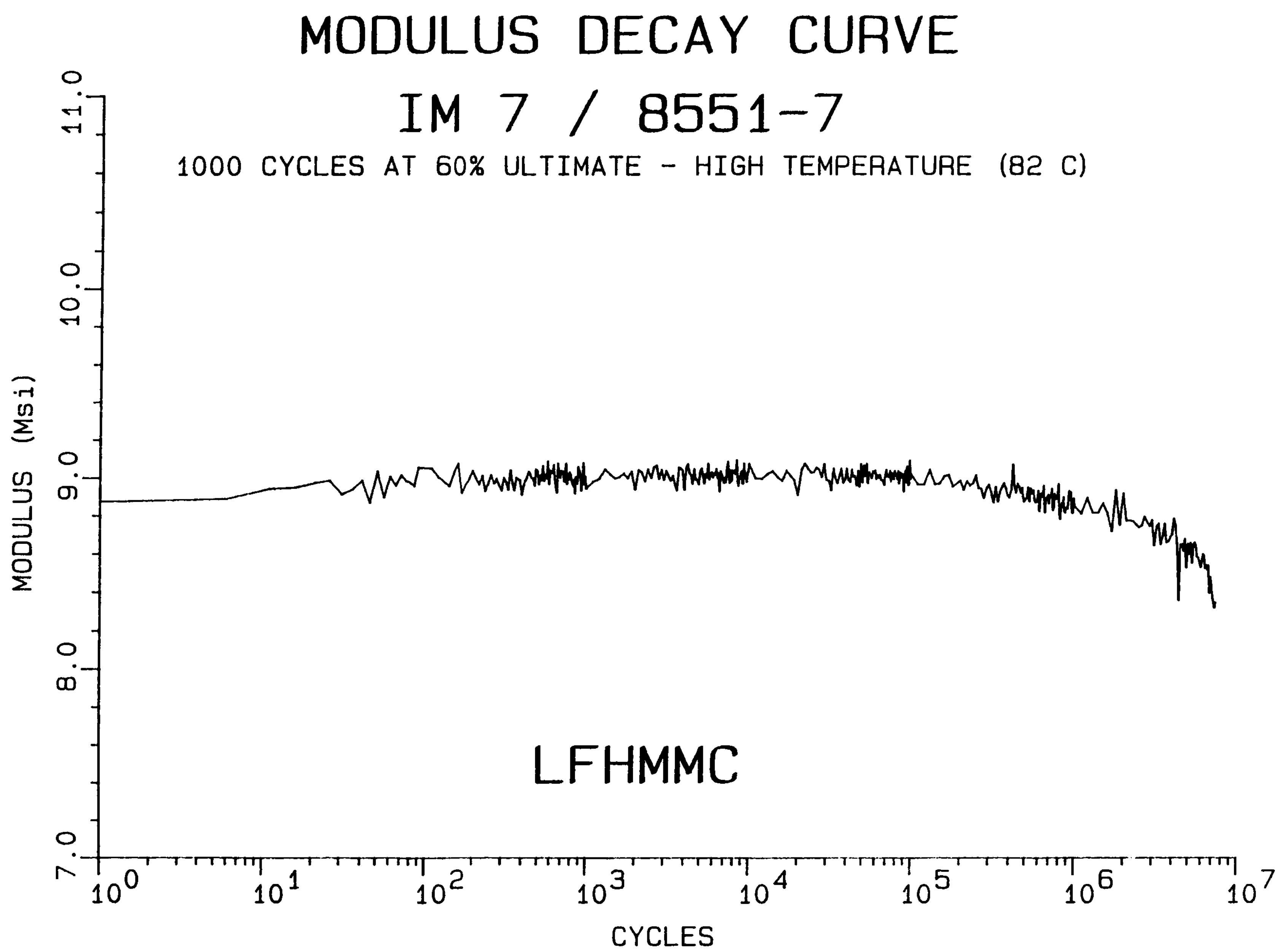
MODULUS DECAY CURVE
IM 7 / 8551-7
1000 CYCLES AT 60% ULTIMATE - HIGH TEMPERATURE (82 C)
MODULUS (Msi)
11.0
10.0
9.0
8.0
7.0
10^0
10^1
10^2
10^3
10^4
10^5
10^6
10^7
CYCLES
LFHMMC

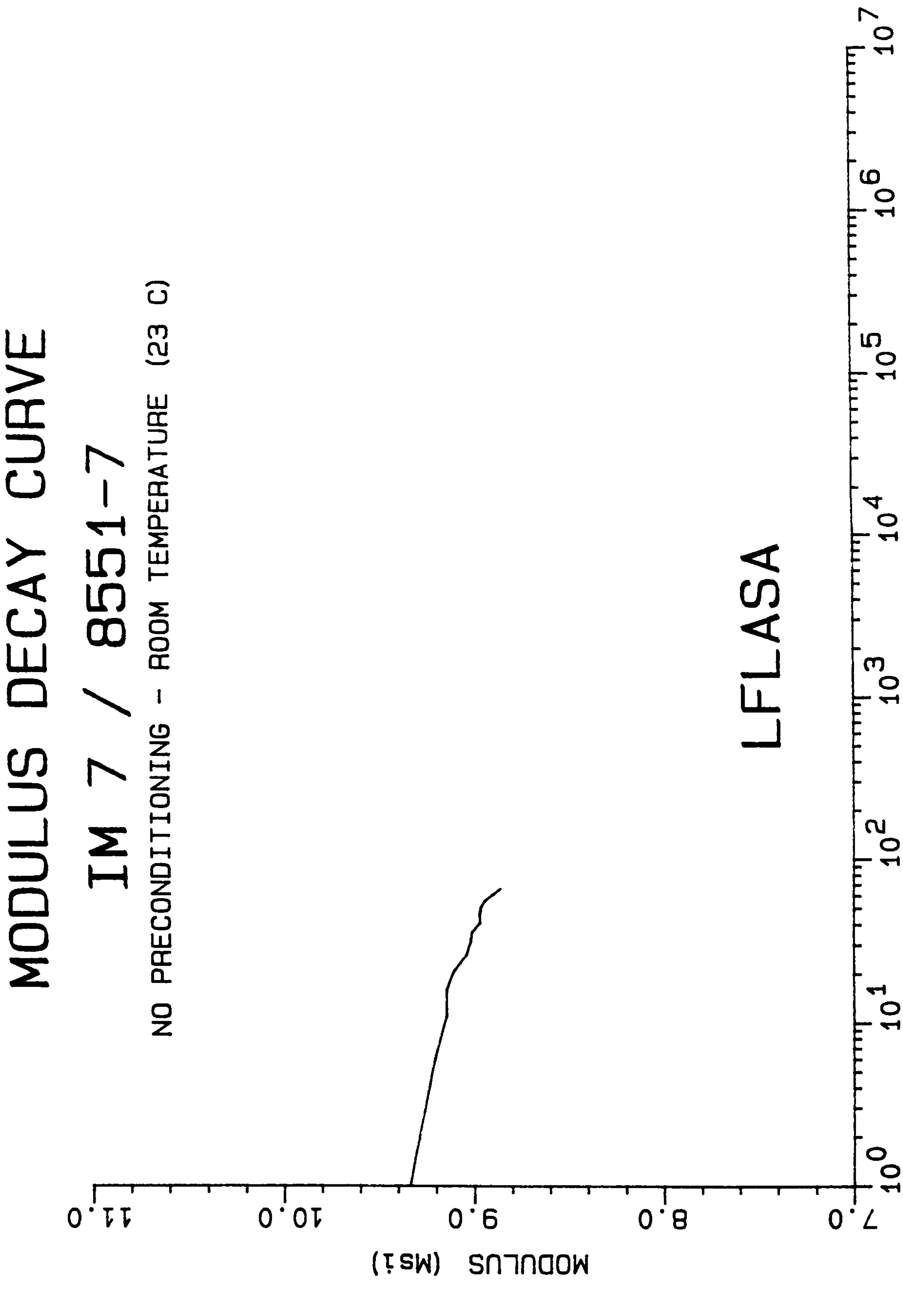
MODULUS DECAY CURVE
IM 7 / 8551-7
NO PRECONDITIONING - ROOM TEMPERATURE (23 C)
LFLASA
MODULUS (Msi)
7.0
8.0
9.0
10.0
11.0
CYCLES
10^0
10^1
10^2
10^3
10^4
10^5
10^6
10^7

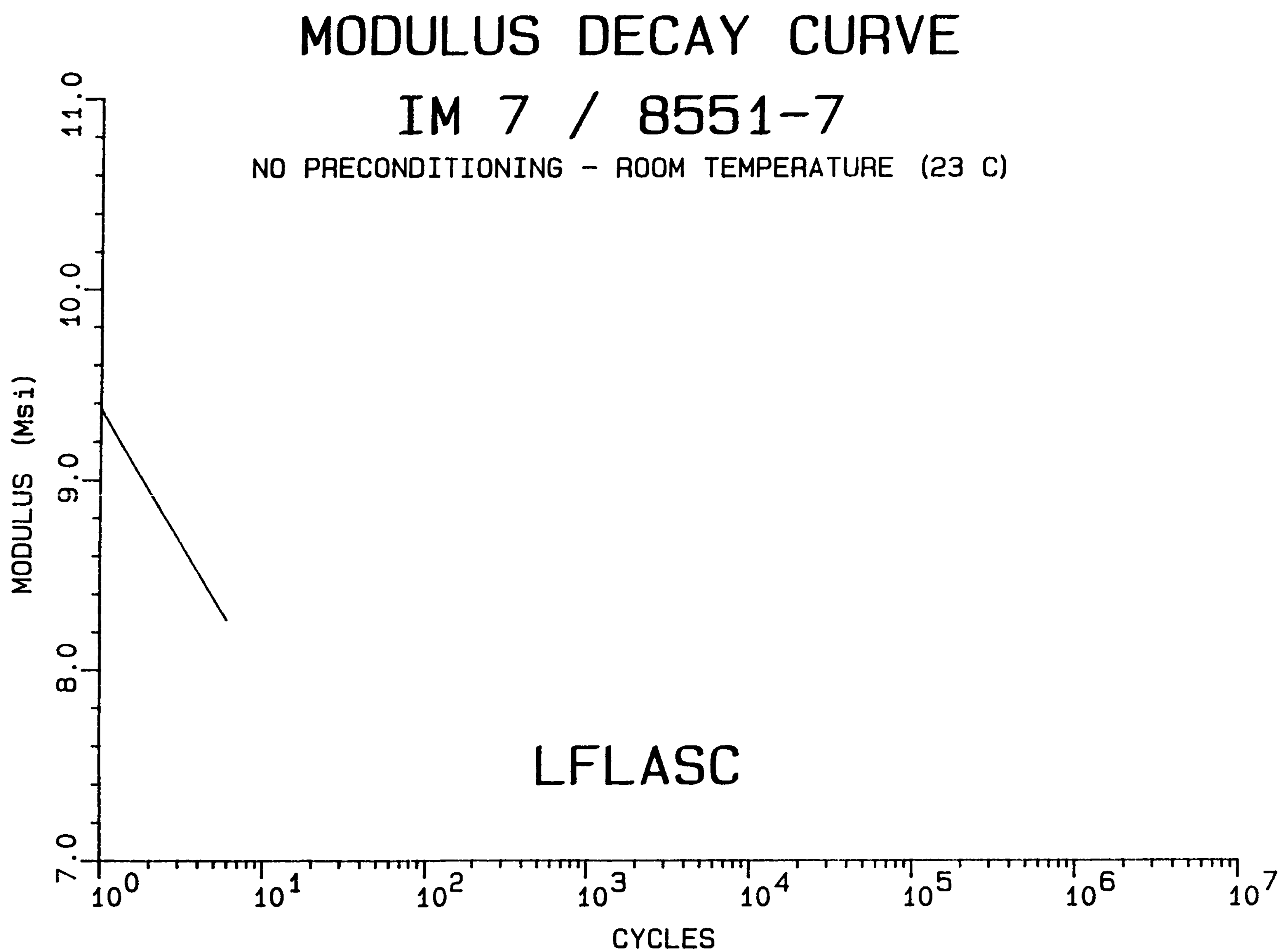
MODULUS DECAY CURVE
IM 7 / 8551-7
NO PRECONDITIONING - ROOM TEMPERATURE (23 C)
LFLASC
MODULUS (Msi)
7.0
8.0
9.0
10.0
11.0
CYCLES
10^0
10^1
10^2
10^3
10^4
10^5
10^6
10^7

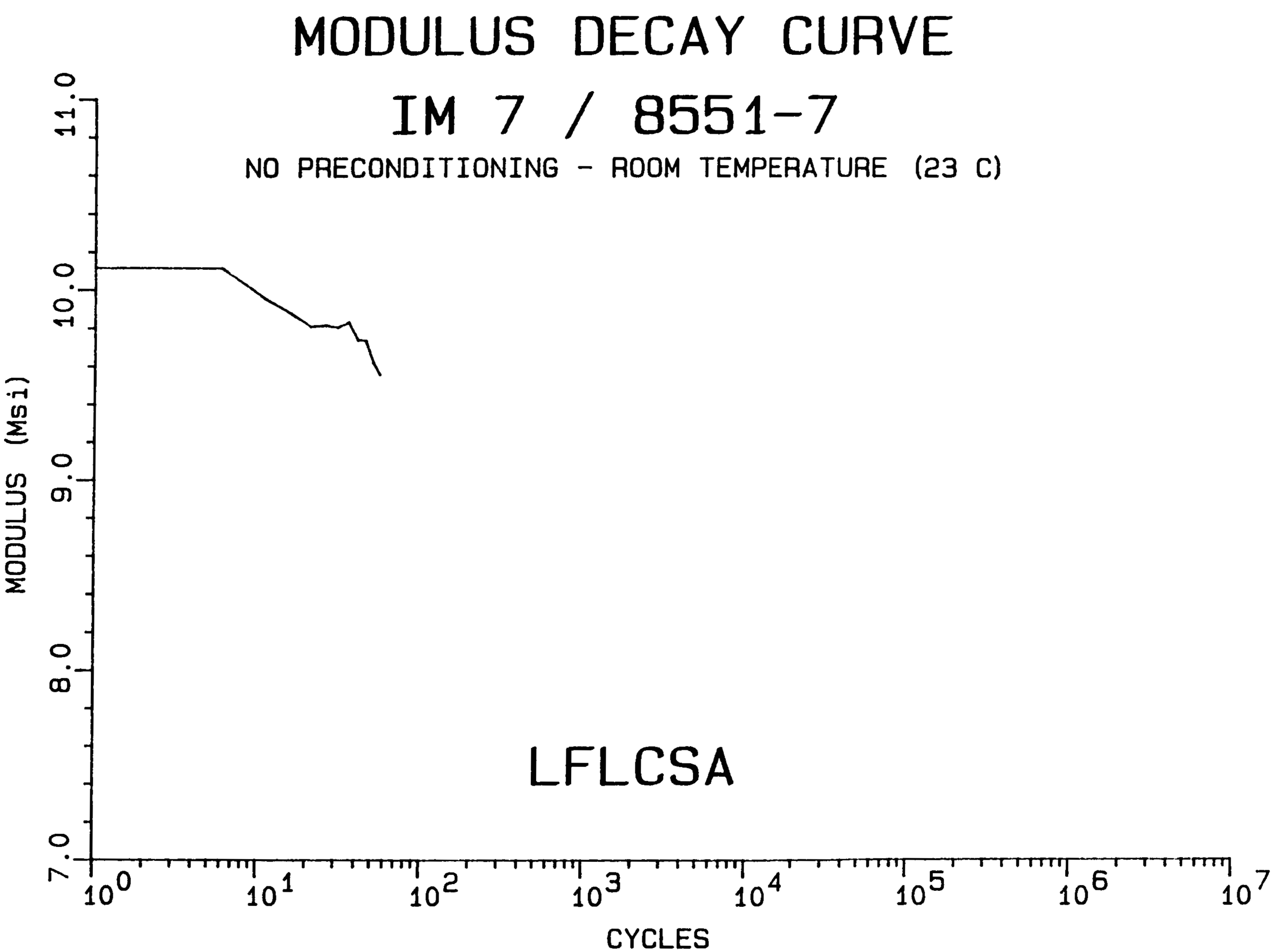
MODULUS DECAY CURVE
IM 7 / 8551-7
NO PRECONDITIONING - ROOM TEMPERATURE (23 C)
LFLCSA
MODULUS (Msi)
7.0
8.0
9.0
10.0
11.0
CYCLES
10^0
10^1
10^2
10^3
10^4
10^5
10^6
10^7

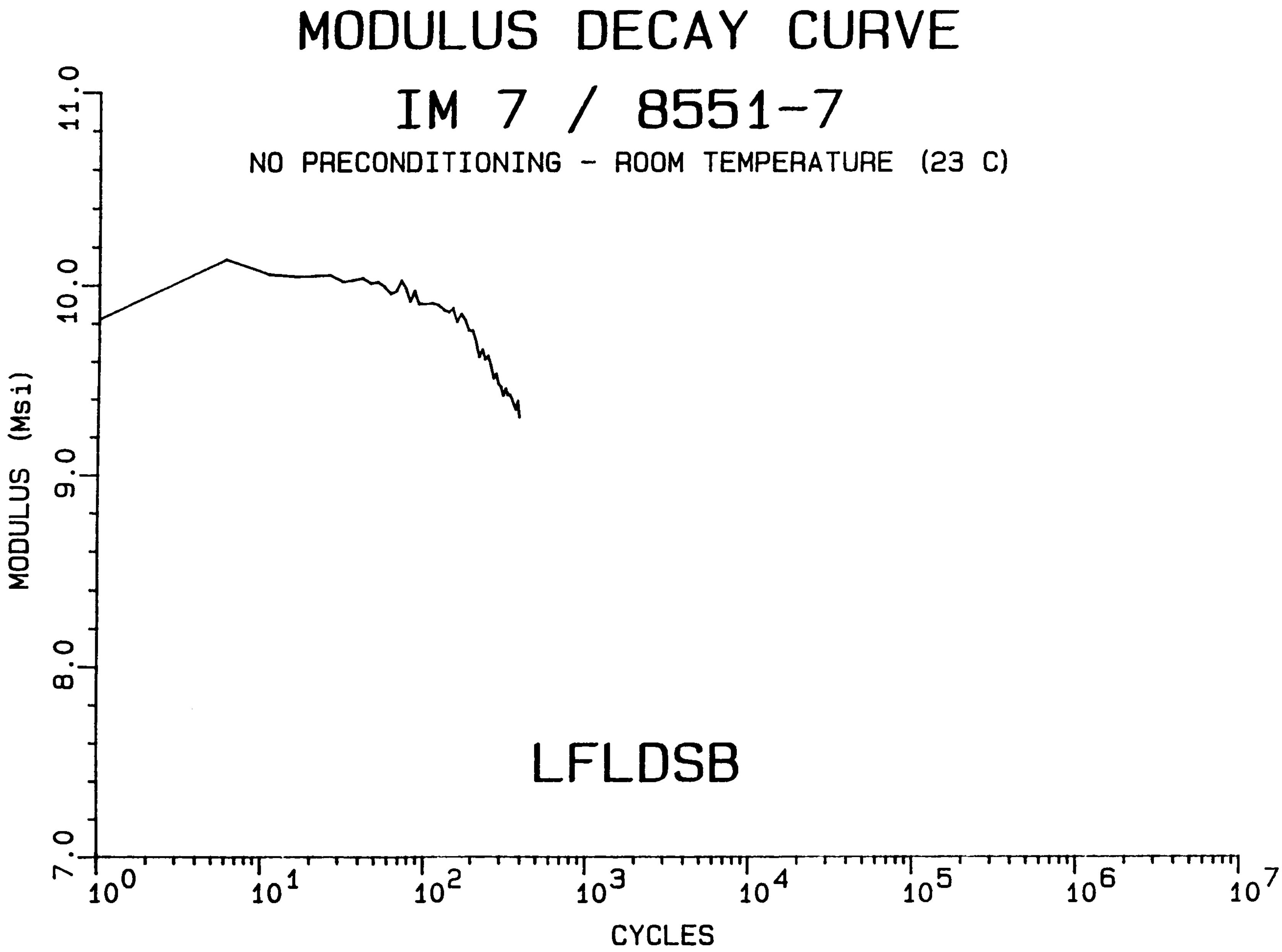
MODULUS DECAY CURVE
IM 7 / 8551-7
NO PRECONDITIONING - ROOM TEMPERATURE (23 C)
LFLDSB
MODULUS (Msi)
11.0
10.0
9.0
8.0
7.0
CYCLES
10^0
10^1
10^2
10^3
10^4
10^5
10^6
10^7

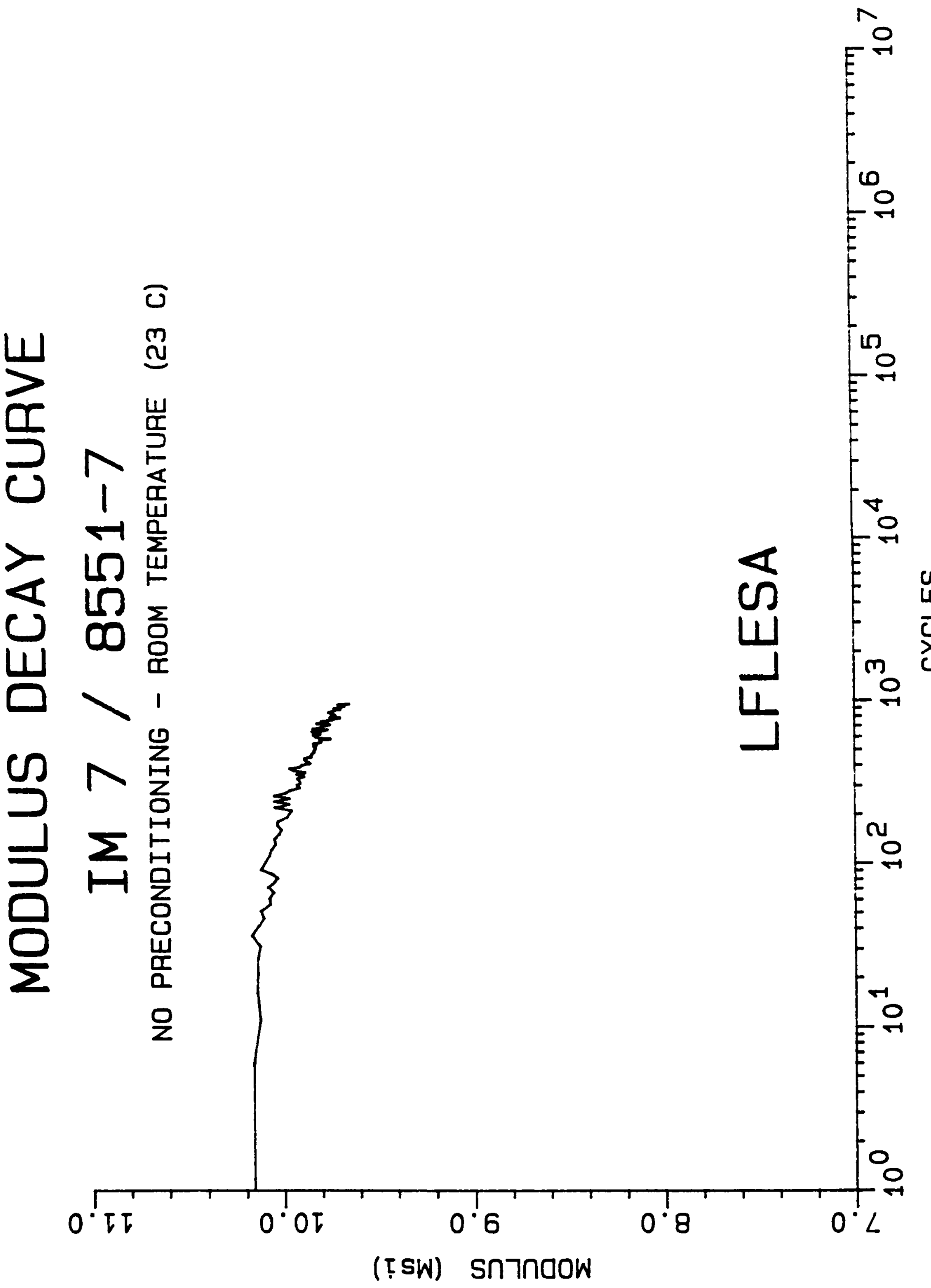

MODULUS DECAY CURVE
IM 7 / 8551-7
NO PRECONDITIONING - ROOM TEMPERATURE (23 C)
LFLESA
MODULUS (Msi)
7.0
8.0
9.0
10.0
11.0
CYCLES
10^0
10^1
10^2
10^3
10^4
10^5
10^6
10^7

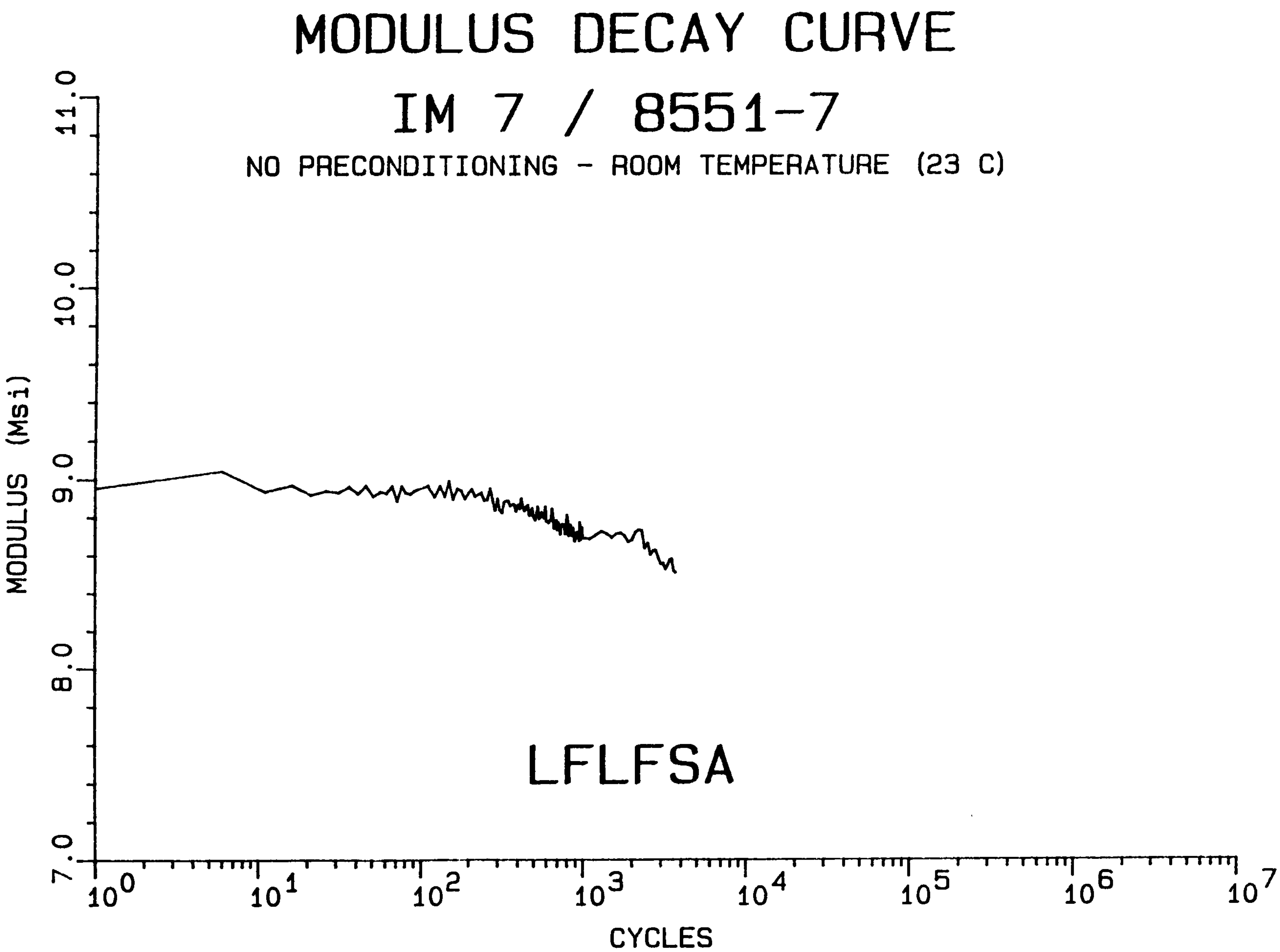

MODULUS DECAY CURVE
IM 7 / 8551-7
NO PRECONDITIONING - ROOM TEMPERATURE (23 C)
MODULUS (Msi)
11.0
10.0
9.0
8.0
7.0
LFLFSA
10^0
10^1
10^2
10^3
10^4
10^5
10^6
10^7
CYCLES

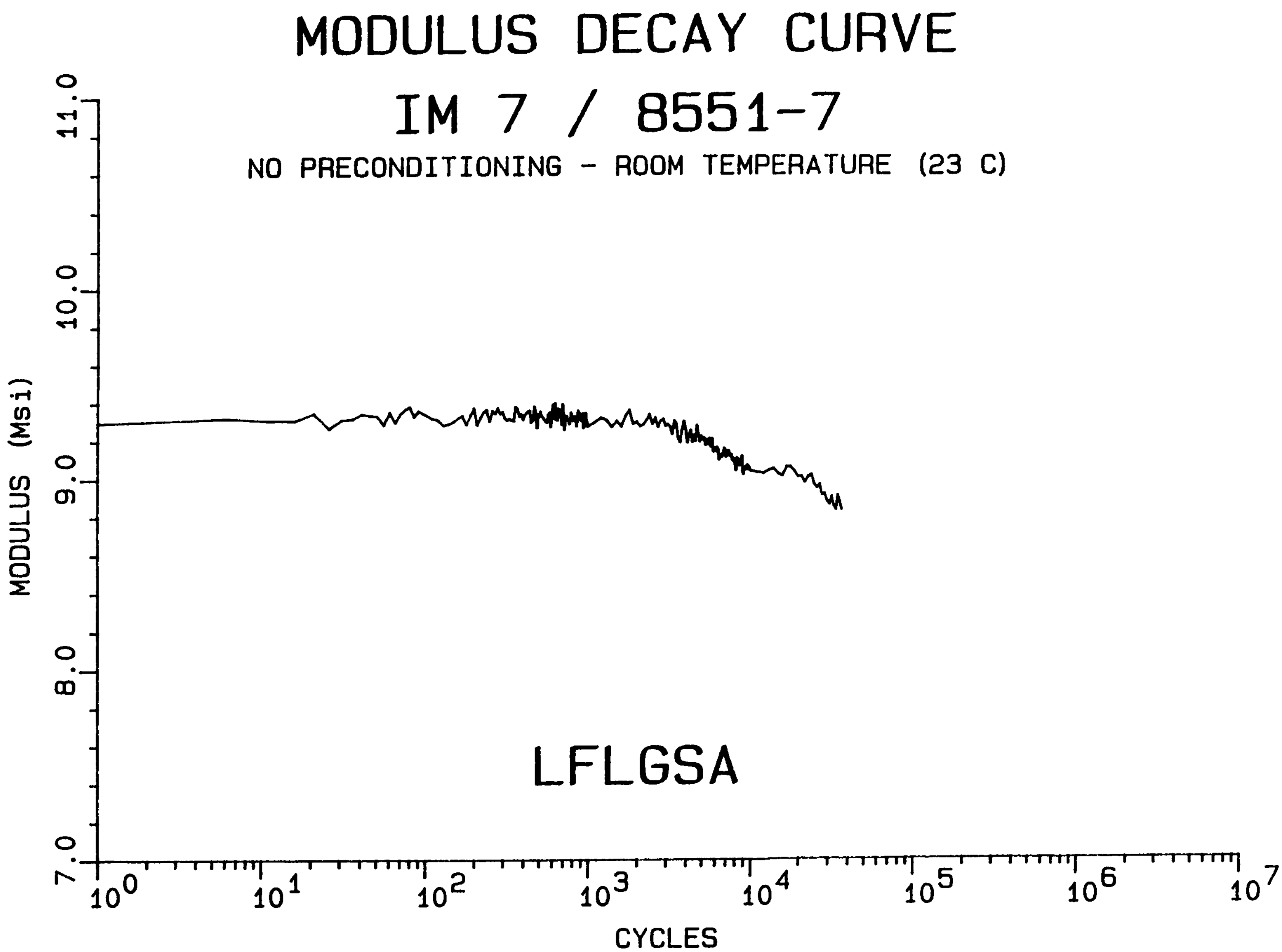

MODULUS DECAY CURVE
IM 7 / 8551-7
NO PRECONDITIONING - ROOM TEMPERATURE (23 C)
LFLGSA
MODULUS (Msi)
7.0
8.0
9.0
10.0
11.0
CYCLES
10^0
10^1
10^2
10^3
10^4
10^5
10^6
10^7

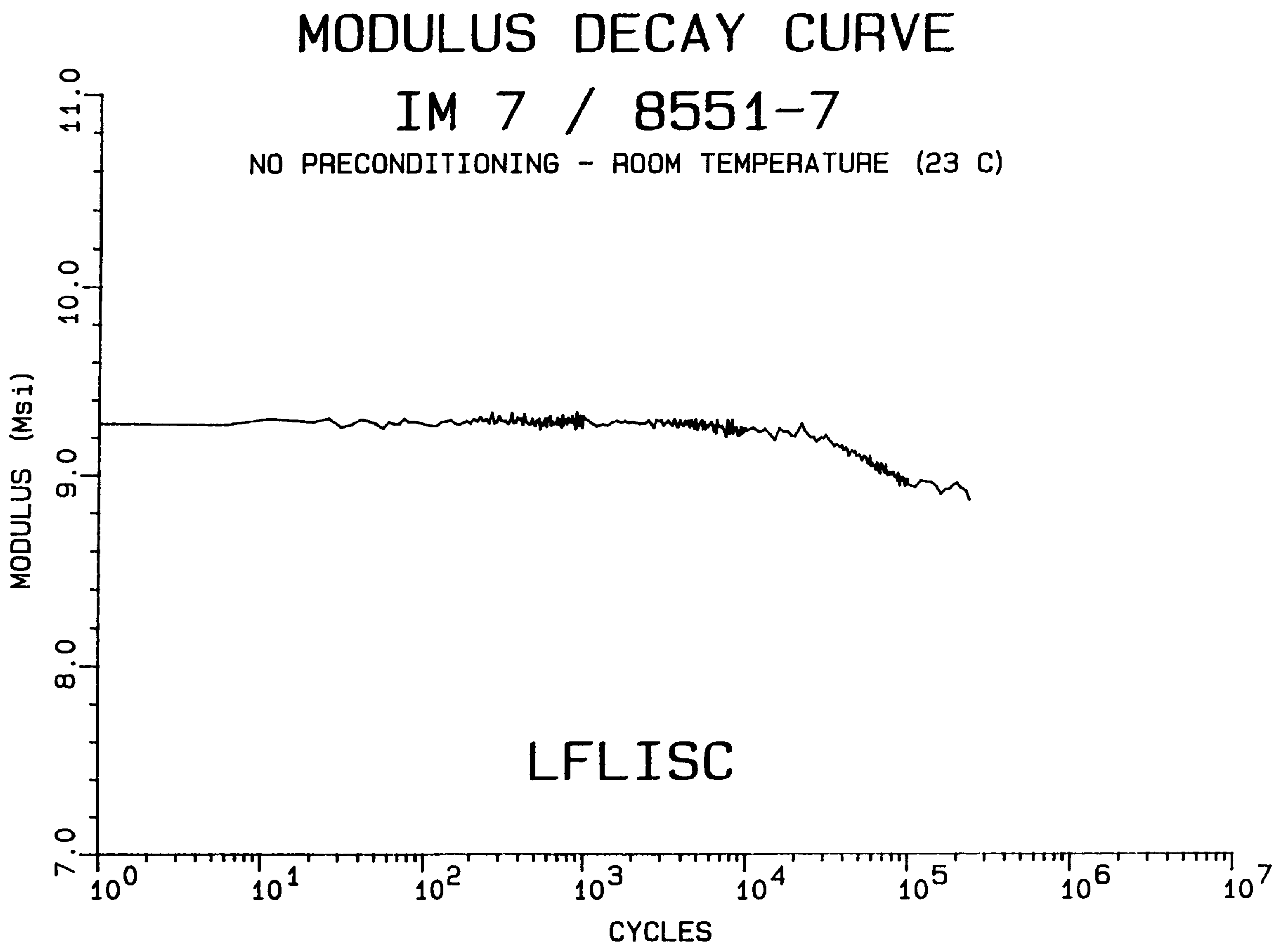

MODULUS DECAY CURVE
IM 7 / 8551-7
NO PRECONDITIONING - ROOM TEMPERATURE (23 C)
LFLISC
MODULUS (Msi)
11.0
10.0
9.0
8.0
7.0
CYCLES
10^0
10^1
10^2
10^3
10^4
10^5
10^6
10^7

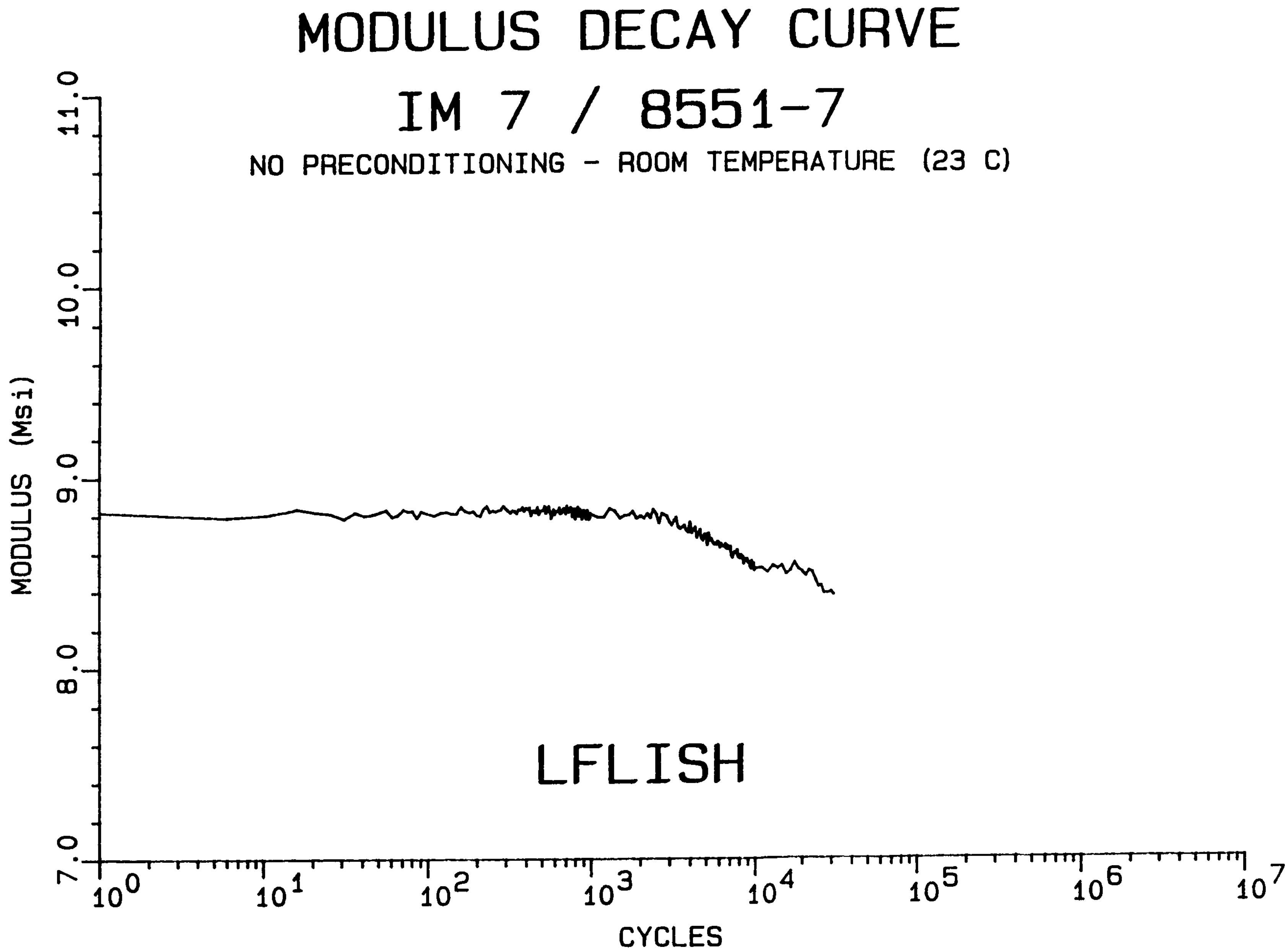
MODULUS DECAY CURVE
IM 7 / 8551-7
NO PRECONDITIONING - ROOM TEMPERATURE (23 C)
MODULUS (Msi)
11.0
10.0
9.0
8.0
7.0
LFLISH
10^0
10^1
10^2
10^3
10^4
10^5
10^6
10^7
CYCLES

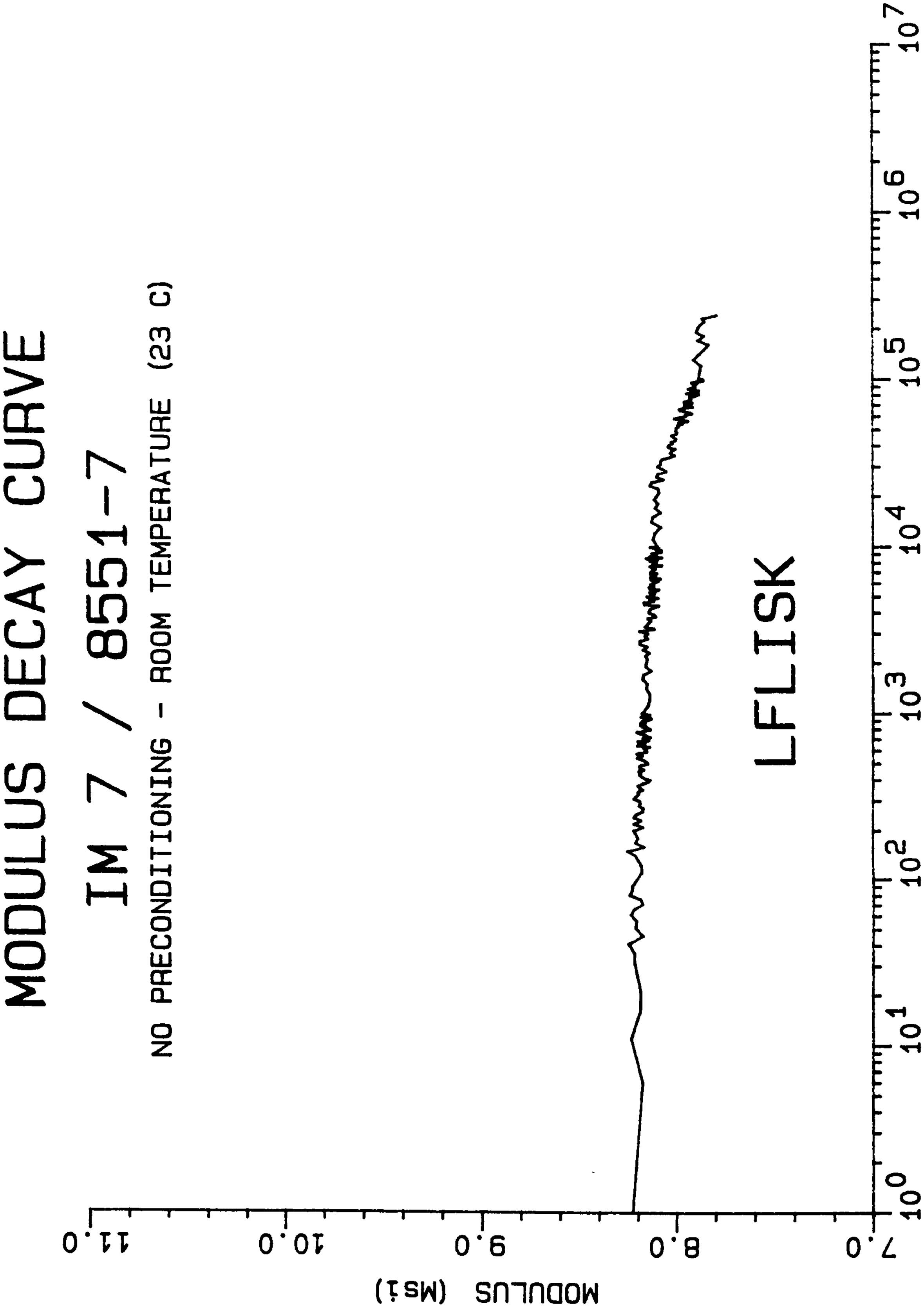
MODULUS DECAY CURVE
IM 7 / 8551-7
NO PRECONDITIONING - ROOM TEMPERATURE (23 C)
LFLISK
MODULUS (Msi)
7.0
8.0
9.0
10.0
11.0
CYCLES
10^0
10^1
10^2
10^3
10^4
10^5
10^6
10^7

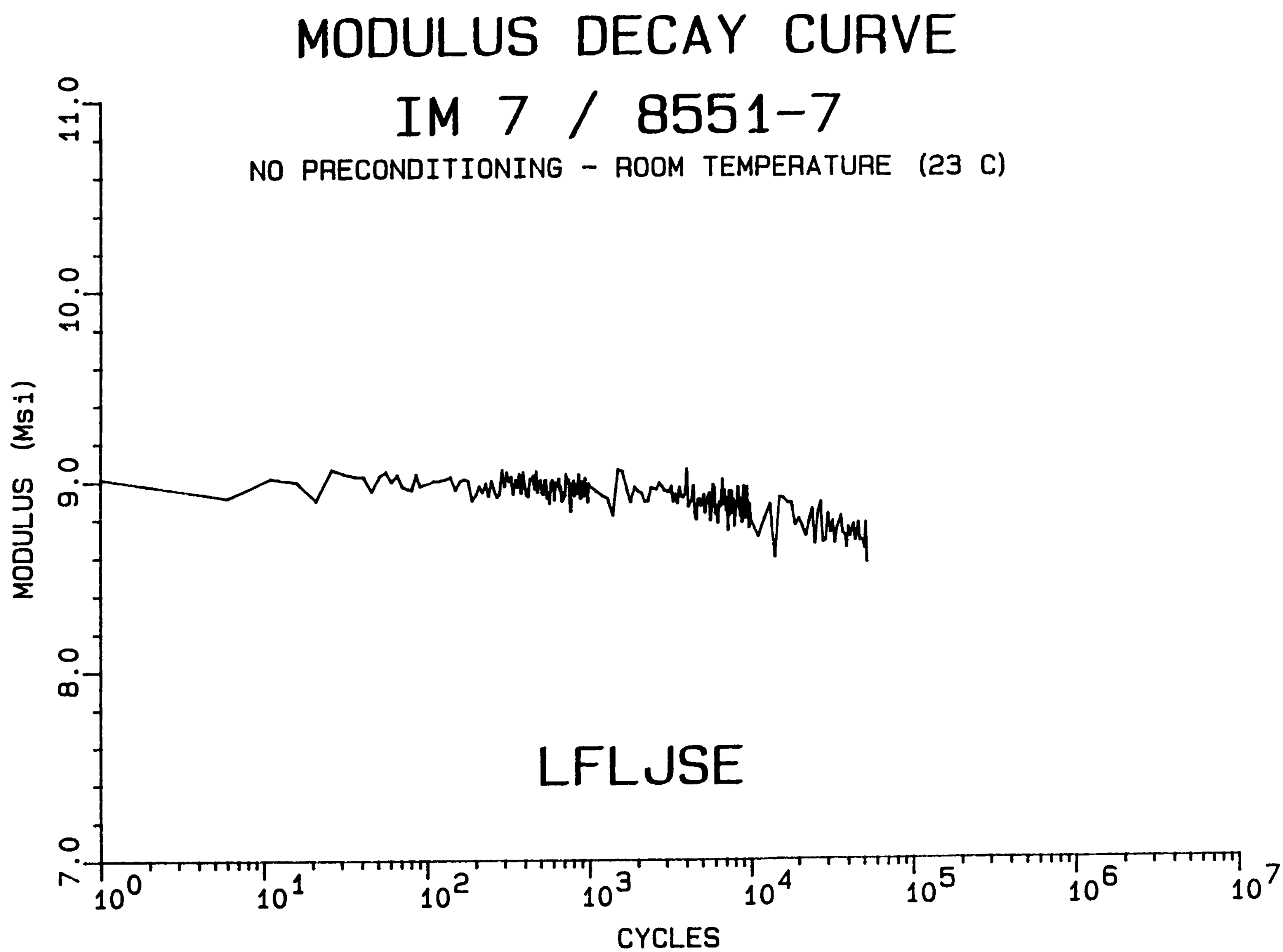
MODULUS DECAY CURVE
IM 7 / 8551-7
NO PRECONDITIONING - ROOM TEMPERATURE (23 C)
MODULUS (Msi)
11.0
10.0
9.0
8.0
7.0
LFLJSE
10^0 10^1 10^2 10^3 10^4 10^5 10^6 10^7
CYCLES

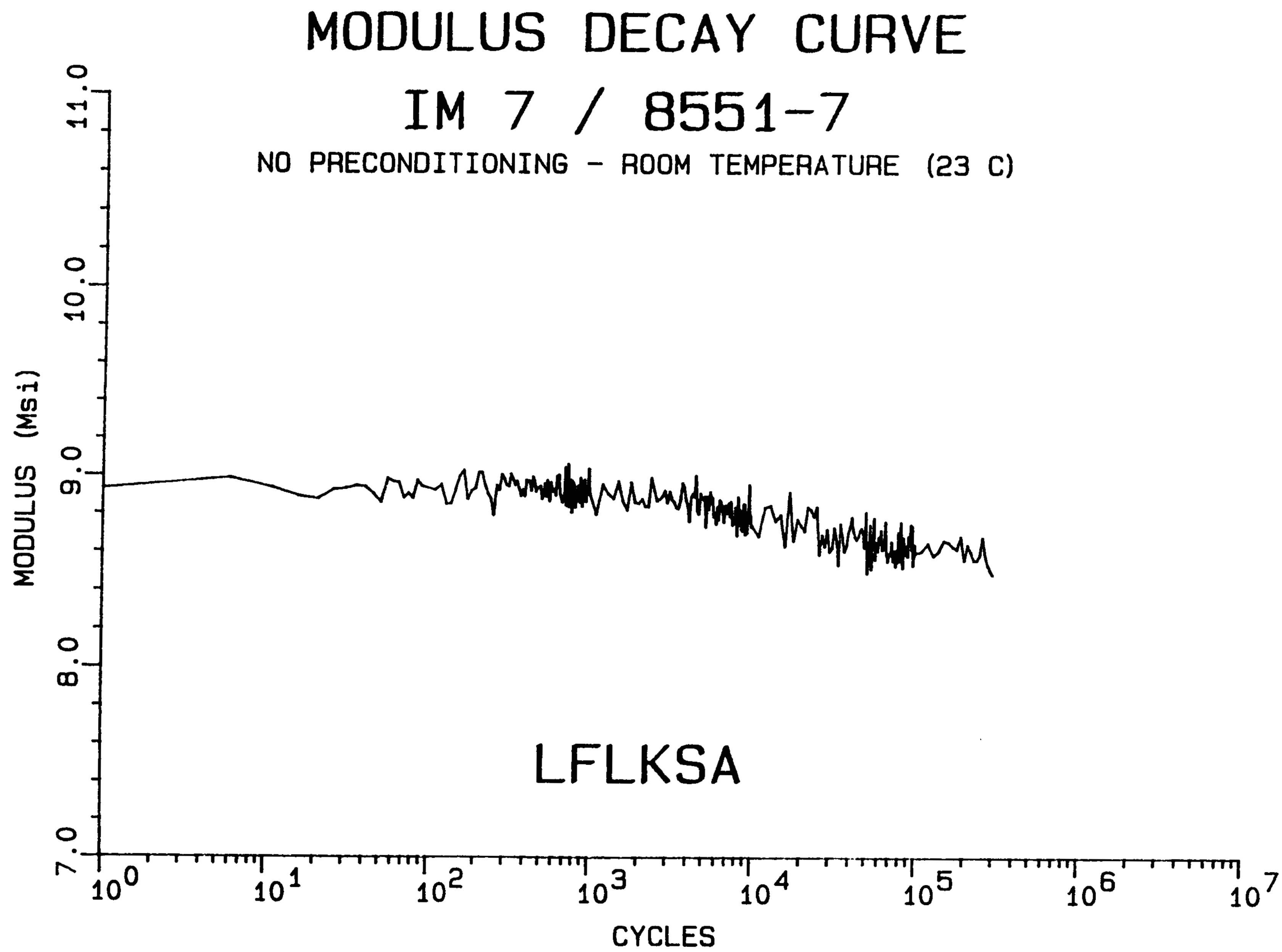
MODULUS DECAY CURVE
IM 7 / 8551-7
NO PRECONDITIONING - ROOM TEMPERATURE (23 C)
MODULUS (Msi)
11.0
10.0
9.0
8.0
7.0
LFLKSA
10^0
10^1
10^2
10^3
10^4
10^5
10^6
10^7
CYCLES

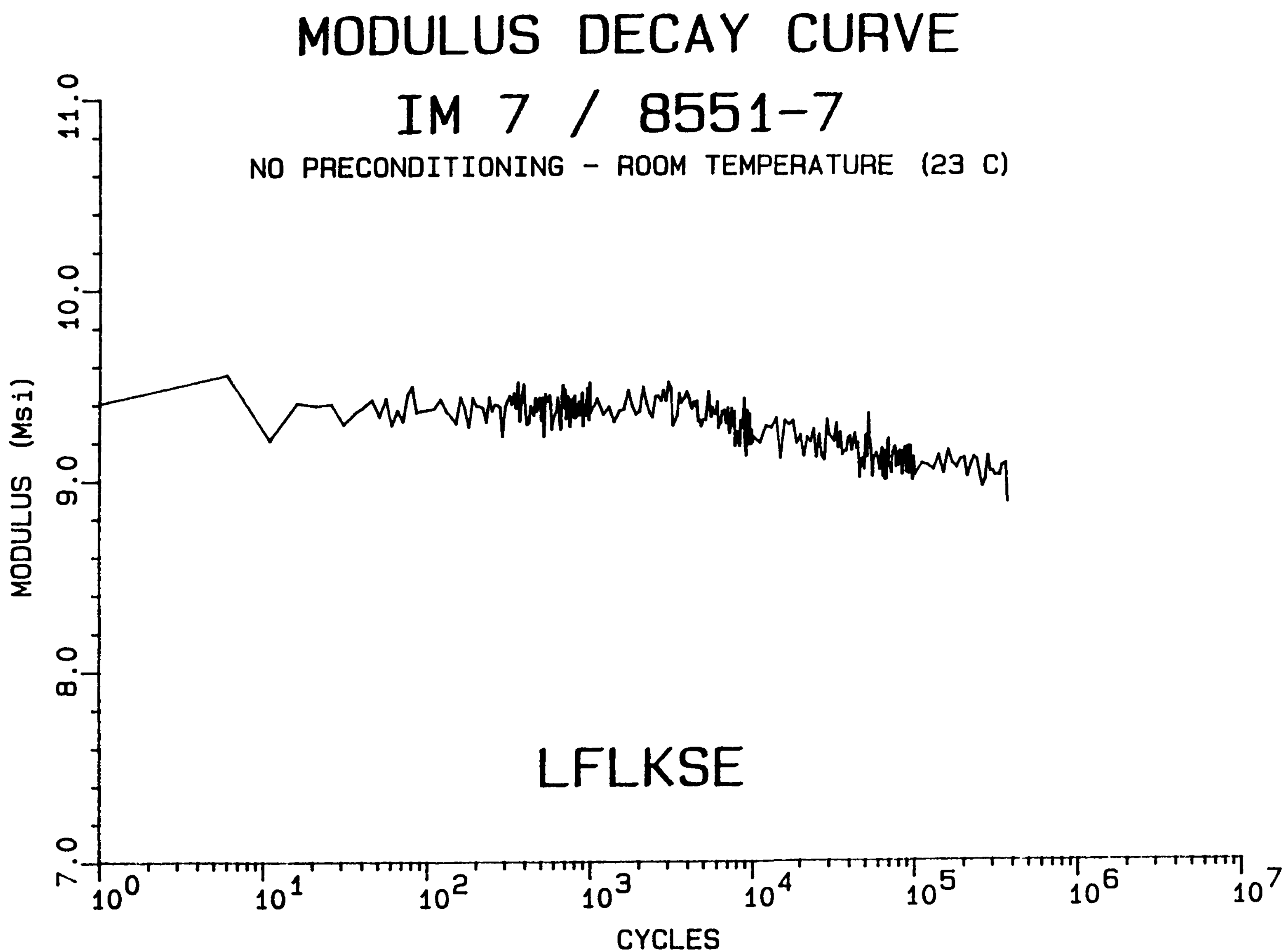
MODULUS DECAY CURVE
IM 7 / 8551-7
NO PRECONDITIONING - ROOM TEMPERATURE (23 C)
LFLKSE
MODULUS (Msi)
7.0
8.0
9.0
10.0
11.0
CYCLES
10^0
10^1
10^2
10^3
10^4
10^5
10^6
10^7

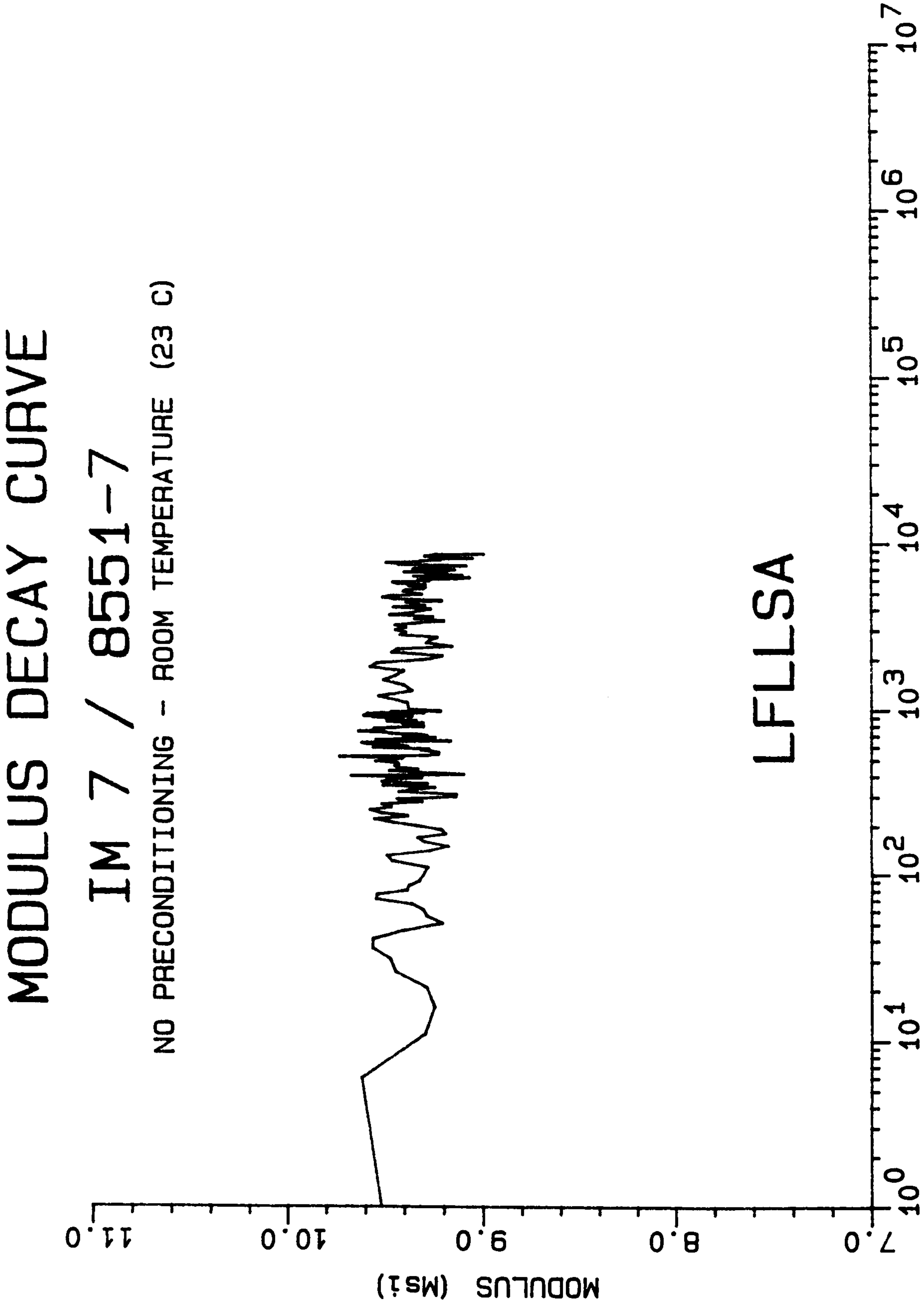
MODULUS DECAY CURVE
IM 7 / 8551-7
NO PRECONDITIONING - ROOM TEMPERATURE (23 C)
LFLLSA
MODULUS (Msi)
11.0
10.0
9.0
8.0
7.0
CYCLES
10^0
10^1
10^2
10^3
10^4
10^5
10^6
10^7

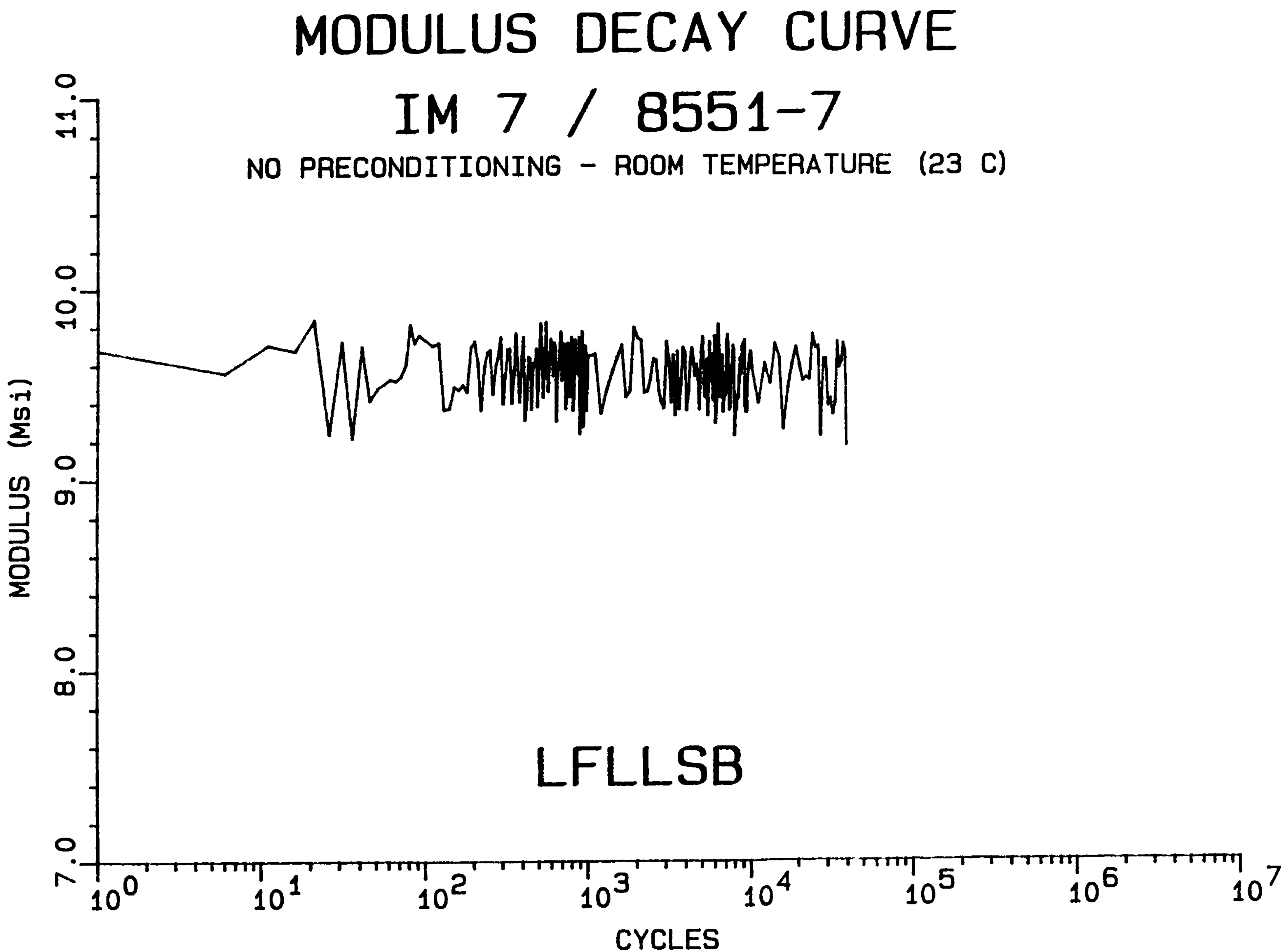

MODULUS DECAY CURVE
IM 7 / 8551-7
NO PRECONDITIONING - ROOM TEMPERATURE (23 C)
MODULUS (Msi)
7.0
8.0
9.0
10.0
11.0
10^0
10^1
10^2
10^3
10^4
10^5
10^6
10^7
CYCLES
LFLLSB

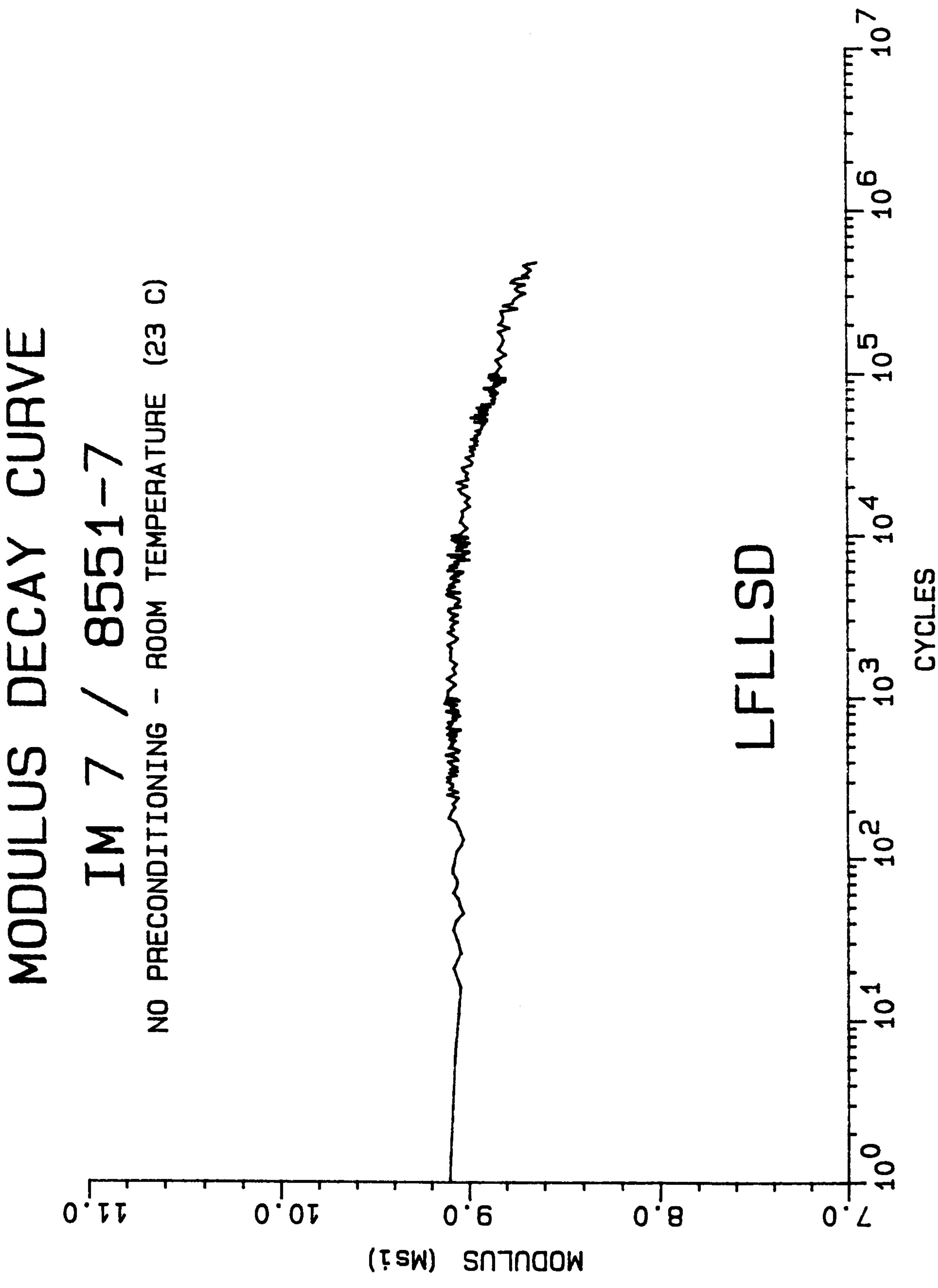

MODULUS DECAY CURVE
IM 7 / 8551-7
NO PRECONDITIONING - ROOM TEMPERATURE (23 C)
LFLLSD
CYCLES
MODULUS (Msi)
7.0
8.0
9.0
10.0
11.0
10^0
10^1
10^2
10^3
10^4
10^5
10^6
10^7

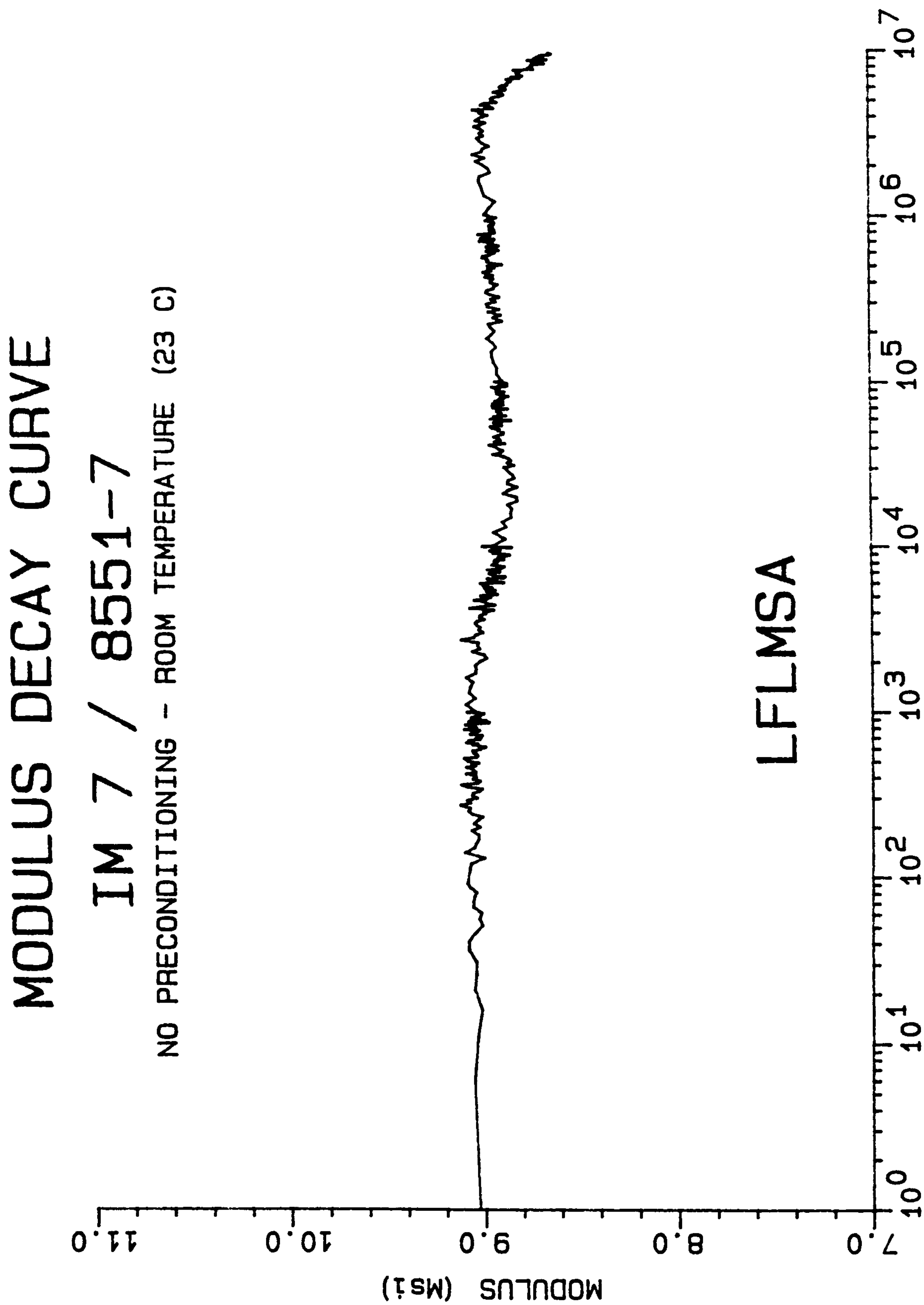
MODULUS DECAY CURVE
IM 7 / 8551-7
NO PRECONDITIONING - ROOM TEMPERATURE (23 C)
LFLMSA
MODULUS (Msi)
7.0
8.0
9.0
10.0
11.0
CYCLES
10^0
10^1
10^2
10^3
10^4
10^5
10^6
10^7